PERIMETRY UPDATE 1996/1997

Navigation Menu

PERIMETRY UPDATE 1996/1997

Proceedings of the
XIIth International Perimetric Society Meeting
Würzburg, Germany, June 4–8, 1996

edited by Michael Wall and Anders Heijl

KUGLER PUBLICATIONS
Amsterdam / New York

ISBN 90-6299-139-4

Distributors

For the U S A and Canada:
DEMOS
386 Park Avenue South, Suite 201
New York, NY 10016
Telefax (+212) 683-0072

For all other countries
Kugler Publications
P.O. Box 11188
1001 GD Amsterdam, The Netherlands

TABLE OF CONTENTS

Reliability and artifacts

Psychophysics

Glaucoma

Clinical observations

Miscellaneous

PREFACE

The Twelfth Annual Symposium of the International Perimetric Society was held in Würzburg, Germany, June 4-8, 1996. There again were interesting and informative scientific sessions. As usual, an exceptionally well-coordinated social program was enjoyed by all. In the scientific sessions, papers and discussions of posters were interleaved within ten sessions: Epidemiology, Neural Networks, Visual Field Progression; Cataract and Diffuse Loss; Clinical Observations I and II; Blood Flow and Nerve Fiber Layer Analysis; New Methods of Perimetry; Image Analysis and Glaucoma; Perimetric Techniques Reliability; Artifacts and Instruments; and Psychophysics and Electrophysiology. The many excellent presentations attest to the continued fine perimetry research on five continents. Again, at this meeting, two sessions were devoted to ophthalmic imaging; this field continues to advance.

One hundred and seven presentations were given, 55 were platform presentations and 52 were given as posters. Nineteen countries were represented.

We wish to thank those members of our executive committee, who helped with peer-review of the submitted manuscripts: President John Wild, Vice President Yoshiaki Kitazawa, Treasurer Fritz Dannheim, Past Secretary Richard Mills, Group Chairman Evanne Casson, Bernard Schwartz, Jörg Weber, William Hart, Avinoam Safran, Balwantray Chauhan and Enrico Gandolfo, and Members-at-Large Mario Zulauf and Elliot Werner. The XII Annual IPS Symposium was hosted by Eugen Gramer of Würzburg with much help from Fritz Dannheim. A special thanks goes to Diane Anderson of the University of Iowa Department of Ophthalmology for proofing and editing the manuscripts. We also thank Joey Haug, of the office of the secretariat, for her efforts in the organization of this monograph.

We are all looking forward to our next meeting, The XIII International Visual Field Symposium in Lago di Garda, Italy, September 6-9, 1998.

The Editors

NEW METHODS OF PERIMETRY

CONTRAST SENSITIVITY PERIMETRY IN EXPERIMENTAL GLAUCOMA
Investigations with degenerate gratings

RONALD S. HARWERTH and EARL L. SMITH, III

College of Optometry, University of Houston, Houston, TX, USA

Abstract

Visual field defects from experimental glaucoma occur earlier with Gabor patch stimuli than with standard perimetry using Goldmann III white stimuli. To investigate the mechanisms underlying the visual deficits for grating stimuli, the authors studied the changes in contrast sensitivity produced by the combined effects of experimental glaucoma and variable spatial sampling for Gabor patches. Psychometric functions for grating contrast were measured using degenerated Gabor patches (5%-85% stimulus blanking) for central vision and three locations in each visual field quadrant (3x3°, 9x9° and 15x15°) during the course of unilateral glaucoma in five rhesus monkeys. The authors found that the control functions for contrast sensitivity versus grating degeneration were exponential with a rapid decline in sensitivity when the stimulus blanking was greater than 50% of the pixels. Experimental glaucoma caused a uniform downward shift in the monkeys' contrast sensitivity versus degeneration functions, without displacement along the stimulus degeneration axis. Thus, the results were compatible with a model in which visual field defects caused by glaucomatous damage were due to a reduction in the sensitivities of detection mechanisms, without an increase in internal noise.

Introduction

Static threshold perimetry has become the standard functional test for the clinical diagnosis and assessment of treatment for glaucoma.[1,2] However, the well-known discrepancies between morphological and functional measurements of optic nerve damage[3,4] have suggested that threshold perimetry with the standard Goldmann III white stimulus is not the optimal test for early visual field defects. As a consequence, many investigations of alternative methods have been reported, most of which have used stimulus parameters that were presumed to reflect functions of neural mechanisms affected early in the disease. These studies have found improved sensitivity using perimetry paradigms based on the detection of color,[5-10] motion,[11-14] spatial resolution,[15-19] temporal resolution,[20-24] or contrast sensitivity.[25-30] However, in spite of positive preliminary data, only a few of the new techniques have gained acceptance for clinical perimetry.[7,18]

The best demonstration of an improvement in perimetric methodology would be

Address for correspondence: Ronald S. Harwerth, College of Optometry, University of Houston, Houston, TX 77204-6062, USA

Perimetry Update 1996/1997, pp. 3–12
Proceedings of the XIIth International Perimetric Society Meeting
Würzburg, Germany, June 4–8, 1996
edited by M. Wall and A. Heijl

based on a prospective study of glaucoma, but such studies are difficult because of the low rate of conversion of glaucoma suspects to glaucoma patients.[31-33] As an alternative approach, we wanted to determine whether, instead of research on patients, it would be more efficient to conduct preliminary studies of perimetry procedures on macaque monkeys with experimentally induced, unilateral glaucoma. Our initial investigations[30] have involved behavioral perimetry with Gabor patch stimuli.[34] The Gabor stimuli were chosen because they are spatially localized stimuli[35] that could be incorporated into existing methods of visual field analysis,[36-39] and their spatial profiles can be adjusted to match the receptive field properties of subpopulations of ganglion cells.[40] Thus, it seemed likely that contrast sensitivity with Gabor patches would be a sensitive test for functional defects caused by glaucoma. This prediction was confirmed by our preliminary studies[30] demonstrating an earlier appearance of visual field defects caused by experimental glaucoma for perimetric measurements with Gabor patches than with Goldmann III white stimuli.

Examples of the results of these investigations are shown in Figure 1 for two of the monkeys. The upper portion of each graph is a plot of the animal's intraocular pressure (IOP) history, with each of the experimental laser treatments indicated by a vertical dashed line. The lower parts of the graphs present comparisons of derived mean deviation (MD) perimetric indices for visual fields with either Gabor patches (circles) presented on a video monitor, or Goldmann III white stimuli (squares) using a Humphrey Field Analyzer. In all cases, the Gabor stimulus revealed statistically significant visual field defects earlier than the Goldmann III stimulus. The difference in the time courses of field defects is especially marked for subject OHT-10. It should also be noted that, within the resolution of the experimental data, Gabor patch perimetry produced significant MD defects whenever the monkey's IOP was greater than approximately 30 mmHg. This empirical correlation between IOP and MD defects suggested that one component of the Gabor patch visual field defects may be a pressure-induced neural dysfunction, rather than a loss of optic nerve fibers.[41]

The clinical implications for different mechanisms of visual field defects are substantial, therefore, the investigations to be described here were undertaken to differentiate between these two types of perimetric field defect. The experiments utilized spatially sampled (degenerate) stimuli,[42-46] which are defined by a selective occlusion of a proportion of the stimulus so that only samples of the target are visible.[46] The effect of spatial sampling for a redundant stimulus, *e.g.*, a sine-wave grating, is to add broadband masking noise and to reduce the effective stimulus contrast.[44] It has been shown that the visual sensitivities of normal observers are remarkably resilient to random stimulus degeneration,[44-46] but the effect may be more marked for subjects with a retinal pathology because the pathological process could add a source of internal noise that would combine with the controlled, sampling noise. For this reason, we studied the combined effects of experimental glaucoma and stimulus degeneration to determine whether IOP-induced reductions in visual sensitivity could be differentiated from visual field defects caused by optic nerve degeneration using Stiles' classical model for threshold-versus-intensity functions.[47-49]

Methods

The subjects were adult male rhesus monkeys (*Macaca mulatta*) who had been trained for behavioral perimetry.[50] Experimental glaucoma of the monkeys' right eyes was induced by argon laser trabeculoplasty following established procedures.[52-54]

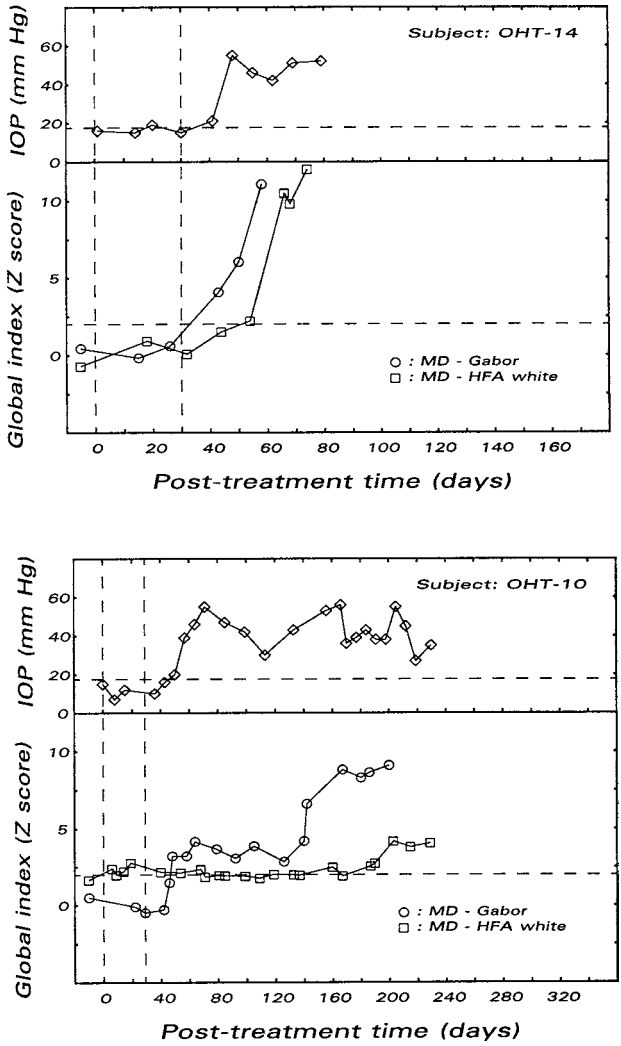

Fig. 1. Intraocular pressures (*diamonds*) and mean deviation (MD) perimetry indices (*circles and squares*) as a function of time following argon laser treatment to induce experimental glaucoma in monkeys. The times for the initial and second laser treatments are indicated by the dashed vertical lines. The dashed horizontal line in the upper graph for each subject shows the mean intraocular pressure for the control eye, for comparison to the experimental eye (*diamonds*). The dashed horizontal line in the lower graph for each subject demarcates two standard deviations from the mean (95% confidence limit) for the derived MD perimetric indices for contrast sensitivity perimetry (*circles*) and conventional clinical perimetry (*squares*).

Typically, the initial laser treatment (nominal laser parameters: 50 μm spot size, 500 msec duration, 1 W power) involved 75-100 burns over 270° of the trabecular meshwork. The subsequent treatments, with at least three-week intervals between treatments, involved 50-75 burns over a 180° segment of the drainage angle. Laser treatments were administered until the monkey's IOP was elevated reliably on weekly measurements with applanation tonometry.

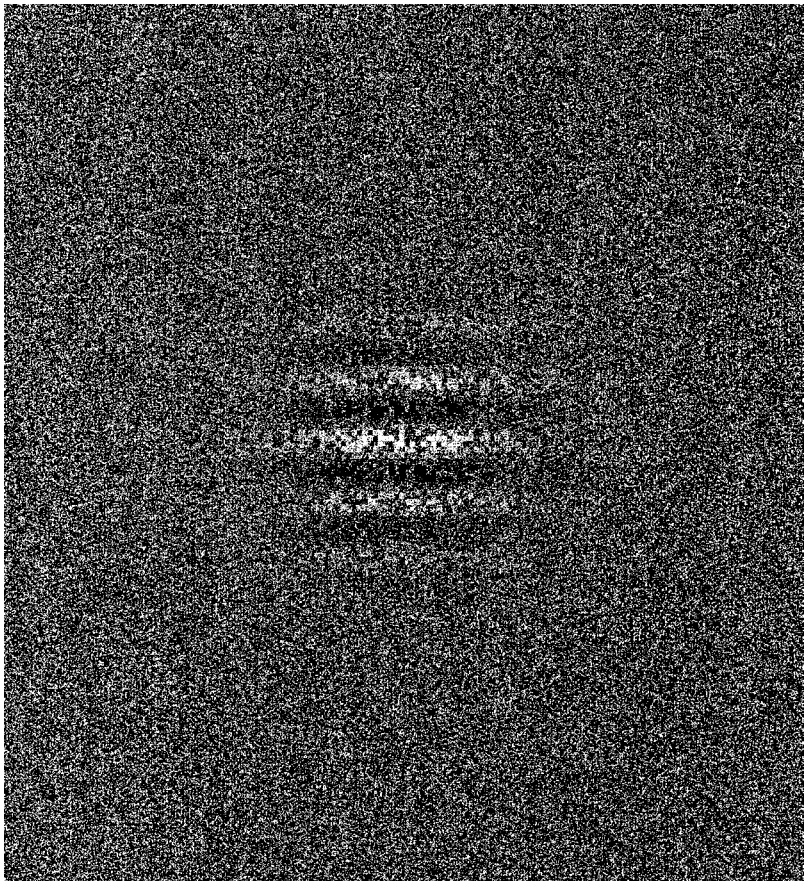

Fig. 2. A simulation of the degenerated Gabor patch stimuli, with 50% pixel blanking, used for experimental perimetry on monkeys with experimental glaucoma.

The methods for behavioral perimetry have been described previously.[50,51] The subjects were trained for both conventional clinical perimetry with an adapted Humphrey Field Analyzer (HFA)[50] and for an experimental perimetry procedure utilizing video images of Gabor patches. The Gabor patch stimuli were generated by a Cambridge Research Systems VSG graphics board, presented on a 20" video monitor (Nanao Corporation) and viewed through a +3 D lens at a distance of 33 cm. Gabor patches of one octave bandwidth[35] were composed of a 1 cycle/deg horizontal carrier grating multiplied by a 2-D gaussian envelope. The stimulus contrast was specified as the contrast of the carrier grating. Decreased spatial sampling of the Gabor stimulus was accomplished by blanking arrays of pixels to the mean luminance of the video screen (usually 2x2 pixel arrays, each pixel subtended 5.7 arcmin). An example of a Gabor patch with 50% degeneration is illustrated in Figure 2.

For the full visual field plots, contrast thresholds were measured at 44 test locations which coincided with the retinal co-ordinates (without correction for the flat video screen) of the HFA 24-2 Threshold Program over the central 30° (vertical) by 48° (horizontal) of the visual field. In some sessions, rather than complete visual

fields, data for psychometric functions were obtained at the fixation point and three locations along the 45° diagonal (3x3°, 9x9°, and 15x15°) of each visual field quadrant. Frequency-of-seeing data were obtained for stimuli with various amounts of stimulus degeneration (0 to 84% of the stimulus blanked), and these data were fit with a Weilbull function to determine slope and position (contrast threshold) of the psychometric function.

Results

Control data for the effects of stimulus degeneration with a centrally fixated stimulus are presented in Figure 3. The data from this monkey are consistent with control data from the other monkey subjects and with published data from humans[44-46] in showing that spatial sampling had little effect on the detection thresholds until more than 50% of the stimulus area had been deleted. With greater degeneration, the monkey's contrast sensitivity decreased exponentially to a contrast sensitivity value of 1 (100% contrast) with 100% degeneration, as is demonstrated by the exponential function fitted to the data.

These pretreatment data for the effects of experimental external stimulus noise provided the baseline function for a model to predict the effects of adding pathological noise in glaucoma. We assumed that the model for the combined effects of internal and external noise was a straightforward application of Stiles' 'rules of independence' for threshold-versus-intensity functions.[47-49] The model, illustrated in Figure 3, predicts independent horizontal or vertical displacement of the degeneration functions when glaucoma causes visual field defects. First, if the effect of experimental glaucoma is to decrease the sensitivities of the detection mechanisms, without an overall addition of internal noise, then the degeneration function should be simply displaced downward, as is illustrated by the dashed line in Figure 3. Alternatively, if the effect of elevated IOP is to increase the internal noise within the detection mechanisms, then the degeneration function should be uniformly displaced leftward to reflect the additional noise, as is illustrated by the dot-dashed line in Figure 3. Of course, both effects could occur and cause a downward and leftward shift in the function, but the magnitude of the leftward shift should still reflect the amount of pathological noise.

Representative results of the effects of experimental glaucoma are shown in Figure 4. The figure presents subject OHT-14's pretreatment data (circles) and his post-treatment data collected during a one-week period starting at either 45 days (squares) or 60 days (diamonds) after the first laser treatment (see Fig. 1, upper plot, for the monkey's IOP history and visual fields data). The individual graphs in Figure 4 represent central vision and 12 peripheral retina test locations on the oblique meridians (3x3°, 9x9° and 15x15°) in each visual field quadrant. Over the time course of these measurements, the experimental glaucoma caused a substantial reduction in the monkey's contrast sensitivity for non-degenerated stimuli and at some test locations, the detection threshold was near 100% contrast. Most importantly, the best-fit exponential functions for the stimulus degeneration data collected during this period represented purely vertical shifts in the functions. Similar data were obtained for the other subjects, thus the results were compatible with a reduction in the sensitivities of the detection mechanisms, rather than an increase in the internal noise of the mechanisms caused by glaucomatous damage.

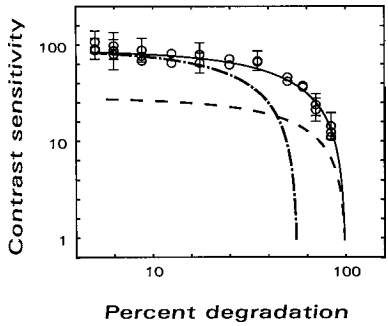

Fig. 3. Contrast sensitivity as a function of stimulus degradation of the Gabor patch, *i.e.*, the percent of the stimulus area blanked to the mean luminance of the video screen. The data represent the means and ±1 SD of the contrast sensitivity measurements. The dashed and dot-dashed lines represent two predictions of the effects of experimental glaucoma (see text for details).

Discussion

These investigations have demonstrated that behavioral assessments of visual functions in monkeys with experimental glaucoma represent a viable approach to the development of new perimetry procedures. The monkey model provides an efficient approach because their functional defects progress quite rapidly following the laser-induced elevation of IOP, which in most cases reached 40 to 60 mmHg. The animals' pressure-induced visual field defects developed as diffuse losses in sensitivity which were reflected as significant increases in the mean deviation (MD) perimetric index for both conventional perimetry with the Goldmann III white stimuli and the experimental perimetry procedure with Gabor stimuli. This result is also in agreement with findings from conventional perimetry on patients with open-angle glaucoma.[2,39,55-57] Thus, in general, the visual field defects from experimental perimetry in monkeys seem analogous to visual field defects in human glaucoma patients, but the monkey model offers several experimental advantages. For example, the investigations are prospective, with pre-glaucoma measurements and time-course data available for each subject. In addition, the natural progression of visual field defects can be followed to an end-state without confounding therapeutic intervention. Also, physiological or morphological experiments can be conducted to determine the physiological basis for visual defects.[58-60]

In clinical practice, perimetric visual field defects are used as a gauge of glaucomatous optic nerve damage and of the success of glaucoma treatment.[61] In some instances, lowering a patient's IOP results in an improvement of visual fields, but in other cases, visual fields either do not improve or continue to deteriorate.[41,62] Presently, it is not possible to determine which response will occur for any given patient,[41,61] but it should be possible to develop methods to differentiate between permanent and recoverable visual field defects.

We have explored some of the possibilities of contrast sensitivity perimetry and spatial sampling as a procedure to differentiate IOP-induced reductions in visual sensitivity from visual field defects caused by optic nerve degeneration. The results of these studies were equivocal. First, the time course for visual field defects with contrast sensitivity perimetry using Gabor patch stimuli were suggestive of pressure-

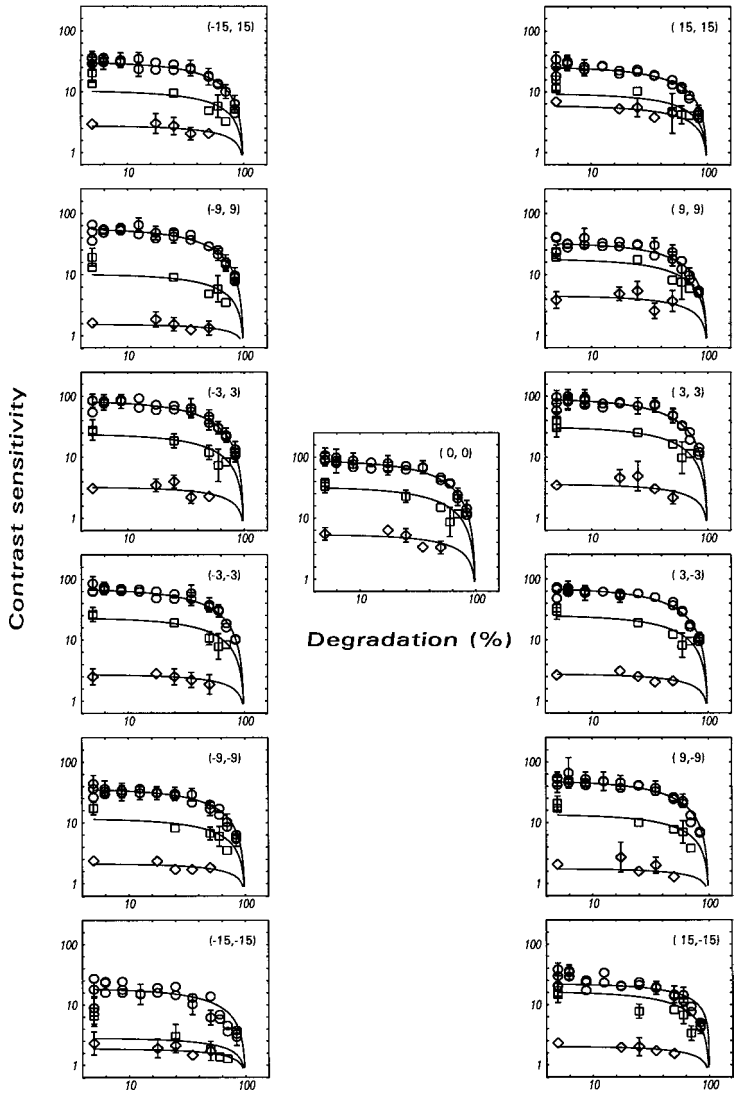

Fig. 4. Stimulus degeneration functions for subject OHT-14 (see Fig. 1 for the subject's IOP history and visual field data). The visual field coordinates for each set of data are given in the upper-right of each of the graphs. Pretreatment baseline data (*circles*) and data collected 45 days (*squares*) or 60 days (*diamonds*) after the initial laser treatment are presented.

induced reductions of contrast sensitivity. The reduced sensitivities were diffuse and produced significant MD defects earlier than defects measured by conventional perimetry. On the other hand, the noise experiments with degenerated gratings indicated that there was a unitary process underlying reduced visual sensitivities from experimental glaucoma. The mechanism of reduced sensitivity, however, cannot be deduced from these functions, and either a reduction in the number of detectors or reduced sensitivities of detectors are compatible with the measurements.

The operation of a unitary mechanism for visual field defects may be correct, but its acceptance without reservation requires additional experiments. The spatial sampling strategy produces noise exclusively in the stimulus, but retinal disease would increase the noise level across the entire visual field.[45] Therefore, measurements with experimental background noise, in addition to stimulus noise, are important to verify the present results.

With respect to the development of perimetry methodology, we found that contrast sensitivity perimetry with narrow-band, spatial frequency-defined Gabor patch stimuli provided earlier evidence of visual field defects than perimetry with the standard white Goldmann III stimulus. Thus, contrast sensitivity perimetry with Gabor stimuli may have a potential usefulness for the early detection of glaucoma. However, the restricted range of Michaelson contrast sets a limit on the measurement of advanced field defects and, because the MD perimetric index is the most sensitive indication of abnormal fields, non-glaucoma related losses of contrast sensitivity may limit its specificity. It seems that additional work with the monkey model will be beneficial before subjecting the procedure to clinical investigations on patients.

Acknowledgments

This study was supported in part by a research grant from Alcon Laboratories, Inc., Fort Worth, TX, USA, and NIH Core Center Grant EY-07551 from the National Eye Institute, Bethesda, MD, USA.

References

1. Anderson DR: Perimetry With and Without Automation, 2nd Edn. St Louis: CV Mosby Co 1987
2. Drance SM: The early structural and functional disturbances of open-angle glaucoma. Ophthalmology 92:853-857, 1985
3. Quigley HA, Addicks EC, Green WR: Optic nerve damage in human glaucoma. III. Quantitative correlation of nerve fiber loss and visual field defects in glaucoma, ischemic neuropathy, papilledema and toxic neuropathy. Arch Ophthalmol 100:135-146, 1982
4. Quigley HA, Dunkelberger GR, Green WR: Studies of retinal ganglion cell atrophy correlated with automated perimetry in human eyes with glaucoma. Am J Ophthalmol 107:453-464, 1989
5. Heron G, Adams AJ, Husted R: Central visual fields for short wavelength sensitive pathways in glaucoma and ocular hypertension. Invest Ophthalmol Vis Sci 29:64-72, 1988
6. Sample PA, Weinreb RN: Progressive color visual field loss in glaucoma. Invest Ophthalmol Vis Sci 33:240-243, 1992
7. Johnson CA, Adams AJ, Casson EJ, Brandt JD: Blue-on-yellow perimetry can predict the development of glaucomatous visual field loss. Arch Ophthalmol 111:645-650, 1993
8. Johnson CA, Adams AJ, Casson EJ, Brandt JD: Progression of early glaucomatous visual field loss for blue-on-yellow and standard white-on-white automated perimetry. Arch Ophthalmol 111:651-656, 1993
9. Harwerth RS, Smith EL, DeSantis L: Perimetric indices for the progression of visual field defects using colored light. Invest Ophthalmol Vis Sci (Suppl) 35:2185, 1994
10. Greenstein VC, Halevy D, Zaidi Q, Koenig KL, Ritch RH: Chromatic and luminance systems deficits in glaucoma. Vision Res 36:621-629, 1996
11. Silverman SE, Trick GL, Hart WM: Motion perception is abnormal in primary open-angle glaucoma and ocular hypertension. Invest Ophthalmol Vis Sci 31:722,729, 1990
12. Bullimore MA, Wood JM, Swenson K: Motion perception in glaucoma. Invest Ophthalmol Vis Sci 34:3526-3533, 1993
13. Trick GL, Steinman SB, Amyot M: Motion perception deficits in glaucomatous optic neuropathy. Vision Res 35:2225-2233, 1995

14. Wall M, Ketoff KM: Random dot motion perimetry in patients with glaucoma and in normal subjects. Am J Ophthalmol 120:587-598, 1996
15. Phelps CD: Acuity perimetry and glaucoma. Trans Am Ophthalmol Soc 82:753-791, 1984
16. Airaksinen J, Tuulonen A, Valimaki J, Alanko HI: High-pass resolution perimetry and retinal nerve fiber layer in glaucoma. Acta Ophthalmol (Kbh) 68:687-689, 1990
17. Sample PA, Ahn DS, Lee PC, Weinreb RN: High-pass resolution perimetry in eyes with ocular hypertension and primary open-angle glaucoma. Am J Ophthalmol 113:309-316, 1992
18. Frisen L: High-pass resolution perimetry: a clinical review. Doc Ophthalmol 83:1-25, 1993
19. Frisen L: High-pass resolution perimetry: central-field neuroretinal correlates. Vision Res 35:293-299, 1995
20. Tyler CW: Specific deficits of flicker sensitivity in glaucoma and ocular hypertension. Invest Ophthalmol Vis Sci 20:204-212, 1981
21. Brussel EM, White CW, Faubert J, Dixon M, Balazsi GA, Overbury O: Multi-flash campimetry as an indicator of visual field loss in glaucoma. Optom Vis Sci 63:32-38, 1986
22. Breton ME, Wilson TW, Wilson R, Spaeth GL, Krupin T: temporal contrast sensitivity loss in primary open-angle glaucoma and glaucoma suspects. Invest Ophthalmol Vis Sci 32:2931-2941, 1991
23. Austin MW, O'Brien CJ, Wishart PK: Forced choice flicker perimetry in glaucoma and ocular hypertension. In: Mills RP, Wall M (eds) Perimetry Update 1994/1995, pp 135-140, Amsterdam/ New York: Kugler Publ, 1995
24. Matsumoto C, Okuyama S, Uyama K, Iwagaki A, Otori T: Automated flicker perimetry in glaucoma. In: Mills RP, Wall M (eds) Perimetry Update 1994/1995, pp 141-146, Amsterdam/ New York: Kugler Publ, 1995
25. Atkin A, Bodis-Wollner I, Wolkstein M, Moss A, Podos SM: Abnormalities of central contrast sensitivity in glaucoma. Am J Ophthalmol 88:205-211, 1979
26. Ross JE, Bron AJ, Clarke DD: Contrast sensitivity and visual disability in chronic simple glaucoma. Br J Ophthalmol 68:821-827, 1984
27. Lundh BL: Central and peripheral contrast sensitivity for static and dynamic sinusoidal gratings in glaucoma. Acta Ophthalmol (Kbh) 63:487-492, 1985
28. Korth M, Horn F, Storck B, Jonas JB: Spatial and spatiotemporal contrast sensitivity of normal and glaucoma eyes. Graefe's Arch Clin Exp Ophthalmol 227:428-435, 1989
29. Lundh BL, Gottvall E: Peripheral contrast sensitivity for dynamic sinusoidal gratings in early glaucoma. Acta Ophthalmol Scand 73:202-206, 1995
30. Harwerth RS, Smith EL: Visual field defects in glaucoma: Gabor patch vs. Goldmann III test targets. Invest Ophthalmol Scand 73:202-206, 1995
31. Armaly MF: Ocular pressure and visual fields: a ten-year follow-up study. Arch Ophthalmol 81:25-40, 1969
32. Graham PA: The definition of pre-glaucoma: a prospective study. Trans Ophthalmol Soc UK 88:153-165, 1969
33. Drance SM, Schulzer M, Thomas B, Douglas GR: Multivariate analysis in glaucoma: use of discriminate analysis in predicting glaucomatous visual field damage. Arch Ophthalmol 99:1019-1022, 1981
34. Swanson WH, Wilson HR, Giese SC: Contrast matching data predicted from contrast increment thresholds. Vision Res 24:63-75, 1984
35. Peli E, Arend LE, Young GM, Goldstein RB: Contrast sensitivity to patch stimuli: effects of spatial bandwidth and temporal presentation. Spatial Vision 7:1-14, 1993
36. Heijl A, Lindgren G, Olsson J: A package for the statistical analysis of visual algorithms for detecting glaucomatous visual fields. Doc Ophthalmol Proc Ser 49:1543-168, 1987
37. Katz J, Sommer A, Gaasterland DE, Anderson DR: Comparison of analytic algorithms for detecting glaucomatous visual field loss. Arch Ophthalmol 109:1684-1689, 1991
38. Bartz-Schmidt KU, Weber J: Comparison of spatial thresholds and intensity thresholds in glaucoma. International Ophthalmol 17:171-178, 1993
39. Wood JM, Burce AS: The value of visual field indices in screening and threshold testing of glaucoma. Glaucoma 15:140-146, 1993
40. Regan D: A brief review of some of the stimuli and analysis methods used in spatiotemporal vision research. In: Regan D (ed) Vision and Visual Dysfunction. Vol 10: Spatial Vision, pp 1-42. Boca Raton: CRC Press 1993
41. Katz LJ, Spaeth GL, Cantor LB, Poryzees EM, Steinmann WC: Reversible optic disk cupping and visual field improvement in adults with glaucoma. Am J Ophthalmol 107:485-492, 1989

42. Nyman G, Greenlee MW, Laurinen P: Sampling irregularity perturbs visual reconstruction. J Opt Soc Am A 5:628-635, 1988
43. Mulligan JB, MacLeod DIA: Visual sensitivity to spatially sampled modulation in human observers. Vision Res 31:895-905, 1991
44. Geller AM, Sieving PA, Green DG: Effect on grating identification of sampling with degenerate arrays. J Opt Soc Am A 9:472-477, 1992
45. Seiple W, Holopigian K, Szlyk JP, Greenstein VC: The effects of random element loss on letter identification: implications for visual acuity loss in patients with retinitis pigmentosa. Vision Res 35:2057-2066, 1995
46. Alexander KR, Xie W, Derlacki DJ, Szlyk JP: Effect of spatial sampling on grating resolution and letter identification. J Opt Soc Am A 12:1825-1833, 1995
47. Stiles WS, Separation of the 'blue' and 'green' mechanisms of foveal vision by measurements of increment thresholds. Proc Roy Soc B 133:418-434, 1946
48. Barlow HB: Increment thresholds at low intensities considered as signal/noise discrimination. J Physiol (Lond) 136:469-488, 1957
49. Kalloniatis M, Harwerth RS, Smith EL, DeSantis L: Colour vision anomalies following experimental glaucoma in monkeys. Ophthalmol Physiol Opt 13:56-67, 1993
50. Harwerth RS, Smith EL, DeSantis L: Behavioral perimetry in monkeys. Invest Ophthalmol Vis Sci 34:31-40, 1993
51. Harwerth RS, Smith EL, DeSantis L: Mechanisms mediating visual detection in static perimetry. Invest Ophthalmol Vis Sci 34:3011-3023, 1993
52. Gaasterland D, Kupfer C: Experimental glaucoma in the rhesus monkey. Invest Ophthalmol Vis Sci 13:455-460, 1974
53. Pederson JE, Gaasterland DE: Laser-induced primate glaucoma. I. Progression of cupping. Arch Ophthalmol 102:1689-1698, 1984
54. Quigley HA, Hohman RM: Laser energy levels for trabecular meshwork damage in the primate eye. Invest Ophthalmol Vis Sci 24:1305-1307, 1983
55. Anderson D: The damage caused by pressure. XLVI Edward Jackson memorial lecture. Am J Ophthalmol 108:185-195, 1989
56. Caprioli J, Sears M: Patterns of early visual field loss in open angle glaucoma. Doc Ophthalmol Proc Series 49:307-315, 1987
57. Glowazki A, Flammer J: Is there a difference between glaucoma patients with rather localized visual field damage and patients with more diffuse visual field damage? Doc Ophthalmol Proc Series 49:317-320, 1987
58. Smith EL, Chino YM, Harwerth RS, Ridder WH, Crawford MLJ, DeSantis L: Retinal inputs to the monkey's lateral geniculate nucleus in experimental glaucoma. Clin Vis Sci 8:113-139, 1993
59. Vickers JC, Schumer RA, Podos SM, Wang RF, Riederer BM, Morrison JH: Differential vulnerability of neurochemically identified subpopulations of retinal neurons in a monkey model of glaucoma. Brain Res 680:23-35, 1995
60. Desatnik H, Quigley HA, Glovinsky Y: Study of central retinal ganglion cell loss in experimental glaucoma in monkey eyes. J Glaucoma 5:46-53, 1996
61. Quigley HA: Open-angle glaucoma. New Engl J Med 328:1097-1106, 1993
62. Tsai CS, Shin DH, Wan JY, Zeiter JH: Visual field global indices in patients with reversal of glaucomatous cupping after intraocular pressure reduction. Ophthalmology 98:1412-1419, 1991

THE ROLE OF SPATIAL AND TEMPORAL FACTORS IN FREQUENCY-DOUBLING PERIMETRY

CHRIS A. JOHNSON and SHABAN DEMIREL

Optics and Visual Assessment Laboratory (OVAL), Department of Ophthalmology, University of California, Davis, Sacramento, CA, USA

Abstract

When a low spatial frequency sinusoidal grating undergoes high temporal frequency counterphase flicker, its perceived spatial frequency is twice its actual spatial frequency (frequency doubling). This percept is believed to be mediated by non-linear magnocellular mechanisms (M*y* cells). Recent studies have shown that contrast thresholds for frequency-doubled stimuli are effective in detecting glaucomatous visual field loss. The purpose of the present study was to determine the contribution and efficacy of spatial and temporal components of the stimulus in distinguishing patients with early to moderate glaucomatous field loss from age-matched normal controls. Four stimulus configurations were employed: *1.* stimuli that produce the frequency-doubling effect (0.25 cycles/degree, 25 Hz counterphase flicker), *2.* a steady 0.25 cycle/degree grating, *3.* a steady 0.5 cycle/degree grating, and *4.* a uniform flickering stimulus (25 Hz). Stimuli were approximately 8° in diameter, and were presented in a 4 x 4 grid over the central 20° radius. Contrast sensitivity was estimated using a modified binary search (MOBS) staircase procedure. Contrast sensitivity for glaucoma patients was reduced in areas of localized field loss for all four stimulus conditions. Frequency-doubling stimuli showed the greatest amount of abnormality, suggesting that sparsely represented large-diameter M*y* cells were isolated by this test, thereby revealing more extensive damage in early to moderate glaucoma.

Introduction

When a low spatial frequency sinusoidal grating undergoes high temporal frequency counterphase flicker, the grating appears to have twice as many light/dark cycles as are physically present, *i.e.*, its spatial frequency appears to be doubled. This phenomenon, often referred to as the frequency-doubling illusion, was first described by Kelly[1,2] and has subsequently been evaluated by many other investigators.[3-7] Since the frequency-doubling effect is produced by a low spatial frequency sinusoidal grating in combination with a high temporal frequency counterphase flicker, it is predominantly mediated by magnocellular (M-cell) mechanisms. The frequency-doubling effect occurs as the result of a non-linearity in the response to contrast,[1,2] possibly by mechanisms performing a full-wave rectification of the stimulus input.[4]

Address for correspondence: Chris A. Johnson, PhD, Optics and Visual Assessment Laboratory, Department of Ophthalmology, 1603 Alhambra Boulevard, Sacramento, CA 95816, USA

Perimetry Update 1996/1997, pp. 13–19
Proceedings of the XIIth International Perimetric Society Meeting
Würzburg, Germany, June 4–8, 1996
edited by M. Wall and A. Heijl

In particular, Maddess and associates[8,9] have attributed the frequency-doubling effect to M*y* cells, a subset of magnocellular mechanisms with non-linear response properties.[10,11] In addition to their non-linear response properties, M*y* cells typically have large diameter axons.

The frequency-doubling effect would seem to be a very promising method of detecting glaucomatous damage, because it has been reported that glaucoma produces a preferential loss of large diameter fibers[12,13] and selective damage to mechanisms in the magnocellular pathway.[14,15] In addition, the M*y* cells consist of a small subset (approximately 20%) of magnocellular mechanisms, and therefore comprise only 3-5% of the total number of optic nerve fibers. Thus, from the standpoint that visual functions mediated by mechanisms with reduced redundancy or sparse representation will more readily identify early glaucomatous losses,[16,17] the frequency-doubling effect also appears to be a strong candidate as an effective screening procedure for glaucomatous damage. Recently, several investigators have found that contrast thresholds for detection of frequency-doubled stimuli are effective in detecting early glaucomatous visual field loss.[8,9,18-20] Sensitivities and specificities ranging from 82% to 95% have been reported for different implementations of contrast sensitivity for frequency-doubled stimuli in glaucoma patients and normals.

The purpose of the present investigation was to examine the significance of the individual spatial and temporal components of the stimulus. The frequency-doubling effect is produced by a low spatial frequency in conjunction with a high temporal frequency, the combination of which is essential for preferentially stimulating the M*y* cells in an optimal fashion. We sought to determine whether contrast sensitivity measures for frequency-doubled stimuli (containing the combination of low spatial and high temporal components) were more effective for detecting glaucomatous visual field loss than contrast sensitivity measures for either the spatial frequency or the temporal frequency components presented individually.

Methods

One eye each of 16 patients with early to moderate glaucomatous visual field loss and one eye each of 16 age-matched normal control subjects were evaluated. Prior to testing, informed consent was obtained from all participants. Glaucoma patients were included if they had a diagnosis of primary open-angle glaucoma, IOP measurements of greater than 21 mmHg in at least one eye prior to treatment, evidence of reproducible early to moderate glaucomatous visual field loss in at least one eye for the Humphrey Field Analyzer 30-2 Program, visual acuity of 20/30 or better OU, no history of other ocular or neurological surgery or disease, and no history of diabetes or other systemic diseases. The glaucomatous visual field loss ranged from a small cluster of abnormal points associated with an early nasal step, a mean deviation (MD) of -1.01 dB, a corrected pattern standard deviation (CPSD) of 2.16 dB, and a glaucoma hemifield test (GHT) within normal limits, to an arcuate nerve fiber bundle defect with an MD of -14.91 dB and a CPSD of 12.76 dB. Normal control subjects were included if they had 20/30 or better visual acuity OU, normal visual fields OU for the Humphrey Field Analyzer 30-2 Program, IOP measures of less than 20 mmHg OU, a normal ophthalmological examination OU, no evidence of diabetes or other systemic diseases, and no prior history of ocular or neurological

Table 1. Characteristics of the normal control and glaucoma patient populations

		Mean	*SD*	*Range*
Normals	Age (years)	67.50	11.09	48 to 85
	MD (dB)	+0.06	1.37	-2.86 to +2.38
	CPSD (dB)	0.92	0.75	0.00 to 2.06
	GHT	15 within normal limits		
		1 borderline		
		0 outside normal limits		
Glaucomas	Age (years)	67.81	10.94	48 to 85
	MD (dB)	-5.77	3.72	-14.91 to -1.01
	CPSD (dB)	5.32	3.07	1.91 to 12.76
	GHT	3 within normal limits		
		2 borderline		
		11 outside normal limits		

disease or surgery. Table 1 lists the characteristics of the normal control and glaucoma patient populations.

Stimuli were presented on a black and white video monitor with specialized control circuitry. The apparatus employed was a prototype of a commercial screening device for detecting glaucomatous visual field loss manufactured by Welch-Allyn, Inc. (Skaneateles, New York). For each test condition, 16 stimuli were presented, four per visual field quadrant. Stimulus size was approximately 8° x 8°. The central 5° of the visual field was excluded. The total duration of each stimulus presentation was two seconds, with a one-second interval between trials. To avoid temporal transients at the beginning and end of each stimulus presentation, the stimuli were presented within a cosine envelope to provide a ramped onset and offset. Contrast sensitivity measurements were obtained using a modified binary search (MOBS) procedure, which is a variant of the conventional staircase method that is more robust to response errors and variability.[21,22] For each trial, the location of the stimulus presentation was randomly selected. Subjects were instructed to depress a response button each time they detected a stimulus being presented (either flicker or sinusoidal bars or both).

To examine the role of spatial and temporal stimulus attributes, four test conditions were employed: *1.* Frequency doubling: stimuli consisted of a 0.25 cycle/degree sinusoidal grating undergoing 25 Hz square wave counterphase flicker; *2.* 0.25 cycle/degree steady grating: stimuli consisted of a steady 0.25 cycle/degree sinusoidal grating with no flicker present; *3.* 0.5 cycle/degree steady grating: stimuli consisted of a steady 0.5 cycle/degree sinusoidal grating with no flicker present – the spatial frequency of this steady grating corresponded to the perceived spatial frequency of the frequency-doubled stimulus; *4.* diffuse flicker: stimuli consisted of a uniform target area (no grating) undergoing 25 Hz square wave flicker. Tests were presented in the above order for half the normal control subjects and glaucoma patients, while the other half had the order of tests reversed. This was done to counterbalance possible learning or fatigue effects which might have been present. Analysis of results indicated that the order of test presentation did not affect contrast sensitivity measures for the four test conditions.

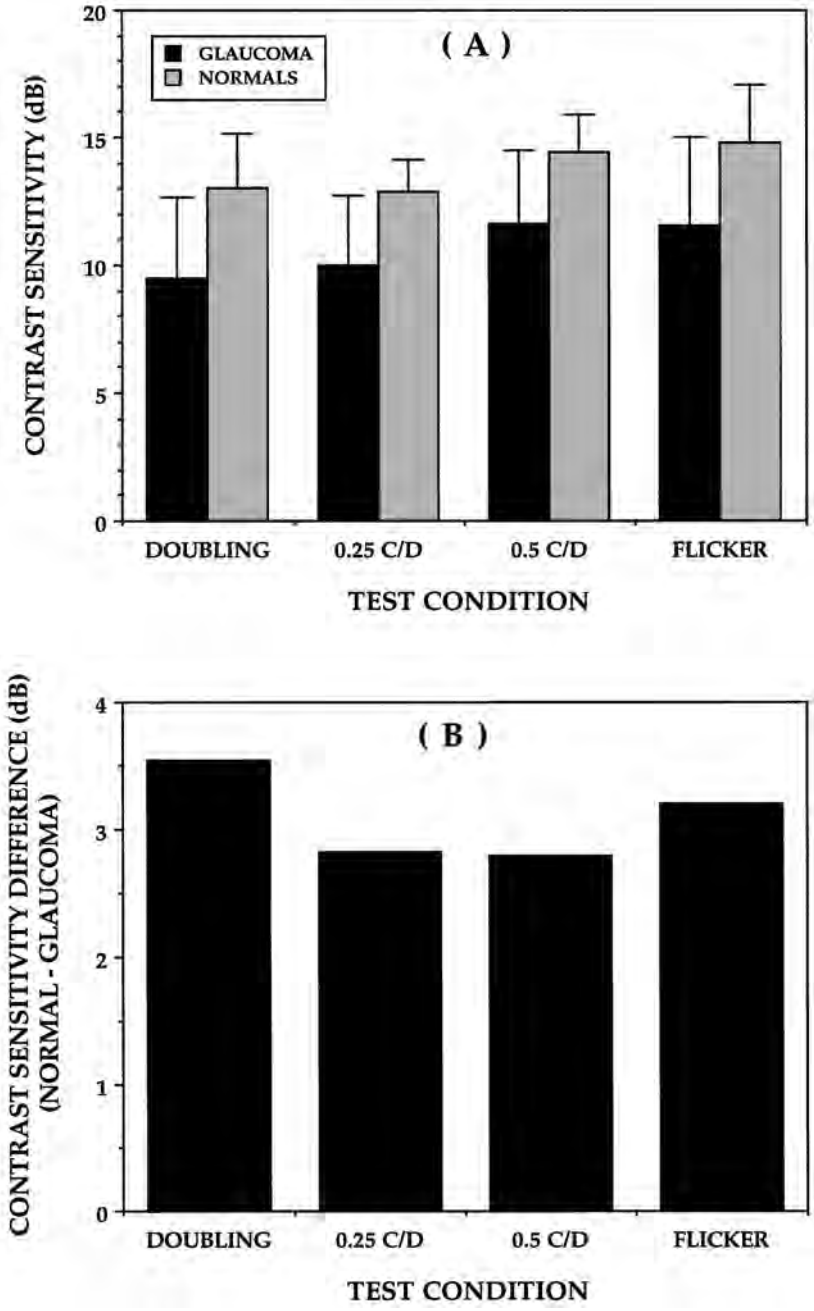

Fig. 1A. Top graph: Average contrast sensitivity (in dB) of the central 20° radius of the visual field for glaucoma patients (solid dark bars) and normal control subjects (stippled gray bars) for each of the four test conditions. The vertical lines atop the bars indicate the standard deviation of measures between subjects. *B. Bottom graph:* Average difference (in dB) for contrast sensitivity measures for normal control subjects and glaucoma patients for each of the four test conditions.

Results

Average contrast sensitivity measurements (in dB) for each of the four test conditions are presented in Figure 1A (top graph) for patients with early glaucomatous visual field loss (solid bars) and normal control subjects (stippled bars). For each individual, the mean contrast sensitivity for the 16 stimulus locations was determined, and these values were averaged for the two subject populations. The vertical lines atop the bars represent the standard deviation of measures among subjects. For each of the test conditions, contrast sensitivity was relatively similar, with the flicker-only condition exhibiting the highest sensitivity and the frequency-doubling stimulus and the 0.25 cycle/degree steady grating demonstrating the lowest contrast sensitivity. Both the 0.25 and 0.5 cycle/degree steady gratings had slightly lower between-subjects variability than the flicker-only and frequency-doubling test conditions. The difference between the glaucoma patients and the normal control subjects was greatest for the frequency-doubling test condition, second greatest for the flicker-alone condition and least for the two steady-state gratings.

This is depicted more readily in Figure 1B (bottom graph), which plots the average difference in contrast sensitivity for normal control subjects and early glaucoma patients for each of the four test conditions. Average contrast sensitivity differences were 3.54 dB for the frequency-doubling stimuli, 3.20 dB for the flicker-only condition, 2.83 dB for the 0.25 cycle/degree steady grating and 2.80 dB for the 0.50 cycle/degree steady grating.

To compare the performance characteristics of the four test conditions, a step-wise (maximum-likelyhood) logistic regression (STATA Statistics program, College Station, Texas) was conducted for each of the four test conditions. The step-wise logistic regression evaluated contrast sensitivity measures from all 16 target locations to determine the ability to separate normal control subjects from glaucoma patients, and sensitivity and specificity values were derived from the logistic regression analyses. For each of the test conditions, the step-wise logistic regression used the default criteria of a significance level of 0.2 or less to enter the model and a significance level of 0.4 or greater to be removed from the model. Approximately half the 16 target locations were included in the model for each of the test conditions, although the specific locations included varied among the test conditions. Figure 2 presents the sensitivity and specificity characteristics for each of the four test conditions. In general, all four of the test conditions demonstrated quite good performance in distinguishing the glaucoma patients from normal control subjects on the basis of their contrast sensitivity measures. The frequency-doubled test condition demonstrated the best performance, with a sensitivity of 93.75% and a specificity of 93.75%. Both the flicker-only and the 0.25 cycle/degree steady grating exhibited a sensitivity of 87.5% and a specificity of 87.5%. The 0.5 cycle/degree steady grating had a sensitivity of 81.25% and a specificity of 87.5%.

Discussion

Our results are consistent with previous investigations that have evaluated contrast sensitivity for frequency-doubled stimuli as a means of screening for glaucomatous visual field loss.[8,9,18-20] In previous investigations, sensitivities and specificities of 82-95% have been reported for the ability of frequency-doubled contrast sensitivity

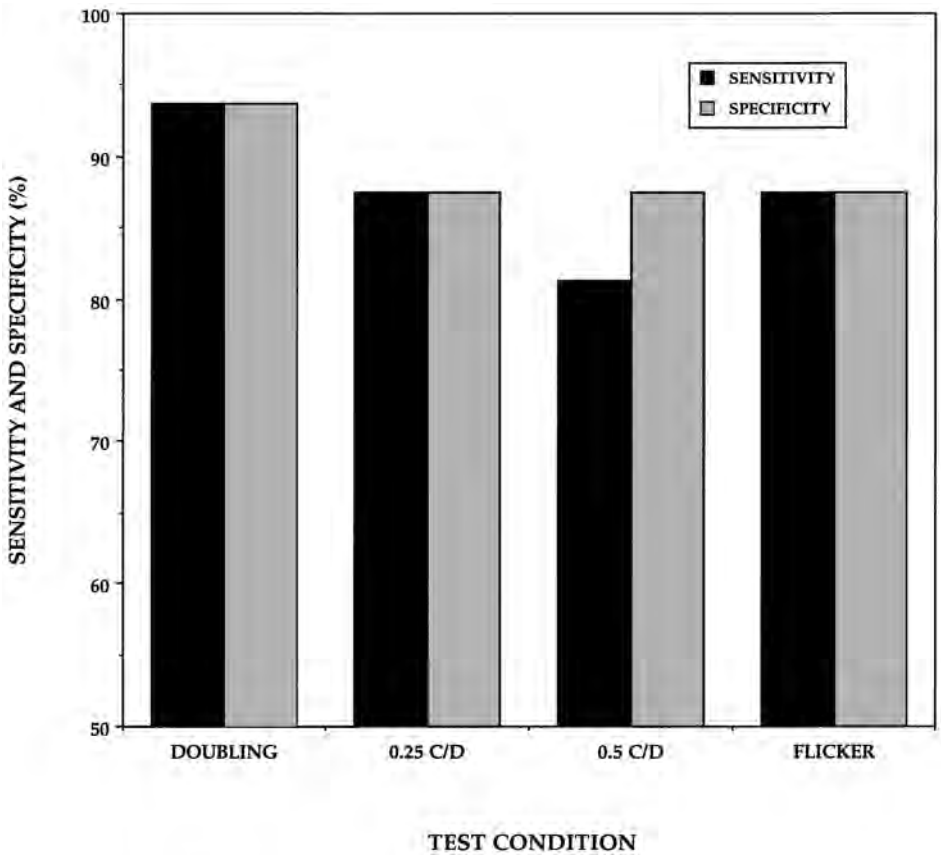

Fig. 2. Sensitivity (solid dark bars) and specificity (stippled gray bars) values for each of the four test conditions, based on the results of a step-wise logistic regression model.

measurements to separate patients with glaucomatous visual field loss from normal subjects.

Although all four test conditions revealed differences in contrast sensitivity between glaucoma patients and normal subjects, the frequency-doubling condition produced the largest difference in contrast sensitivity between glaucoma patients and normal controls, and the highest sensitivity (93.75%) and specificity (93.75%). This indicates that both spatial and temporal frequency properties are important for obtaining optimal performance in this form of contrast sensitivity testing. This is probably due to the greater isolation of M-cell mechanisms produced by the frequency-doubling stimulus parameters, particularly the M-cell mechanisms with non-linear response properties. The results of this investigation, in conjunction with the findings of previous studies, indicate that frequency-doubling perimetry is an effective and efficient means of rapidly screening for glaucomatous visual field loss.

Acknowledgments

Supported in part by National Eye Institute Research Grant No. EY-03424, a Research to Prevent Blindness Senior Scientific Investigator Award, and an Unrestricted Research Support Grant from Research to Prevent Blindness, Inc.

We are grateful to Kimberly Cello and Jacqueline M. Nelson-Quigg for their assistance in testing subjects.

References

1. Kelly, DH: Frequency doubling in visual responses. J Opt Soc Am 56:1628-1633, 1966
2. Kelly, DH: Nonlinear visual responses to flickering sinusoidal gratings. J Opt Soc Am 71:1051-1055, 1981
3. Richards W, Felton TB: Spatial frequency doubling: retinal or central? Vision Res 13:2129-2137, 1973
4. Tyler, CW: Observations on spatial frequency doubling. Perception 3:81-86, 1974
5. Virsu V, Nyman G, Lehtio PK: Diphasic and polyphasic temporal modulations multiply apparent spatial frequency. Perception 3:323-336, 1974
6. Tolhurst, DJ: Illusory shifts in spatial frequency caused by temporal modulation. Perception 4:331-335, 1975
7. Virsu V, Laurinen P: Long-lasting afterimages caused by neural adaptation. Vision Res 17:853-860, 1977
8. Maddess T, Henry GH: Performance of nonlinear visual units in ocular hypertension and glaucoma. Clin Vis Sci 7:371-383, 1992
9. Maddess T, Goldberg, I, Dobinson J, Wine S, James AC: Clinical trials of the frequency doubled illusion as a indicator of glaucoma. Invest Ophthalmol Vis Sci (Suppl)36:S335 (ARVO Abstract), 1995
10. Kaplan E, Shapley RM: X and Y cells in the lateral geniculate nucleus of macaque monkeys. J Physiol 330:125-143, 1982
11. Marrocco RT, McClurkin JW, Young RA: Spatial summation and conduction latency classification of cells in the lateral geniculate nucleus of macaques. J Neurosci 2:1275-1291, 1982
12. Quigley HA, Dunkelberger GR, Green WR: Chronic human glaucoma causing selectively greater loss of large optic nerve fibers. Ophthalmology 95:357-363, 1988
13. Quigley HA, Sanchez RM, Dunkelburger GR, Henaut NL, Baginski TA: Chronic glaucoma selectively damages large optic nerve fibers. Invest Ophthalmol Vis Sci 28:913-918, 1987
14. Chaturvedi N, Hedley-Whyte ET, Dreyer EB: Lateral geniculate nucleus in glaucoma. Am J Ophthalmol 116:182-188, 1993
15. Dandona L, Hendrickson A, Quigley HA: Selective effects of experimental glaucoma on axonal transport by retinal ganglion cells to the dorsal lateral geniculate nucleus. Invest Ophthalmol Vis Sci 32:1593-1599. 1991
16. Johnson CA: Selective versus nonselective losses in glaucoma. J Glaucoma (Suppl)3:S32-S44, 1994
17. Johnson CA: The Glenn Fry Lecture: early losses of visual function in glaucoma. Optomet Vis Sci 72:359-370, 1995
18. Johnson CA, Samuels SJ: Screening for glaucomatous visual field loss with Frequency-Doubling Perimetry. Invest Ophthalmol Vis Sci 38:413-425, 1997
19. Johnson CA: The frequency doubling illusion as a screening procedure for detection of glaucomatous visual field loss. Invest Ophthalmol Vis Sci (Suppl)36:S335 (ARVO Abstract), 1995
20. Johnson CA: Frequency doubling perimetry as a means of screening for glaucomatous visual field loss. Invest Ophthalmol Vis Sci (Suppl)37:S444 (ARVO Abstract), 1996
21. Tyrrell RA, Owens DA: A rapid technique to assess the resting states of the eyes and other threshold phenomena: the modified binary search (MOBS). Behavior Res Meth Instr Computers 20:137-141, 1988
22. Johnson CA, Shapiro LR: A comparison of MOBS (modified binary search) and staircase test procedures in automated perimetry: noninvasive assessment of the visual system, 1989. Tech Digest Ser, Opt Soc Am 7:84-87, 1989

MOTION DETECTION PERIMETRY
Properties and results

MICHAEL WALL, CARIDAD F. BRITO and KIM KUTZKO

Departments of Neurology and Ophthalmology, Veterans Administration Medical Center, Iowa City, and University of Iowa, College of Medicine, Iowa City; IA, USA

Abstract

Motion detection perimetry is a method that measures a subject's ability to detect a correlated shift in position of dots within a circular area against a background of non-moving dots. Motion size threshold is the smallest detectable circular area in which the subject can detect motion. Subjects respond by touching a computer screen with a light pen where they detect motion stimuli. Their localization errors, measured as the number of pixels from target center and reaction times, are then calculated.

Here, the authors report their experience in studying fundamental properties of motion detection perimetry. Regarding the validity of this testing for isolating motion perception, results of a comparison of motion detection thresholds with direction discrimination thresholds, and the effects of increasing motion coherence on lowering of motion detection thresholds, indicate motion perception is being measured by motion detection perimetry. The retest variability, as estimated by the slope of the frequency of seeing curves, appears to be low compared with conventional automated perimetry. A 'floor' effect, or premature cut-off at the low end of the dynamic range, was found for thresholds at test locations close to fixation in version 1 of the software; this has now been remedied. No significant 'ceiling' effect has been observed. The test runs on a personal computer and is similar in ease of administration to other perimetric tests. Results of a survey of patients taking the test reveals a high participation rate, with above average scores on ease of taking the test and maintaining attentiveness.

As with other tests of motion perception, motion detection perimetry is resistant to stimulus blur up to six diopters. The sensitivity appears to be superior to conventional automated perimetry, but the specificity is not yet known. The authors know of no apparent cultural biases inherent in the test, except possibly experience using a personal computer. A database of 100 normals with 20 per decade from ages 20-70 years, is available for interpretation of results. Further studies of sensitivity and specificity are needed to compare motion detection perimetry with conventional automated perimetry.

Introduction

In some fundamental ways, perimetry has changed little since Von Graefe introduced it into clinical medicine in 1856.[1] Progressive evolution of control and standardiza-

Address for correspondence: Michael Wall, MD, University of Iowa, College of Medicine, Department of Neurology, 200 Hawkins Drive #2007 RCP, Iowa City, IA 52242-1053, USA

Perimetry Update 1996/1997, pp. 21–33
Proceedings of the XIIth International Perimetric Society Meeting
Würzburg, Germany, June 4–8, 1996
edited by M. Wall and A. Heijl

tion of the stimulus and background conditions culminated in the Goldmann bowl perimeter. Automation of the testing procedure using the Goldmann perimeter hardware occurred in the 1970s. During the 1980s, we learned much about the strengths and weaknesses of automated perimetry. These studies showed us the important factors and properties that need to be considered when any new perimetric test is introduced. Mae Gordon, PhD, reviewed these factors at the 1995 North American Perimetry Society Meeting.

First, the perimetric test must be valid. In other words, the results must reflect the underlying construct measured. It should be both sensitive for detecting disease and specific; that is, there should be few true normals with abnormal results. Next, the test should be reliable; high agreement between the results at different administrations of the test should occur. The test-retest variability should be low, and the dynamic range of test stimuli should be full enough that there is no 'ceiling' or 'floor' effect. A test should be practical. Administering it should be easy, and the test should have a high participation rate. It should be robust against errors, such as lens, lid and brow artifacts, and blur from refractive error. Lastly, the test should not be culturally biased, and normative standards should be available.

Because some of these factors for conventional automated perimetry can be improved, many types of perimetry have been developed in the past ten years. Computer graphics perimeters, in particular, have evolved. These devices have many advantages since they allow customization of many types of stimuli and test conditions, improved ergonomics and feedback of results to the subjects. With the goal of developing a more sensitive and less variable method of perimetry, we have designed a computer graphics perimeter that measures a subject's motion perception size threshold, localization error and reaction time. Here, we report our experience with this technique and provide information on factors important for a perimetric test.

Methods

We performed motion detection perimetry in a darkened room using an IBM compatible 33 mHz 486 computer for version 1 and a 90 mHz Pentium computer for version 2 with software we have developed. The data for diagnostic sensitivity and validity of the test were done using version 1. The details of this method have been published earlier.[5-7] We used version 2 for all other testing.

The test background for version 2 of motion detection perimetry was composed of 10,000 randomly positioned white dots with 3.26% of pixels illuminated. The dots were one pixel in size and 580 apostils in brightness, *i.e.*, 2.75 log units above the background. The dots were positioned randomly on a gray background with a luminance of 50 apostils using a 640 x 480 pixel VGA video display. The motion targets were circular random dot cinematograms, within which 50% of the dots move centrifugally and 50% move in random directions. The circular target itself was stationary, *i.e.*, dots move within the target. Each trial was composed of ten cinematogram frames displayed in 173 msec. Each dot moved two pixels per frame, giving a velocity of 11.76°/sec. Dots moving out of the circular window were wrapped back to the point 180° from the dot exit position.

To increase the dynamic range of the instrument and eliminate a 'floor effect', the six smallest targets were 'hard-coded' using a smaller dot movement step factor (see Table 1). The targets were of 17 sixes with a diameter step factor of 10^{-1} (1.259). The

angle subtended by the targets ranged from 0.13° to 8.46°. The size of the stimulus varied from trial to trial, and a 2/1 staircase procedure was used to bracket the threshold. The test, therefore, continued until the smallest circle size seen, defined as the size threshold at each test point, was bracketed by the staircase procedure. Stimulus presentation was randomized among the preselected test loci. Fixation was monitored by the visual field technician. For clinical testing, we specified 44 locations; these match the 24-2 Humphrey perimetry test points, except for absence of the top and bottom rows and the two most eccentric points along the nasal horizontal meridian.

Valid responses were defined as having a reaction time greater than 100 msec but less than one second, and having a localization error of no more than 10° from the center of where the target was presented. Testing took place in a dimly illuminated room. The testing distance from the screen was fixed at 22 cm by a lens holder attached to the monitor. The monitor was on an adjustable-height table and was positioned so that a subject was comfortably seated looking slightly down. The 17-inch diagonal monitor gave a 21° test field (42° by 42° total).

A stimulus presentation was initiated when the subject touched a light pen to the midpoint of the bottom of the video display while fixing on a central cross. The stimulus was then displayed. If the subject saw the stimulus, he or she lifted the light pen signaling the response time. He or she then attempted to touch the pen to the position on the video display where the center of the test target was perceived. We used the FTG Data systems high resolution light pen model FT-1000. The reaction time was calculated using a high resolution timer function with 1-10 μsec accuracy.[8] The localization error was calculated using the distance from the target center *x* and *y* pixel coordinates that was corrected for distortion from monitor screen parallax to the *x* and *y* coordinates of where the subject pointed with the light pen. We calculated this error using the method of least square distance (Pythagorean theorem). The subject received visual feedback of the localization error at the end of each trial. In order to maintain attention, when the subject's response came within three pixels of the target center, reinforcement was given as a computer-simulated fireworks display. Subjects took rest breaks between trials by lifting the light pen from the screen. Test times for normals ranged from 12 to 20 minutes.

The subject's appropriate near correction was used. Care was taken to prevent lens rim artifact by asking whether the subject could see white squares on a black background in each corner of the video display while looking at the fixation target.

We evaluated motion detection perimetry's construct *validity* – that its motion targets were processed by motion mechanisms – by comparing sensitivities to motion detection and direction discrimination. We evaluated how the relationship between sensitivity to motion detection and motion direction discrimination varied with visual field eccentricity. The motion targets differed in their direction of movement; the coherent or correlated vector of the motion stimuli moved in either up, down, left or right directions. We tested 20 subjects with no known eye disease, normal eye examinations, and normal conventional automated perimetry. Each subject was tested in a block of trials for motion detection and a block of trials for direction discrimination; these blocks were counterbalanced between observers. We used the method of constant stimuli. Each of seven stimuli sizes was presented 24 times at each of six spatial locations at 2, 12, and 21° along the temporal and nasal horizontal. We assessed sensitivities by computing d' for detection and direction discrimination to reduce response bias effects.[9]

In the detection task, subjects pressed any one of four arrow keys on a computer keyboard when they perceived motion. Besides the seven stimulus sizes used, a 'blank' trial, without motion, was presented 24 times at each location. These 'catch' trials were used to calculate false positive rates. For direction discrimination, the subjects indicated in which direction the targets moved by pressing keys having direction labels; on each trial, subjects were required to enter a response.

Calculation of d´ was done by tabulating false positive rates for each eccentric location tested and converting them to *z* values, where *z* was the inverse of the standard normal distribution. Then, we obtained hit rates (true positives) for each stimulus size, at each test location. These were also converted to *z* values; d´ was set as the difference between these two: d´ = hits-false alarms (true positive rate – false positive rate); d´ were obtained for each stimulus size. The d´ values for discrimination were obtained from Hacker and Ratcliff's tables.[10] These tables give d´ values for multi-alternative response tasks. The d´ values were then submitted to analysis of variance.

The effect of signal strength on motion detection perimetry performance was examined by varying the percentage of dots within the motion target that moved coherently. We gave 29 subjects two motion detection perimetry tests. Subjects took a standard motion detection perimetry test where 50% of the pixel-dots within the motion target moved coherently while the other 50% moved in random directions; they also took a motion detection perimetry test in which only 1% of the dots in the motion targets moved coherently – random motion was perceived. Fifteen of the 29 observers took a third motion detection perimetry test in which 100% of the dots within the motion target moved coherently.

For the data on sensitivity, subjects had motion detection perimetry and conventional automated perimetry (24-2) done on the same day. Point-wise probability plots, similar to those used for the Humphrey Field Analyzer, were generated by tabulating whether the tested point in the patients fell outside the upper 95 or 99th confidence bound of the normal subjects. To be considered abnormal, three contiguous test points had to be abnormal at a $p<0.05$ level or two contiguous points abnormal, one at the $p<0.01$ level in a clinically suspicious area. The two types of perimetry were compared using these plots for the 44 test loci common to both tests. The details of this analysis have been published elsewhere.[7]

Variability was studied by constructing frequency of seeing curves using a technique we have described previously.[11] We compared psychometric functions from a central and peripheral test location of normal subjects with functions from normal sensitivity (by STATPAC®) locations of glaucoma subjects and functions from test locations in glaucoma subjects with 10-20 dB loss on a 24-2 or 30-2 visual field examination. The same protocol was used for motion detection, but subjects were tested at every other dB.

Frequency of seeing curves were computed for conventional automated perimetry using our previously published method.[11] They were constructed for each subject as cumulative gaussian functions and a least squares fit was calculated using the Microsoft Excel solver function. The resulting mean of the fitted distribution corresponded to the 50% correct threshold for the test location (defined as the stimulus intensity corresponding to the 50% frequency of seeing point of the fitted curve). The standard deviation of the cumulative gaussian function is an index of the maximum slope of the frequency of seeing function. A steep slope (low standard deviation) corresponds to a small transition zone between stimuli seen and those not seen, and

therefore a measure of variability. We compared the standard deviations of the cumulative gaussian functions of motion detection perimetry and conventional automated perimetry of glaucoma patients at two test locations: in a normal sensitivity area as determined by Humphrey's STATPAC® software, in an area of 10-20 dB loss. A paired *t* test was used for the comparison.

For the blur experiment, five young normal subjects, age range 24-32 years (mean, 25.4 ± 3.6), with normal uncorrected near acuity, were tested under five conditions in random order: no correction, two, four, six, and eight diopters of added plus lens. Standard motion detection perimetry was performed at 44 test locations. A one-way repeated measures ANOVA was performed to test for differences in motion detection perimetry mean thresholds between the different conditions of added plus lens.

Survey methodology: we gave a questionnaire to 60 consecutive patients and control subjects with an age range of 24-70 years. The results were tabulated by category.

Results

Validity

Does motion detection perimetry test motion perception or local flicker perception? Ideally, one should choose a property of motion for the subject's response, such as direction of motion (direction discrimination). However, since this requires a four-alternative, forced-choice protocol or crossing threshold with a staircase many times and taking the average of the crossings, there is a significant cost in increased testing time. This cost is so high as to be prohibitive for clinical use if the number of test locations used is similar to conventional automated perimetry. We therefore performed two experiments to better understand the mechanisms involved in detecting random dot stimuli.

First, we compared the sensitivity for motion detection and direction discrimination at different eccentricities across the horizontal meridian. Using signal detection theory, we found that the sensitivity, measured as d´, varied (decreased) with eccentricity for both tasks. As can be seen in Figure 1a, sensitivity for motion detection and direction discrimination was different, but the rate of change with eccentricity was the same; this is indicated by the parallel lines seen in the figure.

A replication of this study using five glaucoma patients yielded similar results. As seen in Figure 1b, the relationship between d´ for motion detection and direction discrimination did not vary significantly as a function of eccentricity. The lines appear to come closer at 21°. This is likely due to the visual loss being greatest at this test location with a resultant 'ceiling' effect for the direction discrimination task. Therefore, sensitivity increased linearly as stimulus size increased (r^2 = 0.993). The results of these experiments show that performance on the motion detection task can be used to predict direction discrimination performance in normals and glaucoma patients.

We performed the experiment with varying degree of motion signal strength to determine whether subjects could be simply responding to local flicker rather than motion. If they were just responding to local flicker, varying the percentage of coherently moving dots in a stimulus would have no effect. We used 1, 50 and 100% coherence using version 1 of our software. We found the signal strength affected the

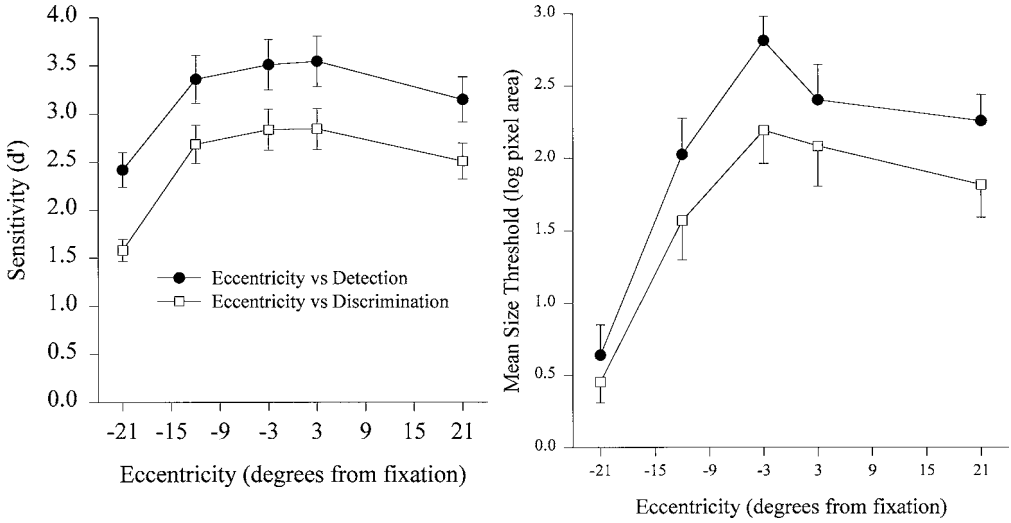

Fig. 1.a. The relationship between motion detection and direction discrimination across eccentricities in normal subjects. Note how sensitivity decreases as a function of eccentricity with the rates of decline being similar. The two-way interaction between test type and eccentricity was not significant. *b.* Similar results are obtained using the same testing paradigm on glaucoma patients.

rate at which thresholds increased with eccentricity (Fig. 2). For 1% coherence, thresholds increased at a rate of 0.063 units of log pixel area/degree of visual field eccentricity (lpa/dvf); the increase was at a rate of 0.045 lpa/dvf for 50% coherence and was 0.033 lpa/dvf for 100% coherence. Thresholds rose at the fastest rate when only random motion was observed and least for fully coherent moving targets: the stronger a target's direction of movement, the smaller the target size that can be detected in the periphery. Signal strength did not significantly affect reaction times or localization errors. Since adding signal reduced thresholds, at least some of the response in motion detection perimetry is due to motion signal. The convergence of the lines of Figure 2 at the 3° test location is probably due to the 'floor' effect of the version 1 software. From the results of these two experiments, we concluded that with motion detection perimetry, it is likely that we were testing detection of a moving stimulus rather than local flicker.

Another test of a method's validity is whether visual field defects are present of the type known to occur when the underlying anatomy is damaged. For example, when the optic nerve is damaged, it is common to have defects that conform to a nerve fiber bundle pattern. Our results from four studies show that motion perimetry yields the expected types of defects relative to the anatomy being damaged. We have observed good correlation between the visual field defects found with motion perimetry and those present with conventional automated perimetry in a variety of optic nerve disorders (see Fig. 5).[5-7,12] The optic neuropathies studied to date are glaucoma and ocular hypertension, optic neuritis and idiopathic intracranial hypertension.

Sometimes, there can be indirect evidence that a new test is more sensitive, as in Figure 6. This shows results from a patient with optic neuritis in the acute phase (a). Conventional automated perimetry (b) in the resolved phase shows full recovery of

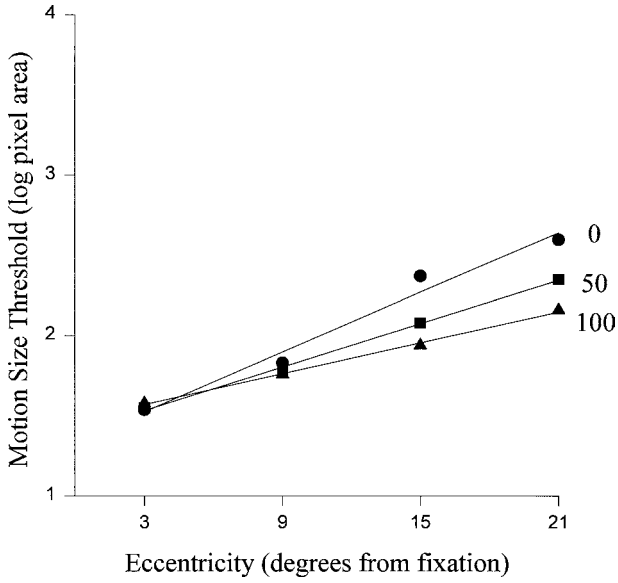

Fig. 2. Mean motion perimetry size thresholds plotted as a function of eccentricity for each coherence level.

function to light sensitivity stimuli. However, motion perimetry (c) performed on the same day shows a superior quadrant defect in the area where there was the most visual loss in the patient's acute phase. The '+' marks the site of the patient's response, the line represents the localization error, and the size of the '+' is proportional to the reaction time. Note the increased localization error in the form of an 'undershooting' of the stimulus position (c) in the upper left quadrant.

Sensitivity and specificity

Motion detection perimetry appears to be more sensitive in detecting visual loss than conventional automated perimetry in various optic neuropathies, including glaucoma and ocular hypertension (Figs. 5, 6).[5-7,12] Examples of nerve fiber bundle-like defects found with motion detection perimetry in patients with normal results on conventional automated perimetry can be found in the last *Perimetry Update*.[7] Our database of 100 normal subjects[6] for these studies was used to calculate confidence bounds for the motion detection perimetry results, and therefore could not be used to calculate the test's specificity.

Reliability and test-retest variability

We used frequency of seeing curves as a measure of the motion detection perimetry's retest variability. The steeper the slope (lower standard deviation), the smaller the transition zone from seen to not seen, the narrower the range of values obtained, and the better the test-retest variability. Our results on three subjects show a steeper slope with motion detection perimetry than with conventional automated perimetry (Fig. 3).

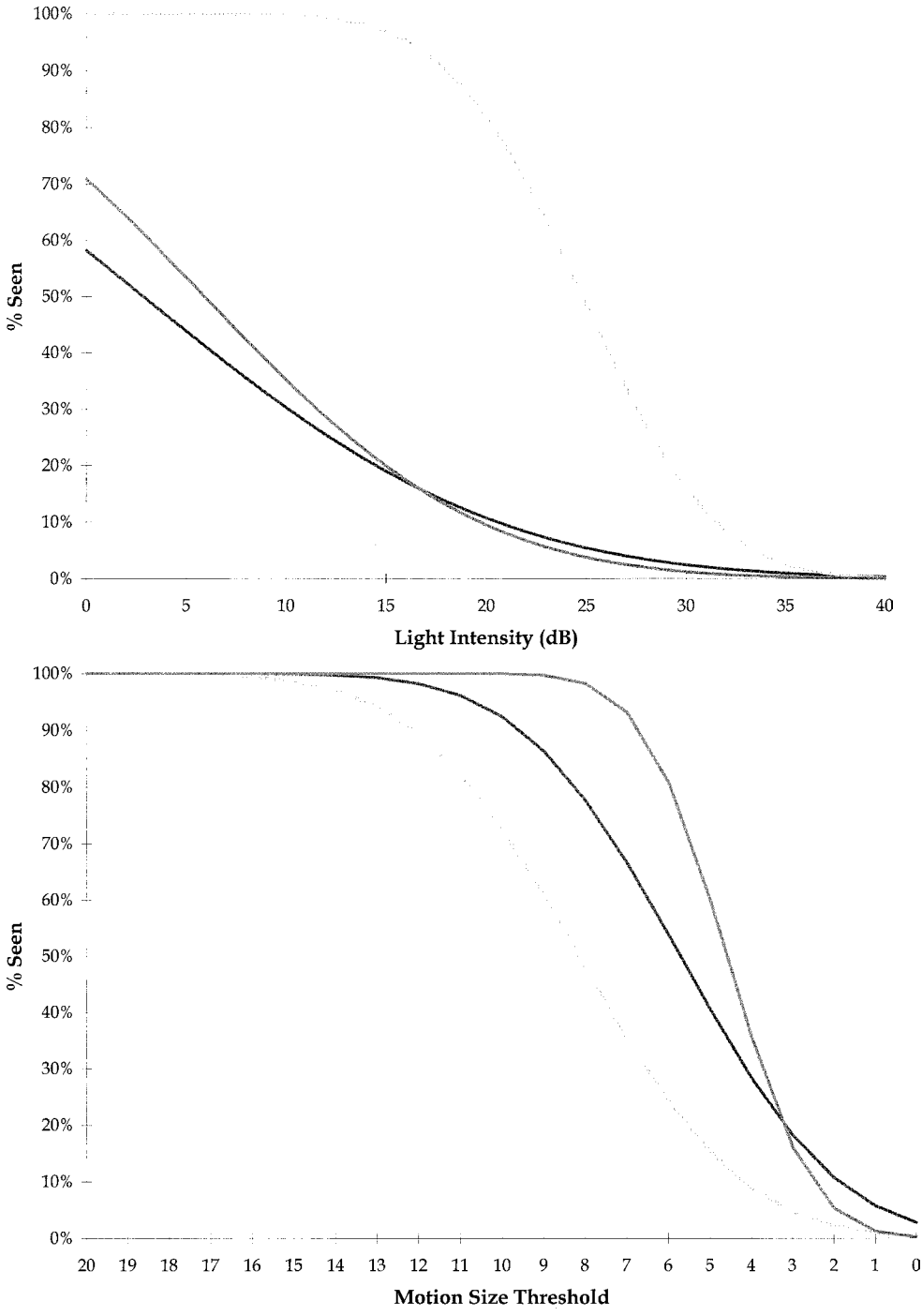

Fig. 3. Frequency of seeing curves in three subjects with glaucoma at test locations with 10-20 dB loss. In *a*, results from conventional automated perimetry are shown. Note how shallow the slopes are, indicating poor test-retest variability. In *b*, the results of motion perimetry on the same patients at the same test locations show much steeper slopes.

Table 1. Hard-coded motion detection perimetry stimuli for the smallest sizes

dB	*Pixel diameter*	*Exact diameter*	*Circle area*	*Dots/circle 4% turned on*	*Minimum dots*	*Maximum dots*	*Frames*	*Pixel step size*
2	2	2.6	3.1	0.1	1	1	2	1
3	3	3.3	5.0	0.2	1	1	2	2
	3	4.1						
	4	*5.2*						
4	5	6.5	19.8	0.8	1	1	3	2
	6	*8.2*	*31.4*	*1.3*	*2+2*	*2+2*	*2*	*2*
5	8	10.4	49.8	2.0	2+2	2+2	6	2
6	10	13.0	78.9	3.2	2+2	2+2	10	2
7	13	16.4	125.1	5.0	3+3	3+3	10	2

Pixel diameter increases as in .1 log units ($10^{.1}$). Rows in italics are stimuli in sequence that are not used because psychophysically (from data using frequency of seeing curves), they are too similar to neighboring stimuli.

In version 1 of the software, a 'floor' effect was found at the test locations close to fixation. That is, there was an artificial cutoff in normal subjects at these test locations because the stimuli were too easy to detect. This has been remedied in version 2 of our software. However, this required changing the coding for the six smallest stimuli (Table 1). We have not observed a significant 'ceiling' effect at the large stimulus end of the dynamic range of motion detection perimetry.

Practicality

The hardware costs of the system are those of an IBM-compatible Pentium computer with a PCI bus and at least eight megabytes of random access memory. We use NEC Multisync 5FG with a 17" diagonal monitor and an ATI Mach 64 graphics card equipped with two megabytes of video random access memory. A custom-built lens holder that fits on the top of the monitor, together with custom-made lenses, are necessary. The light pen can be obtained from FTG data systems.

The results from our questionnaire can be found in Table 2 (10 was the best score). The results show that the test was well understood by subjects, easy to take and administer, and captured the subjects' attention. We found the time needed to instruct older subjects to learn the proper response technique was almost twice that for young subjects. Our subject participation rate was high; it was uncommon to find subjects who were unable to properly complete the test.

Robustness against errors

Errors can be introduced in any subject's test result by failure to keep the light pen perpendicular to the monitor; this was necessary for light capture by the pen. We reduced the frequency of these errors in version 2 of the software by using a brighter background. However, it remains a problem that requires attention by the perimetrist.

As with conventional automated perimetry, lens rim, eyebrow and eyelash artifact can occur. By not testing the top four test locations used by the 24-2 test of conven-

Table 2. Experience of subjects and a perimetrist on 60 consecutive examinations using motion perimetry

	Category	*Average*	*Standard deviation*
Subject	understanding	9.38	0.85
	ease of test	8.73	1.19
	attentiveness	8.05	1.57
	test validity*	8.70	1.49
Perimetrist	cooperation	9.42	0.79
	ease of test	8.95	0.98
	attentiveness	8.37	0.96
	test validity*	8.63	1.09

*Test validity was defined as how well the perimetristic subject thought the test measured her vision

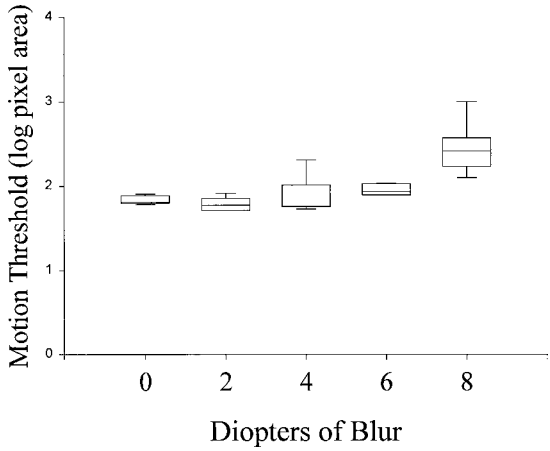

Fig. 4. The relationship between motion perimetry thresholds and diopters of blur. Note how motion perimetry is resistant to blur up to six diopters.

tional automated perimetry, the occurrence of these perimetric artifacts was less likely.

Unlike conventional automated perimetry, motion detection perimetry is robust against errors due to improper refraction. Figure 4 shows little effect of blur up to six diopters. At eight diopters, mean thresholds rose ($p<0.001$, repeated measures ANOVA).

To eliminate guessing errors, we require that subjects touch the computer monitor within 10° of target center for the trial to be counted as 'seen'. In addition, we retest outlying thresholds if the value differs by more than two stimulus sizes from its neighbors.

Normative standards

We have published version 1 data on normals.[7] We have now tested 100 ocular normals using version 2 of the software; this group is broken down into 20 subjects per decade from age 20 to 70 years. As with version 1, motion thresholds increase with age.[7]

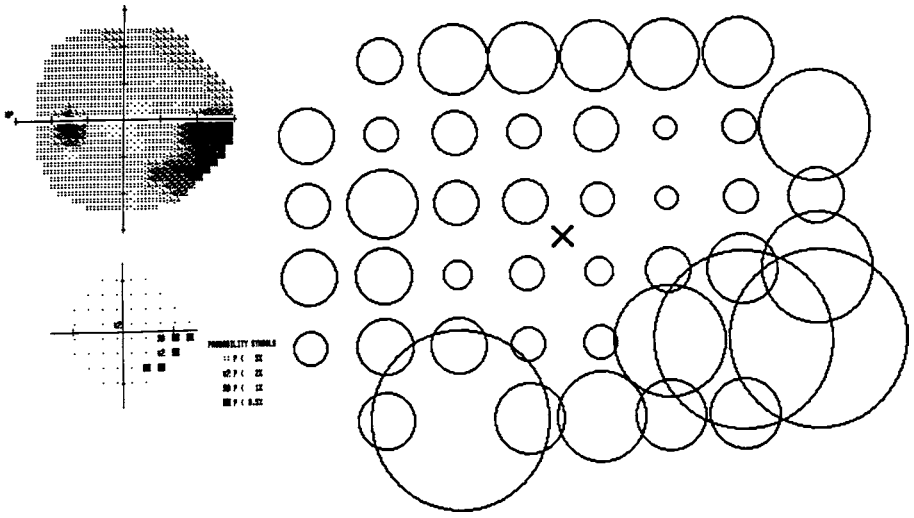

Fig. 5. A glaucoma patient has a typical inferior arcuate defect to both motion perimetry and conventional automated perimetry.

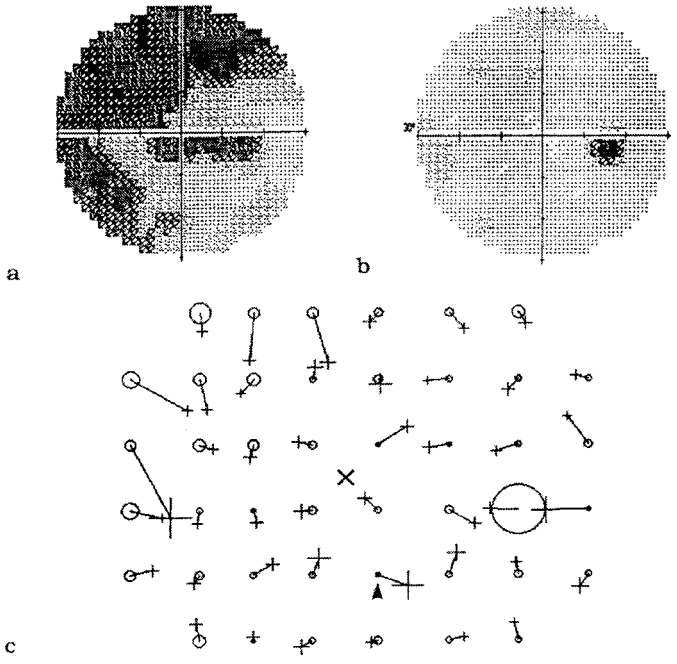

Fig. 6. Perimetry in an optic neuritis patient. *a.* Initial conventional automated perimetry. Note the visual loss in the superior quadrant. *b.* Conventional automated perimetry result months later, after recovery. *c.* Motion perimetry at the time of the test shown in *b*; note the high thresholds (larger circle sizes) in the left superior quadrant.

Discussion

Regarding Mae Gordon's standards for perimetric tests, motion detection perimetry results appear to reflect the underlying construct that is measured – motion perception. The finding that the relationship between motion detection and direct discrimination was not affected by eccentricity or visual field damage implies that both responses are processed by the motion system. In addition, these results demonstrate in both normals and glaucoma subjects that testing motion detection allows prediction of direction discrimination results. The data on adding signal to the stimulus also show that using random dot cinematograms for motion detection was not simply a task of local flicker perception.

Motion detection perimetry was sensitive for detecting disease. Its specificity has not yet been determined. Our experience, though, is that few ocular normals have nerve fiber bundle-like defects. The test-retest variability appears to be low in normals and glaucoma patients, as shown by our data on frequency of seeing curves. Although in version 1 of the software there was a 'floor effect', this has been corrected in version 2. No significant 'ceiling' effect has emerged. Based on the survey data, motion detection perimetry was easy to administer and had a high participation rate. It was robust against refractive error with a tolerance to blur of up to six diopters. False positive responses are reduced by requiring the subject touch of the monitor within 10° of target center for the trial to count as 'seen'. Normative standards of 100 subjects are available and the test does not appear to be culturally biased. Further studies of sensitivity and specificity are necessary to fully compare motion detection perimetry with conventional automated perimetry.

Acknowledgments

This study was supported in part by a VA merit review and an unrestricted grant to the Department of Ophthalmology from Research to Prevent Blindness, New York, NY, USA.

References

1. Von Graefe A: Ueber die Untersuchung des Gesichtsfeldes bei amblyopischen Affectionen. Von Graefe's Arch Ophthalmol 2:258-298, 1856
2. Frisén L: Computerized perimetry: possibilities for individual adaptation and feedback. Doc Ophthalmol 69:3-9, 1988
3. Frisén L: A computer graphics visual field screener using high-pass spatial frequency resolution targets and multiple feedback devices. Doc Ophthalmol Proc Ser 42:441-446, 1987
4. Frisén L: High-pass resolution perimetry: a clinical review. Doc Ophthalmol 83:1-25, 1993
5. Wall M, Montgomery EB: Using motion detection perimetry to detect visual field defects in patients with idiopathic intracranial hypertension: a comparison with conventional automated perimetry. Neurology 45:1169-1175, 1995
6. Wall M, Ketoff KM: Random dot motion detection perimetry in glaucoma patients and normal subjects. Am J Ophthalmol 120:587-596, 1995
7. Wall M: Motion detection perimetry in optic neuropathies. In: Mills RP, Wall M (eds) Perimetry Update 1994/1995, pp 111-118. Amsterdam/New York: Kugler Publ 1995
8. Designing a high-resolution timer function. Inside Microsoft C 2(6):1-7, 1992
9. Gescheider GA: Psychophysics: Method, Theory, and Application. Hillsdale NJ: Lawrence Erlbaum 1985
10. Hacker MJ, Ratcliff R: A revised table of d' for m-alternative forced choice. Perception & Psychophysics 26:168-170, 1979

11. Wall M, Maw RJ, Stanek KE, Chauhan BC: The psychometric function and reaction times of automated perimetry in normal and abnormal areas of the visual field in glaucoma patients. Invest Ophthalmol Vis Sci 37:878-885, 1996
12. Wall M, Jennisch CJ, Munden PM: Motion detection perimetry identifies nerve fiber bundle-like defects in ocular hypertension. Arch Ophthalmol 115:26-33, 1997

STIMULUS ORIENTATION CAN AFFECT MOTION SENSITIVITY IN GLAUCOMA

MARK C. WESTCOTT[1], FREDERICK W. FITZKE[1] and ROGER A. HITCHINGS[2]

[1]*Institute of Ophthalmology;* [2]*Moorfields Eye Hospital; London, UK*

Abstract

Purpose: To investigate the effect of stimulus orientation on motion detection thresholds in primary open-angle glaucoma (POAG) patients and controls.
Methods: Line displacement thresholds were measured for a 2° × 2 min arc stimulus moving parallel, perpendicularly, or at 45° to the orientation of the retinal nerve fiber layer (NFL), in a randomized order in eight normal controls and 17 POAG patients with reproducible glaucomatous Humphrey 24-2 field defects. Motion measurements were made at one of two locations in the visual field at an eccentricity of 15°.
Results: There was no effect of orientation on the motion detection thresholds in the controls. At the test location, the patients showed a range of motion displacement thresholds from normal to severely elevated. There was more marked threshold elevation for stimulus movement perpendicular to the NFL, compared to movement parallel to the NFL. This difference was significantly greater for patients with more pronounced threshold elevations (Spearman rank correlation coefficient of the difference in the thresholds at perpendicular orientation and parallel orientation versus the mean threshold was significant: $r = 0.55$, $p < 0.005$).
Conclusion: The authors have identified an orientation dependence sensitivity to motion in some patients with glaucoma. This effect may be useful in improving the sensitivity and specificity of motion sensitivity testing in identifying early glaucomatous damage.

Introduction

Abnormalities of motion detection have been shown to occur early in glaucoma using a variety of different stimuli.[1-5] We have previously identified significantly elevated motion detection thresholds in glaucoma patients using a line displacement test.[1,2] We have also detected line displacement sensitivity losses in glaucoma in areas of the visual field which appear normal using conventional Humphrey luminance testing and these findings have been confirmed by other workers.[1,5] Furthermore, we have demonstrated that elevated displacement thresholds can predict the future development of conventional visual field loss at the same locality with good sensitivity and specificity in initially normal fellow eyes of normal-tension glaucoma patients.[6] These investigations of displacement thresholds in glaucoma have been obtained

Address for correspondence: F.W. Fitzke, Department of Visual Science, Institute of Ophthalmology, 11-43 Bath Street, London EC1V 9EL, UK

Perimetry Update 1996/1997, pp. 35–42
Proceedings of the XIIth International Perimetric Society Meeting
Würzburg, Germany, June 4–8, 1996
edited by M. Wall and A. Heijl

using vertical line stimuli undergoing horizontal displacements. Other stimuli that have been used are random dot kinetograms, using stimuli in which the signal component moves in either a horizontal direction or one of four cardinal directions.[3,4,7] The aim of this study was to investigate the effect of the orientation of the stimulus motion on the displacement thresholds in normals and glaucoma, as we are not aware of any previous studies specifically directed at this question.

Although mediated by motion sensitive pathways, line displacement thresholds may in addition be influenced by local luminance loss. Previous investigators have identified the existence of fine slit-like scotomas, beyond the resolution of conventional perimetry, that correspond to the orientation of retinal nerve fiber layer defects.[8-10] We postulate that displacements of a line stimulus into a slit-like scotoma would contribute to impaired motion sensitivity, and that this effect would depend on the orientation of the line stimulus relative to the orientation of the slit-like scotoma. We hypothesize that the motion sensitivity of a line stimulus moving in a parallel direction to the nerve fiber layer would be less influenced by an underlying fine slit-like scotoma orientated along the axis of the nerve fiber, as illustrated by Figure 1a, than a stimulus moving perpendicular to the NFL and thus into the slit-like scotoma (Fig. 1b).

The aim of this study is to test the hypothesis.

Patients and methods

Seventeen patients with an established diagnosis of primary open-angle glaucoma (POAG) and eight age-matched normal controls were prospectively recruited for this study. All patients had documented intraocular pressures above 21 mm Hg, glaucomatous optic disc cupping and early but reproducible glaucomatous visual field defects on Program 24-2 of the Humphrey Visual Field Analyzer. All controls had a normal ocular examination, intraocular pressures under 21 mm Hg and normal Humphrey 24-2 fields (normal glaucoma hemifield test and global indices within 95% CI for normal subjects) in both eyes.

All patients and controls had a corrected visual acuity in both eyes of >6/9 achieved with less than ±4 diopters (D) spherical equivalent and less than 2 D of astigmatism. Patients with significant ocular pathology other than glaucoma were excluded.

The glaucoma patients had a mean age of 64.9 years with an SD of 7.4, and the control group 58.9 with an SD of 9.8 (non-significant difference at 0.05 level).

Peripheral line displacement thresholds were measured using a test described previously.[1,2] A PC-generated 2° × 2 min line is projected on a green phosphor display viewed at 1.24 meters. The background luminance is set at 7 C/m^2 and the stimulus luminance at 27 C/m^2. The stimulus is presented in the superotemporal or inferotemporal fields at 15° eccentricity on the 30 or 330 meridian. The line stimulus undergoes instantaneous oscillatory displacements of magnitudes 0–18 min arc at a fixed constant frequency of 2.5 Hz. The subject is instructed to press a response button if movement is seen. Frequency of seeing curves are generated for ten magnitudes of displacement from 0 to 18 min arc, each presented ten times. A Probit fit analysis is applied and the displacement corresponding to 50% seen is taken as the threshold. A gimbal system was constructed to enable the monitor to be rotated through 360°. This allowed us to alter the orientation of the line and hence the

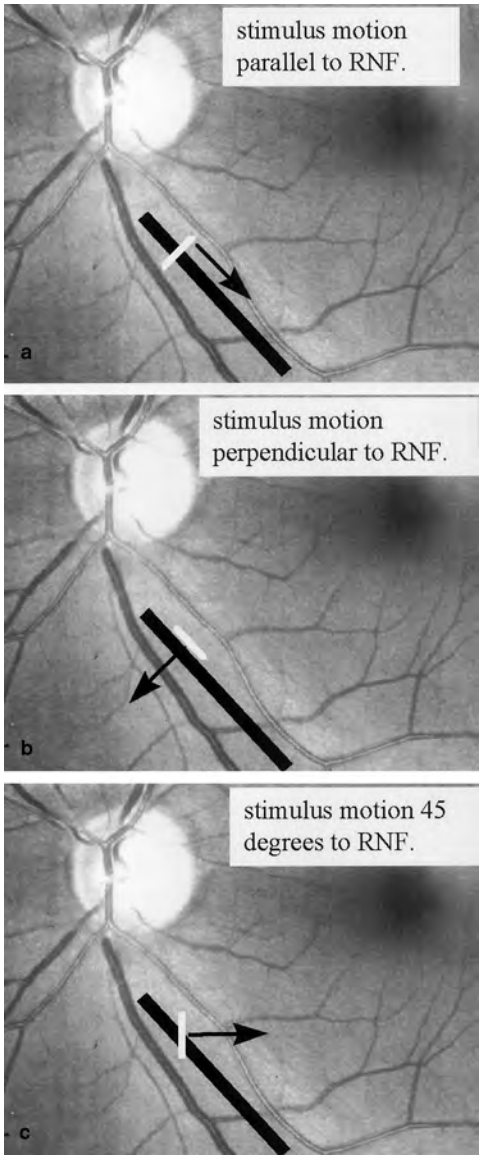

Figs. 1a to c. Left eye motion test in superotemporal field: vertical line stimulus shown in white superimposed on fundus image. The arrow shows the direction of the stimulus displacement, in relation to hypothetical slit-like scotoma orientated along the axis of the retinal nerve fiber layer shown in black. *a.* Stimulus motion parallel to orientation of retinal nerve fibers. *b.* Stimulus motion perpendicular to orientation of retinal nerve fibers. *c.* Stimulus motion 45° to orientation of retinal nerve fibers.

direction of the stimulus motion to an accuracy of within 1°, whilst keeping all other properties of the test constant. Patients underwent motion measurements in one glaucomatous eye in either the superotemporal location (14 patients) or in the inferotemporal location (three patients). Controls underwent motion sensitivity testing in one randomly chosen eye, all in the superotemporal location. All subjects

underwent an initial baseline motion sensitivity test with the stimulus in the vertical position undergoing horizontal motion (designated 0° axis). This was followed by tests with the stimulus rotated counterclockwise by 45°, 135° and 0° (*i.e.*, baseline again) with appropriate rest breaks, in a randomized order to avoid any consistent bias in learning or fatigue.

Analysis

Motion measurements were classified according to the direction of stimulus movement with respect to the orientation of the retinal nerve fibers at the test site. Figures 1a, b and c show the position of the stimulus for a motion test in the superotemporal field of the left eye: movement along the 135° meridian is labeled as 'motion parallel' to the retinal nerve fibers, stimulus movement along the 45° meridian is labeled as 'motion perpendicular' to the retinal nerve fibers, and stimulus movement along the 0° meridian is labeled as 'motion at 45°' to the retinal NFL. This analysis is a valid supposition, assuming that the orientation of the retinal nerve fibers at the test location lies between 22.5° and 90° from the horizontal reference line.

We evaluated the Humphrey 24-2 luminance at the test site by examining the threshold sensitivities at the four Humphrey 24-2 test locations closest to the motion site. We defined the Humphrey 24-2 luminance at the motion test site as being abnormal if at least one of these four locations was contiguous with a hemifield cluster of depressed locations consisting of at least three adjacent depressed points on the STATPAC-2 pattern deviation plot with one point having a probability of $p < 1\%$ and two adjacent points having a probability of $p < 2\%$.[11]

Results

The patients had early glaucomatous Humphrey 24-2 field loss with repeatable focal arcuate losses or a nasal step usually limited to one hemifield. The mean of the MDs of the Humphrey 24-2 fields of the glaucoma group was -4.87 dB, SD ± 3.37 dB, (range +3.37 to -10.10 dB) which was significantly different from the control mean MD of -0.65 dB, SD ± 1.11 dB (range +1.11 to -2.24 dB). (*t* test significant at $p < 0.001$.)

Fifteen of the seventeen patients had normal Humphrey luminances of the four closest Humphrey test locations to the motion test site, according to our definition (see analysis section), whilst two patients had scotomas extending into the motion test site.

Table 1 shows the mean motion displacement thresholds for the glaucoma and control groups for the orientations tested. The motion tests are classified according to the direction of the stimulus movement relative to the orientation of the retinal nerve fibers (RNF).

The means of the motion thresholds of the controls lie within our normal range of values for this test for all orientations tested.[2]

The means of the motion displacement thresholds of the glaucoma group were significantly elevated compared to the means of the control group for all orientations tested. There was a statistically significant negative linear correlation between the motion thresholds and the mean of the luminance thresholds at the four Humphrey

Table 1. Mean motion displacement thresholds and standard deviations in min arc for glaucoma and control groups by orientation, with statistical comparison between groups using Student's *t* test

Direction of motion relative to RNF	*Controls (min arc)*	*Glaucoma (min arc)*	*Controls versus glaucoma*
45° (1st measurement)	6.4 ± 1.2	11.7 ± 3.8	$t = 5.18$ $p < 0.001$
45° (2nd measurement)	5.0 ± 1.5	10.0 ± 4.3	$t = 4.25$ $p < 0.001$
Perpendicular	5.2 ± 1.8	11.3 ± 5.2	$t = 4.32$ $p < 0.001$
Parallel	5.6 ± 1.5	9.8 ± 3.7	$t = 3.04$ $p = 0.006$

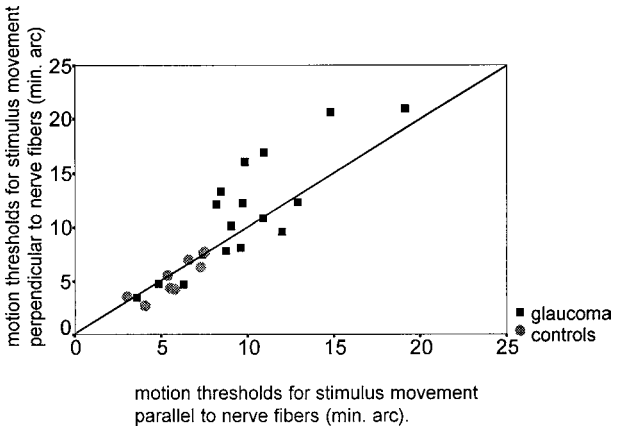

Fig. 2. Scatterplot of subject's thresholds for stimulus motion perpendicular versus motion parallel to retinal nerve fibers, with the line of unity.

24-2 test locations nearest the test site although the degree of correlation was poor ($r^2 = 0.22$, $p = 0.02$). There was no significant linear correlation between the motion thresholds and the Humphrey MD.

To illustrate the individual orientation-dependent variability we plotted the thresholds for stimulus motion perpendicular to the RNF against stimulus motion parallel to the RNF for all subjects (Fig. 2).

For quantitative analysis, we plotted the difference in the thresholds for stimulus motion perpendicular and parallel to the RNF versus the mean of the thresholds (Fig. 3). The zero on the *y* ordinate represents no difference between the motion threshold for motion perpendicular and parallel to the retinal NFL.

For subjects with normal motion thresholds (up to 8.6 min arc, equivalent to mean + 2 SD of controls), there is no orientation dependence, with all differences lying close to the zero ordinate.

In contrast, in patients with abnormally elevated motion thresholds (above 8.6 min arc), a number of the patients lie a considerable distance above the zero ordinate, with the motion threshold for stimulus motion perpendicular to the NFL more severely elevated compared to motion parallel to the NFL. Figure 3 also shows a trend of increasing elevation of motion threshold for stimulus motion perpendicular compared to parallel to the NFL (data points above zero ordinate) in patients with more pronounced threshold elevations. A Spearman rank correlation test showed that this was highly statistically significant ($r = 0.55$, $p < 0.005$). Thus increasing threshold

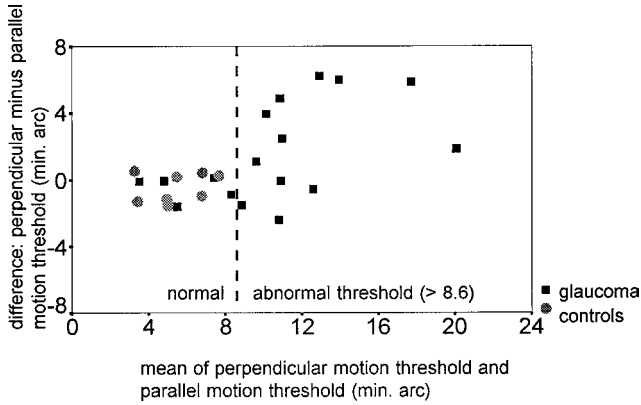

Fig. 3. Difference versus mean plot of motion thresholds for stimulus motion perpendicular and parallel to retinal nerve fibers. Subjects with normal motion thresholds lie to left of vertical reference lines of 8.6 min arc.

elevation is associated with increasing elevation of the motion threshold for motion perpendicular compared to parallel to the nerve fiber layer.

However, this analysis does not take into account smaller differences in the thresholds which may be proportionally more important at the lower range of threshold values. To correct for this, we calculated the proportional difference in the thresholds for perpendicular and parallel stimulus motion according to:

Proportional difference (Pn) = perpendicular – parallel motion threshold / perpendicular + parallel motion threshold

A proportional difference value of 0 represents no difference between the perpendicular and parallel thresholds, +1 represents maximally elevated perpendicular threshold relative to parallel, -1 maximally elevated parallel threshold relative to perpendicular.

Figure 4 is a plot of the proportional difference versus the mean of the perpendicular and parallel thresholds for all subjects. A ranked Spearman correlation test again showed a significant positive correlation between the proportional difference (Pn) and the mean. For all subjects (Spearman ranked correlation coefficient $r = 0.555$, $p = 0.004$). Reference lines indicate the mean ±2 SD of the controls, with no controls lying outside this range. However, five of the glaucoma patients lie above the control mean +2 SD. These patients have a proportionally elevated motion threshold of at least 15% for stimulus motion perpendicular to the RNF compared to stimulus motion parallel to the RNF. No patients have a proportional difference below the mean -2 SD of the controls. We reviewed the results to identify any distinguishing characteristics of these five patients who showed the most pronounced orientation effect. There was no consistent order in the sequence of the tests performed in the five which may have influenced the results. Of these five patients with the most pronounced orientation effect, one had a scotoma extending to the four Humphrey 24-2 test locations closest to the site of motion testing, one had a nasal Humphrey field defect distant to the motion test site, and three patients had normal Humphrey field in the hemifield of the motion test. Although there was a weak correlation between the motion threshold and the Humphrey luminance at the motion test site,

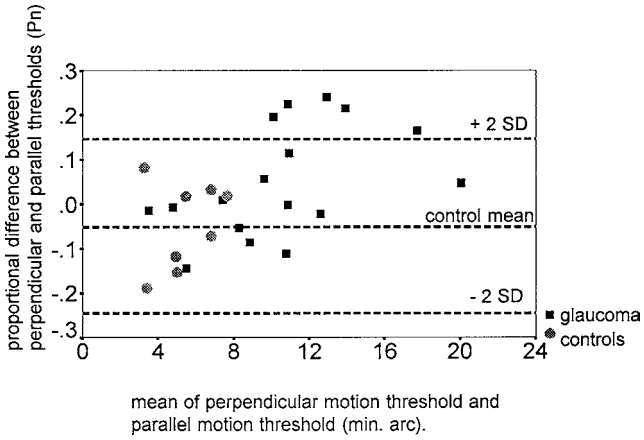

Fig. 4. Proportional difference versus mean plot of motion thresholds for stimulus motion perpendicular and parallel to retinal nerve fibers.

there was no significant correlation between the difference in the motion thresholds of the orientations tested and the Humphrey luminance at the motion test site.

Discussion

The aim of this study is to investigate the effect of stimulus orientation on motion detection thresholds in controls and patients with POAG. We performed tests of motion sensitivity using a line displacement test, with the line stimulus orientated parallel or perpendicularly to the orientation of the retinal NFL corresponding to the site of motion testing. We did not identify any clinically significant differences between the thresholds at perpendicular and parallel orientations in the controls, or in patients with normal motion thresholds. In patients with elevated motion thresholds, there was more marked threshold elevation for stimulus movement perpendicular to the NFL, compared to movement parallel to the NFL. This difference was statistically significantly greater for patients with more pronounced threshold elevations.

In five patients the motion thresholds for stimulus motion perpendicular to the retinal NFL were proportionately elevated by over 15%, compared with motion parallel to the NFL. This proportional elevation exceeded the 95% confidence limits we obtained with our controls. We did not identify any patients who demonstrated a proportional elevation of the threshold for motion parallel compared to perpendicular of this magnitude.

Although factors such as fatigue and learning may affect an individual's performance during the tests we think this is unlikely to explain this affect as the order in which the motion tests were performed was randomized, and we could not find any consistent order effects in the test sequence in these patients. There were no differences in the degree of astigmatic and spherical error in these patients (which was low in all groups) nor were there marked differences in the Humphrey luminance at the test site between the patients who showed an orientation effect and those who did not.

We hypothesize that this effect is explained by the interaction of the stimulus with fine slit-like luminance loss orientated along the RNF, on a much finer scale than is identifiable with conventional perimetry. We postulate that the motion sensitivity of a line stimulus in a parallel direction to the NFL would be less influenced by fine slit-like luminance loss orientated along the axis of the nerve fiber, as illustrated by Figure 1a, than a stimulus moving perpendicular to the NFL and thus into the luminance loss (Fig. 1b). According to this hypothesis, any effect of orientation on the motion threshold may be predicted by the underlying orientation of the retinal NFL at the site of testing. The results of this study are based on a small number of subjects tested so far, and we are at present testing further patients in multiple locations of the visual field to test this hypothesis and to see if any orientation effect is useful in improving the sensitivity and specificity in glaucoma.

Acknowledgments

Supported by the Friends of Moorfields, International Glaucoma Association and the Medical Research Council.

References

1. Fitzke FW, Poinoosawmy D, Ernst W, Hitchings RA: Peripheral displacement thresholds in normals, ocular hypertensives and glaucoma. In: Greve EL, Heijl A (eds) Seventh International Visual Field Symposium, pp 447-452. Dordrecht: Martinus Nijhoff/Dr W Junk Publ 1987
2. Fitzke FW, Poinoosawmy D, Nagasubramanian S, Hitchings RA: Peripheral displacement thresholds in glaucoma and ocular hypertension. In: Heijl A (ed) Perimetry Update 1988/89, pp 399-405. Amsterdam/Milano: Kugler & Ghedini 1989
3. Silverman SE, Trick GL, Hart WM: Motion perception is abnormal in primary open-angle glaucoma and ocular hypertension. Invest Ophthalmol Vis Sci 31/4:722-729, 1990
4. Bullimore MA, Wood JM, Svenson K: Motion perception in glaucoma. Invest Ophthalmol Vis Sci 34/13:3526-3533, 1993
5. Johnson CA, Marshall D, Eng KM: Displacement threshold perimetry in glaucoma using a Macintosh computer system and a 21-inch monitor. In: Mills RP, Wall M (eds) Perimetry Update 1994/1995, pp 103-110. Amsterdam/New York: Kugler Publ 1995
6. Baez KA, McNaught AI, Dowler JGF, Poinoosawmy D, Fitzke FW, Hitchings RA: Motion detection threshold and field progression in normal tension glaucoma. Br J Ophthalmol 79:125-128, 1995
7. Wall M, Ketoff K: Random dot motion perimetry in patients with glaucoma and in normal subjects. Am J Ophthalmol 120:587-596, 1995
8. Åsman P, Heijl A, Olsson J, Rootzén H: Spatial analyses of glaucomatous visual fields: a comparison with traditional field indices. Acta Ophthalmol (Kbh) 70:679-686, 1992
9. Weber J, Ulrich H: A perimetric nerve fibre bundle map. Int Ophthalmol 15:193-200, 1991
10. Tuulonen A, Lehtola J, Airaksinen PJ: Nerve fiber layer defects in normal visual fields. Ophthalmology 100:587-598 1993
11. Plitz JR, Drance SM, Douglas GR, Milkelbergh FS. The relationship of peripheral vasospasm, diffuse and localized visual field defects, and intraocular pressure in glaucomatous eyes. In: Mills RP, Heijl A (eds) Perimetry Update 1990/1991, pp 465-472. Amsterdam/New York/ Milano: Kugler & Ghedini 1991.

SHORT-WAVELENGTH AUTOMATED PERIMETRY AND MOTION AUTOMATED PERIMETRY IN GLAUCOMA*

PAMELA A. SAMPLE, CHARLES F. BOSWORTH, INCI IRAK and ROBERT N. WEINREB

Glaucoma Center and Visual Function Laboratory, University of California at San Diego, La Jolla, CA, USA

Abstract

Purpose: To compare short-wavelength automated perimetry (SWAP), a test favoring detection by the parvocellular pathways of vision, and motion automated perimetry (MAP), a test favoring the magnocellular pathways, in the same eyes.

Methods: Subjects were 20 glaucoma suspects and 12 glaucoma patients, compared to age-matched normal databases. SWAP was carried out with the usual protocol (24-2). Motion coherence thresholds were measured with 14 random dot targets which covered the 24-2 field area.

Results: SWAP and MAP were correlated by visual field location (whole field, r = -0.59, p<0.0000), and especially in the superior field (r = -0.75, p<0.0000), although there was a small percentage of individuals with defect results on only one test or with visual field defects on the two tests which did not overlap. ANOVA showed a significant effect of diagnosis for both tests (SWAP p<0.0000; motion p<0.0003), with glaucomas significantly different from normals. Although suspects were not significantly different, 30% had abnormal fields with SWAP and 20% with MAP.

Conclusions: Both tests successfully identified glaucoma eyes and a percentage of the suspects, and they were highly correlated. These results suggest that damage due to glaucoma is localized and non-selective for either the parvocellular or magnocellular type ganglion cell axons, and that there may be individual differences in which type of ganglion cell shows damage first.

Acknowledgment

This study was supported in part by National Eye Institute grant EY-08208 (Dr. Sample).

*The full article will be published elsewhere

Address for correspondence: Pamela A. Sample, PhD, Department of Ophthalmology, 0946, University of California, San Diego, La Jolla, CA 92093-0946, USA

Perimetry Update 1996/1997, p. 43
Proceedings of the XIIth International Perimetric Society Meeting
Würzburg, Germany, June 4–8, 1996
edited by M. Wall and A. Heijl

BLUE-ON-YELLOW PERIMETRY IN PATIENTS WITH OCULAR HYPERTENSION

HIDETAKA MAEDA, YOSHIAKI TANAKA and TORAO SUGIURA

Department of Ophthalmology, Kobe University, Kobe, Japan

Abstract

The authors report the visual field pattern of blue-on-yellow (B/Y) perimetry in ocular hypertensives. The ocular hypertensive group showed a radical sensitivity loss around the peripheral visual field in B/Y perimetry, and diffuse retinal sensitivity loss could be detected by B/Y perimetry, whereas no visual field defect could be seen with white-on-white (W/W) perimetry in ocular hypertensives. Visual field defects resembling early glaucomatous changes could be shown with B/Y perimetry in some ocular hypertensives.

Introduction

Several investigators[1-3] have assessed the role of color vision in the diagnosis of glaucoma, and studies indicate that blue color vision deficits appear early in the disease. Blue-on-yellow (B/Y) perimetry assesses the S-cone visual field under yellow adaptation. Glaucomatous visual field defects can be detected earlier and are shown to be larger in B/Y perimetry compared to standard white-on-white (W/W) perimetry.[4] We have evaluated the visual fields of patients with ocular hypertension using a modified Humphrey automated perimeter (Model 640).

Materials and method

Retinal sensitivities of 20 eyes of patients with ocular hypertension and of 15 normal controls were measured with B/Y perimetry and compared to those measured with W/W perimetry. Examinations with W/W and B/Y perimetry were conducted using program 30-2 of a modified Humphrey Field Analyzer (Humphrey Instruments, San Leandro, CA). Patients under 50 years of age were selected in order to exclude the effect of cataract and retinal sensitivity loss with aging. All patients had a best-corrected visual acuity of better than 20/40, refractive errors of less than three diopters of spherical equivalent. The standard W/W perimetry test was performed with 10 candela/m^2 background and size III (4 mm^2) stimulus.[5] B/Y perimetry

Address for correspondence: Hidetaka Maeda, MD, Department of Ophthalmology, Kobe University School of Medicine, 7-5-2 Kusunoki-cho, Chuo-ku, Kobe-shi, Hyougo-ken 650, Japan

Perimetry Update 1996/1997, pp. 45–48
Proceedings of the XIIth International Perimetric Society Meeting
Würzburg, Germany, June 4–8, 1996
edited by M. Wall and A. Heijl

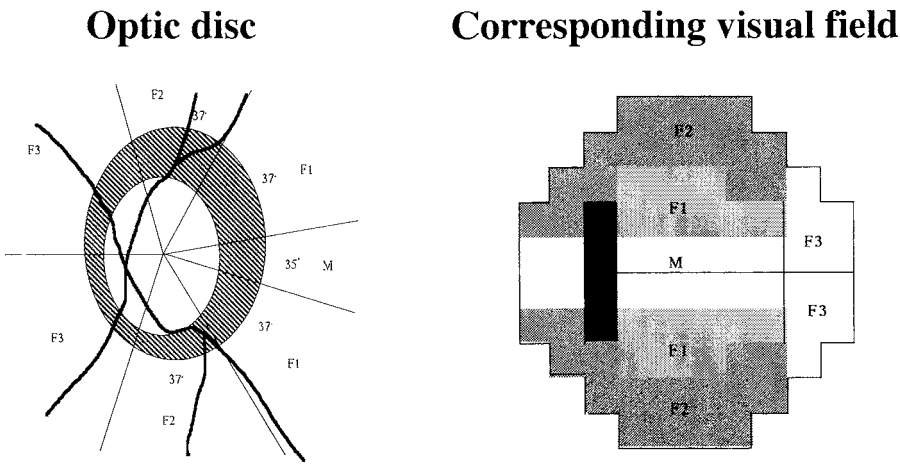

Fig. 1. Division of visual field (left eye).

Table 1. Average retinal sensitivity in each area

White-on-white (W/W)					*Blue-on-yellow (B/Y)*				
Area		*Normal*	*OHT*	*p value*	*Area*		*Normal*	*OHT*	*p value*
M	superior	34.9±1.4	34.1±1.4	NS	M	superior	30.9±1.8	30.0±1.8	NS
	inferior	36.1±1.7	34.4±1.5	NS		inferior	31.2±1.7	30.9±1.5	NS
F1	superior	30.4±1.1	33.6±1.6	NS	F1	superior	29.2±1.5	28.4±1.2	NS
	inferior	35.0±1.1	33.9±1.1	NS		inferior	29.7±1.7	29.2±1.2	NS
F2	superior	31.5±1.4	31.2±1.7	NS	F2	superior	26.7±2.9	24.8±1.8	0.05*
	inferior	32.8±0.9	32.3±1.3	NS		inferior	28.5±1.7	26.6±1.3	0.05*
F3	superior	32.5±1.6	32.6±1.8	NS		inferior	28.0±1.7	27.2±1.9	NS

(Mean ±SD)

measurements were obtained with a 200 cd/m^2 yellow background and a size V (64 mm^2) blue stimulus. We divided the retinal nerve fiber layer into seven anatomical regions and compared the average retinal sensitivities in the corresponding visual field displays (Fig. 1).

Results

There was no significant difference in age and refraction between the two groups. Distribution of retinal sensitivities measured with W/W and B/Y are given in Table 1 and Figure 2. In normal subjects, these mean data showed a parallel slope in both groups. Mean difference of sensitivity measured with B/Y was about 4.5 dB lower than that measured with W/W perimetry. However, the ocular hypertensive group showed a marked sensitivity loss of the peripheral visual field (F2 area) with B/Y perimetry. In three of 20 ocular hypertensive eyes, glaucomatous visual field defects

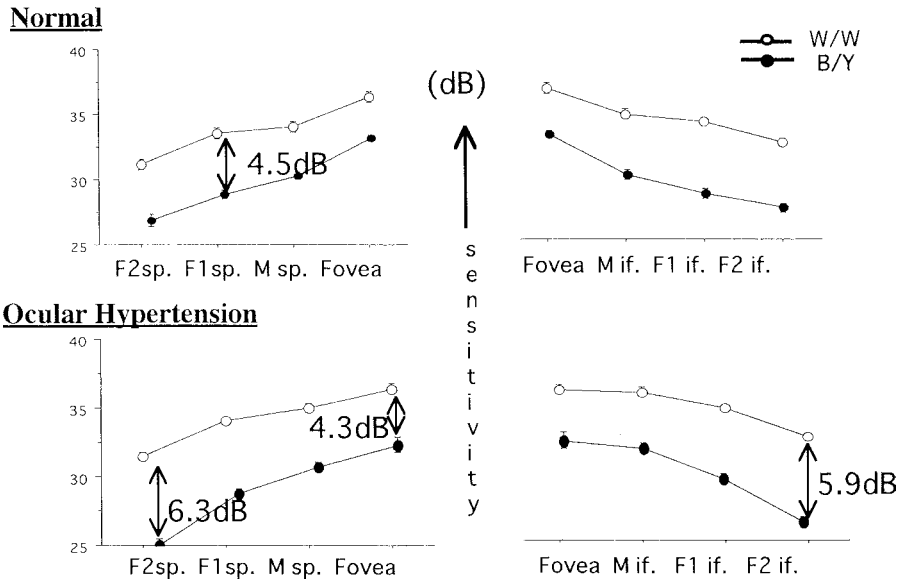

Fig. 2. Distribution of retinal sensitivity between W/W and B/Y.

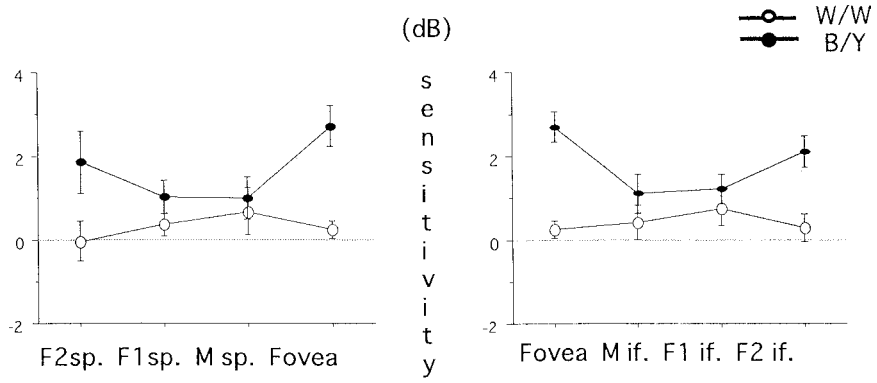

Fig. 3. Difference in sensitivity between W/W and B/Y.

were only detected with B/Y perimetry, while none of the visual field defects were detected with W/W perimetry.

Discussion

We have evaluated the central visual field of patients with ocular hypertension using B/Y perimetry. Previous investigators have reported that the most noticeable difference between W/W and B/Y perimetry is the sensitivity loss in the 10-20° area in ocular hypertensives with B/Y perimetry.[6] In our study, diffuse retinal sensitivity loss could be detected by B/Y perimetry, whereas no visual field defect was seen with

W/W perimetry in ocular hypertensives. Moreover, the ocular hypertensive group showed a marked sensitivity loss of the peripheral visual field with B/Y perimetry. Visual field defects resembling early glaucomatous changes could be shown with B/Y perimetry in some ocular hypertensives.

References

1. Sample PA, Weinreb RN: Progressive color visual field of glaucoma. Invest Opthalmol Vis Sci 33:2068-2071, 1992
2. Felius J, De Jong LAMS, Van den Berg TJTP, Greve EL: Functional Characteristics of blue-on-yellow perimetric threshold in glaucoma. Invest Opthalmol Vis Sci 36:1665-1674, 1995
3. Sample PA, Weinreb RN: Color perimetry for assessment of primary open-angle glaucoma. Invest Opthalmol Vis Sci 31:1869-1876, 1990
4. Johnson CA, Adams AJ, Casson EJ, Brandt JD: Progression of early glaucomatous visual field loss as detected by blue-on-yellow and standard white-on-white automated perimetry. Arch Ophthalmol 111:651-656, 1993
5. Johnson CA, Adams AJ, Casson EJ, Brandt JD: Blue-on-yellow perimetry can predict the development of glaucomatous visual field loss. Arch Opthalmol 111:645-650, 1993
6. Gunji H, Kitahara K, Takahashi G-I: Automated perimetry for a blue test light on an intense white background in glaucoma. In: Heijl A (ed) Perimetry Update 1994/1995, pp 97-102. Amsterdam/New York: Kugler Publ 1995

MASS SCREENING FOR VISUAL FIELD DEFECTS WITH SNOWFIELD CAMPIMETRY
Results of a field study using local TV broadcasting

A.C. GISOLF[1], J. KIRSCH[2], H.K. SELBMANN[2], E. ZRENNER[3] and U. SCHIEFER[3]

[1]Süddeutscher Rundfunk (SDR), Mannheim; [2]Institute for Medical Information Processing (IMI), Tübingen; [3]University Eye Hospital, Department II, Tübingen; Germany

Abstract

Snowfield campimetry immediately transforms usually negative scotomas into perceivable visual field defects.[1-4] The suitability of this method for mass screening was tested by broadcasting this stimulus to home TV sets. In cooperation with the 'Süddeutscher Rundfunk' (SDR), as well as several health insurance companies ('AOK Baden-Württemberg' and RVO-Kassen'), approximately 300,000 viewers were addressed in this local test.

Results of this pilot project are shown diagrammatically in Figure 1. There were 531 calls for questionnaires, which were additionally used for documenting subsequent ophthalmological examinations. Of these, 127 usable questionnaires were returned to the Institute for Medical Information Processing (IMI). In 78 cases, the ophthalmologists did not confirm a lesion of the visual pathway; however, in 49 subjects, they detected scotomas, which were already known to them in 25 cases. Glaucomatous optic neuropathology and macular degeneration were the most frequent pathological ophthalmological findings causing white noise field defects.

A detailed interpretation of the results, as well as aspects evaluating the costs and benefit of this study, are recorded elsewhere.[5]

Acknowledgment

Supported by the 'AOK-Baden-Württemberg' and 'RVO' health insurance companies, as well as 'Kassenärztliche Vereinigungen Nord-Württemberg, Südwürttemberg, Nordbaden und Südbaden'.

Address for correspondence: A.C. Gisolf, Süddeutscher Rundfunk (SDR), Wilhelm-Varnholt-Allee 5, D-68165 Mannheim, Germany

Perimetry Update 1996/1997, pp. 49–50
Proceedings of the XIIth International Perimetric Society Meeting
Würzburg, Germany, June 4–8, 1996
edited by M. Wall and A. Heijl

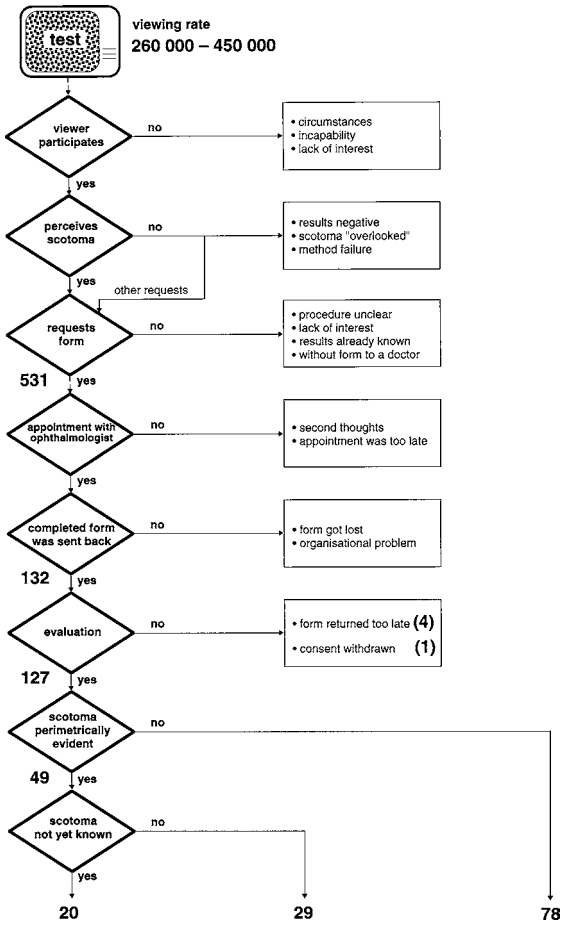

Fig. 1. Diagram illustrating the course and results of the TV mass screening test using snowfield campimetry. Reasons for non-responding are also listed.

References

1. Aulhorn E, Köst G: Rauschfeldkampimetrie: eine neuartige perimetrische Untersuchungsmethode. Klin Mbl Augenheilk 192:284-288, 1988
2. Aulhorn E, Köst G: Noise-field campimetry: a new perimetric method (snow campimetry). In: Heijl A (ed) Perimetry Update 1988-89, pp 331-336. Amsterdam/Milano: Kugler & Ghedini Publ 1989
3. Schiefer U, Pfau U, Selbmann HK, Wilhelm H, Zrenner E: Sensitivität und Spezifität der Rauschfeldkampimetry. Ophthalmologe 92:156-167, 1995
4. Schiefer U: Rauschfeldkampimetry. Stuttgart/Berlin/Köln: Kohlhammer Verlag 1995
5. Schiefer U, Gisolf AC, Kirsch J, Selbmann HK, Zrenner E: Rauschfeld-Screening – Ergebnisse einer Fernseh-Feldstudie zur Detektion von Gesichtsfelddefekten. Ophthalmologe 1996 (submitted for publication)

PUPIL PERIMETRY WITH THE OCTOPUS 1-2-3

SACHIKO OKUYAMA, CHOTA MATSUMOTO, ATSUSHI IWAGAKI, TAKUYA OTSUKI and TOSHIFUMI OTORI

Department of Ophthalmology, Kinki University School of Medicine, Osaka-Sayama City, Osaka 589, Japan

Abstract

Pupil perimetry was performed in normal subjects and glaucoma patients using the Octopus 1-2-3 perimeter. The amplitude of pupil constriction and the constriction rate were determined in ten normal subjects on the upper nasal 135° meridian using stimulus sizes 3 and 5, stimulus intensities 0 (4000 asb), 2, 4, 6, 8 and 10 dB, and a background luminance of 0 and 3 asb. The amplitude of pupil constriction was also measured in glaucoma patients for the same test points of the Octopus Program 38 using stimulus size 5, a stimulus intensity of 6 dB (approximately 1000 asb) and a background luminance of 3 asb.

It was found that the inter- and intra-individual variations of the amplitude of pupil constriction were large. In order to ensure a dynamic range large enough for pupil perimetry in the central 30° visual field, the stimulus intensity needs to be higher than 8 dB with a background luminance of 3 asb and stimulus size 5. Abnormal points detected by pupil perimetry corresponded well to those of standard Octopus perimetry in glaucoma patients. It was, however, impossible to detect small scotomata under the above-mentioned conditions.

Introduction

Standard perimetry is a subjective examination during which results depend on the alertness of the subject. The measurements of involuntary responses, such as pupillography and electroretinography, and the measurement of the visually evoked potential have been used to evaluate the visual field objectively. Other investigators have reported the results of experiments of pupil perimetry.[1-13] Since 1990, several pupil perimeters combined with automated perimeters have been developed.[14-18] In recent studies, each pupil constriction (not pupillary threshold) has been quantified. However, examination conditions suitable for pupil response perimetry have not been fully investigated. The purpose of this study was to look at reproducible examination conditions for clinical investigations.

Address for correspondence: Sachiko Okuyama, MD, Department of Ophthalmology, Kinki University School of Medicine, 377-2 Ohno-Higashi, Osaka-Sayama City, Osaka 589, Japan

Perimetry Update 1996/1997, pp. 51–58
Proceedings of the XIIth International Perimetric Society Meeting
Würzburg, Germany, June 4–8, 1996
edited by M. Wall and A. Heijl

Subjects and methods

Pupil perimetry was performed using a modified Octopus 1-2-3 perimeter and a 486/33 mHz IBM compatible personal computer. The amplitude of pupil constriction and the constriction rate were determined in ten normal subjects in the upper nasal field on the 135° meridian. Test points were located at 0, 4, 8, 12, 16, 20, 24 and 28°. We used stimulus sizes 3 and 5, stimulus intensities of 0 (4000 asb), 2, 4, 6, 8 and 10 dB, and a background luminance of 0 and 3 asb. Stimulus duration was 200 msec and inter-stimulus interval was approximately 3 seconds. Each test point was measured three times under each test condition.

We evaluated the maximum and minimum values of both the amplitude of pupil constriction and the constriction rate of three pupillary responses under various test conditions. The amplitudes were given by the number of pixels of the CCD camera which measured the pupil area. The constriction rate was given by the amplitude of constriction divided by the pupil size in the beginning of the light reflex. We calculated the arithmetic mean of the constriction rates obtained in ten normal subjects at each test point under the above-mentioned conditions.

Using stimulus size 5, a stimulus intensity of 6 dB (approximately 1000 asb) and a background luminance of 3 asb, we also measured the amplitude of pupil constriction at 77 test points in the central 30° visual field in normal subjects and glaucoma patients. The arrangement of these test points was almost the same as that of the Octopus Program 38. The amplitude of pupil constriction was measured twice at each test point, and the larger pupil response was evaluated.

Results

Measurements on the 135° meridian of the central 30° visual field under various test conditions in ten normal subjects

Figure 1 shows the profiles of the arithmetic means of the constriction rate obtained in ten normal subjects for six kinds of stimulus intensities, stimulus sizes 3 and 5, and background luminances of 0 and 3 asb. The profiles for each stimulus intensity were nearly parallel to each other. When stimulus intensity decreased, the constriction rate decreased. Constriction rates were smaller at a background luminance of 3 asb than at 0 asb. Constriction rates for stimulus size 3 were also smaller than those for stimulus size 5. In addition, the profiles obtained at a background luminance of 3 asb were steeper in the central 4° visual field than those obtained at 0 asb.

Figure 2 shows the profiles of the maximum constriction rate of three measurements. Only results obtained with a stimulus intensity of 6 dB are shown. The inter-individual variability was large, and larger with a background luminance of 0 asb than with a background luminance of 3 asb. In some normal subjects, using stimulus size 3 and a background luminance of 3 asb, it was not possible to detect any pupil responses at some test points in the central 30° visual field despite triplicate measurements. Even when the stimulus intensity was 0 dB, the average constriction rate was smaller than 10% in ten normal subjects at the two most peripheral test points (as shown in Fig. 1).

Figure 3 shows the profiles of the minimum constriction rate of three measurements for each normal subject with stimulus size 5 and a background luminance of

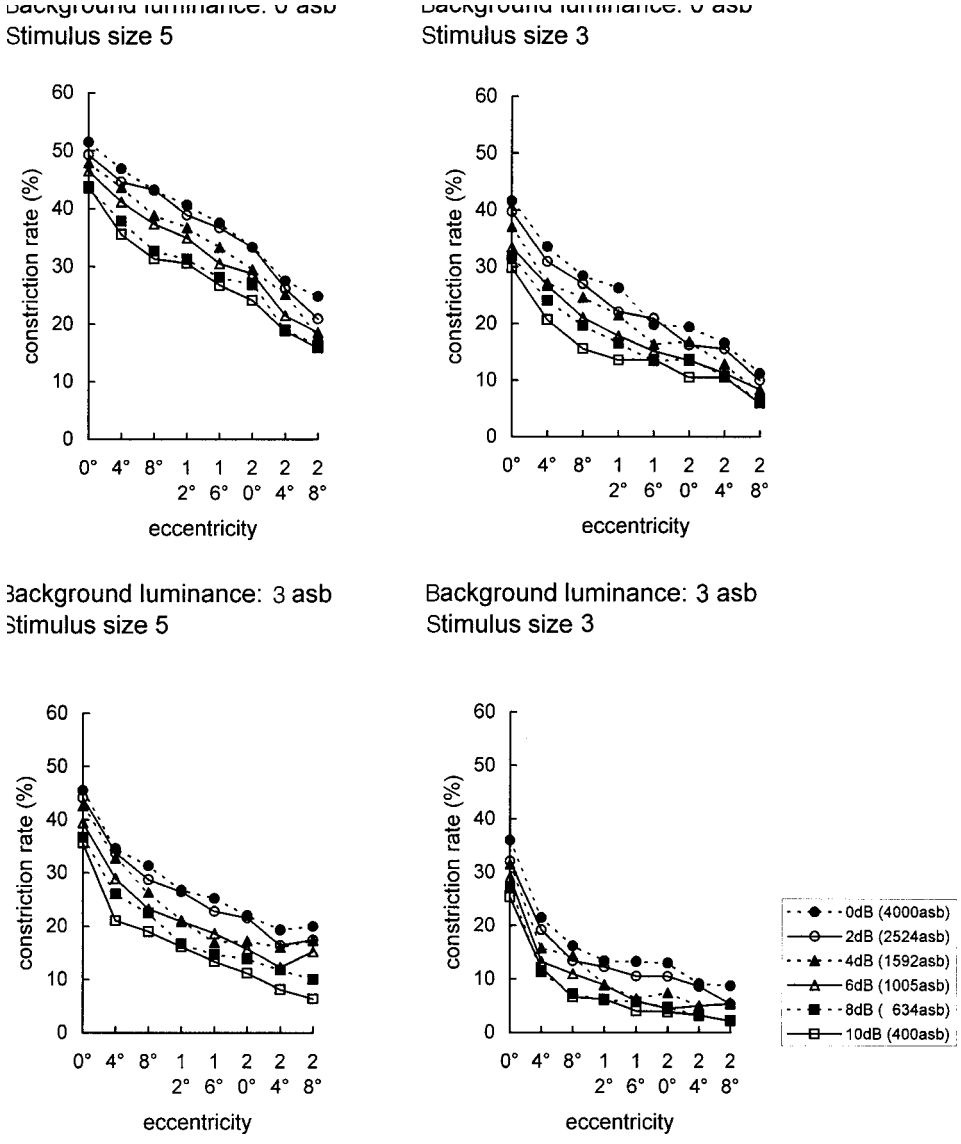

Fig. 1. Profiles of the arithmetic means of the constriction rate of ten normal subjects on the 135° meridian for six stimulus intensities, two stimulus sizes and two background conditions.

3 asb. Results are shown for stimulus intensities of 4, 6 and 8 dB. With stimulus intensities of 8 dB or less, almost no or only very small pupil responses were often observed at the points further than 10° from the point of fixation.

We calculated the differences between the maximum and minimum constriction rates for each subject at each test point with stimulus size 5, a stimulus intensity of 6 dB and a background luminance of 3 asb. The arithmetic mean of these differences values was 7.0% (SD 5.0%).

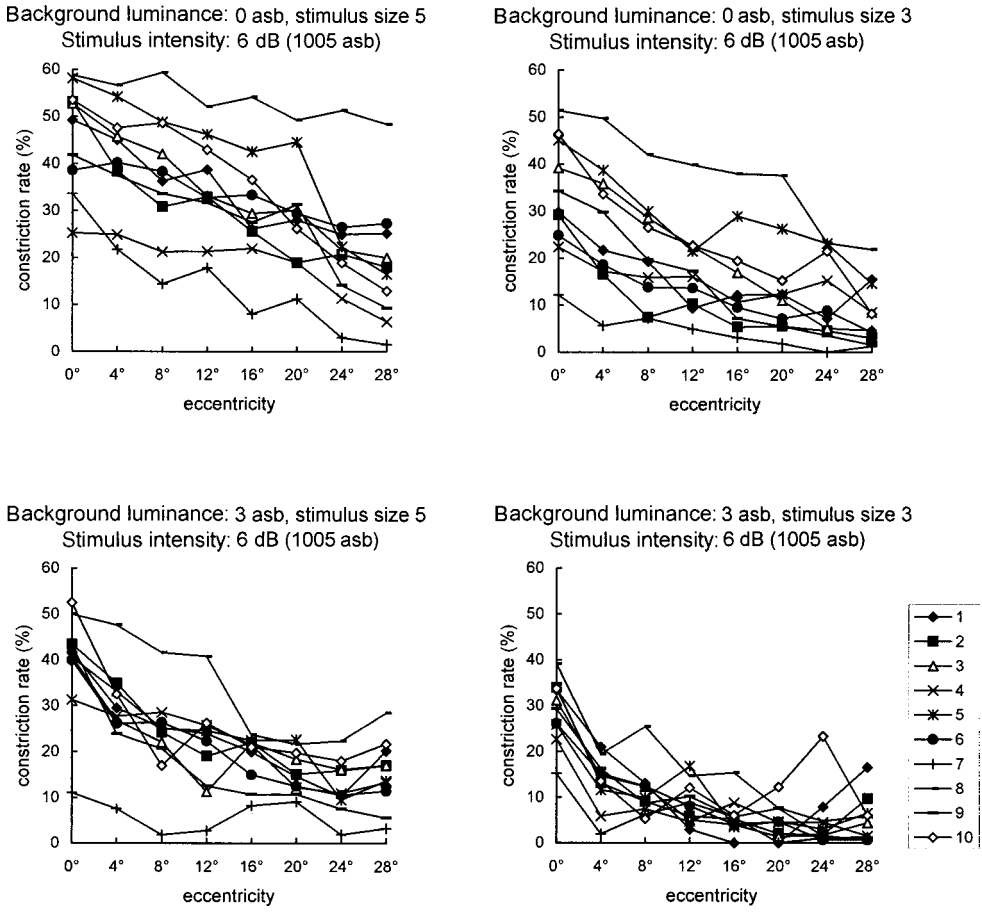

Fig. 2. Profiles of the maximum constriction rate of three measurements for two stimulus sizes at two different background luminances. Stimulus intensity was 6 dB.

Measurement of the central 30° visual field with stimulus size 5, a background luminance of 3 asb and a stimulus intensity of 6 dB

Figure 4 shows the traces of the pupillogram, the value table of the amplitude of pupil constriction and its gray scale in a 38-year-old normal male. The pupil responses were large enough to be detected at all test points in the central 30° visual field. The blind spot was not detected under the above-mentioned conditions.

The clinical case of a 54-year-old female with primary open-angle glaucoma (POAG) is reported. The results of the Octopus standard differential light-sense perimetry are shown in Figure 5, and the results of pupil perimetry with stimulus size 5, a background luminance of 3 asb and a stimulus intensity of 6 dB are shown in Figure 6. Abnormal points detected by pupil perimetry corresponded well with those of standard Octopus perimetry. However, it was impossible to detect small scotomata by pupil perimetry under the above-mentioned conditions.

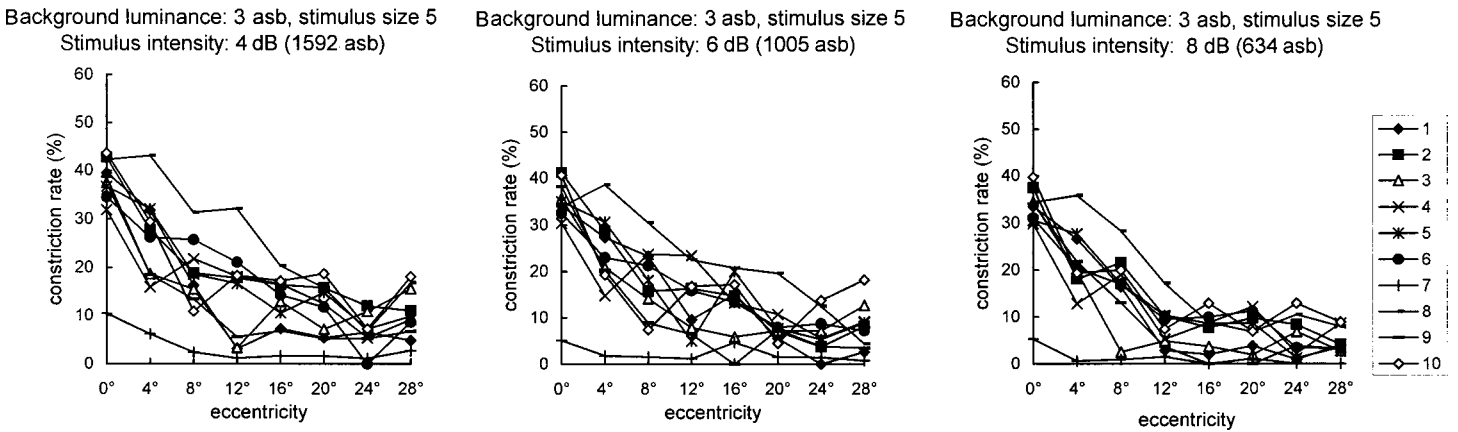

Fig. 3. Profiles of the minimum constriction rate of three measurements in normal subjects (stimulus size: 5, background luminance: 3 asb, stimulus intensity: 4, 6 and 8 dB).

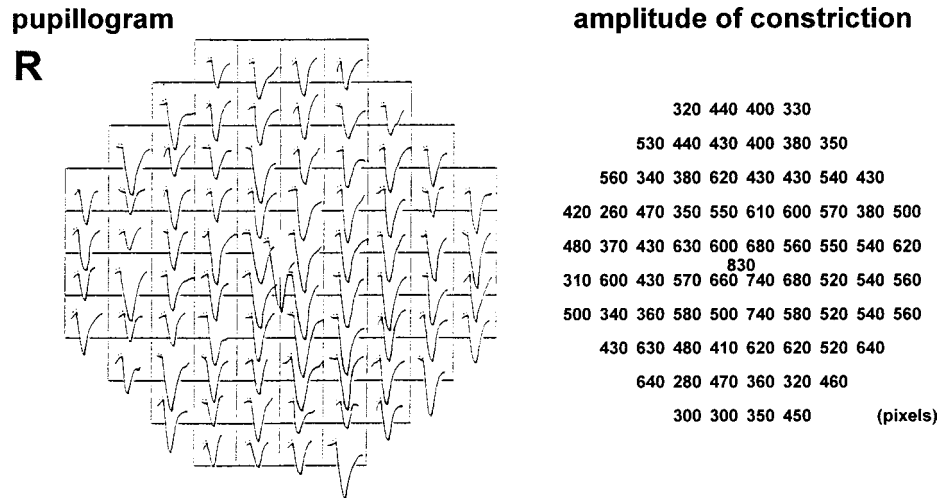

Fig. 4. An example of pupil perimetry in a normal subject.

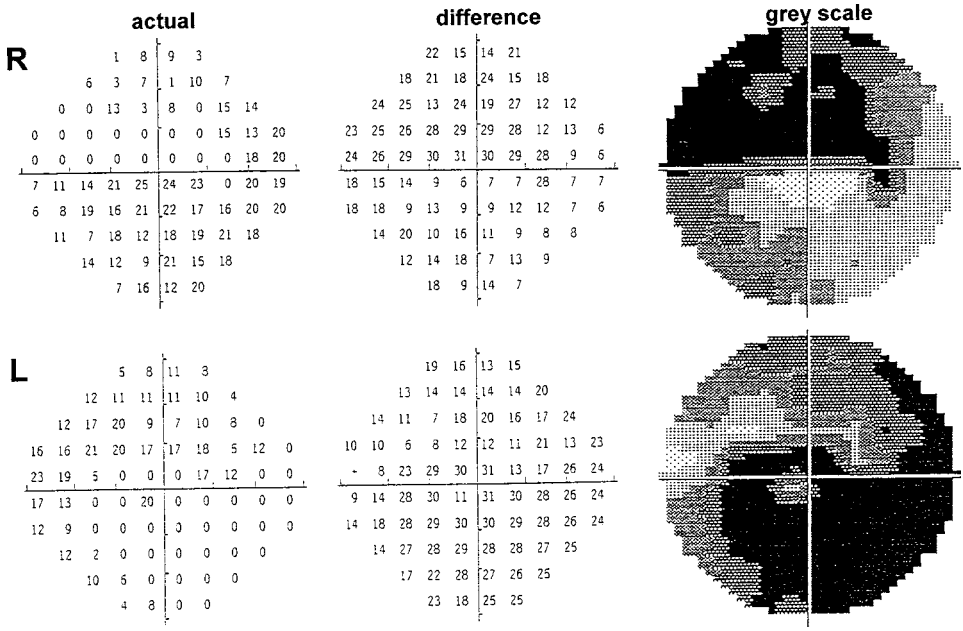

Fig. 5. Actual value tables, difference tables and gray scale of Octopus differential light threshold perimetry in a patient with POAG.

Discussion

A background luminance of 3 asb and stimulus size 3 did not seem to provide us with the best conditions for pupil perimetry in the central 30° visual field when the Octopus 1-2-3 was used. Under these conditions, pupil responses were too small to be detected constantly.

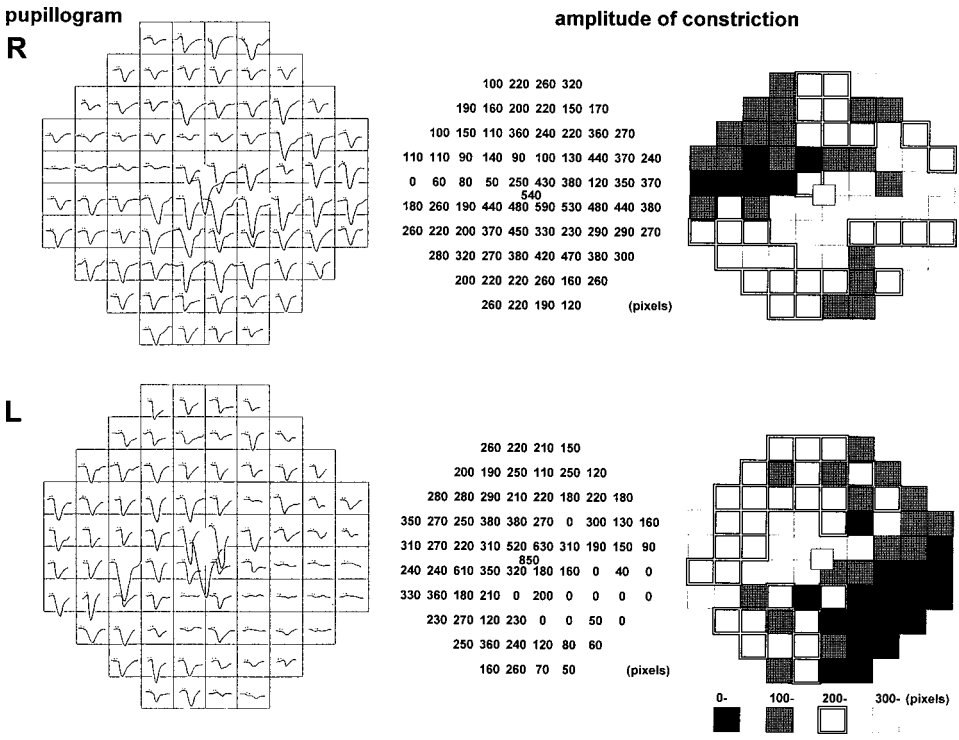

Fig. 6. Map of the pupillogram, value tables of the amplitude of pupil constriction and its gray scale of pupil perimetry in the same patient shown in Figure 5.

On the other hand, with a background luminance of 0 asb, it is possible that the exposed retinal area cannot be localized because of scattering of the stimulus light. Particularly when stimulus size 5 was used, pupil perimetry near the fixation point gave very large responses, so that sometimes the pupil size did not recover completely before the next stimulus light was exposed. In addition, the inter-individual variability using a background luminance of 0 asb was larger in normal subjects than that obtained with a background luminance of 3 asb. Therefore, it was difficult to compare the actual amplitude values among different subjects. Evaluation of the pattern deviation might be useful in these cases.

With a background luminance of 3 asb and stimulus size 5, stimulus intensity may have to be higher than 8 dB in order to obtain a constant pupil response. However, extremely high stimulus intensities cannot be recommended since they lead to disturbingly high pupil recovery times. Thus, we used a background luminance of 3 asb, stimulus size 5 and a stimulus intensity of 6 dB in this study. These examination conditions were very similar to those reported by Kardon *et al.*[16], who used a modified Humphrey Field Analyzer.

However, a normal subject No. 7 (a 38-year-old male), as seen in Figures 2 and 3, showed considerably poor pupil responses under the conditions we used clinically. He showed better pupil responses, which were detectable in the central 30° visual field, with a background luminance of 0 asb and stimulus size 5. Therefore, if some

patients show poor pupil responses in the broad test area under usual test conditions, we may have to look for some other conditions.

The present study of glaucoma patients suggested that pupil perimetry was a useful method for detecting visual field defects objectively. However, it was impossible to detect small scotomata by pupil perimetry under our examination conditions. If we use a stimulus smaller than size 5, smaller perifoveal scotomata may become detectable. However, high suprathreshold stimulus intensities are necessary to detect pupil responses in the peripheral 30° field.

We believe that automated pupil response perimetry with the Octopus 1-2-3 is more practical for objective perimetry than manual pupil threshold perimetry. However, the software for pupil perimetry using the Octopus 1-2-3 should be improved, for example, with regard to analysis of the data and automatic repetition of the measurement of the test points affected by blinking.

References

1. Harms H: Grundlagen, Methodik und Bedeutung der Pupillenperimetrie für die Physiologie und Pathologie des Sehorgans. Graefe's Arch Clin Exp Ophthalmol 149:1-68, 1949
2. Bresky RH, Charles S: Pupil motor perimetry. Am J Ophthalmol 68:108-112, 1969
3. Sugita K, Sugita Y, Mutsuga N, Takaoka Y: Pupillary reflex perimeter for children and unconscious patients. Rinsho Ganka 24:517-523, 1970
4. Narasaki S, Noguchi J: Videopupillographic perimetry: I. The apparatus for objective measurement of visual field. J Jpn Ophthalmol Soc 76:1639-1645, 1972
5. Narasaki S, Noguchi J: Videopupillographic perimetry: II. Findings and its method used in human and rabbits eyes. J Jpn Ophthalmol Soc 77:1278-1310, 1973
6. Narasaki S, Kawai K, Kubota S, Noguchi J: Video-pupillographic perimetry: III. Reformed perimeter. J Jpn Ophthalmol Soc 79:1765-1769, 1975
7. Mamada N: A pupillometric perimeter. Rinsho Ganka 27:71-80, 1973
8. Mamada N: A pupillometric perimeter: II. Clinical application. J Jpn Ophthalmol Soc 77:1311-1324, 1973
9. Aoyama T, Kani K: Pupillographic perimetry. J Jpn Ophthalmol Soc 79:1247-1255, 1975
10. Aoyama T: Pupillographic perimetry: the application to clinical cases. J Jpn Ophthalmol Soc 81:1527-1538, 1977
11. Jensen W: A description of the objective perimetry. Graefe's Arch Clin Exp Ophthalmol 201:183-191, 1976
12. Hellner KA, Jensen W, Müller-Jensen A: Video-processing pupillography as a method for objective perimetry in pupillary hemiakinesia. Doc Ophthalmol Proc Ser 14:221-226, 1977
13. Hellner KA, Sautter H: Pupillen- und Lichtsinnperimetrie bei Hell- und Dunkeladaptation. Klin Mbl Augenheilk 173:653-657, 1978
14. Alexandridis E, Krastel H: New equipment for pupillographic perimetry. Neuro-Ophthalmology 73:235-248, 1990
15. Fankhauser F II, Flammer J: Puptrak 1.0: a new semiautomated system for pupillometry with the Octopus perimeter: a preliminary report. Doc Ophthalmol 73:235-248, 1990
16. Kardon RH, Aydin-Kirkali P, Thompson HS: Automated pupil perimetry: I. Pupil field mapping in patients and normal subjects. Ophthalmology 98:485-496, 1991
17. Turtschi S, Bergamin O, Dubler B, Schötzau A, Zulauf M: Pupillenperimetrie mit dem Octopus 1-2-3: erste Erfahrungen. Klin Mbl Augenheilk 204:398-399, 1994
18. Bergamin O, Turtschi S, Schötzau A, Hendrickson PH, Flammer J, Zulauf M: Pupil perimetry with the Octopus 1-2-3: first experience. In: Mills RP, Wall M (eds) Perimetry Update, 1994/1995, pp 125-129. Amsterdam/New York: Kugler Publ 1995

AGE, GENDER AND TEST LOCATION IN PUPIL PERIMETRY

OLIVER BERGAMIN, ANDREAS SCHÖTZAU, STEPHANIE TURTSCHI, BIRGITTA HENZI, PHILLIP HENDRICKSON and MARIO ZULAUF

University Eye Clinic, Basel, Switzerland

Abstract

Purpose: To evaluate the effect of age and gender on visual-field eccentricity in healthy volunteers.
Methods: Pupil perimetry was performed on 100 healthy volunteers with a modified Octopus 1-2-3. Stimulus parameters were Goldmann size V, intensity 1632 cd/m^2, duration 200 msec, background illumination 0 cd/m^2, and interstimulus interval 3 sec. Pupillometric parameters were velocity of contraction, redilation velocity, latency, duration of contraction, implicit time, pupillary diameter before (=PD max) and after contraction (=PD min) and amplitude. Age, gender, test location (=three independent variables) and PD max as covariate, and pupillometric parameters, were investigated by analysis of variance.
Results: No three-way interaction was found among the independent variables. No two-way interactions were observed with variable test location. An age/gender interaction was observed for all investigated parameters, *i.e.*, the age effect was more pronounced in males than in females. All pupillometric parameters showed the significant main effect for test location to be strongest for duration of contraction (F=27.41) and for amplitude (F=22.77), weaker for implicit time (F=15.33) and for velocity of contraction (F=13.01), and minimal for latency time (F=4.784), and redilation velocity (F=4.371). Latency increased, while amplitude, velocity of contraction, duration of contraction, and redilation velocity decreased with eccentricity.
Conclusions: Areas closer to the center have the greatest pupillomotor response. These results revealed that this holds true especially for the pupillary contraction amplitude and duration, but less for latency time. Age effect is more important than gender in terms of pupil size and latency, but similar in amplitude.

Introduction

In static perimetry, the differential light sensitivity is determined. Stimuli of variable light intensity are presented. The tested subjects respond to a seen stimulus by pressing a button.[1] In pupil perimetry, the same test set-up is used, but the pupillary light reflex (PLR) replaces the response button. Pupil perimetry is an objective way to test visual function, a source of additional information in case of impaired cooperation,[2,3] and is less stressful for the patient.[4] In addition, other qualities can be

Proprietary interest category: N.

Address for correspondence: Mario Zulauf, MD, University Eye Clinic, PO Box, CH-4012 Basel, Switzerland

Perimetry Update 1996/1997, pp. 59–65
Proceedings of the XIIth International Perimetric Society Meeting
Würzburg, Germany, June 4–8, 1996
edited by M. Wall and A. Heijl

measured, *i.e.*, the velocity of information transmission of the optic nerve is diminished in patients with multiple sclerosis[5] and those with optic nerve atrophy.[6] Also, the pupillary system is influenced by the autonomic nerve system.[7] Pupillography has been used to study alertness of individuals with sleep disorders.[8,9] Many other factors influence the outcome of the pupillary light reflex as a retinal function. As in standard perimetry, age[10] and eccentricity[11] affect pupil perimetry. The aim of the present study was to evaluate the effect of age, gender, and eccentricity to obtain detailed normal value data in pupil perimetry.

Material and methods

One hundred and seven subjects entered the study. Seven were excluded because normal-tension glaucoma was diagnosed (one), too many blinking artifacts were present (three), the subject did not complete the test (one), or pupil size was less than 3 mm (two). Therefore, 50 left and 50 right eyes of 43 males and 57 females were included. The subjects' age averaged 38.1 ±14.1 years. Two age groups were investigated in order to obtain stable and consistent age effects: the older group's age ranged from 46 to 62 years, and the younger group's from 20 to 38 years. Informed written consent was obtained from each subject prior to testing, according to the Ethical Commission of the University of Basel. Each subject underwent a routine eye examination, including best corrected visual acuity, IOP measurement, slit-lamp examination, and indirect ophthalmoscopy. In addition, swinging flash light, direct and consensual PLR, pupil reaction to convergent eye movement, and accommodation, were tested. Retroillumination of the iris through the pupil investigated a possible lack of iris pigmentation. Inclusion criteria were normal eye history and examination. Exclusion criteria were systemic and local diseases (inflammation, autonomic neuropathy) or medications which affect the pupil, previous eye surgery, visual acuity of <20/25, IOP of >21 mmHg, or an abnormal direct, consensual or accommodative PLR.

A slightly modified Octopus 1-2-3 was remote-controlled by a 486/40-MHz personal computer, measuring the pupil size at a rate of 50 Hz. The fixation target consisted of a small, dim, red point that was positioned to coincide with the subject's far point to avoid accommodation. The subjects completed a test program as illustrated in Figure 1. Testing time for the 129 stimuli was approximately 400 seconds. The following stimulus parameters were chosen: stimulus size Goldmann V (=1.72°) with a constant stimulus intensity of 1632 cd/m^2 being presented for 200 msec, the interstimulus interval was three seconds, and background illumination was 0 cd/m^2. No acoustic cue was presented between stimuli to trigger blinking.

The median of all investigated parameters of each test location was calculated to receive solid and stable individual values, therefore, balanced interpersonal results were obtained. All pupillometric parameters were normally distributed for both age and gender groups. Furthermore, the analysis of variance (ANOVA) model resulted in normal distributed residuals. Normal distribution of residuals is a prerequisite for performing ANOVA. A software algorithm was developed that describes the pupil response after each stimulus and marks the beginning of each PLR by a curve-fitting technique.[12] Age, gender, and test locations were considered as independent variables. PD max (= covariate) and the following pupillometric parameters were investigated by ANOVA: velocity of contraction, redilation velocity, latency, duration of

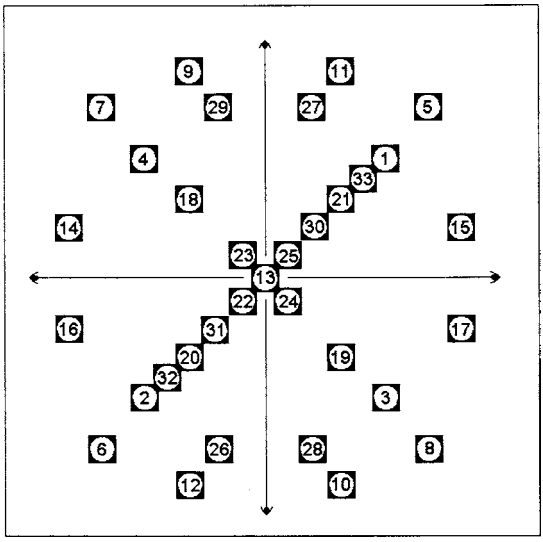

Fig. 1. Order of stimulus presentation of the test program. The length of the arrows represents the 30° visual field.

contraction, implicit time (=sum of the two mentioned before), pupillary diameter after contraction, and amplitude.

Results

First, interactions between independent variables are presented. Thereafter, the four subgroups (young females, old females, young males, and old males) are investigated in relation to the test locations. Moreover, the eccentricities' influence on the pupillometric parameters is described.

No significant three-factor interaction was observed among the independent variables of age, gender, and test location. No significant two-factor interactions were found between age/test location and gender/test location. Figure 2 shows that the subgroups' lines seldom crossed each other. A two-factor age/gender interaction was observed in all parameters, *i.e.*, the age effect was more pronounced in males than in females.

With regard to the main effect test location, PD max, amplitude, and latency are plotted in function to the test locations, as shown in Figure 2. The results on pupil size (=PD max) are illustrated in Figure 2a and summarized in Table 1. Young males had the largest pupils, and then young females, while old males, and even more so old females, had small pupils. This is true of all test locations investigated. The difference between age groups was 0.68 mm, and between gender groups 0.28 mm.

In Figure 2a, test location -26/4 stands out by presenting comparatively small pupil sizes. As presented in Figure 1, -26/4 was stimulated straight after 0/0. Following stimulation of the central test location, pupillary recovery time was too short. As shown in Figure 2b, amplitudes were largest in young men, followed by young females, old men and, finally, old females. The difference between age groups was

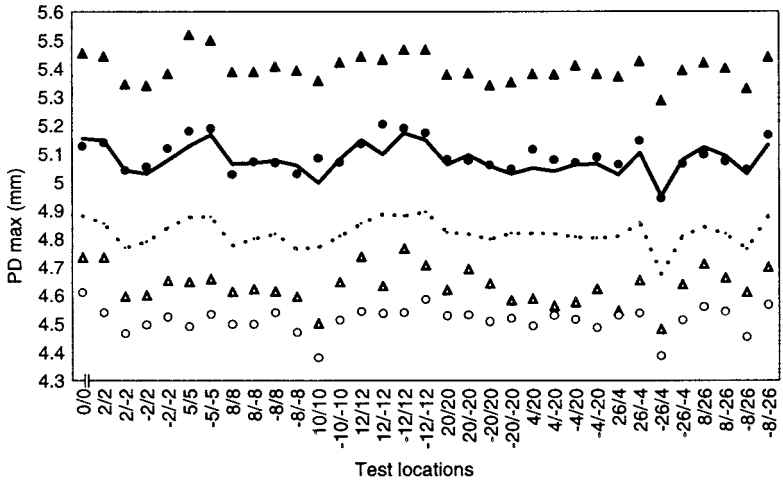
PD max (mm)
5.6
5.5
5.4
5.3
5.2
5.1
5
4.9
4.8
4.7
4.6
4.5
4.4
4.3
0/0
2/2
2/-2
-2/2
-2/-2
5/5
-5/-5
8/8
8/-8
-8/8
-8/-8
10/10
-10/-10
12/12
12/-12
-12/12
-12/-12
20/20
20/-20
-20/20
-20/-20
4/20
4/-20
-4/20
-4/-20
26/4
26/-4
-26/4
-26/-4
8/26
8/-26
-8/26
-8/-26
Test locations

a

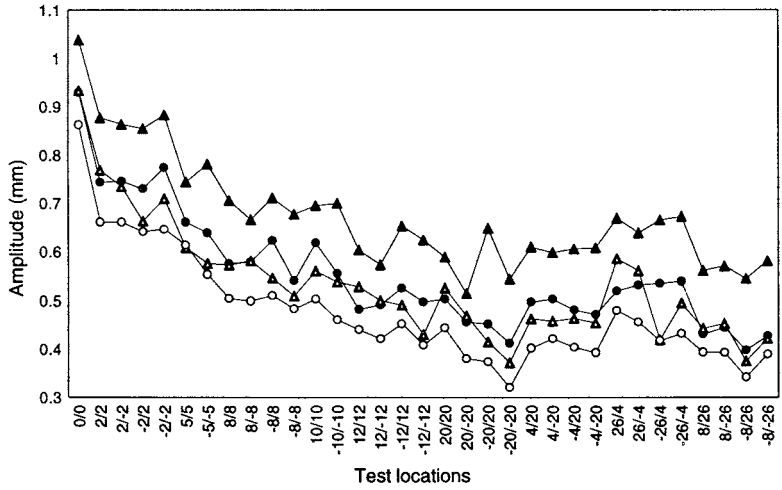
Amplitude (mm)
1.1
1
0.9
0.8
0.7
0.6
0.5
0.4
0.3
0/0
2/2
2/-2
-2/2
-2/-2
5/5
-5/-5
8/8
8/-8
-8/8
-8/-8
10/10
-10/-10
12/12
12/-12
-12/12
-12/-12
20/20
20/-20
-20/20
-20/-20
4/20
4/-20
-4/20
-4/-20
26/4
26/-4
-26/4
-26/-4
8/26
8/-26
-8/26
-8/-26
Test locations

b

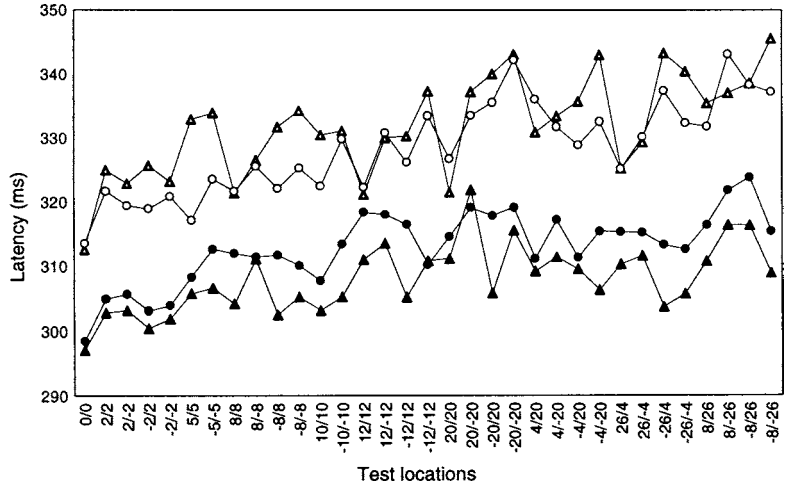
Latency (ms)
350
340
330
320
310
300
290
0/0
2/2
2/-2
-2/2
-2/-2
5/5
-5/-5
8/8
8/-8
-8/8
-8/-8
10/10
-10/-10
12/12
12/-12
-12/12
-12/-12
20/20
20/-20
-20/20
-20/-20
4/20
4/-20
-4/20
-4/-20
26/4
26/-4
-26/4
-26/-4
8/26
8/-26
-8/26
-8/-26
Test locations

c

on average 0.116 mm; that between gender groups, on average, 0.100 mm. A similar order of differences among subgroups was observed for PD max, PD min, velocity of contraction, and redilation velocity. Similarly, the age effect was always stronger than the gender effect in these parameters. An exception to this order of subgroups was observed for latency (Fig. 2c): the smallest latencies were present in young men, increasing in young females and older females, and longest in old males. However, the difference between gender groups was minimal (2.1 msec) compared to the difference in age groups (19.1 msec). All pupillometric parameters showed a significant main effect for test location. Table 2 shows the numerical order of the factors, which indicates the effect's power on the pupillometric parameters.

Discussion

The pupil perimetric results are influenced by many physiological factors, *viz.*, the stimulus (intensity, duration, size, wavelength, eccentricity), cortical influences (alertness, sleep, emotion) and individual factors, such as age, refraction, and pupil size.[13] The present study investigates the three important factors: age, gender, and test location. The results showed no interactions between test location and gender, *i.e.*, both males and females resulted in the same pattern of pupillomotor response within the visual field. This gender difference was observed in both age groups. Also, no age/test location interaction was found in the present study; in other words, the age effect in pupillomotor response was similar for all test locations. This is in contrast to standard perimetry.[10,11] However, static perimetry is a psychophysical test, whereas pupil perimetry is based on the PLR and, therefore, on different anatomical pathways. Furthermore, background illumination is set to 0 instead of 4 asb and strongly suprathreshold stimuli are presented.

The present study confirms that pupillomotor response was weaker in peripheral test locations.[4] Figure 2 shows an increased latency and a decreased amplitude with eccentricity. Also velocity of contraction, duration of contraction, and redilation velocity decreased towards the periphery.

As illustrated in Figure 2 and summarized in Table 1, the following numerical order was observed in parameters with dimension mm and mm^2/sec: young males, young females, old males, old females. Therefore, age effects are stronger than the observed differences between gender. Similarly, latency had a very strong age effect.

Nevertheless, the results of the present study might help us understand individual variation in healthy subjects, which is a prerequisite for detecting pathological changes in the pupillary pathway. However, further studies to elucidate other effects on pupil perimetry are required.

←
Fig. 2. The means of the pupillometric parameters PD max (*a*), amplitude (*b*), and latency (*c*) on the y axis are in function of the 33 test locations (x axis) ordered by eccentricity. All parameters are separated by age group, and gender. In Figure 2a, there are no connecting lines between the symbols for better observation. See the parallelism between both gender groups.

▲ males, younger age group ● females, younger age group
▵ males, older age group ○ females, older age group
– males, both age groups ..... females, both age groups

Table 1. The horizontal listed pupillometric parameters are calculated in means for each age group and for each gender group. The smallest number for all parameters is given at the last column as valid cases

	Velocity of contraction (mm^2/sec)	*Redilation velocity (mm^2/sec)*	*Latency (msec)*	*Duration of contraction (msec)*	*Implicit time (msec)*	*PD max (mm)*	*PD min (mm)*	*Amplitude (mm)*	*Valid N*
Younger males	20.35	7.35	308.4	408.9	717.3	5.416	4.739	0.678	790
Younger females	16.03	5.61	312.8	399.5	712.3	5.101	4.544	0.558	934
Older males	13.91	4.70	332.1	413.8	745.9	4.641	4.108	0.533	554
Older females	12.27	4.12	328.4	398.1	726.5	4.513	4.039	0.474	859
Younger	18.01	6.41	310.8	403.8	714.6	5.246	4.633	0.609	1724
Older	12.91	4.35	329.9	404.3	734.2	4.563	4.066	0.499	1413
Males	17.70	6.26	318.0	411.0	729.2	5.097	4.479	0.616	1344
Females	14.23	4.90	320.4	398.8	719.1	4.820	4.302	0.518	1793
All groups	15.72	5.48	319.4	404.1	723.5	4.939	4.378	0.561	3137

Table 2. The pupillometric parameters are calculated by ANOVA with main effect test location and with covariate PD max

	MS effect	*df error*	*MS error*	*F*	*p level*
Duration of contraction	74284	3146	2710.3	27.41	<0.001
Amplitude	1.3071	3146	0.0574	22.77	<0.001
Implicit time	51844	3146	3382.1	15.33	<0.001
Velocity of contraction	543.87	3162	41.792	13.01	<0.001
Latency time	3075.4	3163	642.92	4.784	<0.001
Redilation velocity	22.848	3005	5.2273	4.371	<0.001

df: degree of freedom; MS: mean square; F: factor

Acknowledgments

Supported by the Swiss National Fund, grant #3200-43624.95 and the Commission for the Promotion of Applied Research, grant #2569.1.

References

1. Bebie H, Fankhauser F, Spahr J: Static perimetry: strategies. Acta Ophthalmol (Kbh) 54:325-332, 1976
2. Kardon RH: Pupil perimetry. Curr Opin Ophthalmol 3:565-570, 1992
3. Lowenstein O, Kawabata H, Loewenfeld IE: The pupil as an indicator of retinal activity. Am J Ophthalmol 57:569-596, 1964
4. Kardon RH, Kirkali PA, Thompson HS: Automated pupil perimetry: pupil field mapping in patients and normal subjects. Ophthalmology 98(4):485-495, 1991
5. Van Dieman HA, Van Dongen MM, Nauta JJ, Lanting P, Polman CH: Pupillary light reflex latency in patients with multiple sclerosis. Electroencephalogr Clin Neurophysiol 83(3):213-219, 1992
6. Alexandridis E, Argyropoulos T, Krastel H: The latent period of the pupil light reflex in lesions of the optic nerve. Ophthalmologica 182:211-217, 1981
7. Heller PH, Perry F, Jewett DL, Levine JD: Autonomic components of the human pupillary light reflex. Invest Ophthalmol Vis Sci 31(1):156-162, 1990
8. Löwenstein O, Feinberg R, Loewenfeld IE: Pupillary movement during acute and chronic fatigue: a new test for the objective evaluation of tiredness. Invest Ophthalmol 2:138, 1963
9. Wilhelm B, Wilhelm H: Die Pupille als Schlaf-Wach Indikator: Diagnose der Einschlafgefährdung mittels Pupillographie. Z Prakt Augenheilk 1:185-189, 1994
10. Haas A, Flammer J, Schneider U: Influence of age on the visual field in normal subjects. Am J Ophthalmol 101:199-203, 1986
11. Zulauf M, LeBlanc RP, Flammer J: Normal visual fields measured with Octopus Program G1. I. Differential light sensitivity at individual test locations. Graefe's Arch Clin Exp Ophthalmol 232:509-515, 1994
12. Bergamin O, Turtschi S, Schötzau A, Hendrickson Ph, Flammer J, Zulauf M: Pupil perimetry with the Octopus 1-2-3: first experience. In: Mills RP, Wall M (eds) Perimetry Update 1994/1995, pp 125-129. Amsterdam/New York: Kugler Publ 1995
13. Loewenfeld IE: The Pupil: Anatomy, Physiology and Clinical Applications. Ames: Iowa State University Press; Detroit: Wayne State University Press 1993

MEASUREMENTS FOR DESCRIPTION OF VERY EARLY GLAUCOMATOUS FIELD DEFECTS

C.T. LANGERHORST, L.L. CARENINI, D. BAKKER and M.A.C. DE BIE-RAAKMAN

Department of Ophthalmology, Glaucoma Unit, Academic Medical Center of the University of Amsterdam, Amsterdam, The Netherlands

Abstract

In patients with suspected or (very) early glaucoma, the central 30° visual fields were compared with the corresponding 10° fields. Of 971 hemifields analyzed retrospectively, and 291 hemifields analyzed prospectively, in approximately 10% of cases the 10° field showed more or more severe glaucomatous defects than were suspected on the basis of the 30° fields. It seems advisable also to perform a 10° visual field in patients with a questionable defect located in the center of the 30° field.

Introduction

In our clinic for glaucoma patients and patients with ocular hypertension or suspect glaucoma, we regularly examine the visual field with a full-threshold program for the central 30°, and a suprathreshold test for the periphery. Threshold testing for the central 10° is performed additionally when (possible) defects are found in the 10° area on the 30° field. It was noticed that sometimes the central 10° visual field seemed to show an early glaucomatous defect more clearly than the 30° field.

Although, for example, testing of the central 10° field is well suited for monitoring central islands, and is a sensitive way of detecting progression in already known defects,[1] not much is known about its usefulness for detecting early loss close to the center of the field. Very early defects close to the center were found to occur in normal-pressure glaucoma patients.[2]

In order to investigate the possible benefit of examining the central 10° field for the identification of early glaucomatous defects, we undertook a retrospective analysis of available fields in a large data base. In this retrospective group, the reason for making a 10-2 field was either a very central defect in the (other) hemifield or a questionable defect in the analyzed hemifield. This population might be biased towards those patients already showing central defects in the 30° field. It would also be of interest to study 10° fields in patients not already showing central defects.

Address for correspondence: Christine T. Langerhorst, MD, PhD, Department of Ophthalmology G2-221, Academic Medical Center, Meibergdreef 9, 1105 AZ Amsterdam, The Netherlands

Perimetry Update 1996/1997, pp. 67–73
Proceedings of the XIIth International Perimetric Society Meeting
Würzburg, Germany, June 4–8, 1996
edited by M. Wall and A. Heijl

Therefore, the central 10° field was also prospectively performed as a routine test in an unselected number of glaucoma suspects, in addition to a 30° field test.

Methods

As part of our routine practice, all patients visiting our glaucoma clinic are entered into a computer-based registration system. Data entered are: name, date of birth, date of examination, diagnosis and diagnostic code. For each eye, the stage of the visual field defects is registered according to the modified classification of Greve and Aulhorn,[3] for upper and lower field halves separately.

For the retrospective evaluation, all patients (eyes) were considered who met the following criteria: diagnosis of ocular hypertension (pressures over 21 mmHg, no abnormalities), glaucoma suspects (suspect disc, no field defects) or early glaucoma (Stages 0, I, and II of the Greve classification); visual field examinations performed with the Humphrey Field Analyzer; both a 30-2 and a 10-2 field available; reliability parameters within normal limits. In this manner, 545 patients were eligible, with a mean age of 65 years.

When more than one field was available, the first one was used for further analysis. Each field thus obtained was then scored with objective criteria into: no defect (Class 0), minimal defect (Class 1), early defect (Class 2), moderate defect (Class 3), and severe defect (Class 4). The objective criteria used were those described by Sponsel *et al.*[4], adapted from the original classification of Hodapp *et al.*[5] For each field, the upper and lower halves were judged separately. The criteria of Sponsel were more or less divided by two and then applied to the field halves. A precise description of the classification per field half is given in Table 1.

A total of 971 hemifields was thus available for retrospective classification and analysis. In addition, 291 hemifields of 121 patients or suspects (with Greve classification 0-II; mean age 63 years) were tested with the 30-2 Program and the 10-2 Program in a prospective manner. They were scored in the same way as the retrospective group.

Results

Of the 971 hemifields analyzed retrospectively, 408 30-2 fields were graded Class 0. Of the corresponding 10-2 fields, 347 were graded Class 0, seven Class 1, 30 Class 2, 19 Class 3, and five Class 4. Of the 66 30-2 fields graded as Class 1, 12 10-2 fields were also graded Class 1, 15 Class 2, and five Class 3. An overview of the classifications is given in Table 2.

Of the 291 hemifields analyzed prospectively, 150 30-2 fields were graded Class 0. Of the corresponding 10-2 fields, six were graded Class 2, and five Class 3. Of the 14 30-2 fields graded as Class 1, four corresponding 10-2 fields were graded Class 2 or 3. The classification grades of the prospectively tested group are shown in Table 3.

Table 1. Visual field scoring criteria for Humphrey 30-2 and 10-2 hemifields

Class 0 (no defect)
Glaucoma hemifield test within normal limits and CPSD >5% confidence limit. Also less than 3 points <5% probability

Class 1 (minimal defect)
Glaucoma hemifield test outside normal limits or CPSD <5% confidence limit. And/or a total of 3 points (clustered) <5% probability, of which at least one point <1% probability

Class 2 (early defect)
Glaucoma hemifield test outside normal limits or CPSD <5% confidence limit. And/or a total of 4-9 points <5% probability, with a minimum cluster of 3 points, of which less than 5 points <1% probability; and no point in the central 5 degrees less than 15 dB

Class 3 (moderate defect)
Glaucoma hemifield test outside normal limits or CPSD <5% confidence limit. And/or a total of 10-19 points <5% probability, with a minimum cluster of 3 points, of which less than 10 points <1% probability; and no point in the central 5 degrees of 0 dB; and only one hemifield may have 2 points <15 dB in the central 5 degrees

Class 4 (severe defect)
Glaucoma hemifield test outside normal limits and CPSD <5% confidence limit. Number of points exceeding the criteria of Class 3

Note: the individual probability plots were used for scoring; edge-points were not counted for the 30-2 fields; edge-points were included for the 10-2 fields; mean defect was not taken into account; CPSD: corrected pattern standard deviation

Table 2. Classification of 971 hemifields analyzed retrospectively. The grades of the 30-2 fields are given from top to bottom, for the 10-2 fields from left to right

30° field	*10° field*					
	Class 0	*Class 1*	*Class 2*	*Class 3*	*Class 4*	*Total*
Class 0	347	7	**30**	**19**	**5**	408
Class 1	34	12	**15**	**5**	**0**	66
Class 2	102	14	60	25	15	216
Class 3	41	7	31	23	47	149
Class 4	18	1	12	13	88	132
Total	542	41	148	85	155	971

Table 3. Classification of 291 hemifields analyzed prospectively. The grades of the 30-2 fields are given from top to bottom, for the 10-2 fields from left to right

30° field	*10° field*					
	Class 0	*Class 1*	*Class 2*	*Class 3*	*Class 4*	*Total*
Class 0	137	2	**6**	**5**	**0**	150
Class 1	8	2	**3**	**1**	**0**	14
Class 2	23	3	16	9	6	57
Class 3	14	0	4	19	6	43
Class 4	3	0	8	6	10	27
Total	185	7	37	40	22	291

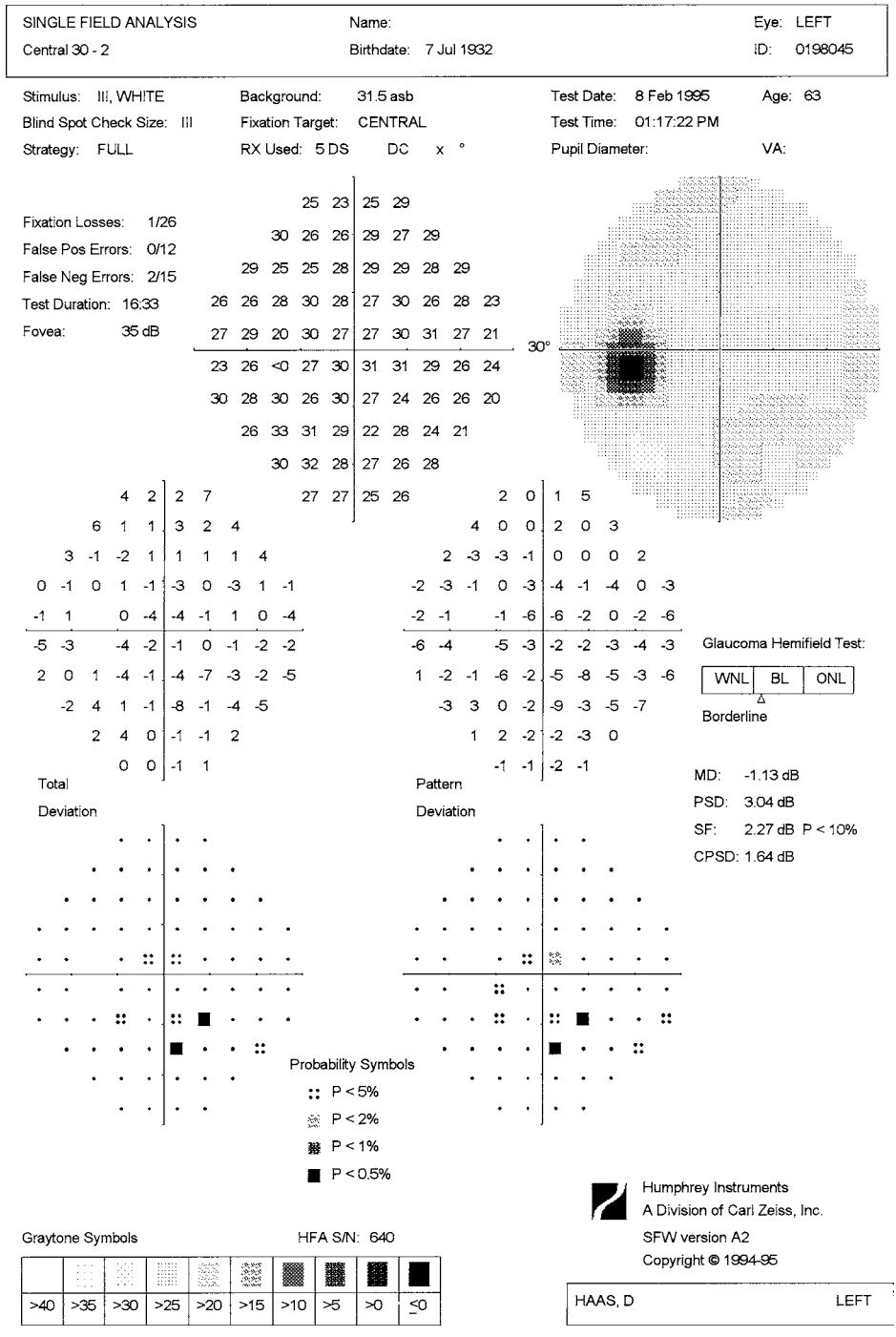

Fig. 1a. Thirty-degree visual field with no defect in the upper hemifield and Class 2 in the lower hemifield.

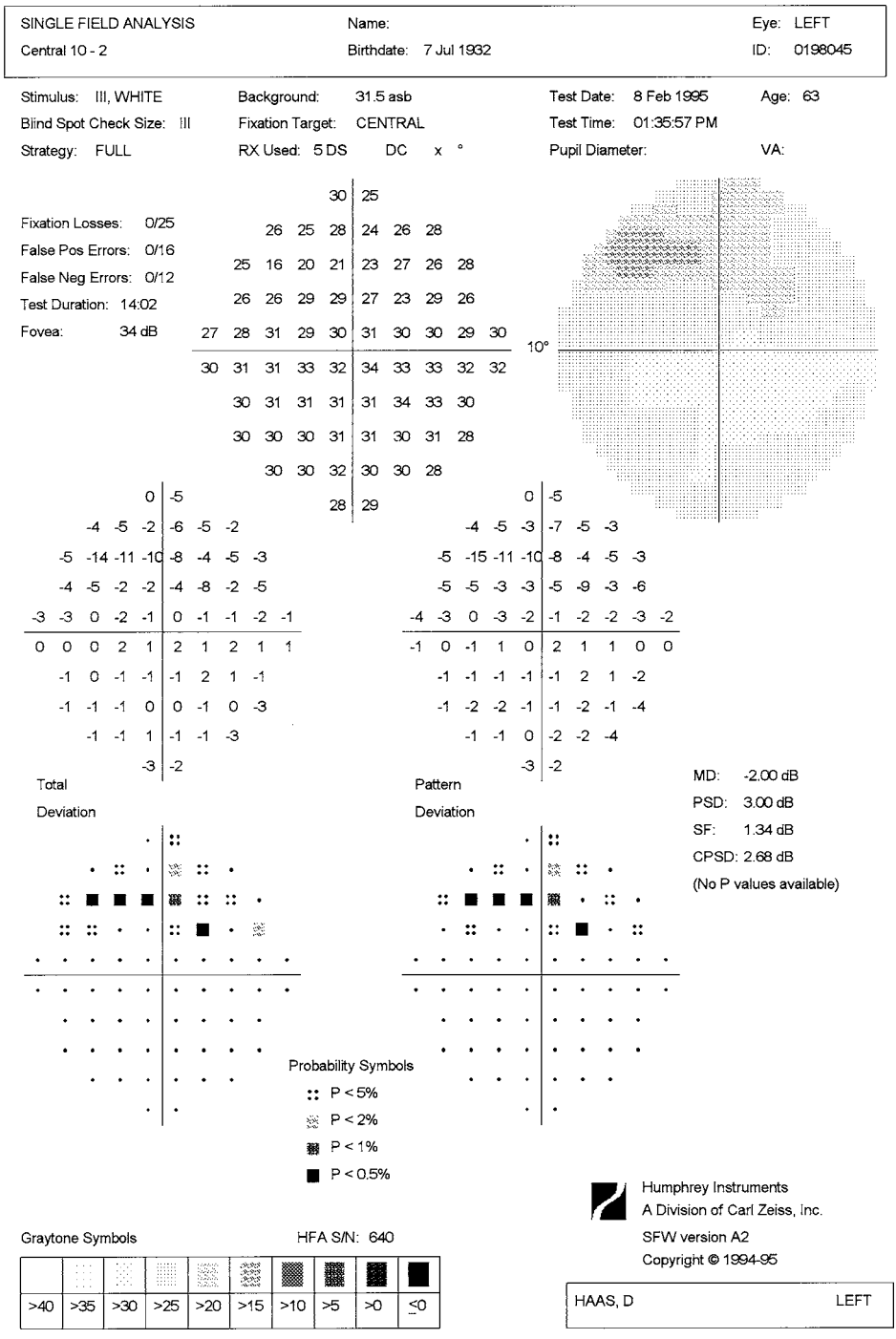

Fig. 1b. Ten-degree central examination of the same visual field as in Fig. 1a. The upper hemifield was scored as Class 3 and the lower hemifield as Class 0.

Discussion

The purpose of this study was to see whether the central 30° visual field test sometimes underestimates (very) early glaucomatous defects, in comparison to a 10° central field test. Looking at the summary of data in the classification (Tables 2 and 3), a number of observations can be made. First of all, it is clear that for most hemifields the scores for the 30-2 field and the 10-2 field were the same. However, some fields scored higher in the 30-2 examination, and others scored higher in the 10-2 examination. This could, of course, partly be due to the well-known fluctuation of the visual field. In order to investigate the effect of fluctuation, the same scoring system would have to be applied to several 30-2 fields in the same eye performed in a short timespan, and likewise to the 10-2 fields. This was not done in our study. Therefore, we do not know the exact size of the fluctuation effect. Secondly, it must be realized that those hemifields scoring in a higher class with the 30-2 field than with the 10-2 field are most likely those with defects outside the 10° central area. However, we were interested in underestimation with the 30-2 examinations, and therefore any data pertaining to higher 30-2 scores were not given further consideration.

For the purpose of our study, it was very interesting to consider why 10-2 fields might show more severe staging than 30-2 fields. First, there is a geometrical argument. Any defect location on the 30-2 field will, on average, be magnified nine times on the 10-2 field and is, therefore, more likely to score in a higher class. This could indeed be the case, but reproducibility studies would have to be carried out to obtain more insight into this phenomenon. There is also a stochastical argument, in the case of small defects. Because of the larger sampling distance in the 30-2 fields, small defects have a higher chance of being missed. The magnification of the 10-2 field yields a nine-times greater chance of detecting even a small glaucomatous defect. This would be a good reason for performing a detailed central field examination.

For practical clinical purposes, the size of the severe underestimation of glaucomatous defects by the 30-2 field would be very interesting. Therefore, we chose to study those hemifields judged to be in Classes 0 or 1 with the 30-2 field, but in Classes 2 to 4 with the 10-2 field. In the retrospective group, this was the case in 74 of 474 hemifields (15.6%) and, in the prospective group, in 15 of 164 hemifields (9.1%). The difference between these figures may represent the bias mentioned in the introduction. A typical example of underestimation with the 30-2 field is presented in Figure 1 (upper hemifield).

The overall magnitude of underestimation of early glaucomatous field defects by a 30° field would then seem to be about 10%. Because we found this rather a large percentage, we looked at our data in another way. We selected those 30-2 fields from the retrospective and the prospective groups which had scored Class 0 in both hemifields, and looked at the corresponding 10-2 scores. In 147 normal 30° fields, glaucomatous defects Classes 2 to 4 were scored in 12 cases with the 10° field examination (8.2%).

Conclusions

A 30° field performed in patients with suspected or early glaucoma may underestimate the presence or severity of a defect in up to 10% of cases. It would seem to

be advisable also to perform a 10° visual field in all cases in which there is any doubt as to the presence of a defect location in the center of the 30° field.

References

1. Weitzman ML, Zeyen T, Caprioli J: High resolution central visual field to detect progressive glaucomatous damage. In: Mills RP, Wall M (eds) Perimetry Update 1994/1995, pp 71-72. Amsterdam/New York: Kugler Publ 1995
2. Poinoosawmy D, McNaught AI, Fitzke FW, Hitchings RA: Location of early field deterioration in glaucoma suspects. In: Mills RP, Wall M (eds) Perimetry Update 1994/1995, pp 289-297. Amsterdam/New York: Kugler Publ 1995
3. Greve EL: Performance of computer assisted perimeters. Doc Ophthalmol 53:343-380,1982
4. Sponsel WE, Rich R, Stamper R, Higginbotham EJ, Anderson DR, Wilson MR, Zimmerman TJ: Prevent Blindness America visual field screening study. Am J Ophthalmol 120:699-708, 1995
5. Hodapp E, Parrish RK, Anderson DR: Clinical Decisions in Glaucoma, pp 52-61. St Louis: CV Mosby 1993

A NEW FUNDUS PERIMETER BY WHICH THE TARGET CAN AUTOMATICALLY PURSUE EYE MOVEMENT

YASUHIRO NISHIDA[1], KAZUTAKA KANI[1], TOYOTAKA MURATA[1], KOZO OKAZAKI[2] and SHINICHI TAMURA[3]

[1]Department of Ophthalmology, Shiga University of Medical Science, Otsu; [2]Department of Electrical and Electronics Engineering, Faculty of Engineering, Fukui University, Fukui; [3]Medical School, Osaka University, Osaka; Japan

Abstract

In order to remove the influence of eye movements and stably stimulate the same retina during fundus perimetry,[1-4] a new infrared fundus perimeter has been developed. This system is composed of three parts: the fundus camera, the pursuit device, and the target device. Sending the infrared fundus image from the camera to the pursuit device, a pursuit point in the fundus is decided on a pursuit device display. The real time position of the pursuit point can be calculated using the pursuit device computer. Even if there are eye movements, and the coordinates of the fundus change in the display during the examination, the position where the stimulating target will be displayed on the monitor can be controlled by the target device receiving a signal from the pursuit device and the stimulating target pursuing the same retinal point. This makes it possible to stably stimulate the same retina during the examination. Using the new fundus camera, the quality of the infrared fundus image is also improved.

Introduction

Using ordinary perimetry, it is impossible to identify which area is stimulated on the fundus. We developed an infrared television fundus perimeter[2,3] which makes it possible to identify the points where stimulation on the fundus occurs during the examination. There were two problems. One was that the quality of the infrared image of the fundus was poor. The other was that the reproducibility of the examination was not strong because it was very difficult to stably stimulate the same retina due to small eye movements. In order to resolve these problems, we have developed a new fundus perimeter.

Instruments

The new fundus perimeter is composed of an infrared fundus camera with a CCD camera, a pursuit device, and a target device with a color liquid crystal monitor, as

Address for correspondence: Yasuhiro Nishida, MD, Department of Ophthalmology, Shiga University of Medical Science, Seta, Tsukinowa, Otsu 520-21, Japan

Perimetry Update 1996/1997, pp. 75–79
Proceedings of the XIIth International Perimetric Society Meeting
Würzburg, Germany, June 4–8, 1996
edited by M. Wall and A. Heijl

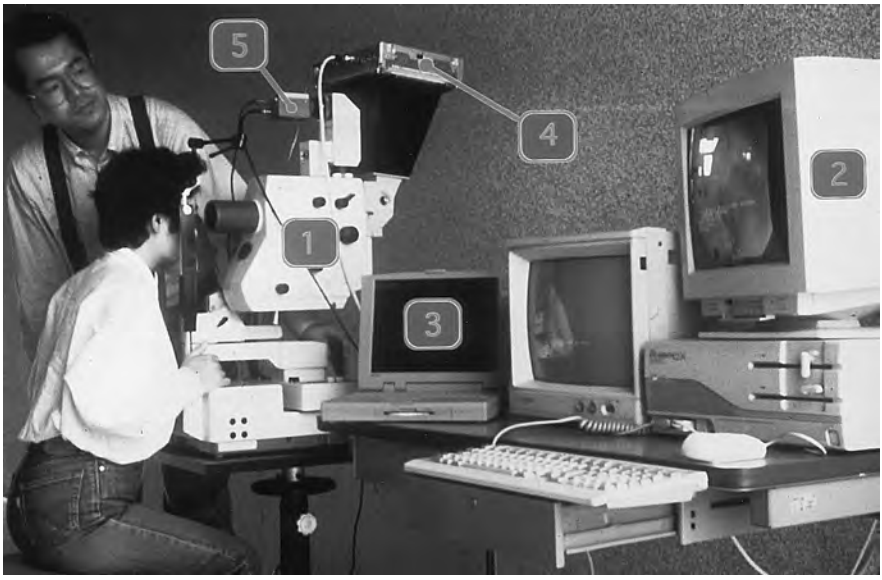

Fig. 1. The system for a new fundus perimetry. 1. Infrared fundus camera; 2. pursuit device; 3. target device; 4. CCD camera; 5. color liquid crystal monitor.

shown in Figure 1. The infrared fundus camera, TRC-501A, was manufactured by Topcon, Japan. Using a dichroic mirror in the camera allows us to divide the system so that we can observe the fundus while also displaying the stimulating target for the subject. The pursuit device is a computer system with a special program and a special picture board, manufactured by the Disco Company, Japan. The target device is a computer system with a special program developed using Visual Basic by Microsoft. The color liquid crystal monitor, an LMD-1040XC, was manufactured by Sony. The pixel number of this color monitor for the target display is 640 x 480 x 3, and 167 x 10^5 colors can be displayed.

Methods

The block diagram of this system is shown in Figure 2. The infrared image of the fundus is transmitted to the pursuit device through the CCD camera. At first, using the computer mouse in the pursuit device, the pursuit point in the fundus can be decided upon on a display, by enclosing it with a frame, as shown in Figure 3. The optic disc is adequate for the pursuit point in the fundus. The real time position of the pursuit point enclosed with the frame in the display is calculated by the pursuit device during the examination. The signals of this position are transmitted from the pursuit device to the target device through the RS-232C. The position where the stimulating target will be displayed on the color monitor can be changed by adjusting the position of the pursuit point. So the target can always stimulate the same retina by adjusting for eye movements, as shown in Figure 4.

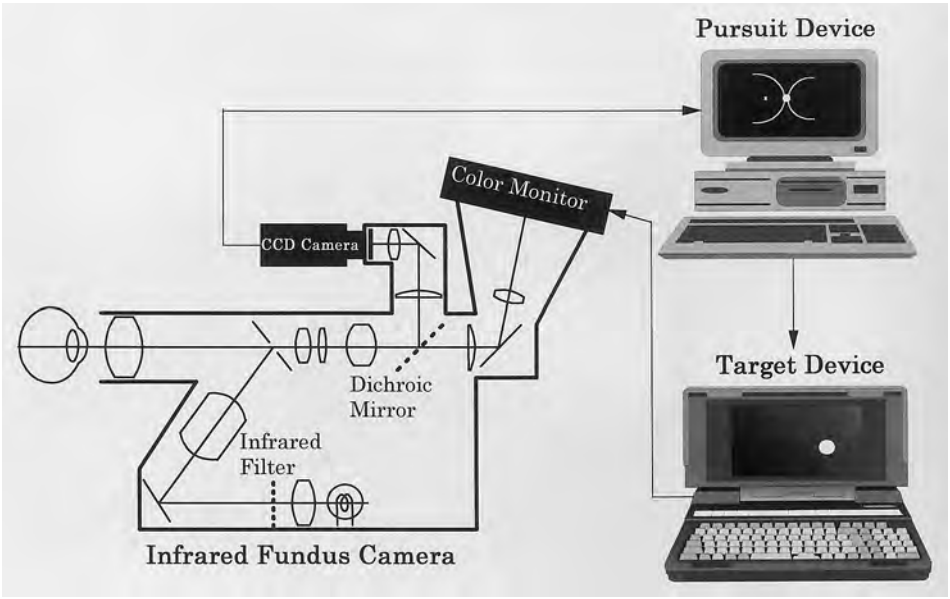

Fig. 2. Block diagram of the fundus perimeter.

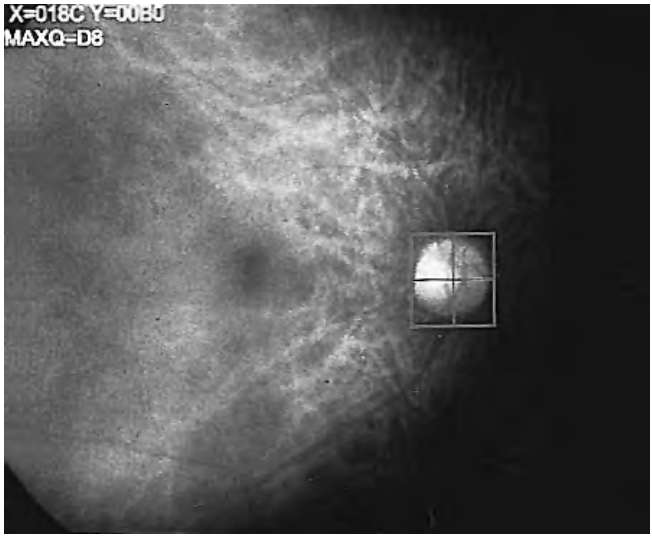

Fig. 3. The pursuit point. The pursuit point is decided by enclosing it with a frame using the pursuit device mouse. The optic disc is adequate for the pursuit point on the fundus.

Results and discussion

As shown in Figure 5, by employing the new infrared fundus camera, the quality of the fundus image is much improved. The stimulated retina can be observed in detail, and accurate pursuit is possible. The maximal picture angle of this camera is 50°, which is a little small for perimetry on the peripheral retina.

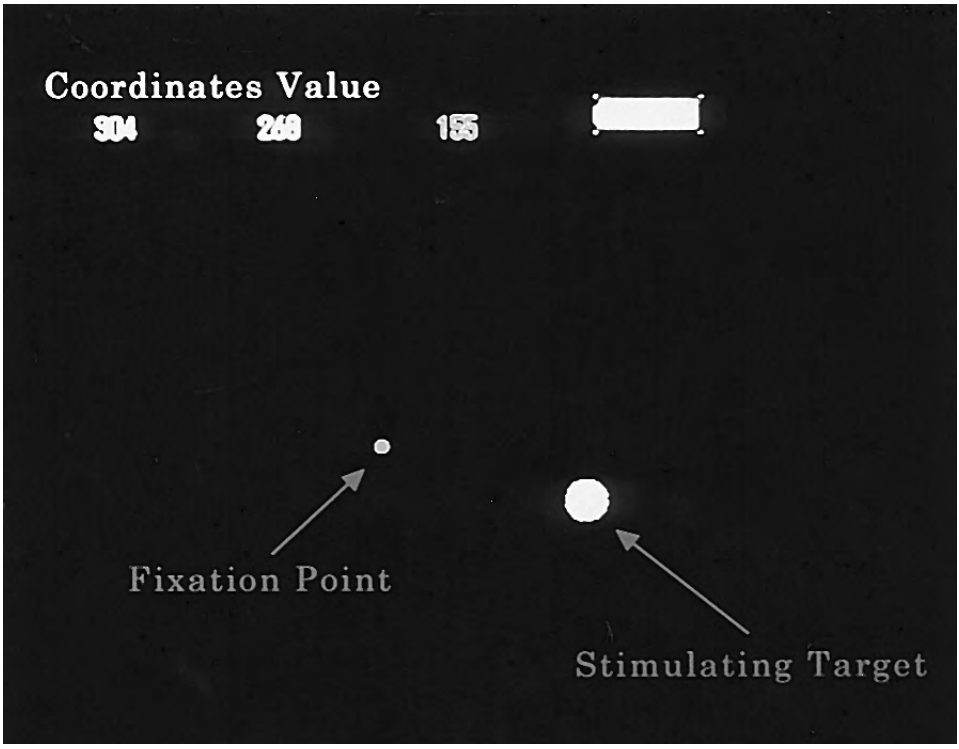

Fig. 4. The stimulating target on the color monitor. The position of the target can be changed on the monitor by adjusting the pursuit point position on the fundus.

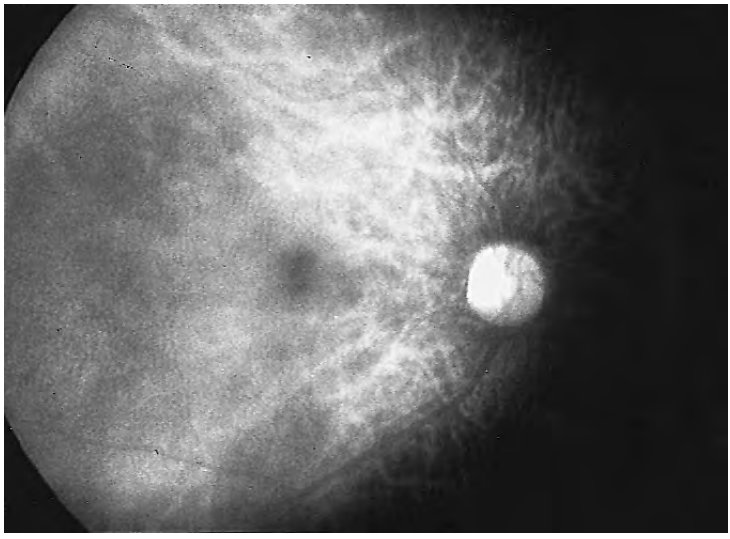

Fig. 5. The infrared fundus image. The quality of the image is much improved.

The sampling number of the pursuit device is about ten times per second. So the position of the pursuit point can be calculated even if there are frequent eye movements. Pursuit during small eye movements can also be carried out, because the minimal amount of the pursuit is one pixel of the CCD camera, which has a visual angle of about six minutes.

From our experiences with this experiment, using Visual Basic makes it possible for amateur programmers to develop programs for target sequence stimulation. Using a high resolution color monitor and the special program for the target stimulation, it is thought that various kinds of stimulation may be possible. Fortunately, various kinds of perimetry can be used.

Conclusions

This new fundus perimeter makes it possible to stably stimulate the same point on the fundus, even if there are eye movements. We think it will be possible to detect many small scotomata in the fundus and to investigate the relationship between fundus lesions and retinal sensitivity[1-4] using this perimetry. This new method of fundus perimetry has great potential.

References

1. Inatomi A: Fundus perimetry and overlap of the nasal and temporal visual field. Jpn Rev Clin Ophthalmol 71:528-532, 1977
2. Kani K, Eno N, Abe K, Ono T: Perimetry under television ophthalmoloscopy. Doc Ophthalmol Proc Ser 14:231-236, 1977
3. Kani K, Ogita Y: Fundus controlled perimetry. Doc Ophthalmol Proc Ser 19:341-350, 1979
4. Ogita Y, Sotani T, Kani K, Imachi J: Fundus controlled perimetry in optic neuropathy. Doc Ophthalmol Proc Ser 26:279-285, 1981

THE SCANNING LASER OPHTHALMOSCOPE AND ITS APPLICATIONS IN FUNDUS PERIMETRY
Our experiences

R. DE NATALE[1], G. PAOLO[2] and A. CRESTANI[2]

[1]University Eye Clinic of Verona; [2]Schio Eye Department, U.L.S.S. n. 4 Alto Vicentino (Vi); Italy

Abstract

Fundus perimetry, performed with the scanning laser ophthalmoscope (SLO), is a very sensitive technique for the study of localized retinal lesions. Six patients affected by age-related macular degeneration, macular hole and peripapillary atrophy, were examined. The authors used a staircase strategy to delineate the borders of the retinal lesion. Fundus perimetry, in these cases, is preferable to conventional bowl perimetry for documenting the functional conditions of the retina surrounding a lesion.

Introduction

Conventional bowl perimetry does not always permit exact topographical correspondence between the light stimulus and the corresponding retinal site. This aspect of traditional perimetry may represent a limit when we need to address a stimulus to specific restricted retinal zones. This problem is particularly noticeable with a localized retinal lesion, such as age-related macular degeneration, where it is important to know the functional conditions of the retina surrounding the lesion.

Precise topographical correspondence between light stimulus and retinal site may be reached by means of fundus perimetry.[1] The scanning laser ophthalmoscope allows a real-time perimetric examination to be performed while viewing the functional answer of the explored retinal point.[2,3]

The high sensitivity of this perimetric method needs to be supported by good reproducibility.[4,5] It helps to characterize the scotomata of different localized retinal lesions.

Material and methods

First, we investigated the reproducibility of this perimetric method. For this purpose, ten healthy subjects, six females and six males, with a mean age of 40 ± 5 years,

Address for correspondence: Renato De Natale, MD, University Eye Clinic of Verona, Pizzale Stefani, Verona, Italy

Perimetry Update 1996/1997, pp. 81–83
Proceedings of the XIIth International Perimetric Society Meeting
Würzburg, Germany, June 4–8, 1996
edited by M. Wall and A. Heijl

were studied. All subjects underwent fundus perimetry performed with the scanning laser ophthalmoscope (SLO).

Five test points along the 0-180 meridian were explored. The first test point was positioned around 200 μm above the fovea. The second and third points were at the nasal and temporal anatomical borders of the macula. The fourth test point was positioned 200 μm from the temporal border of the optic disc. The fifth test point was symmetrical to the fourth with respect to the fovea. A staircase strategy with stimulus size Goldmann No. III was used. A HeNe laser source was used to produce the light stimulus with a background luminance of 10 cd/m^2. The fundus was visualized with the help of an infrared beam.

Each subject underwent two examination sessions. The coefficient of variation (CV) was used to calculate the reproducibility of the method. Also, Student's *t* test was used to compare the results of the two sessions.

Six patients, two affected by age-related macular degeneration, two by a disciform stage, and two by macular hole degeneration, were studied. The patients had a mean age of 58 ± 7 years, and central visual acuity ranged from 0.1 to 0.7. All the patients underwent fundus perimetry with the SLO. A series of test points, along the inner and outer borders of the retinal lesion, was explored. The staircase threshold strategy with stimulus size No. III was used.

Results

Fundus perimetry, performed in a group of healthy subjects, did not show any statistically significant difference (Student's *t* test) between the first and second examination sessions. The CV showed good reproducibility of the method.

Differential light sensitivity, as measured by the SLO, presents different characteristics according to the retinal disease studied. An absolute scotoma from the retinal lesion, close to healthy retinal areas with elevated light sensitivity, was present in a case of age-related macular degeneration. The scotoma appeared deep and hollow, with a steep border.

In a case of peripapillary atrophy, the scotoma's characteristics were different. We found an absolute defect that progressively improved in retinal areas with higher sensitivity up to normal. Good correspondence between the extension and position of the scotoma and retinal depigmentation was observed.

Performing fundus perimetry in retinal lesions, such as those studied by us, is not time-consuming. It does not expose the patient to heavy stress, as when exploring the whole visual field, and it ensures good information on the functional status of the perilesional retina. It is, therefore, possible to delineate the exact borders of the scotomata, excluding the rest of the visual field.

Discussion

Fundus perimetry, performed with an SLO, still presents some problems. First, the machine was conceived as a viewing device, with the perimetric program being added later, and still having to be operated manually. Exploring few test points, as we did, does not take much time. However, it requires good facility with the machine and considerable technical support. The main difficulties met by the operator were

problems with always stimulating the same retinal point. The machine used for this study was aided by a digitalization system, which allowed the light stimulus to be addressed exactly to the same retinal point.

An arteriole venous crossing, the optic disc and the fovea, may be used as reference points by the examiner. The infrared visualization system allows the perimetric examination to be followed, with the retinal point stimulated being watched. This does not appear to be an important function. This perimetric method allows identification of very small retinal sites of new fixation points so that they can be avoided during laser photocoagulation.

We believe that implementing the actual perimetric program of this machine would broaden its use in the study of localized retinal lesions.

References

1. Trantas NG: Applications et résultats d'un moyen simple d'examen de la photosensibilité de la rétina. Bull Soc Ophthalmol Fr 55:499-513, 1955
2. Timberlake GT, Mainster MA, Webb RH, Hughes GW, Tremple CL: Retinal localization of scotomata by scanning laser ophthalmoscopy. Invest Ophthalmol Vis Sci 22:91, 1982
3. Hert O, Miller A, Buser A: Threshold perimetry under fundus control with the scanning laser ophthalmoscope. Ger J Ophthalmol 1:374,250, 1992
4. Orciuolo M, Varano M, Giuliano MA: Perimetria SLO. Min Oftalmol 36:277-283, 1994
5. Panta G, Randazzo DA, Ott JP, Nicoletti GA, Uva MG, Reibaldi A: Scanning laser ophthalmoscope e fundus perimetria. Min Oftalmol 36:285-289, 1994

PERIMETRIC TECHNIQUES

EVALUATION OF A NEW INTERACTIVE THRESHOLD STRATEGY IN NORMAL SUBJECTS

BOEL BENGTSSON[1], ANDERS HEIJL[1] and JONNY OLSSON[2]

[1]Department of Ophthalmology, Malmö University Hospital, Malmö; [2]Department of Mathematical Statistics, University of Lund, Lund; Sweden

Aim

We have developed a new strategy for threshold determination of visual fields.[1] A family of entirely new algorithms are incorporated in the new strategy. The goal was to achieve the same high test performance as the Full Threshold algorithm of the Humphrey perimeter, often referred to as a modern perimetric gold standard, but with a considerably reduced testing time.

The new interactive strategy includes some novel concepts:

a. Models of the visual field are constructed before the actual test starts. These models are based on *a priori* knowledge, such as age-corrected normal threshold values, frequency-of-seeing curves and interpoint correlations between threshold values.

b. All response results, positive as well as negative, are added to the models and used for calculation of threshold values and threshold error estimates. These are continuously calculated at all test point locations during the test, using maximum likelihood techniques. By predetermining acceptable magnitudes of errors in threshold estimates, staircase procedures can be interrupted before the required sequences of stimulus alterations are brought to an end. This results in limitations of stimulus exposures.

c. After the test, all threshold estimates are recalculated using information on the frequencies of false answers gathered during the test.

d. Frequencies of false positive and negative answers are estimated in new ways.[2,3]

Our goal was to achieve the same high test performance as the Full Threshold of the Humphrey perimeter, but with a considerably reduced testing time.

Methods

An evaluation was performed in normal subjects, and the results of the new interactive strategy were compared with the standard Full Threshold and FASTPAC strat-

Address for correspondence: Boel Bengtsson, Department of Ophthalmology, Malmö University Hospital, Malmö, Sweden

Perimetry Update 1996/1997, pp. 87–88
Proceedings of the XIIth International Perimetric Society Meeting
Würzburg, Germany, June 4–8, 1996
edited by M. Wall and A. Heijl

egies, using the 30-2 test point pattern. The same perimeter was used for all visual field tests. Twenty eyes of 20 healthy volunteers were tested twice with each of the three strategies on three separate occasions. The order of the test strategies was randomized and masked. All subjects had experience with Humphrey perimeter threshold tests.

The test results were analyzed as test-retest variances and average testing times of the two tests for each subject. Differences between strategies were compared, using analysis of variance.

Results

The new interactive strategy had on average significantly lower ($p = 0.0014$) test-retest variance than FASTPAC, 1.59 dB^2 compared to 2.61 dB^2, and slightly lower than Full Threshold ($p = 0.1136$ with 2.12 dB^2. The interactive algorithm used significantly less testing time ($p < 0.001$) compared to both Full Threshold and Fastpac. The average testing time was reduced by 50% compared to Full Threshold and by approximately 15% compared to Fastpac.

Discussion

The current evaluation thus showed that, in the tested population, the new strategy met our goals. It was as accurate or better than the Full Threshold algorithm, and considerably better than FASTPAC. Maintaining high accuracy is important for the calculation of normal limits and, consequently, for the sensitivity of the test. The new tests were obtained with a substantial reduction of testing time, particularly compared to the Full Threshold algorithm.

If it is possible to accept larger measurement errors, as with FASTPAC, the testing time may be reduced even further. These new principles, applied in the interactive strategies, can be used in any type of threshold strategy, regardless of stimulus color, size or step sizes used in staircases of stimulus intensities or other modifications.

References

1. Olsson J, Bengtsson B, Heijl A, Rootzén H: New thresholding algorithms for automated perimetry. In: Mills RP, Wall M (eds) Perimetry Update 1994/1995, p 365. Amsterdam/New York: Kugler Publ 1995
2. Olsson J, Rootzén H, Heijl A: Maximum likelihood estimation of the frequency of false positive and false negative answers from the up-and-down staircases of computerized threshold perimetry. In: Heijl A (ed) Perimetry Update 1988/1989, pp 245-251. Amsterdam/Milano: Kugler & Ghedini Publ 1989
3. Olsson J, Bengtsson B, Heijl A, Rootzén H: Improving estimation of false-positive and false-negative responses in computerized perimetry. In: Mills RP, Wall M (eds) Perimetry Update 1994/1995, p. 219. Amsterdam/New York: Kugler Publ 1995

A NEW STRATEGY FOR AUTOMATED PERIMETRY
First clinical results

MARKUS M. SCHAUMBERGER, ELISABETH GLASS, GREGOR-K. ELBEL and BERNHARD J. LACHENMAYR

Section of Psychophysics and Physiological Optics, University Eye Hospital, Munich, Germany

Abstract

'ZAPP', a new strategy for automated perimetry is presented, in which threshold determination is based on a 'mean likelihood' algorithm. Using a video screen campimeter, this new method is compared to a standard 4/2 dB full threshold strategy. A study of 40 subjects (20 normal subjects, 20 patients) showed a statistically significant reduction of 7.8% in the necessary number of presentations with this new strategy (normal subjects: 7.7%, patients: 8.0%). A mean difference in mean sensitivity ($MS_{4/2} - MS_{ZAPP}$) of -0.96 ± 0.97 dB was found (normal subjects: -1.13 dB, patients: -0.78 dB). Linear regression analyses gave good to excellent linear correlation between MS values (r^2 value: 0.65 to 0.95). Variability in repeated measurements was found to be identical. These results show that the new strategy ZAPP requires significantly fewer stimulus presentations than the commonly used 4/2 dB double-bracketing strategy to obtain comparable threshold values of equal inter-test variability.

Introduction

One of the limiting factors in the clinical use of automated visual field tests is the duration of these tests in combination with the subject's fatigue:[1,2] fluctuations in the measured differential light sensitivity thresholds increase with increasing examination time.[3,4] This results in deteriorated diagnostic quality of visual field results. Therefore, in order to reduce examination time, several fast strategies for automated light-sense perimetry have been presented.[5-8]

We are in the process of developing a new strategy named 'ZAPP'. The aim of the present study was to test the prototype of this new strategy in a small clinical study and to compare these results with the commonly used 4/2 dB double-bracketing strategy.

Address for correspondence: Dipl.-Phys. Markus Schaumberger, Section of Psychophysics and Physiological Optics, University Eye Hospital, Mathildenstrasse 8, D-80336 Munich, Germany

Perimetry Update 1996/1997, pp. 89–96
Proceedings of the XIIth International Perimetric Society Meeting
Würzburg, Germany, June 4–8, 1996
edited by M. Wall and A. Heijl

Methods

Scheme of the new strategy ZAPP

Visual field examination is divided into two parts. First, sensitivity thresholds at 12 selected locations of the visual field are determined. These threshold values serve as a basis to estimate an individual 'hill of vision' for the subject being tested. This is achieved by means of two-dimensional polynomials fitted to the 12 determined thresholds, using the algorithm presented by Humpert and Witte.[9]

From this two-dimensional surface, threshold estimates for the entire visual field can be computed. These estimates are used as optimum individual starting values for the threshold determination at the remaining test grid locations in the second phase of the test. Subjects do not experience any interruption. Within each phase, the location of the next presentation is completely random.

The threshold algorithm used in both phases was derived from QUEST[10] and one of its variants, ZEST.[11] To determine the next stimulus intensity to be presented at each test grid point, the mean of the current probability density function (pdf) specific for this point is used. Each pdf is calculated based on an *a priori* pdf, using logistic functions[12] to represent the 'frequency-of-seeing' curve of the subject. Both *a priori* pdf and logistic function have parameters specific for visual field location and age. The *a priori* pdf represents the distribution of thresholds in normal visual fields. All these normal data have been evaluated from an earlier normal value study using the 'method of constant stimuli'.[13]

Determination of a single threshold is terminated when a given level of 'accuracy' is reached, as described by the standard deviation of the posterior pdf. The final threshold value is then calculated as the mean of the posterior pdf, after correction according to the *a priori* pdf to exclude any influence of the *a priori* pdf. Further details of the new strategy and the threshold algorithm can be found elsewhere.[14]

4/2 dB double-bracketing strategy

The 4/2 dB double-bracketing strategy used here largely corresponds to the algorithm incorporated in the Humphrey Field Analyzer (HFA)[15] but with one major exception: the 'next neighbor' method to determine starting values for yet to be tested grid points has not been included. Not to put this strategy at a disadvantage, visual field tests are divided into two parts as described for ZAPP. Here, the same four visual field locations used by the HFA to determine the height of the individual 'hill of vision' are tested in the first phase. Individual threshold estimates are then calculated as described above.

Perimetric system

All visual field tests were performed on a video screen campimeter, based on a computer graphic system using a high-resolution 21" monitor for stimulus presentation, which was calibrated with regard to a standard background luminance of 10 cd/m^2, so that a stimulus range of 23 dB was feasible (dB defined according to the standard definition in light-sense perimetry[16]). Further details of the video screen campimeter will be published elsewhere.[17]

Subjects

Twenty normal subjects with a mean age of 38.0 ± 10.1 years (25-56 years; median 36 years) and 20 patients from our clinic with a mean age of 54.0 ± 16.3 years (23-81 years; median 55 years) were included in the study. Normal subjects had to fulfil the following inclusion criteria:
– corrected visual acuity of ≥ 0.8
– intraocular pressure of ≤ 21 mmHg
– no media opacities or abnormalities of the fundus
– no history of severe ocular trauma or ocular surgery
– no family history of glaucoma or any inheritable ocular disease
– no history of poorly controlled hypertension, diabetes mellitus, multiple sclerosis, cerebrovascular attacks or epilepsy

If both eyes fulfilled the inclusion criteria, one was selected randomly. Normal subjects also had to have fixation losses (determined using the Heijl-Krakau method[18]) and false positive/negative errors of ≤ 33% in the visual field tests performed in this study. Five of the normal subjects had no previous experience with automated perimetry.

In the patient group, the tested eye was selected according to the following characteristics:
– corrected visual acuity of ≥ 0.4
– visual field defects established during an earlier visual field test with an automated perimeter

If both eyes fulfilled the criteria, the eye showing more distinct visual field defects in earlier tests was selected. There were no restrictions regarding the type of ocular pathology or patients' errors (false positive/negative errors, fixation losses).

All subjects had to have a refractive error of ≤ ±5 DS and ≤ 2 DC, a pupil diameter of ≥ 2 mm, and should not have ingested any psychiatric drugs in the 24 hours prior to field testing. Informed consent was obtained from each subject before recruiting them for the study.

Test procedure

Each subject had to undergo two consecutive visual field tests in random order within one session: one with the 4/2 dB double-bracketing strategy, the other with ZAPP. A 6° rectangular grid consisting of 76 points of up to 30° eccentricity, similar to Program 30-2 of the HFA,[15] plus foveal testing was used (stimulus size Goldmann III). Twelve of the normal subjects had two additional sessions within a maximum time interval of three weeks after the first session.

Each session began with a short demonstration so the subject could familiarize himself with the test set-up. Between the two tests, a minimum break of five minutes was given. Visual field testing could be interrupted upon the subject's request. A complete session lasted for about 45 minutes.

Data analysis

Mean sensitivity (MS) was calculated as the unweighted mean of the sensitivity values at 74 test locations (excluding two test points next to the blind spot, similar to STATPAC[19]) plus fovea. The number of presentations only included stimuli pre-

Table 1. Mean ± standard deviation of mean sensitivity (MS) and the number of presentations for both strategies in the entire sample and each subgroup (*p* values of Wilcoxon matched-pair signed-rank tests)

	4/2 dB strategy	*ZAPP*	*p value*
Entire sample			
MS (dB)	13.97 ± 4.11	14.93 ± 4.33	<0.001
presentations	347.82 ± 35.02	320.58 ± 37.94	<0.001
Normal subjects			
MS (dB)	16.95 ± 1.40	18.08 ± 1.77	0.001
presentations	322.50 ± 15.04	297.70 ± 26.73	0.002
Patients			
MS (dB)	11.00 ± 3.75	11.78 ± 3.80	0.002
presentations	373.15 ± 30.66	343.45 ± 33.73	0.026

sented to determine thresholds. Visual field results of repeated testing were analyzed as follows: for each subject at each grid point, the standard deviation of threshold values multiple measured by each strategy was calculated. The mean standard deviation for each subject and each strategy was calculated as described for MS. Subsequent Δ values were calculated as $\Delta x = x_{4/2} - x_{ZAPP}$. Due to the fact that most of the variables were not normally distributed, non-parametric tests were applied. Statistical analysis was performed using programs SPSS/PC+ 5.0.1 and SPSS for Windows 6.1.[20]

Results

The mean ± standard deviation of MS and the number of presentations in the entire population and both subgroups – normal subjects and patients – are shown in Table 1 for both strategies, as are the significance values of Wilcoxon matched-pair signed-rank tests. Boxplots of the results are presented in Figures 1 and 2.

Highly significant differences in MS between the 4/2 dB double-bracketing strategy and ZAPP were found in the entire sample (ΔMS = -0.96 ± 0.97 dB, $p<0.001$) as well as in normal subjects (ΔMS = -1.13 ± 1.05 dB, $p<0.001$) and patients (ΔMS = -0.78 ± 0.88 dB, $p=0.002$). The number of presentations required to determine a single visual field was reduced by close to 8% with ZAPP compared to the 4/2 dB strategy. A higher reduction was found in the patient group, although this difference between subject groups was not statistically significant (all subjects: 7.8%, $p<0.001$; normal subjects: 7.7%, $p=0.002$; patients: 8.0%, $p=0.026$). No significant age effect was found for any difference between the strategies in the entire population or in both subgroups.

Correlation of mean sensitivity between the strategies

Linear regression analyses were performed to test the comparability of mean sensitivity values, as determined by the strategies. Table 2 lists the relevant data and Figure 3 illustrates the results. Good to excellent linear correlation was found for the entire sample, as well as for normal subjects or patients only. Slopes equalled 1.0 within one standard error in all analyses.

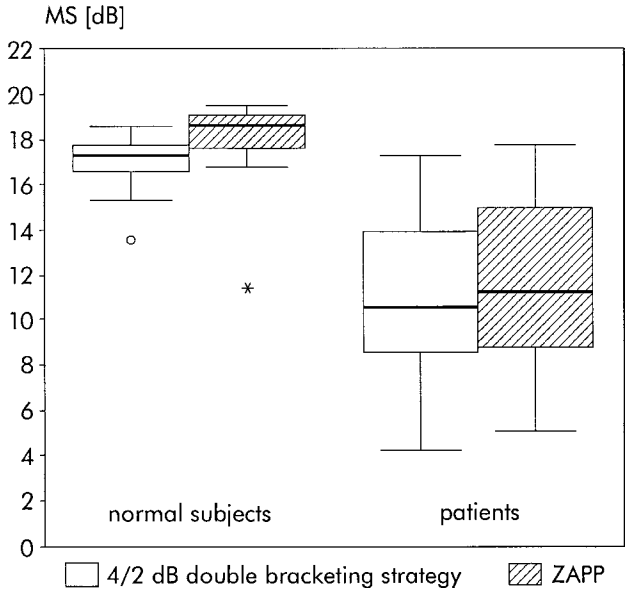

Fig. 1. Boxplots of mean sensitivity (MS) of normal subjects and patients determined by the 4/2 dB double-bracketing strategy and by ZAPP.

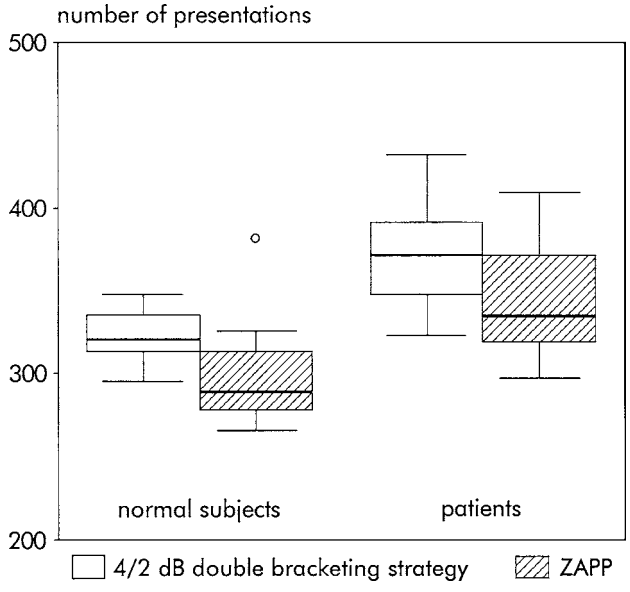

Fig. 2. Boxplots of the number of presentations of a single visual field test of normal subjects and patients required by the 4/2 dB double-bracketing strategy and by ZAPP.

Table 2. Linear regression analyses of mean sensitivity for both strategies in the entire sample and in each subgroup (MS_{ZAPP} was the dependent, $MS_{4/2}$ the independent variable)

	r^2 *value*	*slope ± SE*	*p value*
Entire sample	0.95	1.03 ± 0.04	<0.001
Normal subjects	0.65	1.02 ± 0.18	<0.001
Patients	0.95	0.98 ± 0.06	<0.001

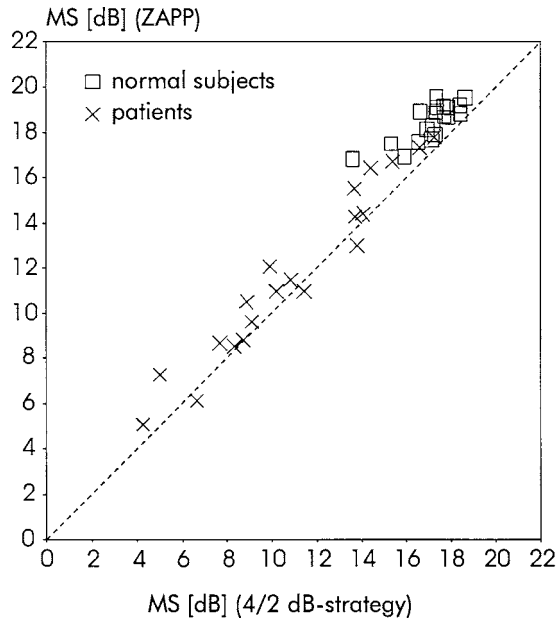

Fig. 3. Mean sensitivity (MS) of normal subjects and patients, as determined by the 4/2 dB double-bracketing strategy in comparison to values determined by ZAPP (dashed line indicates line of identity).

Inter-test variability

Figure 4 shows boxplots of the mean standard deviations of triple measured thresholds of 12 normals subjects for both strategies, as described in the 'Method' section above. Obviously, there is no difference between the strategies (Δmean SD = 0.01 ± 0.20 dB, Wilcoxon matched-pair signed-rank test: p=0.875).

Discussion

Our results show that the new strategy ZAPP requires significantly fewer stimulus presentations (close to 8% less) compared to the commonly-used 4/2 dB double-bracketing strategy. The mean sensitivity values determined with ZAPP are about 1 dB higher than those for the 4/2 dB strategy. This can be explained by a characteristic of the double-bracketing strategy used in this comparison (and, for example,

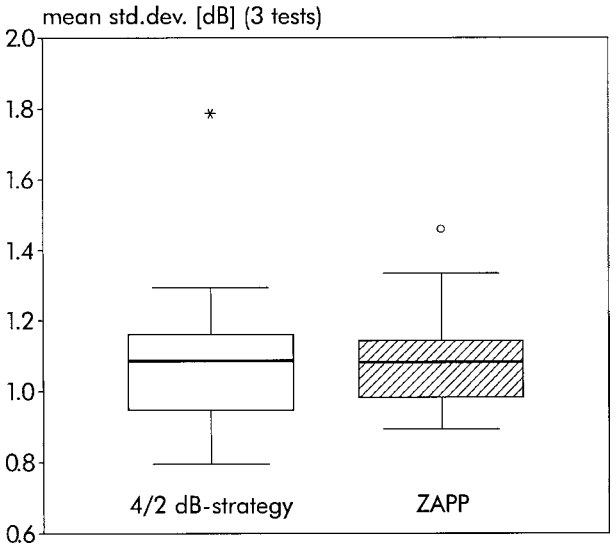

Fig. 4. Boxplots of mean standard deviations of the thresholds of 12 normal subjects measured three times within a maximum time interval of three weeks with the 4/2 dB double-bracketing strategy and with ZAPP.

in the HFA[15]): the threshold is defined as the last seen stimulus value. Taking into account the final step size of 2 dB, in contrast to the minimum step size of 1 dB for ZAPP, this explains the deviation found. In conjunction with good to excellent linear correlation of the MS values of both strategies with slopes close to 1, this indicates that sensitivity values determined by ZAPP are in good agreement with standard strategy values. These statements are valid both for normal subjects and for patients showing various visual field defects. Inter-test variability of thresholds determined in separate sessions as described by mean standard deviations is equivalent for both strategies.

Further clinical tests with ZAPP still have to be carried out in order to compare its performance with the results of other new strategies, such as FASTPAC[21-23] and the DSE strategy,[24-26] with regard to short-term fluctuations and efficiency.

Acknowledgments

This study was supported by the German Research Foundation (Grant No. La 517/6-1, 6-2, 6-3). The authors thank Mrs Hedi Degmair, MTA, for the clinical organization of the study, performing most of the visual field tests, and permanently motivating patients to participate in this study.

References

1. Johnson CA, Adams CW, Lewis RA: Fatigue effects in automated perimetry. Appl Optics 27:1030-1037, 1988
2. Hudson C, Wild JM, O'Neill EC: Fatigue effects during a single session of automated static threshold perimetry. Invest Ophthalmol Vis Sci 35:268-280, 1994

3. Heijl A: Time changes of contrast thresholds during automatic perimetry. Acta Ophthalmol (Kbh) 55:696-708, 1977
4. Searle AET, Wild JM, Shaw DE, O'Neill EC: Time-related variation in normal automated static perimetry. Ophthalmology 98:701-707, 1991
5. Johnson CA, Shapiro LR: A rapid heuristic test procedure for automated perimetry. In: Mills RP, Heijl A (eds) Perimetry Update 1990/1991, pp 251-256. Amsterdam/Milano: Kugler & Ghedini Publ 1991
6. Moss ID, Hudson C, Dengler-Harles M, Wild JM, Whitaker DJ, O'Neill EC: A 3 dB step single crossing algorithm for threshold automated perimetry [Abstract]. Invest Ophthalmol Vis Sci 33(Suppl):969, 1992
7. Olsson J, Bengtsson B, Heijl A, Rootzén H: New thresholding algorithms for automated static perimetry. In: Mills RP, Wall M (eds) Perimetry Update 1994/1995, p 265. Amsterdam/New York: Kugler Publ 1995
8. Weber J: Eine neue Strategie für die automatisierte statische Perimetrie [in German]. Fortschr Ophthalmol 87:37-40, 1990
9. Humpert A, Witte FO: Gestützte Flächen: Optimalanpassung einer Polynomfläche an ein Wertefeld [in German], mc pp 108-114. Munich: Franzis-Verlag GmbH, 1989
10. Watson AB, Pelli DG: QUEST: a bayesian adaptive psychometric method. Percept Psychophys 33:113-120, 1983
11. King-Smith PE, Grigsby SS, Vingrys AJ, Benes SC, Supowit AJ: Efficient and unbiased modifications of the QUEST threshold method: theory, simulations, experimental evaluation and practical implementation. Vision Res 34:885-912, 1994
12. Harvey LO: Efficient estimation of sensory thresholds. Behav Res Meth Instrum Comput 18:623-632, 1986
13. Elbel GK, Schaumberger MM, Lachenmayr BJ: Psychometric functions in light sense perimetry. Influence of eccentricity and mathematical modelling in normal subjects [Abstract]. German J Ophthalmol 3:301, 1994
14. Schaumberger M: Entwicklung einer neuen Strategie für die automatisierte Perimetrie. Doctoral thesis, Faculty of Medicine, Ludwig-Maximilians-Universität, Munich, Germany 1997 (in preparation)
15. Haley MJ: Field Analyzer Fibel [in German]. Karlsruhe: Allergan Humphrey GmbH 1987
16. Lachenmayr BJ, Vivell PMO: Perimetry and its clinical correlations, p 12. Stuttgart/New York: Georg Thieme Verlag 1993
17. Elbel GK, Schaumberger MM, Lachenmayr BJ: Psychometric functions and frequency-of-seeing curves for light-sense perimetry. German J Ophthalmol (submitted for publication)
18. Heijl A, Krakau CET: An automatic static perimeter, design and pilot study. Acta Ophthalmol (Kbh) 53:293-310, 1975
19. Heijl A, Lindgren G, Olsson J: A package for the statistical analysis of visual fields. In: Greve EL, Heijl A (eds) Seventh International Visual Field Symposium, Amsterdam, September 1986, pp 153-168. Dordrecht/Boston/Lancaster: Martinus Nijhoff/Dr W Junk Publ 1987
20. Norusis MJ, SPSS Inc: SPSS for Windows: Base System User's Guide, Release 6.0 + SPSS 6.1 for Windows Update. Chicago: SPSS Inc 1993 and 1994
21. Flanagan JG, Moss ID, Wild JM, Hudson C, Prokopich L, Whitaker D, O'Neill EC: Evaluation of FASTPAC: a new strategy for threshold estimation with the Humphrey Field Analyzer. Graefe's Arch Clin Exp Ophthalmol 231:465-469, 1993
22. O'Brien C, Poinoosawmy D, Wu J, Hitchings R: Evaluation of the Humphrey FASTPAC threshold program in glaucoma. Br J Ophthalmol 78:516-519, 1994
23. Schaumberger M, Schäfer B, Lachenmayr BJ: Glaucomatous visual fields. FASTPAC versus full threshold strategy of the Humphrey Field Analyzer. Invest Ophthalmol Vis Sci 36:1390-1397, 1995
24. Vivell PMO, Lachenmayr BJ, Zimmermann P: Vergleichsstudie verschiedener perimetrischer Strategien [in German]. Fortschr Ophthalmol 88:819-823, 1991
25. Weber J, Klimaschka T: Test time and efficiency of the dynamic strategy in glaucoma perimetry. German J Ophthalmol 4:25-31, 1995
26. Zulauf M, Fehlmann P, Flammer J: Perimetrie mit der normalen Octopus-Strategie und der 'dynamischen' Strategie nach Weber – Erste Ergebnisse bezüglich Reproduzierbarkeit der Messungen bei Glaukompatienten. Ophthalmologe 93:420-427, 1996

TWO DIFFERENT TECHNIQUES FOR OBTAINING ANSWERS IN AUTOMATED PERIMETRY

S. LUTZ[1], T.J. DIETRICH[1], N. BENDA[2], B. SELIG[1], U. SCHIEFER[1] and I. DAUM[3]

[1]University Eye Hospital, Department II; [2]Department of Medical Biometry; [3]Department of Medical Psychology; Tübingen, Germany

Abstract

Subjects and methods: So far, all computer perimeters use the same technique for obtaining the patient's answers: seeing the stimulus, the patient presses a button; if there is no response within a specific time period, the stimulus will be counted as not perceived (yes-time-out method). In this study, an alternative method was used: subjects answer by pressing one of two different buttons after each stimulus is presented (forced yes-no method). The different light sensitivity (DLS) for bright stimuli (32 min of arc) was evaluated at 26 test locations within the central 30<o> of the visual field using a computer monitor and a modified 4/2-staircase strategy. Threshold estimation was performed using the maximum-likelihood method.

Results: Sixty-one healthy subjects (aged 20-30 years) were examined on two days using both methods. The DLS thresholds with the forced yes-no method were on average 0.11 dB above those measured within the yes-time-out method; this was a statistically significant, but not clinically relevant, difference. There was no significant difference in the reproducibility. The forced yes-no method resulted in a higher number of incorrect answers in the catch trials ($p<0.05$, Wilcoxon signed rank test for the differences).

Conclusions: Compared to the conventional yes-time-out method, the forced yes-no method showed no differences of any relevance either for threshold level or for reproducibility. With regard to the responses to the catch trials, as an index for correct answering, the forced yes-no method yielded worse results than the traditional one.

Acknowledgment

Supported by the Tübingen Fortüne Program (Nos. 97 and 167).

Address for correspondence: S. Lutz, MD, University Eye Hospital, Department II, Schleichstrasse 12-16, D-72076 Tübingen, Germany

Perimetry Update 1996/1997, p. 97
Proceedings of the XIIth International Perimetric Society Meeting
Würzburg, Germany, June 4–8, 1996
edited by M. Wall and A. Heijl

DISCRETE STRATEGIES IN PERIMETRY

J. PÄTZOLD[1], N. BENDA[1], U. SCHIEFER[2] and T.J. DIETRICH[2]

[1]Department of Medical Biometry; [2]University Eye Hospital, Department II; Tübingen, Germany

Abstract

A common but frequently neglected problem in perimetry results from a discrete set of possible stimulus intensities as a result of physical circumstances. In electronic campimetry, such discrete steps depend on the restricted number of shades of gray which can be presented by the graphic board. In the region of interest – close to the threshold – often only a few intensities are available. Therefore, the values demanded by the strategy have to be replaced by luminances that can really be presented.

This problem raises the question of whether such modifications impair the quality of threshold estimation. To answer this question, computer simulations employing a logistic regression model for the binary response were conducted to determine the mean squared error of threshold estimation for a 4-2-1 strategy (used by the Tübingen Computer Campimeter, TCC), assuming both an ideal situation with infinite resolution and a real situation with several given resolutions.

The simulation results indicated that there was no relevant worsening of the estimation, even comparing a simple 24-bit graphic board (256 shades of gray) with an ideal screen (continuous grayscale). This result was due to the fact that such a strategy was not a uniformly optimal procedure. An optimized strategy should be affected by the resolution of the graphic board. To demonstrate this, we also calculated the *a posteriori* mean squared error of threshold estimation using a Bayes strategy and taking into account prior information. In this case, a higher resolution uniformly improved the threshold estimate.

Acknowledgment

Supported by the Tübingen Fortüne Program (Nos. 97 and 167).

Address for correspondence: J. Pätzold, Department of Medical Biometry, Westbahnhofstrasse 55, D-72070 Tübingen, Germany

Perimetry Update 1996/1997, p. 99
Proceedings of the XIIth International Perimetric Society Meeting
Würzburg, Germany, June 4–8, 1996
edited by M. Wall and A. Heijl

OPTIMIZING DISTRIBUTION AND NUMBER OF TEST LOCATIONS IN PERIMETRY

KEIKO SUGIMOTO, ANDREAS SCHÖTZAU, OLIVER BERGAMIN and MARIO ZULAUF

University Eye Clinic, Basel, Switzerland

Abstract

Purpose: Are short programs useful for glaucoma screening? The authors investigated Program G1x with Octopus 1-2-3, which allows the examination of various numbers of test locations, *i.e.*, 16, 32, 45, or all 59 test locations.
Material and methods: Using 99 visual fields of glaucomatous or glaucoma-suspect right eyes, the authors compared the mean defect (MD) and loss of variance (LV) of the global visual field with (a) the MD and LV of the stages of the G1x Program; and (b) the MD and LV of newly created stages, on the basis of seven publications.
Results: The results showed that Stage 1 of Program G1x underestimated the visual field damage present in the entire field. These newly created stages revealed higher correlation with MD and LV of the entire visual field and also detected more defects.
Conclusions: The use of the first stage only (16 test locations) of G1x is not advisable. At least 32 test locations, *i.e.*, stages 1 and 2, are recommended. A prospective study is required to evaluate the validity of the newly created stages.

Introduction

The examination time to test both eyes with the standard program, G1x, is between 30 and 50 minutes. A shorter examination time would increase patient acceptance; difficulties regarding concentration and fatigue[1-6] might then diminish. There are two techniques for saving time: optimizing the examination strategy or modifying the number of test locations and their spatial distribution. The latter was chosen for this study. A retrospective study by Zeyen *et al.*[7] showed that 12 optimally chosen test locations produce a sensitivity and specificity of 80%. Introducing up to 26 test locations in the discriminate analysis only increased sensitivity and specificity to 89%! Similar retrospective studies based on a small, highly selected number of test locations showed astonishingly good results.[7-13] These studies have in common that they include only test locations with optimal diagnostic power. Nevertheless, it seems logical that longer examinations should lead to more precise and reproducible results. Yet, several studies contradict this assumption, *e.g.*, studies describing the effects of

Address for correspondence: Dr. med. Mario Zulauf, Universitäts-Augenklinik Basel, Mittlere Strasse 91, Postfach, CH-4012 Basel, Switzerland

Perimetry Update 1996/1997, pp. 101–105
Proceedings of the XIIth International Perimetric Society Meeting
Würzburg, Germany, June 4–8, 1996
edited by M. Wall and A. Heijl

fatigue.[3] Although not all studies noted a fatigue effect,[5] Heijl and Drance[2] reported greater fatigue effects in glaucoma patients than in normals. Diagnostically, this could be important and does again favor short programs.

Retrospective studies on Octopus[7] and Zeiss-Humphrey perimeters[13,14] show the high diagnostic value of test locations between 20 and 30° of eccentricity. In this respect, the distribution of test locations in Program G1x is not well chosen, as it examines the test locations with the greatest diagnostic value during the last stage.[7] Additionally, the sensitivity of many test locations within one stage correlate are very similar to each other.

Methods

This study reports on 99 visual fields of a practising ophthalmologist, meeting the following inclusion criteria: a minimum of two G1x visual fields/eye; diagnosis: glaucoma or glaucoma-suspect.

The G1x Program examines 59 test locations in four stages within 26°.[15] Each stage consists of 16, 16, 13, and 14 test locations. The Octopus standard strategy was chosen. The coordinates of the test locations are presented in Table 1. Four new alternative stages were created on the basis of seven studies.[7,16-21] All seven studies investigated the test locations most affected by glaucoma. Four test locations were removed, and four new test locations added, taking into account the results of these seven studies. The following test locations were chosen (Stage 1 new): 3, 8, 9, 10, 15, 18, 19, 21, 35, 40, 41, 42, 49, 50, 51 and 56.

Results

As summarized in Tables 2 and 3, Stage 1 of G1x (the first 16 test locations) underestimates the damage present in the entire visual field. Tables 4 and 5 reveal that the newly created stages included similar defective areas.

Discussion

The present results discourage stopping the test after one stage, *i.e.*, 16 test locations, as the tendency is to underestimate the defects which are present only in later stages of Program G1x. This might be partially due to the effects of fatigue. However, current normal values do not take this into account. A number of studies reported on astonishingly high sensitivities and specificities with only a few test locations.[7-13] However, these studies all select the best test locations retrospectively. Therefore, the practical value of these studies is limited.

To the best of our knowledge, this is the first study to investigate how programs with few test locations really perform in a clinical setting. The *a priori* selected new stages performed better than the current stages. The better selection of test locations (based on the analysis of seven studies[7,16-21]) may have led to the favorable performance of the new stages. However, prospective studies are needed to test their sensitivities and specificity in a real clinical setting.

Table 1. Coordinates of the 59 test locations of Program G1x

Test locations	*Coordinates*	*Test locations*	*Coordinates*
1	(- 8/+26)	31	(- 2/- 2)
2	(+ 8/+26)	32	(+ 2/- 2)
3	(-20/+20)	33	(+ 8/- 2)
4	(-12/+20)	34	(-26/- 4)
5	(- 4/+20)	35	(-20/- 4)
6	(+ 4/+20)	36	(-14/- 4)
7	(+12/+20)	37	(-.4/- 4)
8	(+20/+20)	38	(+ 4/- 4)
9	(- 4/+14)	39	(+22/- 4)
10	(+ 4/+ 4)	40	(- 8/- 8)
11	(-20/+12)	41	(+ 8/- 8)
12	(-12/+12)	42	(+26/- 8)
13	(+12/+12)	43	(- 3/- 8)
14	(+20/+12)	44	(+ 3/- 8)
15	(- 8/+ 8)	45	(-20/-12)
16	(- 2/+ 8)	46	(-12/-12)
17	(+ 2/+ 8)	47	(+12/-12)
18	(+ 8/+ 8)	48	(+20/-12)
19	(+26/+ 8)	49	(- 4/-14)
20	(-26/+ 4)	50	(+ 4/-14)
21	(-20/+ 4)	51	(-20/-20)
22	(-12/+ 4)	52	(-12/-20)
23	(- 4/+ 4)	53	(- 4/-20)
24	(+ 4/+ 4)	54	(+ 4/-20)
25	(+22/+ 4)	55	(+12/-20)
26	(- 8/+ 2)	56	(+20/-20)
27	(- 2/+ 2)	57	(- 8/-26)
28	(+ 2/+ 2)	58	(+ 8/-26)
29	(+ 8/+ 2)	59	(0/ 0)
30	(- 8/- 2)		

Table 2. Mean defect (MD, dB) of 99 right eyes, with mean MD of the four G1x stages and of the entire G1x Program

	Mean (dB)
Stage 1	-0.17
Stage 2	0.34
Stage 3	0.47
Stage 4	1.04
Entire G1x	0.40

Table 3. Loss of variance (LV, dB^2) of 99 right eyes, mean LV of the four G1x stages and of the entire G1x Program

	Mean (dB^2)
Stage 1	9.44
Stage 2	14.29
Stage 3	11.03
Stage 4	15.19
Entire G1x	13.01

Table 4. Mean defect (MD, dB) of 99 right eyes, of the newly created stages, MD of the first two stages and of the entire G1x Program

	Mean (dB)
Stage 1 new	0.42
Stages 1+2 new	0.29
Stage 1 G1x	-0.17
Stages 1+2 G1x	0.08
Entire G1x	0.40

Table 5. Loss of variance (LV, dB^2) of 99 right eyes, of the newly created stages, LV of the first two stages and of the entire G1x Program

	Mean (dB^2)
Stage 1 new	15.75
Stages 1+2 new	14.09
Stage 1 G1x	9.44
Stages 1+2 G1x	12.02
Entire G1x	13.01

Acknowledgments

Supported by the Swiss National Fund Grant No. 3200-43624.95

References

1. Heijl A: Time changes of contrast thresholds during automatic perimetry. Acta Ophthalmol (Kbh) 55:696-708, 1977
2. Heijl A, Drance SM: Changes in differential threshold in patients with glaucoma during prolonged perimetry. Br J Ophthalmol 67:512-516, 1983
3. Hudson C, Wild JM, O'Neill EC: Fatigue effects during a single session of automated static threshold perimetry. Invest Ophthalmol Vis Sci 35:268-280, 1994
4. Johnson CA, Adams CW, Lewis RA: Fatigue effects in automated perimetry. Appl Optics 27:1030-1037, 1988
5. Marra G, Flammer J: The learning and fatigue effect in automated perimetry. Graefe's Arch Clin Exp Ophthalmol 229:501-504, 1991
6. Zulauf M, Flammer J, Signer C: The influence of alcohol on the outcome of automated static perimetry. Graefe's Arch Exp Ophthalmol 224:525-528, 1986
7. Zeyen T, Caprioli J, Zulauf M: Priority of test locations for automated perimetry in glaucoma. Ophthalmology 100:518-522, 1993
8. Funkhouser A, Fankhauser F, Hirsbrunner H: A comparison of eight test location configurations for estimating G1 mean defect values. Jpn J Ophthalmol 33:295-329, 1989
9. Gonzalez de la Rosa M, Abreu Reyes JA, Gonzalez Sierra MA: Rapid assessment of the visual field in glaucoma using an analysis based on multiple correlations. Graefe's Arch Clin Exp Ophthalmol 228:387-391, 1990
10. Henson DB, Chauhan BC, Hobley A: Screening for glaucomatous visual field defects: the relationship between sensitivity, specificity and the number of test locations. Ophthalmic Physiol Opt 8:123-127, 1988
11. Krakau CET: Visual field testing with reduced sets of test points: a computerized analysis. Doc Ophthalmol 73:71-80, 1989

12. Rabin S, Kolesar P, Podos SM, Wilensky JT: A visual-field screening protocol for glaucoma. Am J Ophthalmol 92:530-535, 1981
13. Weber J, Distelhorst M: Perimetric follow-up in glaucoma with a reduced set of test points. Ger J Ophthalmol 1:409-414, 1992
14. Weber J, Kosel J: Glaukomperimetrie- die Optimierung von Prüfungsrastern mit einem Informationsindex. Klin Mbl Augenheilk 189:110-117, 1986
15. Messmer C, Flammer J: Octopus Program G1x. Ophthalmologica 203:184-188, 1991
16. Chauhan BC: Cluster analysis in visual field quantification. Doc Ophthalmol 69(1):25-39, 1988
17. Gramer E: Zur Topographie früher glaukomatöser Gesichtsfeldausfälle bei der Computerperimetrie. Klin Mbl Augenheilk 180:515-532, 1982
18. Heijl A, Lundquist: The location of earliest glaucomatous visual field defects documented by automatic perimetry. Doc Ophthalmol Proc Ser 35:153-158, 1983
19. Hamado H, Furuno F, Matsuo H: A method for objective evaluation of the results of perimetry by Friedmann Analyser 2 and its application with glaucoma. Acta Soc Ophthalmol Jpn 87(12):1480-1488, 1983
20. Mandava S, Caprioli J, Zulauf M: A glaucoma pattern index to quantify glaucomatous visual field loss. J Glaucoma 1:178-183, 1992
21. Anton A, Maquet JA, Pastor JC: Value of logistic discriminant analysis for interpreting initial visual field defects. 1996 (in press)

FUNDUS ORIENTED PERIMETRY
A new concept for increasing the efficiency of visual field examination

U. SCHIEFER[1], G. STERCKEN-SORRENTI[1], T.J. DIETRICH[1], M. FRIEDRICH[1] and N. BENDA[2]

[1]University Eye Hospital, Department II; [2]Department of Medical Biometry; Tübingen, Germany

Abstract

This new method (patent pending) uses a digitized fundus image of the tested subject as a basis for 'construction' of an individual grid of perimetric stimuli.

The procedure is illustrated schematically in Figure 1: First, the fundus image is down-loaded from the data carrier (diskette, photo-CD, etc.), depicted on a control monitor, and mirrored if necessary with the help of a new type of software. Assuming central fixation, the foveola of the fundus image is aligned to the center of the perimetric field using a cross hair. During a second step, the blind spot, which has previously been determined by means of kinetic perimetry, is interactively superimposed onto the optic disc of the fundus image by automatic activation of rotary and zoom routines. This method allows direct adaptation of the perimetric procedure to the individual fundus morphology, *i.e.*, stimuli may be individually condensed or repeatedly presented in regions of special morphological pathology (nerve fiber bundle defects, etc.). On the other hand, test points can be removed from locations of reduced evidence (*e.g.*, blood vessels).

Preliminary results of this new technique have been reported elsewhere: in order to check its precision, the method was used to detect angioscotomas in normal test subjects.[1] Additionally, the advantages of a locally condensed test grid for detection and precise evaluation of photographically documented nerve fiber bundle defects could be demonstrated.

Acknowledgments

Supported by Tübingen Fortüne Program Nos. 97 and 167.
The authors are indebted to Miss B. Selig for her careful execution of the perimetric examinations and to Mrs G. Jany for her support in preparing the graphics.

Address for correspondence: U. Schiefer, MD, University Eye Hospital, Department II, Schleichstrasse 12-16, D-72076 Tübingen, Germany

Perimetry Update 1996/1997, pp. 107–109
Proceedings of the XIIth International Perimetric Society Meeting
Würzburg, Germany, June 4–8, 1996
edited by M. Wall and A. Heijl

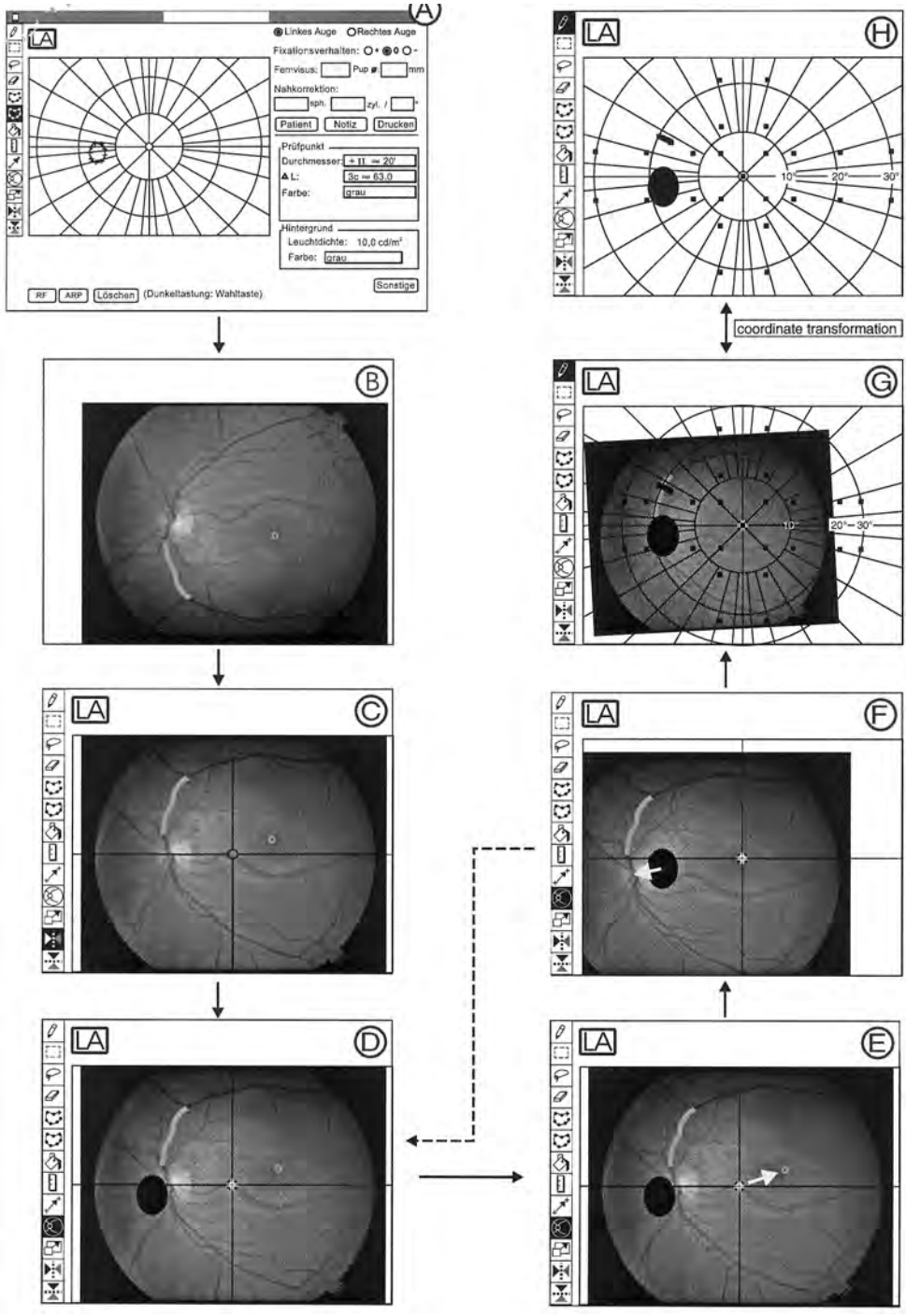
A
LA
Linkes Auge
Rechtes Auge
Fixationsverhalten:
Fernvisus:
Pup ø
mm
Nahkorrektion:
sph.
zyl.
Patient
Notiz
Drucken
Prüfpunkt
Durchmesser:
Farbe:
grau
Hintergrund
Leuchtdichte:
Farbe:
RF
ARP
Löschen
(Dunkeltastung: Wahltaste)
Sonstige
B
C
D
E
F
G
H
10°
20°
30°
coordinate transformation

Reference

1. Schiefer U, Stercken-Sorrenti G, Dietrich TJ, Friedrich M, Benda N: Fundus-orientierte Perimetric: Evaluation eines neuen Gesichtsfeld-Untersuchungsverfahrens bezüglich der Evaluation von Angioskotomen. Klin Mbl Augenheilk 209:394, 1996

←
Fig. 1. Sequence of the single steps in fundus oriented perimetry (FOP).
A. Detection of blind spot (kinetic perimetry with large stimulus of high contrast).
B. Fading-in of the digitized fundus image on the control monitor (via network, disc, other storage media, or photo-CD, etc.). Relevant structures have already been outlined if necessary.
C. Graphical processing of the fundus image (*e.g.*, mirroring along the horizontal or vertical axis).
D. Fading-in of the individual manual perimetric result (blind spot, see *A*), as well as the center of the visual field (specially marked by a cross hair).
E. Manual alignment of the visual field center to the foveola of the digitized fundus image by horizontal and/or vertical translation of the cross hair (blind spot is thereby moved equidirectionally).
F. Manual superposition of the initially registered blind spot onto the optic disc of the digitized fundus image; in this way, a rotary as well as a zoom function for the faded-in fundus image is activated (steps *D* to *F* have to be repeated if necessary).
G. After completion of the alignment procedures mentioned above, a coordinate system corresponding to the depicted fundus image is faded in. Subsequently, an individual, fundus-oriented perimetric grid can be created on the screen of the control monitor. Alternatively, an already existing stimulus grid can be called and modified if necessary. For this reason, single-space or highlighted groups of test points can be positioned, shifted or erased.
H. As a final step, coordinate transformation of the stimulus positions created on the digitized fundus image is performed to adapt the grid to the given device (VDU/flat screen or bowl perimeter), observing (spherical) trigonometric rules. [This step has not yet been performed as a routine – Benda *et al.*, in preparation.]

IS RAPID ASSESSMENT OF THE VISUAL FIELD IN GLAUCOMA USING MULTIPLE CORRELATIONS USEFUL? An evaluation of Delphi perimetry

P.K. WISHART and A.S. KOSMIN

Glaucoma Clinic, St Paul's Eye Unit, Royal Liverpool University Hospital, Liverpool, UK

Abstract

Purpose: To evaluate Delphi perimetry which uses multiple correlations and linear regressions to produce a statistical estimation of the visual field in glaucoma, from a determination of the sensitivities of four critical points of the visual field.[1]

Method: Patients with glaucoma or ocular hypertension underwent Humphrey visual field analysis (HVFA) with Program 24-2, and also Delphi perimetry. All eyes had good visual acuity, were reliable subjects at perimetry and were free of ocular abnormalities, with the exception of glaucoma. The normality of the Humphrey visual fields was judged by glaucoma hemifield test and STATPAC 2 probability analysis. Delphi perimetry fields were considered abnormal if mean deviation was worse than -2 dB or mean scotoma probability was greater than 10%.[2] The extent, defect depth and location of any field loss identified by HVFA was compared to the decibel maps and mean scotoma probability maps of the Delphi fields.

Results: Two hundred and fifty-nine eyes of 196 patients met the criteria for inclusion in the study and, of these, HVFA showed glaucomatous defects in 120 eyes and normal fields in 139 eyes. The sensitivity for the detection of glaucomatous visual field loss by Delphi perimetry was 78% and the specificity for the test was 91%. However, Delphi perimetry consistently failed to detect glaucomatous field loss that was confined to the paracentral area and small nasal steps. Twenty-six eyes with such defects were classed as normal by Delphi perimetry and, in a further 27 eyes, Delphi perimetry, although abnormal, failed to predict central visual field loss that posed a threat to fixation.

Conclusions: Delphi perimetry has reasonable sensitivity and specificity for a rapid method of detecting glaucomatous visual field loss, but its inability to detect central visual field loss is a severe drawback. The addition of two more critical points above and below fixation, and the use of a larger database of glaucoma patients for the statistical estimation, may improve its usefulness.

References

1. Gonzalez de la Rosa M, Abreu Reyes JA, Gonzalez Sierra MA: Rapid assessment of the visual field in glaucoma using an analysis based on multiple correlations. Graefe's Arch Clin Exp Ophthalmol 228:387-391, 1990
2. Gonzalez de la Rosa M: Personal communication. October 1993

Address for correspondence: P.K. Wishart, MD, Glaucoma Clinic, St Paul's Eye Unit, Royal Liverpool University Hospital, Liverpool, UK

Perimetry Update 1996/1997, p. 111
Proceedings of the XIIth International Perimetric Society Meeting
Würzburg, Germany, June 4–8, 1996
edited by M. Wall and A. Heijl

EVALUATING THE DELPHI SYSTEM FOR RAPID ASSESSMENT OF VISUAL FUNCTION USING THE HUMPHREY PERIMETER

T.D. QUACH[1], B.V. NGUYEN[1], W. ROWE ELLIOTT III[1], R.M. REDMOND[2] and W.E. SPONSEL[1]

[1]University of Texas Health Science Center, San Antonio, TX, USA; [2]Scarborough Hospital, Scarborough, North Yorkshire, UK

Abstract

Purpose: This study was conducted to compare Delphi perimetry with concomitant Humphrey 30-2 visual fields of individuals with early, moderate, or severe open-angle glaucoma, and of an age-related control group to assess the utility of the Delphi program as a rapid screening test for glaucoma.
Methods: A total of 31 single eyes of glaucoma patients and eight single eyes of age-related subjects with no ocular disease were evaluated using both the Delphi perimetry and Humphrey Full Threshold 30-2 visual field. Of the 31 glaucomatous eyes, five were classified as having early Humphrey visual field loss, ten were classified as moderate, and 16 as severe, according to the Prevent Blindness America adaptation of the Hodapp, Parrish Anderson criteria (see Table 1).
Results: Delphi perimetry required an average of 1.1 minute per eye, compared with 15.6 minutes with the Humphrey 30-2 Full Threshold algorithm. There was a strong correlation between Humphrey and Delphi mean deviation (r=0.75; p<0.0001), and of Humphrey corrected pattern standard deviation (CPSD) with Delphi mean scotoma probability (r=0.84; p<0.0001). Using a cut-off of >3 SD (to obviate false positives) from the mean Delphi scotoma probability value for the control group, the Delphi successfully detected 93.8% of those with severe Humphrey glaucomatous field loss. Using the same cut-off criteria, the Delphi detected 74.2% of all grades of Humphrey 30-2 glaucomatous field loss.
Conclusions: The Delphi appears to be capable of detecting three-quarters of eyes with any degree of glaucomatous field loss (and more than nine out of ten with severe field loss) in 7% of the time required to perform Humphrey 30-2 Full Threshold perimetry, without the likelihood of producing false positive diagnoses. The Delphi concept of rapidly testing four epidemiologically-determined glaucoma-specific points appears to have potential utility for population screening.

Introduction

Open-angle glaucoma accounts for over 13% of blindness in the US, and is one of the three most common causes of visual loss. Traditional systems for detecting glaucoma before severe neural loss has occurred are expensive and time-consuming, thus limiting the access of many individuals to early diagnosis and treatment. In search

Address for correspondence: W.E. Sponsel, MD, Department of Ophthalmology, The University of Texas Health Science Center, S.A., 7703 Floyd Curl Drive, San Antonio, TX 78284-6230, USA

Perimetry Update 1996/1997, pp. 113–118
Proceedings of the XIIth International Perimetric Society Meeting
Würzburg, Germany, June 4–8, 1996
edited by M. Wall and A. Heijl

of a less expensive diagnostic tool, a new software program called Delphi has recently been developed that takes much less time than standard thresholding perimetry. This Delphi software exploits epidemiological information to elicit glaucoma-specific data in the form of a very abbreviated visual field test, using the Humphrey perimeter's hardware.[1]

Using mathematical principles and a large epidemiological database, the Delphi system has been designed to exploit four specific loci in the visual field which are depressed with high frequency among glaucomatous eyes, but which are rarely affected among age-related normal eyes. Multiple linear regression is used to extrapolate a presumptive image of the visual field from these few diagnostically powerful points, which alone produce a 98% correlation with actual fields. Testing additional loci tends to produce progressively less relative information and increases the risk of false positive results.

The particular attraction of this method is its tendency to minimize both testing time and false positives, since normal eyes outnumber diseased eyes by a factor of 50:1 in the population at large. Even a slight tendency to produce false positives in a screening setting can ameliorate the value of a diagnostic test, regardless of its purported capability to detect diseased eyes. Put simply, even if sensitivity is perfect, specificity needs to exceed 98% for true-positives merely to equal the number of false-positives in a glaucoma screening exercise; even at 99% specificity, at least one-third of failures would not be expected to have disease. A test with 90% specificity (which is a value often quoted in the literature) would, at very best, incorrectly fail six non-diseased eyes for every eye with true glaucomatous field loss in a typical population, largely defeating the purpose of the screening exercise.

With these principles in mind, the objective of this study was to compare Delphi perimetry with concomitant Humphrey 30-2 visual field analysis among a population with a range of glaucomatous visual pathology, and a group of age-related normal subjects. An adaptation of the Hodapp, Parrish, Anderson criteria,[2] recently adopted by Prevent Blindness America for grading visual field loss (Table 1),[3] was applied to obtain a test population with a reasonably balanced distribution of normal, early, moderate, and severe disease, for correlation of visual field indices, and estimation of diagnostic sensitivity for each category of visual loss.

Patients and methods

Testing was performed at the Audie Murphy Veterans Administration Medical Center in San Antonio, Texas. Informed consent was obtained from all participants, in accordance with the tenets of the Declaration of Helsinki, and with the approval of the Institutional Review Board of the University of Texas Health Science Center. Thirty-nine eyes of 39 subjects, all male, were classified by Hodapp, Parrish, Anderson criteria into four groups. Group 1 consisted of nine age-related individuals with no ocular disease; Group 2 of individuals with early glaucomatous defects in the tested eye; Group 3 of those with moderate field defects; and Group 4 of those with severe glaucomatous visual field loss. Humphrey Full Threshold and Delphi perimetry were performed in random sequence, and always within less than a three-day interval.

Table 1. Humphrey visual field rating criteria

Groups	*Characteristics*
Severe visual field loss	Mean defect worse than -12 dB, or on the pattern deviation plot 37 or more points depressed at or below 5%, or 20 or more points depressed at or below 1%, or one or more points in the central 5° at 0 dB, or hemifield point pairs in the central 5° at or below 15 dB
Moderate visual field loss	Mean defect between -12 dB and -6 dB, or on the pattern deviation plot 18 to 36 points depressed at or below 5%, or 10 to 19 points depressed at or below 1%, and no points in the central 5° at 0 dB, and no hemifield pairs in the central 5° at or below 15 dB
Early visual field loss	Mean defect greater than -6 dB, and on the pattern deviation plot at least three arcuate depressed points, and 17 to 7 points depressed at or below 5%, and 10 or fewer points depressed at or below 1%, and no points in the central 5° at 0 dB, and no hemifield pairs in the central 5° at or below 15 dB
N1 field	Defects do not meet early criteria

Adapted from Hodapp, Parrish and Anderson[2]

Results

Thirty-one eyes of glaucoma patients and eight normal eyes were studied. Of the glaucomatous eyes, five were classified as having early Humphrey defects, ten as moderate, and 16 as having severe glaucomatous Humphrey fields.

The time required for the two tests differed markedly. Humphrey Full threshold 30-2 testing required an average of 15.6 minutes per eye tested, excluding setting-up time, while the Delphi program required only 1.1 minute per eye on average.

Correlations of Humphrey mean deviation with Delphi mean deviation across the normal and diseased population range showed significant association (r=0.75; p<0.0001; Fig. 1). A similar analysis comparing Humphrey corrected pattern standard deviation (CPSD) with Delphi mean scotoma probability was even stronger (r=0.84; p<0.0001, Fig. 2). Thus, the estimates of both global and focal visual field loss produced by the abbreviated Delphi program tended to show quite strong numerical agreement with the more detailed Humphrey measurements, although the Delphi tended to truncate more than a third of the data for both its indices at or near zero.

To evaluate the potential utility of the Delphi in screening, Groups 1 to 4 (according to Humphrey field status) were plotted against Delphi scotoma probability (which had shown the better correlation with Humphrey). Because the age-related normal group was small in this pilot study, in order to maximize presumptive specificity, a conservative cut-off limit of 3 SD (*i.e.*, 3 x 0.43 units) from the mean (0.35 units) of the normal eye group (Group 1) was adopted. The distribution of this data is shown in Figure 3. Using the criteria defined above, a diagnostic sensitivity of 74.2% existed for all grades of glaucoma (*i.e.*, Groups 2, 3 and 4, cumulatively). Sensitivity for moderate and severe disease only (*i.e.*, Groups 3 and 4) was only marginally

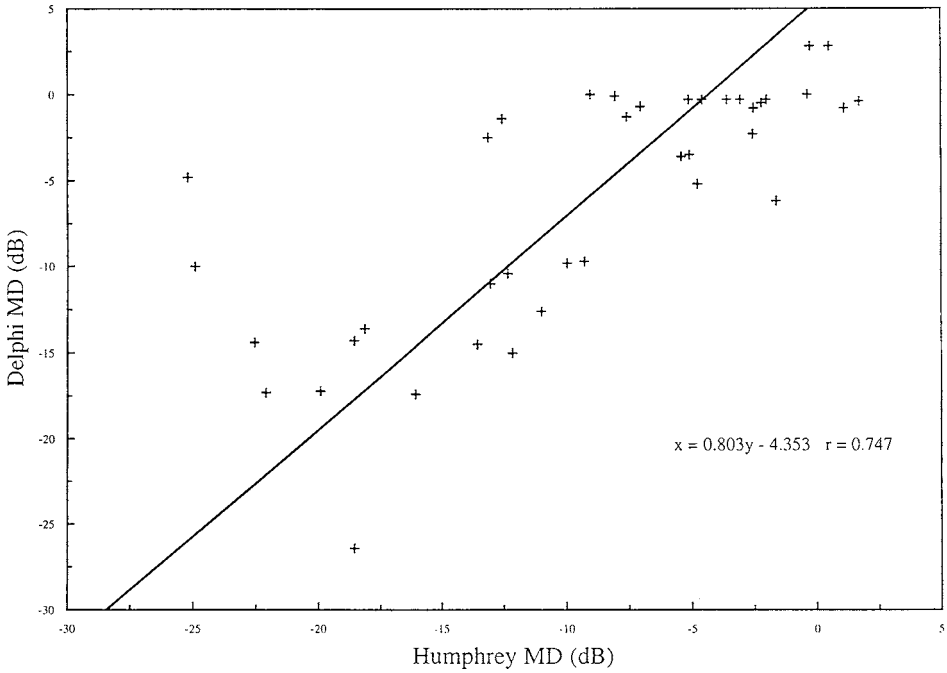

Fig. 1. Linear correlation of Humphrey mean deviation (MD) versus Delphi MD among the 39 subjects tested.

better at 76.2%. Sensitivity of the Delphi for detecting severe disease (Group 4) was very high (93.8%) with only one false negative among the 16 eyes.

Discussion

This preliminary assessment of the effectiveness of the Delphi software suggests the technique may have potential utility as a population screening tool. Testing of a much larger normative database is necessary before any true estimate of the technique's specificity can be determined. The present study does verify that its sensitivity, with conservative application of the available normal data, would qualify the method as an appropriate screening technique according to recently defined criteria of the Prevent Blindness America Glaucoma Advisory Committee (Screening Subcommittee; Robert Stamper, Chair). Obviously, if the method is to have utility for screening, the concept must be transposed into a much lower-cost, portable device. The developer of the Delphi system has apparently undertaken to develop a variety of novel approaches for applying the technique with 'appropriate technology' in mind.

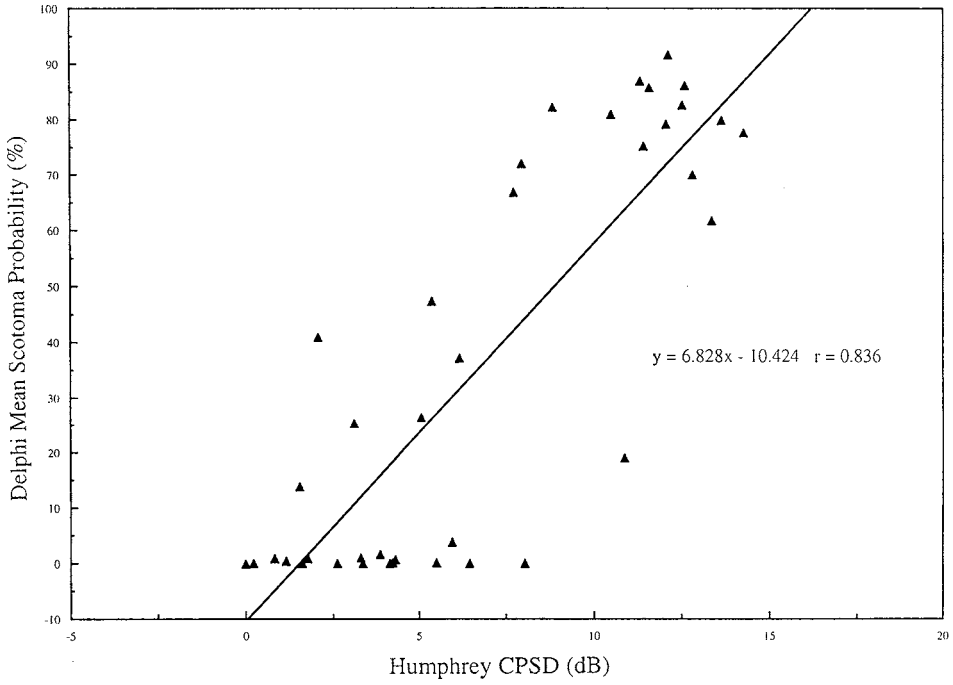

Fig. 2. Linear correlation of Humphrey corrected pattern standard deviation (CPSD) versus Delphi mean scotoma probability among the 39 subjects tested.

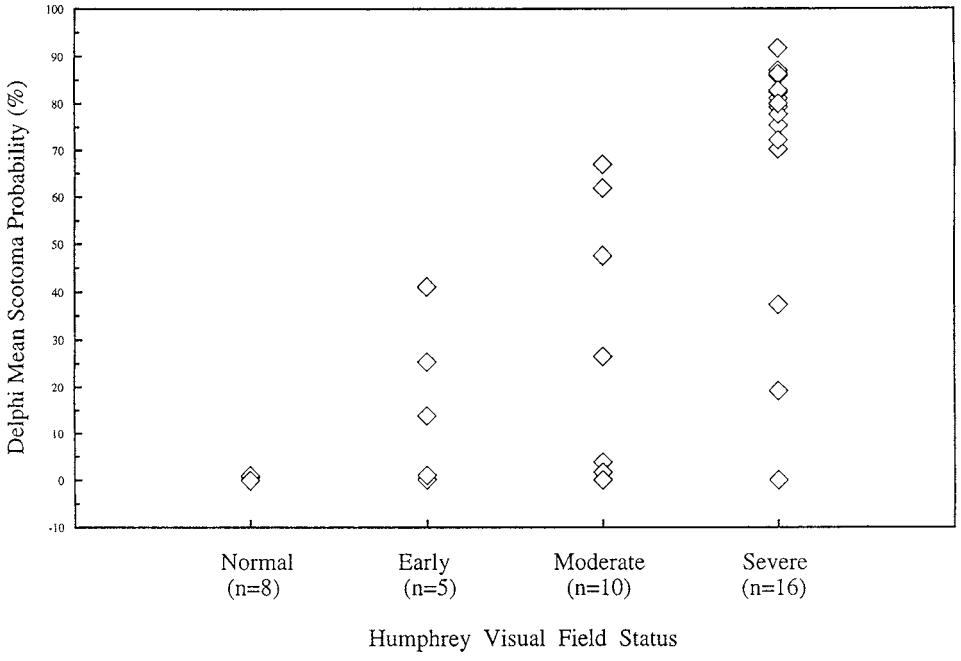

Fig. 3. Distribution of Delphi mean scotoma probability values among the four groups, graded according to their Humphrey 30-2 status using the Hodapp, Parrish, Anderson criteria (see Table 1).

Acknowledgments

Supported by a Lions Sight Research Scholarship, Delphi Perimetry, and an unrestricted grant from Research to Prevent Blindness. Charles Ballentine provided extensive technical assistance.

References

1. Gonzalez de la Rosa M, Gonzalez Sierra MA: Rapid assessment of the visual field in glaucoma using an analysis based on multiple correlations. Graefe's Arch Clin Exp Ophthalmol 228:387-391, 1990
2. Hodapp E, Parrish RK II, Anderson DR: Clinical Decisions in Glaucoma, pp 52-61. St Louis MO: CV Mosby 1993
3. Sponsel WE, Ritch R, Stamper R, Higginbotham EJ, Anderson DR, Wilson MR, Zimmerman T: Prevent Blindness America Visual Field Screening Study. Am J Ophthalmol 120:699-708, 1995

ACCURACY OF TENDENCY-ORIENTED PERIMETRY WITH THE OCTOPUS 1-2-3 PERIMETER

MANUEL GONZÁLEZ DE LA ROSA, ANGELES MARTINEZ, MANUEL SANCHEZ, CARMEN MESA, LUIS CORDOVÉS and MARÍA JOSÉ LOSADA

Hospital Universitario de Canarias, Universidad de La Laguna, Spain

Abstract

Using the tendency-oriented perimetry (TOP) algorithm, each test point is examined only once. The patient's response is used to calculate the threshold in the specific test location and in the adjacent area, conditioning the intensity of the following stimuli. Test points that have already been examined are also influenced by the surrounding test area when examined later. Fifty-two eyes (29 male and 23 female; mean MD 10.06 dB, SD ±7.47) of 42 patients (mean age 54.1 years, SD ± 18.9) with different diagnoses and defect levels (12 normals, 22 glaucomatous, eight neuropathies, ten chorioretinal lesions) were examined with TOP and Program 32 of the Octopus 1-2-3 perimeter. With the TOP program, the MD values were 1.65 dB higher on average than the values obtained with Program 32. Using a linear regression equation, the following results were obtained: total MD (r=0.96), MD of each square (r=0.92-0.96), LV (r=0.91), and the individual threshold values (r=0.84). In conclusion, the TOP algorithm produced comparable results to those obtained with the conventional bracketing strategy, with the advantage that it only takes one-fifth or one-sixth of the time. With the TOP program, the thresholds obtained were slightly higher than those with Program 32, in a proportion similar to the known threshold reduction due to the 'fatigue effect' during long examinations.

Introduction

Tendency oriented perimetry (TOP) is a novel approach to visual field exploration, which utilizes each of the subject's responses, not only to deduce the differential light threshold of the visual field location where the stimulus is shown (traditional approach), but also to generate the threshold of neighboring locations.

The anatomical and topographical relationship of the defects determine proximal interdependence or 'tendencies' among the thresholds of neighboring zones of the visual field. These tendencies are examined and utilized by this strategy to obtain an estimate of the whole group of thresholds.

With the TOP strategy, the subject's response generates a group of 'vectors' applied to the position in question, as well as to surrounding test locations. During the exploration, when one of the positions adjacent to the first test location is exam-

Address for correspondence: Manuel González de la Rosa, C/. 25 de Julio No. 34, 38004 Santa Cruz de Tenerife, Spain

Perimetry Update 1996/1997, pp. 119–123
Proceedings of the XIIth International Perimetric Society Meeting
Würzburg, Germany, June 4–8, 1996
edited by M. Wall and A. Heijl

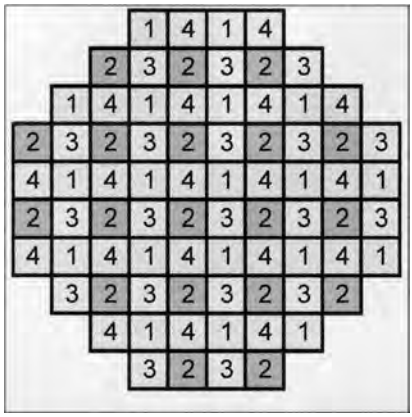

Fig. 1. The four exploration submatrices of the TOP program.

ined, the subject's response will influence the interpretation of that particular threshold, as well as the neighboring test locations, including the first one. In other words, the threshold estimation of a given test location in the visual field is obtained by information coming from that position's exploration and from that provided by all the surrounding test locations.

Material and methods

The program was developed based on the TOP algorithm for the Octopus 1-2-3 perimeter, using the same pattern values for normal thresholds and their test standard parameters: Goldmann spot III with exposure times of 0.1 seconds. The test positions of the standard Program 32 were divided into four submatrices (numbered 1 to 4 in Fig. 1), each separated by 12°.

The first submatrix exploration was in a random sequence of points, using a light intensity equal to half (8/16) the corrected normal threshold for the patient's age at each test point. The patient's answer 'seen' or 'not seen' generated either positive or negative 'vectors' equal to one-fourth (4/16) of the patient's normal age mean sensitivity (MS) value. With these vectors from the first submatrix, new vectors were obtained for the whole 32 matrix by interpolation, and these were added to the initial values.

The answers to the second, third and fourth submatrices also modified the 32 matrix in the same way as described above, adding or subtracting a vector obtained by interpolation to the previous values, equal to 3/16, 2/16 or 1/16 of the normal MS value, corrected for the patient's age, respectively.

Fifty-two eyes (29 male and 23 female; mean MD 10.06 dB, SD ± 7.47) of 42 patients (mean age 54.1 years, SD ± 18.9) with different diagnoses and defect levels (12 normals, 22 glaucomatous, eight neuropathies, and ten chorioretinal lesions) were examined with TOP and Program 32 of the Octopus 1-2-3 perimeter.

Table 1.

	32 versus TOP Octopus 123	*30-2a versus 30-2b Humphrey*
MD	0.96	0.93 r
	1.95	2.22 e.e. (dB)
MD(SN)	0.96	0.93 r
	2.51	2.34 e.e
MD(IN)	0.94	0.92 r
	2.76	2.82 e.e. (dB)
MD(ST)	0.92	0.92 r
	2.8	2.37 e.e. (dB)
MD(IT)	0.96	0.9 r
	2.09	2.63 e.e. (dB)
LV	0.91	0.7 r
	11.96	16.85e.e. (dB^2)
Thresholds	0.84	0.84 r
	5.38	4.41 e.e. (dB)

r: correlation coefficient; e.e.: error of estimation (dB)

Results

Excellent correlation was found between the MD values, the MD of each quadrant, LV, and individual thresholds of the two methods (Table 1).

With the TOP program, MD values were 1.65 dB higher on average than the values obtained with Program 32. This difference was lower than for normal subjects. The appearance of the grayscale maps was similar for both procedures. In Figures 2 and 3, the scattergrams of the MD and LV values obtained by using the two procedures can be seen.

Discussion

As an additional piece of data to be compared with results obtained in the present study, Table 1 shows the correlation of two other tests performed with the Humphrey Program 30-2 over a short time period in a group of 80 affected eyes (with ocular hypertension or glaucoma) and obtained in a parallel study. The comparison should be used for orientation only due to the fact that the data came from two independent groups using different instruments. To elucidate, a comprehensive comparative study must be performed in the future on the same group or population and using the same perimeter.

The results of this work confirm earlier results obtained with computer simulation and applied to visual field data on file.[1] Other authors have searched for shorter threshold procedures to explore the visual field.[2-9] Their approach was either to decrease the number of locations tested or to select only those locations which would seem to give more useful information. More recently, Humphrey Instruments, with the aid of the FASTPAC strategy, has attempted to shorten the testing time by reducing the staircase step size from 4 to 3, but at the cost of increased short-term fluctuation and reducing the precision of the mean deviation (MD) measurement.[10-2]

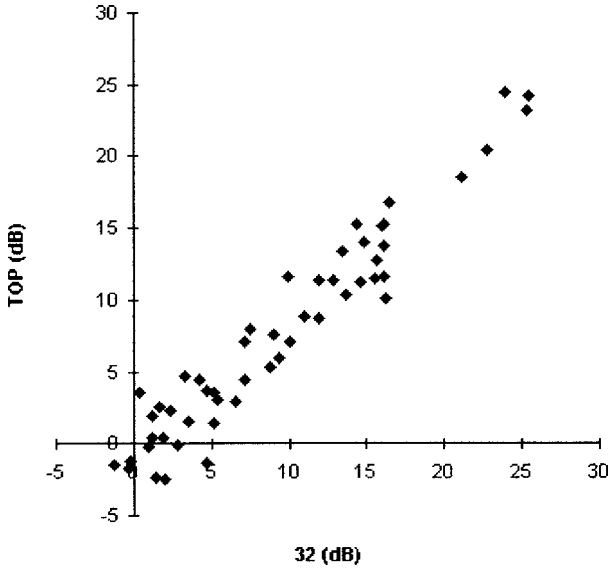

Fig. 2. Scattergram of the MD values.

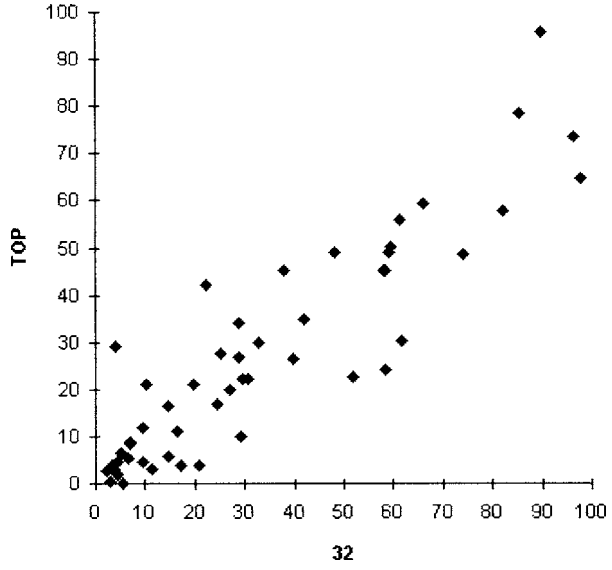

Fig. 3. Scattergram of the LV values.

The TOP strategy does not reduce the number of examined test positions; on the contrary, it utilizes a single question per location, and generates comparable results to those obtained with the conventional bracketing strategy, and with the added advantage that it only takes one-fifth or one-sixth of the time. With the TOP program, the mean sensitivity (MS) can therefore be 1-1.5 dB higher and the mean defect (MD) 1-1.5 lower, compared with the indices obtained during long conventional examinations. This is mainly due to the fact that a short examination avoids

the 'fatigue effect' (retinal neuronal tiredness caused by keeping a still uniform position for a long time). This difference is higher in older persons and it increases test specificity (reduces the number of false pathological cases).

The borders of steep scotomas (for example, hemianopsia) become slightly blurred. In other cases, this blurring is only apparent and is caused by the fact that the TOP algorithm has less tendency to produce extreme results among fluctuating values of threshold.

The TOP algorithm is less sensitive to isolated errors in the patient's response and is very sensitive to clustered defects. Thus, if scotomas should be detected, it is very unlikely that we will be dealing with false pathological results.

Acknowledgments

The authors thank Dr. Patricia Kishi for her assistance in translating and structuring the manuscript.

References

1. González de la Rosa M, Bron A, Morales J, Sponsel W: TOP perimetry. A theoretical evaluation. Vision Res 36:88, 1996 (Sup. Jermov)
2. Funkhouser A, Fankhauser F, Hirsbrunner H: A comparison of three methods for abbreviating G1 examinations. Jpn J Ophthalmol 33:288-294, 1989
3. Funkhouser A, Fankhauser F, Hirsbrunner H: A comparison of eight test location configurations for estimating G1 mean defect values. Jpn J Ophthalmol. 33:295-299, 1989
4. Krakau C: Visual field testing with reduced sets of test points: a computerised analysis. Doc Ophthalmol 73:71-80, 1989
5. Vedy J, Queguiner P, Mouly A, Lagrange C, Riviere B: Le score périmétrique dans l'aire de Bjerrum. Ophtalmologie 4:295-297, 1990
6. Gonzalez de la Rosa M, Abreu Reyes J, Gonzalez Sierra M: Rapid assessment of the visual field in glaucoma using an analysis based on multiple correlations. Graefe's Arch Clin Exp Ophthalmol 228:387-391, 1990
7. Gonzalez de la Rosa M, Hernandez Brito A, Quijada Fumero E: Campimetria para glaucoma explorando cuatro puntos. Arch Soc Esp Oftalmol 62:93-98, 1992
8. Gonzalez de la Rosa M, Sanchez Mendez M, Mesa Moreno C, Mantolán Sarmiento C, Martín Barrera F: Mathematical model of the glaucomatous visual field: evaluation of the 'Delphi' procedure. Paper presented at the Xth International Perimetric Society Meeting. Kyoto, Japan 1992
9. Gonzalez de la Rosa M, Salazar M, Sanchez Mendez M, Hernandez Brito A: A practical visual field exploration device: the Delphi program. Chibret Int J Ophthalmol 10:7-12, 1994
10. Flanagan J, Wild J, Trope G: Evaluation of FASTPAC, a new strategy for thresholds estimation with the Humphrey field analyzer, in a glaucomatous population. Ophthalmology 100:949-954, 1993
11. Flanagan J, Moss I,Wild J, Hudson C, Prokopich L, Whitaker D, O'Neill EC: Evaluation of FASTPAC, a new strategy for threshold estimation with the Humphrey field analyzer. Graefe's Arch Ophthalmol 231:465-469, 1993
12. O'Brien C, Poinoosawmy S, Wu J, Hitchings R: Evaluation of the Humphrey FASTPAC thresholds program in glaucoma. Br J Ophthalmol 78:516-519, 1994

CLINICAL EVALUATION OF HFA II (MODEL 750) IN GLAUCOMA PATIENTS

AIKO IWASE, KAZUMASA OKADA, TETSUYA YAMAMOTO and YOSHIAKI KITAZAWA

Department of Ophthalmology, Gifu University of Medicine, Gifu, Japan

Abstract

The new model of the Humphrey Field Analyzer (model 750 HFA II) is compact, having a non-spherical bowl but the same program as the standard model 600 series (HFA I). It has been reported that the results obtained with model 750 are not significantly different from those of the standard model. The authors attempted to evaluate the features of the new model and to compare the results of both models. Thirty eyes of 30 glaucoma patients and ten eyes of ten ocular hypertension patients were tested by both models using the central 30-2 Program. All had stable intraocular pressure (IOP) and reproducible visual fields with high reliability factors when examined with the HFA I. Three eyes (0.75%) showed poor reliability factors (fixation loss, false positive, false negative) with the HFA II and seven eyes (17.5%) were judged to be 'low reliability' by the gaze-tracking system, the method of continuously monitoring the direction of the patient's eye. No significant differences were noted between the two models in the sensitivity of the points in the central 24°, but significant differences existed in the most peripheral points of the central 30-2 test. MD and PSD were smaller with HFA II than with HFA I ($p<0.01$). The test time was shorter with HFA II than with HFA I ($p<0.01$). The gaze-tracking system proved to be useful for monitoring fixation closely.

Introduction

The new model of the Humphrey Field Analyzer (model 750, HFA II) is compact, having a non-spherical bowl, but the same test programs as the standard model 600 series (HFA I). It has been reported that the results obtained with the HFA II are not significantly different from those obtained with the HFA I. We attempted to evaluate the features of the new model and compared the results of both models.

Material and methods

Thirty eyes of 30 glaucoma patients and ten eyes of ten ocular hypertension patients were tested using both perimeter models. Subjects ranged from 37 to 75 years of age (mean, 41 years), and there was a male/female distribution of 18/22. All had stable

Address for correspondence: Aiko Iwase, MD, Department of Ophthalmology, Gifu University of Medicine, 40 Tsukasa-machi, Gifu-shi, Gifu 500, Japan

Perimetry Update 1996/1997, pp. 125–128
Proceedings of the XIIth International Perimetric Society Meeting
Würzburg, Germany, June 4–8, 1996
edited by M. Wall and A. Heijl

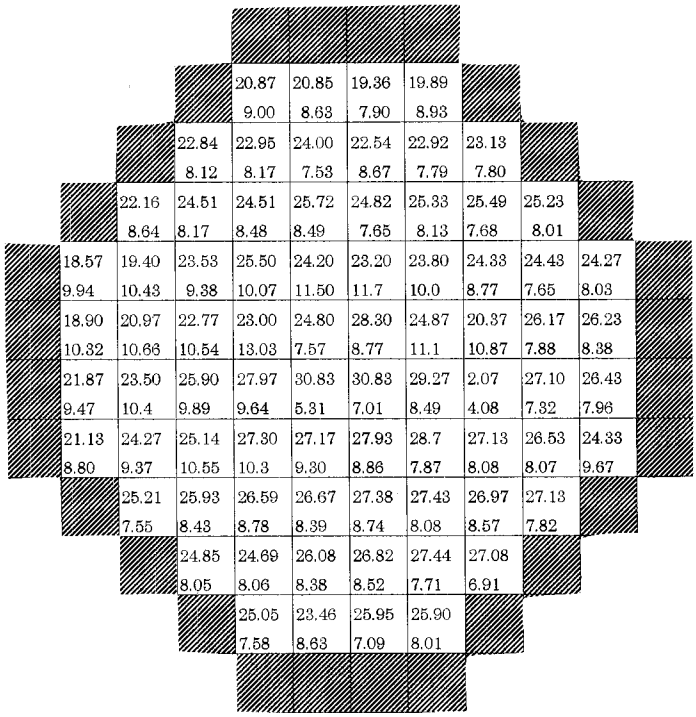

Fig. 1. Boxes represent the test locations of the central 30-2 Program of the HFA 630 (right eyes). The top number is the mean sensitivity and the bottom number the standard deviation (n=30).

intraocular pressure (IOP), no change in medications, and reproducible visual fields with high reliability when examined with the HFA I. All tests were performed within one month; testing order between HFA I and HFA II was randomized. The results with the HFA I were used as a standard for comparison.

Results

Three eyes were excluded because of the low reliability on testing with the HFA II, and seven eyes were excluded because of excessive errors on gaze tracking. Therefore, 30 eyes were included in the analysis. The results obtained with each perimeter model are shown in Figures 1 and 2. No significant difference was noted between the two models for the thresholds within the central 24°, but a significant difference was noted in the most peripheral points of the central 30-2 test (Fig. 2).

MD and PSD were lower with HFA II than with HFA I (p<0.01) (Table 1). Test time was shorter with HFA II than with HFA I (p<0.01) (Table 2). Some eyes with good reliability using standard parameters showed lower reliability with the gaze-tracking system. For example, one eye showed good fixation at the beginning of the test, but worse fixation towards the end. Unfortunately, we have no standards against which to measure patient gaze tracking, so we are forced to evaluate it subjectively.

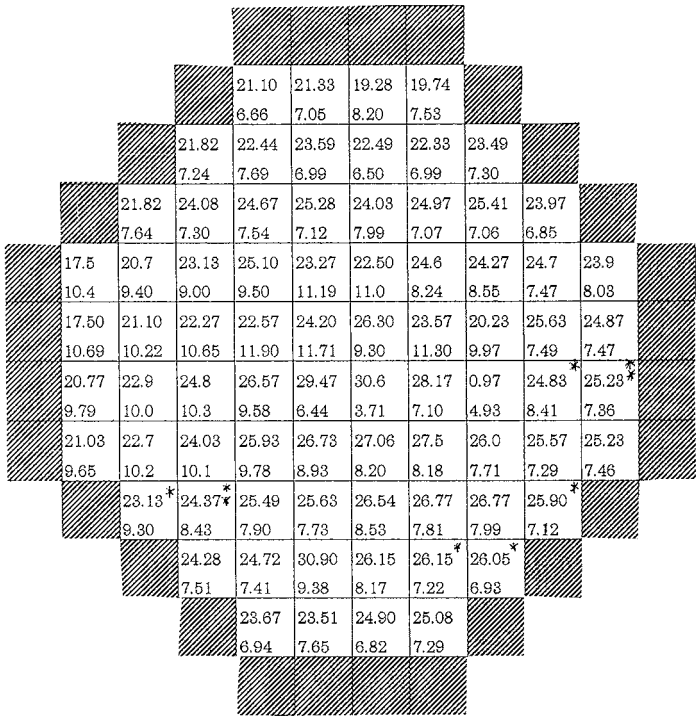

Fig. 2. Boxes represent the test locations of the central 30-2 Program of the HFA 750 (right eyes). The top number is the mean sensitivity and the bottom number the standard deviation (n=30). *p<0.05; **p<0.01.

Table 1. Global indices

	Model 630 (HFA I)	*Model 750 (HFA II)*
MD (dB)	-4.58 ± 7.45	-5.21 ± 7.33*
PSD (dB)	-5.09 ± 3.09	4.54 ± 4.11*
SF (dB)	1.94 ± 1.15	1.60 ± 0.77
CPSD (dB)	4.25 ± 4.22	3.88 ± 4.31

*p<0.05

Table 2. Test time (seconds)

HFA 630 (HFA I)	891 ± 214
HFA 750 (HFA II)	813 ± 160*

*p<0.01

Discussion

The HFA II is a compact perimeter that is convenient to use. There are statistically significant differences in the global indices generated by the two models. The tests were carried out within one month, so that long-term fluctuation may have played a role in the generation of the differences, but the real basis for these differences remains unknown. The gaze-tracking system provides much information on eye position during the test, but still requires normative studies to define acceptable norms of eye position deviation.

Reference

1. Humphrey Field Analyzer CAB User's Guide. Carl Zeiss Japan Group 1995

STATPAC VERSUS DICON FIELDVIEW STATISTICAL ANALYSES*
A pilot study

PETER ÅSMAN

Department of Ophthalmology, Malmö University Hospital, Malmö, Sweden

Abstract

Purpose: Probability maps constitute a widely accepted standard for visual field interpretation. The aims of the present study were to examine a newly developed perimetric statistical package, FieldView, for the Dicon perimeter, and to compare this package to the Humphrey STATPAC package. FieldView calculates a total deviation probability map resembling the one calculated by STATPAC. These maps depict measured threshold values graphically in terms of the significance reached. Furthermore, both programs calculate height-adjusted deviation maps (FieldView HOV-Delta [hill of vision] plot, and STATPAC pattern deviation map). In these, abnormality is based on the resulting deviations in dB values (FieldView) or test point significance (STATPAC).

Material and methods: One normal and one patient group were studied. All study subjects had previous perimetric experience. The normal group consisted of 23 eyes of 23 subjects with a mean age of 63 years (range, 27-83 years), and all were normal on ophthalmological examination, IOP <22 mmHg. The patient group consisted of 31 eyes of 31 subjects with a mean age of 72 years (range, 28-87 years); 24 of these patients had primary open-angle glaucoma and the remaining seven cerebrovascular disease verified by CT or MRT scans. A Humphrey 30-2 FASTPAC threshold test and a Dicon 76-point threshold test (Program 9, LD400 perimeter) were performed in random order during one test session. The normal visual field models (age correction and significance limits) applied in the FiewView and STATPAC programs were compared. For each subject, the FieldView and STATPAC printouts were compared with respect to *1.* the number of significant test points in the total deviation probability map, including sensitivity and specificity estimates; *2.* the number of abnormal points in the STATPAC pattern deviation probability map and the FieldView HOV-Delta map; and *3.* the ability to detect the physiological blind spot (measured threshold at x≈15, y≈-3).

Results: The correction of measured threshold values for age were negligible in FieldView analyses compared to STATPAC analyses (*e.g.*, at x=3, y=27). The age-corrected normal threshold value remained 24 dB from 20-80 years of age, while it decreased from 27 to 19 dB in the STATPAC program. Probability map significance limits were jagged and generally larger in the center than in the periphery, in sharp contrast to the STATPAC limits. In the normal group, the STATPAC total probability maps behaved as expected, while the FieldView probability maps yielded numerous false-positive defects (*e.g.*, altogether there were 19 test points reaching 1% significance in the STATPAC total deviation probability maps [17 points were expected statistically], while the Fieldview probability maps showed 81 such points). Separation between the 23 normals and the 31

*The full article will be published elsewhere

Address for correspondence: Peter Åsman, MD, PhD, Department of Ophthalmology, Malmö University Hospital, S-205 02 Malmö, Sweden

Perimetry Update 1996/1997, pp. 129–130
Proceedings of the XIIth International Perimetric Society Meeting
Würzburg, Germany, June 4–8, 1996
edited by M. Wall and A. Heijl

Table 1. Sensitivity and specificity (%) for various significance limits in probability maps

Significance limit (%)	*STATPAC sensitivity*	*specificity*	*FieldView sensitivity*	*specificity*
5	94	78	94	39
2	94	87	97	52
1	94	91	97	65
0.5	94	91	97	61

patients was significantly better ($p<0.05$, standard log likelihood ratio test for large samples) with STATPAC than with FieldView total deviation probability maps for each level of significance in the probability maps (Table 1).

Furthermore, the STATPAC maps were often superior to the FieldView maps in correctly categorizing field defects as glaucomatous or neurological. The mean threshold in the blind spot point among the normal subjects was 3.4 dB in the Humphrey printouts compared to 17.3 dB in the dicon printouts.

Conclusions: The results with the STATPAC total deviation probability map agreed well with the statistically expected outcome in the normal group. The FieldView probability map, on the other hand, resulted in an unacceptably high number of false-positive defects. FieldView significance limits were in sharp contrast to widely published data on physiological threshold variability. The diagnostic precision of STATPAC printouts was superior to those of FieldView. The ability of the Humphrey perimeter to detect small scotomas (*e.g.*, the blind spot) was superior to that of the Dicon perimeter. The Dicon perimeter uses a moving fixation light, which might account for some of the differences obtained in the present study. The importance of carefully selected normal material and a statistically sound approach for defining normative limits in automated threshold perimetry is stressed.

Acknowledgments

This study was supported by grants from the Herman Järnhardt Foundation, Inez and Joel Carlsson's Foundation, and Ingeborg and Ernst Ydman's Foundation, Malmö, Sweden.

CATARACT AND DIFFUSE VISUAL FIELD LOSS

DIFFUSE VISUAL FIELD LOSS AND GLAUCOMA
Initial experience from the early manifest glaucoma trial*

PETER ÅSMAN, ANDERS HEIJL and the EMGT STUDY GROUP

Department of Ophthalmology, Malmö University Hospital, Malmö, Sweden

Abstract

Purpose: To evaluate the components of diffuse visual field loss in patients with early glaucoma and reproducible localized field defects.

Material and methods: The authors studied 140 visual field tests of 140 patients with early manifest glaucoma. All patients were part of their ongoing Early Manifest Glaucoma Trial (EMGT). The vast majority of patients was recruited by means of mass screening of the population of Malmö, Sweden. Intraocular pressure and disc photographs were used to select individuals with suspected glaucoma to be scheduled for a post-screening visit. In these, a diagnosis of glaucoma was made if two consecutive field tests showed a reproducible field defect (glaucoma hemifield, Glaucoma Hemifield Test (GHT) classification[1] 'outside normal limits' [or 'borderline' in conjunction with corresponding optic disc damage] in the same sector on two consecutive tests). Patients with lens opacities exceeding LOCS II (NI, CII, PI), non-glaucomatous field loss, a VA of less than 0.5, significant ametropia, previous or current glaucoma treatment, or proliferative or preproliferative diabetic retinopathy, were ineligible. All patients underwent two consecutive threshold perimetry tests before the Humphrey 30-2 full-threshold field used in this study was obtained.

Visual field results obtained from 88 normal subjects, randomly selected from the healthy population of Malmö, were used as normal reference material. These normal subjects are part of the Humphrey STATPAC normal database,[2,3] and all had previous perimetric experience before the study fields were obtained.

Two aspects of visual field status were evaluated: the general sensitivity level of the visual field (diffuse component), and the extent of localized field loss (localized component). The diffuse component was estimated with the general height (GH) index, which is the seventh-highest deviation from the age-corrected normal threshold value within the central 24°. Localized field loss was measured with the Glaucoma Hemifield Test (GHT) analysis. The GHT compares visual field results across the horizontal meridian in five mirror-image pairs of sectors. Such differences are labelled 'borderline' if exceeding the $p<0.03$ significance limit. Localized field loss was graded according to the number of such abnormal sectors in the Glaucoma Hemifield Test.

Results: In eyes with mild field loss, *i.e.*, fields with no more than one abnormal GHT sector, GH values did not differ from those in the STATPAC normal database. With the increasing size of localized field loss, GH gradually decreased below that found in normal eyes.

*The full article will be published elsewhere.

Address for correspondence: Peter Åsman, MD, PhD, Department of Ophthalmology, Malmö University Hospital, S-205 02 Malmö, Sweden

Perimetry Update 1996/1997, pp. 133–134
Proceedings of the XIIth International Perimetric Society Meeting
Würzburg, Germany, June 4–8, 1996
edited by M. Wall and A. Heijl

Conclusions: These results indicate that the very earliest visual field changes in glaucoma are usually *purely* localized and not associated with any significant diffuse field loss. In later stages, a diffuse component of visual field loss is gradually superimposed on the increasing localized loss.

References

1. Åsman P, Heijl A: Glaucoma Hemifield Test: automated visual field evaluation. Arch Ophthalmol 110:812-819, 1992
2. Heijl A, Lindgren G, Olsson J: Normal variability of static perimetric threshold values across the central visual field. Arch Ophthalmol 105:1544-1549, 1987
3. Heijl A, Lindgren G, Olsson J: A package for the statistical analysis of visual fields. Doc Ophthalmol Proc Ser 49:153-168, 1987

NEW GLAUCOMA CHANGE PROBABILITY MAPS TO SEPARATE VISUAL FIELD LOSS CAUSED BY GLAUCOMA AND BY CATARACT

ANDERS HEIJL[1], BOEL BENGTSSON[1], PETER ÅSMAN[1] and MICHAEL PATELLA[2]

[1]Department of Ophthalmology, Malmö University Hospital, Sweden; [2]Humphrey Instruments, San Leandro, CA, USA

Introduction

Identification of visual field progression in glaucoma patients is crucial for the management of the disease. High random variability between tests complicates the task. Another problem is development of increasing cataract. Most techniques used for interpretation of visual field deterioration cannot separate visual field loss caused by glaucoma from that caused by cataract.

We have previously reported empirical measurements of the inter-test variability[1] found in glaucomatous fields. The findings were used for designing the Glaucoma change probability maps,[2] based on the total deviation. Such change probability maps signal whether threshold changes from baseline exceed expected random variability, and thus the maps provide an interpretation aid for the detection of significant changes at individual test point locations. Unfortunately, the maps are influenced by progressive cataract.

We developed a new type of Glaucoma change probability map intended to separate localized glaucomatous field progression from media-induced diffuse progression. These new change probability maps are based on the Statpac pattern deviation maps.

An evaluation was performed on data from glaucoma patients who had undergone cataract surgery.

Material

All patient records with a diagnosis of glaucoma or suspected glaucoma, where the patient had undergone cataract surgery with intraocular lens implantation, were retrieved. Studied eyes had at least two baseline and two follow-up tests, obtained with

Address for correspondence: Anders Heijl, MD, Department of Ophthalmology, Malmö University Hospital, S-205 02 Malmö, Sweden

Perimetry Update 1996/1997, pp. 135–137
Proceedings of the XIIth International Perimetric Society Meeting
Würzburg, Germany, June 4–8, 1996
edited by M. Wall and A. Heijl

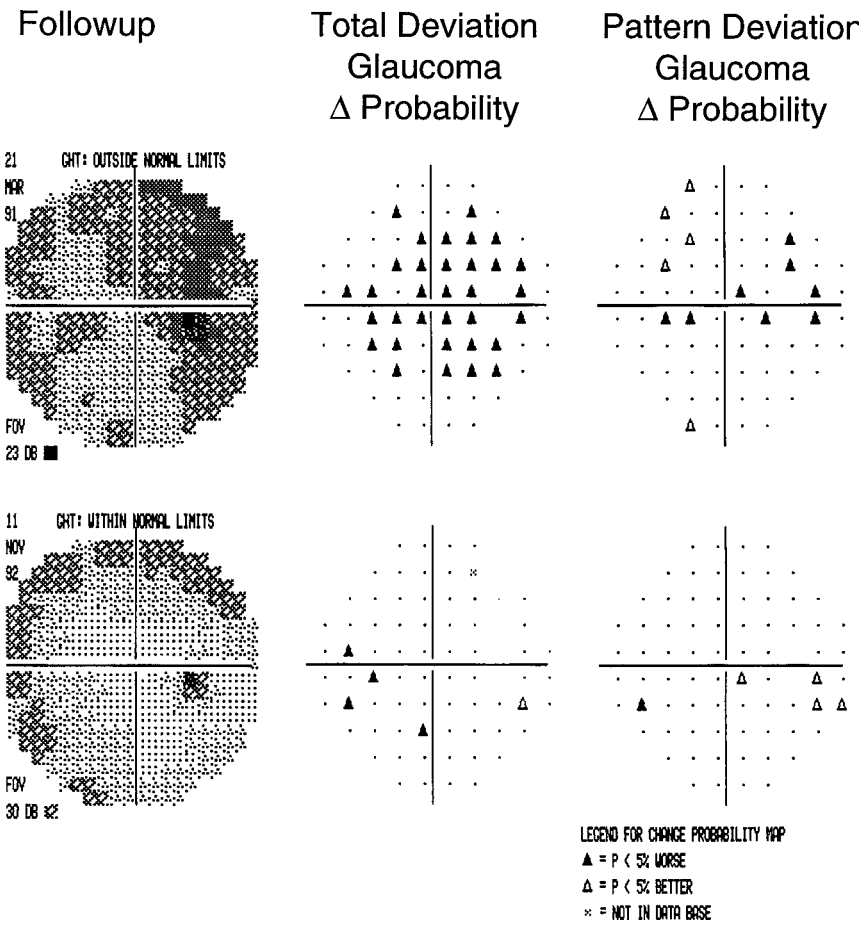

Fig. 1. Two follow-up tests obtained before (*top*) and after (*bottom*) cataract surgery in the same eye. Filled triangles indicate test point locations with significant deterioration compared to baseline tests ($p<0.05$). Obvious differences are seen between the traditional total deviation-based change probability maps (*left*) and the new pattern deviation-based change probability maps (*right*) in the field obtained before surgery. After surgery, the two probability maps are similar to each other and also rather similar to the pre-surgery pattern deviation-based map.

the HFA 30-2 full-threshold program. The follow-up fields had to be obtained both before and after cataract surgery. Forty-seven eyes of 38 patients fulfilled these criteria. Four eyes were excluded because baseline fields were so severely damaged that a majority of test points could not be calculated as stable or deteriorating in the change probability maps ('not in database'). Forty-three eyes of 35 patients then remained. The patients were 14 men and 21 women with a mean age of 74.6 years (range: 52-85). The last follow-up field examination before cataract surgery had been obtained 0-30 months before surgery (mean: 6.4 months). The first field test post-surgery was obtained two to 18 months after the operation (mean: 7.9 months).

Methods

Glaucoma change probability maps were calculated and printed for all eyes, both the old type, based on total deviation, and the new type, based on pattern deviation. All significantly deteriorated points in the two change probability maps of follow-up fields obtained before and after cataract surgery were counted. This was done in both types of change probability maps and total deviation maps, as well as pattern change probability maps. The number of significantly deteriorated points would be expected to decrease after surgery if the change probability maps were influenced by progressive cataract. Therefore, we counted differences for significantly deteriorated points between the two follow-up fields for each type of change probability map.

Results

Cataract surgery significantly changed the number of points indicated as being significantly deteriorated in the old total deviation Glaucoma change probability maps. After surgery, the number of such points decreased by an average of 11.2 ($p<0.001$, *t* test). Using the new method based on pattern deviations, such changes were negligible (average increase of 0.4 significantly deteriorated points).

Discussion

Thus, the common and disturbing effect of increasing cataract was almost eliminated using the new pattern deviation-based change probability maps. In our retrospective material, the intervals between visual field examinations were quite long. It is therefore likely that true glaucomatous progression sometimes occurred between pre- and post-surgery fields. If present, such true deterioration would tend to mask the artificial improvement caused by cataract surgery when using the old maps. Therefore, we expect that our analysis tends to understate any advantages found in the new maps. The new interpretation tool can facilitate differentiation between progressive glaucomatous visual field loss and deterioration caused by increasing cataract.

References

1. Heijl A, Lindgren A, Lindgren G: Test-retest variability in glaucomatous visual fields. Am J Ophthalmol 108:130-135, 1989
2. Heijl A, Lindgren G, Lindgren A, Olsson J, Åsman P, Myers S, Patella M: Extended empirical statistical package for evaluation of single and multiple fields in glaucoma: Statpac 2. In: Mills RP, Heijl A (eds) Perimetry Update 1990/1991, pp 305-315. Amsterdam/Milano: Kugler & Ghedini Publ 1991

INFLUENCES OF CATARACTS ON GLAUCOMATOUS VISUAL FIELD CHANGES

CHIHARU MATSUMOTO[1], TETSURO OGAWA[2], HIROTAKA SUZUMURA[1], HIROSHI INOUE[2] and NATSUKO KIMURA[1]

[1]Department of Ophthalmology, Tokyo Medical College Hospital; [2]Department of Ophthalmology, Hachioji Medical Center, Tokyo Medical College; Tokyo, Japan

Abstract

The influence of cataracts on glaucomatous visual field changes was investigated in 51 eyes of 35 glaucoma patients. The glaucomatous visual field changes revealed by Program 24-2 of the Humphrey Field Analyzer before and after cataract surgery were evaluated. The postoperative stages of the glaucomatous visual field changes (Aulhorn classification) remained unchanged in 70 of 102 hemifields. Isolated scotomata disappeared in three hemifields and appeared in ten hemifields for the first time after surgery. In these 102 hemifields, 86 had a generalized reduction of sensitivity and this number decreased to 58 after surgery. Postoperative pattern standard deviation (PSD) and corrected pattern standard deviation (CPSD) increased in most of the eyes, although mean deviation (MD) improved. When comparing the cumulative sensitivity curves, the diffuse visual field damage caused by cataracts was classified into three types: a constant increase, a lesser increase, and an inconsistent increase in sensitivity. These results indicated that the influence of cataracts on glaucomatous visual field change was not only seen as a generalized reduction of sensitivity (not always homogeneous), but also as blurring of the glaucomatous visual field changes, although cataract had little influence on the stage of glaucomatous visual field change in the majority of glaucoma patients.

Introduction

Absorption of light by the lens has the effect of a filter (decrease of retinal illumination), and diffusion of light causes a ground-glass effect (gradation or shading of the retinal image). The sensitivity curve is reduced by the decrease of retinal illumination, and degradation of the retinal image gives rise to a deterioration of contrast and a decrease of sensitivity. If a cataract is present, a mesopization of the sensitivity curve results from these effects. It has been reported that, based on perimetric results, diffuse lens opacity causes a generalized reduction of retinal sensitivity, and that local lens opacity causes a localized reduction of retinal sensitivity.[1] Increase of a cataract in glaucoma will modify glaucomatous visual field changes, due to alteration in lens opacity.[2] It is therefore important for the diagnosis and management of

Address for correspondence: Chiharu Matsumoto, MD, Department of Ophthalmology, Tokyo Medical College Hospital, 6-7-1, Nishishinjuku, Shinjuku-ku, 160 Tokyo, Japan

Perimetry Update 1996/1997, pp. 139–145
Proceedings of the XIIth International Perimetric Society Meeting
Würzburg, Germany, June 4–8, 1996
edited by M. Wall and A. Heijl

glaucoma to understand how cataracts influence glaucomatous visual field changes. However, there are very few reports evaluating the influence of cataracts on glaucomatous visual field changes using automated perimetry.[3] We investigated the influence of cataracts on the glaucomatous visual field changes before and after phacoemulsification and aspiration (PEA) of cataract and intraocular lens (IOL) implantation.

Material and methods

The material consisted of 51 eyes of 35 glaucoma patients of average age (73.3±8.4 years), who had glaucomatous visual field changes corresponding to glaucomatous optic disc changes and had not undergone surgical treatment for glaucoma. There were cortical cataracts in 29 eyes and nuclear cataracts in 22, and they all underwent cataract surgery with PEA and IOL implantation. Their pupil diameters were more than 3 mm in the pre- and postoperative periods.

The visual field changes revealed by Program 24-2 of the Humphrey Field Analyzer were evaluated to determine the stage of glaucomatous visual field change, isolated scotomata, generalized reduction of sensitivity, global indices, and cumulative sensitivity curves, within six months pre- and postoperatively.

Results

Stages of glaucomatous visual field changes

The pre- and postoperative stages of glaucomatous visual field changes are shown in Figure 1. The postoperative stage of glaucomatous visual field change (Aulhorn classification) remained unchanged in 70 of 102 hemifields (68.6%), improved in 23 (22.6%), and progressed in nine (8.8%).

Isolated scotomata and generalized reduction of sensitivity

Scotomata were detected in 13 hemifields in the gray scale before surgery. After surgery, the scotomata remained unchanged in ten hemifields, disappeared in three, and appeared for the first time in ten (Table 1). In the 102 hemifields, 86 (84.3%) had a generalized reduction of sensitivity and this number decreased to 58 (56.9%) after surgery (Table 2).

Postoperatively, scotomata appeared for the first time in ten of 89 hemifields not detected before surgery and disappeared in three of 13 hemifields detected before surgery.

There was a generalized reduction of sensitivity in 58 hemifields even after surgery.

Global indices

There were significant differences between the average foveal sensitivities and the average mean deviations (MD), although there were no significant differences between the average pattern standard deviations (PSD), the average corrected pattern

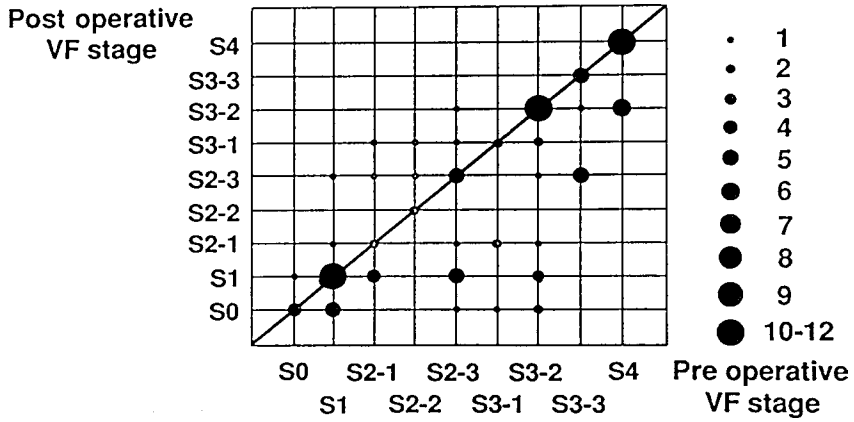

Fig. 1. Scatter diagram of the stages of glaucomatous visual field changes pre- and postoperatively (Aulhorn classification). Seventy hemifields showed unchanged stages pre- and postoperatively.

Table 1. Number of hemifields in which scotomata were or were not detected

	Detected	*Not detected*
Preoperatively	13	89
Postoperatively	20	82

Table 2. Number of hemifields in which a generalized reduction of sensitivity was or was not detected

	Detected	*Not detected*
Preoperatively	86	16
Postoperatively	58	44

Table 3. Average global indices pre- and postoperatively

	Preoperatively	*Postoperatively*	*p value*
Foveal sensitivity	25.8±6.5	31.0±5.5	<0.01*
MD	-13.23±6.24	-9.40±5.82	<0.01*
PSD	6.29±2.91	7.03±3.49	<0.08
CPSD	5.51±3.26	6.37±3.61	<0.08
SF	2.32±1.46	2.19±1.27	<0.46

*Statistically significant. MD: mean deviation; PSD: pattern standard deviation; CPSD: corrected pattern standard deviation; SF: short-term fluctuation

standard deviations (CPSD), and the average short-term fluctuations (SF) before and after surgery. While foveal sensitivity and MD improved after surgery, PSD and CPSD increased (Table 3). There were no significant correlations between the differences in the indices before or after surgery, the type of cataract, or the preoperative stage of glaucomatous visual field changes.

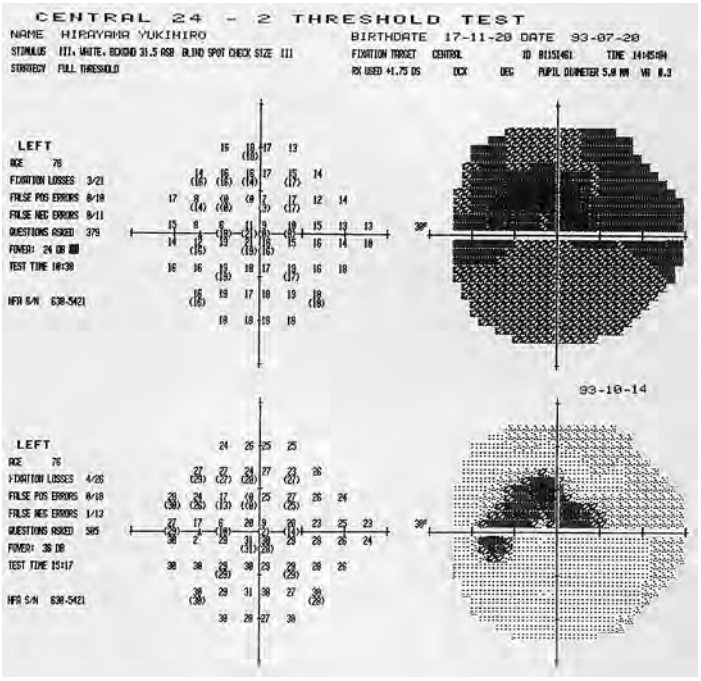

Fig. 2a. The visual fields of a patient with NTG in type A. *Top:* preoperatively; *bottom:* postoperatively.

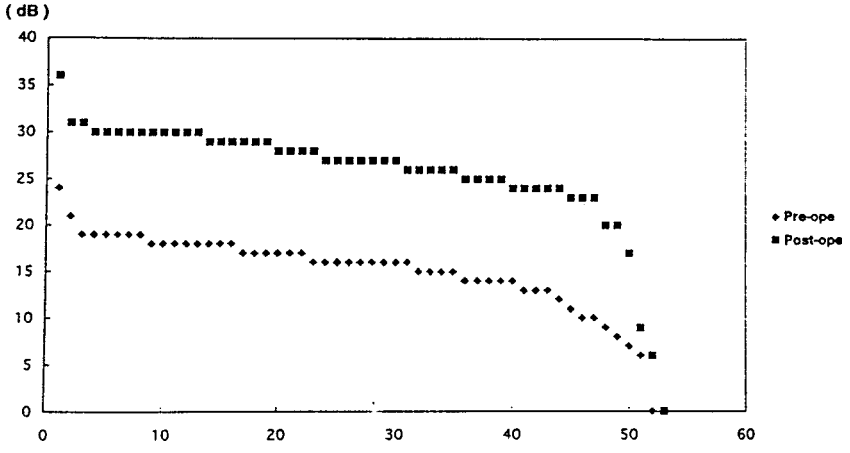

Fig. 2b. Cumulative sensitivity curves of Figure 2a (type A). This type showed a constant increase in sensitivity.

Alteration of the cumulative sensitivity curves

The retinal sensitivities before and after surgery in 53 examination points, excluding two points corresponding to the blind spot, were used to make cumulative curves. When comparing the cumulative curves before and after surgery, they were classified

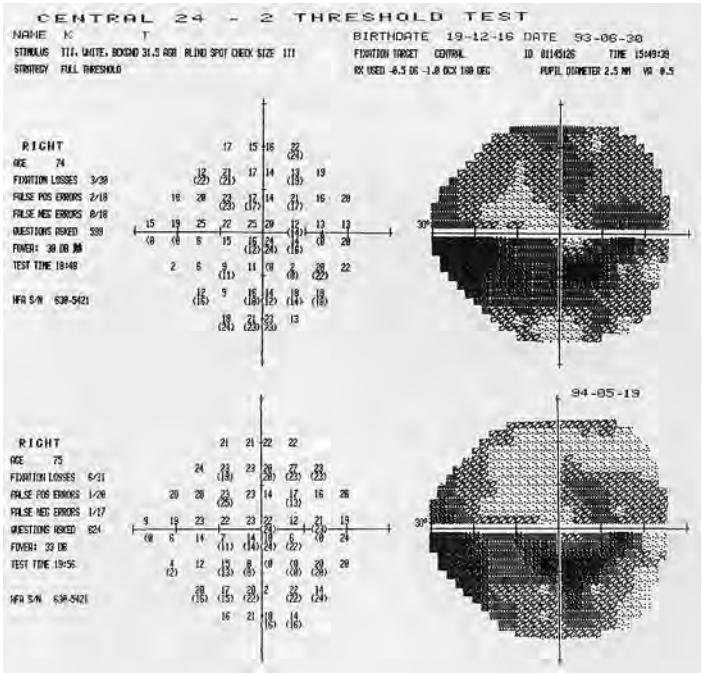

Fig. 3a. The visual fields of a patient with POAG in type B. *Top:* preoperatively; *bottom:* postoperatively.

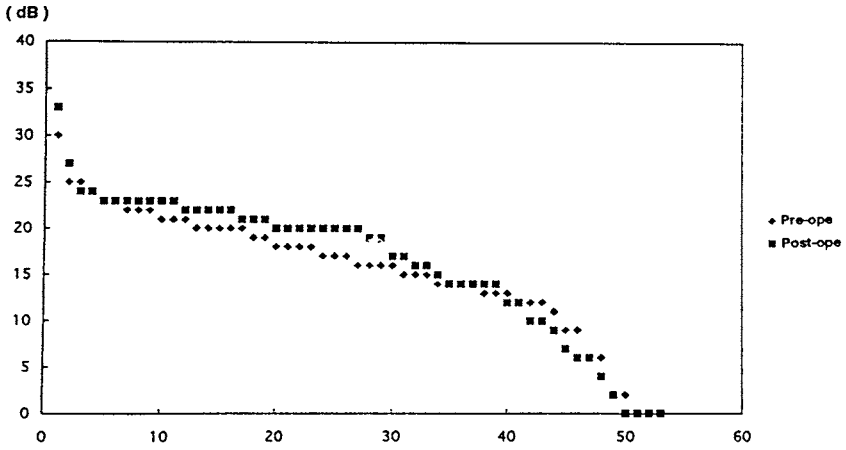

Fig. 3b. Cumulative sensitivity curves of Figure 3a (type B). This type showed less increase in sensitivity.

according to the following types (Figs. 2, 3 and 4): a constant increase in sensitivity in 22 eyes (43.1%) was shown as type A, a lesser increase in sensitivity in 14 eyes (27.5%) was shown as type B, and an inconsistent increase in sensitivity in 15 eyes (29.4%) was shown as type C.

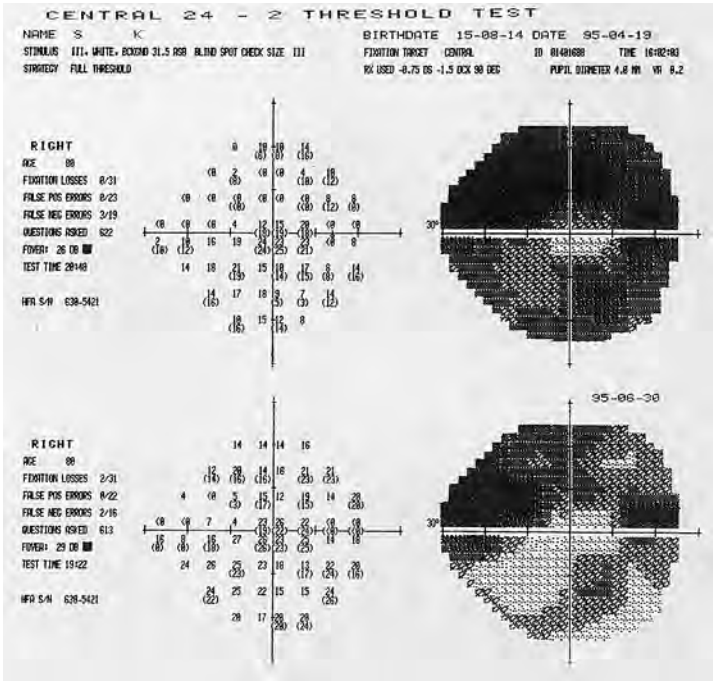

Fig. 4a. The visual fields of a patient with POAG in type C. *Top:* preoperatively; *bottom:* postoperatively.

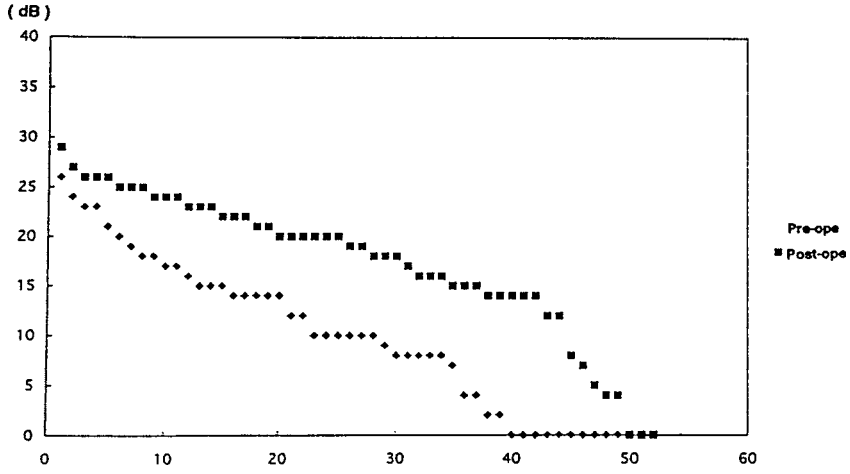

Fig. 4b. Cumulative sensitivity curves of Figure 4a (type C). This type showed an inconsistent increase in sensitivity.

Discussion

In this study, we found that most of the generalized reduction of sensitivity in glaucomatous eyes with cataract was caused by glaucoma, due to the fact that a gener-

alized reduction in sensitivity still existed in 56.9% of glaucomatous eyes even after surgery. Half the isolated scotomata detected after surgery had not been detected before surgery and most of the eyes had increased PSD and CPSD after surgery, although there were no statistical differences in PSD and CPSD before or after surgery. These results indicate that cataracts caused not only a generalized reduction of sensitivity, but also blurring of glaucomatous visual field changes. However, the stage of glaucomatous visual field loss, using the Aulhorn classification, remained unchanged postoperatively in most of the eyes. This result suggests that cataracts have little influence on the stages of glaucomatous visual field loss.

On the other hand, when comparing the retinal sensitivities using the cumulative curve, as in a previous report,[3] it was found that, while cataracts caused diffuse visual field change, the effects were not always homogeneous.

References

1. Greve EL: Single and multiple stimulus static perimetry in glaucoma; the two phases of visual field examination. In: Lens IX Preretinal Factors, pp 206-209. The Hague: Dr W Junk Publ 1973
2. Urner-Bloch U: Simulation of the influence of lens opacities on the perimetric results; investigated with orthoptic occluders. Doc Ophthalmol Proc Ser 49:23-31, 1987
3. Guthauser U, Flammer J: Quantifying visual field damage caused by cataract. Am J Ophthalmol 106:480-484, 1988

DIFFUSE VISUAL FIELD LOSS IN OPEN-ANGLE GLAUCOMA

BALWANTRAY C. CHAUHAN[1,2], RAYMOND P. LEBLANC[1], ALYSON M. SHAW[3], ANGELA B. CHAN[1] and TERRY A. MCCORMICK[1]

Departments of [1]Ophthalmology, [2]Physiology and Biophysics, and [3]Faculty of Medicine, Dalhousie University, Halifax, Nova Scotia, Canada

Abstract

Purpose: To determine the frequency of repeatable diffuse loss as the only form of visual field damage in patients with early to moderate open-angle glaucoma in a prospective follow-up study.

Methods: The study contained 113 patients (median age: 64 years; range 17 to 89 years) who were tested at six-monthly intervals with Program 30-2 of the Humphrey Field Analyzer. Cumulative defect curves were generated for all visual fields (median per patient: 7; range 4 to 9). After randomizing the order and removing all patient information, two observers independently rated each visual field as being 'normal' or showing 'diffuse', 'localized' or 'diffuse and localized' loss. The authors defined repeatable diffuse loss as occurring when at least two-thirds of the fields in the follow-up were classified as 'diffuse'.

Results: On entry, 94 (83.2%) patients had at least 6/7.5 visual acuity. Fourteen patients (12.4%) had repeatable diffuse loss according to the cumulative defect curves. After reviewing their clinical charts, the authors excluded despite good visual acuity, six of these patients because of early lens changes and three because of a suggestion of localized loss (on pattern deviation probability plots) in addition to the predominantly diffuse loss. The remaining five (4.4%) patients had repeatable diffuse loss, which was probably due solely to open-angle glaucoma.

Conclusion: While diffuse visual field loss is exaggerated by factors other than glaucoma in the majority of patients, it can occur repeatedly in a small number of patients as the only sign of visual field damage.

Acknowledgment

This study was supported by grant #MT-11357 from the Medical Research Council of Canada, Ottawa, Canada.

Each author states that he/she has no proprietary interest in the development or marketing of these or competitive pieces of equipment.

Address for correspondence: Balwantray C. Chauhan, PhD, Department of Ophthalmology, Dalhousie University, 1335 Queen Street, Halifax, Nova Scotia, Canada B3J 2H6

Perimetry Update 1996/1997, p. 147
Proceedings of the XIIth International Perimetric Society Meeting
Würzburg, Germany, June 4–8, 1996
edited by M. Wall and A. Heijl

OPTIC DISC AND NERVE FIBER LAYER IMAGING

VALIDITY OF MEASUREMENTS WITH CONFOCAL SCANNING LASER DOPPLER FLOWMETRY

BALWANTRAY C. CHAUHAN[1,2] and FRANK M. SMITH[3]

Departments of [1]Ophthalmology, [2]Physiology and Biophysics, and [3]Anatomy and Neurobiology, Dalhousie University, Halifax, Nova Scotia, Canada

Introduction

Confocal scanning laser Doppler flowmetry is a promising new technique for estimating retinal and optic nerve head hemodynamics.[1] It has considerable clinical appeal since it can be carried out rapidly through natural pupils yielding perfusion maps of the imaged area with high spatial resolution.

While the technique, using the Heidelberg Retina Flowmeter (HRF, Heidelberg Engineering GmbH, Heidelberg, Germany), has good reproducibility,[1,2] its validity has not been established. It is important to determine the practical operating range of the HRF in addition to the linearity of measurements obtainable within this range. The purpose of this study was to derive a series of calibration curves using known fluid flow rates in glass capillaries of varying internal diameters.

Material and methods

Capillaries

A custom-made pipette puller with a single-coil heating element (18 ga. nichrome wire) was used to make capillaries from borosilicate glass tubing blanks (external diameter 1.7 mm). In order to ensure laminar flow through the capillary, the puller was set up to produce a center section of the desired diameter over at least 3 cm leaving segments of each end of the blank at the original diameter. We used 12 capillaries with internal diameters ranging from 705 to 25 μm. Internal diameters were measured using a Wild M5 microscope (Leica AG, Heebrugg, Switzerland) and a micrometer eyepiece.

Each author states that s/he has no proprietary interest in the development or marketing of these or competitive pieces of equipment.

Address for correspondence: Balwantray C. Chauhan, PhD, Department of Ophthalmology, Dalhousie University, 1335 Queen Street, Halifax, Nova Scotia, Canada B3J 2H6

Perimetry Update 1996/1997, pp. 151–154
Proceedings of the XIIth International Perimetric Society Meeting
Würzburg, Germany, June 4–8, 1996
edited by M. Wall and A. Heijl

Experimental set-up

Silastic tubing (internal diameter 1.0 mm) was slipped over each end of the capillary. One end was coupled to either a 25, 50 or 100 µl gas-tight syringe with a Luer-lock tip (Hamilton Company, Reno, NV) using a Luer-lock tapering tubing connector. The capillary was clamped at each end in a custom-built holder which was attached to the head-rest mount of the HRF.

The circuit first was primed with skim milk using a 1 ml disposable syringe. The filled gas-tight syringe was then connected to an infusion pump (SP200i, World Precision Instruments, Inc., Sarasota, FL) to infuse the capillary with skim milk at flow rates ranging from 1 to 2000 µl/hour. In order to minimize any hysteresis effects, a minimal length of silastic tubing from the syringe to capillary was used. The volume of the circuit from the connector tip to the capillary was around 15 µl.

After each experiment, the angle between the axis of the capillary and that of the HRF was carefully measured in order to compute the velocity vector parallel to the HRF axis.

Image acquisition

A custom-built lens holder was attached to the objective tube of the HRF. We used a +25 D lens for the initial experiments and a +90 D Volk lens with the smaller diameter capillaries. With the latter set-up and the HRF focus at 0 D, the image resolution, measured with an etched micrometer slide, was 9.43 microns/pixel (approximately the same as the *in vivo* resolution with a 10° scan angle).

We perfused the capillary with up to 18 different flow rates. We obtained five scans at each flow rate (single scans for first three capillaries) and waited at least 20 minutes at a new flow rate before image acquisition.

Data analysis

We used a 4 x 4 pixel measurement window to obtain the hemodynamic parameters at two locations. We measured at the same locations for the subsequent flow rates. Spearman's correlation coefficient was used to assess the correlation between the actual flow rate from the infusion pump and the mean HRF measured flow rate.

Results

There was a highly significant linear relationship between the HRF measured flow rate and the actual flow rate (r = 0.94 to 0.99 where multiple measurements were made). Since the flow rate through the capillary was constant for each setting on the infusion pump, the actual velocity can be determined by the following equation:

$$\text{velocity} = (4 \times \text{flow})/(\pi \times \text{diameter}^2)$$

The angle between the axis of the capillary and that of the HRF was between 12° and 20°. The HRF measured velocity as a function of the actual velocity vector parallel to the HRF axis superimposed for the different capillaries is shown in Figure 1. The data show that all but two calibration curves have almost identical slopes.

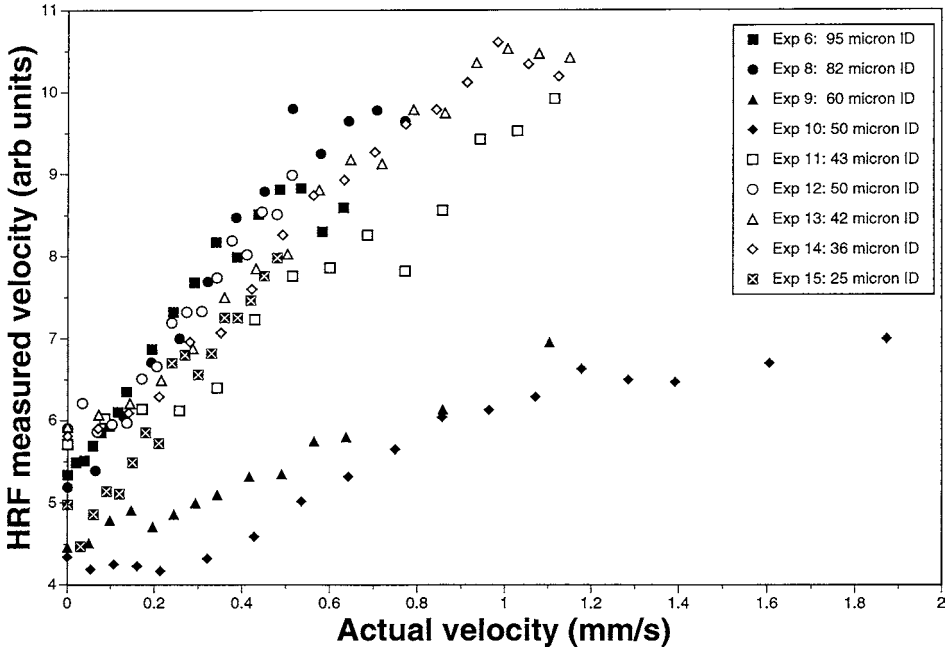

Fig. 1. Heidelberg Retina Flowmeter measured velocity as a function of the known velocity for one location in nine capillaries where five measurements for each flow rate were taken. Internal diameters are shown in the inset.

Hence, in different diameter capillaries with different flow rates, HRF estimates of velocity are generally accurate and increase linearly with actual velocity. There was a saturation effect at around 0.8 to 1.0 mm/sec, indicating that measurements beyond this value are not reliable.

Conclusions

Our study suggests that flow measurements with the HRF are linearly related to actual flow in a model system. Since the detector frequency of any laser Doppler flowmeter has a finite maximum, there is a corresponding maximum velocity that can be resolved. The HRF has a detector frequency of 2000 Hz, and our experiments suggest that the maximum detectable velocity is around 0.8-1.0 mm/sec (or 2.3-3.4 mm/sec in the plane of the capillary). These experiments therefore suggest that the HRF measures reliably and linearly in the range of velocities previously reported in the ocular microcirculation.[3]

Since experiments in glass capillaries have obvious differences compared to *in vivo* conditions, these results must be confirmed in *in vitro* and *in vivo* studies which are currently under way.

Acknowledgments

This study was supported by grants MT-11357 (BCC) and MA-11622 (FMS) from the Medical Research Council of Canada, a grant from the Camp Hill Medical Centre Research Fund (BCC), and a Scholarship from the Heart and Stroke Foundation of Canada (FMS).

References

1. Michelson G, Schmauss B: Two dimensional mapping of the perfusion of the retina and optic nerve head. Br J Ophthalmol 79:1126-1132, 1995
2. Chauhan BC, MacDonald CA, Rafuse PE: Variability of measurements in the retinal circulation using confocal scanning laser flowmetry. Invest Ophthalmol Vis Sci 36(Suppl):S109, 1995
3. Arend O, Wolf S, Harris A, Reim M: The relationship of macular microcirculation to visual acuity in diabetic patients. Arch Ophthalmol 113:610-614, 1995

REPRODUCIBILITY AND THE EFFECT OF OPERATOR-DEPENDENT VARIABLES IN IMAGING WITH THE NERVE FIBER ANALYZER II*

RICHARD P. MILLS, JAMES F.G. STEWART, YASUKO TAKAHASHI and MARTHA MOTUZ LEEN

Department of Ophthalmology, University of Washington, Seattle, Washington, USA

Abstract

The Nerve Fiber Analyzer II (NFA) (Laser Diagnostic Technologies, Inc., San Diego, CA, USA) is a computerized polarimeter designed for measuring the thickness of the peripapillary nerve fiber layer. Results from the previous model of the instrument (Nerve Fiber Analyzer I) proved to be very operator-dependent, so this study was designed to determine whether such operator dependence was also a feature of the NFA II.

Methods: To assess reproducibility, both eyes of five normal subjects were imaged on five occasions during a two-week period by each of three ophthalmic photographers. Three images of each eye were taken by each photographer during each examination (90 total images for each subject).

To assess operator-dependent variables, good quality baseline images were studied from a randomly chosen eye in ten glaucoma patients, and from both eyes in ten normal subjects. In the recommended analysis routine, the operator positions a green measurement ellipse set at a specified distance from a blue ellipse which is manually approximated to the edge of the optic disc. In all subsequent images of the same eye, the instrument positions the ellipses in the same position. The authors used three methods of positioning the inner ellipse:

1. Standard circle: a 60-pixel radius inner circle was centered on the optic disc.
2. Fitted oval: the inner ellipse was adjusted to outline the optic disc as closely as possible (manufacturer's recommendation). Focal correction was not used.
3. Fitted oval with correction: as in No. 2, except that focal correction was applied.

Data were recorded with outer measuring ellipse sizes from 1.2 disc diameters (DD), increasing by 0.1 DD increments to 2.3 DD, or until part of the measurement circle lay outside the image. The effects of decentration of the inner ellipse in the four primary directions was measured using a 1.75 DD measurement ellipse.

*After further patient acquisition and data analysis, the full paper will be published elsewhere.

No proprietary interest

Address for correspondence: Richard P. Mills, MD, University of Washington, Ophthalmology, Box 356485, Seattle, WA 98195-6485, USA

Perimetry Update 1996/1997, pp. 155–156
Proceedings of the XIIth International Perimetric Society Meeting
Würzburg, Germany, June 4–8, 1996
edited by M. Wall and A. Heijl

Results: The study of reproducibility of multiple images with the NFA II in normals produced a coefficient of variation of 4.9% with single images and 3.7% with baseline images made from three single images. Variation due to photographer or session effect was low, in contrast to experience with the NFA I.

There was no significant difference (p=0.48) in total integral nerve fiber thickness when a standard circle was used instead of fitting the disc, with or without focal correction. The effect of decentration of the ellipse did not appreciably affect the total integral result with decentrations up to 25% of the disc radius, but did so above that degree of decentration.

In every eye studied, there was a steady rise in the total integral with increasing diameter of the measurement ellipse. Nerve fiber layer thickness variation among normal individuals is lessened if a standard 60 pixel diameter inner ellipse is used to define 'disc diameter' rather than the true disc diameter, which varied from 1.24 to 2.17 mm in the authors' series. However, this effect is less apparent if the total integral is divided by the circumference of the measurement ellipse (mean total integral). Wide interindividual variation in total integral is not explained by variations in disc size, however.

Conclusions: In terms of total integral NFL thickness, it is not particularly important whether the shape of the measurement ellipse is defined by setting the inner ellipse to either a standard circle or an oval fitted to the disc margin. Focal correction makes little difference in total integral (although it does when other derivative calculations are performed). The inner circle centration is not critically important, as long as it is within 1/4 disc diameter of centered.

Since total integral increases with distance from the disc, NFA integral results using different settings cannot be compared. Total integral values have good reproducibility, even across experienced operators.

Acknowledgments

Supported in part by NIH Grant EY01730, and in part by an award from Research to Prevent Blindness, Inc. (New York, NY).

CORRELATION OF NERVE FIBER LAYER THICKNESS AS EVALUATED BY THE HEIDELBERG RETINA TOMOGRAPH AND OPTIC DISC HEMORRHAGE LOCATION

ALAIN BÉCHETOILLE, HÉLÈNE BRESSON-DUMONT and MALEK SLIM

Centre Hospitalier Universitaire d'Angers, Angers, France

Abstract

Background: The presence of hemorrhages on the optic nerve head is considered to be evidence of ischemic mechanisms in glaucoma patients. It is of clinical interest to establish a correlation between disc hemorrhages and thinning of the retinal nerve fiber layer (RNFL) in the corresponding area, as evaluated by the Heidelberg Retina Tomograph (HRT).
Methods: Twenty patients (24 eyes) with open-angle glaucoma, including patients with normal pressure and those with increased intraocular pressure, who were found to have a disc hemorrhage during routine disc photography, were enrolled in this study. All disc hemorrhages were observed between one and 72 months prior to enrollment. Mean RNFL thickness in a 10° sector corresponding to the hemorrhage was measured using the HRT and compared to the mirror-image position on the other side of the horizontal meridian. Mean RNFL thickness was also measured in the two 10° sectors surrounding the hemorrhage's 10° sector and a mean gradient of thickness was calculated between the hemorrhage site and that of the two adjacent sectors, positive (Δ+) and negative (Δ-).
Results: Mean RNFL was found to be significantly decreased in the 10° sector corresponding to the disc hemorrhage compared to the mirror image: n=24, 55±90 μm versus 140±110 μm, p=0.0001. There was a gradient between the thickness of the RNFL at the hemorrhage site and that of the two adjacent sectors: n=24, Δ- = 15±80 μm, Δ+ = 35±80 μm, p=0.012. However, the thickness gradient between the hemorrhagic zone and the adjacent sectors decreased with time when comparing recent RNFL hemorrhages occurring less than 14 months before the HRT examination, and old hemorrhages occurring more than 14 months before the HRT.
Conclusions: RNFL thickness was significantly smaller in areas of disc hemorrhages than in corresponding mirror-image areas of the disc circumference. It is possible that disc hemorrhages are clinical markers for the progression of localized RNFL defects. However, further investigation of this relationship is necessary.

Introduction

Hemorrhages on the optic disc associated with glaucoma were first described by Jannik Petersen Bjerrum in 1889 and, after a long period of silence, they were reintroduced by Stephen Drance in 1970.[1,2] Since then, they have been the subject of many publications, and their importance as an essential feature of glaucomatous optic

Address for correspondence: Alain Béchetoille, MD, Centre Hospitalier Universitaire d'Angers, 4 rue Larrey, 49033 Angers Cedex 01, France

Perimetry Update 1996/1997, pp. 157–161
Proceedings of the XIIth International Perimetric Society Meeting
Würzburg, Germany, June 4–8, 1996
edited by M. Wall and A. Heijl

neuropathy seems to have been growing steadily. They are encountered not only in primary open-angle glaucoma but also in normal-pressure glaucoma, ocular hypertension and retinal vein occlusion, but very seldom in normal eyes. Although some advocate a mechanical origin of the hemorrhages, most clinicians see in them a trace of an ischemia/reperfusion event, somewhere within the microcirculatory network irrigating the retinal nerve fiber layer (RNFL), with the likelihood of consequences for this structure.

Hemorrhages are generally superficial, flame-shaped or splinter-like, and pointed towards the exterior of the disc, but they can occasionally be round and deeper. They are generally located infero- or superotemporally along arcuate fiber bundles, with no obvious relationship with major retinal vessels.[3-7] In addition, they are transient, but recurrent. Consequently, the probability of their detection – between 5 and 10% of all glaucoma patients – increases with the number of observations, and this led Bengtsson and Krakau to put forward the hypothesis that most glaucoma patients are bleeders at one moment of the evolution of the disease. Others think that there are bleeders and non-bleeders among glaucoma patients.[8-12]

Currently, our knowledge of disc hemorrhages is limited. We do not exactly know the time-course of their occurrence. There is a fair amount of evidence to indicate that hemorrhages appear early in the course of the disease. They are correlated with localized, neuroretinal rim notches, circumscribed perimetric loss and RNFL defects. However, we quite frequently observe hemorrhages at one edge of a sector-shaped RNFL defect, or even in front of a slit-like defect, raising the idea of considering hemorrhage an early marker of a localized glaucomatous defect.[7,13-19]

The purpose of this study was to investigate the correlation between disc hemorrhages and thinning of the RNFL in the corresponding area, using the Heidelberg Retina Tomograph (HRT). The HRT provides rapid and reproducible measurements of optic disc tomography, as well as calculation of a number of disc parameters. Among the latter, the distance between a ‘reference plane’ and the retinal surface is used to evaluate the mean thickness of the RNFL. We adopted the reference plane defined parallel to the peripapillary retinal surface and located 50 mm posteriorly to the retinal surface at the papillo-macular bundle.

Methods

Twenty patients (ten females and ten males; mean age, 66.5 years) (24 eyes), with open-angle glaucoma, including ten patients with normal-pressure glaucoma and 12 with increased intraocular pressure, who were found to have a disc hemorrhage during routine disc photography, were enrolled in this study. Twelve hemorrhages were located temporosuperiorly, 12 temporoinferiorly. All disc hemorrhages were observed one to 72 months prior to enrollment. HRT measurement of RNFL thickness was at the level of the scleral ring. Mean RNFL thickness in a 10° sector corresponding to the hemorrhage was measured using the HRT and compared to the mirror-image position on the other side of the horizontal meridian. RNFL thickness was also measured in the two 10° sectors surrounding the hemorrhage’s 10° sector, in an attempt to determine whether hemorrhages were located at the edge of the RNFL, thinning down progression. Version 1.10 of the Heidelberg software was used with the Wilcoxon test for statistical analysis (Fig. 1).

a.

b.

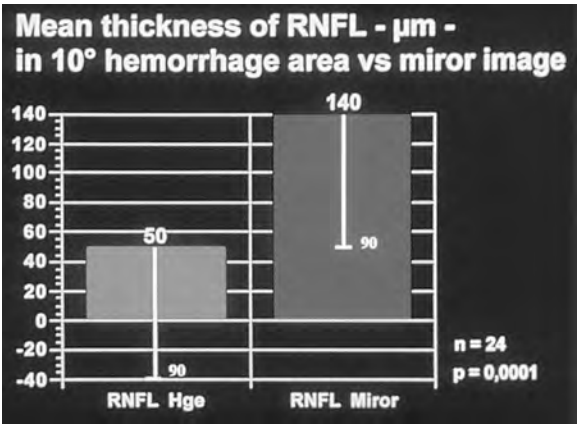

Fig. 1a. Splinter-like hemorrhages on the optic disc located at the edge of a RNFL defect. *b.* HRT measured RNFL thickness (in µm) is decreased at the level of the hemorrhage when compared to the mirror image on the other side of the horizontal meridian..

Results

Mean RNFL was found to be significantly decreased in the 10° sector corresponding to the disc hemorrhage compared to the mirror image: n=24, 55±90 µm versus 140±110 µm, p=0.001 (Table 1). There is a gradient between the thickness of the RNFL at the hemorrhage site and that of the two adjacent sectors: n=24, Δ- = 15±80 µm, Δ+ = 35±80 µm, p=0.012 (Table 2). However, the thickness gradient between the hemorrhagic zone and the adjacent sectors decreased with time ($p \leq 0.01$) when comparing recent RNFL hemorrhages occurring less than 14 months before the HRT examination (n=13, Δ- = 25±90 µm, Δ+ = 45±95 µm), and old hemorrhages occurring more than 14 months before HRT (n=11, Δ- = 15±120 µm, Δ+ = 20±130 µm) (Δ- [recent versus old]:$p \leq 0.1$; Δ+ [recent versus old]: $p \leq 0.01$).

Table 1. Mean thickness of RNFL in the hemorrhage's 10° sector versus mirror image

	Hemorrhage (μm)	*Mirror image (μm)*
Recent*	50 ± 110	145 ± 100
Old**	70 ± 140	135 ± 130
All**	55 ± 90	140 ± 110

*p=0.0001; **p=0.001

Table 2. Mean negative (Δ-) and positive (Δ+), gradient of thickness of RNFL in hemorrhage and adjacent sectors in recent, old, and all hemorrhages

	Adjacent sector (Δ-) (μm)	*Adjacent sector (Δ+) (μm)*
Recent	25 ± 90	45 ± 95
Old	15 ± 120	20 ± 130
All	15 ± 80	35 ± 80

Δ- [recent versus old]: $p \leq 0.1$; Δ+ [recent versus old]: $p \leq 0.01$

Conclusions

RNFL thickness was significantly smaller in areas of disc hemorrhages than in corresponding mirror-image areas of the disc circumference. There was a gradient between the thickness of the RNFL at the hemorrhage site and that of the two adjacent sectors. This would indicate that nerve fiber layer (NFL) hemorrhage may be a precursor or a marker of visual fiber loss. With time, the hemorrhage site itself becomes included in the area of fiber loss. Thus, fresh NFL hemorrhages probably indicate areas where NFL loss will occur secondarily. Older hemorrhages simply mark the site where NFL damage has already been done. However, further investigation of this relationship is necessary.

References

1. Bjerrum JP: Om en tillfojelse til den saedvanliga synsfeltsundergelse samt sunsfelt ved glaukom. Nord Ophthalmol Tidschr (Kbh) 2:141-185, 1889
2. Drance S, Begg IS: Sector haemorrhage: a probable acute ischaemic disc change in chronic simple glaucoma. Can J Ophthalmol 5:137-140, 1970
3. Kottler MS, Drance SM: Studies of haemorrhages of the optic disc. Can J Ophthalmol 11:102-105, 1976
4. Airaksinen PJ, Mustonen E, Alanko HI: Optic disc haemorrhages: analysis of stereophotographs and clinical data of 112 patients. Arch Ophthalmol 1(99):1795-1801, 1981
5. Drance SM: Disc hemorrhages in the glaucomas. Surv Ophthalmol 33(5):331-337, 1989
6. Collignon J, Borlon A: Optic disc hemorrhages and glaucoma. In: Béchetoille A (ed) Normal Pressure Glaucomas, pp 119-130. Angers: Japperenard 1990
7. Jonas JB, Xu L: Optic disk hemorrhages in glaucoma. Am J Ophthalmol 118(1):1-8, 1994
8. Gloster J: Incidence of optic disc haemorrhages in chronic simple glaucoma and ocular hypertension. Br J Ophthalmol 65:452-456, 1981
9. Bengtsson B, Holmin C, Krakau CE: Disc haemorrhage and glaucoma. Acta Ophthalmol (Kbh) 59:1-14, 1981

10. Bengtsson B: Optic disc hemorrhages preceding manifest glaucoma. Acta Ophthalmol (Kbh) 64(4): 450-454, 1990
11. Hendrickx KH, Van den Eden A, Rasker MR, Hoyng PFJ: Cumulative incidence of patients with disc hemorrhages in glaucoma and the effect of therapy. Ophthalmology 101(7):1165-1172, 1994
12. Drance S, Fairclough M, Butler D, Kottler MS: The importance of disc haemorrhage in the prognosis of chronic angle glaucoma. Arch Ophthalmol 95:226-228, 1977
13. Susana R, Drance S, Douglas G: Disc haemorrhage in patients with elevated intraocular pressure occurrence with and without field changes. Arch Ophthalmol 97:284-285, 1979
14. Airaksinen PJ, Mustonen E, Alanko HI: Optic disc haemorrhages precede retinal nerve fibre layer defects in ocular hypertension. Acta Ophthalmol (Kbh) 2(59):627-641, 1981
15. Kitazawa Y, Shirato S, Yamamoto T: Optic disc haemorrhage in low-tension glaucoma. Ophthalmology 93(6):853-857, 1986
16. Heijl A: Frequent disc photography and computerized perimetry in eyes with disc haemorrhage. Acta Ophthalmol (Kbh) 64:274-281, 1986
17. Tuulonen A, Takamoto T, Ching WUD, Schwartz B: Optic disc cupping and pallor measurements of patients with a disc hemorrhage. Am J Ophthalmol 103:505-511, 1987
18. Diehl DLC, Quigley HA, Miller NR, Sommer A, Burnez EN: Prevalence and significance of optic disc hemorrhage in a longitudinal study of glaucoma. Arch Ophthalmol 108(4):545-550, 1990
19. Krakau CET: Disk hemorrhages and retinal vein occlusions in glaucoma. Symposium Ocular blood flow in the progression and therapy of glaucoma. Surv Ophthalmol (Suppl)38:S18-S22, 1994
20. Mikelberg FS, Parfitt GM, Swindale N, Graham SL, Drance SM, Gosine R: Ability of the Heidelberg Retina Tomograph to detect early glaucomatous visual field loss. J Glaucoma 4:242-247, 1995

NERVE FIBER LAYER THICKNESS EVALUATIONS IN THE UPPER AND LOWER RETINAL HALF USING THE NERVE FIBER ANALYZER I
A clinical study

S. SERGUHN[1] and E. GRAMER[2]

[1]University Eye Hospital, Ulm; [2]University Eye Hospital, Würzburg; Germany

Abstract

Purpose: Questions evaluated: *1.* Is there a conformity between the up-down asymmetry of visual field loss (VFL) and the up-down asymmetry of nerve fiber layer thickness (NFLT), calculated by laser polarimetry (LP)? *2.* Is there any asymmetry in NFLT between the upper and lower retinal halves in normals?
Methods: 1. Thirty-eight eyes of 38 glaucoma patients with VFL up-down asymmetry were examined. NFLT was measured by LP, using the Nerve Fiber Analyzer (NFA I), VFL by using the Octopus Perimeter (Program 31 or 32). By changing NFA software, it was possible to calculate NFLT separately in the upper and lower halves of the retina. The authors divided the glaucomatous eyes into groups with small, medium or large up-down visual field asymmetry. *2.* NFLT was examined in the upper and the lower retinal halves in 62 healthy eyes of 62 control subjects.
Results: 1. In eyes with small up-down asymmetries of VFL, there was a greater conformity between the up-down asymmetry of VFL and the up-down asymmetry of NFLT (ten of 14 eyes), than in eyes with medium (seven of 12 eyes) or large size (six of 12 eyes). *2.* In healthy eyes, NFLT was approximately 6% higher in the lower than in the upper half of the retina. *3.* Even when this NFLT asymmetry in normals was taken into consideration, glaucomatous eyes with a large asymmetry of VFL showed only a slightly higher conformity (seven of 12 eyes).
Discussion: In about 40% of glaucomatous eyes, there was no conformity between the up-down asymmetry of VFL and the up-down asymmetry of NFLT. Therefore, staging of the glaucomatous disease by LP (software version 06/93) does not seem to be possible.

Introduction

The Nerve Fiber Analyzer I (NFA I) allows a measurement of the retinal nerve fiber layer thickness (NFLT). The conformity of measured NFLT with the stage of visual field loss (VFL) in glaucoma patients has not yet been tested. Staging of glaucomatous damage with laser polarimetry (LP) could be faster and more independent of patient cooperation than perimetric measurements. The purpose of this study was to investigate: whether there is any difference between NFLT in the upper and the lower

Address for correspondence: Prof Dr. med. Dr. jur. E. Gramer, University Eye Hospital Würzburg, Josef Schneider Strasse 11, D-97080 Würzburg, Germany

Perimetry Update 1996/1997, pp. 163–171
Proceedings of the XIIth International Perimetric Society Meeting
Würzburg, Germany, June 4–8, 1996
edited by M. Wall and A. Heijl

retinal halves in normals; and whether there is any conformity between the up-down asymmetry of VFL and the up-down asymmetry of NFLT in glaucoma patients.

Methods

After a verbal explanation, all patients agreed to be examined with the NFA I.

Healthy eyes

NFLT was examined in 62 healthy eyes of 62 control subjects. In 23 healthy eyes of 23 patients (Group 1), we performed a biomicroscopical and an automated visual field examination. These eyes, *e.g.*, second healthy eyes in cases of perforating injury in the other eye, had their NFLT examination carried out by a first examiner. In 39 healthy eyes of 39 controls (Group 2), no perimetry was performed. Examination of this control group was carried out by a second examiner. Measurement results from healthy eyes were analyzed separately for Group 1 and 2, and for both groups together.

Glaucomatous eyes

Thirty-eight eyes of 38 glaucoma patients (30 eyes with POAG, eight with LTG) were examined. Inclusion criteria for glaucoma patients were a defined up-down asymmetry of VFL in earlier visual fields, no eye diseases other than glaucoma and a refractive error $<\pm 3$ diopters (D).

NFLT measurements[1,2] in retinal halves using NFA I
NFLT measurements were performed using the Nerve Fiber Analyzer I (NFA I) (Laser Diagnostic Technologies, San Diego, CA). The retina is examined using a low intensity infrared laser beam (780 nm). While penetrating the nerve fiber layer, polarization of the laser beam is changed proportional to NFLT.[1] After reflection in deeper retinal layers, the backscattered light is analyzed by means of a polarization sensitive detector within NFA I. NFLT is calculated using the change of the polarization of the laser beam. The polarizing quality of the cornea is compensated by a special method which has not yet been published. We changed the software of the NFA I, so that NFLT values could be calculated separately for the upper and the lower retinal halves. After imaging the optic disc using the 15° scan angle, the examiner defines a measurement circle around the papilla approximately 1.5x the optic disc diameter.

Perimetry
Computerized perimetry was performed with the Octopus Perimeter 201 (Program 31 or 32), or with the Humphrey Perimeter (Program GG).[3] Mean VFL per test point was calculated for the upper and the lower visual hemifields, while excluding the test points in the region of the blind spot.

Calculation of hemifield quotients for VFL and NFLT
An asymmetry index for VFL (glaucoma hemifield index, GHI) and NFLT (retinal asymmetry index, RAI) was calculated using measurement values from upper and

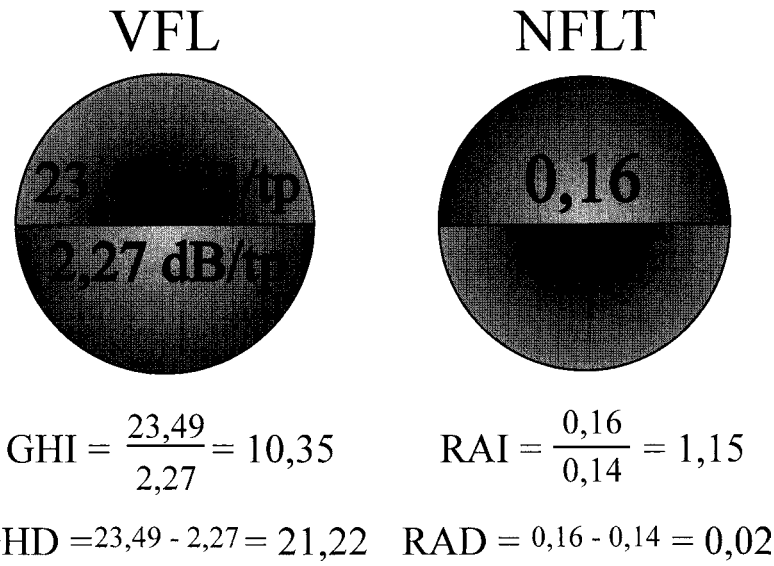

Fig. 1. GHI/RAI and GHD/RAD of the right eye of a patient with POAG. VFL in the upper visual hemifield was 23.49 dB/test point, in the lower visual hemifield 2.27 dB/test point. The NFLT value in the upper retinal half was 0.16, in the lower retinal half 0.14. Therefore, we calculated a GHI of 10.35 (GHD of 21.22 dB/test point) and a RAI of 1.15 (RAD of 0.02). A larger VFL in the upper visual hemifield corresponded with a lower NFLT value in the lower retinal half and *vice versa*.

lower visual hemifields or retinal halves (shown in Fig. 1). The asymmetry index shows the loss of the lower visual hemifield, or retinal half, directly as a percentage of the upper half. The GHI was defined as a quotient of the mean VFL of the upper to lower visual hemifields. The RAI was defined as a quotient of NFLT of the upper to lower retinal halves.[4,6]

Calculation of hemifield differences for VFL and NFLT

An asymmetry difference for VFL (glaucoma hemifield difference, GHD)[7,8] and NFLT (retinal asymmetry difference, RAD) was calculated using measurement values from the upper and lower visual hemifields, or retinal halves (shown in Fig. 1). The GHD was defined as the difference of the mean VFL values of the upper and lower visual hemifields. The RAD was defined as the difference of the mean NFLT of the upper and lower retinal halves.[4,5]

Definition of asymmetry of VFL

We divided the glaucomatous eyes corresponding to the degree of VFL asymmetry into three groups by using the following arbitrary definition of GHI:

Group 1 (up-down asymmetry of VFL <1:2 (*n*=14))
Group 2 (up-down asymmetry of VFL >1:2 and <1:5 (*n*=12))
Group 3 (up-down asymmetry of VFL >1:5 (*n*=12))

Statistical methods

Correlation between GHI and RAI was tested by regression analysis. Spearman's coefficient was calculated. The difference in NFLT between the upper and lower

Table 1. NFLT in the upper and lower retinal halves of 62 normals

Groups	*Average NFLT value (mm^2)*	*Average RAI*	*Quantity of larger NFLT value*	*Probability p (Wilcoxon test)*
Examiner/Group 1 (n=23)				
Upper retinal half	0.219±0.049	0.94	(upper>lower retinal half) 6	0.046
Lower retinal half	0.234±0.043		(lower>upper retinal half) 17	
Examiner/Group 2 (n=39)				
Upper retinal half	0.326±0.052	0.942	(upper>lower retinal half 10	0.00395
Lower retinal half	0.348±0.054		(lower>upper retinal half) 29	
All (n=62)				
Upper retinal half	0.286±0.072	0.942	(upper>lower retinal half) 16	0.00022
Lower retinal half	0.306±0.075		(lower>upper retinal half) 46	

retinal halves in healthy eyes was tested using the Wilcoxon test. Moreover, we tested all eyes, whether a larger VFL in one visual hemifield corresponded to a smaller NFLT in the corresponding retinal half, or *vice versa*. The relative quantity of conformity between NFLT and VFL was calculated.

Results

Healthy eyes

Asymmetry of NFLT between the upper and the lower retinal halves

In 46 healthy eyes of 62 subjects (74%), there was a thicker NFLT in the lower than in the upper retinal halves. The NFLT in the lower retina was on average 6.9% (0.286±0.072 mm^2 in the upper retina and 0.306±0.075 mm^2 in the lower retina) thicker compared to the upper retina (Table 1). This asymmetry of NFLT between the upper and lower retinal halves in normals was significant (Wilcoxon test, p=0.00022). The average RAI was 0.942 and described a physiological asymmetry of NFLT which was used as a correction factor.

There were significantly larger NFLT values in the lower than in the upper retinal halves in 23 healthy (top), 39 healthy (middle) and all 62 healthy (bottom) eyes. Average NFLT was 6.9% greater in the lower than in the upper retinal halves in normals

Glaucomatous eyes

Correlation of VFL (GHI, GHD) and NFLT (RAI, RAD)

We found a significant correlation between the NFLT values in the upper and the lower retinal halves and the corresponding VFL. There was a significant correlation between GHI and RAI: Spearman's coefficient (r=0.4714, p=0.0028 (p<0.05)) (Table 2). There was a significant correlation between GHD and RAD: Spearman's coefficient (r=0.3629, p=0.025 (p<0.05)) (Table 2). In 23 of 38 eyes (62%), there was a smaller peripapillary NFLT in the retinal half with larger VFL in the corresponding visual hemifield (Table 2). There was a higher conformity in the group with small VFL asymmetry (ten of 14 eyes) than in the groups with medium (seven of 12 eyes) or large (six of 12 eyes) (Table 2). Asymmetry groups also differed as to the stage

Table 2. Conformity of VFL and NFLT for groups with different asymmetry in VFL with and without correction factor

Asymmetry of VLF	*Mean glaucoma hemifield difference (GHD) (dB/TP)*	*Eyes/patients*	*Without 'correction factor'*		*With 'correction factor'*	
			Spearman coefficient	*Conformity (No. of eyes)*	*Spearman coefficient*	*Conformity (No. of eyes)*
Small asymmetry <1:2	-1.694±4.767	14	*r*=-0.495 *p*=0.16	10 of 14	*r*=-0.1958 *p*=0.5638	8 of 14
Medium asymmetry >1:2 and <1:5	4.747±-7.086	12	*r*=0.2067 *p*=0.57	7 of 12	*r*=0.2587 *p*=0.4747	7 of 12
Large asymmetry >1:5	10.995±-9.683	12	*r*=0.0699 *p*=0.85	6 of 12	*r*=0.3846 *p*=0.2886	7 of 12
All	4.347±-8.874	38	*r*=0.4718 *p*=0.0025	23 of 38	*r*=0.4665 *p*=0.0032	22 of 38

of the disease, because the group with a small VFL asymmetry (GHI) showed a smaller average GHD than the group with medium or large asymmetries of VFL (GHI) (Table 2). When considering the identified NFLT asymmetry in normals, an equal conformity between larger VFL in one visual hemifield and smaller peripapillary NFLT in the corresponding retinal half was found in the three asymmetry groups. Conformity between RAI and GHI did not differ significantly in the group with small VFL asymmetry (eight of 14 eyes) and the groups with medium (seven of 12 eyes) or large (seven of 12 eyes) asymmetries. Furthermore, in 16 of 38 eyes (42%) there was no conformity between the up-down asymmetry of VFL and the up-down asymmetry of NFLT (Table 2).

In the case of a low GHI, examined glaucomatous eyes also showed a low average GHD and *vice versa*. Therefore, larger VFL asymmetry corresponded to a larger total VFL per test point, *i.e.*, advanced glaucomatous disease. Without the correction factor, conformity of asymmetry of VFL and NFLT values decreased in advanced stages of the disease, while with the correction factor, an equal conformity was found in all three asymmetry groups. Total conformity without and with correction factor was only 62% (58%).

Discussion

Healthy eyes

A surprising result was that we found a 6.9% larger NFLT in lower than in upper retinal halves in normals (Table 1). This physiological asymmetry of NFLT values is not verified by earlier histological examinations of the peripapillary NFLT.[9,10] In contrast to our LP measurement results, histological NFLT measurements of normal primates' eyes[9] showed larger NFLT in upper than in lower retinal halves (Fig. 2).

This study cannot answer the question whether *in vivo* measured LP NFLT values correspond to actual NFLT. Histological examinations of the peripapillary nerve fiber layer more often showed thicker nerve fiber axons within the inferior than within the superior papillomacular bundle.[9] It is not known whether this could cause an asymmetry of absolute NFLT values. Histological examinations of the course of the peripapillary nerve fibers showed that peripheral nerve fiber axons are located in the deeper retinal layers and in the peripheral parts of the optic nerve head, whereas peripapillary nerve fiber axons are located in the superficial retinal layers and in the central parts of the optic nerve head.[11] These results are verified by our own examinations of glaucomatous VFL.[12] No asymmetry of the peripapillary nerve fibers has been found between the superior and inferior papillomacular bundles.[11,13] Therefore, LP NFLT measurements do not seem to be disturbed by different courses of the peripapillary nerve fibers in the superior and inferior papillomacular bundles. Perhaps the evaluated asymmetry of NFLT values in normals is caused by LP itself. LP NFLT measurements only seem to be possible if the peripapillary nerve fibers are arranged in a parallel position. One explanation for the asymmetry of NFLT values in normals could be differences in the parallelism of the peripapillary nerve fibers between the superior and inferior papillomacular bundles. From our anatomical knowledge, we expected to see larger NFLT values in the temporal-superior and temporal-inferior parts around the optic nerve head. The largest NFLT values by LP, however, were found along the vertical axis through the optic nerve head. Earlier examinations using

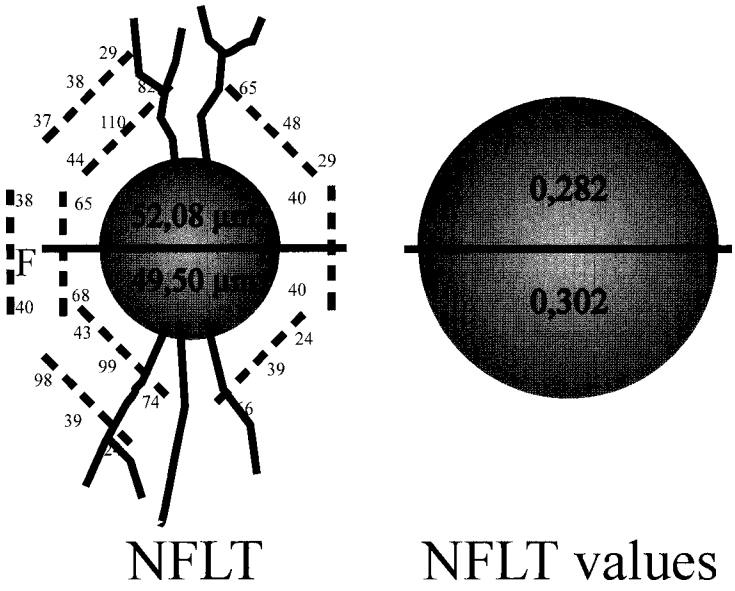

Fig. 2. A combination of print-wise NFLT measurements in the upper and lower retinal halves of nine healthy primates eyes (*left*) and the LP NFLT value of 62 normals in the upper and lower retinal halves (*right*). Histological NFLT measurements of the healthy primates eyes showed larger NFLT in the upper than in the lower retinal halves, in contrast to LP measurements. (Modified according to Quigley and Addicks.[9])

the optic nerve head analyzer (ONHA) (Rodenstock, Munich, Germany) and laser-scanning-tomography[5,14-17] showed a typical 'double-hump' configuration[15,16] with humps temporally-superior and temporally-inferior. In earlier studies, we used the height difference (HD) value of the nerve fiber layer between Elschnig's ring and the peripapillary retina as a value for NFLT, and found this value to depend on the age of the patients.[17] Compared with this absolute HD value, the asymmetry index (RAI) did not depend on age. If RAI differs from our evaluated asymmetry of NFLT values in normals, it might be used as an indicator of a starting glaucomatous disease[18] and increase the validity of a retinal hemifield index.

Glaucomatous eyes

Our hypothesis was that there is a correlation between VFL in one visual hemifield and a loss of NFLT in the corresponding retinal half.[19,20] Examination of 38 glaucomatous eyes showed a correlation between VFL and NFLT values (Table 2), so that a connection between the measurement value calculated by LP and NFLT appeared possible. However, our results suggested that the diagnostic validity of LP diminished with the increasing stage of the glaucomatous disease because an increasing asymmetry of VFL (GHI) did not correspond to an increasing asymmetry of NFLT (RAI). The larger the asymmetry in VFL (GHI), the smaller the conformity with the RAI. Perhaps in advanced stages of the disease with increased loss of nerve fibers, LP measurements are increasingly influenced by the polarizing quality of other structures (for example, the cornea).[2] Surprisingly, an eye with absolute VFL in one

hemifield did not show a zero value for NFLT in the corresponding retinal half (see Fig. 1). Also, in advanced stages of the disease, the small conformity could have been caused by the exclusively used 30° visual field, since a possible large and asymmetrical peripheral VFL would not be quantified. A disadvantage of asymmetry indices is that a large GHI could even be caused by a small and asymmetrical VFL. Yet our conclusions seem to be correct, since we also found a significant correlation using asymmetry differences (GHD, RAD).[4] Moreover, in the present study, the examined glaucomatous eyes with a small GHI also showed a small average GHD and *vice versa* (Table 2). Therefore, greater VFL asymmetry corresponded to a larger total VFL per test point, indicating an advanced stage of the glaucomatous disease. An additional use of asymmetry indices seems to be reasonable. Because of missing standard values of LP measurements, our evaluated asymmetry of NFLT in normals was used as a correction factor. This improved the conformity of VFL and NFLT in the group of patients with large VFL asymmetries (Table 2). Nonconformity was still present between the up-down asymmetry of VFL (GHI) and the up-down asymmetry of NFLT (RAI) in 16 of 38 examined glaucomatous eyes (42%).

We conclude that LP does not seem to allow staging of the glaucomatous disease.[21] Possibly, conformity between the up-down asymmetry of VFL and the up-down asymmetry of NFLT could be improved by using the changed software of the NFA (NFA II).

Acknowledgments

This study describes in parts the results of the dissertation of S. Serguhn. The authors wish to thank Dr I. Haubitz for her advice on the statistical analysis. The authors also thank Dr U. Harbarth (Laser Diagnostic Technologies, San Diego, CA) for the necessary changes to the software of the Nerve Fiber Analyzer I.

References

1. Dreher AW, Reiter K: Scanning laser polarimetry of the retinal nerve fiber layer. In: Goldstein DH, Chipman RA (eds) Polarization Analysis and Measurements, pp 34-41. Proceedings SPIE 1746, 1992
2. Rohrschneider K, Burk ROW, Kruse F, Völcker HE: Zur Bestimmung der retinalen Nervenfaserschichtdicke in vivo mittels Laser-Polarimetrie. Klin Mbl Augenheilk 203:200-205, 1993
3. Roesen B, Gramer E: Perimetrie mit einem glaukomspezifischen Prüfpunktraster: eine Pilotstudie mit dem GG-Programm. Ophthalmologe 92:506-510, 1995
4. Serguhn S, Gramer E: Läßt sich mittels Laser-Polarimetrie durch in vivo Messung der retinalen Nervenfaserschichtdicke das Ausmaß des Glaukomschadens quantifizieren? Eine klinische Studie. Ophthalmologe 93:527-534, 1996
5. Serguhn S, Gramer E: Is middle relative height of the peripapillary retina, calculated by laser scanning tomography, a measurement value for nerve fiber layer thickness in glaucoma? A clinical study. Invest Ophthalmol Vis Sci 36/4:4513, 1995
6. Serguhn S, Gramer E: Evaluation of measurements of retinal nerve fiber layer thickness with polarization technology for methods of automated analysis of upper and lower retina in glaucoma: a clinical study. Invest Ophthalmol Vis Sci 35/4:1345, 1994
7. Åsman P, Heijl A: Evaluation of methods for automated hemifield analysis in perimetry. Arch Ophthalmol 110:820-826, 1992
8. Åsman P, Heijl A: 'Glaucoma hemifield test': automated visual field evaluation. Arch Ophthalmol 110:812-819, 1992
9. Quigley HA, Addicks EM: Quantitative studies of retinal nerve fiber layer defects. Arch Ophthalmol 100:807-814, 1982

10. Skaf M, Barron E, Heller K, Varma R: Retinal nerve fiber layer thickness in normal human eyes. Invest Ophthalmol Vis Sci 37/4:5043, 1996
11. Minckler DS: The organization of nerve fiber bundles in the primate optic nerve head. Arch Ophthalmol 98:1630-1636, 1980
12. Gramer E, Althaus G: Quantifizierung und Progredienz des Gesichtsfeldschadens bei Glaukom ohne Hochdruck, Glaucoma simplex und Pigmentglaukom. Klin Mbl Augenheilk 191:184-198, 1987
13. Minckler DS, Ogden TE: Primate arcuate nerve fiber bundle anatomy. In: Greve EL, Heijl A (eds) Doc Ophthalmol Proc Ser, Vol 49, pp 605-612. Dordrecht: Martinus Nijhoff, Dr W Junk 1987
14. Burk ROW, Rohrschneider K, Kruse FE, Völcker HE: Laser Scanning Tomographie der Papille. In: Gramer E (ed) Glaukom: Diagnostik und Therapie, pp 113-119. Stuttgart: Enke Verlag 1990
15. Caprioli J: The contour of the juxtapapillary nerve fiber layer in glaucoma. Ophthalmology 97:358-367, 1990
16. Caprioli J, Ortiz-Colberg R, Miller JM, Tressler C: Measurement of peripapillary nerve fiber layer contour in glaucoma. Am J Ophthalmol 108:404-413, 1989
17. Maier H, Siebert M, Gramer E, Kampik A: Eine Maßzahl für die Nervenfaserschichtdicke. Messungen mit dem Laser Tomographic Scanner (LTS): eine klinische Studie. In: Gramer E (ed) Glaukom: Diagnostik und Therapie, pp 120-145. Stuttgart: Enke Verlag 1990
18. Gramer E, Tausch M: The risk profile of the glaucomatous patient. Curr Opin Ophthalmol 6(2):78-88, 1995
19. O'Brien C, Schwartz B, Takamoto T: Correlation of optic disc cupping, pallor and retinal nerve fiber layer thickness with visual field loss in chronic open angle glaucoma. In: Mills RP, Heijl A (eds) Perimetry Update 1990/1991, pp 15-22. Amsterdam/New York: Kugler Publ 1991
20. Takamoto T, Schwartz B, Nangia V: Relation of asymmetrical differences of visual fields between open angle glaucoma eyes with measurements of optic disc cupping, pallor and retinal nerve fiber layer thickness. In: Mills RP, Heijl A (eds) Perimetry Update 1992/1993, pp 215-223. Amsterdam/New York: Kugler Publ 1993
21. Tjon-Fo-Sang MJ, Lemij HG: The correlation between visual fields and NFL thickness as determined with the Nerve Fiber Analyzer (NFA). Invest Ophthalmol Vis Sci 37/4:5042, 1996

MEAN PALLOR VALUE OF THE OPTIC DISC
A new parameter in automated disc analysis with the optic nerve head analyzer

MICHAEL SIEBERT and EUGEN GRAMER

University Eye Hospital, Würzburg, Germany

Introduction

Compared to recent confocal examination techniques the optic nerve head analyzer (ONHA) determines the pallor of the optic disc, as well as the well-known parameters of optic disc topography, such as rim area and cup/disc ratio.[1-5]

Purpose

Our aim was to describe the measurement of optic disc pallor and calculate the mean pallor value (MPV) of the optic disc. The clinical relevance of this pallor measurement is demonstrated and discussed with regard to the following questions: *1.* Is there a difference in MPV among healthy eyes, ocular hypertensives (OH) and eyes with primary open-angle glaucoma (POAG)? *2.* Is there a larger MPV in eyes with deterioration of visual fields in OH and POAG? *2.* What additional information and limitations can be expected using MPV in the long-term follow-up of glaucoma patients and glaucoma suspects?

Methods

Two special photographs of the fundus are taken for measurement of optic disc pallor: one with green and one with red illumination. The intensity of reflected green and red light is measured, and a pallor value is calculated for about 1000 pixels in the area of the optic nerve head.

The pallor value is twice the intensity of the reflected green light divided by the sum of the intensities of green and red light. Therefore, the range of pallor values is from zero to two:

Address for correspondence: M. Siebert, MD, University Eye Hospital, Josef-Schneider-Strasse 11, D-97080 Würzburg, Germany

Perimetry Update 1996/1997, pp. 173–178
Proceedings of the XIIth International Perimetric Society Meeting
Würzburg, Germany, June 4–8, 1996
edited by M. Wall and A. Heijl

$$PV = \frac{2 * \text{intensity (reflected green light)}}{\text{intensity (reflected green light)} + \text{intensity (reflected red light)}}$$

Zero implies pure reflection of red light and no reflection of green light. A higher pallor value results from a larger amount of green light being reflected, while only some of the red light is sent back from the disc, for example, by the surface of a pale structure such as the lamina cribrosa.

The different pallor values for all pixels in the area of the optic disc are color-coded on the computer screen. Elements with predominant reflection of red light have small pallor values and are depicted in red, orange or yellow. With increasing pallor, the pixels are shown in green, blue, violet, grey and white (Figs. 1 and 2).

The part of each pallor value-range related to the total area of the optic disc is determined by the computer, resulting in a histogram of pallor values. Additionally, we calculated a new parameter, called the mean pallor value (MPV), of the optic disc in order to obtain a single number to characterize the color (suggesting vitality) of the optic nerve head.

$$MPV = \frac{\Sigma(\text{pallor values of all pixels in the area of the disc})}{\text{number of disc pixels}}$$

The mean pallor value was calculated from double examinations with the ONHA in 99 eyes of 99 patients, 34 healthy eyes, 12 ocular hypertensives, and 53 eyes with POAG. The Mann-Whitney test was used to detect differences in MPV in patients with different diagnoses. The same analysis was carried out for the cup/disc ratio (CDR) values of these patients.

A long-term follow-up of the visual fields was carried out after initial double measurement of the MPV in 33 patients with well-controlled intraocular pressure: ten ocular hypertensives and 23 eyes with POAG. The follow-up range was two to 5.5 years, with an average of 3.6 years (±1.1 years (SE)).

The visual field tests were performed by computerized perimetry either with the Octopus 201 (Program 32) or the Humphrey Field Analyzer (Program 30-2).

A significant visual field loss was assumed with a defect of >4 dB in more than four test points or a defect of >9 dB in more than two test points, disregarding test points in the area of the blind spot. In ocular hypertensives, the development of a visual field defect was defined as a transition from normal visual field to significant visual field loss. The criteria for deterioration of visual fields in glaucoma were either a doubling in total loss or an increase in total loss of at least 200 dB. The Mann-Whitney test was used to determine significant differences in MPV in eyes with or without deterioration of visual fields.

Results

The average MPV was 0.28 (±0.07 (standard error (SE)) in healthy eyes and 0.32 (±0.05 (SE)) in ocular hypertensives, a statistically significant difference. The mean pallor value was higher in ocular hypertensives than in healthy eyes ($p<0.05$). The

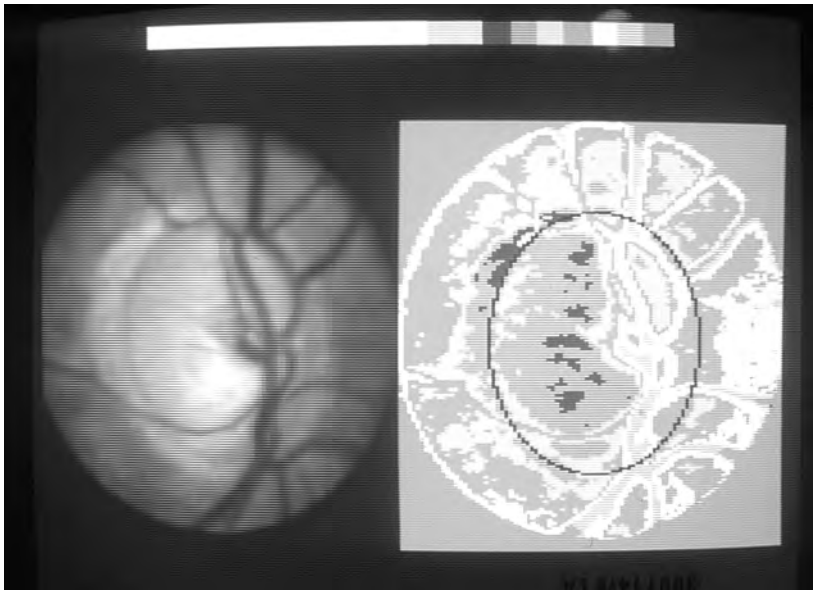

Fig. 1. Optic disc of a glaucoma patient. Pallor map (right) and fundus photograph (left) as shown by the optic nerve head analyzer (ONHA).

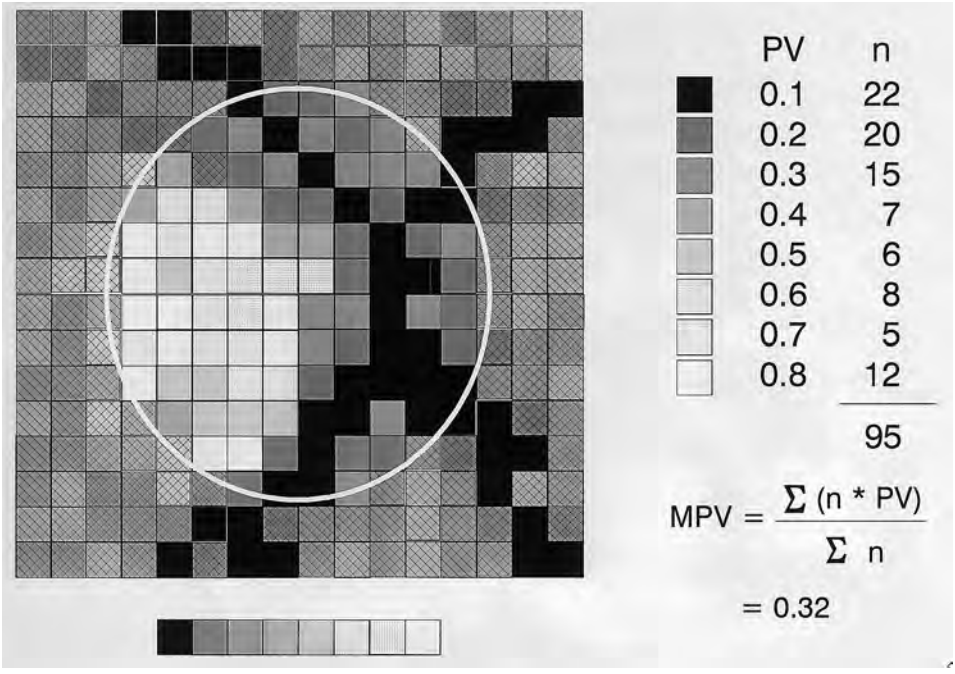

Fig. 2. Schematic drawing demonstrating the subdivision of the examined fundus area into picture elements (pixels). Structures with different pallor values are depicted in different colors. A pallor value histogram and the calculation of the MPV is shown.

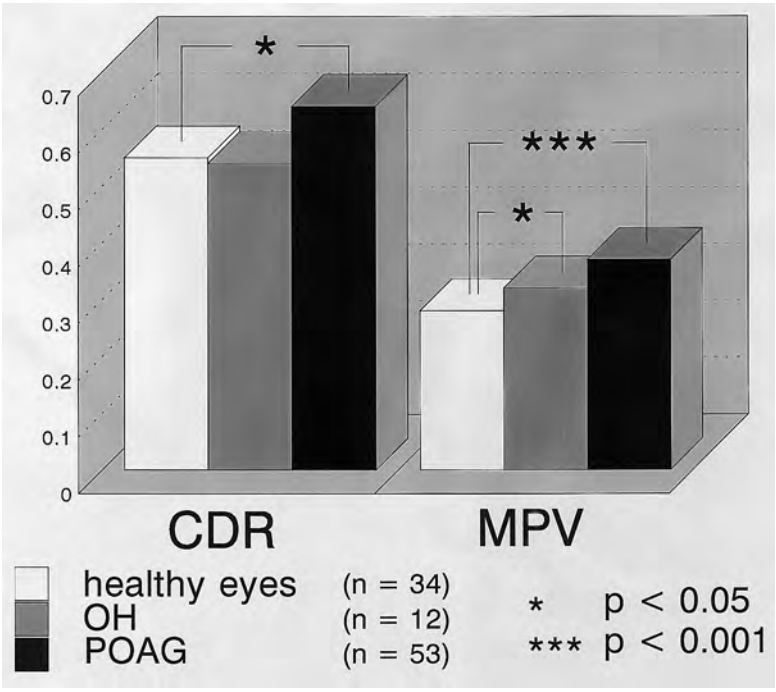

Fig. 3. Mean values for cup/disc ratio (CDR) and mean pallor value (MPV) in healthy eyes (*n*=34), ocular hypertensives (OH) (*n*=12), and eyes with primary open-angle glaucoma (POAG) (*n*=53).

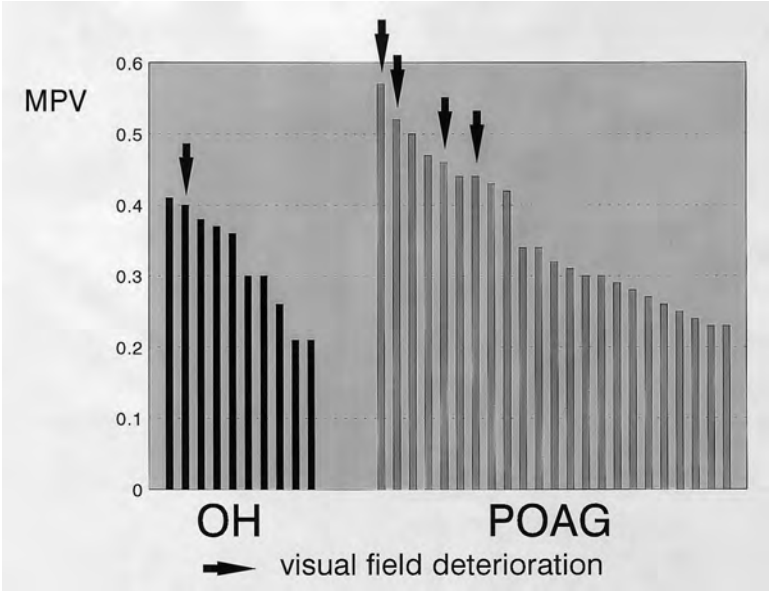

Fig. 4. Mean pallor values in ocular hypertensives (OH) and eyes with primary open-angle glaucoma (POAG) with or without deterioration of the visual fields during the follow-up period.

MPV in eyes with POAG was 0.37 (±0.09) (mean value ±SE), this also being significantly higher than in healthy eyes ($p<0.001$) (Fig. 3).

In contrast to these results, the cup/disc ratio was about the same in healthy eyes, with an average of 0.55 (±0.15), and in ocular hypertensives with an average of 0.54 (±0.23). As expected by the definition of glaucoma, the CDR was significantly higher in the glaucoma group compared to healthy eyes, with an average of 0.64 (±0.16; $p<0.05$) (Fig. 3).[6]

The long-term follow-up of visual fields revealed an increase in visual field loss in five of 33 patients (one OH, four POAG) in spite of controlled IOP (<22 mmHg). In ocular hypertensives, MPV was 0.40 in the eye developing visual field defect compared to 0.31 (±0.07) (mean ±SE) in nine eyes, also being classified as ocular hypertensives at the end of the follow-up period (Fig. 4). In POAG, the average MPV of 0.50 (±0.06) in four eyes with deterioration was significantly higher than 0.33 (±0.08) in 19 eyes with no deterioration ($p<0.005$).[7] Those eyes with a tendency to deteriorate showed a higher MPV at the beginning of the observation period compared to those with no deterioration.

Discussion

In accordance with our results, when evaluating the area of pallor as a ratio of disc area, other researchers have found this parameter to be greater in glaucomatous eyes than in ocular hypertensive eyes, and ocular hypertensives to have greater areas of pallor than normal eyes.[8]

In a follow-up study of 54 eyes of 29 ocular hypertensives, Kitazawa *et al.* found that seven eyes which developed glaucomatous visual field loss had a significantly greater pallor area/disc area ratio on initial examination compared to 47 eyes which did not develop visual-field loss.[9] Our results are in good agreement with these findings. Although, in our study there was no statistically significant difference in visual field defects, there was a clear tendency for higher total loss values in the eyes with POAG to develop further visual field deterioration compared to the eyes with non-progressive visual field defects. This supports the clinical observation that eyes with greater glaucomatous damage are predisposed to further deterioration.

Pallor is often used to characterize the vitality and integrity of the optic nerve head. Different techniques are applied to obtain a measurement value of optic disc pallor.[10-14]

Interpretation of a pallor map (Fig. 1) raises the same problems as interpretation of visual fields in automated perimetry. There is a lot of information (for each test point at least one measurement value) and, in order to handle all these data, the information is compressed into single numbers such as total loss (TL) or mean defect (MD), and some of the information is lost. The same happens when we transform about 1000 pallor measurements to get the MPV. Therefore, evaluation of the MPV is simply one more step in the still unresolved problem of determining which optic cup parameters will best serve to distinguish glaucomatous eyes from normal eyes, especially those in early stages of the disease.[15]

Follow-up of pallor in circumscribed areas of the optic disc may be useful in determining the pathogenesis of the glaucomatous damage, but many difficulties must be overcome before being able to obtain good evaluation of optic disc pallor in longitudinal studies, for example, changes in lens opacity and the problem of identifying corresponding pixels.

Pallor measurements of the type used with the ONHA are useful for the comparison of groups of patients. The new parameter MPV could be important for indicating progressive disease in glaucoma patients. On the other hand, in a single patient, these measurements did not appear to be sensitive or specific indicators of early glaucoma.[4,16]

Conclusions

An increase in optic disc pallor, as shown by a higher MPV in ocular hypertensives compared to healthy eyes, seems to be an early pressure-induced disc change and might precede a significant increase in CDR or detectable visual field defects.

The long-term follow-up of visual fields shows that an initially high MPV might be a risk factor for visual field decay.

References

1. Burk ROW, Rohrschneider K, Kruse FE, Völcker HE: Laser-Scanning-Tomographie der Papille. In: Gramer E (ed) Glaukom: Diagnostik und Therapie, pp 113-119. Stuttgart: F Enke Verlag 1990
2. Maier H, Siebert M, Gramer E, Kampik A: Eine Maßzahl für die Nervenfaserschichtdicke: Messungen mit dem Laser Tomographic Scanner (LTS). In: Gramer E (ed) Glaukom: Diagnostik und Therapie, pp 120-145. Stuttgart: F Enke Verlag 1990
3. Gramer E, Siebert M: Optic nerve head measurements: the optic nerve head analyzer: its advantages and its limitations. Int Ophthalmol 13:3-13, 235, 1989
4. Siebert M, Gramer E: Reproduzierbarkeit und klinische Anwendbarkeit der Meßergebnisse mit dem Optic Nerve Head Analyzer: Klinische Studien. In: Gramer E (ed) Glaukom: Diagnostik und Therapie, pp 96-107. Stuttgart: F Enke Verlag 1990
5. Siebert M, Gramer E, Leydhecker W: Die Reproduzierbarkeit der Papillenmeßwerte bei der Untersuchung mit dem Optic Nerve Head Analyzer. Spektrum Augenheilk 2/4:167-176, 1988
6. Siebert M, Gramer E, Leydhecker W: Papillenabblassung: ein Frühzeichen des Glaukoms: eine klinisch kontrollierte Untersuchung von Papillenblässe und Papillenexkavation bei Glaucoma simplex, okulärer Hypertension und gesunden Augen mit dem Optic Nerve Head Analyzer. Klin Mbl Augenheilk 194:433-436, 1989
7. Siebert M, Gramer E: Hoher mittlerer Blässewert der Papille: Ein Risikofaktor für die Gesichtsfeldverschlechterung bei Glaukom und okulärer Hypertension: Eine Pilotstudie mit dem Optic Nerve Head Analyzer (ONHA). Ophthalmologe 92:506-510, 1995
8. Nagin P, Schwartz B: Detection of increased pallor over time using computerized image analysis in untreated ocular hypertension. Ophthalmology 92:252, 1985
9. Kitazawa Y, Tomita G, Shirato S: Image analysis of the optic disc of the ocular hypertensive eyes: a follow-up study. In: Gramer E (ed) Glaukom: Diagnostik und Therapie, pp 93-95. Stuttgart: F Enke Verlag 1990
10. Carassa RG, Schwartz B, Takamoto T: Increased preferential optic disc asymmetry in ocular hypertensive patients compared with control subjects. Ophthalmology 98(5): 681-691, 1991
11. Coulangeon LM, Plane C, Sole P, Menerath JM: Recent developments in medical therapy of POAG with beta blocking agents. Bull Soc Belge Ophtalmol 244:135-146, 1992
12. Lee SY, Shin DH, Spoor TC, Tsai CS, Kim C, Lee SH: Quantitative evaluation of optic disc pallor in pseudotumor cerebri patients. Graefes Arch Clin Exp Ophthalmol 230(2):107-110, 1992
13. Peigne G, Schwartz B, Takamoto T: Differences of retinal nerve fiber layer thickness between normal and glaucoma-like optic disks (physiological cups) matched by optic disk area. Acta Ophthalmol (Kbh) 71(4):451-457, 1993
14. Schwartz B, Takamoto T: Measurement of retinal nerve fiber layer thickness and its functional correlations with the visual field. Bull Soc Belge Ophtalmol 244:61-72, 1992
15. Varma R, Spaeth GL: The Optic Nerve in Glaucoma. Philadelphia, PA: JB Lippincott Co 1993
16. Assad A, Caprioli J: Digital image analysis of optic nerve head pallor as a diagnostic test for early glaucoma. Graefes Arch Clin Exp Ophthalmol 230(5):432-436, 1992

MAPPING STRUCTURAL TO FUNCTIONAL DAMAGE IN GLAUCOMA*

NORIKO YAMAGISHI, ALFONSO ANTON, PAMELA A. SAMPLE, LINDA ZANGWILL, INCI IRAK, ANN LOPEZ, MARCIA DE SOUZA LIMA and ROBERT N. WEINREB

Glaucoma Center and Visual Function Laboratory, Department of Ophthalmology, University of California, San Diego, La Jolla, CA, USA

Abstract

Purpose: To evaluate the spatial relationship between functional and structural damage in glaucoma patients using short-wavelength automated perimetry (SWAP) and the Heidelberg Retina Tomograph (HRT).

Methods: Subjects were 14 glaucoma patients who met the following inclusion criteria: *1.* open-angle glaucoma, *2.* only focal damage on the optic disc, and *3.* only focal damage on SWAP. Short-wavelength visual fields were obtained on a Humphrey Visual Field Analyzer (Model 620, San Leandro, CA), using Program 24-2. The SWAP visual field was divided into 21 zones corresponding to the 'perimetric nerve fibre bundles' (Weber and Ulrich, 1990). Test points were compared with a normative database. The optic disc was assessed with a confocal scanning laser ophthalmoscope (Heidelberg Retina Tomograph, Heidelberg, Germany). Measurements were calculated in 10° sectors and compared with a normative database (n=52) using a new calculation, the rim area ratio (RAR). The RAR takes the individual's rim area at each sector and divides it by their total rim area. This corrects for individual differences in disc size and shape. The resulting spatial relationship of structural and functional damage is described by a frequency map. A spatial relationship between the deepest defect zone in SWAP and the most defective sector in the optic disc was also obtained.

Results: The mean number of damaged zones in SWAP was four (4±2.9), and the mean number of damaged rim sectors was five (5±1.9). Fifty percent of the patients had one cluster, 36% had two clusters and 14% had three clusters of optic disc sectors outside the 99% normal percentile limits. All eight patients with only superior hemifield defects had inferior rim defects, and all three patients with only inferior hemifield defects had superior rim defects. Two patients with simultaneous superior and inferior hemifield defects had simultaneous superior and inferior optic disc defects. One patient with simultaneous superior and inferior hemifield defects had only inferior rim defects.

Conclusions: Although individual differences exist, focal defects in optic discs and in SWAP can be related with this objective and quantitative mapping technique.

Acknowledgments

This study was supported in part by National Eye Institute grants EY 08208 (PS), EY 11008 (LZ), and EY 11158 (RNW), and Fondo de Investigaciones Sanitarias 95/5039 (AA).

*The full article will be published elsewhere.

Address for correspondence: Pamela A Sample, PhD, Department of Ophthalmology, University of California, San Diego, 9500 Gilman Drive, La Jolla, CA 92093-0946, USA

Perimetry Update 1996/1997, p. 179
Proceedings of the XIIth International Perimetric Society Meeting
Würzburg, Germany, June 4–8, 1996
edited by M. Wall and A. Heijl

RELIABILITY AND ARTIFACTS

NECESSITY OF SUPERVISION DURING HUMPHREY PERIMETRY*

ROSITA E. VAN COEVORDEN, RICHARD P. MILLS and HOWARD S. BARNEBEY

Department of Ophthalmology, University of Washington, Seattle, Washington, USA

Abstract

It is generally acknowledged that patient performance on computerized perimetry improves with active, continuous technician involvement. For most clinical practices, such involvement is an expensive requirement, and there is considerable interest in abandoning it, at least for some patients who seem to be able to perform well unsupervised. The release of the new version of the Humphrey Field Analyzer (HFA II), with its improved ergonomic design, has prompted speculation that patients may more easily be left alone for testing with the new device. This study was designed to answer three questions: *1.* Does patient performance improve with supervision, as expected? *2.* Does the HFA II require less patient supervision than the HFA I? *3.* What patient characteristics predict poor unsupervised performance?

Methods: An unselected series of patients undergoing Humphrey visual field testing for glaucoma, glaucoma suspect, or neuro-ophthalmic indication was eligible for the study. Patients were excluded if they had visual acuity worse than 0.3 or an MD worse than -15 dB in the study eye, because such patients usually have trouble with fixation or attentiveness and clearly require technician supervision. Patients were not excluded if they had no prior perimetric experience or if they had co-morbidities precluding optimal performance. All patients giving their informed consent were tested with the 30-2 Full Threshold test with standard parameters. The eye to be tested (OD or OS), the device to be used (HFA I or HFA II), and the order of testing (supervised and unsupervised) were randomly selected.

In all tests, patients were oriented to testing, including how to pause the test by holding down the response button, and were given the demonstration test if they were novices. The foveal threshold test and the first 30-60 seconds of the full test were performed with the technician present, giving reminders, and recentering the patient. The test proceeded either unsupervised with the technician absent, or supervised with continuous active technician involvement, as specified by the randomization schedule.

Results: One hundred and twenty-eight patients completed testing, 69 on the HFA I and 59 on the HFA II. Twenty-one of 256 tests were unreliable by the manufacturer's criteria ('XX' flag). Overall,

*After further patient acquisition and data analysis, the full paper will be published elsewhere.

No proprietary interest.

Address for correspondence: Richard P. Mills, MD, University of Washington, Ophthalmology, Box 356485, Seattle, WA 98195-6485, USA

Perimetry Update 1996/1997, pp. 183–184
Proceedings of the XIIth International Perimetric Society Meeting
Würzburg, Germany, June 4–8, 1996
edited by M. Wall and A. Heijl

there was a positive effect of supervision on reliability ($p<0.02$) after adjusting for the effect of intrapatient correlation. There was no significant difference between the HFA I and HFA II on the effect of supervision on reliability (Fisher's exact test).

There was no significant effect of supervision on mean defect (MD), pattern standard deviation (PSD), corrected pattern standard deviation (CPSD), or test time. There was no differential effect of supervision on these indicators between the two HFA models.

Logistic regression modelled the following variables to reliability (*n* in parentheses):

supervised (128) versus unsupervised (128)

age over 70 years (44) versus age ≤70 years (84)

prior visual fields ≤2 (67) versus prior fields >2 (61)

post-primary educational level on a continuous scale, range 2-22

HFA I (69) versus HFA II (59)

After removal of the insignificant variables, two predictors of a reliable visual field remained: supervision ($p<0.01$) and age ≤70 years ($p<0.008$). The probability of a reliable test in patients aged ≤71 years improved from 91% unsupervised to 96% supervised, while in patients older than 70 years, the probability of a reliable test improved from 76% to 88%. A similar logistic regression on mean defect produced no significant predictors from among the same variables listed above.

Discussion: Supervision has a positive effect on reliability. From a pragmatic standpoint, however, the incremental improvement in probability of a reliable test with supervision in patients under 70 years is only 5%, while in patients over 70 years, it is 12%. Thus, a case could be made for allowing patients under 70 years with fair to good visual acuity and less than severe visual field loss to perform visual field testing without supervision (but with proper orientation). If testing were unreliable on the first eye, retesting of that eye and the fellow eye with supervision on the same or a subsequent day could be performed. Such retesting would involve fewer office resources than routinely requiring supervision for all visual field tests.

Supervision did not significantly affect MD, PSD, CPSD, or test time. No differential effect of the HFA I or II on the effect of supervision on any parameter could be demonstrated. Unfortunately, no patient demographic feature we studied other than age under 70 years could predict whether testing could safely be done unsupervised.

Acknowledgments

Supported in part by NIH Grant EY01730, and in part by an award from Research to Prevent Blindness, Inc. (New York, N.Y.).

FALSE-POSITIVE PEAK OF THE BEBIE CURVE AS A RELIABILITY PARAMETER

MARIO ZULAUF, CHRISTOPH BECHT and DENNIS BERNOULLI

University Eye Clinic, Basel, Switzerland

Abstract

Purpose: To develop a reliability parameter based on the left-side elevation of the Bebie curve observed in subjects with positive responses to catch trials.
Material and methods: The parameter, 'false-positive peak' (FPP), was developed on 552 visual fields (G1, 59 points, first phase, Octopus 201) of both eyes of 138 healthy volunteers. From the mean defect of the six highest ranks of the Bebie curve (10%), the defect value of rank 15 (percentile 25) was subtracted to account for diffuse damage. The clinical validity of FPP was tested on a second set of 290 similar visual fields of 58 glaucomatous eyes of 29 subjects.
Results: In glaucomatous fields, FPP averaged 2.35 dB (0.3-11 dB). FPP correlated with the percentage of false-positive responses (r^2=0.34; p<0.001). Mean FPP of each eye correlated with the long-term fluctuation (r^2=0.47; p<0.001). Compared with false-positive responses, the FPP of each eye correlated on average more highly with the index loss variance (LV: r^2=0.35 versus r^2=0.26; p<0.05; Wilcoxon). The differences for the correlation coefficients of false-positive responses and FPP with the index, mean defect (MD), were not significant (r^2=0.29 and r^2=0.23, respectively; p<0.1, Wilcoxon).
Conclusions: The 'false-positive peak' is a reliability parameter, supplementing the false-positive rate on catch trials and requiring no additional test time.

Introduction

The advent of automated perimetry has enhanced the accuracy and standardization of perimetric results. Nevertheless, the outcome of automated perimetry still depends on the performance of the subjects. In automated perimetry, there are several parameters which may be used to assess performance, *i.e.*, reliability of the visual field. Testing for false-positive responses is a standard feature of most automated perimeters.[1,2] Such catch trials are intended to quantify the subject's avidity, eagerness, ease, and tolerance level to respond to stimuli. A false-positive answer occurs when no stimulus is presented during a certain time period, but a response is given. Many false-positive answers may indicate an anxious or eager subject.

The authors have no proprietary interest in the hard- and software used in this study.

Address for correspondence: Mario Zulauf, MD, University Eye Clinic, P.O. Box, CH-4012 Basel, Switzerland

Perimetry Update 1996/1997, pp. 185–190
Proceedings of the XIIth International Perimetric Society Meeting
Würzburg, Germany, June 4–8, 1996
edited by M. Wall and A. Heijl

The percentage of false-positive answers averages 2.8%. Most test subjects do not give any false-positive responses.[3] Therefore, one or two errors may be tolerable, whereas three or more false answers are alarming. Clinical assessment of catch trials is rather difficult and may be inaccurate because the gradations used to estimate the subject's reliability are too large. Indeed, the observed correlation coefficient of r=0.34 between sensitivity and percentage of false-positive responses led to the conclusion that false-positive answers do not estimate the subject's cooperation reliably.[4] In this study, a 10% increase in false-positive answers to catch trials usually resulted in an increase in mean sensitivity of 1.5 dB. Therefore, a subject's cooperation has a clinically significant effect on the outcome of perimetry. The need to quantify reliability effectively is further accentuated by the fact that visual fields are not usually tested and interpreted by the same person.

Currently 5-10% of the presented stimuli are reserved to test the subject's reliability. Increasing the number of stimuli devoted to this task is not advisable. Several statistical procedures to evaluate reliability have been proposed which do not require additional test time. A sophisticated mathematical procedure has been reported to replace false-positive and false-negative responses.[5] It has been proposed to quantify the subject's reliability by adding up the inconsistent responses given during the bracketing procedure.[6] Another proposed alternative to evaluate reliability is based on the number of stimuli required to finish a given examination program.[7]

The aim of this study was to develop a reliability parameter complementary to false-positive catch trials, based on the often-observed 'false-positive peak' (FPP) of the Bebie curve.[8] The clinical validity of FPP was evaluated using a set of glaucomatous visual fields.

Material and methods

The study was performed according to the regulations of the University of Basel Ethical Commission. Written informed consent to participate in the study was obtained from each volunteer.

Rationale

False-positive responses generally result in artificially high sensitivity values. In gray-scale presentations, these are known as 'white scotomas'. In Bebie curves, these result in a peak to the left of the curve. This peak could be quantified as an adjunctive reliability parameter to the number of false-positive responses in catch trials. Ideally, such an index includes all test locations which present such artificially high sensitivities, but the peak is of variable width, *i.e.*, wider when many false-positive responses are given. Visual-field defects should not influence such a parameter. Therefore, the new parameter might be standardized for the diffuse defect often observed in glaucomatous visual fields.[9-15] Only one research group seldom found diffuse visual-field defects in glaucoma.[16] Inconsistent terminology might explain the discrepancies. The term 'homogenous defect' refers to a uniform decrease in sensitivity in all test locations, which is the extreme of a 'diffuse defect', where a large number of adjacent test locations are quite similarly affected and the gestalt of the defects are not arranged in any retinotopic or neurotopic pattern.

Table 1. Background statistics for data set to develop FPP. The results are given for the fourth visual field of each of 138 normal, healthy volunteers

	Average	*Median*	*Range*
Mean sensitivity (MS)	28.7 dB	28.9 dB	22.3-32.4 dB
Mean defect (MS)	-0.47 dB	-0.60 dB	-4.2-4.5 dB
Loss variance (LV)	4.1 dB^2	3.23 dB^2	1.6-34.5 dB^2
Corrected LV (CLV)	1.9 dB^2	1.3 dB^2	0.17-30.9 dB^2
Short-term fluctuation (SF)	1.4 dB	1.4 dB	0.8-2.5 dB
Number of stimuli presented	487	492	453-567
False-positive responses	2.7%	0%	0-35.3%
False-negative responses	0.5%	0%	0-14.3%

Table 2. Background statistics for the data set to evaluate the clinical validity of the reliability parameter FPP: 290 visual fields of glaucoma patients, Program G1, data on all three phases, Octopus 201

	Average	*Median*	*Range*
Mean sensitivity (MS)	25.4 dB	25.4 dB	16.7-33 dB
Mean defect (MS)	1.3 dB	1.2 dB	-5.3-8.6 dB
Loss variance (LV)	13.6 dB^2	7.1 dB^2	1.5-95.2 dB^2
Corrected LV (CLV)	10.0 dB^2	3.9 dB^2	0-92.3 dB^2
Short-term fluctuation (SF)	1.9 dB	1.7 dB	0.9-5.0 dB
Number of stimuli presented	542	535	448-722
False-positive responses	4.6%	3%	0-44%
False-negative responses	1.5%	0%	0-20%

Development of the reliability parameter FPP

The G1 normal value database was evaluated by one of the authors (CB).[17] All 552 visual fields (G1, 59 points, first phase only, Octopus 201) of 138 normal, healthy volunteers who completed four tests, were included. Details of the evaluation have been described elsewhere.[17] Most subjects were new to automated perimetry on the first test. Background information on the visual fields studied is summarized in Table 1. The mean and median of each of the 59 ranks of the Bebie curve were calculated and plotted (not presented in this publication). The total variation expressed as the average variance of all 552 measurements (*i.e.*, the interindividual and intra-individual variation) of each of the 59 ranks of the Bebie curve was calculated and plotted (not presented in this publication).

Clinical evaluation of the reliability parameter FPP

A second set of 290 similar visual fields in 58 glaucomatous eyes of 29 subjects treated with beta blockers was evaluated to determine the clinical validity of FPP.[18] Details of the evaluation have been described elsewhere.[19] All subjects had performed automated visual fields previously. Background information on the visual fields studied is summarized in Table 2.

Results

Development of the reliability parameter FPP

The results were similar for each of the four test sessions. The results of the fourth test are shown in the Tables. The peak to the left of the mean Bebie curve, as well as the median Bebie curve, is approximately 9 ranks wide (not presented in this publication). This coincides with our clinical experience. In spite of this, the average of ranks 1 to 6 were chosen to quantify the peak. The mean defect of ranks 1 to 6 averaged –3.6 dB (median = –3.6 dB; standard deviation = 1.6 dB; range: –9.8-1.5 dB).

The average variation of each rank of the Bebie curve is minimal for ranks 10 to 20. Rank 15 is chosen to standardize FPP as this might be an appropriate estimate of a diffuse defect or general sensitivity level. Rank 15 averaged -1.7 dB (median = 1.9, standard deviation = 1.4 dB; range: –5.5-3.0 dB). FPP as the difference between rank 15 and the average of rank 1–6 averaged 1.9 dB (median = 1.7 dB; standard deviation = 0.8 dB; range: -0.7-5.5 dB).

Clinical evaluation of the reliability parameter FPP

In the second data set of 290 glaucomatous visual fields, FPP averaged 2.35 dB (median 2.17; standard deviation = 1.3 dB; range: 0.3-11 dB). FPP correlated with the percentage of false-positive responses (r^2=0.34; p<0.001). Mean FPP of each eye correlated with the long-term fluctuation LF_{ho+he} (r^2=0.47; p<0.001).[20] Compared with the percentage of false-positive responses, FPP of each eye correlated on average more highly with the index loss variance (LV: r^2=0.35 versus r^2=0.26, p<0.05, Wilcoxon). The differences for the correlation coefficients of false-positive responses and FPP with the mean defect (MD) were not significant for the p<0.05 level (r^2=0.29 and r^2=0.23, respectively; p<0.1, Wilcoxon).

Discussion

The reliability parameter false-positive peak (FPP) correlates moderately well with the percentage of false-positive responses to catch trials, *i.e.*, FPP is related to false-positive responses but might contain information of its own. FPP demonstrates a gaussian distribution. In contrast to the percentage of false-positive responses, FPP permits a continually graduated estimate of reliability. FPP compares quite favorably with the percentage of false-positive responses, as FPP explains long-term fluctuation of the visual field at least as well as false-positive responses do. In addition, the new parameter does not require extra test time. FPP requires little computational time and can be applied to already stored visual fields.

A previous report presented a visual field with a false-positive peak and 55% false-positive answers.[21] In that example, rank 15 of the Bebie curve had a sensitivity of -3 dB and was also affected by false-positive answers. In that case, rank 27 (percentile 50) would have been appropriate. Standardization of the peak by rank 15 would have resulted in an unwanted reduction of FPP. This was a very rare case, and the case with the highest observed FPP in this study is presented in Figure 1. Rank 15 was chosen to avoid influences of large local defects. If only a central island of

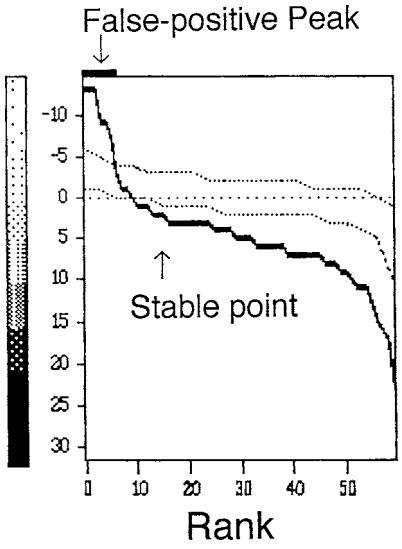

Fig. 1. The 'false-positive peak' is defined as the difference of: rank 15 (2 dB) – the average ranks 1 to 6. The values for this extreme example are 2 dB for rank 15 and 7 dB for the peak, FPP = 5 dB.

the visual field of less than 15 test locations remains, FPP cannot be calculated. In such cases, false-positive responses are the appropriate choice to evaluate the subject's cooperation. These do not depend on retinal sensitivity.[22] In conclusion, FPP does not replace, but rather complements, false-positive responses.

FPP was developed, and its clinical validity examined, in visual fields tested with Program G1.[23] All 59 test locations included in the study are measured with the standard Octopus test strategy.[24] The Humphrey standard strategy retests a test location, if the threshold is more than 4 dB from the expected value (which is based on the threshold of a neighboring test location).[2] This would result in a decrease of FPP. Therefore, normative data for FPP depend on details of the test strategy. However, adaptation to programs with other grid sizes and numbers of test locations should be easy. Instead of ranks 1-6, the test locations above percentile 10 are chosen. Similarly, instead of rank 15, percentile 25 is chosen.

Further details will be presented elsewhere.

Acknowledgments

This work was supported in part by The Swiss National Fund, grant #32-43624.95. Thanks are extended to Phillip Hendrickson for proofreading the text.

References

1. Fankhauser F: Problems related to the design of automatic perimeters. Doc Ophthalmol 47(1):89-138, 1979

2. Heijl A: The Humphrey Field Analyzer: construction and concepts. Doc Ophthalmol Proc Ser 42:77-84, 1985
3. Zulauf M, Flammer J, LeBlanc RP: Normal visual fields measured with Octopus program G1. I. Differential light sensitivity at individual test locations. Graefe's Arch Clin Exp Ophthalmol 232:509-515, 1994
4. Lee M, Zulauf M, Caprioli J: The influence of patient reliability on visual field outcome. Am J Ophthalmol 117:756-761, 1994
5. Olsson J, Rootzén H, Heijl A: Maximum likelihood estimation of the frequency of false positive and false negative answers from the up-and-down staircases of computerized threshold perimetry. In: Heijl A (ed) Perimetry Update 1988/89, pp 245-251. Amsterdam/Milano: Kugler & Ghedini Publ 1989
6. Lee M, Zulauf M, Caprioli J: A new reliability parameter: inconsistent responses. J Glaucoma 2:279-284, 1993
7. Zulauf M, Caprioli J, Boeglin RJ, Lee M: Number of stimuli as a reliability parameter in perimetry. German J Ophthalmol 1:86-90, 1992
8. Bebie H, Flammer J, Bebie Th: The cumulative defect curve: separation of local and diffuse components of visual field damage. Graefe's Arch Clin Exp Ophthalmol 227:9-12, 1989
9. Werner RB, Drance SM: Early visual field disturbances in glaucoma. Arch Ophthalmol 95:1173-1175, 1977
10. Anctil JL, Anderson D: Early foveal involvement and generalized depression of the visual field in glaucoma. Arch Ophthalmol 102:363-370, 1984
11. Glowazki A, Flammer J: Is there a difference between glaucoma patients with rather localized visual field damage and patients with more diffuse visual field damage? Doc Ophthalmol Proc Ser 49:317-320, 1987
12. Chauhan BC, Drance SM, Douglas GR, Johnson CA: Visual field damage in normal-tension and high-tension glaucoma. Am J Ophthalmol 18(6):636-642, 1989
13. Gross RL, Spaeth GL: Early detection of glaucoma. Ophthalmol Clin N Am 4:747-755, 1991
14. Araie M, Yamagami J, Suzuki Y: Visual field defects in normal-tension and high-tension glaucoma. Ophthalmology 100(12):1808-1814, 1993
15. Mutlukan E: Diffuse and localized visual field defect to automated perimetry in primary open angle glaucoma. Eye 9:745-750, 1995
16. Åsman P, Heijl A: Diffuse visual field loss and glaucoma. Acta Ophthalmol (Kbh) 72(3):330-338, 1994
17. Becht CN: Entwicklung eines neuen Zuverlässigheitsparameters in der automatischen Perimetrie: False-positive Peak. Inauguraldissertation zur Erlangung der Doktorwürden, Medizinische Fakultät der Universität Basel 1996
18. Kaiser HJ, Flammer J, Messmer Ch, Stümpfig D, Hendrickson Ph: Thirty-month visual field follow-up of glaucoma patients treated with betablockers. J Glaucoma 1:153-155, 1992
19. Bernoulli DD: Anwendung eines neuen Zuverlässigkeitsparameters in der automatisch Perimetrie: False-positive Peak. Inauguraldissertation zur Erlangung der Doktorwürden, Medizinische Fakultät der Universität Basel 1996
20. Bebie H, Fankhauser F, Spahr J: Static perimetry: accuracy and fluctuations. Acta Ophthalmol (Kbh) 54:339-348, 1976
21. Zulauf M, Caprioli J: Fluctuation of the visual field in glaucoma. In: Caprioli J (ed) Glaucoma Update. Ophthalmol Clin N Am 4:692, 1991
22. Jenni F, Flammer J: Experience with the reliability parameter of the Octopus automated perimetry. Doc Ophthalmol Proc Ser 49:601-603, 1987
23. Flammer J, Jenni A, Bebie H, Keller B: The Octopus glaucoma G1 program. Glaucoma 9:67-72, 1987
24. Bebie H, Fankhauser F, Spahr J: Static perimetry: strategies. Acta Ophthalmol (Kbh) 54:325-332, 1976

THE INFLUENCE OF TARGET BLUR ON PERIMETRIC THRESHOLD VALUES IN AUTOMATED LIGHT-SENSITIVE PERIMETRY AND FLICKER PERIMETRY

CHOTA MATSUMOTO, SACHIKO OKUYAMA, ATSUSHI IWAGAKI, TAKUYA OTSUKI, KOJI UYAMA and TOSHIFUMI OTORI

Department of Ophthalmology, Kinki University School of Medicine, Osaka-Sayama, Osaka, Japan

Abstract

The influence of refractive defocusing and artificial media opacities on perimetric threshold values was studied with light-sensitive perimetry and flicker perimetry. The authors examined 15 eyes of 15 normal subjects and 12 eyes of 12 glaucoma patients with both a light-sensitive perimeter and a flicker perimeter, using various degrees of refractive defocusing and artificial media opacities. Perimetric threshold values were determined in normal subjects by the use of spherical plus lenses of +2, +4, +6, +8 and +10 diopters, and occlusion diffusers of densities of 1.0, 0.8, 0.6, 0.4, 0.1 (Ryser, Switzerland). Glaucoma patients were tested with an occlusion diffuser of a density of 0.1. Light-sensitive perimetry was performed using SARGON and Octopus 201, Program 32. Flicker perimetry was performed using the Octopus 1-2-3 and its remote software package with the authors' own programs. These examinations were performed using target size 3. Diffuse sensitivity loss was detected in light-sensitive perimetry when spherical plus lenses and occlusion diffusers were used. However, there was no significant sensitivity loss when flicker perimetry was performed under the same conditions. Flicker perimetry was less influenced by refractive defocusing and artificial media opacities than by light-sensitive perimetry.

Introduction

It is known that light-sensitive perimetry, which measures the differential light sensitivity in the visual field, is affected by the blurring of test targets, such as refractive defocusing or media opacities.[1-5] Previous investigators have reported that flicker perimetry is less influenced by refractive defocusing and artificial media opacities than light-sensitive perimetry.[6-11] Using the Octopus 1-2-3 (Interzeag) and its remote software package, we developed a strategy for automated flicker perimetry to measure the critical fusion frequency (cff) in the central field. We have already reported that this flicker perimetry provides us with a more sensitive perimetric method than traditional light-sensitive perimetry for detecting early glaucomatous visual field

Address for correspondence: Chota Matsumoto, MD, DSc, Department of Ophthalmology, Kinki University School of Medicine, Ohno-Higashi, Osaka-Sayama City, Osaka 589, Japan

Perimetry Update 1996/1997, pp. 191–200
Proceedings of the XIIth International Perimetric Society Meeting
Würzburg, Germany, June 4–8, 1996
edited by M. Wall and A. Heijl

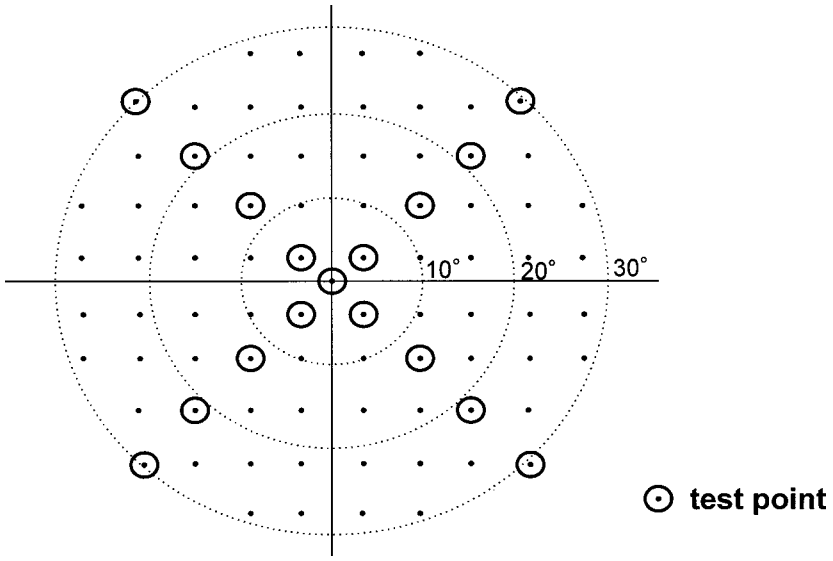

Fig. 1. Arrangement of the test points for light-sensitive perimetry and flicker perimetry. Each test point was tested twice.

loss.[12,13] The aim of the present study was to investigate the influence of target blur on perimetric threshold values in light-sensitive perimetry and our flicker perimetry.

Subjects and method

Normal subjects

Fifteen eyes of 15 normal subjects were examined by both light-sensitive and flicker perimetry, using various degrees of refractive defocusing and artificial media opacities. The inclusion criteria for normal subjects were as follows: corrected visual acuity of ≥ 20/20; refractive errors of ≤ 3.0 D (spherical) and ≤ 2.0 D (cylindrical); pupil diameter of ≥ 3.0 mm; intraocular pressure of ≤ 21 mmHg; clear optical media and normal fundi; no systemic diseases which were likely to affect visual function; and no family history of glaucoma. The mean age of our study population was 25.7±2.8 years (minimum: 21 years; maximum: 35 years). Informed consent was obtained from all subjects.

Light-sensitive perimetry was performed with the Octopus 201. For the present study, we designed a special program to test 17 points in the central 30° visual field using the SARGON program (Fig. 1). Each test point was tested twice. Light-sensitive perimetry was performed with a stimulus size 3, under a background luminance of 4 asb. The duration of each target stimulus was 100 msec. Flicker perimetry was performed using our original program for Octopus 1-2-3 and its remote software package.[12] The arrangement of the test points was the same as that for the test points of the Octopus SARGON program. Flicker perimetry was performed with a stimulus size 3, under a background luminance of 31.5 asb. The duration of each target stimulus was one second. Perimetric threshold values were determined by the use of

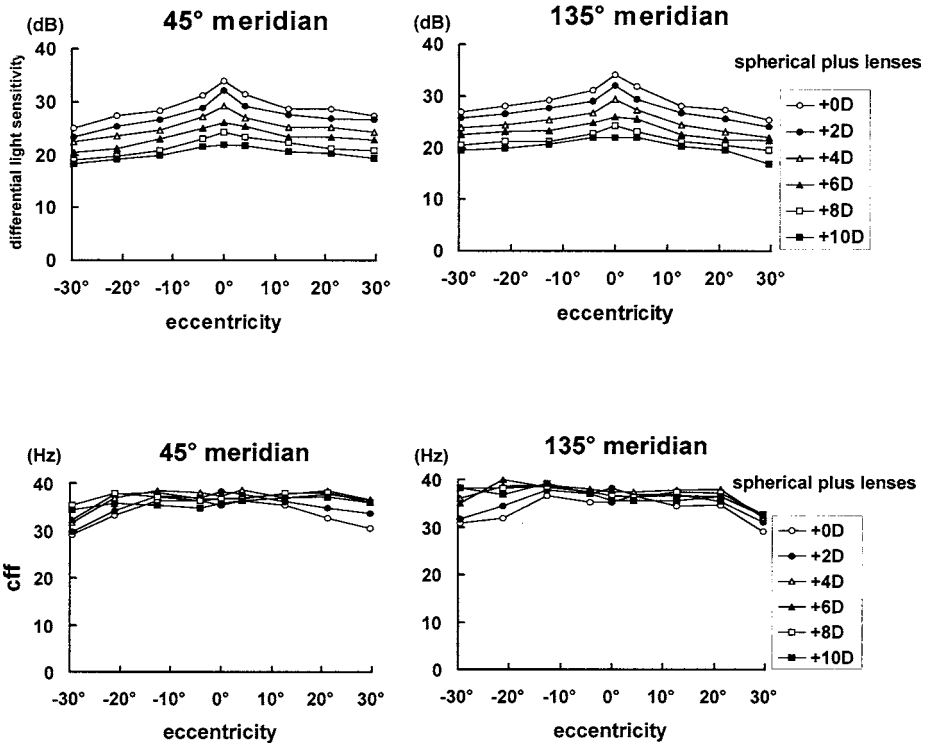

Fig. 2. The influence of refractive defocusing on the perimetric threshold value in light-sensitive perimetry (*upper*) and in flicker perimetry (*lower*).

spherical plus lenses of +2, +4, +6, +8 and +10 diopters, and occlusion diffusers of Nos. 1.0, 0.8, 0.6, 0.4, and 0.1 densities (Ryser, Switzerland).

Glaucoma patients

Measurement was carried out in a total of 12 eyes of 12 subjects; seven eyes of seven patients with primary open-angle glaucoma, and five eyes of five patients with normal-tension glaucoma. The stages of their visual field loss were as follows: four eyes with stage 1, five eyes with stage 2, and three eyes with stage 3, according to Aulhorn's classification modified by Greve.[14] The mean age of the study population was 58.2±6.5 years (minimum: 51 years; maximum: 73 years). The inclusion criteria for glaucoma patients were as follows: corrected visual acuity of ≥ 20/20; refractive errors of ≤ 5.0 D (spherical) and ≤3 D (cylindrical); pupil diameter of ≥ 3.0 mm, and clear optical media. Informed consent was obtained from all patients. Light-sensitive perimetry was performed with the Octopus 201, Program 32. Flicker perimetry was performed in the same test locations as the Octopus Standard Program 38. Light-sensitive perimetry and flicker perimetry were performed with and without occlusion diffuser No. 0.1.

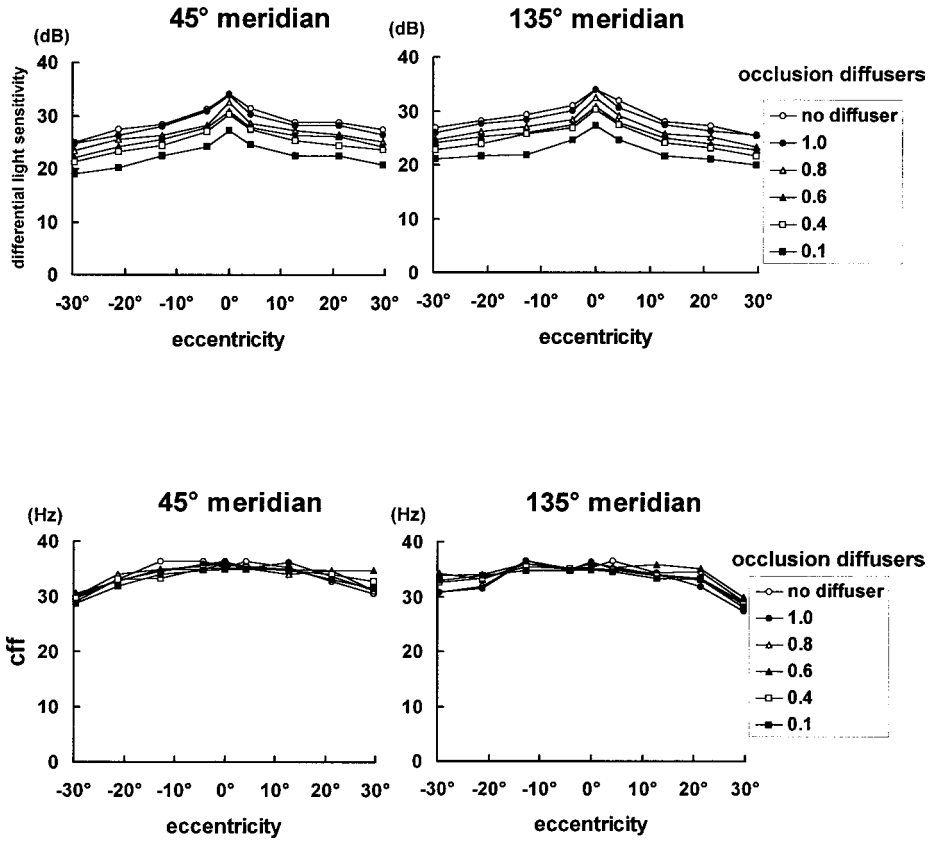

Fig. 3. The influence of artificial media opacities on the perimetric threshold value in light-sensitive perimetry (*upper*) and in flicker perimetry (*lower*).

Results

Normal subjects

Differential light sensitivity decreased markedly with the increase of refractive defocusing (Fig. 2, upper row). However, flicker perimetry was less influenced by the use of spherical plus lenses than light-sensitive perimetry (Fig. 2, lower row). Furthermore, the cff increased slightly at the test locations in the 20-30° visual field. Differential light sensitivity decreased markedly with the increase of artificial media opacities (Fig. 3, upper row), but flicker perimetry was less influenced by the use of occlusion diffusers than light-sensitive perimetry (Fig. 3, lower row).

Figure 4a shows the influence of the additional spherical plus lenses for light-sensitive perimetry and flicker perimetry at the test locations of 0°, 4°, 13°, 21°, and 30°. Differential light sensitivity decreased with the increase of diopters of spherical plus lenses at all test points. Especially, differential light sensitivity decreased markedly at the test location of 0°. On the other hand, the values of cff were less influenced by additional spherical plus lenses than those of differential light sensi-

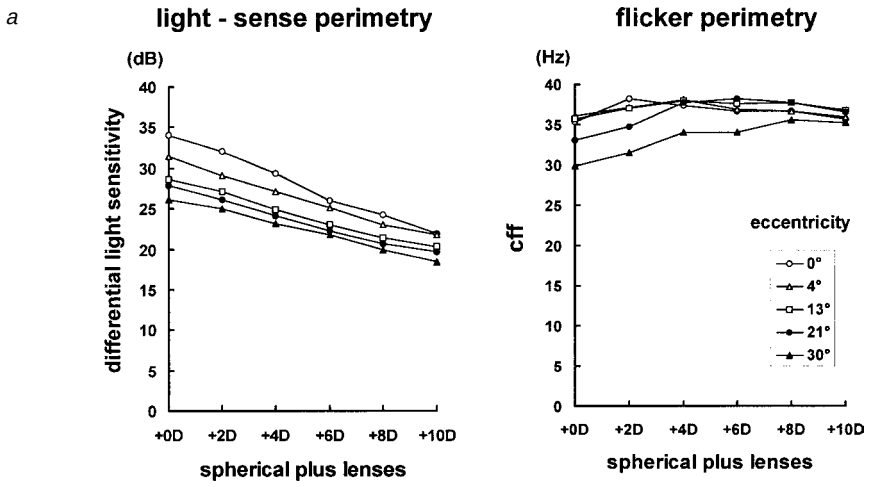

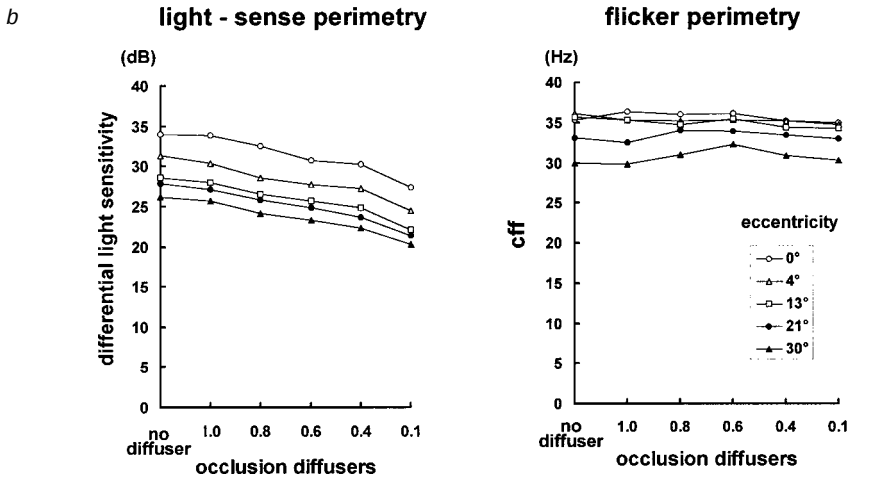

Fig. 4a. The influence of the additional spherical plus lenses for light-sensitive perimetry (*left*) and flicker perimetry (*right*) at the test locations of 0°, 4°, 13°, 21°, and 30°.

Fig. 4b. The influence of the additional occlusion diffusers for light-sensitive perimetry and flicker perimetry (*left*) at the test locations of 0°, 4°, 13°, 21°, and 30°.

tivity. Moreover, the cff increased slightly at the 21° and 30° test points. Figure 4b shows the influence of the use of occlusion diffusers on light-sensitive perimetry and flicker perimetry at the same test locations. Differential light sensitivity decreased with the increase of densities of occlusion diffusers at all test points. However, the values of cff was less influenced by the use of occlusion diffusers than differential light sensitivity.

Glaucoma patients

Case 1 was a 59-year-old male with primary open-angle glaucoma. The intraocular pressure in his right eye was 23 mmHg, in his left eye 22 mmHg. The cup/disc ratio in his right eye was 0.6, in his left eye 0.7. His right eye showed a small depression in the upper Bjerrum area on light-sensitive perimetry and flicker perimetry (Fig. 5). When occlusion diffuser No. 0.1 was used, diffuse sensitivity loss was detected by light-sensitive perimetry (Fig. 5a). However, perimetric threshold values of the flicker field were almost the same with occlusion diffuser No. 0.1 (Fig. 5b).

Case 2 was a 56-year-old female with primary open-angle glaucoma. The intraocular pressure in her right eye was 29 mmHg, in her left eye 29 mmHg. The cup/disc ratio in her right eye was 0.7, in her left eye 0.8. Abnormal test points were detected in the lower nasal visual field of her right eye on light-sensitive perimetry and flicker perimetry (Fig. 6). By the use of occlusion diffuser No. 0.1, diffuse loss was accentuated and it was very difficult to diagnose the pattern of visual field with light-sensitive perimetry (Fig. 6a). Under the same condition of flicker perimetry, the cff slightly increased and the number of the abnormal test points decreased. However, clear definite visual field loss in the lower nasal field was detected by flicker perimetry compared to light-sensitive perimetry (Fig. 6b).

In all the glaucoma patients, diffuse sensitivity loss was detected with light-sensitive perimetry in the presence of artificial media opacities. However, there was no significant change of cff in four eyes and only a slight increase of cff in eight eyes with flicker perimetry under the same conditions.

Discussion

Refractive defocusing and media opacities create test target blurring and retinal image degradation in visual field testing. The results of the present study show that the cff is less influenced by refractive defocusing and artificial media opacities than by differential light sensitivity. Strong refractive blur or very dense artificial media opacities cause general depression in traditional light-sensitive perimetry, but there was no effect or only a slight increase of the cff in our flicker perimetry.

Previous investigators also reported that flicker perimetry is less influenced by refractive defocusing and media opacities.[6-11] Nakabayashi developed a 'Direct Flicker Device' for testing the retinal and neurological function in patients with cataracts or other optical disturbances.[8] Tyler measured foveal flicker sensitivity with and without a refractive blur of +10 diopters of spherical lens.[10] He could not find a statistically significant loss of foveal flicker sensitivity. He explained that the edge effect of test targets did not provide a detectable contribution to flicker sensitivity. Lachenmayr and Gleissner measured the cff in their flicker perimetry using five kinds of spherical plus lenses and three kinds of diffusers.[11] They also reported that flicker perimetry in the central visual field was fairly resistant to retinal image degradation.

→

Fig. 5a. Case 1. The grayscale and the comparison of light-sensitive perimetry with (*lower*) and without (*upper*) an artificial occlusion diffuser.
Fig. 5b. Case 1. The value table and the probability of flicker perimetry with (*lower*) and without (*upper*) an artificial occlusion diffuser.

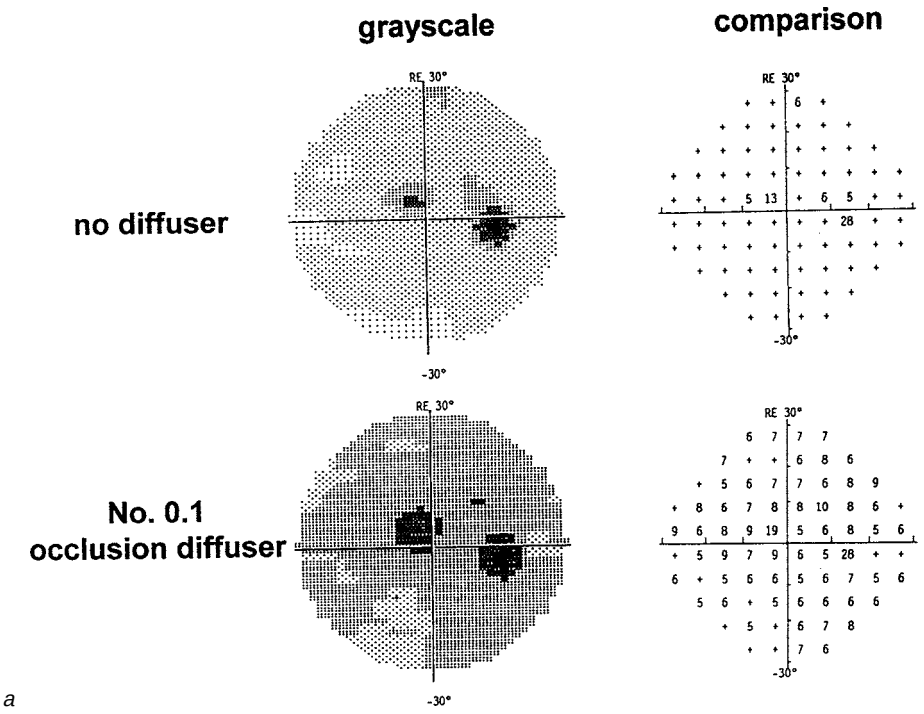
grayscale
comparison
no diffuser
No. 0.1
occlusion diffuser
RE 30°
-30°

a

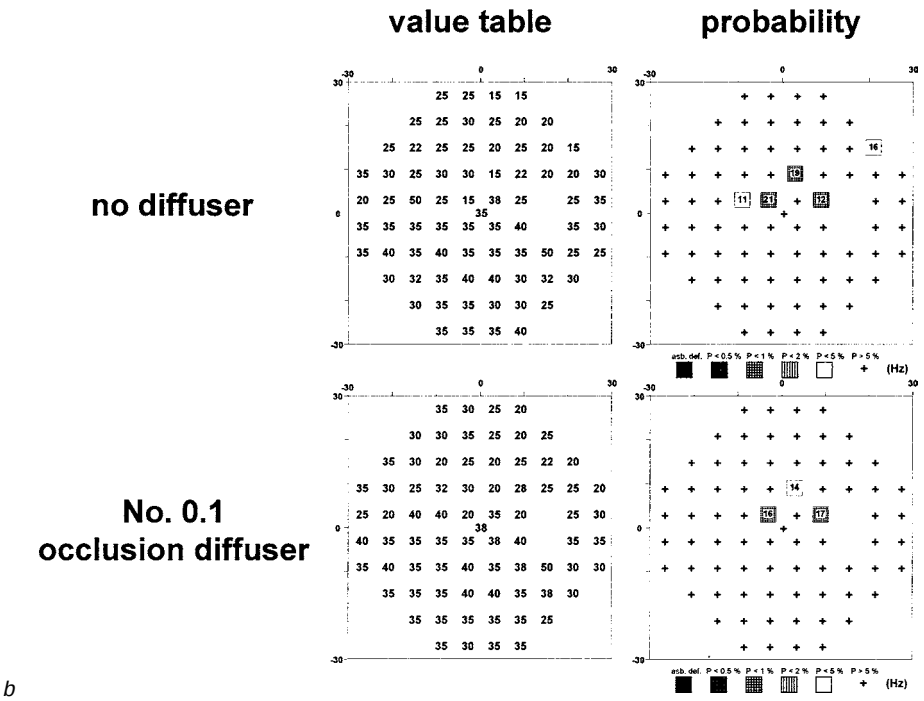
value table
probability
no diffuser
No. 0.1
occlusion diffuser
asb. def. P<0.5% P<1% P<2% P<5% P>5%
(Hz)

b

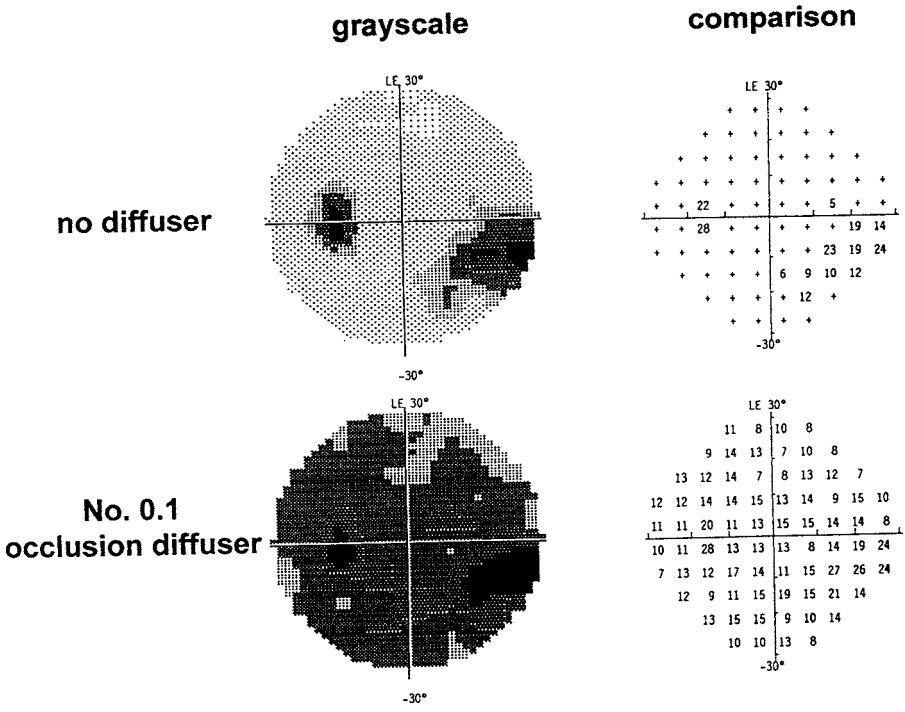
grayscale
comparison
no diffuser
No. 0.1
occlusion diffuser
LE 30°
-30°

a

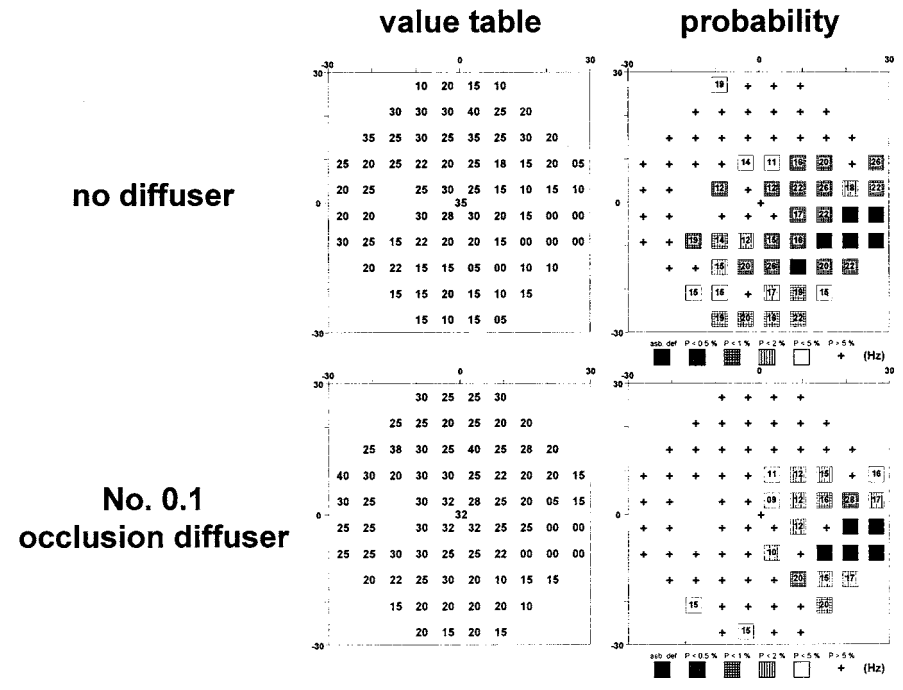
value table
probability
no diffuser
No. 0.1
occlusion diffuser
(Hz)

b

They explained that this phenomenon was due to their symmetrical modulation of 100% around the mean luminance level and a large target size (1° visual angle). However, we measured the flicker fields using bright suprathreshold targets of 4000 asb and also target size 3. One possible explanation for this phenomenon could be that flicker perimetry uses the same average intensity of flicker stimulus during the examination. However, light-sensitive perimetry uses a very dim stimulus for detecting the threshold level which is easily affected by retinal image degradation.

The results of the present study also show a slight increase of cff under the condition of strong refractive blur or very dense artificial media opacities. Furthermore, this effect is accentuated by a greater amount of refractive blur than by artificial media opacities. We assume that this phenomenon is due to the enlargement of the appearance of the target size by defocusing of the retinal image. In our study, enlargement of the target size was recognized in all subjects with the use of spherical plus lenses. Sensitivity for detecting visual field defects slightly decreases when there is a strong refractive blur or very dense media opacities in flicker perimetry. On the other hand, there is a very small artificial cff loss under these conditions. This resistance of flicker perimetry to retinal image degradation seems to be a definite advantage in evaluating retinal and neurological functions in clinical practice.

References

1. Weinreb RN, Perlman JP: The effect of refractive correction on automated perimetric thresholds. Am J Ophthalmol 101:706-709, 1986
2. Eichenberger D, Hendrickson PH, Robert Y, Gloor B: Influence of ocular media on perimetric results: effect of simulated cataract. Doc Ophthalmol Proc Ser 49:3-8, 1986
3. Heuer DK, Anderson DR, Knighton RW, Feuer WJ, Gressel MG: The influence of simulated light scattering on automated perimetric threshold measurements. Arch Ophthalmol 106:1247-1251, 1988
4. Urner-Bloch U: Simulation of the influence of lens opacities on the perimetric results; investigated with orthoptic occluders. Doc Ophthalmol Proc Ser 49:23-32, 1986
5. Uyama K, Matsumoto C, Okuyama S, Otori T: The influence of target blurring and simulated opacity of the ocular media on automated perimetric thresholds. J Jpn Ophthalmol Soc 97:994-1001, 1993
6. Nakabayashi M: Studies on flicker fusion fields by Iso-frequency method. Fol Ophthalmol Jpn 10:845-856, 1959
7. Otori T, Hohki T, Nakao Y: Central critical fusion frequency in neuro-ophthalmological practice. Doc Ophthalmol Proc Ser 19:95-100, 1978
8. Nakabayashi M: 'Direct Flicker Device' for inferring a post-optical visual function covered with optical disturbances. Fol Ophthalmol Jpn 29:1460-1464, 1978
9. Iwagaki A, Otsuji O, Okuyama S, Matsumoto C, Nakao Y, Otori T: Analysis of the normal value of critical fusion frequency using the modified central CFF-meter. Jpn J Clin Ophthalmol 48:952-953, 1994
10. Tyler CW: Analysis of normal flicker sensitivity and its variability in the visuogram test. Invest Ophthalmol Vis Sci 32:2552-2560, 1991
11. Lachenmayr BJ, Gleissner M: Flicker perimetry resists retinal image degradation. Invest Ophthalmol Vis Sci 33:3539-3542, 1992

←
Fig. 6a. Case 2. The grayscale and the comparison of light-sensitive perimetry with (*lower*) and without (*upper*) an artificial occlusion diffuser.

Fig. 6b. Case 2. The value table and the probability of flicker perimetry with (*lower*) and without (*upper*) an artificial occlusion diffuser.

12. Matsumoto C, Uyama K, Okuyama S, Uyama R, Otori T: Automated flicker perimetry using the Octopus 1-2-3. In: Mills RP (ed) Perimetry Update 1992/1993, pp 435-440. Amsterdam/New York: Kugler Publ 1993
13. Matsumoto C, Okuyama S, Uyama K, Iwagaki A, Otori T: Automated flicker perimetry in glaucoma. In: Mills RP, Wall M (eds) Perimetry Update 1994/1995, pp 141-146. Amsterdam/ New York: Kugler Publ 1993
14. Greve EL, Langerhorst CT, Van den Berg TTJP: Perimetry and other function tests in glaucoma. In: Cairns JE (ed) Glaucoma, pp 37-77, London: Grune & Stratton 1986

EFFECT OF DISLOCATED AND TILTED CORRECTION GLASSES ON PERIMETRIC OUTCOME
A simulation using ray-tracing

W. FINK[1], U. SCHIEFER[2] and E.W. SCHMID[1]

[1]Institute for Theoretical Physics; [2] University Eye Hospital, Department II; Tübingen, Germany

Adequate correction is an essential prerequisite for precise perimetry. Therefore, not only the correct glasses have to be chosen, but also their positioning should be properly determined. Otherwise, a distortion of the stimulus grid, as well as a (area enlarging/reducing) distortion of the stimuli themselves, can occur. Therefore, scotomata may be simulated in visual fields which are purely optically evoked (so-called refraction scotoma[1]), because the light stimulus is mapped on an enlarged/reduced retinal area, thereby reducing/increasing light density.

Ray-tracing[2] algorithms are capable of simulating, quite realistically, the optical properties of the human eye and other optical corrections (glasses, IOLs, contact lenses, etc.). Patterns of point sources are used as objects. Based on an improved Gullstrand eye model, the path of light rays is calculated between the point source and the retina through the refractive media obeying Snellius' law.[3] The image formed on the retina is projected back to a screen at the distance of the object so as to simulate image interpretation by the brain.

Even though the correct glasses may be positioned in the right way, the refraction scotomata mentioned above can also occur in the presence of high ametropia, namely high myopia and hyperopia, *e.g.*, aphakia. In the case of high myopia, regional polyopia ('Bildverdoppelung') is caused (see, Fig. 1a), whereas in the case of high hyperopia, an annular scotoma can occur (see, Fig. 1b).[4,5]

To show this, we have calculated the effects on the mapping of a stimulus grid of the Tübingen automated perimeter (TAP). We have demonstrated changes in both size and spatial translation of the blind spot in myopic and hyperopic patients. As far as the perimetric results are concerned, the size of the blind spot is increased and its position is transferred to higher eccentricities for myopic patients. This is due to the wide-angle effect of a bi-concave correction glass. Therefore, the blind spot is detected with stimuli of higher eccentricities compared to an emmetropic normal. However, in the hyperopic case, the size of the blind spot is reduced, and its position is transferred to lower eccentricities because of the magnification effect of a

Address for correspondence: Dr. W. Fink, Institute for Theoretical Physics, Auf der Morgenstelle 14, D-72076 Tübingen, Germany

Perimetry Update 1996/1997, pp. 201–204
Proceedings of the XIIth International Perimetric Society Meeting
Würzburg, Germany, June 4–8, 1996
edited by M. Wall and A. Heijl

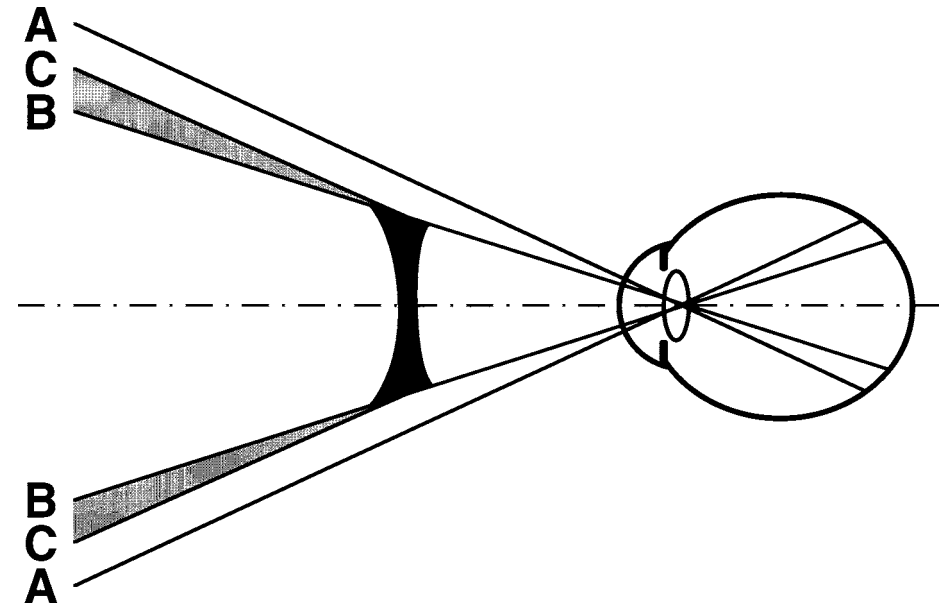

a

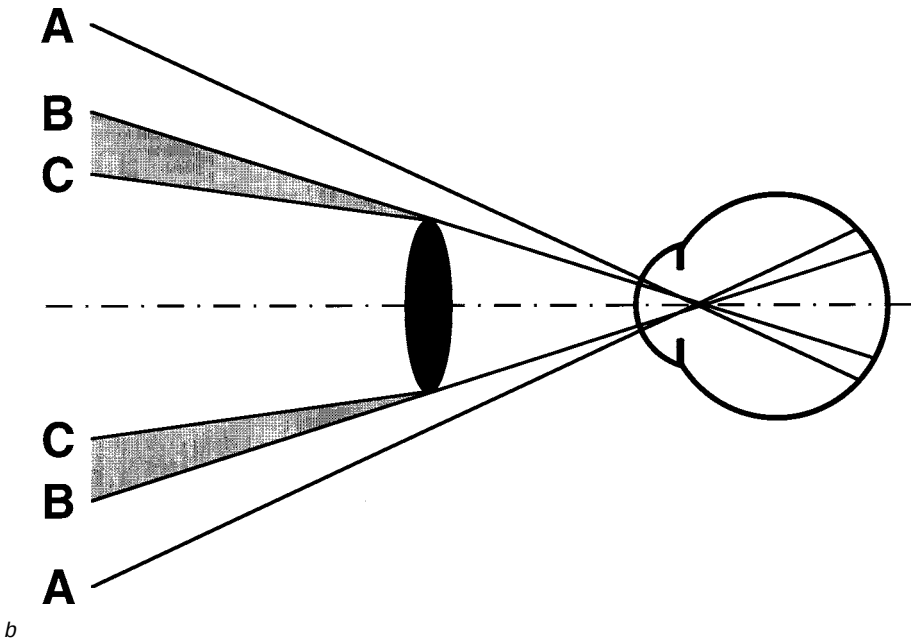

b

Fig. 1a. Formation of purely optically evoked regional polyopia. *b.* Formation of purely optically evoked annular scotoma. *c.* Original TAP stimulus grid. *d.* Distortion of the stimulus grid and of the stimuli – simulated (eye-glass corrected myopia of -11 D). *e.* Distortion of the stimulus grid and of the stimuli – simulated (eye-glass corrected hyperopia/aphakia of +13.5 D).

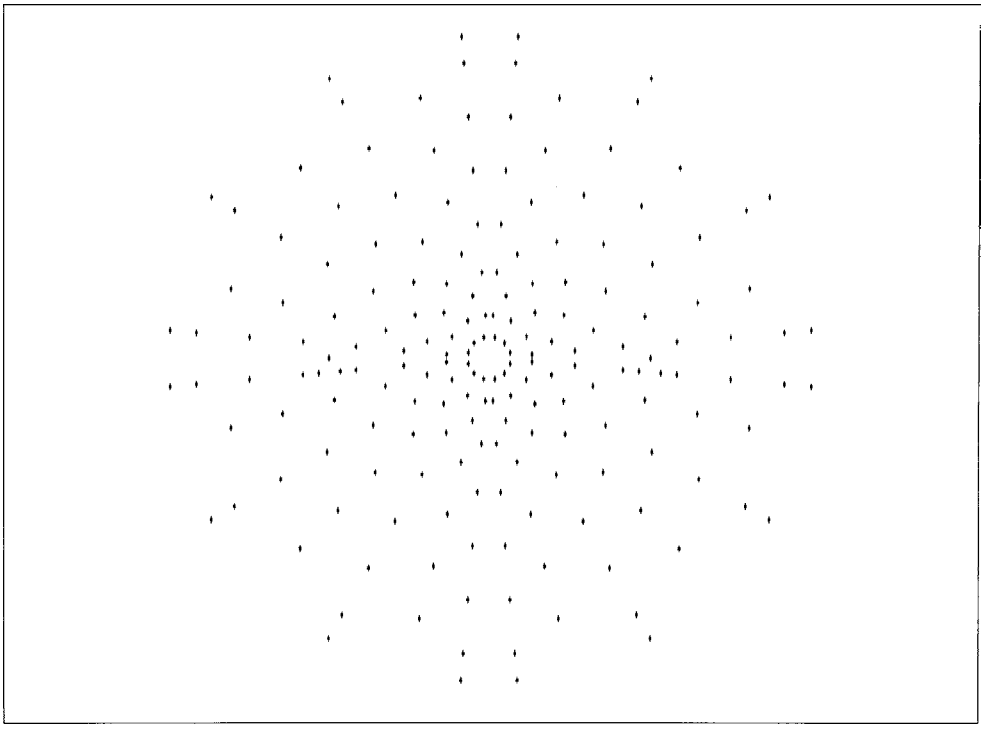

Fig. 1c.

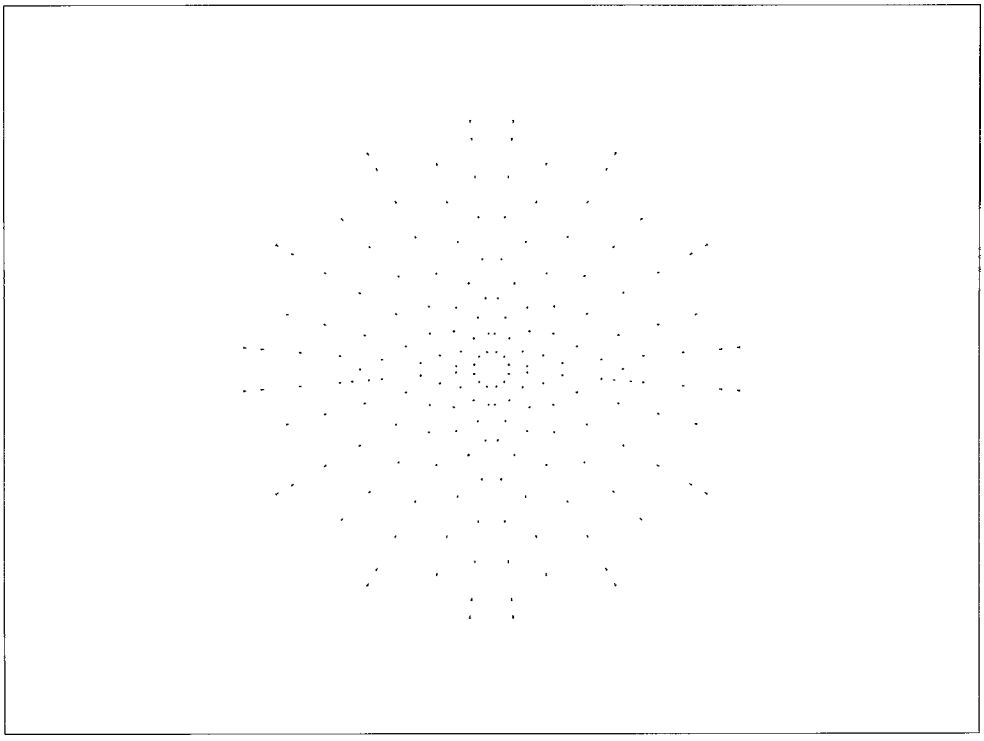

Fig. 1d.

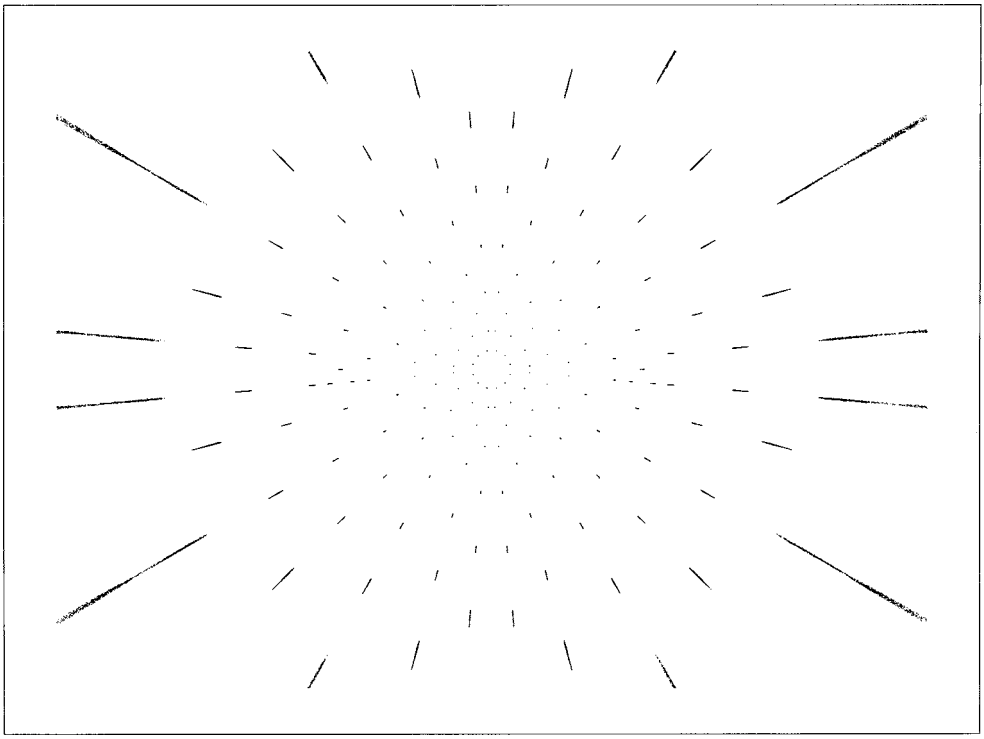

Fig. 1e.

bi-convex correction glass. Thus, detection of the blind spot is performed with stimuli of lower eccentricities compared to an emmetropic normal (see, Figs. 1c, d and e).

Furthermore, it is possible to visualize the influence of tilted and vertically and horizontally dislocated correction glasses, resulting in an asymmetric distortion of both the stimulus grid and the stimuli themselves. In perimetry, a reduction of the distortions shown so far may be achieved by using contact lenses for optical correction instead of eye-glasses.

Ray-tracing is a useful tool for visualization and analysis in ophthalmological research. Therefore, it may contribute to a better understanding of the effects of optically-caused mapping errors on perimetric results.

References

1. Aulhorn E, Durst W: Die Bedeutung der Perimetrie des blinden Flecks für die klinische Diagnostik. Fortschr Ophthalmol 84:631-634, 1987
2. Born M, Wolf E: Principles of Optics, 5th edn. Oxford: Pergamon Press 1975
3. Fink W, Frohn A, Schiefer U, Schmid EW, Wendelstein N: A ray tracer for ophthalmological applications. Ger J Ophthalmol 5:118-125, 1996
4. Fink W, Frohn A, Schiefer U, Schmid EW, Wendelstein N, Zrenner E: Visuelle Abbildung bei hohen Ametropien: Computergestützte Simulation mittels strahlenoptischer Rechnungen. Klin Mbl Augenheilk 208:472-476, 1996
5. Handbuch für Augenoptik, 3rd Edn, p 180. Oberkochen, Germany: Carl Zeiss 1987

APPARENT GLAUCOMATOUS VISUAL FIELD DEFECTS CAUSED BY DERMATOCHALASIS

M.K. BIRCH, A.S. KOSMIN and P.K. WISHART

Glaucoma Clinic, St Paul's Eye Unit, Royal Liverpool University Hospital, Liverpool, United Kingdom

Purpose: To quantify the effect of dermatochalasis on the central visual field and thus to assess the potential of this common upper lid abnormality to confound diagnostic perimetry in glaucoma.

Methods: We identified a series of ocular hypertensive patients with dermatochalasis who demonstrated reproducible central field loss by Humphrey automated perimetry Program 24-2. We confirmed dermatochalasis as the cause of the field loss by demonstrating reversal following taping up the upper lid or blepharoplasty.

Results: Central field loss due to dermatochalasis was identified in 12 eyes of seven ocular hypertensive patients. All demonstrated restriction of the superior field, most marked temporally in ten eyes and in continuity with the blind spot in five eyes. Extension of the defect below the horizontal meridian was seen in four eyes. The average mean deviation was -5.88 dB and average mean sensitivities were reduced at all points including fixation in the superior vertical meridian. The degree of depression increased with eccentricity from fixation.

Conclusions: Dermatochalasis causes more marked restriction of the superior central field than equivalent ptosis. Consequently cosmetically mild dermatochalasis may cause marked central field defects which may confound diagnostic perimetry in glaucoma.

References

1. Hacker HD, Hollsten DA: Investigation of automated perimetry in the evaluation of patients for upper lid blepharoplasty. Ophthalmic Plastic Reconstruct Surg 8(4):250-255, 1992
2. Meyer DR, Stern JH, Jarvis JM: Evaluating the visual field effects of blepharoptosis using automated static perimetry. Ophthalmology 100:651-659, 1993

Address for correspondence: M.K. Birch, MD, Glaucoma Clinic, St Paul's Eye Unit, Royal Liverpool University Hospital, Liverpool, UK

Perimetry Update 1996/1997, p. 205
Proceedings of the XIIth International Perimetric Society Meeting
Würzburg, Germany, June 4–8, 1996
edited by M. Wall and A. Heijl

FITTING ANGIOSCOTOMAS

N. BENDA[1], T.J. DIETRICH[2] and U. SCHIEFER[2]

[1]Department of Medical Biometry; [2]University Eye Hospital, Department II; Tübingen, Germany

Abstract

Using a special perimetric grid, thresholds can be estimated along a line of test points crossing the supposed angioscotoma. To fit angioscotomas, a two-stage analysis which employs these single estimations is compared with a model which incorporates the threshold as a function of position into the probabilistic description of the binary response (stimulus seen/not seen). A special function based on hyperbolic tangents is proposed, the parameters of which describe depth, position and width of the angioscotoma, and can be estimated by the method of maximum likelihood. As an example, the authors present the evaluation of data collected from 13 ophthalmologically normal subjects with the Tübingen computer campimeter (TCC) using bright stimuli (12´). In subjects with detectable angioscotomas, they found scotoma depths of between 1 and 8 dB.

Introduction

To judge a visual field examination correctly, possible nuisance effects such as angioscotomas should be described as clearly as possible. First attempts at quantification used threshold estimations for different test points near the supposed angioscotoma.[1,2]

Threshold estimation of a single test point is rather uncertain when employing only a few stimulus presentations. Therefore, a better description should be based on a probabilistic model using all responses simultaneously, and including the luminance difference sensitivity (lds) threshold as a function of stimulus position.

Methods

Based on a digitized fundus image, a line of closely spaced test points, which crosses an isolated vessel nearly perpendicularly, can be incorporated into a perimetric grid.[3] We present two approaches to fit angioscotomas:

Two-stage fitting estimates single thresholds, and then uses these estimates to fit an appropriate function (here by least squares regression).

Address for correspondence: N. Benda, Department of Medical Biometry, Westbahnhofstrasse 55, D-72070 Tübingen, Germany

Perimetry Update 1996/1997, pp. 207–210
Proceedings of the XIIth International Perimetric Society Meeting
Würzburg, Germany, June 4–8, 1996
edited by M. Wall and A. Heijl

One-stage fitting incorporates stimulus intensity *and* position into the probabilistic description of the binary response (stimulus seen/not seen).
If ϕ measures the distance from a test point on a line crossing a retinal vessel to a fixed point of reference on this line, the threshold near the vessel can be described by

$$\mu(\phi) = a - b\phi + h\left(\tanh\left[\left(\frac{\phi - c}{\delta}\right)^2\right] - 1\right),$$

where a-$b\phi$ describes the linear trend of the threshold near the vessel and beside the scotoma, c the center of angioscotoma and h the scotoma depth at the center. 2δ gives a measure of scotoma width.

Two-stage fitting uses the separately estimated thresholds to fit $\mu(\phi)$, *e.g.*, by least squares estimation corresponding more or less to a 'visual fit'. It does not consider differences in the precision of the single estimates, which may yield misleading results.

One-stage fitting uses a logistic regression model, where the probability of stimulus perception depends on stimulus intensity and $\mu(\phi)$. Here, the unknown parameters a, b, c, h and δ are estimated directly by maximum likelihood, considering *all* responses and the position ϕ of the test point.

Thirteen ophthalmologically normal subjects were examined by the TCC using bright stimuli (12´) on a VDU and a 4-2-1 dB strategy with four reversals. By means of fundus-oriented perimetry, individual perimetric grids were created, including a line of 24 closely spaced test points crossing a large retinal vessel nearly perpendicularly and corresponding to one meridian. Therefore, we set distance ϕ equal to the eccentricity of the test point.

Results

An angioscotoma was detected in six subjects, and a reasonable fit was achieved by one-stage fitting. In one of these subjects (No. 1), we found an important difference between the two fitting methods (see Fig. 1). In Subject 1, a 24-year-old woman, scotoma width was estimated at 0.9° by the one-stage fitting and 0.4° by the two-stage fitting. Since vessel diameter derived from fundus image was about 0.6° and the angioscotoma is more likely to be wider than the respective vessel,[4] one-stage fitting seems to yield the better estimate.

The one-stage fit apparently does not care about the low single threshold estimate at 17° eccentricity. Interestingly enough, this single estimate turns out to be particularly uncertain, due to a very low slope of the estimated psychometric function at this point (0.05 l/dB). Therefore, two-stage fitting seems to be rather misleading, taking less confident single estimates 'too seriously'.

In another case (Subject 3), two-stage fitting could not be carried out reasonably, because the subject did not perceive any stimulus at one of the test points. In four of these cases, the two-fitting method yielded similar results. Angioscotoma width and depth estimations evaluated by one-stage fitting are given in Table 1. The remaining seven subjects did not show any reasonable angioscotoma fit, either with one-stage or with two-stage fitting, or with 'visual fit'.

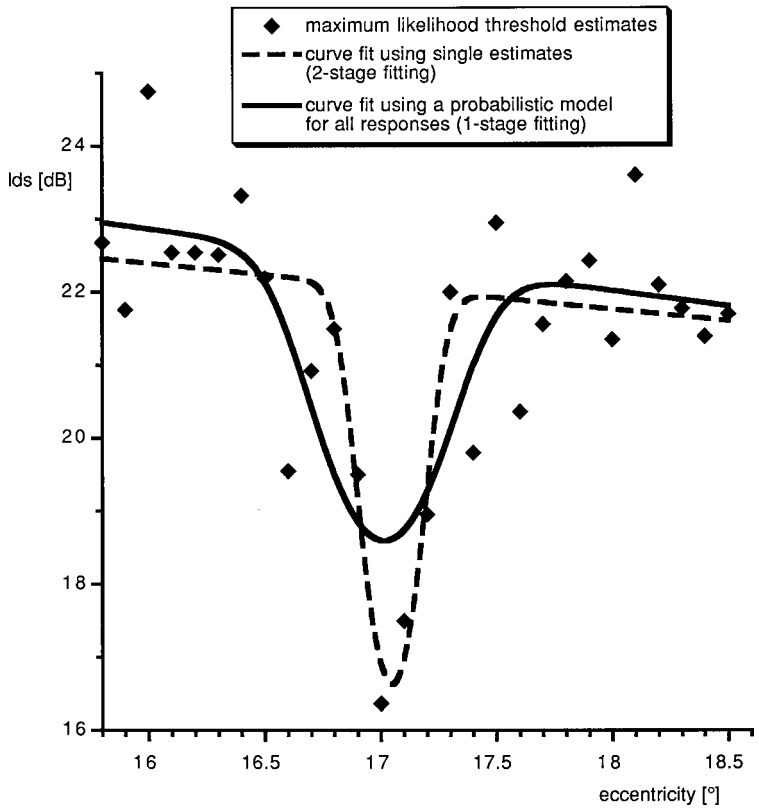

Fig. 1. Angioscotoma fitting using two different approaches.

Table 1. Estimated angioscotoma widths and depths in six ophthalmologically normal subjects

Subject	*Width (°) (2δ)*	*Approximate 95% confidence interval*	*Depth (dB) (h)*	*Approximate 95% confidence interval*
1	0.9	[0.4, 1.5]	3.8	[2.5, 5.9]
2	0.4	[0.3, 0.6]	4.8	[3.2, 6.6]
3	0.3	[0.2, 0.8]	8.4	[4.4, 12.4]
4	0.9	[0.3, 1.3]	6.0	[4.6, 7.6]
5	0.4	[0.2, 0.6]	3.5	[1.6, 5.8]
6	0.6	[0.03, 1.2]	0.8	[0.1, 1.5]

Discussion

One-stage fitting of angioscotomas is preferable to a two-stage fitting, which handles single threshold estimates, such as observations. Numerically, evaluation can be difficult, due to a higher dimensional optimization problem, which is rather demanding if the number of binary observations is small.

However, using this method, we found reasonable estimates of angioscotoma

width and depth, although we only evaluated the data from one perimetric session for each subject. The combination of several examinations of the same subject should improve estimation.

Conclusions

Using a probabilistic model, which simultaneously considers all responses to stimulus presentations at a line of test points crossing a retinal vessel, angioscotomas can reasonably be described. Two-stage procedures dealing with single threshold estimates often yield similar results but can also be misleading.

Acknowledgment

Supported by the Tübingen Fortüne Program Nos. 97 and 167.

References

1. Zulauf M: Quantification of angioscotoma. Ophthalmologica 200:203-209, 1990
2. Zulauf M: Beitrag zur Angioskometric: Stimulus-Grösse und Programmwahl. Klin Mbl Augenheilk 192:613-618, 1988
3. Schiefer K, Benda N, Stercken-Sorrenti G, Dietrich TJ, Friedrich M: Fundus-orientierte Perimetrie. Evaluation eines neuen Gesichtsfeld-Untersuchungsverfahrens bezüglich der Detektion von Angioskotomen. Klin Mbl Augenheilk 208:62-71, 1996
4. Dubois-Poulsen A: Le Champ Visuel, pp 277-299. Paris: Masson 1952

PSYCHOPHYSICS

SPATIAL SUMMATION FOR SELECTED GANGLION CELL MOSAICS IN PATIENTS WITH GLAUCOMA

JOOST FELIUS[1], WILLIAM H. SWANSON[1,2], RONALD L. FELLMAN[3], JOHN R. LYNN[3] and RICHARD J. STARITA[3]

[1]Retina Foundation of the Southwest; [2]University of Texas Southwestern Medical Center; [3]Glaucoma Associates of Texas; Dallas, Texas, USA

Abstract

Irregularities in spatial summation have been found in relative defects of patients with glaucoma,[1] possibly due to recruitment of nearby areas that are less defective, or to detection by other ganglion cell types (normally not sensitive enough to play a substantial role) that have larger receptive fields. The authors addressed this issue by studying summation properties within selected ganglion cell mosaics. In 13 patients with primary open-angle glaucoma and 16 age-similar normals, white-on-white (W-on-W), red-on-white (R-on-W), and blue-on-yellow (B-on-Y) thresholds were measured for sizes I, II, III, IV, and V in four points at 17°, with at least one point in a relative defect. Cycloplegia and refraction were used to control accommodation. A bilinear function was used to describe the transition (at a critical stimulus area, A_c) from complete summation to probability summation. R-on-W summation functions typically were very similar to W-on-W in both groups, whereas responses to B-on-Y stimuli summated to much larger sizes. In patients, most locations with clinically elevated thresholds (W-on-W size III) showed abnormally large A_c.

Introduction

It is well known that in visual field testing of normal eyes, an increase in stimulus size yields an increase in sensitivity (for example, see Sloan,[2] and Wilson[3] and Latham *et al.*[4]). This effect of stimulus size can be unusually large in eyes with glaucoma.[1,5,6] Here, this phenomenon is studied with a range of stimulus sizes in the context of spatial summation in distinct mosaics of ganglion cells.

There have been various approaches to characterize spatial summation functions in normal eyes. One was to analyze peripheral spatial summation data in terms of a critical area. For stimuli smaller than the critical area A_c, sensitivity is proportionally related to stimulus area: a doubling of stimulus area results in a doubling of sensitivity (*i.e.*, half the intensity is needed to reach threshold – 'complete summation'). For stimuli larger than A_c, there is a much smaller increase in sensitivity with stimulus area.[3,7,8] The value of A_c increases with visual eccentricity, and has been hypoth-

Address for correspondence: Joost Felius, PhD, Department of Ophthalmology, University of Michigan, 1000 Wall St., Ann Arbor, MI 48105, USA

Perimetry Update 1996/1997, pp. 213–221
Proceedings of the XIIth International Perimetric Society Meeting
Würzburg, Germany, June 4–8, 1996
edited by M. Wall and A. Heijl

esized to correspond roughly to the area of the receptive field center of a retinal ganglion cell.[9] Thresholds for stimuli that are smaller than A_c would then be mediated through a single ganglion cell, whereas for larger stimuli the responses of several cells are pooled.

Abnormal spatial summation has been reported in visual field testing in patients with glaucoma:[1,5,6] visual fields obtained with targets of Goldmann size V (diameter 1.7°) often show higher detection sensitivities than expected on the basis of standard size III (0.43°) sensitivity. Fellman *et al.*[1] argued that in many cases this effect could be explained by detection of the larger stimuli by surrounding regions in the visual field that are less affected. In some cases, however, they suggested that the effect should be attributed to larger summation areas of the ganglion cells that mediate detection. This could be explained by detection mediated by a different type of ganglion cells (having larger receptive fields), which are normally not sensitive enough to contribute to detection. It must be noted here that the white-on-white (W-on-W) perimetric stimuli used in most studies of spatial summation could potentially be detected by either the parvocellular (midget ganglion cells) or the magnocellular pathway (parasol ganglion cells).

As a next step in understanding the underlying changes that cause abnormal summation in glaucoma, in this study we compared spatial summation functions measured under standard W/W perimetric conditions (for which we do not necessarily know which cell type mediates the detection) with spatial summation functions under test conditions that isolate a single mosaic of ganglion cells. Data were collected from normal and glaucomatous eyes.

Subjects

Thirteen patients with primary open-angle glaucoma (POAG) and 16 normal subjects participated in this study. Patients were recruited from the files of Glaucoma Associates of Texas, based on the following criteria: subjects needed to have early glaucoma, clear ocular media, a visual acuity of 20/30 or better, and reliable performance in visual field testing. The mean age (±1 SD) of the patient group was 67 ± 11 years. Humphrey 30-2 visual fields were used to identify regions with reduced sensitivity. The normal subjects had no known eye diseases, normal visual fields, and a visual acuity of at least 20/20$^-$. The normal group was age-similar to the patient group: 65 ± 9 years.

Methods

Testing was performed with a model 640 Humphrey Visual Field Analyzer (Humphrey Instruments, Inc., San Leandro, CA), using the full-threshold strategy to determine detection thresholds in four locations at 17° eccentricity on the diagonal meridians (Fig. 1). These test locations were selected with the goal that one or two locations would fall in relative defects, and the other locations would fall in areas that appeared normal in standard visual field testing. In four patients, none of the test locations fell in relative defects, and it was necessary to use alternative grid with the test points on different meridians (but at the same eccentricity) such that this goal

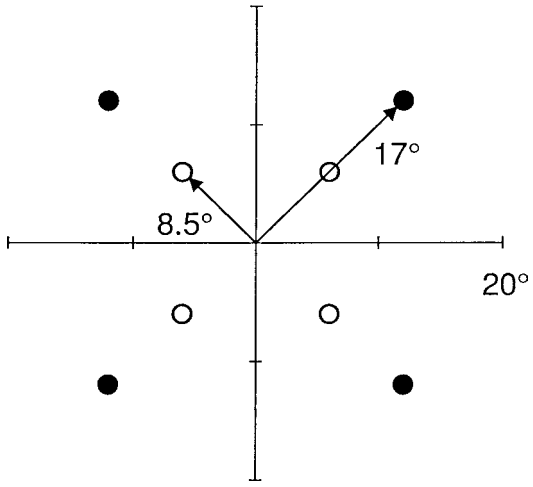

Fig. 1. Test grid of eight locations in the central visual field. Thresholds in the four locations at 17° eccentricity (*filled circles*) were evaluated in this study; the stimuli at 8.5° (*open circles*) served to keep subjects' attention global.

was reached. The test grid also included four locations at 8.5° eccentricity that served to keep the subject's attention global.

Three test conditions were used: W-on-W, using white targets on a 10 cd/m^2 white background; R-on-W, using red targets on a 10 cd/m^2 white background; and B-on-Y, using blue targets on a 100 cd/m^2 yellow background. The W-on-W and B-on-Y conditions corresponded to the Humphrey standard achromatic and blue/yellow test conditions, respectively. For the R-on-W test condition, a red cut-off filter (metameric with 620 nm; Edmunds Scientific, Barrington, NJ) was taped in front of the projection lens of the perimeter.

In each test condition, detection sensitivity was determined for stimuli of Goldmann sizes I, II, III, IV, and V (diameters 0.11°, 0.22°, 0.43°, 0.86°, and 1.7°, respectively) in an interleaved order. This resulted in 15 relatively short test runs, lasting two to three minutes each. One practice test run was given to each subject before the actual testing. Testing was performed monocularly under cycloplegia (1% cyclopentolate), using proper refraction. To verify that refraction was proper for the test distance, visual acuity was tested *in situ* after cyclopleging, with the examiner holding a small eye chart against the back of the perimeter dome.

For all four test locations in all three test conditions in all subjects, the *log* sensitivity versus *log* stimulus area data sets were fit with the following bilinear function:

$$\text{log sensitivity} = \begin{cases} \text{log area} + K & \text{for area} \le A_c \\ 0.25 \text{ log area} + K' & \text{for area} > A_c \end{cases}$$

with the restraint $K' = K + 0.75 \log A_c$ for continuity. This function features complete summation (slope = 1) for stimuli with area smaller than the critical value A_c, and

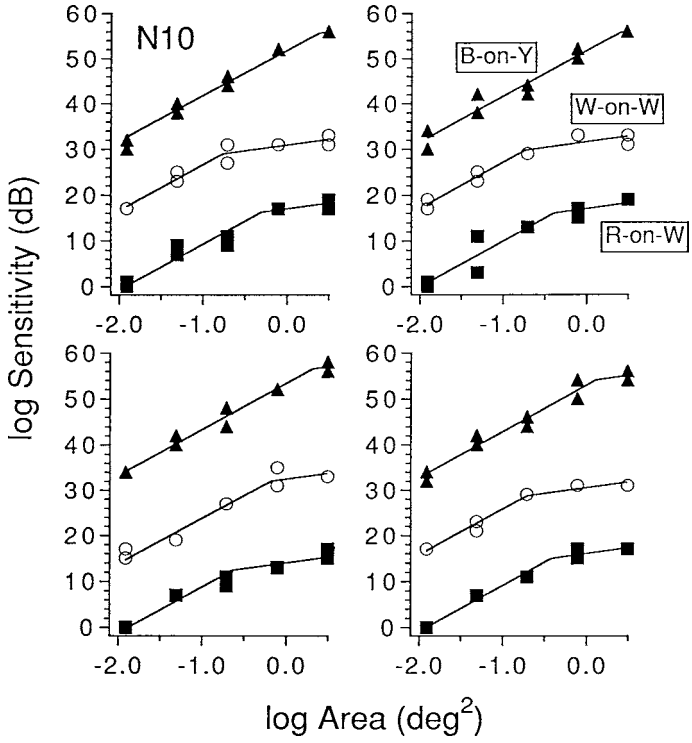

Fig. 2. Results from a normal subject, N10, left eye. Each panel corresponds to one test location at 17° eccentricity: *Upper left:* temporal superior visual field; *upper right:* nasal superior; *lower right:* nasal inferior; *lower left:* temporal inferior. Symbols indicate test condition: *open circles:* W-on-W; *filled squares:* R-on-W; *filled triangles:* B-on-Y. Data from different test conditions are shifted vertically for clarity. Solid lines denote fits of the model function to each of the data sets.

probability summation (slope = 0.25) for larger stimuli. Justification for this choice is given elsewhere.[10] Free parameters were A_c and K.

Results

Figure 2 shows a typical example of the data for a normal subject. Each panel corresponds to one of the locations tested. Different symbols identify the three test conditions; solid lines denote the fit of the bilinear function to the data. A_c for the white stimulus is similar to A_c for the red stimulus in all four locations, whereas for the blue stimulus, A_c is considerably larger.

In most locations in all subjects tested, the empirical function fit the data quite well. In the normal group the function could not be fit to three of the 192 (16 x 4 x 3) data sets due to noise. All data gathered at these three locations in the corresponding subjects were eliminated. Furthermore, due to limitations in the dynamic range of the apparatus, R-on-W thresholds could not be determined in 31% of all locations in all eyes (both groups) for size I; 4% for size II; and 0.9% for size III. For the B-on-Y conditions, thresholds could not be determined in 54% of all loca-

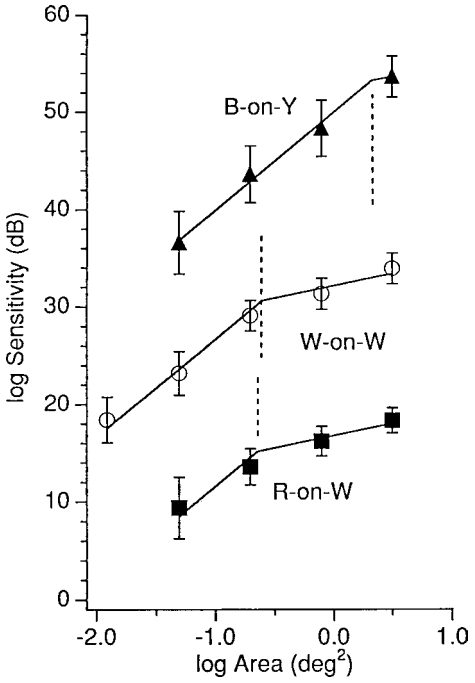

Fig. 3. Mean data from 14 normal eyes. Symbols indicate test condition: *open circles:* W-on-W; *filled squares:* R-on-W; *filled triangles:* B-on-Y. Error bars denote one standard deviation. *Solid lines:* bilinear fits.

tions for size I; 20% for size II; and 4% for size III. In calculating the mean normal data for all three conditions, B-on-Y size I data were omitted because of the large number of locations in which thresholds could not be determined. Two normal eyes had no R-on-W size I and/or B-on-Y size II data, and were omitted. Figure 3 contains the means of the remaining normal data for 14 eyes. Fitting the bilinear function to these data yields similar log A_c for W-on-W conditions (-0.61 log deg^2; diameter 0.56°) and R-on-W conditions (-0.64 log deg^2; diameter 0.54°), whereas for B-on-Y conditions, log A_c is considerably larger (0.33 log deg^2; diameter 1.6°).

An example of the results from a POAG subject is shown in Figure 4. Detection sensitivity tends to be lower for all test conditions, especially in the upper right location, which corresponds to a relative defect in her visual field (Fig. 5). Also, the A_c values for the W-on-W and R-on-W stimuli are larger in the defect location than in the locations where 30-2 sensitivity is still within normal limits.

The resulting parameters for individual data sets are shown in Figure 6. The log expected sensitivity at stimulus size I, rather than K, is plotted against log A_c for clarity, since K and A_c interact. The B-on-Y data are not further evaluated, since a large fraction had A_c at least as large as the largest stimulus size. Furthermore, the sensitivity parameters from the B-on-Y may be influenced by lens density. This might explain at least part of the higher variability in the B-on-Y data as seen in Figure 6. In the W-on-W and R-on-W data, abnormalities in the POAG group are small compared to the variability among normals. In both groups we can see a trend

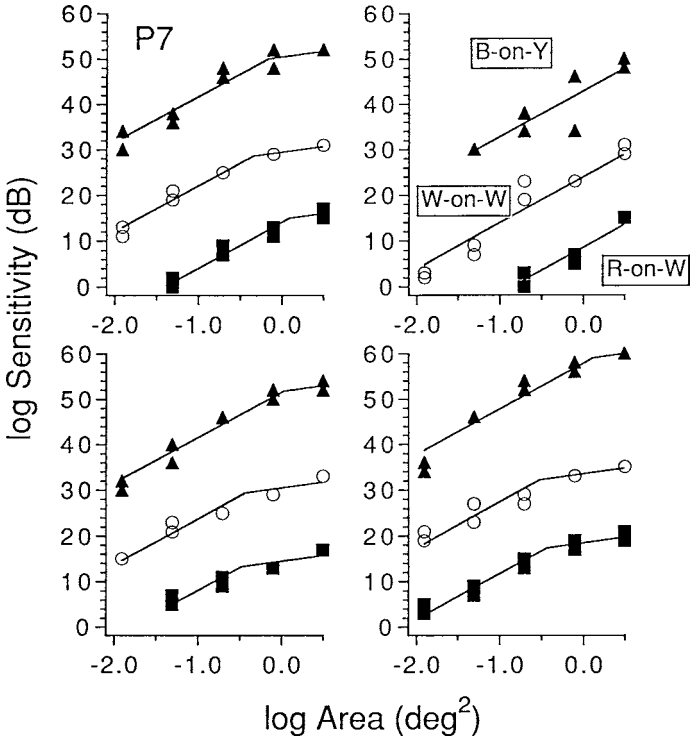

Fig. 4. Results from a POAG patient, P7, left eye. Panels and symbols as in Figure 2. Data from different test conditions are shifted vertically for clarity.

toward larger A_c with decreasing sensitivity. However, for the W-on-W condition, this effect is larger in the POAG group than in the normal group (slopes -10.67 dB/log unit versus -6.65 dB/log unit: $t = 2.69$, $p<0.01$).

Discussion

Spatial summation functions were obtained for W-on-W, R-on-W, and B-on-Y stimuli with sizes ranging from 0.11° to 1.7° diameter. In nearly all locations tested, the bilinear function defined in the 'Methods' section served well for describing the data. In some cases, the value of A_c exceeded the largest stimulus size, and therefore could not be determined.

In an attempt to link the data with particular ganglion cell mosaics through which detection is mediated, we first discuss the normal results. Note that A_c for the B-on-Y condition tends to be much larger than for the other two conditions. It therefore seems reasonable to assume that detection of the B-on-Y stimuli is mediated by a separate ganglion cell mosaic. B-on-Y test conditions such as built into the Humphrey perimeter presumably tap the small bistratified (blue-yellow opponent) ganglion cells.[11-13] Although the W-on-W stimuli, being luminance increments, can be mediated by either the parvocellular pathway or the magnocellular pathway (*e.g.*,

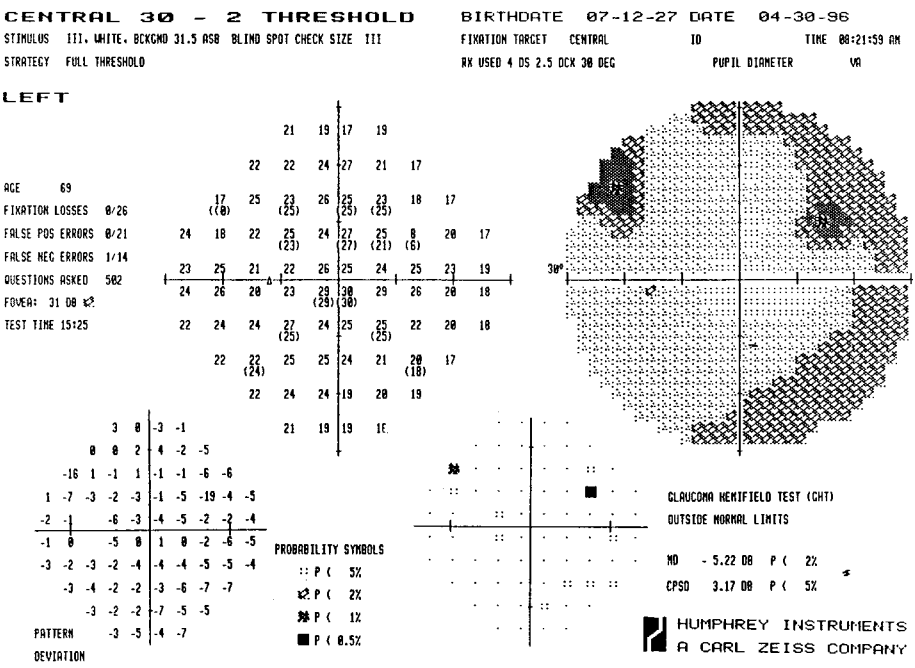

Fig. 5. Humphrey 30-2 visual field for patient P7, left eye.

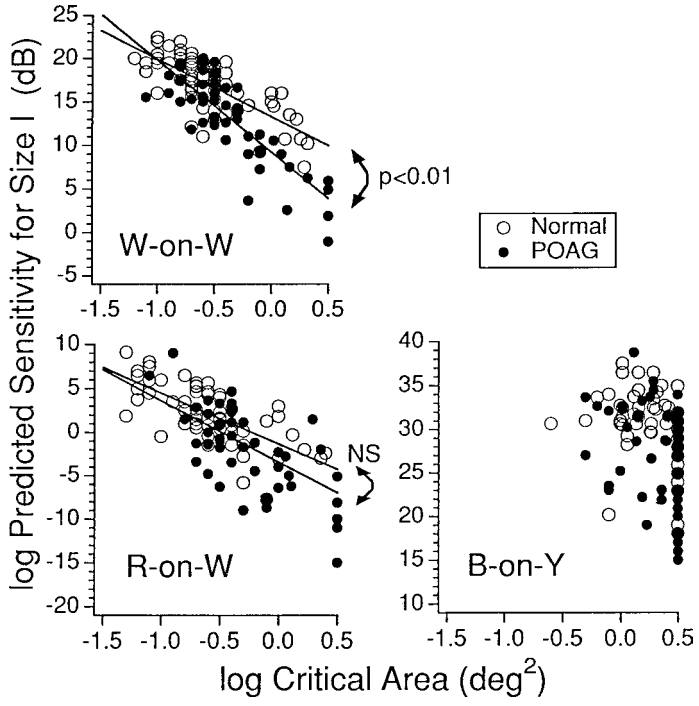

Fig. 6. Fit parameters from all test locations: log A_c (*horizontally*) versus log sensitivity for normals (*open circles*) and POAG patients (*filled circles*). Solid lines are regression lines. *Upper left:* W-on-W; *lower left:* R-on-W; *lower right:* B-on-Y.

Merigan and Maunsell[14]), they are probably mediated by the midget ganglion cells (forming part of the parvocellular pathway), as human ganglion cell dendritic fields of the magnocellular pathway (parasol cells) are similar in size to those of the small bistratified cells,[15] and hence would yield similar A_c as for the B-on-Y condition. Furthermore, the similarity between our W-on-W and R-on-W results suggests that detection is mediated in both conditions by the same ganglion cell mosaic.

However, the mean normal values for A_c found in this study are larger than ganglion cell dendritic fields found in anatomical studies. The A_c values reported here correspond to diameters of 0.54° and 1.6° for the R-on-W and B-on-Y conditions, respectively. Dacey and Petersen[16] reported dendritic field diameters for the midget and parasol cells at 15° eccentricity of 0.14° and 0.66°, respectively. Values for the small bistratified cells are similar to the parasols.[15] This implies that at 15° eccentricity, the Goldmann size I spot covers the area of about one midget dendritic field, and size III about seven midget dendritic fields, whereas spot size V covers about 20 parasol dendritic fields (since the parasol mosaic has an overlap factor of 3.4),[17] or an equal number of small bistratified dendritic fields, since their size and overlap are similar to those of the parasol cells.[15]

It has been argued[18] that cortical processing may result in linear summation of the responses of two to three neighboring ganglion cells. This would make the *cortical* receptive field larger than the ganglion cell dendritic field, and perhaps A_c corresponds to such type of receptive field. Differences in A_c may also be attributed to variation in adaptation state due to differences in mean luminance across studies. Note furthermore that the mean normal values for A_c at the present eccentricity in the W-on-W and B-on-Y conditions are close to test spot sizes III and V, respectively. These spot sizes are commonly used in standard W-on-W and B-on-Y visual field testing. This indicates an equivalence of these forms of perimetry.

A mathematical model of hexagonal mosaics of ganglion cell receptive fields (described elsewhere[10]) on the basis of human and macaque anatomical and physiological data, suggests two causes for variability in A_c. For the midget ganglion cell mosaic, which has no overlap between dendritic fields, shifts in stimulus position with respect to the center of a receptive field result in sensitivity changes. These changes are much larger for small stimuli than for the large stimuli, which leads to larger values for A_c. Positioning shifts resulting from eye movements *e.g.* could thus lead to variability in A_c. Furthermore, dropout of ganglion cells due to aging or disease could also cause a larger reduction in sensitivity for the small spots than for the large spots, again leading to larger values for A_c.

The finding that values of A_c increase much more with decreasing sensitivity in the POAG group than in the normal group, supports the idea that there is an effect of glaucoma on summation area. The finding that the difference between groups is absent for the R-on-W condition, suggests that the effect for the W-on-W condition is due to a shift to other types of ganglion cells that mediate detection: the shift would be towards cells with larger receptive fields at the visual eccentricity studied. Therefore, using perimetric stimulus configurations designed to test a single type of ganglion cells would potentially offer a more accurate measure of ganglion cell function in POAG.

Acknowledgments

The authors wish to thank Marilyn Fiedelman for recruitment of the subjects and for collecting part of the data. This research was supported in part by NIH grant EY07716.

References

1. Fellman RL, Lynn JR, Starita RJ, Swanson WH: Clinical importance of spatial summation in glaucoma. In: Heijl A (ed) Perimetry Update 1988/89, pp 313-324. Amsterdam/Milano: Kugler & Ghedini Publ 1989
2. Sloan LL: Area and luminance of test objects as variables in examination of the visual field by projection perimetry. Vision Res 1:121-138, 1961
3. Wilson ME: Invariant features of spatial summation with changing locus in the visual field. J Physiol 207:611-622, 1970
4. Latham K, Whitaker D, Wild JM, Elliott DB: Magnification perimetry. Invest Ophthalmol Vis Sci 34:1691-1701, 1993
5. Wilensky J, Mermelstein JR, Siegel HG: The use of different-sized stimuli in automated perimetry. Am J Ophthalmol 101:710-713, 1986
6. Weber J, Baltes J: Spatial summation in glaucomatous visual fields. In: Mills RP, Wall M (eds) Perimetry Update 1994/1995, p 63. Amsterdam/New York: Kugler Publ 1995
7. Dannheim F, Drance SM: Studies of spatial summation of central retinal areas in normal people of all ages. Can J Ophthalmol 6:311-319, 1971
8. Inui T, Mimura O, Kani K: Retinal sensitivity and spatial summation in the foveal and parafoveal regions. J Opt Soc Am 71:151-154, 1981
9. Glezer VD: The receptive fields of the retina. Vision Res 5:479-525, 1965
10. Swanson WH, Felius J: Spatial summation for discrete ganglion cell mosaics. Invest Ophthalmol Vis Sci 37:S1074, 1996
11. Sample PA, Taylor JDN, Martinez GA, Lusky M, Weinreb RN: Short-wavelength color visual fields in glaucoma suspects at risk. Am J Ophthalmol 115:225-233, 1993
12. Johnson CA, Adams AJ, Casson EJ, Brandt JD: Blue-on-yellow perimetry can predict the development of glaucomatous visual field loss. Arch Ophthalmol 111:645-650, 1993
13. Felius J, De Jong LAMS, Van den Berg TJTP, Greve EL: Functional characteristic of blue-on-yellow perimetric thresholds in glaucoma. Invest Ophthalmol Vis Sci 36:1665-1674, 1995
14. Merigan WH, Maunsell JHR: How parallel are the primate visual pathways? Ann Rev Neurosci 16:369-402, 1993
15. Dacey DM: Morphology of a small-field bistratified ganglion cell type in the macaque and human retina. Vis Neurosci 10:1081-1098, 1993
16. Dacey DM, Petersen MR: Dendritic field size and morphology of midget and parasol ganglion cells of the human retina. Proc Nat Acad Sci USA 89:9666-9670, 1992
17. Silveira LCL, Perry VH: The topography of magnocellular projecting ganglion cells (M-ganglion cells) in the primate retina. Neuroscience 40:217-237, 1991
18. Thomas JP: Spatial summation in the fovea: asymmetrical effects of longer and shorter dimensions. Vision Res 18:1023-1029, 1978

TEMPORAL SUMMATION IN EARLY GLAUCOMA

PETER HNIK[1], BALWANTRAY C. CHAUHAN[2], STEPHEN M. DRANCE[1] and ANGELA B. CHAN[2]

[1]Department of Ophthalmology, University of British Columbia, Vancouver, BC; [2]Department of Ophthalmology, Dalhousie University, Halifax, NS; Canada

Introduction

Localized visual field defects are the classical functional disturbances of chronic open-angle glaucoma.[1,2] In recent years, many investigators have reported that alternative psychophysical tests detect functional disturbances prior to conventional automated perimetry.[3-5] However, it is not clear whether these disturbances are localized or diffuse in nature. If the earliest damage in glaucoma is a diffuse loss of all retinal ganglion cell subtypes,[6] then a spatially diffuse loss under conditions of maximal stress or minimal redundancy would be expected.

Studying temporal summation characteristics[7] is one method of testing the visual system under varying degrees of stress. The sensitivity to a given stimulus increases with exposure time up to a point when summation is complete (critical duration time) and sensitivity is maximal. A previous study[8] found significantly increased critical duration time in the normal hemifields (defined by conventional perimetry) of glaucoma patients with damage restricted to a quadrant or the other hemifield. That study suggested that, despite normal thresholds, these 'normal' areas did show damage when under stress.

The purpose of this study was to test a group of perimetrically normal eyes of patients with marked glaucomatous visual field damage and disc abnormality in the other eye. We wanted to determine whether the visual fields measured with shorter exposure times would yield diffuse losses compared to a group of age-matched controls.

Methods

Patients and controls

We studied 54 eyes of 54 patients. Thirty-four eyes were from 34 patients with markedly asymmetric glaucoma, in whom the worse eye had marked disc damage

Address for correspondence: Peter Hnik, MD, Department of Ophthalmology, University of British Columbia, Vancouver, BC, Canada

Perimetry Update 1996/1997, pp. 223–226
Proceedings of the XIIth International Perimetric Society Meeting
Würzburg, Germany, June 4–8, 1996
edited by M. Wall and A. Heijl

and extensive localized maximum luminosity glaucomatous field defects. The fellow eyes studied had suspicious optic nerve heads and normal HFA 30-2 visual fields without any localized scotomas, and an MD better than -2.5. None of these eyes were on topical medication and none were aphakic or pseudophakic. The fellow eyes also had to have visual acuities of 6/9 or better (88% were 6/7.5 or better), clear media, and pupils of 3 mm or larger. Twenty eyes were from 20 normal subjects with clear media, normal visual fields, normal optic discs, no family history of glaucoma, and an acuity of 6/7.5 or better.

Testing methods

We first used the Ring Program of the Ophthimus perimeter (HighTech Vision, Göteborg, Sweden) to test the subjects. The Ring Program tests 50 locations in the central visual field, with a stimulus exposure time of 167 msec. We then used the same test pattern to present stimuli at 16.7, 33.4, 50.1, 83.5, 116.9 and 150.3 msec. Each subject was tested with the appropriate near correction. The order of the six tests was randomized, and a break of at least five minutes was allowed between tests.

Statistical analysis

The visual field data were analyzed using an ANOVA with the threshold for each exposure time as the dependent variable. The following model was used:

threshold = group + location + group x location + patient (group) + error

The F ratio for the group effect was derived by dividing the sum of squares for the group effect by that of the nested term. We assumed statistical significance when $p < 0.05$.

Results

There were 34 glaucoma patients and 20 healthy controls in the sample. There were no significant differences ($p<0.05$) in age [mean (± SD) patients: 62.1 (±11.94); controls: 63.0 (±10.35) years] or in the mean threshold of the standard Ring test [mean (± SD) patients: 3.74 (±1.05); controls: 3.16 (±1.06) dB].

The mean point-wise thresholds for each exposure time for the two groups is shown in Figure 1. The difference plot shows that the largest difference between the groups is at 16.7 msec exposure time. The group differences are significant for all exposure times, except for that at 150.3 msec (Table 1). The interaction term (group x location) was significant only for the 150.3 msec exposure times, indicating that the difference between the groups across locations was predominantly uniform.

Discussion

Our study shows that perimetrically normal fellow eyes of patients with uni-ocular glaucoma have temporal summation abnormalities compared to age-matched controls. Since the difference between the groups was uniform, our study suggests that the temporal summation abnormalities are diffuse in nature.

Receptive fields of retinal ganglion cells are widely overlapping.[9] Under many

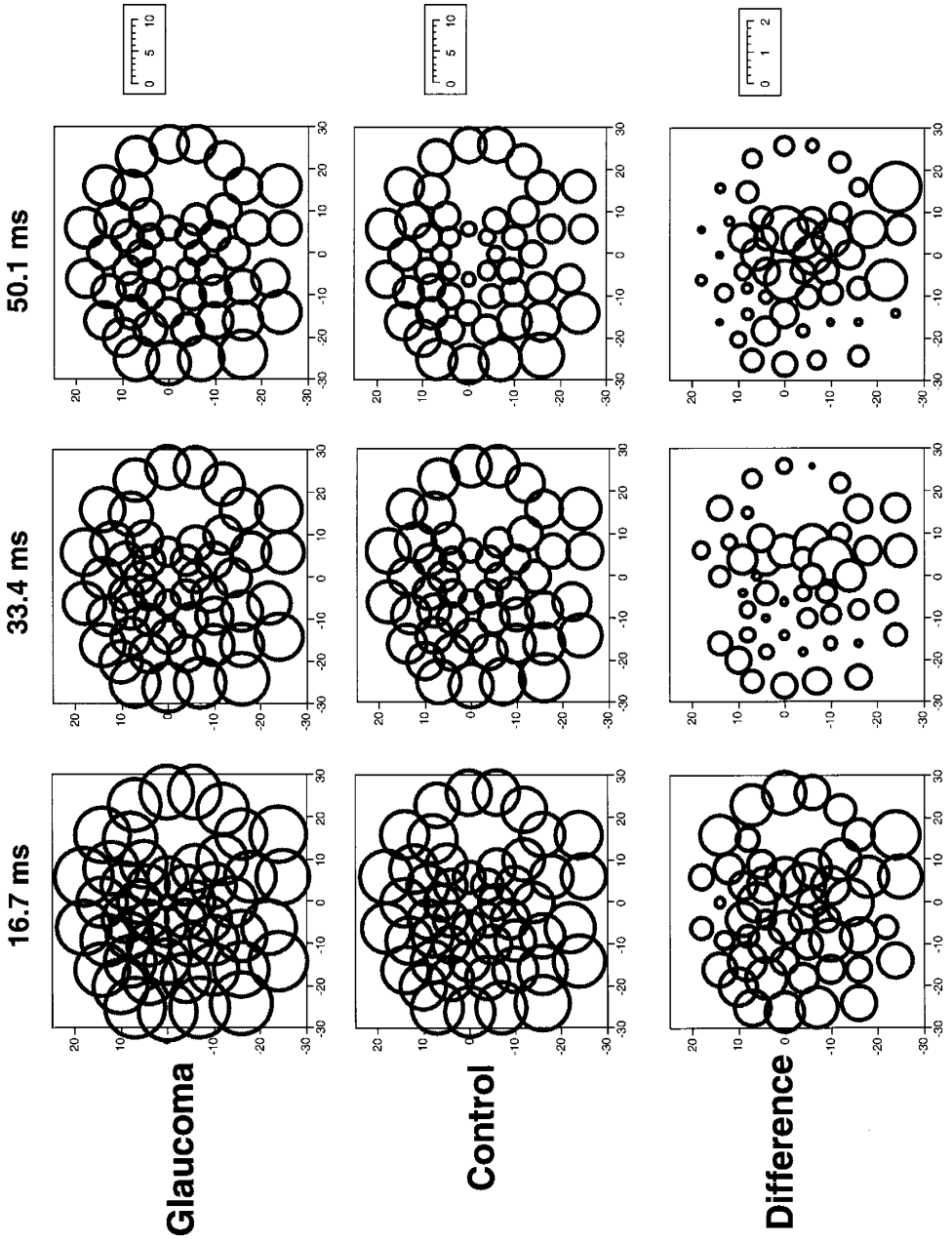
16.7 ms
33.4 ms
50.1 ms
Glaucoma
Control
Difference
0 5 10
0 5 10
0 1 2

Fig. 1.

Table 1. Results (*p* values) from the ANOVA of thresholds

	Stimulus exposure time (msec)					
Independent term	*16.7*	*33.4*	*50.1*	*83.5*	*116.9*	*150.3*
Group	0.002	0.054	0.039	0.014	0.032	0.422
Group x location	0.304	0.136	0.091	0.213	0.192	0.005

conditions, including conventional automated perimetry, these cells exhibit considerable redundancy.[6] Under conditions of minimal redundancy or stress, when only a portion of these cells are stimulated or when an integrated response is required,[10] early losses may become apparent. Studies of temporal summation essentially modulate the level of stress where the shortest exposure time should reveal the maximal difference between the two groups. This was confirmed by our study. We also showed that, at the longest exposure time (150.3 msec), when testing is done with minimal stress, the group difference in thresholds was not significantly different.

The fellow eyes of the uni-ocular glaucoma patients are at high risk of developing glaucomatous visual field loss. The fellow eyes which we studied had suspicious optic disc appearances. Our study suggests that these eyes have already suffered subclinical functional loss, which is predominantly diffuse in nature. A follow-up of these patients may show if and when visual field loss by conventional perimetry will become apparent.

References

1. Aulhorn E, Harms H: Early visual field defects in glaucoma. In: Leydhecker W (ed) Glaucoma Symposium, Tutzing Castle, pp 151-186. Basel: Karger 1967
2. Drance SM: The early field defects in glaucoma. Invest Ophthalmol 8:84-91, 1969
3. Casson EJ, Johnson CA, Shapiro LR: Longitudinal analysis of temporal modulation perimetry in early glaucoma and comparison with white-on-white and blue-on-yellow perimetry [ARVO Abstract]. Invest Ophthalmol Vis Sci (Suppl)33:1384, 1992
4. Johnson CA, Adams AJ, Casson EJ, Brandt JD: Blue-on-yellow perimetry can predict the development of glaucomatous visual field loss. Arch Ophthalmol 111:645-650, 1993
5. Sample PA, Taylor JDN, Martinez G et al: Short wavelength color visual fields in glaucoma suspects at risk. Am J Ophthalmol 115:225-233, 1993
6. Johnson CA: Selective versus nonselective losses in glaucoma. J Glaucoma 3:S32-S44, 1994
7. Gilmer TE: The integrating power of the eye for short flashes of light. J Opt Soc Am [A] 27:386-388, 1937
8. Rogers J, Chauhan BC, LeBlanc RP: Temporal summation in glaucoma patients and normal controls using high-pass resolution stimuli. Invest Ophthalmol Vis Sci (Suppl)35:2189, 1994
9. Perry VH, Oehler R, Cowley A: Retinal ganglion cells that project to the dorsal lateral geniculate nucleus in the macaque monkey. Neuroscience 12:1101-1123, 1984
10. Drum BA, Severns M, O'Leary DK et al: Selective loss of pattern discrimination in early glaucoma. Appl Opt 28:1135-1144, 1989

FLICKER RESOLUTION PERIMETRY IN GLAUCOMA

ROGER S. ANDERSON[1] and COLM J. O'BRIEN[2]

[1]Department of Optometry, University of Ulster, Coleraine, N. Ireland; [2]Department of Ophthalmology, University of Edinburgh, Edinburgh, Scotland

Introduction

Thibos *et al.*[1] demonstrated that, whereas the minimum angle of detection (MAD) for a sinusoidal grating is equal to the underlying receptive field radius, the minimum angle of resolution (MAR) is equal to the receptive field spacing (= $1/\sqrt{}$density assuming a square array). This means that peripheral grating resolution is directly related to the density of the underlying sampling array, in particular the coarsest array which is the retinal ganglion cells. Measurements of peripheral resolution have yielded results that compare closely with the predicted performance based on anatomical counts of ganglion cell density.[2]

We developed a novel perimeter which uses sinusoidal gratings to measure the density of different groups of ganglion cells in the peripheral retina. Previous measurements of peripheral resolution have predominantly employed stationary gratings which stimulate the parvocellular ganglion cells (P cells). Our perimeter, in addition to stationary gratings, uses gratings that flicker (sinusoidal phase reversal) at 30 Hz in order to stimulate a population of ganglion cells that includes a larger number of magnocellular cells (M cells). This allows us to measure not only the loss of P and M ganglion cells separately in glaucoma, but also, more importantly, the relative loss of one type over the other, in order to see if a selective loss occurs.

Methods

Peripheral resolution was measured using high contrast sinusoidal gratings at 12 different visual field locations (four at 10°, eight at 20° eccentricity) in three age-matched groups comprising eight normals, seven ocular hypertensives (OHTs) and eight glaucoma patients. Stimuli were generated on an 18-inch high resolution monitor with a central fixation cross. The procedure was a two alternative forced choice where the subject had to decide whether the grating orientation was horizontal or vertical by pressing one of two buttons. The target was either stationary or flickered at 30 Hz. Target location, orientation and the presence of flicker was random and a

Address for correspondence: Dr. Roger S. Anderson, Department of Optometry, School of Biomedical Sciences, University of Ulster, Coleraine, Co. Londonderry BT52 1SA, N. Ireland

Perimetry Update 1996/1997, pp. 227–228
Proceedings of the XIIth International Perimetric Society Meeting
Würzburg, Germany, June 4–8, 1996
edited by M. Wall and A. Heijl

3/1 reversal strategy was employed. Threshold spatial frequency in cycles/degree was calculated as the mean of four reversals for each stimulus. The mean resolution across all twelve locations was calculated for each subject for both the flickering and non-flickering stimuli.

Results

Without flicker, resolution was lower in glaucoma patients than OHTs, and in OHTs than normals. These differences were significant (ANOVA 5% level).

With 30 Hz flicker, resolution was lower in all groups than without flicker, and again, lower in glaucoma patients than OHTs, and in OHTs than normals. However, this time the difference between groups was larger.

When the ratio of flicker/non-flicker resolution was calculated at each location and averaged for each subject, performance was again significantly lower in glaucoma patients than OHTs, and in OHTs than in normals. This relative loss was particularly apparent in the early glaucoma patients and high risk OHTs, indicating a selective loss of flicker sensitive ganglion cells.

The pattern of loss generally corresponded closely with the pattern of loss measured by the Humphrey 24-2 Program. However, in some OHTs and patients with early glaucoma, deficits in resolution were noted in parts of the field that appeared 'normal' in the Humphrey field.

Conclusions

This new perimeter could detect early localized loss of ganglion cell density in patients with glaucoma and high risk ocular hypertension. These losses were more apparent when the stimulus flickered at 30 Hz.

Up to now, evidence for a selective loss of M cells in glaucoma has been of a mainly anatomical nature. Resolution measurements using this new perimeter provide strong psychophysical evidence for a selective loss of M cells in glaucoma in that resolution was measured both with and without flicker in the same subject and showed a greater loss of performance for the flickering stimulus in glaucoma patients.

It may be that the ratio of M to P cell density proves to be a better indicator of the presence of glaucoma than the density of either cell type alone. This new perimeter may in future aid the early detection of glaucoma by not only detecting early localized loss of ganglion cells, but by detecting a selective loss of one type of cell over the other.

References

1. Thibos LN, Cheney FE, Walsh D: Retinal limits to the detection and resolution of gratings. J Opt Soc Am A 4:1524-1529, 1987
2. Anderson RS, Wilkinson MO, Thibos LN: Psychophysical localization of the human visual streak. Optom Vis Sci 69:171-174, 1992

AGEING CHANGES IN AUTOMATED PERIMETRY
A comparison of flicker and luminance sensitivity in normal subjects

ALAN S. KOSMIN[1], MICHAEL W. AUSTIN[2], COLM J. O'BRIEN[3], NOLAN COTA[1] and PETER K. WISHART[1]

[1]St. Paul's Eye Unit, Royal Liverpool University Hospital, Liverpool; [2]Singleton Hospital, Swansea; [3]Princess Alexandra Eye Pavilion, Edinburgh; UK

Abstract

Flicker perimetry detects glaucomatous visual field defects earlier than traditional luminance-based systems. Visual function declines with age and this is taken into account by currently available computerized automated perimetry systems. The effects of age on flicker sensitivity, however, have yet to be fully elucidated. The authors have used one custom-built computerized automated perimeter to obtain threshold values for both flicker and luminance sensitivity at corresponding visual field locations in 60 normal subjects. In their subjects, both flicker and luminance sensitivity declined in a gradual and linear fashion with age until the sixth decade. In the seventh and eighth decades, luminance sensitivity continued to decline much as before. Flicker sensitivity, however, deteriorated much more rapidly. While flicker perimetry has promise for the early detection of glaucoma in the middle aged, it may be of limited value for diagnosis in the elderly and in the measurement of progression of field loss.

Introduction

The retinal ganglion cells whose axons project to the magnocellular layers of the lateral geniculate nucleus suffer preferential loss in early glaucoma.[1] These nerve fibers are concerned with the processing of information from stimuli of high temporal contrast, *e.g.*, flicker and movement.[2] Flicker perimetry has been shown to detect defects in the visual fields of glaucoma sufferers earlier than traditional luminance-based systems.[3-5]

Visual function in general is known to decline with age and currently available perimeters, such as the Humphrey Visual Field Analyzer and Octopus perimeter, depend on reference to a known pattern of deterioration of luminance sensitivity for identification of abnormally low areas of sensitivity and also for any subsequent statistical analysis.[6]

The purpose of this study was to investigate the effects of age on luminance and flicker sensitivity using the same instrument for each type of test.

Address for correspondence: Michael W. Austin, FRCS, FRCOphth, Department of Ophthalmology, Singleton Hospital, Sketty, Swansea SA2 8QA, UK

Perimetry Update 1996/1997, pp. 229–233
Proceedings of the XIIth International Perimetric Society Meeting
Würzburg, Germany, June 4–8, 1996
edited by M. Wall and A. Heijl

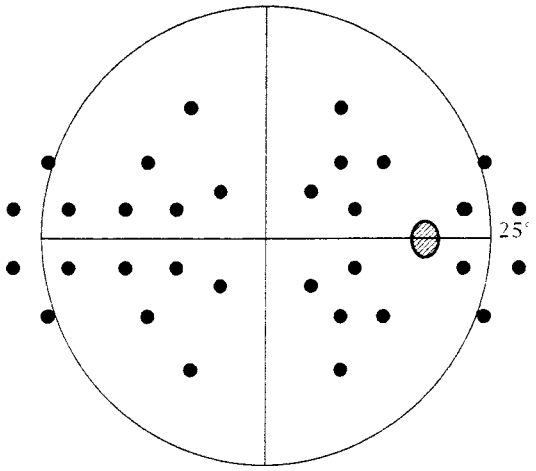

Fig. 1. Visual field locations (as for right eye).

Subjects

Sixty subjects were studied (ten per decade for the third to eighth decades, 42 females, 18 males). All had normal findings on ocular examination, including VA >6/12, IOP <21 mmHg, clear media, normal optic discs and normal visual fields, using the Humphrey Visual Field Analyzer. Potential subjects were excluded if there was a history of ocular or neurological disease or surgery, diabetes, or the systemic administration of any medication known to have ocular side-effects.

Methods

Our perimeter has been described previously.[7] The same 32 visual field locations were used for both luminance and flicker tests (Fig. 1).

Luminance thresholds were obtained using a 4-2-dB staircase, 200-μsec stimulus illumination time and 31.5-asb background illumination.

Critical flicker fusion frequency thresholds were obtained using an 8-4-Hz staircase, 1-sec stimulation time, 31.5-asb background, and a novel forced choice strategy specially devised for our perimeter and described previously (Fig. 2).[8] This strategy requires the subject to respond to the perception of the flicker of the stimulus. Groups of four LEDs were illuminated in a pseudo-random sequence. Only one of the four was made to flicker during any one stimulus presentation. The mean luminance of all four LEDs in the group was kept constant during stimulus presentation. The subjects indicated the perception of flickering stimuli by the use of a joystick. All subjects had experience with both the flicker and luminance tests prior to the study. The data for each subject were acquired in four separate sessions to minimize any effects of fatigue.

Fixation was monitored throughout the tests via a telescope behind the fixation target and also by the method of Heijl and Krakau.[9] Pupil diameter was measured prior to testing in all subjects; no pupil had a diameter of less than 2.5 mm, and in no case was pupillary dilation required.

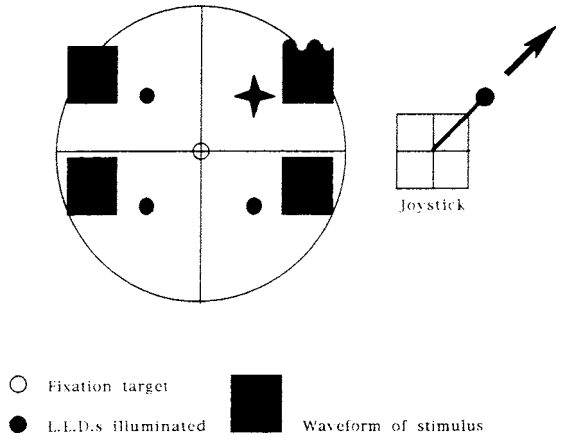

Fig. 2. Forced choice flicker perimetry.

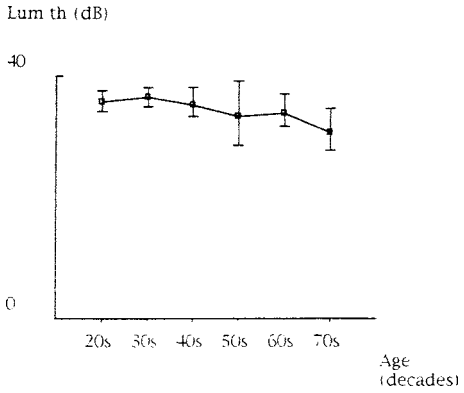

Fig. 3. Luminance threshold (dB ± SD).

Results

The mean (whole field) values for luminance and flicker sensitivity (± SD) are shown plotted by decade in Figures 3 and 4.

Discussion

Luminance sensitivity is known to deteriorate with age in a gradual and linear fashion, and our study confirms this. The effects of age on flicker sensitivity remain more controversial, previous workers having reported both deterioration and relative preservation of function.[10,11] Our subjects exhibited a gradual decline in flicker sensitivity until the sixth decade. In the seventh and eighth decades, flicker sensitivities declined steeply. This accelerated decline may be due to an age-related preferential decline in the numbers and/or function of magnocellular retinal ganglion cells. 'Pre-retinal' factors such as age-related miosis and cataract also need to be considered.

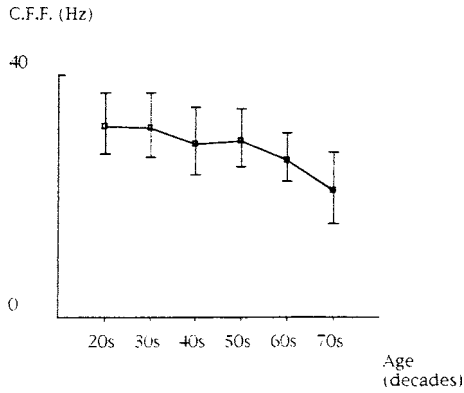

Fig. 4. Critical flicker frequency (Hz ± SD).

Small pupil size adversely affects flicker sensitivity.[12] It is our practice to dilate pupils smaller than 2.5 mm prior to perimetry but this was not required in this study. Similarly, lens opacities reduce threshold values for conventional differential light sensitivity perimetry and especially for newer short wavelength techniques. Flicker sensitivity, however, has been shown to be relatively robust to simulated media opacity.[13] One important difference between the data for luminance and flicker sensitivity was the thresholding strategy used. It is possible that the older patients found the forced choice strategy difficult and that this artifactually affected the threshold values. It was, however, generally the case that the subjects enjoyed the test and, from previous studies,[5,7,8] the forced choice strategy has been found to be more 'user friendly' than the luminance threshold method. In addition, each flicker threshold was double-checked as part of the test algorithm. We conclude therefore that the deterioration we have observed is most likely to be due to loss of magnocellular ganglion cell function. It is of interest that the histopathological work of Repka and Quigley also suggests a relatively more rapid decline for large ganglion cell numbers with age.[14]

While flicker perimetry has promise for the earlier detection of glaucoma in the middle-aged (particularly when there is associated ocular hypertension),[15,16] a decline in flicker sensitivity with age may limit the value of this technique for both diagnosis and monitoring of progression in older patients.

Acknowledgment

Supported in part by The International Glaucoma Association.

References

1. Quigley HA: Chronic glaucoma selectively damages large optic nerve fibres. Invest Ophthalmol Vis Sci 28:913-920, 1987
2. Livingstone M, Hubel DH: Psychophysical evidence for separate channels for the perception of form, movement and depth. J Neurosci 7:3416-3468, 1987
3. Lachenmayr BJ, Rothbacher H, Gleissner M: Automated flicker perimetry versus quantitative

static perimetry in early glaucoma. In: Heijl (ed) Perimetry Update 1988/89, pp 341-347. Amsterdam/Milano: Kugler & Ghedini Publ 1989
4. Casson EJ, Johnson CA: Temporal modulation perimetry in glaucoma and ocular hypertension. In: Mills RP, Heijl (eds) Perimetry Update 1992/1993, pp 443-450. Amsterdam/New York: Kugler Publ 1993
5. Austin MW, O'Brien C, Wishart PK: Flicker perimetry using a luminance threshold strategy at frequencies from 5-25 Hz in glaucoma, ocular hypertension and normal controls. Curr Eye Res 13(10):717-724, 1994
6. Brenton RS, Phelps CD: The normal visual field on the Humphrey Visual Field Analyzer. Ophthalmologica 193:56-74, 1986
7. Austin MW, O'Brien C, Wareing P, Hammond P, Wishart PK: A prototype flicker perimeter. In: Mills RP, Heijl A (eds) Perimetry Update 1992/1993, pp 603-606. Amsterdam/New York: Kugler Publ 1993
8. Austin MW, O'Brien CJ, Wishart PK: Forced choice flicker perimetry in glaucoma and ocular hypertension. In: Mills RP, Wall M (eds) Perimetry Update 1994/1995, pp 135-140. Amsterdam/New York: Kugler 1995
9. Heijl A, Krakau CET: An automated perimeter for glaucoma visual field screening and control. Graefe's Arch Clin Exp Ophthalmol 197:13-23, 1987
10. Lachenmayr BJ, Kojetinsky S, Ostermaier N et al: The different effects of aging on normal sensitivity in flicker and light sense perimetry. Invest Ophthalmol Vis Sci 35:2741-2748, 1994
11. Casson EJ, Johnson CA, Nelson-Quigg JM: Temporal modulation perimetry: the effects of aging and eccentricity in normals. Invest Ophthalmol Vis Sci 34:3096-3102, 1993
12. Brenton RS, Thompson HS, Maxner C: Critical flicker fusion. In: Wall M, Sadun AA (eds) New Methods of Sensory Visual Testing, pp 29-52. New York: Springer-Verlag 1989
13. Lachenmayr BJ, Gleissner M: Flicker perimetry resists retinal image degradation. Invest Ophthalmol Vis Sci 33:3539-3542, 1992
14. Repka MX, Quigley HA: The effect of age on normal human optic nerve fiber number and diameter. Ophthalmology 96:26-32, 1989
15. Kothe AC, Flanagan JG, Lovasik JV: Scotopic and photopic CFF during manipulation of the IOP. In: Mills RP, Heijl A (eds) Perimetry Update 1990/1991, pp 391-394. Amsterdam/New York: Kugler 1991
16. Lachenmayr BJ, Drance SM: The selective effects of elevated intraocular pressure on temporal resolution. Ger J Ophthalmol 1:26-31, 1992

A THREE-POINT VERNIER ALIGNMENT TEST WITH REMARKABLE PROPERTIES

JAY M. ENOCH

School of Optometry, University of California at Berkeley, Berkeley, CA, USA

Abstract

The 'three-point Vernier alignment test' allows assessment of vision through dense ocular media disorders (including mature cataracts where no window through the disorder is present). The test has now been *a*. refined; *b*. shown to work on an applicable patient cohort at Aravind Eye Hospital, Madurai, India; *c*. applied to a separate study of normals and macular degeneration patients (6/60 or worse), with or without a pseudo-nuclear cataract (6/60); and *d*. prepared for a clinical study. This three-point Vernier alignment test, applied to normals, has also been shown to be virtually unaffected by age; and if the test is conducted above threshold level (and without disability glare), then test luminance, contrast, veiling glare and stimulus size (within bounds) do not affect measured outcomes. This very sensitive test could serve as a reference or 'gold standard' for vision testing. The test has been adapted to perimetry and exhibits fall-off in sensitivity with eccentricity equal to or greater than the increment threshold. Macular disorders and anomalies of fixation affect the results.

Introduction

Westheimer introduced the term 'hyperacuity' into vision research literature to describe a class of vision response functions which, under ideal conditions, have thresholds of 3-8 arcsec.[1-5] As a class, these tests/responses all assess the relative position of one object relative to one or more other objects, and are processed differently by the CNS from other visual displays. The term hyperacuity refers to hyper-acute perceptions, not to extremely fine visual acuity. The Vernier alignment test, often termed Vernier acuity, is one of the hyperacuities. This test is considered in this paper.

For years, we have studied this response function as a means of assessing vision through dense media opacities.[6-10] No matter how dense a media disorder, if retinal function behind the media anomaly (leukoma, mature cataract, and aqueous or vitreous scattering bodies or blood) is intact, the individual is able to detect the presence of a bright source of light (*e.g.*, a flashlight) and point to it. This capability is termed 'projection'. If there are two or more such points of light, and they are discernable,

Address for correspondence: Prof. Jay M. Enoch, School of Optometry, University of California at Berkeley, Berkeley, CA 94720-2020, USA

Perimetry Update 1996/1997, pp. 235–239
Proceedings of the XIIth International Perimetric Society Meeting
Würzburg, Germany, June 4–8, 1996
edited by M. Wall and A. Heijl

one from the other(s), we can ask the patient, do you see 'x' points of light? If so, is the top one to the left or right of the bottom one, or is the central test point in line with two other fixed points of light? These are tests of Vernier alignment. No matter how degraded the image, observers can make these judgments with remarkable skill. Because that skill falls off with eccentricity from the central fovea (perhaps even more steeply than visual acuity), by assessing performance at such tests, we can determine the integrity of the foveal vision, and from a different point of view, measure a Vernier alignment visual field.[10]

Such determinations (as a group) are valuable. If there is markedly reduced visual capability *behind* an advanced media anomaly, after successful surgery, the patient, doctor, and family are all highly disappointed. Thus, it is important to assess, prior to surgery, the situation which exists, and to make decisions for or against surgery in advance, or at least to approach surgery with realistic expectations.

In the developing world,[11,12] such measurements are doubly meaningful, because the numbers of individuals requiring surgery are measured in millions, and resources/ surgeons to treat patients are limited. In such settings, it is a matter of triage, *i.e.*, the surgeon will say, I can perform x procedures per day, week or year; which patients shall I operate upon and/or which ones will benefit from the surgery? In these settings, with few exceptions, only one eye is treated. Thus, it is of consequence to know which of two eyes has the better prognosis for a good visual outcome after treatment.

Because large patient cohorts with reasonably common and consistent disorders are available, this research is best conducted in a developing world setting. I and my co-workers have succeeded in performing preliminary and back-up testing at Berkeley, and field studies at the Aravind Eye Hospital in Madurai, India.[13-17] These investigations are not simple from several points of view. Such experiences have been detailed elsewhere (see, for example, Refs. 13-17). One important point is that the two-point Vernier test (line up one point of light directly above a second point of light) proved to be difficult to administer at Aravind. Patients with limited education had difficulty differentiating between superimposition and vertical alignment of two points. The concept of 'vertical' proved somewhat complex to grasp, and maintenance of proper head orientation became a problem. As a result, we successfully utilized a three-point Vernier alignment task (line up a central point of light exactly in line with two fixed points of light). This greatly simplified the task.

Based on folk traditions, we can also face considerable malingering, *i.e.*, a meaningful number of patients seek to bias the results in favor of (mainly), or against, surgery (often as a result of fear or awareness of failure of surgery in other individuals), and for or against treatment of a specific eye. Many individuals believe the surgeon will not operate if there is evidence of function in an eye! They never ask the logical question: what is the point of performing surgery if there is no vision behind the advanced cataract?

So saying, we have been gratified by results achieved to date, and have been systematically preparing for a more extensive clinical study conducted by local ophthalmologists working with technicians.

Age as a factor

For some time, we have been aware of discrepancies between the ages of subjects employed at Berkeley (dominated by students) in preliminary studies, and the ages of patient groups tested in India. The latter are much older – or so it seemed. The question is complicated by the fact that cataracts develop 14-18 years earlier in India than in developed nations (this is not a simple issue). Our patients in India commonly look about 20 years older than their actual ages! Discussing this issue with Sheila West of Johns Hopkins University, she pointed out to me that she was once amazed to have seen a woman apparently in her mid-to-late sixties nursing a child. Clearly, this is not possible. I have since encountered the same thing.

My colleagues and I set out to study the age factor systematically.[18-22] To our surprise, we found for both the two- and three-point Vernier alignment tests (as tested by us) there was remarkably little (or no) meaningful alteration in this visual response function with age among our observers (20-90+ years). Many responses feeding into the same neural/visual system are affected by aging (visual acuity, contrast sensitivity, visual field extent, increment sensitivity, etc.). When we performed these studies, we were not aware of recent related research by Odom *et al.*[23] or that of Elliott *et al.*[24] It is not immediately clear why age does not markedly affect measured outcomes, but the issue is important. Westheimer argues that perhaps the response system is acting as a differential amplifier, *i.e.*, measuring differences in relative position, regardless of the values of input functions (see, for example, Refs. 20 and 22). This topic needs to be revisited in detail.

Constancies (relative)

If individual points of light can be discerned, the retina is normal, and no matter how degraded the image, responses to this test are only slightly affected relative to normal performance with sharp imagery. *Note:* Without the examiner commenting, the observer performs a center of gravity assessment of the blurred image of each point of light observed, and compares their locations, one to the other(s). Collectively, these factors imply that the judgment is largely based on low spatial frequency judgments. Alterations in luminance, veiling glare, contrast, and size (angular extent) of each light source are not highly sensitive factors in defining these visual responses. Other studies support these observations. For example, Wehrhahn and Westheimer have studied the effect of contrast.[25-27] These statements assume that testing is being carried out at super-threshold levels, disability glare is not a factor, and there are bounds within which these statements apply.

Taken together, and with the limits just discussed, the three- (or two-) point Vernier alignment function proves to be remarkably unaltered/unaffected by age, luminance, contrast, veiling glare, and target size. The Vernier alignment threshold is affected by retinal disease, eccentricity of test locus from fixation, and instability of fixation,[28] and judgments are affected by spurious resolution caused by polyopia or marked astigmatism. Effects of polyopia (*e.g.*, as encountered in posterior subcapsular cataract and related nuclear cataract) and astigmatism can be nullified largely by using a low-pass spatial filter (*e.g.*, a piece of ground glass – ground glass affects all spatial frequencies, but affects high spatial frequencies most).[29,30]

Reference (or gold) standard for vision testing

A number of responsible scientists are calling for improved indices of visual performance in clinical and basic studies of vision (*e.g.*, Charles Schepens at the Pisart Award Ceremony at the Lighthouse, New York, fall 1995). The Vernier alignment test, with its unique properties, offers many advantages as a reference standard for vision testing and control of patient responses. Therefore, we recommend that this test be subjected to broad assessment from this point of view.

Visual acuity,[27] contrast sensitivity, and glare testing often seem to be flawed because many factors affect their measured outcomes, particularly in less experienced hands. However, these tests retain many useful features. We do not recommend that these tests be set aside. Rather, we advocate that they be standardized in a superior manner. The three-point Vernier alignment test can be an effective general control for vision testing in addition to these tests. The Vernier test is simple to perform, readily explained, rapidly applied, and lends itself to video display terminals which are becoming increasingly popular today. Put another way, this test merely requires a bit of added software and a 'mouse'.

References

1. Westheimer G: Visual acuity and hyperacuity. Invest Ophthalmol 14:570-572, 1975
2. Westheimer G, McKee S: Integration regions for hyperacuity. Vision Res 17:89-93, 1977
3. Westheimer G, McKee SP: Spatial configurations for visual hyperacuity. Vision Res 17:941-947, 1977
4. Westheimer G: The spatial sense of the eye. Invest Ophthalmol Vis Sci 18:893-912, 1979
5. Westheimer G: The spatial grain of the perifoveal visual field. Vision Res 22:157-162, 1982
6. Stigmar G: Blurred visual stimuli. II. The effect of blurred visual stimuli on Vernier and stereo acuity. Acta Ophthalmol (Kbh) 49:364-380, 1971
7. Westheimer G, McKee SP: Stereoscopic acuity with defocused and spatially filtered retinal images. J Opt Soc Am 70:772-778, 1980
8. Enoch JM, Williams RA: Development of clinical tests of vision: initial data on two hyperacuity paradigms. Percept Psychophys 33:314-322, 1983
9. Williams RA, Enoch JM, Essock EA: The resistance of selected hyperacuity configurations to retinal image degradation. Invest Ophthalmol Vis Sci 25:389-399, 1984
10. Enoch JM, Williams RA, Essock EA, Fendick MG: Hyperacuity: a promising means of evaluating vision through cataract. In: Osborne NN, Chader GJ (eds) Progress in Retinal Research, Vol 4, pp 67-88. Oxford: Pergamon Press 1985
11. Enoch JM, Barroso L, Huang D: Cataract: a critical problem in the developing world. Optom Vis Sci 70(11):986-989, 1993
12. Enoch JM, Lakshminarayanan V, Azen SP, Barroso L: Vision assessment behind dense cataracts in developing nations: implications for quality of life. In: Sridhar R, Srinivasa Rao R, Lakshminarayanan V (eds) Selected Topics in Mathematical Physics: Professor R. Vasudevan Memorial Volume, pp 462-473. New Delhi: Allied Publishers Ltd 1995
13. Enoch JM, Giraldez-Fernandez MJ, Huang D, Hirosi H, Knowles R, Namperumalsamy P, LaBree L, Azen SP: Vision assessment behind dense cataracts in developing nations. In: Mills RP, Wall M (eds) Perimetry Update, 1994/1995, pp 319-327. Amsterdam/New York: Kugler Publ 1995
14. Enoch JM, Giraldez-Fernandez MJ, Knowles R, Huang D, Hunter A, LaBree L, Azen SP: Hyperacuity test to evaluate vision through dense cataracts: research preliminary to a clinical study. I. Studies conducted at the University of California at Berkeley prior to travel to India. Optom Vis Sci 72(9):619-629, 1995
15. Enoch JM, Knowles R: Hyperacuity test to evaluate vision through dense cataracts: research preliminary to a clinical study. II. Initial trials of the India instrument and HASP protocol at Aravind Eye Hospital, Madurai, India. Optom Vis Sci 72(9):630-642, 1995

16. Singh S, Aravind S, Hirose H, Enoch JM: Hyperacuity test to evaluate vision through dense cataracts: research preliminary to a clinical study. III. Data on normal subjects obtained with and without a pseudo-nuclear cataract 6/60 (20/200) at the Aravind Eye Hospital, Madurai, India. Optom Vis Sci 73(1):62-64, 1996
17. Singh S, Aravind S, Hirose H, Enoch JM, Azen SP: Hyperacuity test to evaluate vision through dense cataracts: research preliminary to a clinical study. IV. Data on patients with macular degenerations and minimal media disorders obtained with and without a pseudo-nuclear cataract 6/60 (20/20) at the Aravind Eye Hospital, Madurai, India. Optom Vis Sci 73(2)125-126, 1996
18. Reich L, Lakshminarayanan V, Enoch JM: Analysis of the method of adjustment for testing potential acuity with the hyperacuity gap test: a preliminary report. Clin Vis Sci 6:451-456, 1991
19. Lakshminarayanan V, Aziz S, Enoch JM: Variation of the hyperacuity gap function with age. Optom Vis Sci 69:423-426, 1992
20. Lakshminarayanan V, Enoch JM: Vernier acuity and aging. Int Ophthalmol 19:109-115, 1995
21. Vilar EY-P, Giraldez-Fernandez MJ, Enoch JM, Lakshminarayanan V, Knowles R: Performance on three point Vernier acuity targets as a function of age. J Opt Soc Am Part A (12(10):2293-2304, 1995
22. Enoch JM, Lakshminarayanan V, Vilar EY-P, Giraldez-Fernandez MJ, Grosvenor T, Knowles R, Srinivasan R: Two vision response functions which vary little with age. In: Adrian W (ed) International Symposium on Lighting for Aging, Vision and Health, pp 39-51. Endorsed by the White house Conference on Aging, Orlando, FL, March 22-23, 1995. New York: Lighting Research Institute 1995
23. Odom JV, Vasquez RJ, Schwartz TL, Linberg JV: Adult Vernier thresholds do not increase with age: Vernier bias does. Invest Ophthalmol Vis Sci 30:1004-1008, 1989
24. Elliott DB, MacVeigh D, Whitaker D: Variations in hyperacuity performance in age. In: Noninvasive Assessment of the Visual System. Opt Soc Am Tech Digest Ser 1991 1:137-140, 1991
25. Wehrhahn C, Westheimer G: How Vernier acuity depends on contrast. Exp Brain Res 80:618-620, 1990
26. Westheimer G, Pettet MW: Contrast and duration of exposure differently affect Vernier and stereoscopic acuity. Proc Roy Soc Lond Ser B 241:42-46, 1990
27. Wilcox WW: The basis for the dependence of visual acuity on illumination. Proc Nat Acad Sci US 18:47-56, 1932
28. Lakshminarayanan V, Knowles RA, Enoch JM, Vasudevan R: Measurement of fixational stability while performing a hyperacuity task using the scanning laser ophthalmoscope: preliminary studies. Clin Vis Sci 7(6):557-563, 1992
29. Baraldi P, Enoch JM, Raphael S: Vision through nuclear and posterior subcapsular cataract. Int Ophthalmol 9:173-178, 1986
30. Baraldi P, Enoch JM: Hyperacuity: successful evaluation of visual function through ocular opacities. In: Fiorentini A, Guyton DL, Siegel IM (eds) Advances in Diagnostic Visual Optics, pp 82-87. Heidelberg: Springer-Verlag 1987

THE DISSOCIATION BETWEEN ACTUAL AND PERCEIVED DEFECTS IN THE VISUAL FIELD, DEMONSTRATED BY A 'DOUBLE' AMSLER GRID TEST
The filling-in phenomenon revisited

AVINOAM B. SAFRAN[1], FLORENCE C. DURET[1], MARC ISSENHUTH[1] and THEODOR LANDIS[2]

[1]Neuro-Ophthalmology Unit; [2]Neurology Clinic; Department of Clinical Neurosciences, Geneva University Hospital, Geneva, Switzerland

Abstract

Affected subjects usually do not perceive their visual field defects. Often, the presence of the scotoma is only recognized indirectly, owing to invisibility of the objects located within the field defect. This has been ascribed to a perceptual completion, consisting of a filling-in of the missing information when parts of the image fall on a blind area.[1]

Results from recent neurophysiological studies indicated that filling-in is generated by mechanisms involved in reorganization of the visual cortex following alterations in sensory input. These mechanisms include expansion of the receptive field in cortical neurons, and changes in efficacy of pre-existing synapses.[2]

Although filling-in shares some similarities with Troxler's effect, these phenomena are different in nature. The latter manifests as a fading of an image projected onto the periphery when fixation is stable and is considered to reflect a local adaptation process, probably occurring at the level of the retina.[3] With filling-in, in contrast, the image surface is, at least in part, progressively invaded by the pattern from neighboring areas, including texture and color. Defective areas in the visual field are affected in a similar way by filling-in.[1]

Filling-in significantly delays the recognition of visual field defects, and hence treatment, especially when scotomas do not affect the foveal function, *i.e.*, when visual acuity is preserved. Filling-in is a major cause of failure to recognize the early stages of simple chronic glaucoma. It also dramatically affects patients with ring scotomas due to pigmentary retinopathy, who often remain unaware of the defect until late in the disease process. It causes underestimation of visual dysfunction due to photocoagulation in diabetic retinopathy, and probably in many other ocular conditions.

Several methods of visual field examination, such as Amsler grids, rely on the subject's perception of the defect against a structured background. As a result, these techniques are markedly affected by filling-in. We recently published[4] a study assessing the use of the Amsler grid in evaluating the completion phenomenon. In 15 patients with macular disorders, we compared the results of delineating central scotomas using a tangent screen and Amsler grids. In all patients, Amsler grids showed apparently smaller defects than the tangent screen. Amsler grids occasionally failed to show any abnormality at all, even in patients with major alterations. We attributed these findings to the

Address for correspondence: Prof. A. B. Safran, Neuro-Ophthalmology Unit, Ophthalmology Clinic, Geneva University Hospital, 1211 Geneva 14, Switzerland.

Perimetry Update 1996/1997, pp. 241–242
Proceedings of the XIIth International Perimetric Society Meeting
Würzburg, Germany, June 4–8, 1996
edited by M. Wall and A. Heijl

filling-in phenomenon. In addition, when two examinations were conducted in succession, we found that the size and location of the defects varied markedly, suggesting that completion is a dynamic process. Amsler grid examination therefore is inappropriate for the screening and follow-up of field defects.

The purpose of our new investigation was to test the possibility of demonstrating the degree of completion using only the Amsler grid, both for plotting the actual borders of the defect and for defining the perceived defect.

We tested five subjects with central scotomas, and three subjects with right homonymous paracentral scotomas. A white-on-black Amsler grid was used, first to delineate the perceived defects against the structured background, then to plot the actual borders of the scotoma using a very small, tangent screen type test point.

We found this form of Amsler grid testing very suitable for delineating actual borders of central and paracentral scotomas. In addition, two of our three patients with homonymous paracentral scotoma volunteered the information that, in the Amsler grid test, the diagonal line crossing the affected area showed a much larger gap than that of the grid pattern. In fact, the diagonal line showed no filling-in. In contrast, diagonals presented in isolation showed a filling-in phenomenon. This demonstrated that filling-in is a complex process involving a variety of mechanisms which can be dissociated and even compete with one another.

The ‘double’ Amsler grid test described in this study is most convenient for delineating both actual and perceived defects. In addition, this technique reveals multiple dissociations, including between perceived and unperceived defects, and between various processes involved in the ‘filling-in’ phenomenon. Theoretical and practical implications of these observations are important.

Acknowledgment

Supported by the Swiss National Fund for Scientific Research, grant #3200-040780.94/1, and by the Sandoz Foundation for Scientific Research.

References

1. Safran AB, Landis T: Cortical plasticity in the adult visual cortex. Implications for the diagnosis of visual field defects and visual rehabilitation. Curr Opin Ophthalmol 7(VI):53-64, 1996
2. Darian-Smith C, Gilbert CD: Topographic reorganization in the striate cortex of the adult cat and monkey is cortically mediated. J Neurosci 15:1631-1647, 1995
3. Aulhorn E, Harms H: Local adaptation. In: Jameson D, Hurvich LM (eds) Visual Psychophysics, Handbook of Sensory Physiology, Vol VII/4, pp 128-129. Berlin: Springer 1972
4. Achard OA, Safran AB, Duret FC, Ragama BS: Role of the completion phenomenon in the evaluation of Amsler grid results. Am J Ophthalmol 120: 322-329, 1995

MACULAR CONTRAST SENSITIVITY FUNCTION CORRELATES WITH AUTOMATED THRESHOLD PERIMETRY

ERKAN MUTLUKAN and BARRY SKARF

Department of Ophthalmology, Henry Ford Health System, Detroit, MI, USA

Abstract

The relationship between light detection thresholds in the central visual field and the contrast sensitivity function in the macula was studied. A novel pocket contrast sensitivity test which presents patterns with 1-2 dB steps and a multidirectional spatial frequency of 5 cycles/degree corresponding to peak human spatial sensitivity was used in the macular field. A forced choice method was used to test 214 eyes (108 right, 106 left) of 114 consecutive patients (mean age 55.3±15.8 years) who were taking Humphrey Visual Field Analyzer 30-2 test with standard parameters. The regression analysis technique was used to study the correlation between the contrast sensitivity function (CSF) and the field indices of mean deviation (MD) and corrected standard pattern deviation (CPSD) as well as the foveal, parafoveal and average macular light thresholds. Results from both eyes individually, as well as interocular differences, were determined. Statistically significant correlations between the CSF and average macular light thresholds (MLT) [CSF=6.20+0.65 MLT; r=0.53, p<0.001), MD [CSF=27+0.38 MD; r=0.42, p<0.001] and CPSD [CSF=26.1-0.44 CPSD; r=0.28, p=0.003] were observed. Also, the interocular difference (D) in macular light thresholds (DMLT) significantly correlated with the asymmetry in contrast sensitivity function (DCSF) [DCSF=0.32+0.62 DMLT; r=0.56, p<0.001]. Similar correlations were identified between the interocular differences in CSF and MD [DCSF=0.29+0.43 DMD; r=0.51, p<0.001] as well as CPSD [DCSF=0.38-0.57 DCPSD; r=0.44, p<0.001]. The results suggest that macular contrast sensitivity testing may predict and complement conventional light sensitivity in the visual field and may be useful in situations where automated threshold perimetry is not possible.

Introduction

Contrast sensitivity function (CSF) is the result of receptive field formation and integrity of parallel channels in the visual system and reflects the balance between the ON and OFF pathways.[1] Threshold perimetry, which also measures the retinal receptive field density, is currently the gold standard in evaluation of neuro-visual system disorder.

However, it is not always possible to perform automated perimetry readily due to its cost, availability, time requirement, dependency on trained personnel and need for high level of patient cooperation. Contrast sensitivity (CS) testing with spatial pat-

Address for correspondence: Erkan Mutlukan, MD, PhD, Department of Ophthalmology, Henry Ford Health System, 2799 West Grand Boulevard, Detroit, MI 48202, USA

Perimetry Update 1996/1997, pp. 243–250
Proceedings of the XIIth International Perimetric Society Meeting
Würzburg, Germany, June 4–8, 1996
edited by M. Wall and A. Heijl

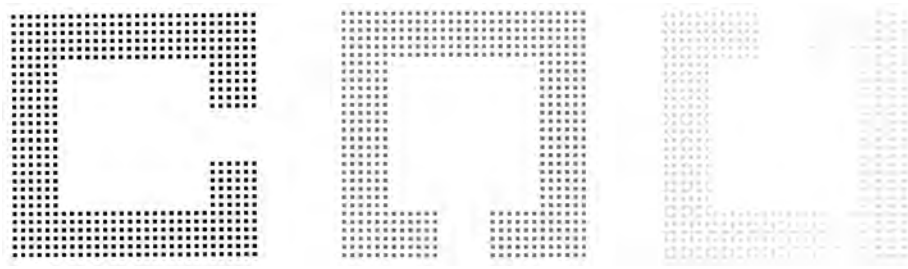

Fig. 1. Examples of contrast test patterns used in the study. Each of a total of 18 'C' patterns is presented on one page of a test book.

Table 1.

Reason for visual field test	*No. of patients*
Glaucoma / ocular hypertension	76
Optic neuritis / multiple sclerosis	15
Pseudotumor cerebri	7
Intracranial tumors	5
Retinal disease	3
Optic nerve menengioma	2
Ischemic optic neuropathy	2
Cerebrovascular accident	2
Intracranial aneurysm	1
Head trauma	1
Total	114

terns has been shown to be of informative value in diagnosis of eye and brain diseases,[2] but, is also used infrequently and only as a complimentary test. Many methods of CSF have little or no impact in routine ophthalmic practice[3] as they require either costly equipment and/or significant time and effort on the part of both the patient and the care provider in busy ophthalmic clinics. A better understanding of the relationship between the results of these two different psychophysical testing approaches may facilitate more widespread and precise visual sensitivity determination in routine eye care practice.

This study describes a novel, portable and quick method of CS testing in the form of a test book, and investigates the relationship between conventional threshold perimetry and the contrast sensitivity function to spatial frequency patterns of varying contrast.

Material and methods

The novel test pattern consisted of square-wave dark spots forming a 'C'-shaped pattern subtending to 5 x 5° in the macular visual field when viewed at 2 feet test distance. The dots forming the test patterns subtend to a spatial frequency of 5 cycles/degree both vertically and horizontally, corresponding to peak human spatial sensitivity (Fig. 1).

The contrast (C) of the dark pattern on white background ranged up to 33 dB with

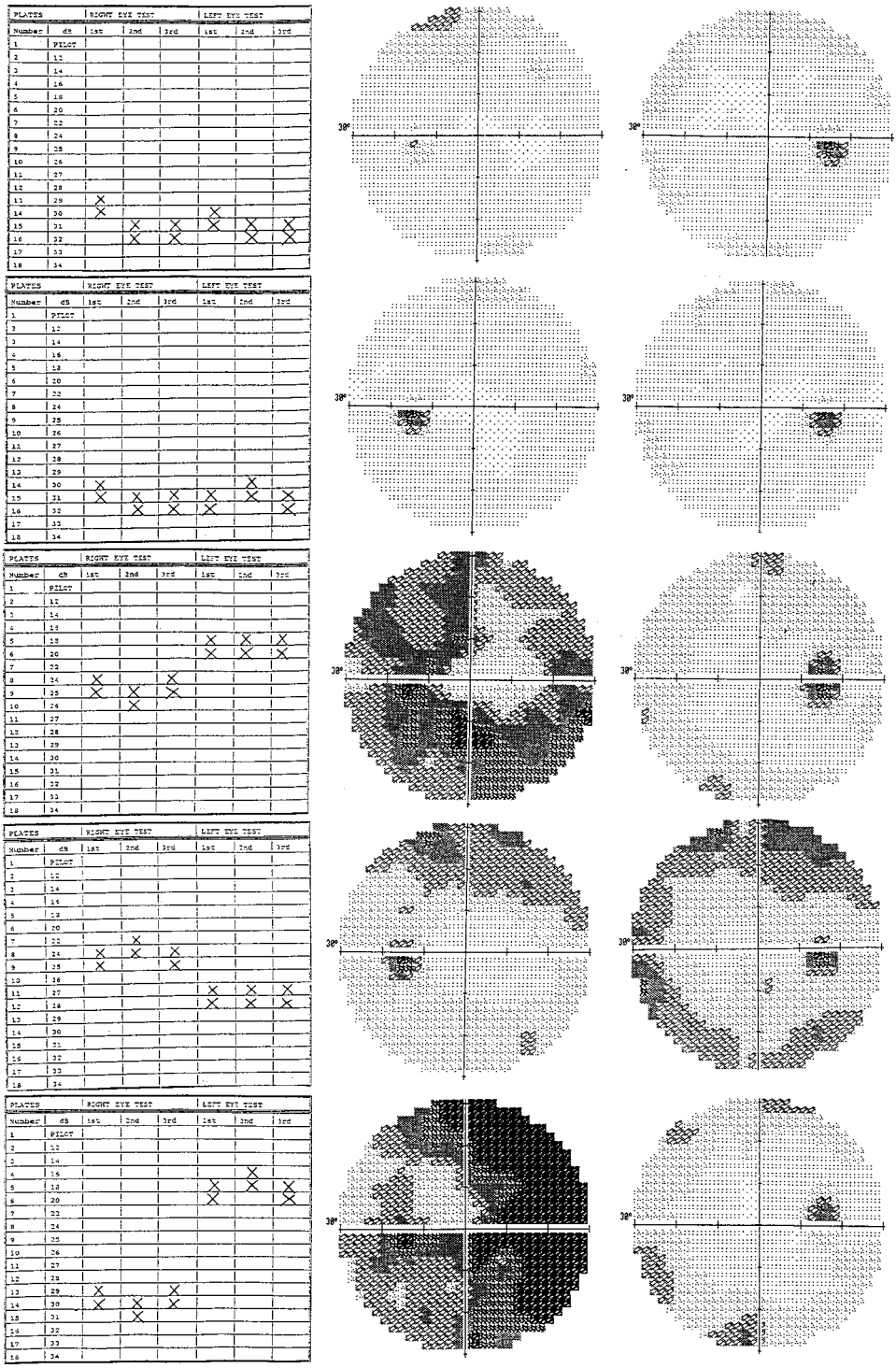

Fig. 2. Contrast sensitivity and perimetric results from a normal (*top*), ocular hypertensive with normal fields (*2nd row*), glaucoma with bilateral and asymmetrical involvement and, resolving optic neuritis (*bottom*).

Table 2. Regression analysis results

Right eyes		
CS	27.1+0.38 MD	r=0.41 p<0.001
CS	26.1-0.44 CPSD	r=0.28 p<0.005
CS	8.36+0.58 MLT	r=0.51 p<0.001
CS	2.41+0.68 FLT	r=0.47 p<0.001
CS	11.3+0.49 PFLT	r=0.49 p<0.001
Left eyes		
CS	26.7+0.37 MD	r=0.35 p<0.001
CS	26.3-0.52 CPSD	r=0.32 p<0.003
CS	6.20+0.65 MLT	r=0.53 p<0.001
CS	-3.65+0.87 FLT	r=0.60 p<0.001
CS	10.7+0.51 PFLT	r=0.47 p<0.001
Interocular asymmetries		
DCS	0.29+0.43 DMD	r=0.51 p<0.001
DCS	0.38-0.57 DCPSD	r=0.44 p<0.001
DCS	0.32+0.62 DMLT	r=0.56 p<0.001
DCS	0.40+0.46 DFLT	r=0.46 p<0.001
DCS	0.33+0.53 DPFLT	r=0.53 p<0.001

CS: contrast sensitivity (in dB); FLT: foveal threshold; PFLT: perifoveal threshold; MLT: macular light threshold; D..: difference in .. (interocular asymmetry); MD: mean deviation (full field); CPSD: corrected pattern standard deviation (full field)

1 to 2 dB steps using Michelson's formula[2] ($C=L_{max}-L_{min}/L_{max}+L_{min}$) and converted to decibels (dB= 20 log C). Each pattern formed a plate as one page of a test book and was presented to the patient in the macular field at the standard test distance. A four choice forced detection method involving the description of the opening location was used. Patients were encouraged to give answers until they guessed incorrectly for two consecutive pattern contrasts. The average between the last correct and first incorrect answers was regarded as the dB score. Each eye was tested three times and the average taken as the final result for that eye. CS tests were performed with refractive correction, standardized test distance and lighting conditions (150 cd/m^2) either before or after automated perimetry.

The study group consisted of 143 consecutive patients who underwent scheduled Humphrey Visual Field Analyzer 30-2 test with standard parameters during their routine clinical evaluation. All patients had refractive error less than ±7.00 diopters (D) with a cylindrical component of less than 2.00 D. The technician who performed contrast sensitivity tests was not aware of the visual field status of patients. Those patients who produced acceptable reliability criteria (*i.e.*, fixation losses <20% and false positives and false negatives <33% of total attempts) were included in the analysis. The diagnosis for those patients is given in Table 1.

The correlation between the CS and various parameters of the perimetric results, namely the foveal thresholds, perifoveal thresholds (*i.e.*, four test points in the innermost circle of the Humphrey 30-2 test grid at 4° from fixation), macular light thresholds (*i.e.*, average of foveal and perifoveal sensitivities) and the field indices of mean deviation (MD) and corrected standard pattern deviation (CPSD) were studied using regression analysis.

The relationship between the CS and automated perimetric results were studied for individual eyes and interocular differences.

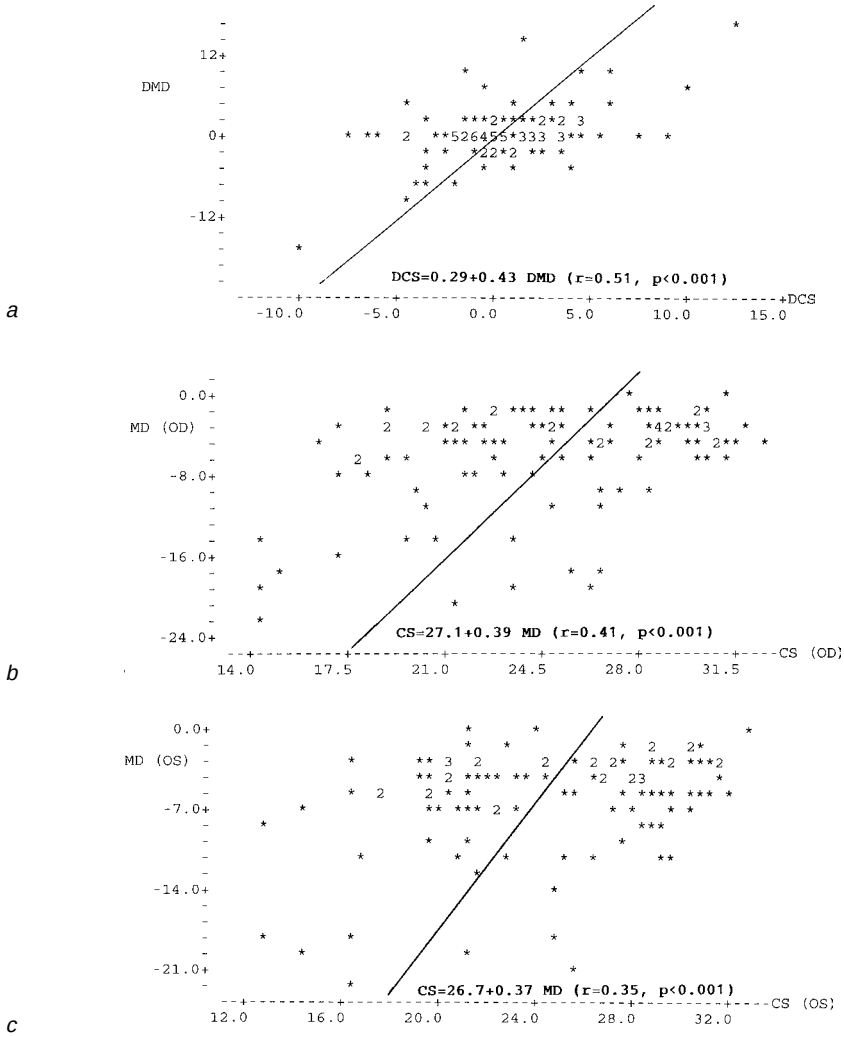

Fig. 3. The relationship between contrast sensitivity (CS) and mean deviation (MD) for individual eyes and interocular differences (in dB). *a.* Interocular differences in contrast sensitivity (DCS) versus differences in mean deviation (DMD). *b.* MD versus CS in right eyes (OD). *c.* MD versus CS in left eyes (OS).

Results

Among 143 consecutive patients who underwent Humphrey perimetry, 214 eyes (108 right, 106 left) of 114 patients (mean age, 55.3±15.8 years) produced acceptable reliability criteria and were included in the evaluation. Low perimetric reliability was observed in one eye of 15 patients (10.5% of the total) and in both eyes of 14 patients (9.8% of the total). The total low reliability rate of 20.3% (43 eyes) in the study group was the result of fixation losses in 20 eyes (47%), false positives in three eyes

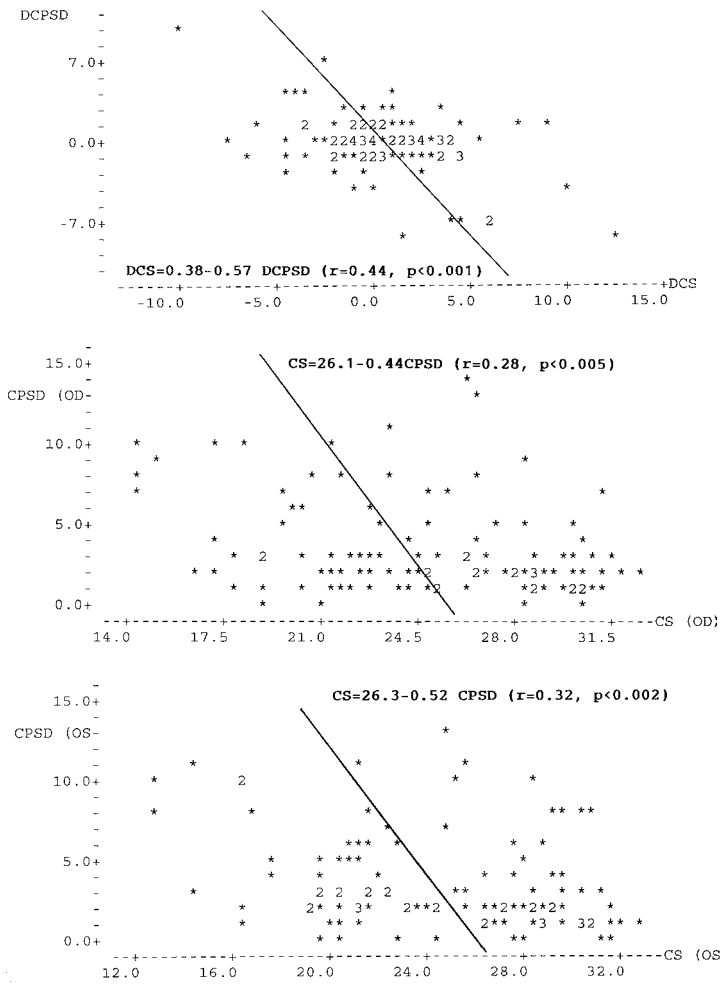

Fig. 4. The relationship between contrast sensitivity (CS) and corrected pattern standard deviation (CPSD) for individual eyes and interocular differences (in dB). *a.* Interocular differences in CS (DCS) versus differences in CPSD (DCPSD). *b.* CPSD versus CS in right eyes (OD). *c.* CPSD versus CS in left eyes (OS).

(7%), false negatives in 16 eyes (37%) and the combination of two abnormal reliability criteria in four eyes (9%).

None of the patients who took the CS test was unable to complete the test procedure.

There was a statistically significant correlation between the contrast sensitivity scores and visual field results from individual eyes. Examples of test results are given in Figure 2.

CS scores had the strongest correlation with foveal light threshold (r=0.60) and macular light threshold (r=0.53) values from Humphrey Perimetry. CS scores had the weakest correlation with CPSD (r=0.28).

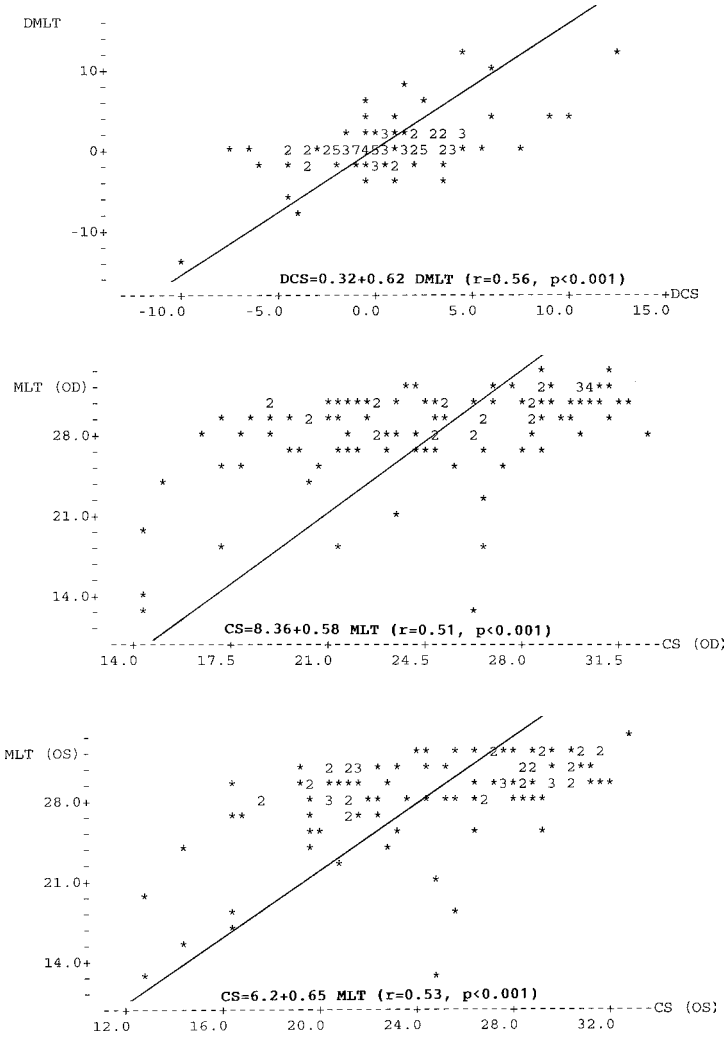

Fig. 5. The relationship between contrast sensitivity (CS) and macular light thresholds (MLT) for individual eyes and interocular differences (in dB). *a.* Interocular differences in CS (DCS) versus differences in MLT (DMLT). *b.* CS versus MLT in right eyes (OD). *c.* CS versus MLT in left eyes (OS).

In general, correlations between interocular differences in CS and visual field scores were stronger than those observed between scores from individual eyes (Table 2, Figs. 3, 4 and 5).

Discussion

A quick, portable and low cost CS test, as described above, may facilitate more accurate visual function assessment in busy clinics, especially when there is no

significant Snellen acuity loss.[4] As it is considered superfluous to conduct contrast testing at high or low spatial frequencies and the testing should focus on the peak sensitivity (4-5 cycles/degree),[5] the contrast test pattern was tuned for that frequency. A sufficient amount of fine steps have been provided to enable adequate sampling to detect change in CS.[6] A forced choice method was implemented instead of numeric or letter optotypes for the frequency pattern since forced choice procedures provide the highest level of reliability.[7]

Although results suggest significant correlation between full field scores (MD & CPSD) and CS, the relationship was strongest within the macular visual field (*i.e.*, central 10°). Similarly, asymmetry in the CS scores between the eyes had a stronger relationship with interocular visual field asymmetries, suggesting that the test may be most useful in conditions causing unilateral or asymmetrical visual involvement, such as optically degrading conditions (*i.e.*, cataract) and organic visual pathway disease involving macula or optic nerve. The results observed in this study provided evidence that CS and light detection thresholds are inter-related, and it may be possible to predict to some extent the result from either test by testing with the other one. As each clinical vision test measures 'something unique to itself',[8] a perfect correlation between different tests should not be expected. For the same reason, CS testing may reveal a different number of abnormalities than those detected by perimetry. The correlation between CS to gratings and automated (*i.e.*, Octopus) perimetry has been reported in glaucoma using a sophisticated contrast-testing approach.[9] Our findings support the presence of a significant relationship between the results from threshold perimetry and contrast testing in a general patient population also using a more practical approach. The described contrast test procedure takes one to two minutes per eye to complete. Since automated perimetry may not yield useful information in one of five tested individuals due to low reliability, CS testing may prove useful in clinical monitoring of such patients with high efficiency.

In conclusion, macular CS testing correlates with conventional light sensitivity in the visual field, may supplement perimetry, and may be useful in situations where automated threshold perimetry is not possible.

References

1. Schiller PH, Sandell JH, Maunsell JH: Functions of the ON and OFF channels of the visual system. Nature 322:824-825, 1986
2. Nadler MP, Miller D, Nadler DJ (eds): Glare and Contrast Sensitivity for Clinicians. New York: Springer-Verlag 1990
3. Moseley MJ, Hill AR: Contrast sensitivity testing in clinical practice. Br J Ophthalmol 78:795-797, 1994
4. Trobe JD, Beck RW, Moke PS, Cleary PA: Contrast sensitivity and other vision tests in the optic neuritis treatment trial. Am J Ophthalmol 121:547-553, 1996
5. Wilkins AJ, Della Sala S, Somazzi L, Nimmo-Smith I: Age related norms for Cambridge low contrast gratings including details concerning their design and use. Clin Vis Sci 2:201-212, 1988
6. Bailey IL, Bullimor MA, Raasch TW, Taylor HR: Clinical grading and effects of scaling. Invest Ophthalmol Vis Sci 32:422-432, 1991
7. Blackwell HR: Studies of psychophysical methods for measuring visual thresholds. J Opt Soc Am 42:606-616, 1952
8. Aspinall PA: Some methodological problems in testing visual function. Mod Prob Ophthalmol 13:2-7, 1974
9. Zulauf M, Flammer J: Correlation of spatial contrast sensitivity and visual fields in glaucoma. Graefe's Arch Clin Exp Ophthalmol 231:146-150, 1993

GLAUCOMA

IS EARLY DAMAGE IN GLAUCOMA SELECTIVE FOR A PARTICULAR CELL TYPE OR PATHWAY?

SHANNON LYNCH, CHRIS A. JOHNSON and SHABAN DEMIREL

Optics and Visual Assessment Laboratory (OVAL), Department of Ophthalmology, University of California, Davis, Sacramento, CA, USA

Abstract

There is much debate in the literature regarding the nature of early glaucomatous damage. Histopathological studies of optic nerve fibers suggest a selective large fiber loss, examination of the dorsal-lateral geniculate nucleus suggest a selective magnocellular (M-cell) loss, while other investigations suggest a non-selective loss that is due to under-sampling or reduced redundancy of sparsely represented mechanisms. The authors examined these competing hypotheses by performing a series of visual function tests that are believed to be mediated by different neural subpopulations. Short-wavelength automated perimetry (SWAP), red/green opponent process perimetry, low (2 Hz) and high (16 Hz) temporal frequency modulation perimetry, displacement perimetry and standard automated perimetry were performed in a small group of patients with early glaucomatous damage. Overall, the greatest amount of loss was observed with SWAP. In seven out of ten eyes, SWAP deficits were more extensive than those observed with all other test procedures. Although some functions were more greatly affected than others in individual eyes, there were no consistent trends observed, except with SWAP. At the present time, SWAP appears to have the best performance of any of the visual function tests for detection of early glaucomatous damage. These findings do not support the concept that early glaucomatous losses are predominantly due to magnocellular mechanisms or those pathways with the largest fiber diameters. Reduced redundancy or under-sampling provides the most parsimonious explanation of the present findings.

Introduction

The glaucomatous disease process causes damage to the neural elements of the optic nerve and retina. There is still debate, however, as to the pattern of neural loss that constitutes the earliest damage due to glaucoma. Microscopic studies of the optic nerves and retinae of both non-human primates and humans with glaucoma have suggested that there may be a selective loss of larger caliber axons and ganglion cells with larger soma early in the disease process.[1-4] Histological studies of the primate visual system suggest that, at any retinal eccentricity, cells that project to the magnocellular layers of the lateral geniculate nucleus (LGN) have larger soma and

Address for correspondence: Chris A. Johnson, PhD, Optics and Visual Assessment Laboratory, Department of Ophthalmology, 1603 Alhambra Boulevard, Sacramento, CA 95816, USA

Perimetry Update 1996/1997, pp. 253–261
Proceedings of the XIIth International Perimetric Society Meeting
Würzburg, Germany, June 4–8, 1996
edited by M. Wall and A. Heijl

larger caliber axons than cells at a similar eccentricity that project to the parvocellular layers of the LGN.[5-8] This piece of information has led to the conclusion that either larger caliber axons or, perhaps more distinctly, magno ganglion cells, are selectively damaged early in the glaucomatous process. This conclusion is supported by the fact that flicker sensitivity[9-12] and motion sensitivity[13-16] are reduced in ocular hypertension and early glaucoma, both of which are supposedly mediated by the magnocellular division of the retino-cortical projection.[17-19]

Despite evidence suggesting a selective loss of larger caliber axons or magno cells in glaucoma, there is also a wealth of evidence in the literature detailing abnormal color vision, slow frequency flicker sensitivity loss and peripheral spatial resolution deficits.[12,20-26] Color vision is believed to be a specialization of the parvocellular stream of the retino-cortical projection,[27-31] and detection of slowly flickering targets is also believed to be mediated by parvo cells.[17,28] Abnormal color vision and reduced sensitivity to slow flicker should not be seen early in the glaucomatous process if magno cells are being selectively damaged.

Another possible mode of neural damage in early glaucoma is that all retinal ganglion subpopulations are damaged. Since the number of cells in each subpopulation is not equal, it is probable that there is not the same degree of receptive overlap for each of these populations. Functions that are conveyed by sparse classes of cells, *i.e.*, classes showing reduced redundancy, will also show the earliest loss.[32,33]

One method of determining the mode of early neural loss in glaucoma is to conduct a battery of functional tests in the same eyes and to examine the relationships among patterns of loss for these different functions. Only a few investigations have compared different visual function tests in the same glaucoma patients.[12,34] Through an understanding of which subpopulations of neurons convey which functions, inferences as to what neurons are being lost can be reached. Six tests were performed on each eye in this study: standard (white on white) automated perimetry (STD), short-wavelength automated perimetry (SWAP), red on white opponent process perimetry (R/W), displacement threshold perimetry (DTP), low frequency temporal modulation perimetry (2-Hz-TMP) and high frequency temporal modulation perimetry (16-Hz-TMP).

Both STD and R/W are functions that are believed to be conveyed by parvocellular units and, as such, are detectable by many neural elements in the retina. The detection of slow flicker is also believed to be mediated by parvocellular units and this type of stimulus should also be detectable by a great many ganglion cells. SWAP stimuli are believed to be detected by a sparse subclass of parvocellular neurons that have slightly larger caliber axons than red-green opponent parvo cells. As such, SWAP stimuli are usually detected by a much smaller number of ganglion cells than an STD stimulus. SWAP stimuli can be detected by other ganglion cells but with greatly reduced sensitivity. Motion detection is believed to be mediated by magnocellular neurons, as is the detection of fast flicker.

It follows then that DTP and 16-Hz-TMP stimuli are probably detected by magnocellular units. These cells are less numerous than parvo cells in the visual system[35] and tend to have larger axon diameters at any given retinal eccentricity.

In conducting this study and measuring many functions in each eye, we were testing three hypotheses of early neural loss in glaucoma. Each hypothesis makes different predictions as to the extent of damage that would be seen in each of the functional tests. The hypotheses are outlined below.

Hypothesis 1. Early glaucomatous loss occurs selectively for large diameter fibers. This predicts that loss will be

greatest with 16-Hz-TMP and DTP
intermediate with SWAP
least with 2-Hz-TMP, R/W and STD

Hypothesis 2. Early glaucomatous loss occurs selectively for magno or parvo mechanisms. This predicts that loss will be

Magno loss greatest with 16-Hz-TMP and DTP
intermediate with 2-Hz-TMP, SWAP and R/W
least with STD

Parvo loss greatest with 2-Hz-TMP, SWAP and R/W
intermediate with 16-Hz-TMP and DTP
least with STD

Hypothesis 3. Early glaucomatous loss is non-selective, but damage becomes evident earlier for non-redundant systems. This predicts that loss will be

greatest with SWAP, 16-Hz-TMP and DTP
intermediate with R/W
least with 2-Hz-TMP and STD

Methods

Ten eyes of eight subjects with early glaucomatous visual field loss or with a high risk of developing glaucoma (risk > 0.75 for a logistic regression model[36]) were tested. Both eyes of all subjects had a best corrected visual acuity of 20/40 or better and an intraocular pressure of greater than 21 mmHg before any treatment. Refractive errors had to be less than five diopters spherical equivalent and less than three diopters of cylinder. All subjects wore an appropriate near correction during the functional testing. Patients were excluded if they had a history of ocular or neurological disease or surgery, diabetes, or any condition other than glaucoma that may have affected their visual field sensitivity. All eyes were tested with six different functional tests, described briefly below.

1. STD (white on white) was performed with a Humphrey Visual Field Analyzer using the 30-2 test with standard parameters.
2. SWAP was performed on a modified Humphrey Visual Field Analyzer. The test uses the 30-2 pattern and logic. However, the modifications consisted of using a short wavelength Goldmann size V target (2°) displayed against a bright (200 cd/m^2) yellow background.[23,37]
3. Opponent process perimetry (R/W) was also performed using the 30-2 test pattern of a modified Humphrey Visual Field Analyzer. This modification consisted of introducing a red interference filter (peak 620 nm) into the stimulus path and using a Goldmann size V (2°) target.[38] Using a larger target has been shown to bias detection in favor of opponent mechanisms.[39]
4. DTP uses a large screen (21-inch) computer VDU controlled by a 24-bit color video card. Testing was performed at equivalent locations to those used by the 30-2 pattern of the Humphrey Visual Field Analyzer without the most peripheral 16 points. Stimulus luminance was 50 cd/m^2 and background luminance was 10 cd/m^2. This technique is described in detail elsewhere.[40]

5/6. TMP was performed using an LED perimeter constructed in the author's labora-

tory. This perimeter uses a bowl (luminance 100 cd/m^2) with recessed LED stimuli (1.5° diameter) which were equated in luminance to the background. This allowed temporal modulation to be performed about the background intensity, the stimulus wave form being one second of sinusoidal modulation with a cosine envelope to avoid temporal transients. Temporal modulation contrast sensitivity was measured at 45 locations in the central 27° (11 per quadrant and one at the fovea) at a low temporal frequency (2 Hz) and a high temporal frequency (16 Hz) using a modified binary search (MOBS) procedure. Subjects were instructed to respond by button press when they detected a stimulus flickering in the field. Each test took approximately 15 minutes. More details of this technique can be found elsewhere.[12]

All results were compared to age-matched normal data which have been collected for each test in the author's laboratory. Points exceeding the normal 95% and 99% confidence limit were compared for each test.

Results

No single test procedure showed the most extensive amount of loss in all ten eyes studied. SWAP revealed the most extensive loss in seven of the ten eyes, although all test procedures showed the most or second most amount of loss in at least two out of the ten eyes. This is shown graphically in Figure 1. In this figure, black bars depict tests that showed the most extensive loss in a particular eye, whereas cross-hatched bars depict tests that showed the second most extensive damage in a given eye. Although the cohort was relatively small, patterns of loss fell into three general categories. The first pattern of loss was seen in the majority of eyes tested. In this group, SWAP test results showed more extensive loss than the other five test procedures used. Figure 2 shows test results from an eye that fell into this category. In this figure, for each test procedure, white stimulus locations indicate results that were within age-matched normal limits. Stippled locations indicate points that were below the lower 5% normal confidence interval and solid black locations indicate points that were below the lower 1% normal confidence interval.

The second pattern of loss was characterized by opponent perimetry (R/W) revealing a greater extent of damage than the other five test procedures. This was seen for one eye in each of two patients. An example of such an outcome is shown in Figure 3. This figure follows the same symbol convention as the previous one.

The third pattern of loss to emerge in this study was characterized by approximately equal reduction of sensitivity with both SWAP and STD. Both these tests showed greater amounts of loss than the other four procedures examined. Figure 4 shows an example of such an outcome.

To compare the spatial location of loss, results were analyzed according to eight nerve fiber bundle regions. If half or more of the locations in a region were beyond normal limits, the region was considered to be abnormal. Since SWAP demonstrated the most consistent and extensive loss, all other tests were compared to it. For each region we determined whether SWAP and other tests agreed (both normal or both abnormal) or disagreed (one normal and one abnormal). The results are presented in Table 1, where a ratio of agreeing to disagreeing regions is shown. In general, there was greater agreement than disagreement between SWAP and other tests.

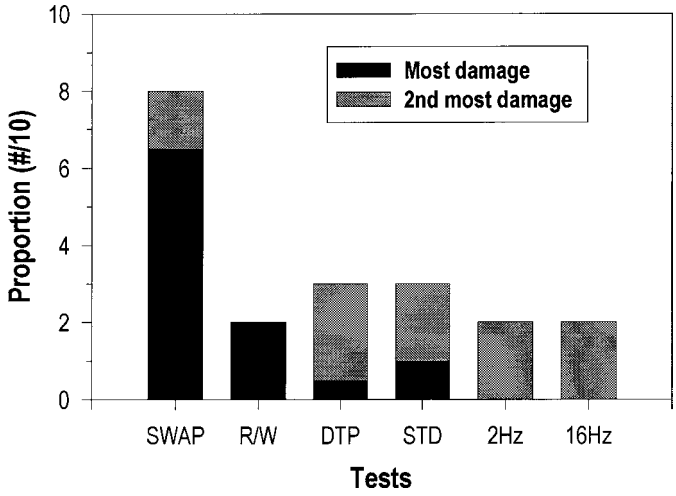

Fig. 1. Summary of the results obtained in the ten eyes. Dark bars indicate that a test showed the most extensive damage in a given eye, cross-hatched bars indicate that a test showed the second most extensive damage in a given eye.

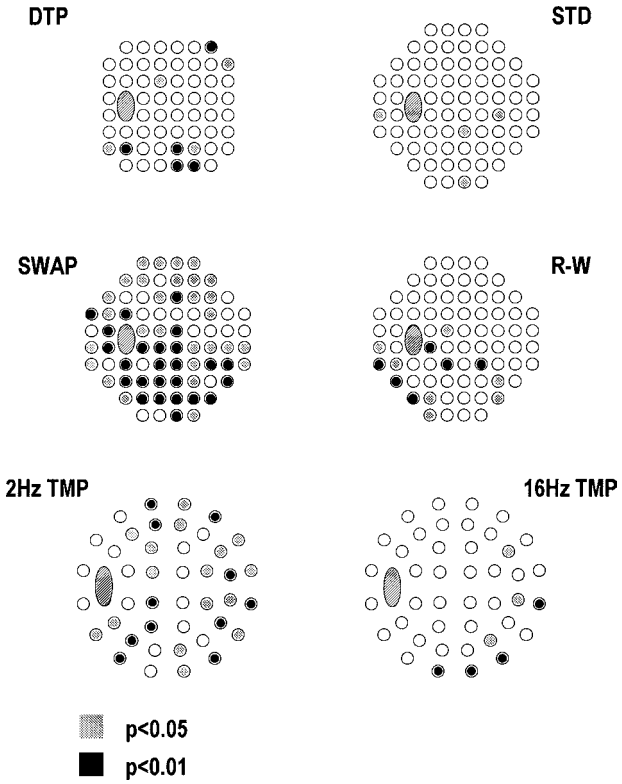

Fig. 2. Results indicative of those obtained in six eyes. SWAP shows the most extensive damage with the other tests showing variable but less extensive damage.

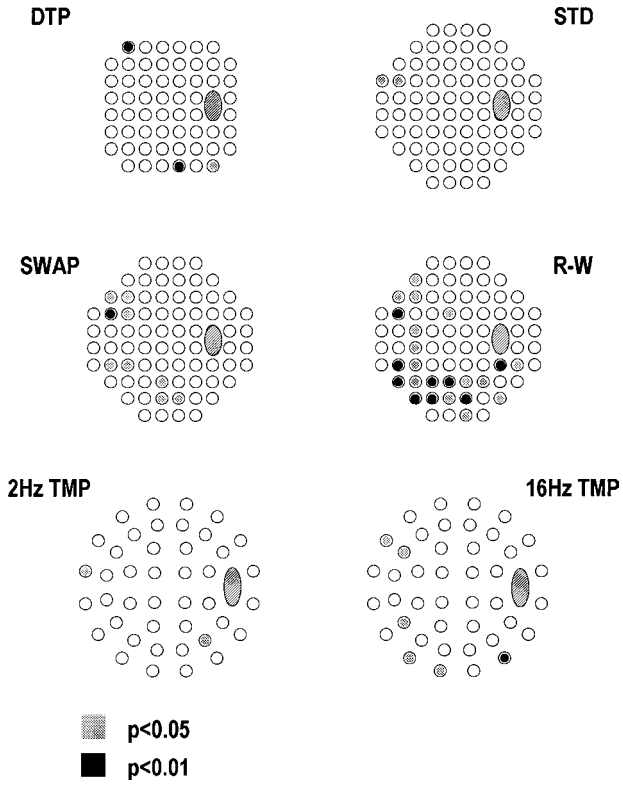

Fig. 3. Results indicative of those obtained in two eyes of two separate subjects. Red on white perimetry shows the most extensive damage with the other tests showing variable but less extensive damage.

Table 1. Ratio of nerve fiber bundle region sensitivities that agree with SWAP assessment versus those regions that disagree with SWAP assessment

Patient ID	*STD*	*R/W*	*DTP*	*2-Hz-TMP*	*16-Hz-TMP*
502 OD	5:3	5:3	3:5	7:1	5:3
502 OS	3:5	3:5	3:5	5:3	5:3
503 OD	7:1	5:3	7:1	8:0	5:3
504 OD	3:5	3:5	4:4	6:2	4:4
504 OS	3:5	1:7	6:2	2:6	6:2
505 OS	6:2	6:2	7:1	6:2	6:2
506 OD	5:3	5:3	4:4	6:2	4:4
508 OD	3:5	2:6	1:7	2:6	2:6
510 OS	4:4	3:5	3:5	3:5	1:7
511 OS	4:4	7:1	4:4	5:3	7:1
Totals	43:37	40:40	42:38	50:30	45:35

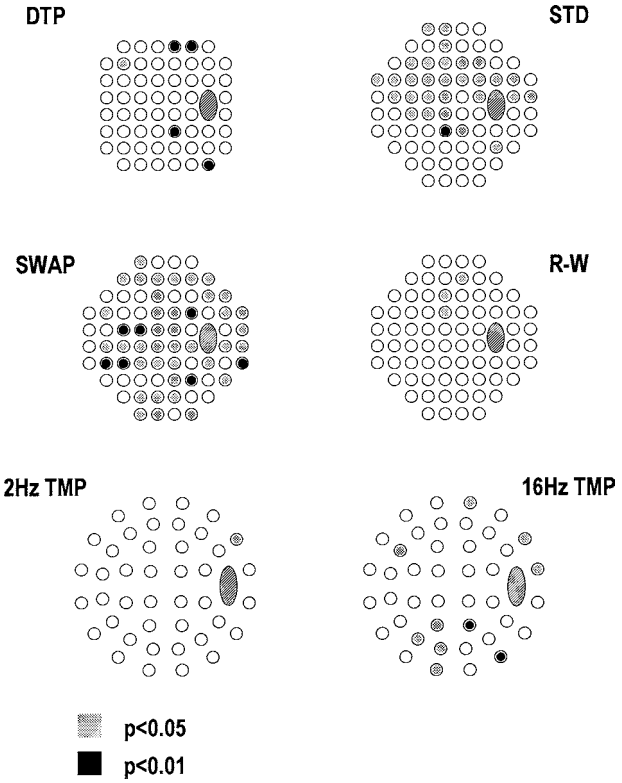

Fig. 4. Results indicative of those obtained in two eyes. SWAP and STD testing show the most extensive damage with the other tests showing variable but less extensive damage.

Discussion

The extent of loss for different visual functions, as well as the spatial correlation of damage among these functions, does not support either a selective loss of large diameter fibers or a selective loss to magnocellular or parvocellular fibers in early glaucoma. The most parsimonious explanation of our findings is that all cell types and fiber sizes are damaged to some degree early in glaucoma, although there may be a moderately greater proportion of damage to some ganglion cell sub-groups. It also appears that early losses are more readily observed for visual functions that have reduced redundancy or decreased functional overlap. At the present time, SWAP appears to be the most effective procedure for detecting early losses of visual function in glaucoma.

Acknowledgments

Supported in part by National Eye Institute Research Grant No. EY-03424, a Research to Prevent Blindness Senior Scientific Investigator Award, and an Unrestricted Research Support Grant from Research to Prevent Blindness, Inc.

References

1. Quigley HA, Sanchez RM, Dunkelberger GR, L'Hernault NL, Baginski TA: Chronic glaucoma selectively damages large optic nerve fibers. Invest Ophthalmol Vis Sci 28:913-920, 1987
2. Quigley HA, Dunkelberger GR, Green WR: Chronic human glaucoma causing selectively greater loss of large optic nerve fibers. Ophthalmology 95:357-363, 1988
3. Glovinsky Y, Quigley HA, Dunkelberger GR: Retinal cell loss is size dependent in experimental glaucoma. Invest Ophthalmol Vis Sci 32:484-491, 1991
4. Glovinsky Y, Quigley HA, Pease ME: Foveal ganglion cell loss is size dependent in experimental glaucoma. Invest Ophthalmol Vis Sci 34:395-400, 1993
5. Schiller PH, Malpeli JG: Properties and tectal projections of monkey retinal ganglion cells. J Neurophysiol 40:428-445, 1977
6. Leventhal AG, Rodieck RW, Dreher B: Retinal ganglion cell classes in the Old World monkey: morphology and central projections. Science 213:1139-1142, 1981
7. Perry VH, Oehler R, Cowey A: Retinal ganglion cells which project to the dorsal lateral geniculate nucleus in the macaque monkey. Neuroscience 12:1101-1123, 1984
8. Rodieck RW, Watanabe M: Survey of the morphology of macaque retinal ganglion cells that project to the pretectum, superior colliculus and parvocellular laminae of the lateral geniculate nucleus. J Comp Neurol 338:289-303, 1993
9. Tyler CW: Specific deficits of flicker sensitivity in glaucoma and ocular hypertension. Invest Ophthalmol Vis Sci 20:204-212, 1981
10. Tytla ME, Trope GE, Buncic JR: Flicker sensitivity in treated ocular hypertension. Ophthalmology 97:36-43, 1990
11. Lachenmayr BJ, Drance SM, Douglas GR, Mikelberg FM: Light-sense, flicker and resolution perimetry in glaucoma: a comparative study. Graefe's Arch Clin Exp Ophthalmol 229:246-251, 1991
12. Casson EJ, Johnson CA, Shapiro LR: Longitudinal comparison of temporal-modulation perimetry with white-on-white and blue-on-yellow perimetry in ocular hypertension and early glaucoma. J Opt Soc Am A 10:1792-1806, 1993
13. Silverman SE, Trick GL, Hart Jr WM: Motion perception is abnormal in primary open-angle glaucoma and ocular hypertension. Invest Ophthalmol Vis Sci 31:722-729, 1990
14. Bullimore MA, Wood JM, Swenson K: Motion perception in glaucoma. Invest Ophthalmol Vis Sci 34:3526-3533, 1993
15. Baez KA, McNaught AI, Dowler JGF, Poinoosawmy D, Fitzke FW, Hitchings RA: Motion detection threshold and field progression in normal tension glaucoma. Br J Ophthalmol 79:125-128, 1995
16. Wall M, Ketoff KM: Random dot motion perimetry in patients with glaucoma and in normal suspects. Am J Ophthalmol 120:587-596, 1995
17. Merigan WH, Maunsell JHR: Macaque vision after magnocellular lateral geniculate lesions. Vis Neurosci 5:347-352, 1990
18. Kremers J, Lee BB, Pokorny J, Smith V: Responses of macaque ganglion cells and human observers to compound periodic waveforms. Vision Res 33:1997-2011, 1993
19. Merigan WH, Byrne C, Maunsell JHR: Does primate motion perception depend on the magnocellular pathway? J Neurosci 11:3422-3429, 1991
20. Adams AJ, Rodic R, Husted R, Stamper R: Spectral sensitivity and color discrimination changes in glaucoma and glaucoma-suspect patients. Invest Ophthalmol Vis Sci 23:516-524, 1982
21. Alvarez SL, Vingrys AJ, King-Smith PE, Perry M, Benes SC, Weber PA: A comparison of sensitivity losses in glaucoma for white and equiluminous colored stimuli. Am J Optom Physiol Optics 65:124, 1988
22. Sample PA, Weinreb RN: Progressive color visual field loss in glaucoma. Invest Ophthalmol Vis Sci 33:2068-2071, 1992
23. Johnson CA, Adams AJ, Casson EJ, Brandt JD: Blue-on-yellow perimetry can predict the development of glaucomatous visual field loss. Arch Ophthalmol 111:645-650, 1993
24. Sample PA, Madrid ME, Weinreb RN: Evidence for a variety of functional defects in glaucoma-suspect eyes. J Glaucoma 3(Suppl):S5-S18, 1994
25. Sample PA, Ahn DS, Lee PC, Weinreb RN: High-pass resolution perimetry in eyes with ocular hypertension and primary open-angle glaucoma. Am J Ophthalmol 113:309-316, 1992
26. Fraser JM, Cioffi GA, Van Buskirk EM: High-pass resolution perimetry and early glaucomatous visual field loss [ARVO Abstract]. Invest Ophthalmol Vis Sci 33(Suppl):1385, 1992

27. Merigan WH: Chromatic and achromatic vision of macaques: role of the P pathway. J Neurosci 9:776-783, 1989
28. Schiller PH, Logothesis NK, Charles ER: Role of the color-opponent and broad-band channels in vision. Visual Neurosci 5:321-346, 1990
29. Kaiser P, Kremers J, Lee BB: Luminance & chromatic activity measured psychophysically in humans and physiologically in monkey ganglion cells [ARVO Abstract]. Invest Ophthalmol Vis Sci 32(Suppl):1115, 1991
30. Merigan WH: For what are the P and M pathways specialized? [ARVO Abstract]. Invest Ophthalmol Vis Sci 33(Suppl):900, 1992
31. Schiller PH, Logothesis NK, Charles ER: Parallel pathways in the visual system: their role in perception at isoluminance. Neuropsych 29:433-441, 1991
32. Johnson CA: Selective versus nonselective losses in glaucoma. J Glaucoma 3(Suppl 1):S32-S44, 1994
33. Drum B, Severns M, O'Leary D, Massof R, Quigley H, Breton M, Krupin T: Selective loss of pattern discrimination in early glaucoma. Appl Opt 28:1135-1144, 1989
34. Lachenmayr BJ, Airaksinen PJ, Drance SM, Wijsman K: Correlation of retinal nerve-fiber-layer loss, changes at the optic nerve head and various psychophysical criteria in glaucoma. Graefe's Arch Clin Exp Ophthalmol 229:133-138, 1991
35. Lennie P, Trevarthen C, Van Essen DC, Wässle H: Parallel processing of visual information, In: Spillmann L, Werner JS (eds) Visual Perception: The Neurophysiological Foundations, p 128. San Diego: Academic Press Inc 1990
36. Hart WM, Yablonski M, Kass MA, Becker B: Multivariate analysis of the risk of glaucomatous visual field loss. Arch Ophthalmol 97:1455-1458, 1979
37. Johnson CA, Adams AJ, Casson EJ, Brandt JD: Progression of early glaucomatous visual field loss as detected by blue-on-yellow and standard white-on-white automated perimetry. Arch Ophthalmol 111:651-656, 1993
38. Johnson CA, Marshall D: Aging effects for opponent mechanisms in the central visual field. Optom Vis Sci 72:75-82, 1995
39. Harwerth RS, Smith EL, DeSantis L: Mechanisms mediating visual detection in static perimetry. Invest Ophthalmol Vis Sci 34:3011-3023, 1993
40. Johnson CA, Marshall DJ, Eng KM: Displacement threshold perimetry in glaucoma using a Macintosh computer system and a 21-inch monitor, In: Mills RP, Wall M (eds) Perimetry Update 1994/1995, pp 103-110. Amsterdam/New York: Kugler Publ 1995

THE ROLE OF RAISED INTRAOCULAR PRESSURE IN THE DEVELOPMENT OF GLAUCOMATOUS OPTIC NEUROPATHY

P.K. WISHART and A.S. KOSMIN

Glaucoma Clinic, St Paul's Eye Unit, Royal Liverpool University Hospital, Liverpool, UK

Abstract

Purpose: To investigate whether elevated intraocular pressure (IOP) is responsible for the development of glaucomatous optic disc damage and visual field loss in at risk patients attending a glaucoma clinic.

Method: Patients attending the Glaucoma Clinic in Liverpool who had been observed to convert from normal to glaucoma while under review over the period 1989-1995 were identified by case retrieval. Stereoscopic optic disc examination by the same observer (PKW) had been recorded in the notes, and serial Humphrey Visual Field Analysis (HVFA) with Program 24-2 was available in most cases. Some of the normotensive subjects had initially undergone manual perimetry followed by HVFA. IOP measurement with Goldmann applanation tonometry and full ophthalmic examination had been conducted at all clinic visits. Cases of secondary glaucoma were excluded.

Results: Eighteen patients (21 eyes) were identified in whom the characteristic visual field and optic disc changes of glaucoma had developed from normal.
(a) IOP: Eleven patients (11 eyes) were ocular hypertensive, five patients (seven eyes) were normotensive, and two patients (three eyes) were initially normotensive, but later developed elevated IOP and glaucoma. In four eyes, IOP was greater than 21 mmHg at the time of conversion (average 31 mmHg).
(b) Disc change: Fourteen eyes developed an acquired pit of the optic nerve (APON), five eyes developed disc hemorrhages, and one eye, disc pallor and increased cup size.
(c) Visual loss: Ten eyes developed an isolated paracentral scotoma involving fixation, seven eyes a nasal step and isolated paracentral scotoma, and four eyes a nasal step alone.

Conclusions: The pattern of optic disc damage and visual field loss seen in both ocular hypertensive and normotensive patients was most commonly that characteristic of the glaucomatous changes associated with low-tension glaucoma, namely the APON[1] and its characteristic paracentral visual field loss.[2] Eighty-one percent of eyes in the series converting to glaucoma had long-term IOP control of 21 mmHg or less, indicating that raised IOP may be less important than other undefined factors in the pathogenesis of glaucomatous optic neuropathy.

Address for correspondence: P.K. Wishart, MD, Glaucoma Clinic, St Paul's Eye Unit, Royal Liverpool University Hospital, Liverpool, UK

Perimetry Update 1996/1997, pp. 263–264
Proceedings of the XIIth International Perimetric Society Meeting
Würzburg, Germany, June 4–8, 1996
edited by M. Wall and A. Heijl

References

1. Javitt JC, Spaeth GL, Katz LJ et al: Acquired pits of the optic nerve: increased prevalence in patients with low-tension glaucoma. Ophthalmology 97:1038-1044, 1990
2. Cashell LF, Ford JG: Central visual field changes associated with acquired pit of the optic nerve. Ophthalmology 102:1270-1278, 1995

INFLUENCE OF CARTEOLOL ON THE VISUAL FIELDS OF PATIENTS WITH NORMAL-TENSION GLAUCOMA

YOSHIAKI TANAKA, HIDETAKA MAEDA and KUNIYOSHI MIZOKAMI

Department of Ophthalmology, Kobe University, School of Medicine, Kobe, Japan

Abstract

Purpose: Investigation of the effect of carteolol treatment on the central visual field of patients with normal-tension glaucoma.
Method: In an age-matched prospective trial, 22 eyes of 22 patients with normal-tension glaucoma were randomly assigned to treatment with carteolol hydrochloride 2% or no treatment. Intraocular pressure and central visual field (Humphrey Central 30-2 grid) were measured at baseline and every three months up to 21 months.
Results: Progression of the corrected pattern standard deviation was less pronounced in the carteolol group than in the control group. This difference was statistically significant.
Conclusion: In this study, carteolol was effective in inhibiting localized deterioration of the visual field.

Introduction

Normal-tension glaucoma (NTG) is a disorder that causes similar optic nerve damage to that in primary open-angle glaucoma (POAG). Its etiology is unknown. While progression of visual field deterioration in patients with POAG is mainly believed to depend on elevated intraocular pressure (IOP), the mechanism of the optic disc damage in NTG is still unknown. Some reports have indicated that the incidence of progression of visual field damage is particularly high in NTG cases with a relatively high IOP. On the other hand, it has been suggested that IOP-lowering therapy using adrenergic β antagonists may increase visual field damage due to undesirable effects on the ocular circulation.[1,2] Whether lowering the IOP by topical administration of β antagonists reduces the risk of visual field deterioration in patients with NTG has not yet been resolved.

The purpose of this study was to investigate the effect of carteolol hydrochloride on the central visual field in patients with NTG. A preliminary mid-term (21-month) report is presented.

Address for correspondence: Yoshiaki Tanaka, MD, Department of Ophthalmology, Kobe University, School of Medicine, 7-5 Kusunoki cho, Chuo-ku, Kobe 650, Japan

Perimetry Update 1996/1997, pp. 265–269
Proceedings of the XIIth International Perimetric Society Meeting
Würzburg, Germany, June 4–8, 1996
edited by M. Wall and A. Heijl

Subjects and methods

Twenty-two eyes of 22 patients with early-stage and intermediate-stage NTG, who gave informed consent, were studied. The average age of the patients was 54.8 years (34-73 years). Except for mild refractive errors, none of the subjects had other ophthalmic diseases or any systemic disorders that would contraindicate administration of the present drug. We adopted the following criteria for NTG:

1. Glaucomatous optic disc changes and corresponding visual field damage.
2. IOP below 21 mmHg, including diurnal variation of IOP.
3. A normal open angle.
4. No intracranial lesions or paranasal sinus diseases causing optic nerve damage.

All topical eye drops were discontinued over a four-week washout period, and one of the following alternatives was randomly selected: *1.* administration of 2% carteolol hydrochloride ophthalmic preparations twice a day (carteolol group); or *2.* observation only without any drug therapy (control group).

IOP was measured using Goldmann's applanation tonometer at the same time of day in all patients.

Visual fields were measured with the Humphrey Field Analyzer Model 630, using the central 30-2 grid. In order to exclude possible training effects, the first results were discarded and the average of two or more measurements from the second field and onwards were adopted as baseline data. Thereafter, the visual field was measured every three months. Moreover, low reliability results, displaying more than 20% false negative, false positive, or fixation losses, were excluded from the analysis.

Temporal changes in the IOP, mean deviation (MD) and corrected pattern standard deviation (CPSD) were compared relative to the baseline. The changes from the baseline values of these three parameters were calculated, and the inter-group differences statistically analyzed using non-parametric methods; a p value below 0.01 was considered statistically significant.

Results

The patient demographics of the two groups are shown in Table 1. There were no statistically significant differences between the two groups with respect to age, IOP, or visual field indices, and thus partition into two groups appears to have been reasonably appropriate. Visual fields, as well as IOPs, were measured in all patients as planned and the results are shown in Figures 1, 2 and 3.

Intraocular pressure (Fig. 1)

During the follow-up period, IOP in the carteolol group was lower than in the control group at six, nine, 12, 15, 18 and 21 months. Compared with the control group, there was a significant reduction of IOP at every point of follow-up, except at six months.

Mean deviation (Fig. 2)

After 21 months, MD had decreased (improved visual field damage) by 0.23 dB on average in the carteolol group, compared with a mean increase (worsening) of 0.12 dB in the control group.

Table 1. Patient demographics

	Carteolol	*Control*	*p value*
No. of cases	14	14	
Age (years)	59.7±12.4	50.5±13.1	0.31
Refraction (D)	-1.74±0.26	-1.43±0.39	0.36
IOP (mmHg)	14.7±1.7	15.0±1.9	0.34
MD (dB)	-2.98±3.17	-2.78±3.14	0.82
CPSD (dB)	5.59±4.79	5.35±3.49	0.43

Mean ± SD. There were no significant differences in age, visual field indices, IOP or other clinical characteristics between the two groups at baseline

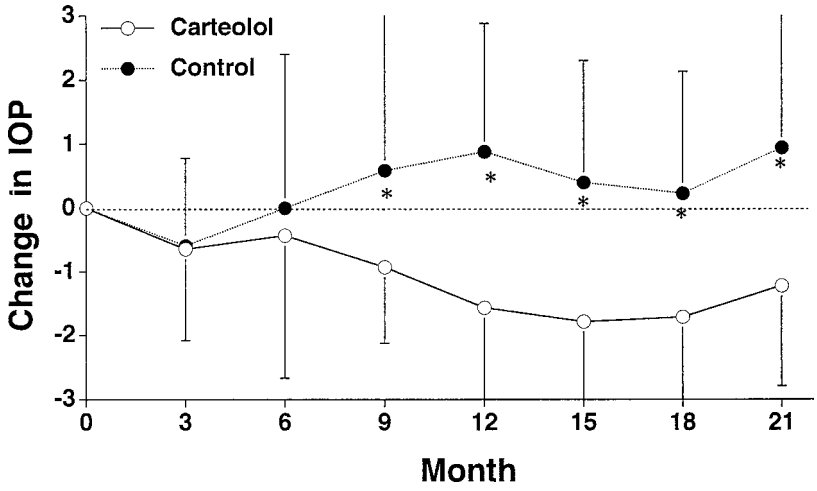

Fig. 1. Change in intraocular pressure. Open circles: carteolol group; closed circles: control group. Increase in 'change in IOP' means increasing IOP. *p<0.05 Mann-Whitney test.

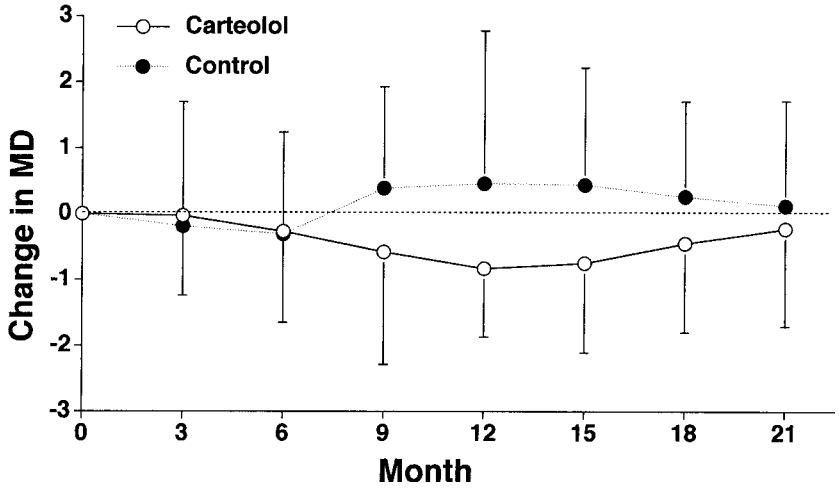

Fig. 2. Change in mean deviation. No significant difference between the two groups.

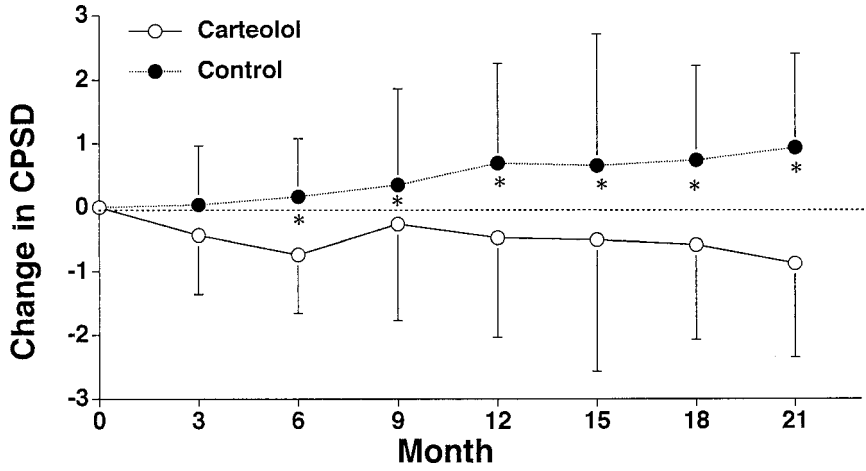

Fig. 3. Change in corrected pattern standard deviation.

Corrected pattern standard deviation (Fig. 3)

After 21 months of medication, CPSD in the carteolol group was clearly less pronounced compared to the control group. That is, more progression of visual field damage was seen in the control group compared to the carteolol group; the difference between the two groups was statistically significant. This fact suggests that instillation of carteolol may decrease the progression of localized visual field deterioration. Likewise, a decrease in CPSD in the carteolol group compared to the control group is indicated by the data shown in Figure 3.

Discussion

Normal-tension glaucoma (NTG) is a disorder that causes optic nerve damage similar to that of primary open-angle glaucoma (POAG). The etiology of NTG is still unknown, and as yet there is no widely accepted theory. IOP, optic nerve head, blood circulation, anatomical weakness of the optic nerve itself, and various other factors have all been suggested to be involved in the progression of visual field damage.[1]

Even among patients with NTG, the progression of visual field damage is significantly faster in the group with a higher IOP, and therefore certain pressure lowering may be necessary.[3] Chandler reported that the progression of visual field damage may be prevented if IOP was lowered to approximately 10 mmHg by drug or surgical therapy.[4]

On the other hand, many investigators have negative opinions with regard to lowering IOP by means of topical medication in patients with NTG.[2,5,6] Levene[2] studied 38 cases with NTG and reported that IOP-lowering agents did not slow the progression of visual field damage. The reason for this failure was considered to be the small IOP-lowering effect encountered.

Ito and Mizokami[7] followed groups treated with timolol and dipibefrine topically for one year, and found that visual field damage increased more often in the timolol group, although no difference in IOP level was seen between the two groups. They

pointed out the possibility that the extent of decreased papillary blood flow caused by timolol was greater than the increased blood flow that could be associated with IOP reduction.

Yamazaki *et al.*[8] reported that retinal blood flow increased within 15 minutes of applying 2% carteolol topically in normal individuals. No significant decrease of IOP was seen during this period. Therefore, it seems that retinal blood flow increased through the pharmacological action of carteolol. Flammer and Drance[9] reported that a group of POAG patients treated with carteolol showed a tendency for improved visual field sensitivity, whereas no significant change was seen in the timolol or placebo groups.

In this study, we conclude that IOP decreased due to carteolol eye drops, compared to the control group. Significantly more progression of visual field damage was seen in the control group compared to the carteolol group.

After 21 months of medication, there was a significant difference between the carteolol group and the control group with regard to the visual field indices. Increase of CPSD in the carteolol group was clearly less pronounced compared to the control group. This could be interpreted to mean that the reduction of IOP by carteolol eye drops inhibited localized visual field deterioration, which is represented by CPSD and not by MD.

The present report is a mid-term analysis of our data. We plan to follow up these patients further in the future.

References

1. Levene RZ: Low-tension glaucoma. In: Cairns JE (ed) Glaucoma. London: Grune and Stratton 1986
2. Levene RZ: Low-tension glaucoma: a critical review and new material. Surv Ophthalmol 24:621-664, 1980
3. Cartwright MJ, Anderson DR: Correlation of asymmetric damage with asymmetric intraocular pressure in normal-tension glaucoma (low-tension glaucoma). Arch Ophthalmol 106:898-900, 1988
4. Chandler PA: Long-term results in glaucoma therapy. Am J Ophthalmol 49:221-246, 1960
5. Anderton SA: The nature of visual field in low tension glaucoma. Heijl A, Greve EL (eds). Doc Ophthalmol Proc Ser 42:383-386, 1986
6. Nakayama T: An analysis of progressive LTG at our clinic. Fol Ophthalmol Jpn 38:1895-1901, 1987
7. Ito M, Mizokami K: A study of topical treatment in low tension glaucoma. Jpn J Clin Ophthalmol 45:323-325, 1991
8. Yamazaki S, Baba H, Tokoro T: Effect of timolol and carteolol on ocular pulsatile blood flow. J Jpn Ophthalmol Soc 96:973-977, 1992
9. Flammer J, Drance SM: Quantification of glaucomatous visual field defects with automated perimetry. Invest Ophthalmol Vis Sci 26:176-181, 1985

IS CALIBRATED TRABECULECTOMY HARMFUL TO VISUAL FUNCTION?

GERHARD WELSANDT and JÖRG WEBER

University of Cologne, Eye Clinic, Cologne, Germany

Abstract

Purpose: To investigate the deterioration of visual function after calibrated trabeculectomy.
Methods: Eighty-one eyes of 69 patients with chronic open-angle glaucoma and various degrees of damage underwent calibrated trabeculectomy.[5] Visual acuity and visual fields were determined before and one to three months after surgery.
Results: Neither the mean change of visual acuity nor that of the visual fields showed a deterioration in visual function. Neither was there a severe drop of function in any of the cases.
Conclusion: Calibrated trabeculectomy is a safe method for preservation of visual function.

Introduction

Deterioration of visual function, even loss of function ('snuff out') is a well-known side-effect of trabeculectomy. We studied this effect by the quantitative analysis of visual acuity and visual function in a larger group of patients who underwent calibrated trabeculectomy.

Patients and methods

Eighty-one eyes of 69 patients (11 female, 70 male eyes; mean age 56.2) with chronic open-angle glaucoma and various degrees of damage (27 with threatened fixation) underwent trabeculectomy. The method of calibrated trabeculectomy[1] was applied to avoid an excessive drop in pressure and prolonged hypotony, as well as hypertony. Visual acuity was determined before surgery, on the day of discharge, and after one to three months. Visual fields (Humphrey Field Analyzer) were performed before and one to three months after the operation. Twelve eyes (15%) were tested with Threshold Program 10-2, 69 (85%) with Program 30-2. The program was the same for both examinations. MD was calculated using the analysis program PeriData. All patients had prior experience with automated perimetry.

Address for correspondence: Priv. Doz. Dr. Jörg Weber, Buchheimerstr. 64, D-51063 Cologne, Germany

Perimetry Update 1996/1997, pp. 271–274
Proceedings of the XIIth International Perimetric Society Meeting
Würzburg, Germany, June 4–8, 1996
edited by M. Wall and A. Heijl

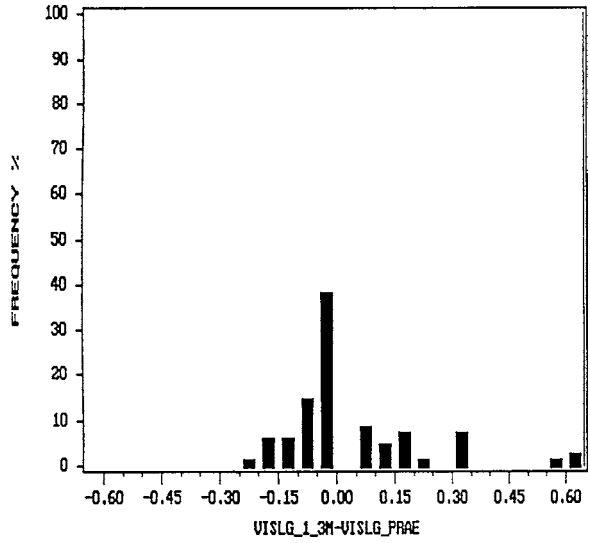

Fig. 1. Visual acuity difference (logarithmic scale): log VA after surgery/log VA before surgery. Mean +0.042; SD <p>0.159; median 0.00.

Results

Complications

Two patients had a transient shallow chamber without corneal touch, all the others maintained a deep anterior chamber.

Visual acuity

On the day of discharge, visual acuity was on average 0.094 (-0.061 log units) lower than preoperatively. After three months, visual acuity (decimal system) had changed in 55 eyes (68%) by 0.1 or less. Fourteen eyes (17%) had improved (maximum +0.5) and 12 eyes (15%) had deteriorated (maximum -0.3). The mean change was +0.022 (= improvement; not significant p=0.2437, t test) (Fig. 1). Using a logarithmic scale, the mean change was +0.042 log units or +0.42 lines (= improvement; significant p= 0.018, t test). (Fig. 1).

Visual fields

The difference in perimetric index MD varied between -5.9 dB and +8.0 dB. The visual field improved on average by 0.04 dB (not significant, p=0.892, t test). The standard deviation of differences was 2.5 dB, which is in the range of long-term fluctuation in glaucoma. There was no case of excessive change in function (Fig. 2).

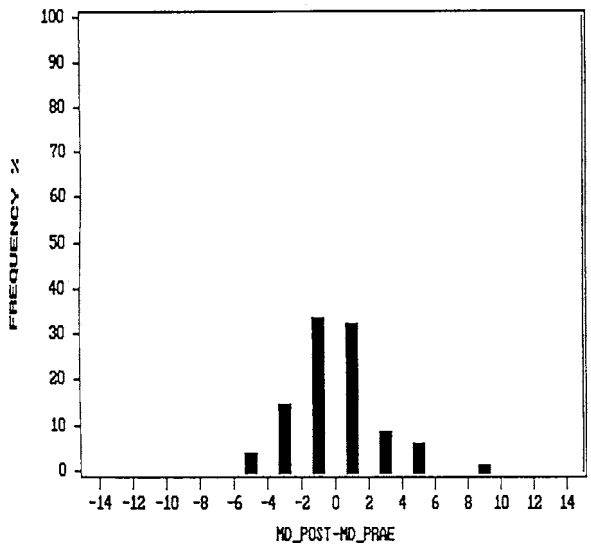

Fig. 2. Visual field difference (index MD): after/before surgery. Mean +0.038; SD <p>2.46; median -0.200.

Discussion

Gandolfi[2] reported an average improvement in mean sensitivity of 1.7 dB after trabeculectomy. Ridings[3] reported more cases of improvement than of deterioration in 34 patients who underwent filtering glaucoma surgery. Boissonnot *et al.*[4] reported similar findings. Similar findings had already been reported by Greve in 1977.[5] In our material, there was only a slight improvement in visual acuity (VA) which was only significant on the logarithmic scales but not on the analogous scales. This may have been due to the fact that all our patients were trained in perimetry. Thus, learning effects were excluded, which may have been responsible for some of the improvement reported in the literature.

The main question in our study was whether there was a severe deterioration of visual function after trabeculectomy. Among our 81 cases, no such case could be found.

Conclusion

Calibrated trabeculectomy is a safe method for preservation of visual function.

References

1. Weber J: Controlled trabeculectomy by intraoperative tonometry. Invest Ophthalmol Vis Sci 36:S20, 1995
2. Gandolfi SA: Improvement of visual field indices after surgical reduction of intraocular pressure. Ophthalmic Surg 26:121-126, 1995

3. Ridings B: Evolution campimétrique post-opératoire précoce après chirurgie filtrante dans les glaucomes chroniques évolués. Ophtalmologie 4:151-153, 1990
4. Boissonnot M, Hirsch AL, Rovira JC, Risse JF: Evolution du champ visuel en périmetrie automatisée dans le glaucome chronique équilibre par trabeculectomie. J Fr Ophtalmol 15:645-650, 1992
5. Greve EL: Pre- and postoperative results of static perimetry in patients with glaucoma simplex. Ophthalmologica (Basel) 175:56-57, 1977

VALIDATION OF A RISK MODEL FOR GLAUCOMATOUS FIELD LOSS
Application to standard automated perimetry and short-wavelength automated perimetry

SHABAN DEMIREL and CHRIS A. JOHNSON

Optics and Visual Assessment Laboratory (OVAL), Department of Ophthalmology, University of California, Davis, Sacramento, CA, USA

Abstract

Hart and colleagues[1] developed a retrospective risk model for development of glaucomatous visual field loss in ocular hypertensives that incorporates four factors: intraocular pressure (IOP), vertical cup-to-disc ratio, age, and family history of glaucoma. Kolker and associates[2] prospectively evaluated this model in a different group of ocular hypertensives. The purpose of this investigation was to determine the validity and generalizability of this risk model by examining the authors' longitudinal data set for 233 ocular hypertensive patients (466 eyes). Risk probabilities were calculated from baseline data using the Hart *et al*. model.[1] In the entire cohort at baseline, 57.76% were low risk (0.0 - 0.2), 12.28% were low to moderate risk (0.21 - 0.4), 6.9% were moderate risk (0.41 - 0.6), 8.84% were moderate to high risk (0.61 - 0.8), and 14.22% were high risk (0.81 - 1.0). Over a four-year time period, 25 eyes developed confirmed glaucomatous visual field loss as determined by standard automated perimetry. Of the 25 eyes that converted in the study period, six (24%) were low risk, five (40%) were low to moderate risk, four (16%) were moderate risk, three (12%) were moderate to high risk, and five (40%) were high risk. A χ^2 analysis showed that the percentage of conversions was significantly different among the risk groups ($p<0.05$) with more converters coming from higher risk groups. The authors also performed their own multivariate logistic regression, using the same four risk factors. The coefficients for each risk factor were similar to those obtained by Hart *et al*. The model was also found to be applicable for SWAP results obtained in these patients with slightly different coefficients. These findings support the validity of the Hart *et al.* model for determining the risk of developing glaucomatous visual field loss in ocular hypertensives.

Introduction

When examining ocular hypertensive patients and those at risk of developing glaucoma, it is useful to establish some quantitative measure of risk. A number of factors need to be considered when developing a glaucoma risk model, but usually intraocular pressure (IOP), disc cupping, family history of glaucoma,[3] and age are included. Such a multifactorial approach was employed by Hart *et al.*[1] Another multi-

Address for correspondence: Chris A. Johnson, PhD, Optics and Visual Assessment Laboratory, Department of Ophthalmology, 1603 Alhambra Boulevard, Sacramento, CA 95816, USA

Perimetry Update 1996/1997, pp. 275–279
Proceedings of the XIIth International Perimetric Society Meeting
Würzburg, Germany, June 4–8, 1996
edited by M. Wall and A. Heijl

factorial study of risk investigated these factors and also examined the importance of cup asymmetry, rim/disc ratio and the presence of a disc crescent.[4] One advantage of the Hart *et al.* glaucoma risk model in comparison to similar approaches is that it was later validated in a prospective study of conversion in a group of glaucoma suspects.[2] Other risk factors, such as low blood pressure and vasospasm,[5-7] high blood pressure to pulse rate ratio,[8] and short wavelength automated perimetry (SWAP) abnormalities,[9-11] have also been investigated with respect to risk of glaucoma development.

The current study was performed to determine whether risk factors for development of glaucomatous visual field loss had similar importance in a separate cohort of glaucoma suspects, and whether this model could also be applied to SWAP visual field loss.

Methods

We examined a longitudinal data set that contained 233 ocular hypertensive patients (466 eyes). To be eligible for inclusion, all subjects had a best corrected visual acuity of 20/40 or better in both eyes and an IOP greater than 21 mmHg before any treatment, also in both eyes. Refractive error had to be less than 5 D spherical equivalent and less than 3 D of cylinder, all subjects wore an appropriate near correction during perimetric testing. Patients were excluded if they had visual field indices outside normal STATPAC 2 limits at baseline, a history of ocular or neurological disease or surgery, diabetes, or any condition other than glaucoma that may have affected their visual field sensitivity. As well as standard (white-on-white) automated visual field assessment (Humphrey Visual Field Analyzer 30-2 fields), subjects also underwent SWAP testing and optic nerve head evaluation.

Baseline risk probabilities were calculated for all subjects using the Hart *et al.* model.[1] The calculated risk probabilities using this model were distributed between zero and one. Coefficients used for the multivariate risk equation were those reported by Hart *et al.*[1]

At the end of the fourth year of the study, eyes that had developed glaucomatous visual field loss were identified on the basis of confirmed abnormal standard automated perimetry results. Fields were considered abnormal if the glaucoma hemifield test (GHT) was outside normal limits or the corrected pattern standard deviation (CPSD) was below the lower 95th percentile of normal. The risk scores of converters were compared to the risk scores of non-converters and analyzed using the χ^2 statistic. The null hypothesis used to calculate expected conversion rates was that all subjects had the same probability of conversion irrespective of their risk score.

We also performed a multivariate logistic regression using the data set collected in our laboratory. This was done to allow comparison of the coefficients for the model parameters obtained by fitting the logistic model to the current data set with coefficients reported by Hart *et al.*[1]

To allow the usefulness of this model to be assessed in relation to SWAP fields, a second multivariate logistic regression analysis was performed using the abnormality of SWAP fields as the dependent variable and the same independent variables as used in the standard perimetry model. This analysis allowed a comparison of the relative importance of parameters in the prediction of SWAP defects to their importance in the prediction of standard (white-on-white) defects.

Table 1. Coefficients of multivariate logistic regression analysis for standard automated perimetry, SWAP and coefficients obtained from Hart *et al.*[1]

Parameter	*Hart (1979)*	*AP*	*SWAP*
Constant	14.64	15.28	5.18
Vertical C/D	-1.22	-2.49	-2.04
IOP	-0.16	-0.11	+0.02
FHx	-1.48	-0.71	+0.01
Age	-0.07	-0.13	-0.05

There are substantial differences between coefficients for standard automated perimetry and SWAP.

Results

In the entire cohort at baseline, 57.76% were low risk (0.0 - 0.2), 12.28% were low to moderate risk (0.21 - 0.4), 6.9% were moderate risk (0.41 - 0.6), 8.84% were moderate to high risk (0.61 - 0.8), and 14.22% were high risk (0.81 - 1.0). Twenty-five eyes converted in the study period. Of these, six (24%) were low risk, five (40%) were low to moderate risk, four (16%) were moderate risk, three (12%) were moderate to high risk, and five (40%) were high risk. A χ^2 analysis showed that conversion of subjects was significantly different from expected ($\chi^2 = 9.99$, df = 4, $p<0.05$), with more medium and high risk patients in the converting group than expected if all subjects had an equal probability of conversion.

In the first multivariate logistic regression analysis, the same four risk factors found to be significant in previous studies, namely vertical C/D ratio, IOP, age and family history of glaucoma, were used. We obtained similar coefficients to Hart and co-workers for each of the variables included in the risk model. The coefficients obtained in the current analysis are compared to those obtained by Hart *et al.*[1] in Table 1.

The risk factor with the highest weighting was vertical C/D ratio (odds ratio = 12.03, $p = 0.025$), followed by age (odds ratio = 1.14, $p<0.001$). Although IOP and family history of glaucoma had positive contributions to the magnitude of risk, the p values obtained for these two risk factors were not below the 0.05 level (IOP: odds ratio = 1.12, $p = 0.13$; family history: odds ratio = 2.04, $p = 0.173$). Receiver operator characteristic (ROC) analysis applied to the logistic model generated an area under the ROC curve of 0.814. In this analysis, a model that could completely separate the two groups would have an area under the ROC curve of 1.0 and a model that only performed at chance level would score 0.5.

A similar analysis was performed for the presence of SWAP defects. The coefficients were different from those obtained from the analysis of standard (white-on-white) field results. These results are also shown in Table 1. Similar to analysis of standard field results, the risk factor with the highest weighting was vertical C/D ratio (odds ratio = 7.69, $p = 0.001$) followed by age (odds ratio = 1.05, $p < 0.001$). IOP and family history contributed little to the logistic risk values (IOP: odds ratio = 0.98, $p = 0.61$; family history: odds ratio = 0.997, $p = 0.99$).

Discussion

From the results obtained in this cohort of ocular hypertensives and previous reports by other authors,[1,2] it appears that the most important predictive factor for the conversion of ocular hypertensives to glaucoma is the vertical C/D ratio. There is some discrepancy as to the relative importance of IOP, age and family history between the current study and previous reports, although they appear to be more important than a host of other marginal risk factors.[1]

Interestingly, 33 of 92 (35.9%) patients converted to glaucoma in at least one eye over a five-year period in the Hart *et al.* study.[1] In the current study, 21 of 233 patients (9.0%) converted in at least one eye. This may reflect a difference in overall risk of the two cohorts at baseline and this may account for the slightly different ranking of the importance of the various risk factors for subsequent development of field loss. Another factor that could account for differences between the two studies is the fact that the original Hart *et al.* study was based on Goldmann kinetic visual fields, and the current study was based on automated static perimetry. Because automated static perimetry detects early glaucomatous loss before Goldmann kinetic perimetry,[12] it is likely that some of the patients in the Hart study had early glaucomatous visual field damage that was not detected at baseline. Despite these minor differences the general findings from two separate groups were similar.

Acknowledgments

Supported in part by National Eye Institute Research Grant #EY-03424, a Research to Prevent Blindness Senior Scientific Investigator Award, and an Unrestricted Research Support Grant from Research to Prevent Blindness, Inc.

References

1. Hart WM, Yablonski M, Kass MA, Becker B: Multivariate analysis of the risk of glaucomatous visual field loss. Arch Ophthalmol 97:1455-1458, 1979
2. Kolker AE, Gordon MO, Kass MA, Becker B, Hart WM, Cooper D, Fitzgerald J, Solish S, Trick G: Prospective estimates of risk versus outcome in ocular hypertensive patients [ARVO Abstracts]. Invest Ophthalmol Vis Sci 31:502, 1990
3. Tielsch JM, Katz J, Sommer A, Quigley HA, Javitt J: Family history and risk of primary open angle glaucoma. Arch Ophthalmol 112:69-73, 1994
4. Quigley HA, Enger C, Katz J, Sommer A, Scott R, Gilbert D: Risk factors for the development of glaucomatous visual field loss in ocular hypertension. Arch Ophthalmol 112:644-649, 1994
5. Perasalo R, Raitta C: Low blood pressure: a risk factor for nerve fiber loss in institutionalized geriatric glaucoma patients. Acta Ophthalmol (Kbh) 68(Suppl 195):65-67, 1990
6. Flammer J: Therapeutic aspects of normal-tension glaucoma. Curr Opin Ophthalmol 4:58-64, 1993
7. Gramer E, Althaus G, Korner U: Are visual field defects in the lower hemifield a risk factor in POAG. In: Mills RP (ed) Perimetry Update 1992/93, pp 81-87. Amsterdam/New York: Kugler Publ 1993
8. Eisner A, Cioffi GA, Campbell HMK, Samples JR: Foveal flicker sensitivity abnormalities in early glaucoma: association with high blood pressure. J Glaucoma 3(Suppl):S19-S31, 1994
9. Johnson CA, Brandt JD, Khong AM, Adams AJ: Short-wavelength automated perimetry in low, medium- and high-risk ocular hypertensive eyes. Arch Ophthalmol 113:70-76, 1995
10. Johnson CA, Adams AJ, Casson EJ. Short-wavelength-sensitive perimetry (SWSP) can predict which glaucoma suspects will develop visual field loss. In: Parel, J-M, (ed) Progress in Bio-

medical Optics: Proceedings of Ophthalmic Technologies II: Bellingham: SPIE Publ 1992
11. Sample PA, Taylor JDN, Martinez G, Lusky M, Weinreb RN: Short wavelength color visual fields in glaucoma suspects at risk. Am J Ophthalmol 115:225-233, 1993
12. Katz J, Tielsch JM, Quigley HA, Sommer A: Automated perimetry detects visual field loss before manual Goldmann perimetry. Ophthalmology 102:21-26, 1995

VISUAL FIELD DAMAGE IN NORMAL-TENSION GLAUCOMA ASSOCIATED WITH VASOSPASM

L. QUARANTA, M. CASSAMALI, N. HAURANIEH and E. GANDOLFO

Centro Glaucoma, Clinica Oculistica, Universitá degli studi di Brescia, Brescia, Italy

Abstract

Purpose: There is some evidence that the nature and progression of disease in normal-tension glaucoma (NTG) may be distinct from other open-angle glaucomas. Moreover, in NTG patients it is possible to differentiate two main groups on the basis of the presence of vasospasm.
Patients/Methods: The authors studied the ocular characteristics of 19 pairs of NTG patients with and without vasospasm who were closely matched for the extent of field damage, pupil size, and visual acuity. The diagnosis of vasospasm was based on the presence of migraine and/or Raynaud's phenomenon, and by means of ocular hemodynamic tests.
Results: For an equivalent extent of damage, the patients in the NTG group with vasospasm had greater areas with normal sensitivity, indicating more localized damage.
Conclusions: NTG patients with vasospasm have more localized damage.

Introduction

Several studies attempting to distinguish between visual field (VF) damage in normal-tension glaucoma (NTG) and high-tension glaucoma have been reported over the last few decades. Patients affected by NTG seem to have more localized damage, and those with a higher IOP have more diffuse VF damage.[1-6] The exact mechanism involved in the onset and progression of damage in NTG is not completely known. Several studies have pointed to the primary role of abnormal ocular and systemic hemodynamics in the genesis and progression of anatomical and functional damage.[7-13] Moreover, some authors have found a significant correlation between ocular blood flow reduction and the extent and characteristics of VF damage.[13]

The aim of the present investigation was to evaluate two groups of patients affected with NTG in order to see whether there was a distinctive VF pattern associated with the presence of an abnormal vascular condition, such as vasospasm. Moreover, we tested the hypothesis that NTG patients with vasospasm have more localized VF damage than patients affected by NTG without vasospasm.

Address for correspondence: Dr Luciano Quaranta, Clinica Oculistica Universitaria, Spedali Civili di Brescia, Piazzale Spedali Civili 1, 25123 Brescia, Italy

Perimetry Update 1996/1997, pp. 281–283
Proceedings of the XIIth International Perimetric Society Meeting
Würzburg, Germany, June 4–8, 1996
edited by M. Wall and A. Heijl

Patients and methods

The patients admitted to this study were taken from the Glaucoma Center at the Department of Ophthalmology, University of Brescia, and were divided into two groups: NTG with vasospasm (v-NTG) and NTG without vasospasm (nv-NTG). For general inclusion into the NTG group, the maximum recorded IOP had to be 21 mmHg or less during diurnal pressure curves (seven IOP measurements from 8.00 a.m. to 8.00 p.m.), and patients must have abnormal optic discs and VF defects. Patients were divided into subgroups on the basis of the presence of vasospasm. The presence of vasospasm was determined by the response to one or more of the following provocative tests: hypercapnia,[11] the cold test,[10] and the behavior of the IOP/pulsatile ocular blood flow trajectory.[12] Moreover, vasospasm was also investigated by means of the ocular blood flow response to oral administration of calcium channel blockers (nimodipine 90 mg *pro die*).[11]

All the patients had a visual acuity of 20/30 or better, a pupil diameter of at least 3 mm during the VF examination, and reliable examinations, using the G1-threshold program on the Octopus-Interzeag perimeter.

Sixty-five NTG patients met the inclusion criteria for the study. Thirty-five patients showed evidence of vasospasm (v-NTG) and 30 did not (nv-NTG). Because the aim of the study was to compare the characteristics of VF damage in the two groups of NTG patients, v-NTG and nv-NTG patients were matched for mean defect, pupil diameter, and visual acuity. In a further analysis, patients were also matched for age and IOP.

The matching procedure resulted in 19 pairs of v-NTG and nv-NTG patients. Only one eye of each patient was selected for analysis, and one examination per eye was analyzed.

The corrected loss of variance (CLV) of each visual field was evaluated in the four quadrants of the VF (nasal and temporal, superior and inferior).

Statistical analysis of the data was performed using Student's *t* test and the paired *t* test. All statistical tests were two-tailed with an alpha value of 0.05.

Results

Age, visual acuity, pupil size, refractive error (spherical equivalent in diopters), and visual field indices of the two groups are summarized in Table 1. The analysis of locations of disturbed clusters revealed no significant preferential distribution of defects in either group. The value of CLV was significantly greater in the v-NTG group than in the nv-NTG group. The v-NTG group had a significantly larger number of normal clusters compared to the nv-NTG group. These data suggest that, in v-NTG, defects are more localized and deeper than those found in the nv-NTG group.

Discussion

Our results provide evidence that patients affected with v-NTG retain more normal VF locations than patients with nv-NTG, suggesting that patients affected with nv-NTG have more diffuse damage than v-NTG. This difference in VF damage is similar to that reported in NTG and primary open-angle glaucoma patients.[1-6]

Table 1. Clinical data (mean ± SEM)

	v-NTG (n=19)	*nv-NTG (n=19)*
Age (years)	64.0 ± 3.5	66.4 ± 4.1
Visual acuity	0.83 ± 0.04	0.87 ± 0.06
Refractive error (spherical equivalent in diopters)	1.2 ± 0.7	1.1 ± 0.4
Pupil size (mm)	3.8 ± 0.4	4.1 ± 0.5
Visual field mean defect (dB)	11.2 ± 3.4	10.7 ± 4.1
Corrected loss of variance (dB)	29.5 ± 6.4*	12.3 ± 3.8*

*Student's *t* test: 2.311; *p*: 0.027

These findings are consistent with the hypothesis that IOP affects VF diffusely, whereas localized defects may be less influenced by a relatively high IOP. In fact, localized defects in v-NTG eyes are sensitive to amelioration after CO_2 or CA^{2+} channel blocker therapy,[11] but are less sensitive to hypotensive therapy (medical or surgical).

In conclusion, our investigation provides evidence that vasospasm associated with glaucoma should be considered as a factor producing optic nerve damage, and may act independently of IOP.

References

1. Drance SM, Douglas GR, Airaksinen PJ et al: Diffuse visual field loss in chronic open angle glaucoma. Am J Ophthalmol 104:577-580, 1987
2. King D, Drance SM, Douglas GR et al: Comparison of visual field defects in normal-tension glaucoma and high-tension glaucoma. Am J Ophthalmol 101:204-207, 1986
3. Motolko M, Drance SM, Douglas GR: Visual field defects in low-tension glaucoma: comparison of defects in low-tension glaucoma and chronic open angle glaucoma. Arch Ophthalmol 100:1074-1077, 1982
4. Drance SM: The visual field of low tension glaucoma and shock-induced optic neuropathy. Arch Ophthalmol 95:1359-1361, 1977
5. Caprioli J, Spaeth GL: Comparison of visual field defects in the low-tension glaucomas with those in the high-tension glaucomas. Am J Ophthalmol 97:730-737, 1984
6. Chauhan BC, Drance SM, Douglas GR, Johnson CA: Visual field damage in normal-tension and high-tension glaucoma. Am J Ophthalmol 108:636-642, 1989
7. Levene RZ: Low tension glaucoma: a critical review and new material. Surv Ophthalmol 24:621-664, 1980
8. Flammer J, Guthauser U, Mahler M: Do ocular vasospasms help cause low-tension glaucoma? Doc Ophthalmol Proc Ser 49:397-399, 1987
9. Phelps CD, Corbett JJ: Migraine and low-tension glaucoma: a case-control study. Invest Ophthalmol Vis Sci 26:1105-1108, 1985
10. Drance SM, Douglas GR, Wijman K et al: Response of blood flow to warm and cold in normal and low-tension glaucoma patients. Am J Ophthalmol 105:35-39, 1988
11. Harris A, Sergott RC, Spaeth GL et al: Color Doppler analysis of ocular vessels blood flow velocity in low tension glaucoma. Am J Ophthalmol 118:642-649, 1994
12. Quaranta L, Manni GL, Donato F, Bucci MG: The effect of increased intraocular pressure on pulsatile ocular blood flow in low tension glaucoma. Surv Ophthalmol 38:S177-S182, 1994
13. Galassi F, Nuzzaci G, Sodi A et al: Color Doppler imaging in evaluation of optic nerve blood supply in normal and glaucomatous subjects. Int Ophthalmol 16:273-276, 1992

VISUAL FIELD DEFECTS AND OCULAR BLOOD FLOW IN GLAUCOMATOUS EYES

ALESSANDRO MAGNASCO[1], LUDOVICA NOVELLA[2], FRANCESCO CALCAGNO[2] and MARIO ZINGIRIAN[1]

[1]University Eye Clinic; [2]Department of Ophthalmology 'Ospedali Galliera'; Genoa, Italy

Abstract

The Langham ocular blood flow (OBF) system is a non-invasive method to calculate the pulsatile ocular blood flow (POBF), which represents 75-90% of the total OBF. Ninety percent of the total OBF depends on the choroidal circulation, and the remaining 10% on the retinal circulation, optic nerve head and blood flow from other parts of the eye. The OBF system consists of a pneumatic tonometer connected to a personal computer which permits the calculation in real time of the pulsatile flow value in μl/min by means of an appropriate software. Sixty-three primary open-angle glaucoma patients aged 56 to 81 years, 25 with glaucomatous visual field defects and 38 with a normal visual field, and 11 normal subjects aged 56 to 78 years, were tested with the 30-2 Program of the Humphrey Visual Field Analyzer. POBF was measured with the Langham OBF system. Glaucomatous eyes with visual field defects showed a significant reduction in POBF compared to the normal eyes. The stages of glaucomatous field defects were not correlated with OBF. These results suggest that OBF may be an important factor in the appearance and progression of glaucomatous visual field defects.

Introduction

Glaucomatous damage to the visual field can be caused by an increase in the intraocular pressure (IOP). However, the existence of glaucomatous damage in the absence of elevated IOP and/or high IOP without detectable damage in the visual field or optic disc indicates that other factors must also be involved in the pathogenesis of glaucoma. Recent studies suggest that the blood flow in the human eye plays a significant role in the pathology of the retina, optic nerve and choroid. In particular, in glaucomatous eyes the survival of retinal ganglion cell axons appears to depend not only on the level of the IOP, but also on other factors such as vascular perfusion of the optic nerve.[1,2] A routine method for measuring ocular blood flow (OBF) became possible with the development of Doppler ultrasound and the Langham OBF system[3] which derives values in μl/min of the pulsatile component of blood flow.[4,5] The pulsatile ocular blood flow (POBF) is the component of the total ocular arterial

Address for correspondence: Alessandro Magnasco, MD, University Eye Clinic, S. Martino Hospital, Pad.9, Largo R. Benzi, 10, 16132 Genoa, Italy

Perimetry Update 1996/1997, pp. 285–288
Proceedings of the XIIth International Perimetric Society Meeting
Würzburg, Germany, June 4–8, 1996
edited by M. Wall and A. Heijl

inflow that causes the rhythmic fluctuation of the IOP and represents about 75-90% of the total OBF. Ninety percent of the OBF depends on the choroidal circulation and the remaining 10% on retinal, optic nerve and other parts of the eye.[6] The present study was designed to compare POBF with glaucomatous visual field defects.

Subjects and methods

Sixty-three primary open-angle glaucoma patients aged 56 to 81 years, 38 with a normal visual field and 25 with glaucomatous visual field defects, and 11 normal subjects aged 56 to 78 years were studied.[7] The criteria used to diagnose primary open-angle glaucoma was an IOP consistently higher than 21 mmHg and a characteristic glaucomatous optic disc cupping. Patients with a history of intraocular surgery, cardiovascular disease, systemic hypertension or hypotension, diabetes mellitus and collagen vascular disease were excluded from the study. The visual field analysis was performed using the 30-2 Program of the Humphrey Visual Field Analyzer. POBF was measured with the Langham OBF system, which includes a pneumatic tonometer connected to a personal computer permitting calculation in real time of the POBF value in μl/min by means of an appropriate software. The values were derived from an analysis of the IOP pulse wave form produced by the amplitude between systolic and diastolic intraocular pressures. Measurements of POBF were performed for two minutes with the 'undisturbed eye' technique[8] with the subject in a supine position,[9,10] and after instillation of 0.4% ossibuprocaine chlorhydrate. In this study, the eyes of the patients were divided into four groups: 22 normal visual field eyes not undergoing therapy; 76 normal visual field eyes undergoing beta-blocker therapy; 15 mild visual field alteration eyes (increased short-term and long-term fluctuation, diffuse depression of sensitivity, absolute defects not in connection with the blind spot) undergoing beta-blocker therapy; and 35 severe visual field defect eyes (arcuate absolute defects in connection with the blind spot, nasal step and extensive absolute defects)[11,12] undergoing beta-blocker therapy.[13,14] The mean POBF of each group was calculated, and Student's *t* test was used for the statistical evaluation.

Results

The POBF clinical measurements in normal and glaucomatous eyes are shown in Tables 1 and 2. In particular, Table 1 shows the POBF values obtained from normal and glaucomatous eyes, with or without visual field defects, undergoing beta-blocker therapy. No significant differences in POBF mean or *t*-test values were found between normal and glaucomatous eyes with a normal visual field; beta-blocker treatment did not seem to have a great influence on POBF. Significant differences in POBF were seen between normal visual field eyes and glaucomatous eyes with visual field defects. In Table 2 the glaucomatous visual field alteration eyes were divided into two classes: mild visual field defect eyes and severe visual field defect eyes. The POBF values showed no significant differences between the two groups, however the POBF of each was significantly decreased compared to normal eyes.

Table 1. Pulsatile ocular blood flow values in normal and glaucomatous eyes

	Normal eyes *(n=22)*	*Glaucomatous eyes with normal visual field* *(n=76)*	*Glaucomatous eyes with visual field defects* *(n=50)*
Age (years)*	67.1±7	66.3±7	67.3±8
POBF (p<0.01) (μl/min)**	770±450	765±470	650±455
POBF (p<0.1) (μl/min)**	770±235	765±260	650±250

*mean ± SD; ** Student's *t* test

Table 2. Pulsatile ocular blood flow values in normal eyes and in glaucomatous eyes with mild and severe visual field defects

	Normal eyes *(n=22)*	*Mild glaucomatous visual field defect eyes* *(n=15)*	*Severe glaucomatous visual field defect eyes* *(n=35)*
Age (years)*	67.1±7	67.9±9	66.7±8
POBF (p<0.01) (μl/min)**	770±450	650±390	660±480
POBF (p<0.1) (μl/min)**	770±235	650±250	660±260

*mean ± SD; ** Student's *t* test

Discussion

In this study the OBF differences observed between normal and glaucomatous visual field defect eyes confirm the importance of vascularization in the pathogenesis of glaucoma.[15] Ocular blood perfusion may be a determining factor in the progression of glaucomatous visual field damage.[16] A series of vascular factors has been outlined which may be important for the pathogenesis of glaucoma: such factors include systemic hypertension, obstruction of the carotid artery, conditions reducing cardiac output and hypertensive angiopathy. Furthermore, vascular disturbances such as migraine may alter the OBF,[17,18] and consequently produce visual field defects. The Langham OBF system is a practical clinical method for assessment of POBF, which does not provide a precise measurement of ocular perfusion, but does provide a summary of the main components which determine the OBF.

Acknowledgment

The authors wish to thank Maura Lodi for her valuable assistance.

References

1. Pillunat LE, Stodtmeister R, Marquardt R, Mattern A: Ocular perfusion pressures in different types of glaucoma. Int Ophthalmol 13:37-42, 1989
2. Flammer J: The vascular concept of glaucoma. Surv Ophthalmol 38 (Suppl, May):S3-S6, 1994

3. Hitchings R: The ocular pulse. Br J Ophthalmol 75:65, 1991
4. Langham ME, To'Mey KF: A clinical procedure for the measurements of the ocular pulse-pressure relationship and the ophthalmic arterial pressure. Exp Eye Res 27:17-25, 1978
5. Silver D, Farrell R: Validity of pulsatile ocular blood flow measurements. Surv Ophthalmol 38 (Suppl, May):S72-S80, 1994
6. Ravalico G, Crocè M, Toffoli G, Pastori G, Calderini S: Variazioni del flusso ematico pulsatile oculare in rapporto all'età. Boll Ocul (Suppl 3)74:501-510, 1995
7. Langham ME, Farrel R, O'Brien V, Silver D, Schilder P: Blood flow in the human eye. Acta Ophthalmol (Kbh) 67 (Suppl 191):9-13, 1989
8. Cambiaggi A, Calcagno F: Il flusso ematico oculare nella sindrome della pseudoesfoliazione: risultati preliminari. Boll Ocul (Suppl 4) 71:515-518, 1992
9. Trew DR, Smith SE: Postural studies in pulsatile ocular blood flow. I. Ocular hypertension and normotension. Br J Ophthalmol 75:66-70, 1991
10. Trew DR, Smith SE: Postural studies in pulsatile ocular blood flow. II. Chronic open angle glaucoma. Br J Ophthalmol 75:71-75, 1991
11. Lachenmayr BJ, Vivell PMO: Perimetry and Its Clinical Correlation, pp 59-90. Stuttgart/New York: G Thieme 1993
12. Zingirian M, Gandolfo E, Capris P: Perimetria: Stato Attuale. Monografie della Società Oftalmologica Italiana, No 1, pp 65-78. Roma: Esam Futura 1990
13. Grajewski AL, Ferrari-Dileo G, Feuer W, Anderson DR: The beta-adrenergic responsiveness of choroidal vasculature. Ophthalmology 98:989-995, 1990
14. Boles Carenini A, Sibour G, Boles Carenini B: Differences in the longterm effect of timolol and betaxolol on the pulsatile ocular blood flow. Surv Ophthalmol 38 (Suppl May): S118-S124, 1994
15. Langham ME: Ocular blood flow and vision in healthy and glaucomatous eyes. Surv Ophthalmol 38 (Suppl, May):S161-S168, 1994
16. Galassi F, Nuzzaci G, Sodi A, Casi P, Cappelli S, Vielmo A: Possible correlation of ocular blood flow parameters with intraocular pressure and visual field alterations in glaucoma: a study by means of color doppler imaging. Ophthalmologica 208:304-308, 1994
17. Rojanapongpun P, Drance SM, Morrison BJ: Ophthalmic artery flow velocity in glaucomatous and normal subjects. Br J Ophthalmol 77:25-29, 1993
18. Corbett JJ, Phelps CD: Migraine and low tension glaucoma. Invest Ophthalmol Vis Sci 26:1101-1104, 1985

FIELDNET: PACKAGE FOR THE SPATIAL CLASSIFICATION OF GLAUCOMATOUS VISUAL FIELD DEFECTS

DAVID B. HENSON[1], SUSAN SPENCELEY[2] and DAVID BULL[3]

[1]Department of Ophthalmology, University of Manchester, Manchester, UK;
[2]School of Computer and Information Science, University of South Australia;
[3]Department of Electrical and Electronic Engineering, University of Bristol, Bristol, UK

Abstract

Purpose: To describe a computer program, FieldNet, which uses artificial neural networks (ANNs) to classify the spatial patterns of visual field loss seen in patients with glaucoma.
Networks: FieldNet incorporates two trained ANNs (Kohonen self-organizing feature maps), one for the superior and one for the inferior hemifield. These networks were trained with pattern deviation data from Program 24-2 of the Humphrey Visual Field Analyzer (HFA). Each record in the training data sets (737 superior and 734 inferior) had two or more defective locations (pattern deviation $p<0.01$) in the relevant hemifield.
Program input: FieldNet runs on an IBM compatible system and accepts 5.25-inch diskettes directly from the HFA. FieldNet will also accept data which has already been converted into an appropriate DOS format.
Program output: The program can run in either an interactive or non-interactive mode. In the interactive mode the program can either step through the file one record at a time, or present a longitudinal sequence of records. In both cases, the perimetrist views a graphical representation of the feature maps and the pattern deviation probability map(s) on the computer monitor. The classification, or, in the case of a longitudinal sequence, the trace pattern, is displayed on the reproduced feature maps.
Applications: To aid the monitoring of progressive loss and to assist in the classification of glaucoma.

Introduction

Glaucoma is known to produce characteristic patterns of visual field loss. Aulhorn and Harms[1] classified 954 eyes with circumscribed defects in the central visual field into eight different groups. The subjective classification being based upon the location, shape and extent of loss. Similar, descriptive classifications have been given by Aulhorn,[2] Aulhorn and Karmeyer,[3] Drance,[4] and, as part of an investigation into progressive loss, by both Hart and Becker[5] and Jay and Murdock.[6]

Address for correspondence: D.B. Henson, PhD, University Department of Ophthalmology, Royal Eye Hospital, Oxford Road, Manchester, M13 9WH, UK

Perimetry Update 1996/1997, pp. 289–298
Proceedings of the XIIth International Perimetric Society Meeting
Würzburg, Germany, June 4–8, 1996
edited by M. Wall and A. Heijl

These subjective classification systems, which are all based upon kinetic data, have a number of shortcomings. The individual classes often lack precise definitions, which can lead to problems of misclassification. The number of classes are invariably small, which limits their usefulness in grading the extent of loss and in monitoring progression, and finally, the classes are often based upon preconceived notions concerning the nature of glaucomatous loss.

Artificial neural networks (ANNs), which are capable of learning from examples, possess a series of attributes that make them particularly useful in the tasks of differentiating and classifying spatial patterns. They have an ability to learn similarities among patterns directly from instances of them, they are capable of using all the data within very large data sets, they have no preconceived notions, and they have an ability to generalize when used to process previously unseen data.

There are two broad classes of ANNs: those which use supervised learning and those which use unsupervised learning. The supervised ANN learns from a training set of data in which each item has already been classified, *e.g.*, normal or glaucomatous. It then learns to reproduce this classification. The back propagation network,[7] which has been used by a number of researchers interested in developing automated systems for the recognition and classification of visual field defects,[8-14] is typical of this type of learning.

The unsupervised ANN, of which the Kohonen self-organizing feature map[15] (SOM) is typical, does not require the training data to be classified. The classification is performed by the network which, during training, groups together inputs which have similar patterns. At the end of the training session, each group is represented by an output node. The number of output nodes and their arrangement is set by the network designers and takes into account the nature of the data, number of examples within the training set and the network's intended application. In this project, the number of output nodes was set to 25 these being arranged in a 5 x 5 square (the feature map). In the case of glaucomatous visual field loss, the input to the SOM is the field data and each of the output nodes within the feature map represents a different type of visual field loss, *e.g.*, arcuate defects and paracentral defects. In comparison to the back propagation network, the Kohonen SOM has received relatively little attention within the ophthalmic literature.[16,17]

Once a SOM has been designed and trained, it can be used quickly to classify new visual field data. Each visual field presented to the trained SOM will maximally activate a single output node. This output node represents the group of visual field defects within the training set which the new defect spatially most resembles.

One of the major advantages of unsupervised networks is that they overcome the criticism that ANNs simply duplicate the pre-conceived judgements of the data classifier(s). A further advantage of the Kohonen SOM is that during training it organizes the output nodes in such a way that neighboring nodes (within the 5 x 5 square) represent similar types of loss. The extremes (very early loss and very advanced loss) often being placed at opposite corners of the feature map. This particular feature can be used to monitor visual field loss. By examining the output nodes of a sequence of visual field records which, when connected together form a trace pattern across the feature map, the direction of movement can be examined to see if it is towards the most defective node, *i.e.*, getting worse.

The spatial patterns of loss within the superior and inferior hemifields show a degree of independence due to the anatomical arrangement of visual fibers at the optic nerve head. When spatially classifying the whole visual field, this arrangement

can result in a certain number of redundant classes in which different combinations of the same superior and inferior hemifield patterns occur.[16] To overcome this problem, the ANNs described in this paper will independently classify the superior and inferior hemifields.

This paper describes a software package, FieldNet, which incorporates two trained Kohonen SOMs (one for the superior and one for the inferior hemifield). The networks have been trained on results from the 24-2 Program of the Humphrey Visual Field Analyzer (HFA). The program runs on an MS-DOS-based computer and accepts data from HFA 5.25-inch diskettes. In its interactive mode, it displays either the classification of a single record or a sequence of records. When displaying the results from a sequence, it also displays their trace patterns across a representation of the feature maps. This paper also describes the data sets used for training the networks.

Methods

The SOM training set was selected from a database of 1316 HFA records collected at Dalhousie University and Moorfields Eye Hospital from both 30-2 and 24-2 programs. All records within the database came from patients with a positive diagnosis of open-angle glaucoma. The diagnosis was based upon the existence of a visual field defect characteristic of glaucoma and/or characteristic changes at the optic nerve head and/or a raised IOP. The database represented an unbiased sample of patients with open-angle glaucoma, with no attempt being made to balance the sample on the basis of visual field loss. Every attempt was made, during collection, to ensure that artefacts due to the rims of correcting spectacle lenses, eyelashes and eyebrows did not occur. The utilization of data from program 24-2 helps to avoid lens rim artefacts.[18]

The test locations used were a subset of those in the HFA, Program 24-2. Excluded were the two locations that normally fall within the blind spot region and the two that are beyond an eccentricity of 24° in the nasal field. This subset contained 25 test locations in both the superior and inferior hemifields. Data from left eyes were flipped around the vertical midline.

The 25 test locations for both the superior and inferior hemifields were converted to pattern deviation probability values,[19] and a cut-off criterion of $p<0.01$ applied to differentiate between normal and defective locations. For inclusion in a training set, the eye had to have two or more defective locations within the respective hemifield. When both eyes of the patient met this criterion, the eye with the largest number of defective locations was selected.

The pattern deviation probability values made use of the results from 134 second visit visual field records from 134 normal patients. The computation followed that described by Heijl *et al.*,[19] with the exception that the distributions of deviation values for each test location took into account both the age and the general height of the visual field. By taking both these factors in account, our distributions were tighter than would have occurred if we had only taken into account age as described by Heijl *et al.*[17] At most field locations, the deviation values formed normal distributions. In other instances, it was necessary to transform the deviation values to reduce the distribution's skew and/or kurtosis. The 1% cut-off values were derived from these distributions after any necessary transformations.

The training set inclusion criterion of two or more defective locations ($p<0.01$)

was used to obtain a good balance of defects within the trained feature maps. The allocation of nodes in a trained SOM will be roughly in proportion to the number of cases within the training set.[16] If, for example, the training set had a large number of eyes with early visual field loss and very few with advanced loss, then the resulting network would allocate a large number of the output nodes to the early loss examples and few to the advanced ones. It is envisaged that FieldNet will be used to assist in the classification of established cases of glaucoma in which some visual field loss already exists. By excluding cases in which there is little, if any, visual field loss, the final network will give a better representation of the classes of visual field loss that exist within established cases.

The final training set for the superior hemifield was composed of 737 records, while that for the inferior hemifield was composed of 734 records. Each training set included only a single record of one eye from each patient.

The 25 test locations, coded as either defective or normal on the basis of the pattern deviation probability values (cut-off criterion $p<0.01$), formed the input to a Kohonen SOM (25 output classes arranged in a 5 x 5 square). The SOM clustered the training data using the learning algorithm of Neural Works Professional II.[20] The SOM cycled through the training set 30 times using a square neighborhood function initialized to a size of 5 x 5 and reducing to 1 x 1 during the training period. The weights connecting each input to each output were scaled between 0 and 100.

An index, representing the relative Euclidean distances of the output node from the most normal and most defective node provides a measure of the extent of loss. This index, which ranges between 0 (normal) and 1 (most defective), ignores the rotational and reflectional differences possible within a map. The index is calculated using the following equation:

$$\textbf{Index} = \frac{\textbf{dist}_i\textbf{(n)}}{\textbf{dist}_i\textbf{(n)} + \textbf{dist}_i\textbf{(d)}}$$

where **n** represents the most normal node, **d** represents the most defective node, **i** represents the output node, and $\textbf{dist}_i\textbf{(n)}$ represents the distance between the output node and the most normal node.

Results

The trained superior and inferior hemifield feature maps are graphically represented in Figures 1 and 2. Each square within each figure represents a particular output node. Within each square, there is a representation of either the superior or inferior hemifield. In the Kohonen SOM, each output node is connected to every test location within the respective hemifield. The strength of each connection (weight) signifies the importance of a particular test location to each node. Figures 1 and 2 graphically represent the strength of these connections at each node to give a representation of the type of field defect each node represents. The 25 nodes/classes are numbered 0-24 from the top left to the bottom right. The numbering does not represent any characteristic of the data.

Figure 3 shows one of the graphical outputs from FieldNet. This type of output occurs when the clinician steps through the individual field records. The screen is

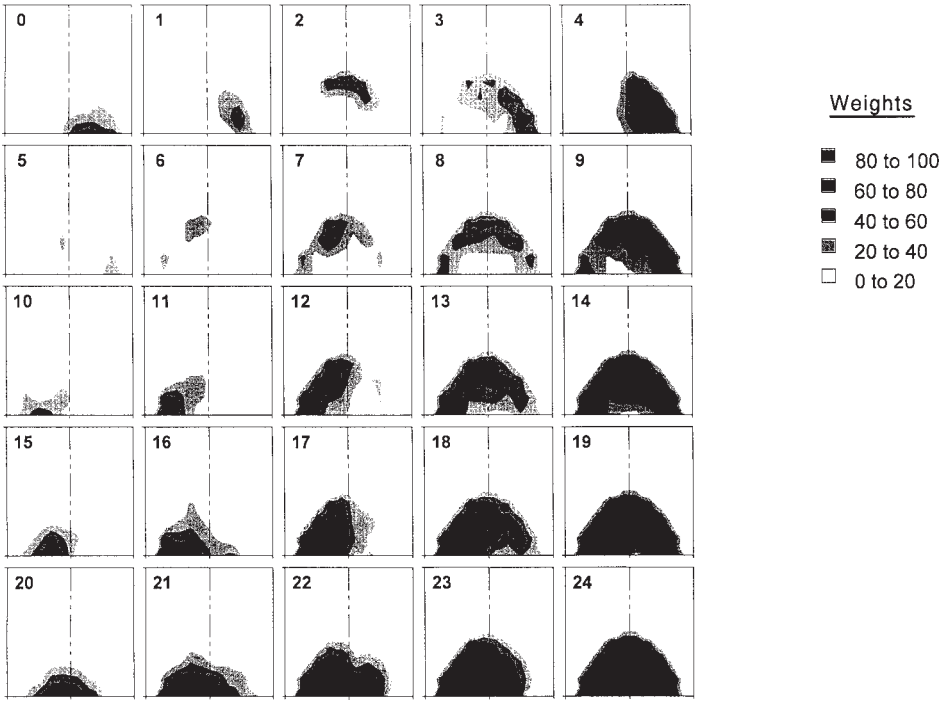

Fig. 1. Graphical representation of a Kohonen self-organizing feature map trained on 737 glaucomatous visual field records from the superior hemifield of program 24-2 of the Humphrey Visual Field Analyzer. Each square represents a single output node (25 arranged in a 5 x 5 matrix). Within each node there is a gray scale representation of the visual field indicating the weight of the connections between each part of the visual field and the respective output node. The weights have been scaled to lie between 0 and 100.

divided into three main sections. Simplified copies of the superior and inferior feature maps are drawn at the top left and top right of the screen. Beneath and to the right of the maps is a representation of the patient's visual field record. Defective locations ($p<0.01$) are presented by light blue squares, while normal locations are represented by mauve squares. In the example given, the patient can be seen to have a superior defect extending across the vertical midline with a normal inferior hemifield.

The defect has been classified by the two networks. It falls into Class 18 (superior hemifield) and Class 8 (inferior hemifield). This information is given at the bottom of the display and by the highlighted squares on the feature maps. The most normal and most defective nodes are differentiated by small solid light blue squares in the upper left hand corner of the respective nodes. The indices representing the extent of loss in the superior and inferior hemifields are also given at the bottom of the display.

Figure 4 shows a sequence of measurements from a patient with a normal superior and inferior hemifield. Eight visual field charts are shown along the bottom of the screen along with the network classes (above and below each field chart). On the feature maps, a trace has been drawn which starts at the node representing the first record and then passes to each subsequent records node to end up in the node

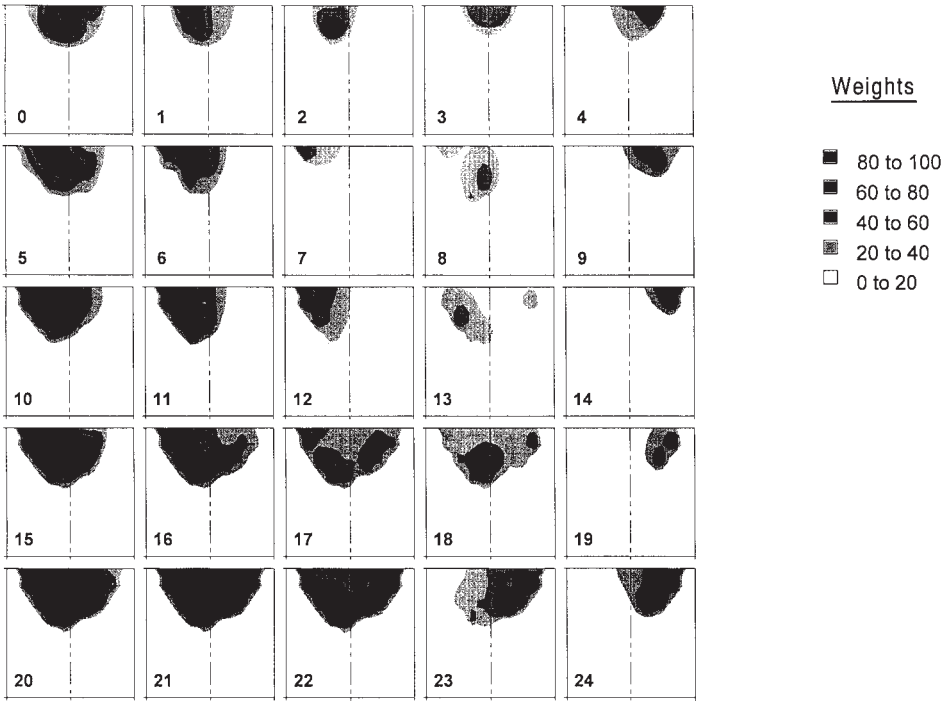

Fig. 2. Graphical representation of a Kohonen self-organizing feature map trained on 734 glaucomatous visual field records from the inferior hemifield of program 24-2 of the Humphrey Visual Field Analyzer. Each square represents a single output node (25 arranged in a 5 x 5 matrix). Within each node there is a gray scale representation of the visual field indicating the weight of the connections between each part of the visual field and the respective output node. The weights have been scaled to lie between 0 and 100.

representing the last visual field record. In the superior hemifield, all results fell within Class 5. In the inferior hemifield, the result started off in Class 8, moved to Class 9 at the fifth visit and to Class 3 on the tenth visit. (Not shown at the bottom of the screen due to limitation of space, the additional field charts can be displayed on a continuation screen.) The trace pattern drawn upon the inferior feature maps shows this movement.

Figure 5 shows the results from a patient with an inferior arcuate defect and a noisy superior hemifield. There are ten records for this patient, the first eight being shown on this screen display. The trace pattern on the superior hemifield shows the noise response with movement taking place among four different output nodes. The start and finish nodes are adjacent to each other. The inferior hemifield shows a gradual shift towards the bottom left hand corner of the map that represents the most advanced loss. This type of trace pattern is indicative of progressive visual field loss.

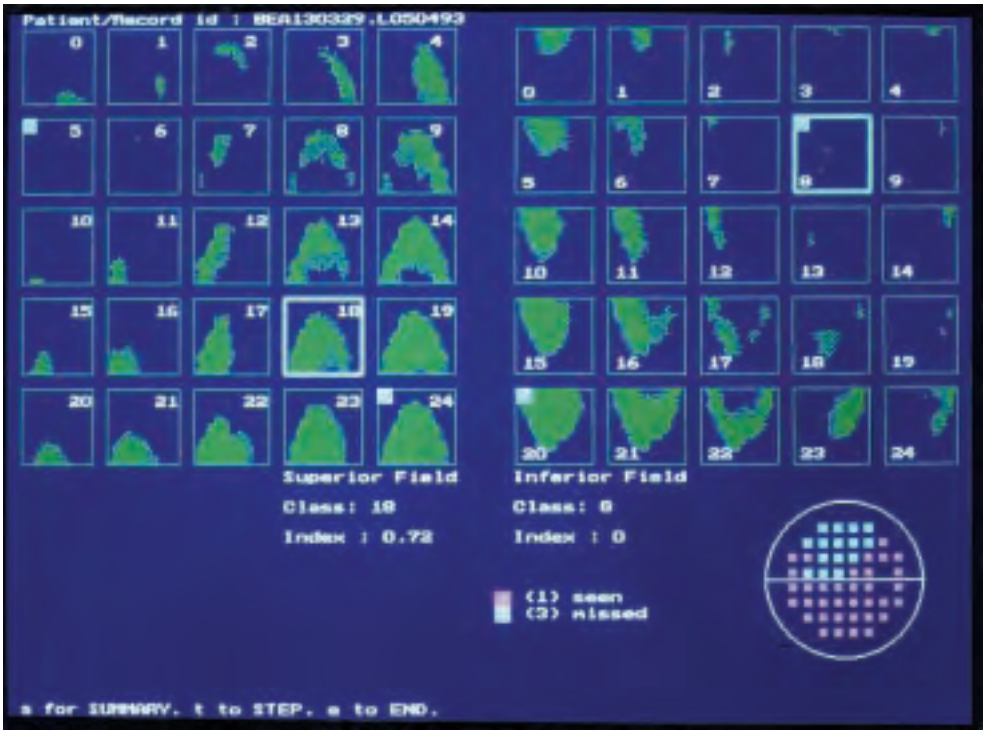

Fig. 3. The graphical output from FieldNet showing the classification of a single visual field record. The pattern deviation probability map ($p<0.01$) is shown in the bottom right hand corner, and the network classifications by the highlighted squares on the reproduced superior and inferior feature maps.

Discussion

FieldNet provides the clinician with a simple, objective means of classifying visual field data from the HFA. This classification is based upon the spatial information contained within the field chart and complements, rather than replaces, the information obtained from packages such as STAPAC-2[19] and Delta.[21]

While there have been a number of papers describing the potential of ANNs to help in the diagnosis and classification of visual field defects, these have not, as yet, found wide acceptance in the clinical environment. This is undoubtedly, in part, related to the problems encountered when trying to design and train ANNs. This process can take a considerable amount of time and requires access to good programming skills. Once trained, networks can be incorporated into relatively simple programs, such as FieldNet, to provide the clinician with a quick and user-friendly method of analysis.

It has been suggested within the literature that glaucoma, rather than being a single disease entity, actually represents a series of different diseases with differing pathogenic mechanisms.[22,23] The subdivision of glaucoma on the basis of visual field measures has been hampered by the lack of a suitable method of spatial classification. Prior methods of spatial classification, which have largely been based on subjective assessments of visual field records, have produced limited numbers of spatial

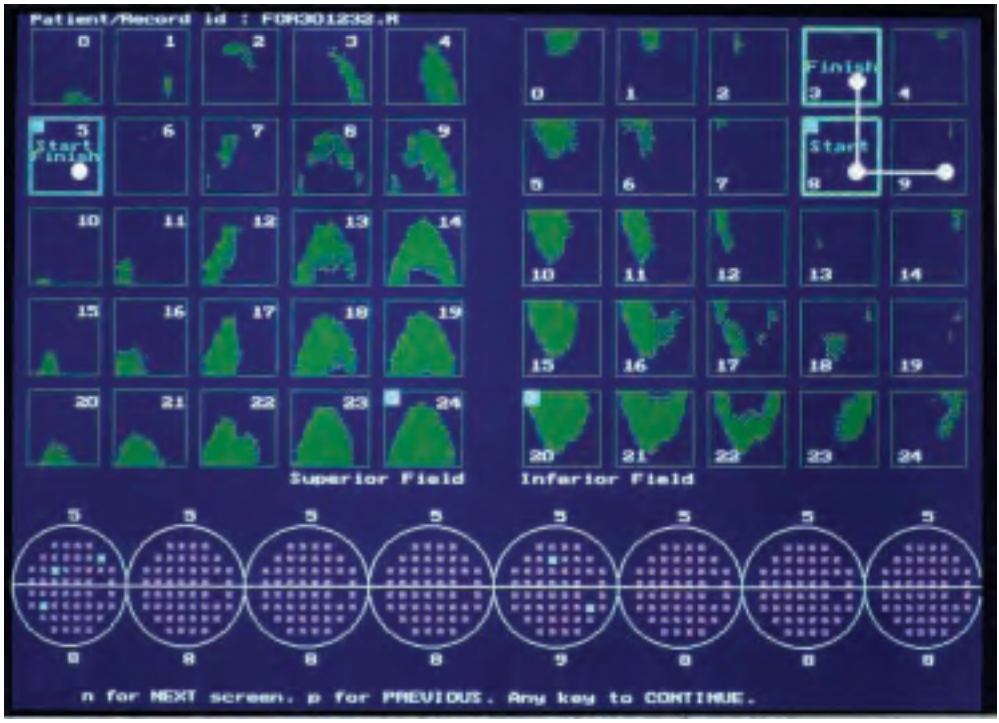

Fig. 4. The graphical output from FieldNet showing the classification of a series of visual field records. The pattern deviation probability maps ($p<0.01$) are arranged in chronological order along the bottom of the figure. The network classifications are printed above and below each field map and represented by the highlighted squares and the white bold line which forms a trace pattern on the reproduced superior and inferior feature maps. This patient has no visual field loss but shows some noise in her inferior classification.

classes that have invariably lacked precise definition. In Aulhorn's classification,[1] there were just eight spatial classes, while in Jay and Murdoch's work,[6] it was confined to five. In other work, defects have often been simply described as localized or diffuse and within or not within five degrees of fixation.[23] Quantification systems based upon an analysis of threshold values do little to help as they invariably take no account of the spatial data. The classification system described in this paper gives a much finer classification of the spatial pattern of loss. The classification system is also objective and avoids misclassifications which result from subjective interpretations. A clear potential for FieldNet is to assist in the recognition of different subclasses of glaucoma.

Mikelberg *et al.*[24] described three ways in which the visual field may progress in glaucoma. Their analysis was based upon a global measure of the visual field plotted over time. Subsequent work[25,26] has shown that the rate of progression is different in different regions of the visual field, and that the application of global measures can obscure significant changes within a specific region. The spatial classification system used in FieldNet has the potential to recognize many different types of progression on the basis of different trace patterns across the feature maps. This provides a further opportunity to recognize different subclasses of glaucoma.

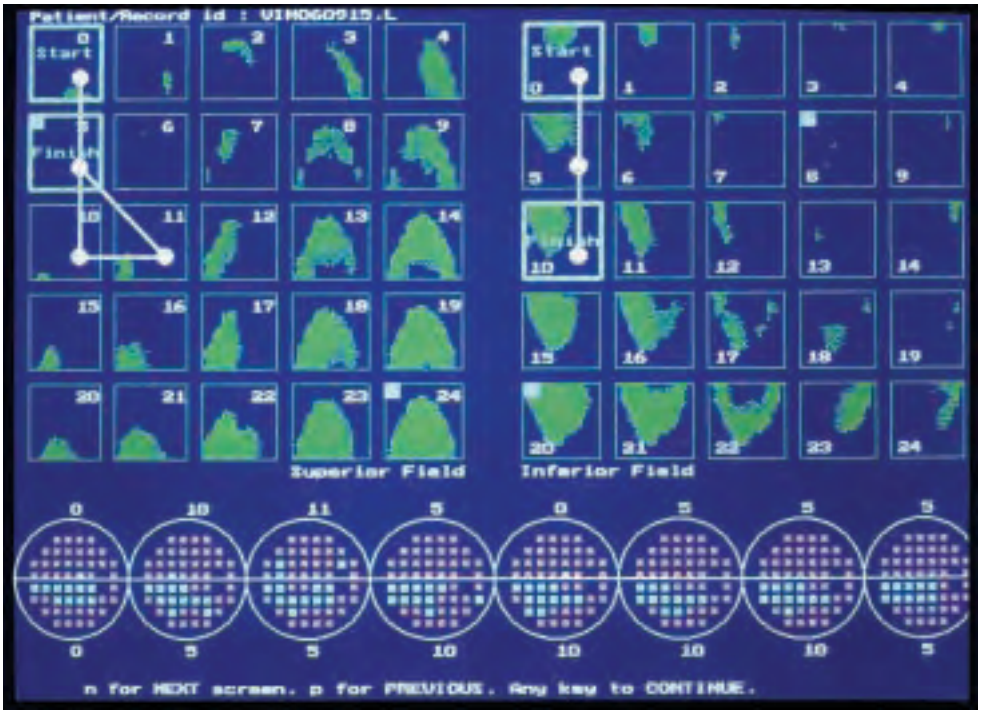

Fig. 5. The graphical output from FieldNet showing the classification of a series of visual field records. The pattern deviation probability maps (p<0.01) for each record are arranged in chronological order along the bottom of the figure. The network classifications are printed above and below each field record and represented by the highlighted squares and the white bold line which forms a trace pattern on the reproduced superior and inferior feature maps. This patient shows enhanced noise in the superior hemifield and a progressive visual field defect in the inferior hemifield.

FieldNet is potentially a very flexible package, able to analyze data from a variety of perimeters, running a range of different programs. The ANNs incorporated within FieldNet determine the range of data it can analyze. At present only ANNs suitable for analyzing Humphrey 30-2 or 24-2 full-threshold programs are made available. It is hoped to extend this work to accept data from other perimeters and programs.

Acknowledgments

This work has been made possible by the kind contribution of visual field data from Mr R. Hitchings and Dr B. Chauhan. We would also like to acknowledge the support of Dr F. Fitzke, Dr A. McNaught, and Mr D. Crabb who helped in the selection of data and discussion of the work. Supported by the UK Engineering and Physical Sciences Research Council (grant number GR/H54393).

References

1. Aulhorn E, Harms H: Early visual field defects in glaucoma. In: Leydhecker W, (ed) Glaucoma. Tutzig Symposium, 1966, pp 151-175. Basel: Karger, 1967
2. Aulhorn E: Comparative visual field study in patients with primary open angle glaucoma and anterior ischemic optic neuropathy. Doc Ophthalmol 22:3-13, 1979
3. Aulhorn E, Karmeyer H: Frequency distribution in early glaucomatous visual field defects. Doc Ophthalmol Proc Ser 14:75-83, 1977
4. Drance SM: The early visual field defects in glaucoma. Invest Ophthalmol Vis Sci 9:84-91, 1969
5. Hart WM, Becker B: The onset and evolution of glaucomatous visual field defects. Ophthalmology 89:268-279, 1982
6. Jay JL, Murdoch JR: The rate of visual field loss in untreated primary open angle glaucoma. Br J Ophthalmol 77:176-178, 1993
7. Rumelhart DE, McClelland JL: Parallel Distributed Processing: Explorations in the Microstructure of Cognition. Vol 1. Foundations. MIT Press 1986
8. Goldbaum MH, Sample PA, White H, Weinreb RN: Discrimination of normal and glaucomatous visual fields by neural network. Invest Ophthalmol Vis Sci 31(Suppl):503, 1990
9. Shields SM, Trick GL: Applying neural networks in glaucoma: prediction of the risk of visual field loss. Invest Ophthalmol Vis Sci 31(Suppl):503, 1990
10. Kelman SE, Perell HF, Autrechy LD, Scott RJ: A neural network can differentiate glaucoma and optic neuropathy visual fields through pattern recognition. In: Mills RP, Heijl A (eds) Perimetry Update 1990/91, pp 287-290. Amsterdam/Milano: Kugler & Ghedini Publ 1991
11. Nagata S, Kani K, Sugiyama A: A computer assisted visual field diagnosis system using neural network. In: Mills RP, Heijl A (eds) Perimetry Update 1990/91, pp 291-295. Amsterdam/Milano: Kugler & Ghedini Publ 1991
12. Spenceley S, Henson DB, Bull DR: Visual field analysis using artificial neural networks. Ophthalmol/Physiol Opt 14:239-248, 1994
13. Goldbaum MH, Sample PA, White H, Cote B, Raphaelian P, Fechtner RD et al: Interpretation of automated perimetry for glaucoma by neural network. Invest Ophthalmol Vis Sci 35:3362-373, 1994
14. Mutlukan E, Keating D: Visual field interpretation with a personal computer based neural network. Eye 8:321-323, 1994
15. Kohonen T: Self-Organization and Associative Memory, 2nd Edn. New York: Springer-Verlag, 1988
16. Henson DB, Spenceley SE, Bull DR: Assessing progressive field loss in glaucoma using a self-organizing feature map. In: Mills RP, Wall M (eds) Perimetry Update 1994/1995, pp 3-11. Amsterdam/New York: Kugler Publ 1995
17. Henson DB, Spenceley SE, Bull DR: Spatial classification of glaucomatous visual field loss. Br J Ophthalmol 80:526-531, 1996
18. Zalta AH: Lens rim artefact in automated threshold perimetry. Ophthalmology 96:1302-1311, 1989
19. Heijl A, Lindgren G, Lindgren A, Olsson J, Åsman P, Myers S et al: Extended empirical statistical package for evaluation of single and multiple fields in glaucoma: STATPAC 2. In: Mills RP, Heijl A (eds) Perimetry Update 1990/91, pp 303-315. Amsterdam/Milano: Kugler & Ghedini Publ 1991
20. Neuralware: Neural Computing: A Technology Handbook for Professional II/Plus and NeuralWorks Explorer. Pittsburgh, PA: Neuralware Inc 1993
21. Bebie H, Fankhauser F: Delta Manual. Zürich: Schlieren, Interzeag AG 1982
22. Speath GL: A new classification of glaucoma including focal glaucoma. Surv Ophthalmol 38:S9-S17, 1994
23. Nicolela MT, Drance SM: Various glaucomatous optic nerve appearances. Ophthalmology 103:640-649, 1996
24. Mikelberg FS, Schultzer M, Drance SM, Lau W: The rate of progression of scotomas in glaucoma. Am J Ophthalmol 101:1-6, 1986
25. O'Brien C, Schwartz B: The visual field in chronic open angle glaucoma: the rate of change in different regions of the field. Eye 4:557-562, 1990
26. Dunbar Hoskins H, Jensvold N, Zaretsky MD, Hetherington J: Rate of progression of discrete areas of the visual field. In: Heijl A (ed) Perimetry Update 1988/89, pp 173-176. Amsterdam/Milano: Kugler & Ghedini Publ 1989

APPLICATIONS OF FRACTAL ANALYSIS TO DIFFERENTIAL LIGHT-SENSITIVE PERIMETRY IN GLAUCOMA PATIENTS AND NORMAL SUBJECTS

YOSHIKI KONO, AIKO IWASE, MIHOKO MAEDA, TETSUYA YAMAMOTO and YOSHIAKI KITAZAWA

Department of Ophthalmology, Gifu University School of Medicine, Gifu, Japan

Abstract

The authors studied the validity of fractal analysis in identifying early-stage glaucomatous visual field demonstrated by differential light-sensitivity perimetry (Humphrey Field Analyzer 630 (HFA)). Further, they studied the relationships between the global indices of HFA and the dispersion index (DI), an index of the fractal analysis.

Forty-six eyes of 37 normal-tension glaucoma (NTG) patients and 118 eyes of 59 normal subjects were studied. Of the 46 NTG eyes, 15 had Aulhorn-Greve classification Stage I and 31 Stage II.

The authors modified the analytical program of Frisén to calculate the DI. The mean rank of DI was 68.4 in normal eyes, 103.5 in Stage I eyes and 125.9 in Stage II eyes, demonstrating a significant difference between the three groups ($p<0.0001$, Kruskal-Wallis test). The mean DI (± standard deviation) was 1.069 ± 0.057 in normal eyes, 1.182 ± 0.234 in Stage I eyes, and 1.256 ± 0.214 in Stage II eyes. Stage I and II glaucomatous eyes showed a significantly higher DI than normal eyes ($p=0.0052$ and $p<0.0001$, respectively, ANOVA and Scheffé's F procedure). Significant correlations were found between the DI and both pattern standard deviation and mean deviation ($rs=0.594$, $p<0.0001$ for PSD; $rs=-0.302$, $p=0.0001$ for MD, Spearman's test).

These results indicate that fractal analysis may be useful for detecting early-stage glaucoma and that the DI is correlated with local visual field defects.

Address for correspondence: Yoshiaki Kitazawa, MD, PhD, Department of Ophthalmology, Gifu University School of Medicine, 40 Tsukasa-machi, Gifu 500, Japan

Perimetry Update 1996/1997, p. 299
Proceedings of the XIIth International Perimetric Society Meeting
Würzburg, Germany, June 4–8, 1996
edited by M. Wall and A. Heijl

A PROFILE OF THE SPATIAL DEPENDENCE OF POINTWISE SENSITIVITY ACROSS THE GLAUCOMATOUS VISUAL FIELD

DAVID P. CRABB[1], FREDERICK W. FITZKE[1], ANDREW I. MCNAUGHT[2] and ROGER A. HITCHINGS[2]

[1]*Department of Visual Science, Institute of Ophthalmology, UCL, London;*
[2]*Glaucoma Unit, Moorfields Eye Hospital, London; UK*

Abstract

Background: Current methods for determining pointwise visual field progression treat each location independently. The authors have recognized that the determination of progression can be improved by applying a spatial (gaussian) filter to the recorded data. This technique, commonly used in image processing, may benefit from better knowledge and quantification of the spatial dependence that exists between the sensitivity of different locations within the visual field.
Purpose: To derive a point-by-point profile of this spatial dependence. This will be used to develop a new adaptive spatial filter customized to each retinal location to further improve the sensitivity of methods for determining field progression.
Methods: Four hundred and forty Humphrey fields of 440 patients with primary open-angle glaucoma were drawn from a large cross-sectional database to provide a wide range of defect severity. All patients had at least three fields prior to the selected field. The sample was divided into two equal samples to provide cross-validation analysis. Multiple regression analysis of sensitivity (dB) values for each location compared to all other locations in the visual field was performed. For each location, a unique set of points with significant dependence, derived using a stepwise technique, were determined and the resulting connections mapped onto the field. The process was repeated with the second set of data.
Results: The connections between highly dependent locations closely follow the architecture of the retinal nerve fiber layer and tend to be between neighboring locations. Connections were generally repeatable in the validation sample.
Conclusions: These results can be used to derive the shape and weighting of a customized spatial filter process for each individual location within the visual field. These spatial techniques could improve methods for determining the rate of change in a series of fields in glaucoma.

Introduction

The determination of glaucomatous change in a series of visual field results is important in the clinical management of a patient, and in the evaluation of which treatments are most effective in arresting progression. The equivocal rate of sensitiv-

Address for correspondence: David Crabb, Department of Visual Science, Institute of Ophthalmology, UCL, Bath Street, London EC1V 9EL, UK

Perimetry Update 1996/1997, pp. 301–310
Proceedings of the XIIth International Perimetric Society Meeting
Würzburg, Germany, June 4–8, 1996
edited by M. Wall and A. Heijl

ity loss, and the variability that exists between field results make this a difficult task. Often, the length of field series available for a patient is insufficient to estimate a true change with confidence. This sparseness of data in time is, however, offset by the quantity of spatial information within a visual field result. This somewhat neglected feature of perimetric data has only recently been incorporated into methods for discriminating glaucomatous from normal fields.[1,2]

Recently, we have recognized that analysis of visual field progression may also be improved by exploiting the spatial characteristics of the data. Both visual field data and digital images are essentially stored by a computer as numerical values on a regular matrix. This analogy suggests that image processing techniques, developed for enhancing the quality of digital images, may be effectively applied to visual field data. Simple filtering methods, utilizing the spatial correlation that exists between individual field locations, can be applied *post hoc* to series of field results to reduce long-term fluctuation.[3] These techniques can also improve the sensitivity of the pointwise linear regression method for predicting visual field progression.[4] Additionally, spatial filtering can quantify the pointwise variability in a field which may be observed as a pre-cursor to further sensitivity loss.[5]

The grid of sensitivity values typically displayed on the results from a field test does not indicate the true functional proximity of retinal locations. Moreover, the dependence in sensitivity between contiguous sites across the field is not uniform. To date the filtering process has been applied to each point in a field using a fixed set of neighboring locations. The gaussian filter generally operates on a fixed 3 × 3 neighborhood (convolution mask) of locations, and may in some cases 'blur' or 'average out' early focal defects. This may not be a clinically significant effect.[6] Nevertheless, this type of filter is probably sub-optimal because the sensitivity of any location may be more dependent on some points than others, both within and possibly outside the rigid 3 × 3 area. The filtering process may benefit from better knowledge and quantification of the topology of the true spatial dependence that exists between the sensitivity of different locations within the glaucomatous visual field. The objective of this study is to derive a point-by-point profile of this spatial dependence with the aim of developing a filter customized to each individual test site.

Methods

Subjects and data

Four hundred and forty Humphrey visual fields of 440 subjects were selected from a large cohort of patients with primary open-angle glaucoma (POAG). All subjects had POAG defined as intraocular pressure (IOP) > 21 mmHg, and optic disc appearance consistent with a clinical diagnosis of POAG. The fields were selected randomly from records kept on computer disks. Patients who had a series of at least four fields in each eye were selected. The most recent visual field of the right eye was selected to give fields with a wide range of defect severity. Fields were not selected if Humphrey reliability parameters were poor. A field was therefore discounted if more than 20% fixation losses or more than 33% FP or FN errors were recorded. All fields had been tested using the size III white stimulus in standard conditions using the 24-2 full threshold program throughout. Information on patient treatment or indicators of coexistence of other ocular pathology were not obtained.

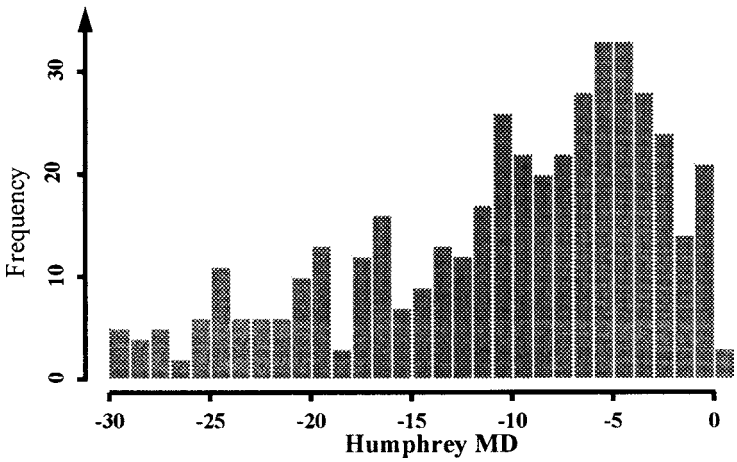

Fig. 1. Distribution of Humphrey MD for all 440 fields.

The median age of the selected patients was 69 years (range 35-91 years). The sample Humphrey mean deviation (MD) of the 440 fields was -9.1 dB (SD: 7.6 dB). The distribution of the Humphrey MD for all the fields, shown in Figure 1, gives an illustration of the range of defect severity within the sample.

Statistical analysis

The visual field data were transferred to a PC via PROGRESSOR software (Institute of Ophthalmology, London, UK) and further analyzed with purpose-written functions using S-PLUS 3.2 for Windows™ (StatSci Europe, MathSoft Inc., Oxford, UK). Where a double determination of threshold had been undertaken at a given test location, the sensitivity was taken as the mean of the values. The two blind spot locations were excluded from further analysis.

Multiple regression analysis was used to determine, for each and every test location, a unique and different set of neighboring points with significant dependence of sensitivity. These are termed the *dependent neighboring locations* for a point. Multiple regression analysis yields a regression model in which the dependent variable or response is expressed as a combination of the explanatory variables.[7,8] Multiple regression analysis was performed separately at each test location (Fig. 2). The dependent variable was simply the sensitivity of the location under consideration. The explanatory variables constituted the sensitivity of the remaining 51 field locations. Significant explanatory variables in each case were determined by a forward stepwise procedure. This technique identifies a subset of all the explanatory variables which best provides an accurate and parsimonious model for the response. This subset is computed by adding variables according to the statistical significance of the improvement in the fit of the model.[8] Strict entry and non-entry cut-off criteria for the stepwise procedure were set at p=0.001 and p=0.01, respectively, to prevent inclusion of variables which have a tiny effect on the response location. The significant explanatory variables give the dependent neighboring locations for each point in the field.

The 440 fields were randomly divided into two equal samples. Therefore, in

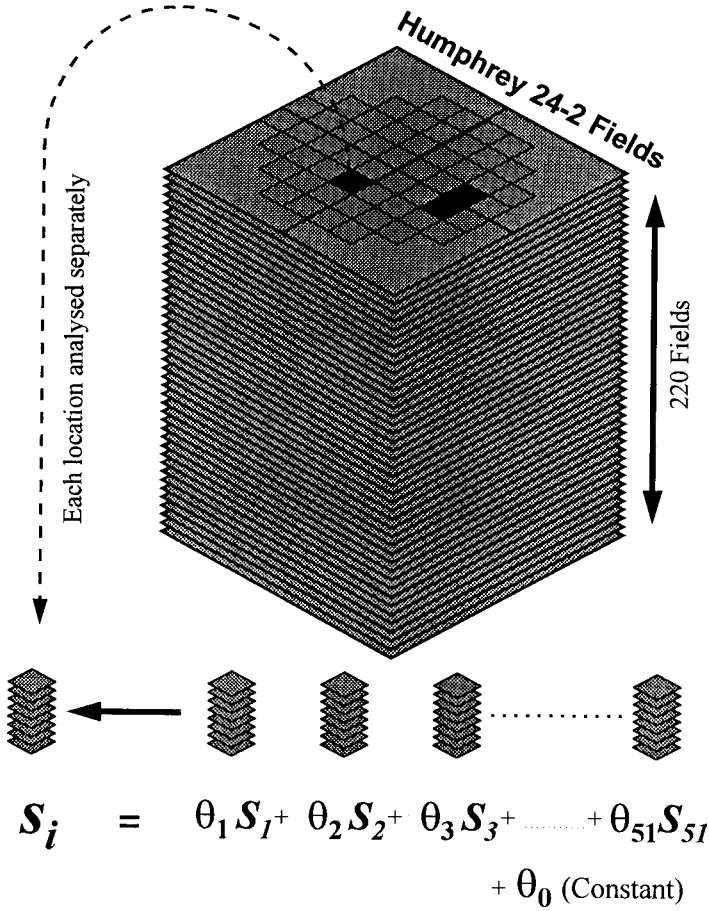

Fig. 2. Schematic diagram describing the multiple regression analysis.

sample A there were 220 sensitivity values for each test location. Multiple regression analysis using forward stepwise selection was performed in turn at each test location using these sensitivity values. Results for each test location, including the significant dependent neighboring locations and their respective regression coefficients, were recorded. Connections between dependent neighboring location and each test point were mapped on a grid of the 24-2 field. This analysis was repeated using the remaining data (sample B; 220 fields). The level of reproducibility in the results from the two samples was assessed.

Results

An example of the results from multiple regression analysis of one location (coded S_{17}) using sample A is given in Table 1. This is the location at Humphrey stimulus location (15°,9°). Three explanatory variables are significant, indicating that the (15°,9°) location is highly dependent on the sensitivity at these locations. The con-

Table 1. Output of results from multiple regression analysis and stepwise procedure applied to the sensitivity of Humphrey location (15°,9°). The location is coded S_{17}. Three significant explanatory variables or dependent neighboring locations were identified by the stepwise procedure. Analysis of variance, regression coefficients, standard errors and associated *p* values for inclusion in the model are shown

Multiple R-value	0.934			
Adj R-value	0.871			
Standard error	3.580			
ANOVA table				
	DF	Sum of squares	Mean square	
Regression	3	18927.287	6309.096	
Residual	216	2769.189	12.820	
MSR (F ratio) =	492.117			
Dependent variable = S_{17}				
Variables in equation	θ	SE.θ	T	*p* value
S_{10}	0.231	0.058	4.012	0.000
S_8	0.273	0.052	5.226	0.000
S_9	0.461	0.062	7.380	0.000
(Constant)	1.583	0.512	3.091	0.002

nections between the set of dependent neighboring locations and the respective test point can be mapped onto a grid of the 24-2 field. Figure 3 illustrates this and additionally shows the dependent neighboring locations for four other test points within the field. In sample A, 40 locations had three dependent neighboring locations, whilst the remaining 12 locations had a set of either two or four dependent neighboring locations. In sample B, 38 locations had three dependent neighboring locations, whilst 13 locations had a set of either two or four (one location in sample B had a total of five dependent neighboring locations). Figure 3 also shows the dependent neighboring locations for the same illustrative set of points using the data from sample B. The connections are generally reproducible. All five of the illustrated locations had at least two dependent neighboring locations that were reproducible in both sample A and B. In fact, 47 of the total 52 locations (90%) had this measure of agreement.

Figure 4 depicts the pattern of all the connections between each point and their respective set of dependent neighboring locations using the data from sample A. Obvious features of this pointwise profile include the independence between locations in the superior and inferior hemifields nasal to the blind spot, and that connections are generally between contiguous points. ‘Diagonal’ and ‘horizontal’ connections suggest agreement between the spatial dependence of sensitivity following the architecture of the retinal nerve fiber layer.

This type of profile of the spatial dependence of pointwise sensitivity coupled with the resultant regression coefficients provide natural solutions to the problem of developing the shape and weighting of a spatial filter customized to each individual location within the visual field. Reconsider, for example, the result of the multiple regression analysis illustrated in Table 1. The Humphrey (15°,9°) location (coded S_{17}) has three dependent neighboring locations derived by the following regression equation:

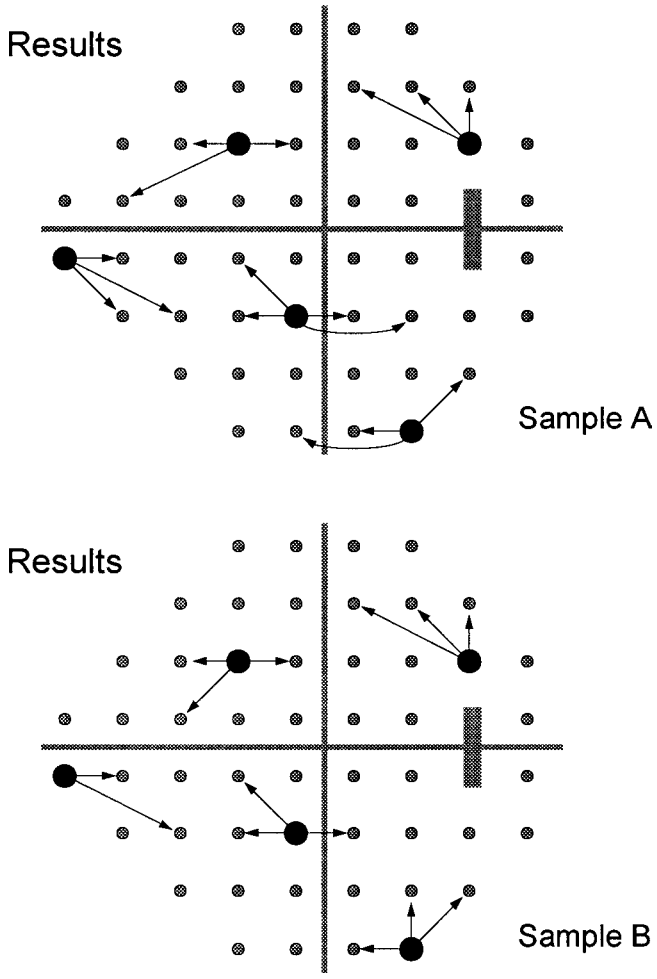

Fig. 3. Examples of significant dependent neighboring locations mapped onto grid of 24-2 field for five test points using data from sample A and sample B.

$$S_{17} = 1.6 + 0.2(S_{10}) + 0.3(S_8) + 0.5(S_9)$$

This equation can be used as a predictor or prognostic indicator of the sensitivity at the Humphrey (15°,9°) location. The regression coefficients can be translated into the convolution weights for a customized filter (Fig. 5). Another example is illustrated in Figure 5.

Discussion

Other workers have investigated the spatial dependence of the pointwise sensitivity across the visual field. Threshold deviations from age-corrected normal values have

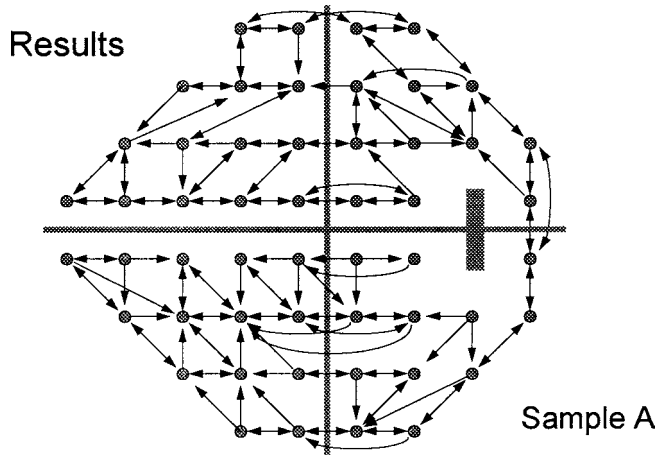

Fig. 4. Representation of connections between each individual point and dependent neighboring location across the whole field using data from sample A. Single and double arrows represent one-way and two-way connections, respectively.

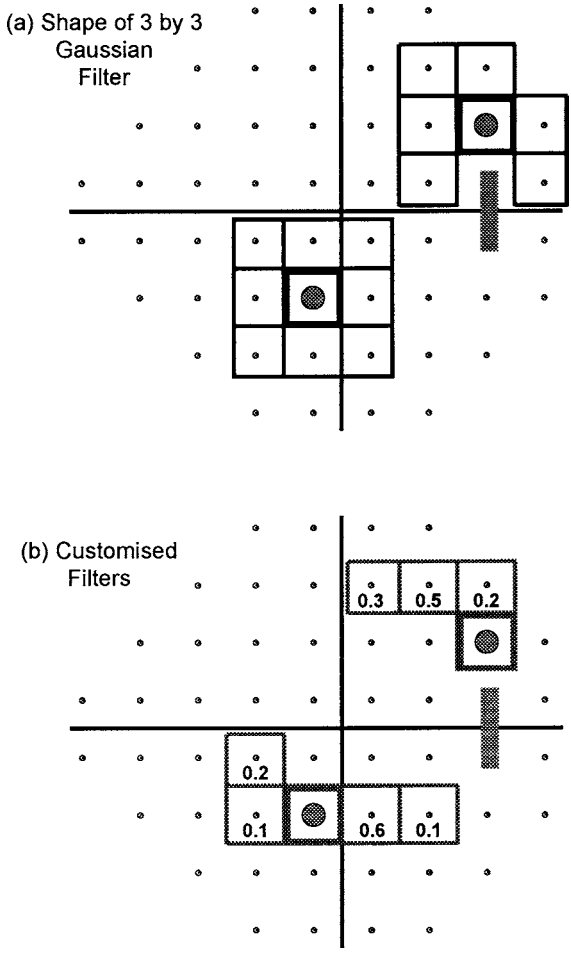

Fig. 5. Comparison of test sites used for (a) simple gaussian filtering and (b) a customized spatial filter. The shape and convolution weights for the customized filter are determined using the pointwise profile of sensitivity dependence determined by stepwise multiple regression analysis.

been shown to be positively correlated between adjacent points in both normals and glaucoma patients.[9,10] Recently, Lachenmayr *et al.*[11] reported similar results in normal subjects using the 2775 pair-wise correlations of sensitivity values of all points in the Humphrey 30-2 field and comparing these to angular distance between locations. Zeyen *et al.*[12] also used pair-wise correlation of sensitivity values to ascertain the dependence between specific locations in a large sample of glaucomatous fields. Results were used in combination with frequency of defective locations to find subsets of points that could be used in staging strategies to reduce test time in Octopus perimetry (program G1).

Mandava *et al.*[13] used statistical cluster analysis of the 1711 pair-wise correlations of sensitivity values from all locations in Octopus perimetry (program G1) to identify groupings of test locations that exhibited similar values. Series of visual fields from normals and patients with stable POAG were then examined using these empirically derived clusters. The authors concluded that these clusters were effective in reducing long-term fluctuation and may allow for an improved method of determining change in a series of fields.

The study described in this paper represents a departure from previous work since we have attempted to determine a different and unique set of neighboring locations for every individual test point within the Humphrey 24-2 field using a sample of 220 glaucomatous eyes. Multiple regression analysis, using a stepwise procedure, was applied in a novel fashion to select a set of most dependent neighboring locations for each site. This stepwise selection technique is particularly advantageous in this case because the explanatory variables are themselves highly correlated. Simply ranking and selecting the highest pair-wise correlation coefficients of sensitivity values would not account for this feature of the data. Additionally, inclusion of a constant value within the multiple regression model allows the use of actual, rather than age-corrected, sensitivity values.

The connections between an individual point and the corresponding dependent neighboring locations generated by the multiple regression analysis can be mapped onto the field. These connections tend to be between adjacent points and generally follow a pattern consistent with the architecture of the retinal nerve fiber layer. These results can be used to derive the shape of a customized spatial filter process for each individual location within the visual field.

Simple filtering techniques have already been applied to visual field data. The process can quantify and reduce the variability or long-term fluctuation in a series of fields and can improve the estimate of the rate of glaucomatous field progression.[3-5] Spatial filters customized to each test location may prove to be more sensitive to the inherent spatial correlation of the sensitivity in the visual field than the simple averaging effect of the 3 × 3 gaussian filter used in previous studies.

It may have been possible to simply evolve a customized filter using clusters of dependent points instituted for other forms of visual field analysis, such as the Glaucoma Hemifield test,[14] or based on previously established patterns of retinal nerve fiber layer clusters.[15,16] However, an empirically based study of a large group of glaucomatous fields should not only describe the spatial dependence that exists between the sensitivity of points due to physiological and pathological sources but, in addition, estimate the component of pointwise dependence arising from the testing strategy of the instrument itself. Moreover, multiple regression coefficients give an estimate of the proportion of dependence provided by each selected location. These

coefficients can be utilized to provide weights for the convolution process using the new customized filter.

The reproducibility of the connections between an individual point and the corresponding dependent neighboring locations in a validation sample of equal number of fields was generally good. This reproducibility may improve further with larger samples. A database of approximately 64,000 visual field records is currently held at the Glaucoma Unit at Moorfields Eye Hospital. Work is under way to repeat this type of investigation with larger groups selected from this corpus of fields, including left eyes and using samples classified by different grades of field loss. The latter may provide evidence of different profiles of spatial dependence across the visual field associated with distinct levels of visual field defect severity. This may allow for the filter process to become *adaptive* whereby appropriate filters may be applied at different stages of the disease progression.

In conclusion, we have demonstrated a method of generating a profile of the spatial dependence of pointwise sensitivity across the glaucomatous visual field. These results can be used to derive a customized spatial filter process for each individual location within the field. Use of filtered values, tailored to the dependence of pointwise sensitivity across the field may improve the sensitivity of methods for detecting and predicting glaucomatous change in a series of fields. Moreover, the difference in sensitivity between the actual and filtered values may detect the increased pointwise variability that is observed as a precursor to temporal change-points in glaucomatous progression. This form of analysis may be incorporated into the pointwise linear regression method used by the PROGRESSOR program[17] to improve the sensitivity of estimating field progression in glaucoma.

Acknowledgments

This work is supported by grants from the Royal National Institute for the Blind, the International Glaucoma Association and the Medical Research Council, UK. The authors thank David Edgar (Applied Vision Research Centre, City University, London) for helpful comments on the manuscript.

References

1. Åsman P: Computer assisted interpretation of visual fields in glaucoma. Acta Ophthalmol (Kbh) 70(Suppl 206):1-47, 1992
2. Åsman P, Heijl A, Olsson J, Rootzén H: Spatial analyses of glaucomatous visual fields: a comparison with traditional field indices. Acta Ophthalmol (Kbh) 70:679-686, 1992
3. Fitzke FW, Crabb DP, McNaught AI, Edgar DF, Hitchings RA: Image processing of computerised visual field data. Br J Ophthalmol 79:207-212, 1995
4. Crabb DP, McNaught AI, Fitzke FW, Hitchings RA: Spatially enhanced modelling of sensitivity decay in low-tension glaucoma. In: Mills RP, Wall M (eds) Perimetry Update 1994/1995, pp 73-81. Amsterdam/New York: Kugler Publ 1995
5. Crabb DP, Edgar DF, Fitzke FW, McNaught AI, Wynn HP: New approach to estimating the variability in visual field data using an image processing technique. Br J Ophthalmol 79:213-217, 1995
6. Viswanathan AC, Fitzke FW, Hitchings RA: Spatial filtering of glaucomatous visual fields using PROGRESSOR for Windows. This Volume
7. Dobson AJ: An Introduction to Statistical Modelling, pp 44-56. London: Chapman and Hall 1983

8. Altman DG: Practical Statistics for Medical Research, pp 336-351. London: Chapman and Hall 1991
9. Heijl A, Lindgren A, Lindgren G: Inter-point correlations of deviations of threshold values in normal and glaucomatous visual fields. In: Heijl A (ed) Perimetry Update 1988/1989, pp 177-183. Amsterdam/Milano: Kugler & Ghedini Publ 1989
10. Heijl A, Åsman P: Clustering of depressed points in the normal visual field. In: Heijl A (ed) Perimetry Update 1988/1989, pp 185-189. Amsterdam/Milano: Kugler & Ghedini Publ 1989
11. Lachenmayr BJ, Kiermeir U, Kojetinsky S: Points of a normal visual field are not statistically independent. Ger J Ophthalmol 4:175-181, 1995
12. Zeyen TG, Zulauf M, Caprioli J: Priority of test locations for automated perimetry in glaucoma. Ophthalmology 100:518-523, 1993
13. Mandava S, Zulauf M, Zeyen TG, Caprioli J: An evaluation of clusters in the glaucomatous visual field. Am J Ophthalmol 114:684-691, 1993
14. Åsman P, Heijl A: Glaucoma hemifield test: automated visual field evaluation. Arch Ophthalmol 110:812-819, 1992
15. Åsman P, Heijl A: Arcuate cluster analysis in glaucoma perimetry. J Glaucoma 2:13-20, 1993
16. Weber J, Ulrich H: A perimetric nerve fibre bundle map. Int Ophthalmol 15:193-200, 1991
17. Fitzke FW, Hitchings RA, Poinoosawmy D, McNaught AI, Crabb DP: Analysis of visual field progression in glaucoma. Br J Ophthalmol 80:40-48, 1996

SPATIAL FILTERING OF GLAUCOMATOUS VISUAL FIELDS USING PROGRESSOR FOR WINDOWS

ANANTH C. VISWANATHAN[1], FREDERICK W. FITZKE[1] and ROGER A. HITCHINGS[2]

[1]*Institute of Ophthalmology, London;* [2]*Moorfields Eye Hospital, London; UK*

Abstract

Background: PROGRESSOR for Windows is a computerized system for the analysis of glaucomatous field progression incorporating a graphical user interface. The software package includes spatial filtering, which has been shown to reduce long-term fluctuation.[1] However, some spatial processing, such as gaussian filtering, may 'blur' early focal defects.
Purpose: To determine the role of gaussian filtering in the early detection of glaucomatous loss.
Methods: Nineteen field series from untreated normal-tension glaucoma patients, which an experienced observer judged as deteriorating, were studied. The time taken from the start of each series until progression criteria (slope worse than -1 dB/year for inner points, -2 dB/year for edge points, $p < 0.05$) were satisfied by at least one retinal location was calculated with and without gaussian filtering.
Results: The unfiltered fields detected progression earlier than the filtered fields in three of the 19 field series (mean 1.18 years, SD 0.30 years). The filtered fields detected progression earlier in five series (mean 1.04 years, SD 1.48 years). Both filtered and unfiltered fields detected progression at the same test in 11 field series. There was no predominance of focal defects in the series where progression was detected earlier by the unfiltered fields.
Conclusions: PROGRESSOR for Windows is a convenient software tool for analyzing glaucomatous field decay. Gaussian filtering reduces long-term fluctuation without delaying the detection of early loss in normal-tension glaucoma.

Introduction

Visual field series obtained by automated perimetry provide both spatial and temporal information about disease progression in glaucoma patients. It is crucial that the rate of progression is accurately quantified since this provides a measure of the need for, and the efficacy of, treatment. This task is hampered by the inherent variability between field tests (long-term fluctuation[1]) which is known to be greater in glaucoma.[2] A promising avenue of research is the application of digital image processing techniques, such as that used to process images obtained by magnetic resonance imaging (MRI) to reduce the 'noise' in the results of computerized perimetry. These spatial filtering techniques take account of the interdependence of neighboring retinal

Address for correspondence: F.W. Fitzke, PhD, Institute of Ophthalmology, 11-43 Bath Street, London EC1V 9EL, UK

Perimetry Update 1996/1997, pp. 311–319
Proceedings of the XIIth International Perimetric Society Meeting
Würzburg, Germany, June 4–8, 1996
edited by M. Wall and A. Heijl

test locations and have been shown to improve the repeatability of automated perimetry by a factor of two[3] and to improve the predictability of glaucomatous decay.[4] However, it is possible that spatial filtering will smooth areas of the field representative of early focal decay, rather than simply noise, and valuable information will be lost.

The PROGRESSOR software[5] performs pointwise linear regression of sensitivity on time and presents the results as a cumulative graphical display (Fig. 1a). Each test location is represented by a bar graph in which each bar represents a successive field test. The length of the bar relates to the depth of defect, and the color of the bar represents the *p* value of the regression slope (Fig. 1b). The pointwise linear model has been demonstrated to provide a valid framework for detecting and forecasting glaucomatous loss[6] and PROGRESSOR has been found to compare favorably with other methods of glaucoma change analysis such as STATPAC-2.[7] PROGRESSOR has recently been updated: the program now runs in a Windows environment and incorporates many new methods of analysis, one of which is the ability to apply spatial filtering to a series of fields (Fig. 2).

This study was designed to investigate, using PROGRESSOR for Windows, whether spatial filtering leads to a clinically significant delay in the detection of glaucomatous field progression.

Methods

Subjects

Patients with untreated normal-tension glaucoma which had been confirmed by phasing were chosen for study as it was felt to be important to analyze the natural history of glaucomatous visual damage in the absence of the potentially confounding effects of therapy. All subjects had visual acuity of 20/40 or better. None had significant ocular pathology apart from normal-tension glaucoma. All subjects were experienced in Humphrey 30-2 tests and able to produce reliable computerized visual fields (less than 30% fixation losses and false negatives and less than 15% false positives). Each had had at least two tests over four months prior to the observation period: this is sufficient to obviate any learning effects[8,9] which may delay the diagnosis of progression.

Patients were chosen whose visual fields appeared to be progressively deteriorating in a typically glaucomatous manner, since it is in these patients that the 'blurring' associated with spatial filtering is most likely to cause delay in the detection of progression. This was done by inspection of STATPAC overview printouts by an experienced observer.

On the basis of the foregoing criteria, 19 eyes from 13 subjects were selected. An indication of the degree of glaucomatous damage in the selected group is given by the following summary measures of the mean deviation (MD) of the initial field in each test series: the mean of the MDs was -6.81 dB (SD 6.01 dB), the median was -5.43 dB and the range was -22.40 dB to +1.07 dB.

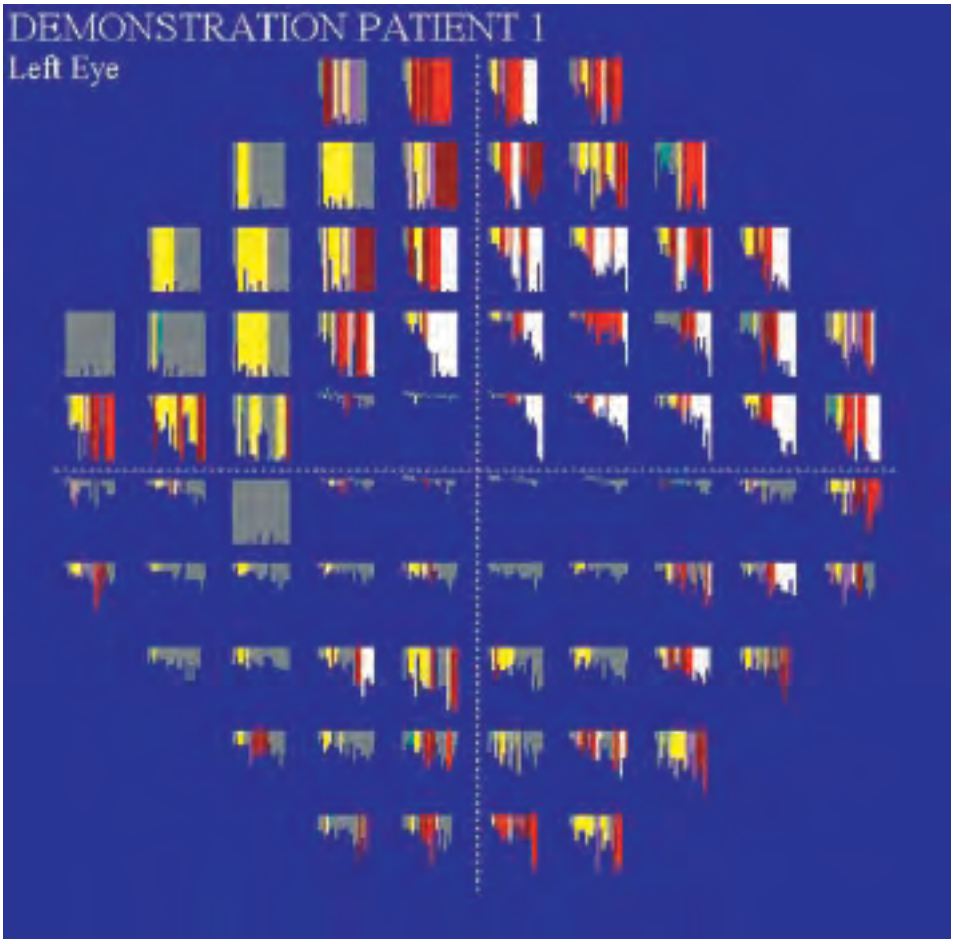

Fig. 1a. Cumulative graphical display from PROGRESSOR for Windows for a progressing normal-tension glaucoma patient.

Testing strategy

All tests were performed on a standard Humphrey automated perimeter. The 30-2 Full Threshold Program with standard 4-2 dB double reversal strategy was used throughout. Tests were performed at intervals of four months.

Progression criteria

PROGRESSOR performs linear regression of sensitivity on time for each test location. For each field in the series, each location is ascribed a change slope (in decibels per year) and a p value for a two tailed t test of the slope against zero (*i.e.*, the null hypothesis of no deterioration). A field series was regarded as progressing if any non-edge location showed a deterioration of 1 dB per year or worse with $p < 0.05$. A

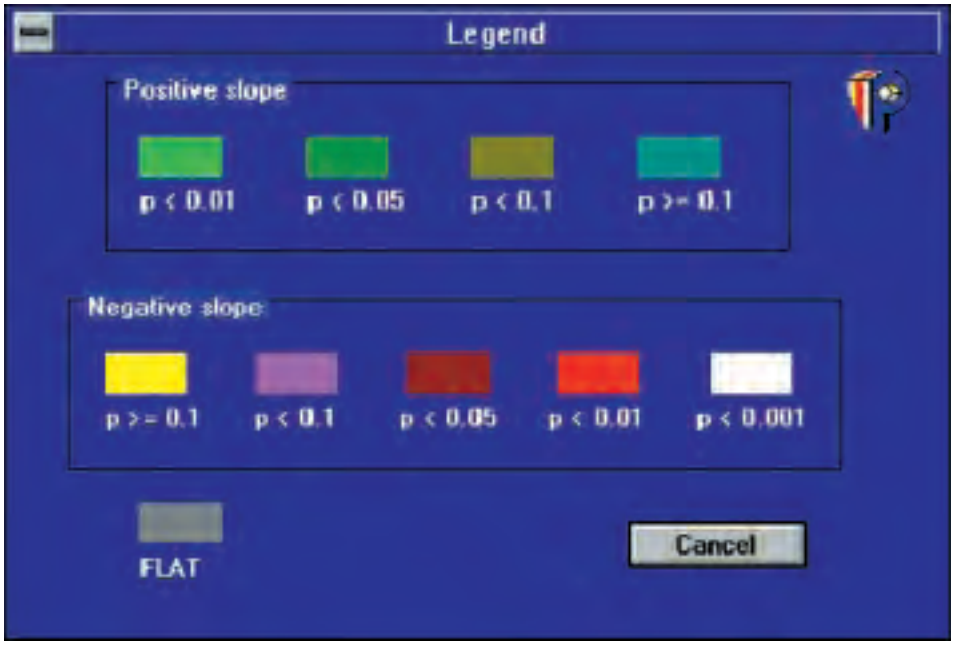

Fig. 1b. PROGRESSOR for Windows legend showing the colors which correspond to each p value of the regression slope.

more stringent slope criterion of 2 dB per year was applied to the edge points of the 30-2 test grid. These slope criteria have been demonstrated to compare closely with the Humphrey STATPAC-2 Glaucoma Change Probability analysis, and the *p* value criterion is stricter than that required to emulate STATPAC-2.[5]

Detection time

The detection time for a field series was defined as the time interval between the initial field and the field when the progression criteria (*vide supra*) were first satisfied.

Spatial filtering

Gaussian low-pass filtering is widely used to remove noise from pixel-based images.[10,11] In order to apply the filter to a 30-2 field, each test location is regarded as the center of a 3x3 neighborhood to which the filter (convolution mask) is applied (Fig. 3). Thus, each point is influenced by the weighted sensitivity of its contiguous neighbors. At the edges of the field the mask is only partial since edge points do not have a full complement of neighbors.

Statistical analysis

For each field series, detection time (*vide supra*) was calculated for both filtered and unfiltered data. Detection times for the unfiltered data were compared with their

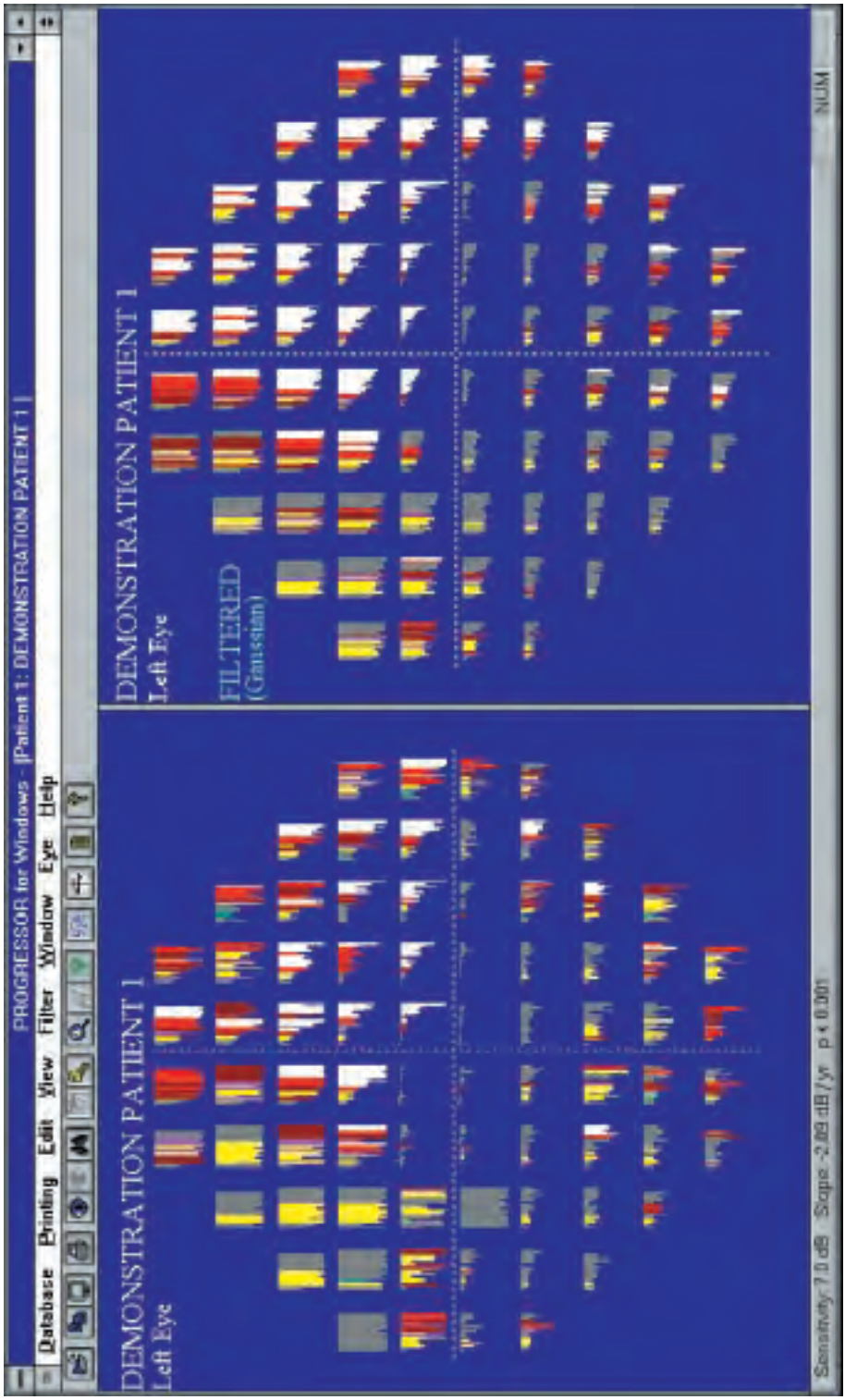

Fig. 2. PROGRESSOR for Windows display showing the results of gaussian filtering.

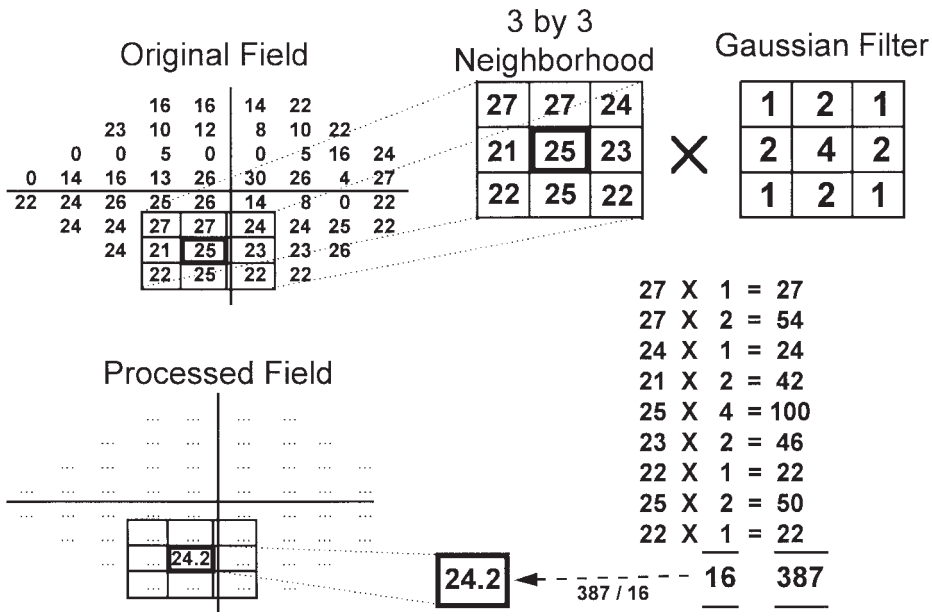

Fig. 3. Gaussian filtering process.

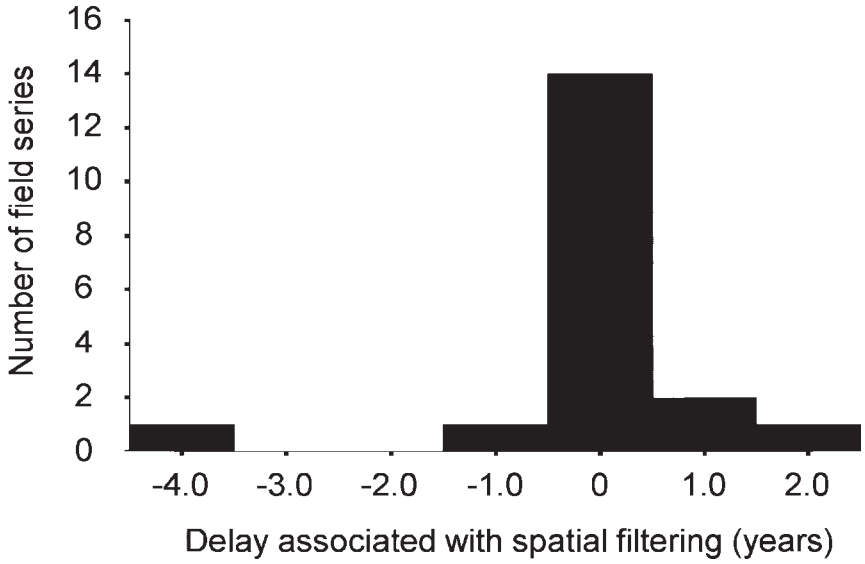

Fig. 4. Histogram of delay in detection time associated with spatial filtering.

correlates for the filtered data using a non-parametric test for paired data from two related samples (Wilcoxon signed rank Z test). In addition, the following summary measures of progression, automatically calculated by PROGRESSOR for Windows, were compared for all field series before and after spatial filtering: number of

progressing points at detection time, mean slope for all test locations at detection time and mean slope for progressing points at detection time.

Statistical analysis was performed using the software package SPSS for Windows version 6.0, except for the power calculation which was performed with Jandel SigmaStat for Windows version 1.0.

Results

Detection times

All field series satisfied the progression criteria both before and after spatial filtering. The unfiltered fields had a mean detection time of 1.077 years (SD 0.985 years) and the filtered fields had a mean detection time of 0.989 years (SD 0.639 years). These are not significantly different ($p = 0.779$, Wilcoxon signed rank Z test). Kolmogorov-Smirnov goodness of fit normality testing yielded $p = 0.260$ for the detection times of the unfiltered data and $p = 0.394$ for the detection times after filtering. On this basis a paired t test is justified and gives $p = 0.709$: a power calculation gives a power of 0.797 to detect a difference of eight months in mean detection time between filtered and unfiltered fields ($\alpha = 0.05$, SD = 0.985 years).

The unfiltered fields detected progression earlier in three field series: for these three series, the mean delay in detection for the filtered fields was 1.18 years (SD 0.30 years). The filtered fields detected progression earlier in five field series: for these series, the mean delay in detection for the unfiltered fields was 1.04 years (SD 1.48 years). Both filtered and unfiltered fields detected progression at the same test in 11 field series. These findings are displayed graphically in Figure 4, which is a histogram of the differences between filtered and unfiltered detection times for each field series. The distribution is centered around zero, which suggests no overall delay associated with filtering.

Number of progressing points at detection time

The mean number of progressing points which satisfied the progression criteria at detection time was 2.95 (SD 1.81) for the unfiltered fields and 3.00 (SD 2.49) after filtering. This difference was not significant ($p = 0.784$, Wilcoxon signed rank Z test).

Mean slope (whole field) at detection time

The mean slope of all test locations at detection time had a mean value of -3.99 dB/years (SD 9.94 dB/years) for the unfiltered fields and -3.76 dB/years (SD 9.84 dB/years) after filtering. This difference was not significant ($p = 0.334$, Wilcoxon signed rank Z test).

Mean slope (progressing points) at detection time

The mean slope of the locations which satisfied the progression criteria at detection time had a mean value of -22.47 dB/years (SD 56.44 dB/years) for the unfiltered fields and -9.15 dB/years (SD 14.14 dB/years) after filtering. This difference was significant at the 5% level ($p = 0.030$, Wilcoxon signed rank Z test).

Discussion

Fluctuation owing to variable patient response and other factors is the main obstacle to the accurate quantification of the results of automated perimetry. Any technique which may reduce this fluctuation is therefore worthy of study. Spatial filtering has been shown to be effective in reducing noise in other two-dimensional digital image processing applications[10,11] and seems to be of benefit in the analysis of glaucomatous visual field progression.[3,4] However, by its very nature, gaussian filtering obscures elements of a digital image which have high spatial frequency. If the digital image concerned is a computerized visual field, these elements are small isolated scotomas and the edges of existing scotomas: these are precisely the areas where progression is most likely to occur first. Thus, it is important to ascertain whether the process of spatial filtering leads to a clinically significant delay in detecting progression, since this would be a high price to pay for improved repeatability and predictability.

This study suggests that gaussian filtering is unlikely to entail a significant delay in the detection of progression.

This study was performed on a highly selected group of patients: the selection criteria were necessarily strict in order to isolate cases in which spatial filtering was most likely to cause a delay in detection. Since detection time was not affected in this group it is likely that other, more stable visual field series will be similarly unaffected. However, further work is required in order to determine whether these results may be generalized to patients with other forms of glaucoma and to those who have received or are receiving medical treatment.

The gaussian filter used in the study was chosen because it is a standard image-processing convolution mask, and has been used in previous work on computerized visual fields.[3,4] However, it is unlikely to be the ideal mask for the special environment of automated perimetry. Firstly, the mask is usually intended for use with pixels which have a range of values (bandwidth) of between 0 and 255: the range of sensitivity values produced by automated perimetry is almost an order of magnitude smaller than this. Secondly, the mask is limited to contiguous neighbors and is symmetrical. This does not conform to our knowledge of the patterns of glaucomatous field loss seen in clinical practice. For example, it seems likely that test locations will be more influenced by the behavior of other locations within the same retinal nerve fiber bundle distribution than by those which are outside it: the closest topological neighbors may not be the closest ‘functional’ neighbors. It is possible that each test location will require its own unique convolution mask for optimum performance. Research is currently being conducted to examine this hypothesis.[12]

The difference between the filtered and unfiltered data with regard to the mean slope of progressing points at detection time reflects the fact that gaussian filtering tends to lessen the slopes of the locations which are progressing at the greatest rate. Notwithstanding this, the fact that both the number of progressing points and the mean slope for the whole field at detection time are not affected by filtering suggests that, for these progression criteria, the overall ‘progression status’ of the field series are retained after filtering.

In summary, previous work has shown spatial filtering to be of potential benefit in the analysis of glaucomatous visual field progression.[3,4] This study has examined the combined use of spatial filtering and pointwise linear regression in the context of a

software package, PROGRESSOR for Windows. The study suggests that the 'blurring' effect inherent in the gaussian filtering process is not clinically significant.

Acknowledgments

Supported by the International Glaucoma Association, London, UK and the Medical Research Council, London, UK.

References

1. Boeglin RJ, Caprioli J, Zulauf M: Long-term fluctuation of the visual field in glaucoma. Am J Ophthalmol 113(4):396-400, 1992
2. Flammer J, Drance SM, Zulauf M: Differential light threshold: short- and long-term fluctuation in patients with glaucoma, normal controls, and patients with suspected glaucoma. Arch Ophthalmol 102(5):704-706, 1984
3. Fitzke FW, Crabb DP, McNaught AI, Edgar DF, Hitchings RA: Image processing of computerised visual field data. Br J Ophthalmol 79:207-212, 1995
4. Crabb DP, McNaught AI, Fitzke FW, Hitchings RA: Spatially enhanced modelling of sensitivity decay in low-tension glaucoma. In: Mills RP, Wall M (eds) Perimetry Update 1994/1995, pp 73-81. Amsterdam/New York: Kugler Publ 1995
5. Fitzke FW, Hitchings RA, Poinoosawmy D, McNaught AI, Crabb DP: Analysis of visual field progression in glaucoma. Br J Ophthalmol 80:40-48, 1996
6. McNaught AI, Crabb DP, Fitzke FW, Hitchings RA: Modelling series of visual fields to detect progression in normal tension glaucoma. Graefes Arch Clin Exp Ophthalmol 233:750-755, 1995
7. McNaught AI, Crabb DP, Fitzke FW, Hitchings RA: Visual field progression: comparison of Humphrey Statpac 2 and pointwise linear regression. Graefes Arch Clin Exp Ophthalmol 1996 (in press)
8. Werner EB, Adelson A, Krupin T: Effect of patient experience on the results of automated perimetry in clinically stable glaucoma patients. Ophthalmology 95:764-767, 1988
9. Werner EB, Krupin T, Adelson A, Feitl ME: Effect of patient experience on the results of automated perimetry in glaucoma suspect patients. Ophthalmology 97:44-48, 1990
10. Gonzales RC, Wintz P: Digital Image Processing, 2nd Edn. Massachusetts: Addison-Wesley 1987
11. Phillips D: Image Processing in C, 1st Edn. Kansas: R&D Publications Inc 1994
12. Crabb DP, Fitzke FW, McNaught AI, Hitchings RA: A profile of the spatial dependence of pointwise sensitivity across the glaucomatous visual field. This Volume

CALCULATION OF A GLAUCOMA PROGRESSION RISK INDEX

EUGEN GRAMER

University Eye Hospital Würzburg, Germany

Abstract

Purpose: Calculation of a glaucoma progression risk index (GPI) to identify at the first visual field examination whether a patient with primary open-angle glaucoma (POAG) and controlled intraocular pressure (IOP) is at risk for further visual field deterioration.
Method: Long-term follow-up with threshold perimetry (Program 31) was performed twice a year in 109 eyes of 109 patients with POAG. Only the period with controlled IOP was evaluated. Using program Delta, it was determined whether or not there was a tendency for deterioration. A deterioration was found in 29 eyes, while 80 eyes showed no change. By means of multiple regression analysis it was evaluated which of the following predictors have the best correlation with the criteria of deterioration or preservation of the visual field: maximum IOP, systolic blood pressure, cup:disc ratio, pre-existing visual field loss (mean loss per test point in the upper hemifield and in the lower hemifield or in the whole field, or mean scotoma depth (TL/TP)).
Results: Low systolic blood pressure was found to be the most important risk factor for further deterioration, in spite of regulated IOP, followed by pre-existing visual field damage and maximum IOP. The regression formula summarizes these three risk factors into a single value, the GPI (a dimensionless number between 1 and 2), which describes the risk of further visual field deterioration in eyes with POAG and regulated IOP. For pre-existing visual field loss in the formula, the loss per test point in the whole field or in the upper hemifield can be used. A lower GPI is more frequent in eyes with a tendency to deteriorate.
Conclusions: The GPI helps to identify at the first visual field examination whether a patient with POAG and controlled IOP is at risk for further visual field deterioration. Due to the multifactorial pathomechanisms involved in glaucoma, the GPI cannot provide an absolute separation between stable and non-stable visual field defects, but it identifies patients with a higher risk of deterioration.

Introduction

The purpose of this study was the development of a formula for calculation of a glaucoma progression risk index (GPI) to identify at the first visual field examination whether a patient with primary open-angle glaucoma (POAG) and regulated intraocular pressure (IOP) is at risk for further visual field deterioration.

Address for correspondence: Professor Eugen Gramer, MD, LLD, University Eye Hospital Würzburg, Josef-Schneider-Strasse 11, D-97080 Würzburg, Germany

Perimetry Update 1996/1997, pp. 321–327
Proceedings of the XIIth International Perimetric Society Meeting
Würzburg, Germany, June 4–8, 1996
edited by M. Wall and A. Heijl

Methods

Long-term follow-up of 109 eyes of 109 patients with POAG and with regulated IOP (21 mmHg or less by medication or operation) was performed twice a year by Octopus perimetry (Program 31 or 33).

Inclusion criteria were: POAG with visual field defects at the start of the observation period, visual acuity of 0.8 or better, refractive error of maximum ±3 diopters and long-term observation with threshold perimetry (Octopus perimeter 201, Program 31 or 33) twice a year. All eyes had IOP values of less than 22 mmHg during the follow-up period. Only the period during which IOP was regulated was evaluated. Information was available on maximum IOP in all eyes. Systolic blood pressure was measured at the Glaucoma Department at the time of the visual field examination. From several blood pressure recordings during the observation time with controlled IOP, we calculated and recorded the mean systolic blood pressure. All eyes had a minimum follow-up of three years with IOP values of 22 mmHg or less during a total observation time of three to eight years. All eyes had open chamber angle. No patients had had earlier systemic or topical steroid therapy. The 109 patients had a follow-up of six to 19 visual field examinations performed with Program 31 or 33 during an observation period of three to eight years, with an IOP of 21 mmHg or less after medical therapy or operation.

With program Delta, comparing mean visual fields at the start and end of the observation period with regulated IOP, it was determined whether or not there was a tendency for deterioration. Figure 1 shows the visual fields of a patient with this tendency.

The influence of the following parameters was evaluated for patients with and without deterioration by means of multiple regression analysis (MRA): maximum IOP (highest IOP ever measured), systolic blood pressure (mean blood pressure values at the time of visual field examinations), cup:disc ratio (CDR), total loss in the whole visual field, mean loss per test point in the upper and lower hemifields, and mean scotoma depth (total loss divided by the number of disturbed test points). These values were taken from the ‘series’ printout of program Delta. If both eyes were being followed up, one eye was selected at random. The diagnostic code was set to 1 for deterioration and 2 for preservation of the visual field. Distribution of the variables mentioned above was examined. Because maximum IOP values did not follow a normal distribution, a correcting logarithmic transformation was applied. MRA showed which of the predictors mentioned above have the best correlation with the criteria: deterioration or preservation of the visual field. The regression formula summarized the significant parameters to a single value (GPI), which describes the risk of further visual field deterioration. For patients with and without visual field deterioration, the frequency of GPI values from 1.2 to 1.9 was calculated.

Results

Systolic blood pressure, mean loss per test point in the upper hemifield and maximum intraocular pressure before treatment were found to be significant predictors for the risk of further visual field deterioration. Systolic blood pressure was found to be the most important risk factor, followed by the pre-existing visual field damage and the maximum IOP. The following formula was used to calculate the glaucoma progression risk index (GPI):

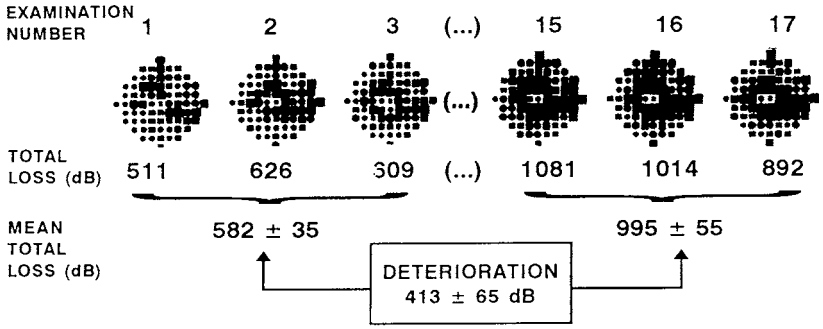

Fig. 1. Visual fields of the right eye of a patient with POAG and regulated IOP, and with significant progression of visual field loss. Mean total loss at the first three examinations (582 ± 35 dB) is compared to mean total loss at the last three follow-up examinations (995 ± 55 dB). Program Delta, mode change, shows the difference (413 ± 65 dB) and calculates the mean difference per test point (in the pathological area) with its confidence interval (-6.4 ± 1.6 dB). As zero happens to be outside this interval, there is statistical evidence (at a level of 5%) to assume a true tendency for deterioration in this visual field. (*t* test: alteration is indicated.)

GPI = -0.34 + 0.0059 x systolic blood pressure -0.017 x pre-existing visual field loss determined by mean loss/test point (dB)(upper hemifield or whole 30° field) + 0.8914 x $\log^{10}$ maximum IOP.

Figure 2 (left) shows a GPI of 1.59 in a patient with visual field deterioration and Figure 2 (right) shows a GPI of 1.95 in a patient with no further deterioration in his visual field.

Figure 3 shows the distribution of GPI values in 29 eyes with deterioration of the visual field (left side), and in 80 eyes with stable visual fields (right side). For quantification of the pre-existing visual field damage, the loss per test point in the upper hemifield was used for GPI calculation.

In Figure 4, the loss per test point in the whole field was used for quantification of the pre-existing visual field loss to calculate the GPI.

The mean GPI in eyes with a tendency for deterioration was 1.55 ± 0.19 using the loss per test point in the upper hemifield (compare Fig. 3, left), or 1.56 ± 0.18 using the loss per test point in the whole visual field (compare Fig. 4, left). In 80 eyes with preserved visual fields, the mean GPI, calculated by using the loss per test point in the upper hemifield, was 1.8 ± 0.2 (compare Fig. 3, right) or 1.81 ± 0.21 using the loss per test point in the whole visual field (compare Fig. 4, right). If the mean loss per test point of all quadrants was used for quantification of the pre-existing visual field loss, we found a small but not significant change in the distribution of the GPI values as shown in Figures 3 and 4. Therefore, the loss per test point in the whole 30° visual field can be used in future for calculation of the GPI. Table 1 shows the frequency of the different GPI values in the 109 patients with or without deterioration shown in Figure 3. A lower GPI was more frequent in eyes with a tendency for the visual fields to deteriorate. For example, a GPI of 1.2 was found in 6.4% of eyes with deterioration, but in only 0.2% of eyes without deterioration. In patients with a GPI of 1.2, the rate of further deterioration was 32.6 times that of patients with less extreme values.

For example, a GPI of 1.2 (or values even further away from the corresponding

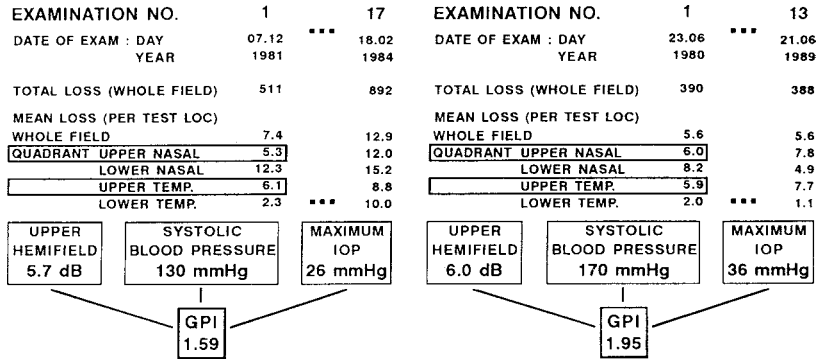

Fig. 2. Calculation of GPI in two patients with POAG and regulated IOP. The patient with significant progression of visual field loss showed a GPI of 1.59 (left) while the patient with no visual field deterioration (right) during follow-up with controlled IOP showed a GPI of 1.95. Program Delta, mode series, provides the following data for each examination: date, total loss, and mean loss per test point both in the whole field and in the quadrants. To calculate the GPI, only data from the first visual field examination were taken into account. The loss per test point in the upper hemifield is the mean of both upper quadrants.

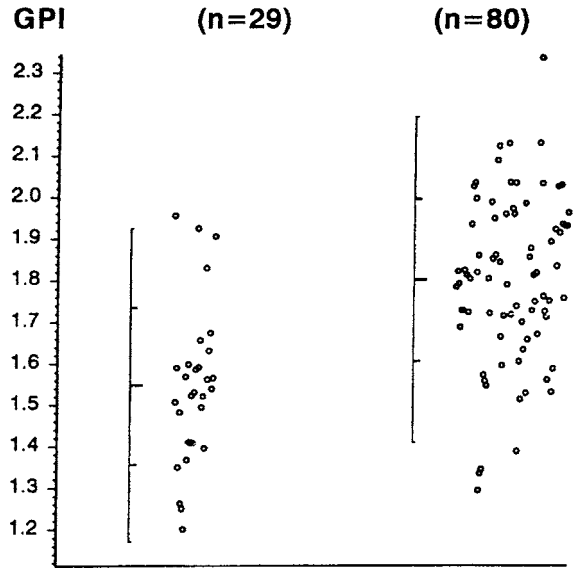

Fig. 3. Distribution of GPI in 29 patients with progressive visual field loss (*left column*) and in 80 patients with no further visual field deterioration (*right column*) during follow-up using pre-existing visual field loss in the upper hemifield.

sample mean) was found in 6.4% of our patients with, and only in 0.2% of our patients without progressive visual field loss, as shown in Table 1. In patients with a GPI of 1.2, the rate of further deterioration was 32.6 times that of patients with less extreme values. To calculate the frequencies of GPI, we normalized the distributions of GPI in patients both with and without progressive visual field loss, by subtracting from each GPI value its sample mean and dividing by its sample standard deviation, as shown in the GPI formula.

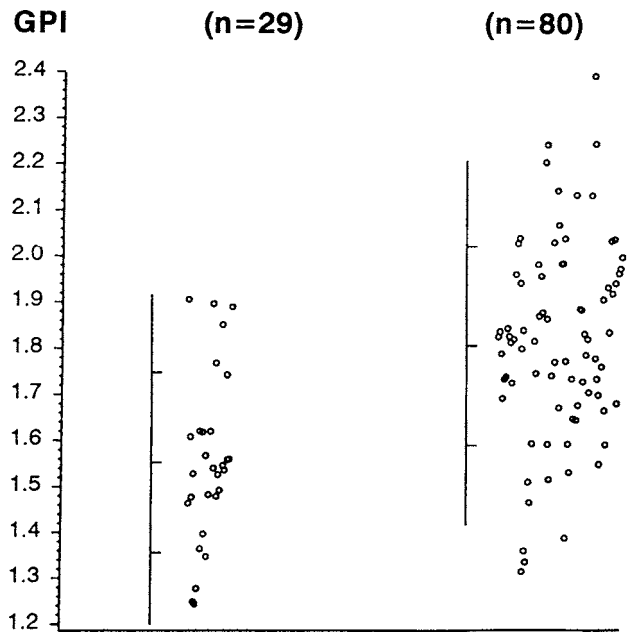

Fig. 4. Distribution of GPI in 29 patients with progressive visual field loss (*left column*) and in 80 patients without further visual field deterioration (*right column*) during follow-up using pre-existing visual field loss in the whole 30° field. When the mean loss per test point was used in the whole field to determine the pre-existing visual field loss, we found no significant change in the mean GPI values compared to eyes in which the pre-existing visual field loss was determined by the mean loss per test point in the upper hemifield only. The loss per test point in the whole field may be used in future for GPI calculation.

Discussion

A low systolic blood pressure was the most important risk factor for further deterioration of visual field defects in eyes with controlled IOP. This is in agreement with the results of our former studies[1-3,10,13] which identified a low systolic blood pressure as a risk factor in low-tension glaucoma (LTG) and POAG.

Pre-existing visual field damage was of importance for the prognosis of further visual field deterioration, confirming the results of an earlier study.[4] The upper hemifield in POAG was found to be more important than the total loss. This can be explained from the topography of visual field loss in POAG. In earlier studies, by means of frequency distributions and quantitatively with program Delta, we showed that in POAG, visual field defects are more frequent in the upper hemifield.[5-8] In spite of this finding, for calculation of the GPI it may be better to use the loss per test point in all quadrants in future, as shown in Figure 4.

The maximum IOP before treatment allows an estimation of the IOP-dependent damage. The practicability and importance of this value was proven in a previous study.[9]

In one single index value, GPI combines these three important risk factors, which have been separately evaluated in earlier studies.[1-10,13] These three risk factors are

Table 1. Frequencies of distinct GPI values in patients with and without progressive visual field loss

GPI	*Frequency (%)*		*Relative risk*
	with progressive visual field loss	*with preserved visual field*	
1.2	6.4	0.2	32.6
1.3	18.7	1.1	21.7
1.4	43.0	4.1	17.9
1.5	79.5	12.4	27.5
1.6	78.0	30.3	8.1
1.7	41.8	60.3	0.5
1.8	18.0	99.2	0.002
1.9	6.2	61.0	0.04

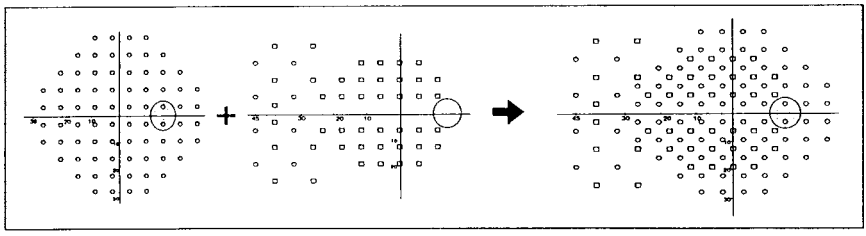

Fig. 5. GG program of the Humphrey-Zeiss perimeter. After standard examination with the 76 test points of Program 30-2 (left), a second examination can be performed, using a grid with 52 test points (center). A combination printout results in a glaucoma specific grid (GG Program) (right). After less examination time, this GG Program shows a better detection probability for early glaucomatous scotomas than a combination of two 6° grids (Program 30-1 and 30-2).

usually weighted by clinical experience, together with further risk factors, such as family history or status of the second eye. GPI now allows summary scoring of these three risk factors, as part of automated perimetry. Therefore, it helps to identify, already at the time of initial perimetric examination, patients who are at risk for further visual field deterioration. Due to the multifactorial pathomechanisms involved in glaucoma,[13,14] GPI cannot provide an absolute separation between stable and non-stable visual field defect, but can identify patients with a higher risk of deterioration. The benefit of GPI is therefore to avoid under-treatment in high-risk patients and over-treatment in low-risk patients.

The glaucoma-specific perimetry (GG Program), shown in Figure 5,[11,12] together with the prognostic message of GPI, may improve the usefulness of the initial visual field examination for determination of the individual target IOP.

Acknowledgment

The author wishes to thank Dr G. Althaus and Dr I. Haubitz for their help in data evaluation and statistical analysis.

References

1. Gramer E, Leydhecker W: Glaukom ohne Hochdruck. Eine klinische Studie. Klin Mbl Augenheilk 186:262-267, 1985
2. Gramer E, Althaus G: Einfluss des systolischen Blutdrucks auf die Lage der Gesichtsfeldausfälle in oberer und unterer Gesichtsfeldhälfte bei Patienten mit Glaucoma chronicum simplex. Ophthalmologe 90:620-625, 1993
3. Gramer E, Althaus G, Körner U: Are visual field defects in the lower hemifield a risk factor in POAG? In: Mills RP (ed) Perimetry Update 1992/93, pp 81-87. Amsterdam/New York: Kugler Publ 1993
4. Gramer E, Althaus G: Zur Progredienz des glaukomatösen Gesichtsfeldschadens. Eine klinische Studie mit dem Programm Delta des Octopus Perimeters 201 zum Einfluss des Vorschadens auf die Gesichtsfeldverschlechterung beim Glaucoma simplex. Fortschr Ophthalmol 85:620-625, 1988
5. Gramer E, Mohamed J, Krieglstein GK: Der Ort von Gesichtsfeldausfällen bei Glaucoma simplex, Glaukom ohne Hochdruck und ischämischer Neuropathie: Indikationen zur vasoaktiven Therapie. In: Krieglstein GK, Leydhecker W (eds) Medikamentöse Glaukomtherapie, pp 115-121. München: JF Bergmann Verlag 1982
6. Gramer E, Gerlach R, Krieglstein GK, Leydhecker W: Zur Topographie früher glaukomatöser Gesichtsfeldausfälle bei der Computerperimetrie. Klin Mbl Augenheilk 180:515-523, 1982
7. Gramer E, Althaus G: Quantifizierung und Progredienz des Gesichtsfeldschadens bei Glaukom ohne Hochdruck, Glaucoma simplex und Pigmentglaukom. Eine klinische Studie mit dem Programm Delta des Octopus-Perimeters 201. Klin Mbl Augenheilk 191:184-198, 1987
8. Gramer E, Althaus G, Leydhecker W: Topography and progression of visual field damage in glaucoma simplex, low tension glaucoma, and pigmentary glaucoma with program Delta of Octopus Perimeter 201. Doc Ophthalmol Proc Series 49:349-363, 1987
9. Gramer E, Althaus G: Bedeutung des erhöhten Augeninnendrucks für den Gesichtsfeldschadens. Eine klinische Studie. Klin Mbl Augenheilk 197:218-224, 1990
10. Gramer E, Althaus G: Calculation of a glaucoma progression risk index (GPI). Invest Ophthalmol Vis Sci 35/4: 2183, 1994
11. Gramer E, Knaut-Spaeth M: Das nasale Gesichtsfeld bei Glaukom. Eine klinische Studie zur glaukomspezifischen Perimetrie. In: Gramer E, Kampik A (eds) Pharmakotherapie am Auge, S, pp 158-183. Heidelberg: Springer Verlag 1992
12. Roesen B, Gramer E: Perimetrie mit einem glaukomspezifischen Prüfpunktraster: eine klinische Studie mit dem GG-Programm des Humphrey-Zeiss-Perimeters. Ophthalmologe 92:564-573, 1995
13. Gramer E: Risk factors in glaucoma. Clinical studies. In: Krieglstein GK (ed), Glaucoma Update V, pp 14-31. Proceedings volume of the Closed Glaucoma Symposium of the Glaucoma Society of the International Congress of Ophthalmology, Quebec, June 22-24, 1994. Heidelberg: Kaden Verlag 1995
14. Gramer E, Tausch M: The risk profile of the glaucomatous patient. In: Krieglstein GK (ed) Glaucoma: Current Opinion in Ophthalmology, Vol 6, No 2, pp 78-88. Philadelphia, PA: Current Science 1995

A COMPARISON OF THREE METHODS FOR DISTINGUISHING BETWEEN DIFFUSE, LOCALIZED AND MIXED VISUAL FIELD DEFECTS IN GLAUCOMA

PAOLO BRUSINI

Department of Ophthalmology, Hospital of San Donà di Piave (VE), Italy

Abstract

The separation of localized and diffuse components of visual field loss is an important step in the functional evaluation of glaucomatous patients. However, there is no general agreement on the methods to assess the type of defect, and even the definition of such defects is controversial. The abilities of three methods (the Humphrey Glaucoma Hemifield Test, the Bebie curve, and the Glaucoma Staging System) were compared with regard to separating diffuse loss from local and mixed loss in a sample of 300 automated visual fields from patients with chronic simple glaucoma with early- to mid-damage. The Glaucoma Hemifield Test is a very efficient method for detecting very slight local sensitivity depressions, but it tends to underestimate the diffuse loss and does not differentiate between localized and mixed defects. The Bebie curve is an easy and useful method for an at-a-glance classification of the state of the visual field, but it can miss very small but significant localized defects. The Glaucoma Staging System allows the user instantly to classify both the type and the severity of visual field defects simply by plotting the mean deviation (MD) and the corrected pattern standard deviation (CPSD) values on a specially designed nomogram. However, it tends to overestimate the diffuse loss and to underestimate small localized defects in the presence of early damage.

Introduction

The separation of localized and diffuse components of visual field loss is an important step in the functional evaluation of glaucomatous patients, since different defects may result from different pathogenetic mechanisms. While localized defects are considered to be a typical perimetric sign of glaucoma damage, a generalized depression of sensitivity is a non-specific finding and may arise from clouded media or miosis. Its presence as a real and isolated sign in chronic glaucoma has been advocated by several authors,[1-5] but has recently been contested by others,[6-8] at least for early glaucoma. These discrepancies may arise, at least in part, from the different terminology and methods used to assess and classify visual field defects. At present, there is no agreement on this important question, and no current method seems to offer the precision required to be chosen as a standard.

Address for correspondence: Dr. Paolo Brusini, Divisione Oculistica, Ospedale Civile, 30027 San Donà di Piave (VE), Italy

Perimetry Update 1996/1997, pp. 329–339
Proceedings of the XIIth International Perimetric Society Meeting
Würzburg, Germany, June 4–8, 1996
edited by M. Wall and A. Heijl

While the definition of localized defects is an easy task, this is not the case when considering diffuse damage. Many methods have been used for its assessment. For example, the perimetric indices mean deviation (MD) and loss of variance (LV),[9] the Bebie cumulative defect curve,[10] the Humphrey STATPAC-2 Glaucoma Hemifield Test (GHT),[8] color-coded probability maps,[11] new specially created indices, such as Langerhorst's general reduction of sensitivity index (GRS)[12] or Funkhouser's diffuse loss index,[13-15] have been proposed. Other methods, even if accurate, need special analytical procedures, which are not readily available.

In this study, we compare the ability of three methods (the Humphrey GHT, the Bebie curve, and the new Glaucoma Staging System (GSS)) to separate diffuse loss from local and mixed loss in a sample of 300 automated visual fields of patients with chronic simple glaucoma with early- to mid-damage.

Material and methods

Three hundred automated visual fields, performed with the Humphrey 30-2 threshold test, were selected retrospectively from 521 patients (aged from 35 to 78 years, mean 59.4) affected by chronic open-angle glaucoma in various stages of severity, from early- to mid-damage. Tests with an MD higher than 10 dB were excluded. Visual acuity was higher than 20/25 in all cases. Only reliable tests without clear artifacts were considered.

Visual fields were classified using Humphrey STATPAC-2 GHT, the Bebie curve, generated with Peridata 6.5 software (Interzeag, Schlieren, Switzerland), and the recent Brusini GSS (patent pending).

The GHT is an expert system based on up-down sensitivity differences, included in the single field analysis page of the Humphrey STATPAC-2 statistical package.[16] Visual field tests are classified into five different groups: (1) 'within normal limits'; (2) 'borderline' (a significant up-down difference at the $p<0.03$ level); (3) 'outside normal limits' (one or more significant up-down sector differences at the $p<0.01$ level or a significant symmetrical defect in each of two mirror-image sectors); (4) 'generalized reduction of sensitivity' (depression below the 0.5% of the point with the seventh highest deviation from normal); and (5) 'abnormally high sensitivity'. The dual statement 'borderline + general reduction of sensitivity' appears when a homogeneous defect is combined with an up-down difference at the $p<0.03$ level.

In this study, visual fields 'outside normal limits' and 'borderline' were considered to have localized defects. Those with 'general reduction of sensitivity' were classified as having a pure diffuse loss. When the statement 'borderline + general reduction of sensitivity' was given, the test was classified as having a mixed defect. It should be noted that in 'outside normal limits' results, the GHT does not check the general reduction of sensitivity, and so it is not possible to distinguish localized from mixed defects.

The Bebie curve represents the cumulative distribution of the local deviations from normal values.[17] All tested point sensitivity values are ranked according to the defect depth, beginning with the best points up to the deepest defects. This type of representation is particularly helpful in separating diffuse loss from local disturbances. Using the Bebie curve, we differentiated the defects into three types using the criteria described in Table 1.

Table 1. Inclusion criteria for distinguishing visual field defects with the Bebie curve

1. *Diffuse loss*
   a. more than 60% of points are under the 95th percentile
   b. the slope should be parallel to the normal curve (a departure from parallel of less than 0.2 dB per location was retained as the maximum permissible)
   c. the plateau of depressed points must start within the first ten ranked locations
   d. no abrupt fall to the right of the curve is under the 95th percentile
2. *Localized defect*
   a. at least 40% of points should be within normal limits
   b. the slope should fall abruptly on the right (these points must be under the 95th percentile)
3. *Mixed defect:* the two components of visual field damage should be present; in particular,
   a. more than 20 locations must have a diffuse defect, as previously described in 1b and 1c
   b. the right segment of the curve must have a steeper gradient (a difference of >5 dB between the mean point of this segment and the end of the diffuse defect segment is required)
   c. cases which cannot be classified in the other two classes should be included here

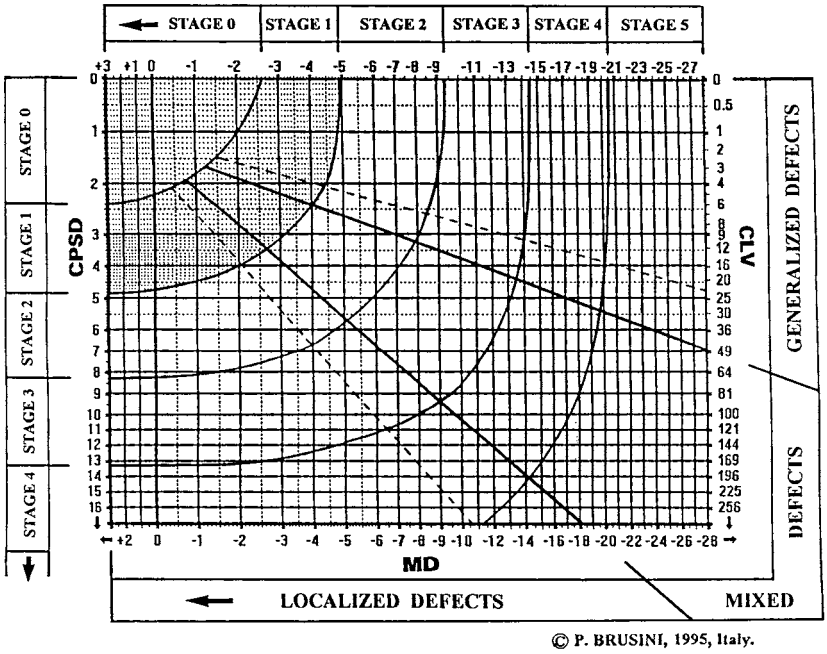

Fig. 1. The Glaucoma Staging System (GSS). The intersection of the MD and CPSD (or CLV) values defines the stage and type of defect.

The GSS has recently been introduced to classify glaucomatous visual field defects.[18] It uses the MD and the corrected pattern standard deviation (CPSD) (or CLV) indices on a Cartesian coordinate diagram. The first index is on the X axis, while the second is on the Y, with CPSD on the left and the corrected loss of variance (CLV) on the right (Fig. 1).

The disease stage is defined by the intersection of the two values. The diagram is arbitrarily divided into six different stages by curvilinear lines: from Stage 0 (completely normal visual fields) to Stage 5 (very low threshold readings with only small remnants of sensitivity). Moreover, every stage, apart from Stage 0, is subdivided

into three classes by two oblique straight lines which separate the visual field defects into three types. The generalized defects are in the upper area, the mixed defects in the central area, and the localized defects in the lower left area. Also, there are two additional broken lines. The first differentiates the purely diffuse (on the top) from the predominantly diffuse defects. The second divides the purely localized (on the bottom, left) from the predominantly localized defects.

With the GSS, the defects were classified as generalized, mixed or localized, according to the nomogram data. To assess the results, reference was made to the criteria shown in Table 2.

Table 2. Reference inclusion criteria

1. *Diffuse loss*
   a. MD>2.5 dB and/or more than 30% of test points depressed as the $p<5\%$ level on the total deviation probability map
   b. CPSD<2.5 dB
   c. the mean deviation of six of the ten best points on the total deviation map (excluding the first four) must be lower than -1 dB (points in the peripheral ring to be excluded)
   d. absence of localized defects, as defined in the following point
2. *Localized defect*
   a. PSD and/or CPSD>MD;
   b. In the pattern deviation probability map:
      cluster of five or more points depressed at the $p<5\%$ level; or
      cluster of three or more points depressed at the $p<2\%$ level; or
      cluster of two or more points depressed at the $p<1\%$ level (or at the $p<2\%$ and $p<0.5\%$, respectively); or
      cluster of four or more points depressed at the $p<5\%$ level with one point at the $p<1\%$ or two points at the $p<2\%$
      The clusters (consisting of horizontally, vertically, or diagonally neighboring depressed points) should be located along the retinal nerve fiber layer. Points located on the peripheral ring were disregarded unless connected to more central and significantly depressed points. Points adjacent to the blind spot were also disregarded unless connected to other significant defects.
   c. In the total deviation probability map:
      no more than four points depressed at the $p<2\%$ level or
      no more than ten points at the $p<5\%$ level, except for the points which are also depressed in the pattern deviation probability map
3. *Mixed defect*
   a. MD>2.5 dB and CPSD (or PSD)>2.5 dB
   b. presence of a localized defect in the pattern deviation probability map, as defined above
   c. more than four points depressed at the $p<2\%$ level or more than ten points depressed at the $p<5\%$ level in the total deviation probability map, in addition to points also significantly depressed in the pattern deviation probability map
   d. the mean deviation of six of the ten best points in the total deviation probability map (excluding the first four) must be lower than -1 dB
   e. defects not classified in the other two groups

Statistical analysis

The contingency table was used to define the correspondence between the reference classes and the classification obtained with the GHT, the Bebie curve, and the GSS. The level of association was estimated with Cramers' V, derived from the χ^2 value

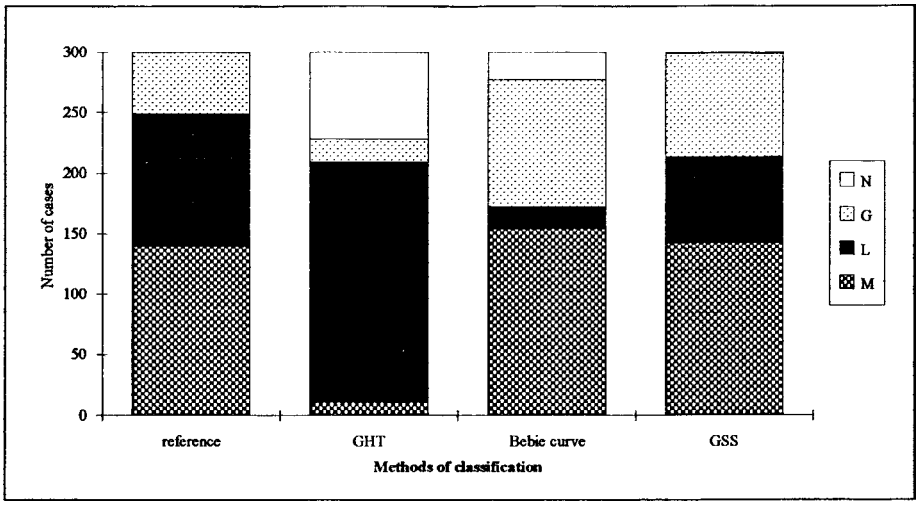

Fig. 2. Distribution of defects according to the various methods of classification. N: within normal limits; G: generalized defect; L: localized defect; M: mixed defect.

(proc freq/χ^2 measures, SAS 1988); the value ranges from -1 to +1, where +1 represents the perfect correspondence and -1 the opposite.

Results

With the reference criteria, the most commonly found defect was the mixed (139 cases, 46.3%), followed by the localized (110 cases; 36.7%), and lastly by the generalized (51 cases, 17%). The distribution of defects among the study population, according to the various methods of classification, is shown in Figure 2.

The correspondence between each classification and the reference criteria for the different types of defect is reported in Table 3.

With the GHT, the generalized damage according to the reference criteria is principally grouped within the normal range (64.7%), and the mixed defects within the 'outside normal limits' (78.4%). The Bebie curve classification closely corresponds to the reference criteria for the generalized defects, while, on the other hand, the localized defects are scattered over all the Bebie curve classes, and particularly within the mixed defects. In more than 20% of cases, a visual field with a localized defect was considered normal according to the Bebie curve.

With the GSS, the reference criteria mixed defects are frequently found in the generalized defect area (23.7%), and the localized in the mixed sector (33.6%). The Cramers' value of association is V=0.45 for the GHT, V=0.53 for the Bebie curve classification, and V=0.66 for the GSS.

Discussion

The subdivision of visual field defects into various types, namely generalized, localized, and mixed, depends on the classification model.

Table 3. Correspondence between the reference criteria and the other classification methods

Reference		*Glaucoma Hemifield Test*				*Bebie curve*				*Glaucoma Staging System*			
		N	*G*	*L*	*M*	*N*	*G*	*L*	*M*	*N*	*G*	*L*	*M*
G	51	33 (64.7%)	13 (25.5%)	1 (2.0%)	4 (7.8%)	0	48 (94.1%)	0	3 (5.9%)	0	49 (96.1%)	0	2 (3.9%)
L	110	21 (19.1%)	0	88 (80.0%)	1 (0.9%)	23 (20.9%)	14 (12.7%)	18 (16.4%)	55 (50.0%)	1 (0.9%)	4 (3.6%)	68 (61.8%)	37 (33.6%)
M	139	18 (13.0%)	6 (4.3%)	109 (78.4%)	6 (4.3%)	0	43 (30.9%)	0	96 (69.1%)	0	33 (23.7%)	3 (2.2%)	103 (74.1%)
Totals		72	19	198	11	23	105	18	154	1	86	71	142

N: normal test; G: generalized defect; L: localized defect; M: mixed defect

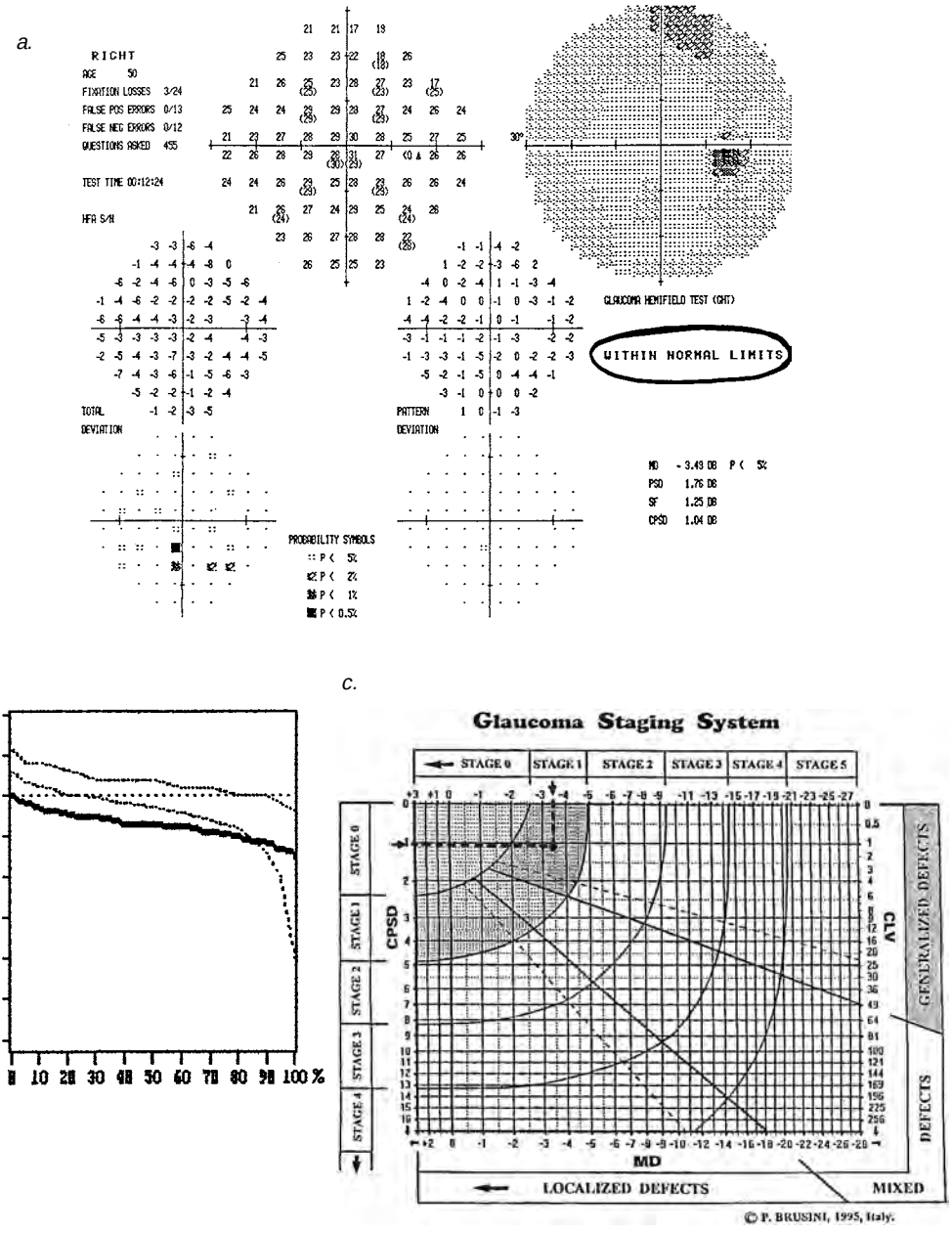

Fig. 3.a. Slight diffuse sensitivity loss in a 50-year-old patient with early glaucoma and clear ocular media. The GHT is 'within normal limits', while both the Bebie curve (*b*) and the GSS (*c*) show a generalized defect.

The criteria used in this study differ slightly from those employed by other authors. For example, Funkhouser[13] used a different length and slope of the depressed curve for estimating diffuse loss with the Bebie curve. Our criteria were stricter, requiring a longer segment of depressed points and a smaller deviation from parallelism with normal curve (0.2 dB per location instead of 0.33 dB). On the other hand, Lachenmayr *et al.*[19] identified a defect as diffuse loss when the Bebie curve fell below the 84th percentile in at least 80% of the values.

The GHT has been programmed to identify the typical glaucomatous defects, namely the localized defects. It classifies as having 'general reduction of sensitivity' only those visual fields with a relatively deep diffuse depression. This system considers slight diffuse loss as a non-glaucomatous defect and systematically classifies it as 'within normal limits'. Mixed defects are included mainly under 'outside normal limits'.

The criteria used as standard reference in this study are, of course, arbitrary and can be criticized. Our definition of diffuse loss is more liberal than the GHT and takes into consideration different points. For example, we required a negative deviation of the six best points, having excluded the first four highest values, which often exhibit artificially high sensitivity. This should result in a more specific classification of diffuse defects, as only those visual fields without (or with very few) normal points are included.

We believe this type of damage, having excluded the presence of a localized defect, could be considered a general defect, even though it may not be entirely homogeneous. This condition has been labelled, perhaps more correctly, as 'widespread loss' by Heijl[20] and has resulted in controversy between supporters and opposers of 'diffuse loss' as a sign of early glaucomatous damage. In any case, it should be stressed that this study was not designed to answer such a question, but only to look for the best method to identify a generalized defect and to distinguish a purely localized depression from a mixed defect. Our visual field sample was composed of early- to mid-damage glaucoma patients with good visual acuity, but we cannot honestly exclude the influence of miosis, cataract, and refractive errors. This may explain, at least in part, the relatively high number of generalized depressions of sensitivity without localized defects (17%) in our population.

Research on the incidence of diffuse loss on selected early glaucoma patients, excluding other possible causes, is in progress. On the other hand, Lachenmayr *et al.*,[19] in a comparative study using light-sense, flicker and resolution perimetry, reported 7.5% of cases with entirely diffuse defects in 106 glaucomatous eyes. In their research, as in our study, mixed defects were found most frequently (53.8%).

The criteria used to define a localized defect were based on previous reports,[21] and were modified to obtain greater sensitivity and specificity. For the classification of mixed defects, the same remarks made for diffuse defects are valid. It should be noted that not all these criteria may be suitable in advanced glaucoma patients. However, in these cases, a precise subdivision of the type of defect is difficult and is of little importance.

The results of this study show that no method is perfect. The GHT is highly sensitive to very small local defects, which might well be ignored by all the other methods of classification. 'Borderline' results should be considered to be strongly suspect if the reliability of the test is good. However, this system tends to underestimate the diffuse loss, which is taken into consideration only when it is very deep, and usually does not differentiate between localized and mixed defects. This is, of

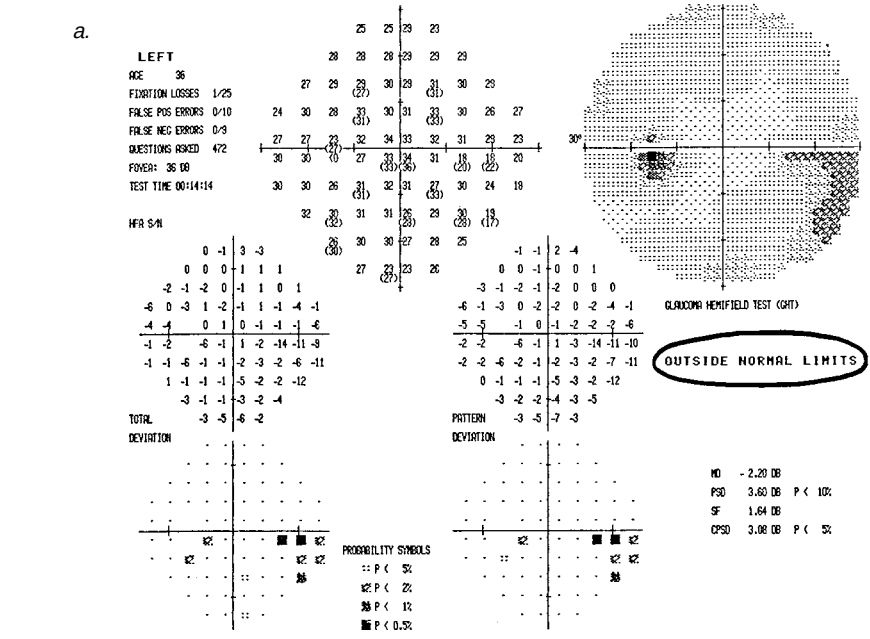

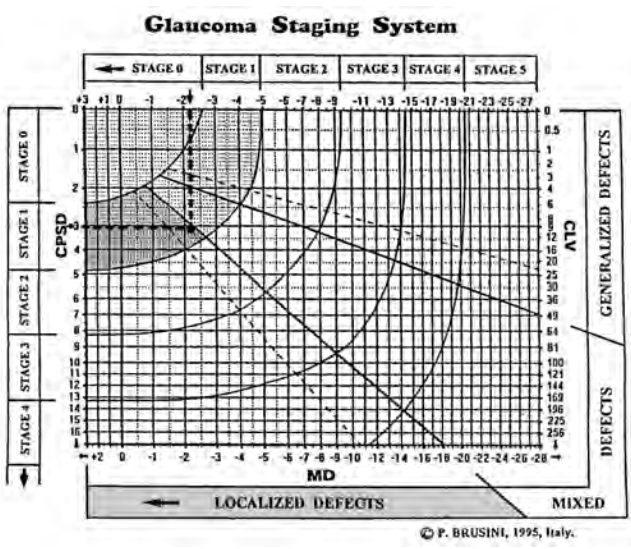

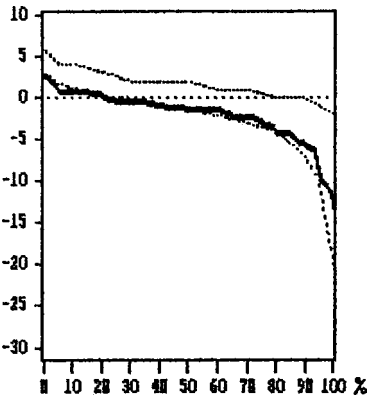

Fig. 4. Small nasal step in a 35-year-old woman. *a.* The GHT statement is 'outside normal limits' and the GSS shows a localized defect (*b*). *c.* The right side of the Bebie curve shows a steep fall, but all points are within the 95th percentile limits.

course, a deliberate choice made by the program designers and has been supported in a number of reports. However, naturally, this decreases the sensitivity of the method in those rare but undoubtedly real cases where a slight general depression is a genuine sign of glaucomatous damage. For example, we could mention a reproducible asymmetry of the MD index in comparison to the other eye with a normal CPSD, together with a corresponding asymmetry of IOP or disc cupping, having excluded other non-glaucomatous causes of such asymmetry of sensitivity (Fig. 3).

The Bebie curve is an easy and useful method for an at-a-glance classification of the visual field state, but it can miss very small, but significant, localized defects. In fact, visual fields with only few disturbed points are usually considered normal and a mixed defect may be classified as diffuse loss if the right end of the curve falls within the 95th percentile limits (Fig. 4).

This is due to the loss of spatial information, as correctly pointed out by Åsman and Olsson.[22] The Bebie curve normative limits are in fact based on values obtained in mid-peripheral areas. So significantly depressed points in the central field may fail to reach the 95% significance limit, which is very low on the right hand of the curve. Moreover, a cluster of clinically significant depressed points is considered in the same way as a group of similarly depressed, but isolated, points.

The GSS allows the user instantly to classify the type and severity of the visual field defects and showed the highest correspondence with the reference criteria. However, as with the Bebie curve, it is not specific for glaucoma damage and does not take into consideration spatial information. It may classify as normals' visual fields with very localized sensitivity depression, if they are not deep enough to affect the CPSD index significantly (one case in our sample). This problem is sometimes related to a high SF, which artificially decreases the value of PSD and produces a low CPSD. This can cause a misclassification of localized defects in the mixed or even in the generalized defect group. In these cases, particularly when the CPSD is 0, it is advisable to use the PSD value, corrected by subtracting a fixed coefficient factor of 0.7 dB (2.5 dB when Octopus LV is used).

A discrete percentage of reference criteria mixed and localized defects was shifted, and classified respectively as generalized and mixed defects by the GSS. This is due to the different definition criteria used by the GSS, which emphasizes even slight widespread depressions of sensitivity and so tends to overestimate the diffuse loss. In any case, purely generalized defects, especially in Stage 1, should be interpreted with caution and considered as glaucomatous only after careful analysis of all clinical patient data. With these limitations, the GSS could be used to assess the severity of functional damage and the characteristics of visual field defects, both in research and in day-to-day clinical practice.

Further research is needed to definitively establish the actual clinical importance of the diffuse defect in early glaucoma damage. The problem becomes even more difficult to solve when a slight opacification of the lens is associated with ocular hypertension and with a suspect cupping of the optic disc. An index of lens opacity, as proposed by Sample *et al.*,[23] could probably help the clinician to differentiate the sensitivity depression due to incipient cataract from actual glaucomatous diffuse loss.

Acknowledgment

The author would like to thank Dr Stefano Filacorda for his valuable help in the statistical analysis

of the data.

References

1. Drance SM: The early structural and functional disturbances of chronic open-angle glaucoma. Ophthalmology 92:853-957, 1985
2. Drance SM, Douglas GR, Airaksinen PJ, Schulzer M, Hitchings RA: Diffuse visual field loss in chronic open-angle and low-tension glaucoma. Am J Ophthalmol 104:577-580, 1987
3. Glowazki A, Flammer J: Is there a difference between glaucoma patients with rather localized visual field damage and patients with more diffuse visual field damage? Doc Ophthalmol Proc Ser 49:317-320, 1987
4. Corallo G, Zingirian M, Gandolfo E et al: Updating the role of diffuse field loss in glaucoma diagnosis. In: Mills RP, Wall M (eds) Perimetry Update 1994/1995, pp 283-287. Amsterdam/ New York: Kugler Publ 1995
5. Drance SM: Diffuse visual field loss in open-angle glaucoma. Ophthalmology 98:1533-1538, 1991
6. Heijl A: Lack of diffuse loss of differential light sensitivity in early glaucoma. Acta Ophthalmol (Kbh) 67:353-360, 1989
7. Langerhorst CT, Van den Berg TJTP, Greve EL: Is there general reduction of sensitivity in glaucoma? Int Ophthalmol 13:71-106, 1989
8. Åsman P, Heijl A: Diffuse visual field loss and glaucoma. Acta Ophthalmol (Kbh) 72:303-308, 1994
9. Caprioli J, Sears M: Patterns of early visual field loss in open angle glaucoma. Doc Ophthalmol 49:307-315, 1987
10. Brusini P, Tosoni C: Use of Bebie curve for perimetric damage staging in glaucoma. Octopus Users' Meeting, Luzern, 22-24 March 1994
11. Åsman P: Color-coded probability maps: separation of field defect types. In: Mills RP, Wall M (eds) Perimetry Update 1994/1995, pp 57-58. Amsterdam-New York: Kugler Publ 1995
12. Langerhorst CT: Automated Perimetry in Glaucoma, pp 88-90. Amsterdam/Milano: Kugler & Ghedini Publ 1988
13. Funkhouser AT: A new diffuse loss index for estimating general glaucomatous visual field depression. Doc Ophthalmol 77:57-72, 1991
14. Funkhouser A, Flammer J, Fankhauser F, Hirsbrunner H-P: A comparison of five methods for estimating general glaucomatous visual field depression. Graefe's Arch Clin Exp Ophthalmol 230:101-106, 1992
15. Funkhouser AT, Fankhauser F, Weale RA: Problems related to diffuse versus localized loss in the perimetry of glaucomatous visual fields. Graefe's Arch Clin Exp Ophthalmol 230:243-247, 1992
16. Heijl A, Lindgren G, Lindgren A, Olsson J, Åsman P, Myers S, Patella M: Extended empirical statistical package for evaluation of single and multiple fields in glaucoma. In: Mills RP, Heijl A (eds) Perimetry Update 1990/1991, pp 303-315. Amsterdam/Milano: Kugler & Ghedini Publ 1991
17. Bebie H, Flammer J, Bebie Th: The cumulative defect curve: separation of local and diffuse components of visual field damage. Graefe's Arch Clin Exp Ophthalmol 227:9-12, 1989
18. Brusini P: Clinical use of a new method for visual field damage classification in glaucoma. Eur J Ophthalmol 6:402–407, 1996
19. Lachenmayr BJ, Drance SM, Douglas GR, Mikelberg FS: Light-sense, flicker and resolution perimetry in glaucoma: a comparative study. Graefe's Arch Clin Exp Ophthalmol 229:246-251, 1991
20. Heijl A: Computerized perimetry in glaucoma management. Acta Ophthalmol (Kbh) 67:1-12, 1989
21. Anderson DR: Automated Static Perimetry. St Louis: Mosby Year Book Inc 1992
22. Åsman P, Olsson J: Physiology of cumulative defect curve: consequences in glaucoma perimetry. Acta Ophthalmol Scand 73:197-201, 1995
23. Sample PA, Esterson FD, Weinreb RN: A practical method for obtaining an index of lens density with an automated perimeter. Invest Ophthalmol Vis Sci 30:786-787, 1989

CLINICAL VALIDITY OF THE BRUSINI GLAUCOMA STAGING SYSTEM*

INCI KOÇAK, MARIO ZULAUF and PHILLIP HENDRICKSON

Department of Ophthalmology, University of Basel, Basel, Switzerland

Abstract

Purpose: To evaluate Brusini charts for the follow-up and classification of glaucomatous visual fields.
Patients and methods: Six hundred and ten visual fields of 64 glaucomatous eyes were studied retrospectively. For each eye, a glaucoma staging system (GSS) sheet was plotted as a scatterplot of mean defect and corrected loss variance (CLV), with guidelines classifying the fields into categories, as follows: normal, localized, mixed, and generalized defects.
Results: Classification was comparable to PeriData analysis in 89% of fields, while 5% were wrongly classified as normal. The 1.3% of fields with marked discrepancies and the 5% of fields with minor ones, mainly presented with high short-term fluctuation, leading to reduced CLV values. In the follow-up evaluation, no change was observed in 59% of eyes, and of those, 30% showed low and 19% high long-term fluctuation (LF), due to impaired reliability. In 3% of eyes, artifacts caused high LF. However, in 8% of eyes with high LF, there was no apparent reason. Changes were observed in 41% of follow-ups. In these, initial improvement (learning and/or therapy effect) was present in 19% of eyes. Deterioration was present in 16% of eyes. After initial improvement, there was no change in 5% of eyes, while deterioration was observed in 11%. In 3.1% of follow-ups, progression was obvious in the PeriData analysis but not in the GSS index-based evaluation.
Conclusion: Brusini charts are useful for classifying and following glaucoma. However, this study suggests implementing current Octopus normal values and the use of loss variance instead of CLV.

Introduction

Automated static perimetry is currently the standard test for identifying and following visual-field defects in a variety of diseases, including glaucoma. Several classification methods have been introduced to evaluate glaucomatous visual-field defects at the onset and during follow-up.[1-5] Recently, Brusini[6] introduced a classification system for glaucomatous visual-field defects called the Glaucoma Staging System (GSS). It is based on the visual-field indices, MD (mean defect for Octopus and mean deviation for Zeiss-Humphrey instruments) and CLV (corrected loss variance for Octopus, which corresponds approximately to the square of corrected pattern stand-

*The authors have no proprietary interest in the hard- and software mentioned.

Address for correspondence: Dr. I. Koçak, Department of Ophthalmology, Hospital of Ankara, 06320 Ankara, Turkey

Perimetry Update 1996/1997, pp. 341–348
Proceedings of the XIIth International Perimetric Society Meeting
Würzburg, Germany, June 4–8, 1996
edited by M. Wall and A. Heijl

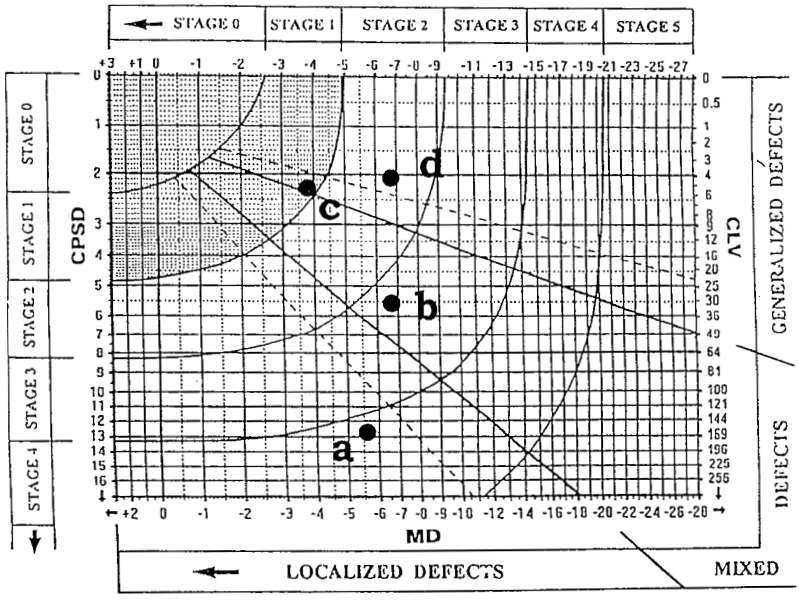

Fig. 1. Brusini Glaucoma Staging System chart. Nomogram for visual-field defect classification and typing. The intersection of the mean defect (MD) or mean deviation (MD) and corrected loss variance (CLV) or corrected pattern standard deviation (CPSD) values defines the stages and type of defect. Figures 2a-d illustrate four examples.

ard deviation (CPSD), to classify the stages and type of glaucomatous visual-field damage as purely or predominantly localized, mixed, or purely or predominantly generalized (Fig. 1).[6]

MD is the arithmetic mean difference between the threshold value and the age-corrected normal value for all test locations. It is sensitive to diffuse damage and is robust to small localized defects.[7] LV represents the local non-uniformity of a visual-field defect. It increases with the depth of scotoma and is helpful in the detection of early defects.[8] An increase of LV requires further evaluation to distinguish true early defects from increased scatter, or both of these.[8] CLV has been proposed to separate real deviations from deviations due to scatter, and remains within normal ranges in cases of increased short-term fluctuation (SF) and uniformly reduced visual fields.[7,9] Previously, Gollamudi *et al.*[5] found that, in general, CLV increases independently from MD, and, in contrast to Brusini, higher MD values do not imply an elevation of CLV variation. Additionally, they used the difference between MD and the square root of CLV to define the stages of glaucoma.

The purpose of this study was to evaluate the clinical validity of GSS to classify single visual fields and to determine changes in series of visual fields in glaucoma.

Patients and methods

Subjects

The visual fields of 32 primary open-angle glaucoma patients (18 males, 13 females) were analyzed retrospectively. The subjects met the following criteria: the intraocular pressure was repeatedly in excess of 23 mmHg, the anterior chamber angles were open gonioscopically, or there was no evidence of other ocular disease contributing to elevated intraocular pressure. Early glaucomatous visual-field defects (CLV > 4 dB^2) were obvious, and the optic disc pathological cupping or visible nerve-fiber defect were evident ophthalmoscopically.

Test protocol

All patients were treated with either timolol maleate 0.5% or Betaxolol 1% eye drops and were experienced with automated perimetry. The therapeutic effects have been described elsewhere.[10,11] All patients had had at least six visual fields within three years for each eye performed by the same perimetrist on the same Octopus 201 perimeter with Program G1.[12] All three phases of Program G1 were always completed.

Visual-field analysis

For each of the 64 eyes, the series of visual fields was plotted on a Brusini GSS chart. This nomogram is arbitrarily divided into six different stages by curvilinear lines:

Stage 0: completely normal visual fields
Stage 1: very subtle defects
Stage 2: moderate field defects
Stage 3: conglomerate defects
Stage 4: very advanced partially absolute defects
Stage 5: very low threshold reading defects

Stages 1-5 are subdivided into three groups: localized, mixed, and generalized visual-field defects. Additionally, the generalized and localized visual-field defects are subdivided into purely diffuse or local (G-, L-), and predominantly diffuse or local (G+, L+) (Fig. 2).

The classification by Brusini GSS was compared on screen with PeriData 7.0.[13] To evaluate the follow-up, all visual fields were grouped into no change (Group A) and change (Group B).

Results

Classification into various defect types

The comparative analysis of 610 visual fields of 32 glaucomatous patients plotted on 64 Brusini GSS charts, agreed with PeriData in 89% (540/610) of the fields. The distribution of the classifications is shown in Table 1. Dissimilar classification was noted in 11% of the fields (70/610). Among those 70 classified dissimilarly, 32 (5%) were wrongly classified as normal by GSS. According to the normal values of the

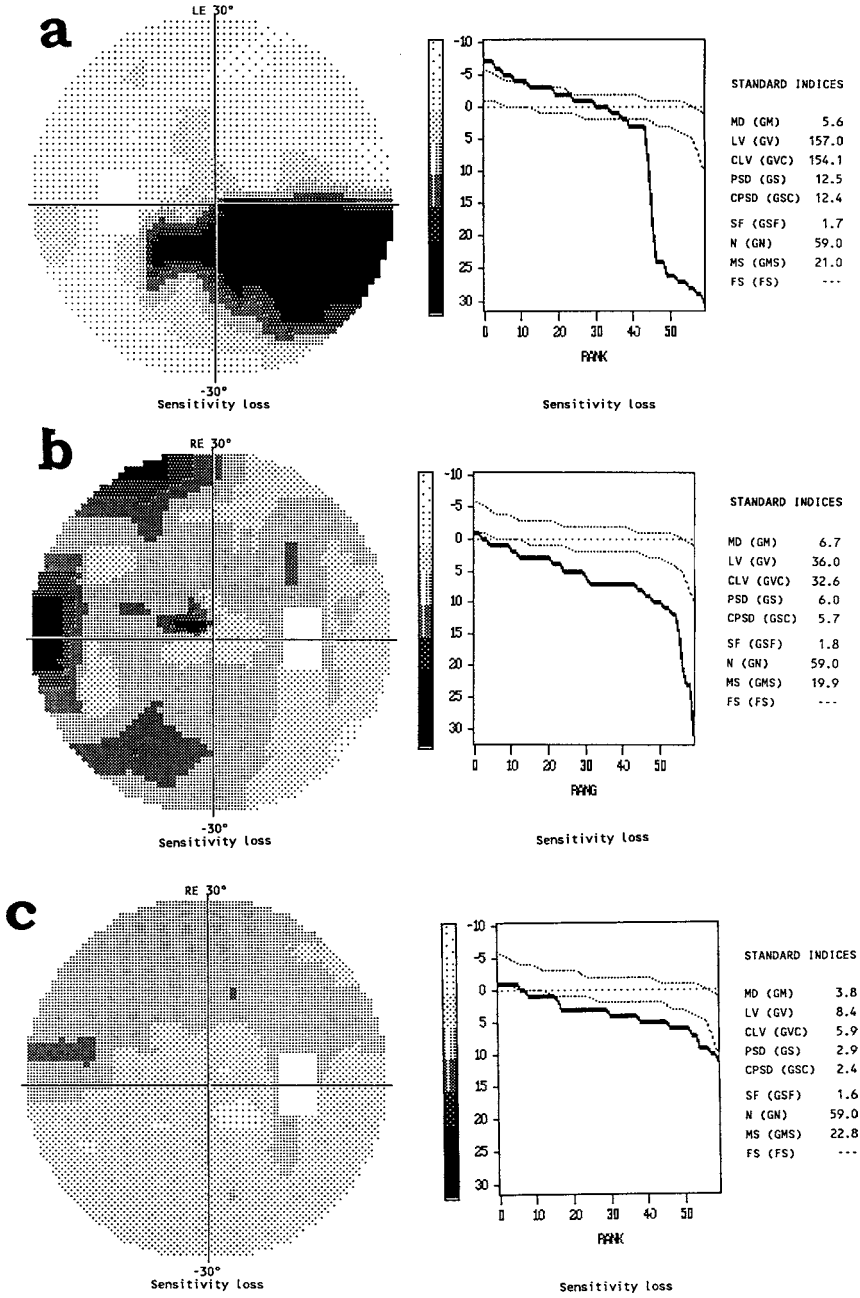

Fig. 2a. PeriData[13] printout of single visual fields of a 72-year-old man with a purely localized visual-field defect (left eye). The defect is obvious on traditional gray-scaled threshold charts and from the Bebie curve, as well as on the Brusini chart (see Fig. 1, where it is indicated as '**a**' on GSS). *b.* Example of a mixed defect which is more obvious on the GSS chart (see Fig. 1 where it is indicated as '**b**' on GSS) than on conventional printouts. *c.* In this glaucomatous field, gray-scaled threshold charts and Bebie curve clearly show that a mostly generalized defect is present (in Fig. 1 it is indicated as '**c**' on GSS). *d.* PeriData[13] printout of a visual field where a defect on GSS is presented as purely generalized (see Fig. 1 where it is indicated as '**d**').

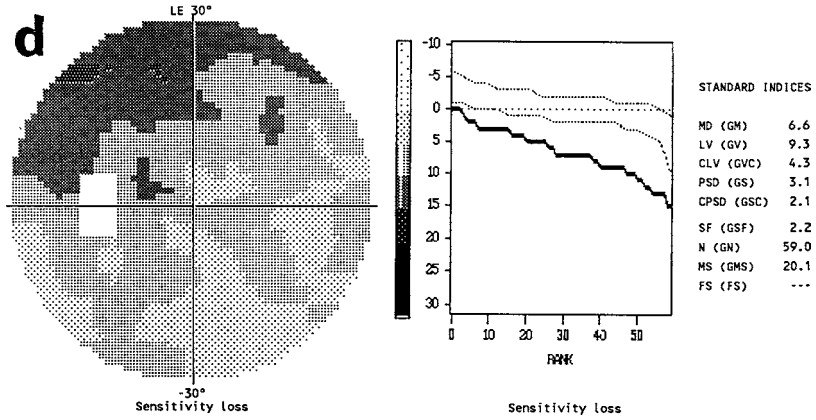

Fig. 2d.

Table 1. Number of fields according to the Glaucoma Staging System (rows) and PeriData 7.0[13] (columns) classifications

	Normal	*L-*	*L+*	*Mixed*	*G+*	*G-*	*Total*
Normal	261	5*	6*	5*	13*	3*	293
L-	1*	49	1*	1*			52
L+		1*	49	2*			52
Mixed			10*	103	3*		116
G+			1*	4*	26		31
G-			3*	3*	8*	52	66
Total	262	55	70	118	50	55	610

L-: purely localized defect; L+: predominantly localized defect; G+: predominantly diffuse defect; G-: purely diffuse defect. The asterisk denotes the 17 fields with considerable discrepancies

visual-field indices of the Octopus (MD ± 2 dB, CLV < 4 dB^2), it was possible to detect these mismatched classifications.[13,14] Marked discrepancies were noticed in eight fields (1.3%). One of these was classified as G+ instead of L+, six were classified as G- instead of either, three L+ and three Mixed, and additionally, one L- was actually Mixed. Almost all these presented with an SF value above 1.7 dB. The other 30 fields (4.7%) presented with minor discrepancies.

Evaluation of the follow-up

Group A represents the follow-up of the visual fields with no changes and includes 38 eyes (59.4%). Figure 3a gives an example for the 29.7% of follow-ups (19/64) with a low LF. However, 17 eyes (26.5%) showed a high LF. High LFs in 12 eyes (18.8%) were due to impaired reliability, either because of poor cooperation of the patient, fatigue effect during the perimetric examination, or an SF value greater than 1.7 dB. However, there was no apparent reason in five follow-ups (8.7%) with a high LF, *i.e.*, no high SF, no fatigue effect, and reliability parameters within the normal range.[7] In two eyes (3.1%), artifacts caused a high LF, namely, incorrect instruction of a patient and inconsistent presence of the blind-spot effect.

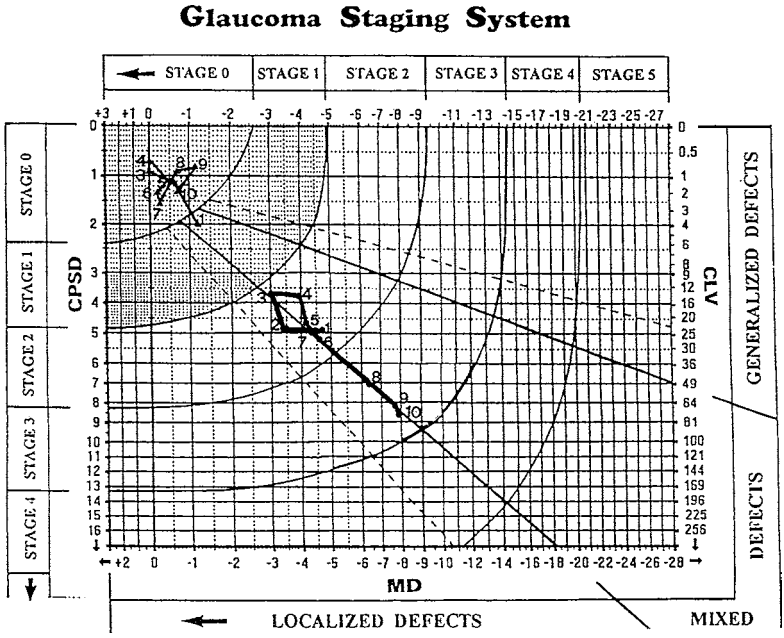

Fig. 3a. Follow-up of visual-field defects in the left eye of a 78-year-old woman showing that they are obviously stable with low LF, while a certain deterioration is easily recognizable on GSS follow-up of the right eye (⊢ ⊢ ⊢ right eye; ▲ ▲ ▲ left eye).

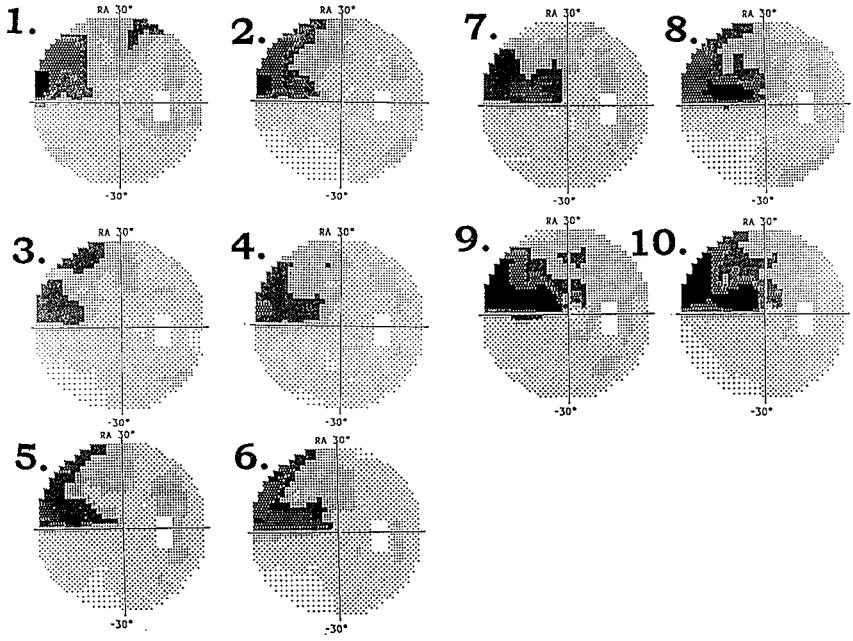

Fig. 3b. PeriData[13] overview printouts summarizing the ten visual fields of the right eye of the same patient.

Group B represents the follow-up of visual-field defects with changes (41%, 26/64 of eyes). Changes in the visual fields can be the learning and/or therapy effect, progression, a combination of both, or, a combination of the learning and/or therapy effect followed by a stable period. In six eyes (9.4%), an improvement was observed due to the learning and/or therapy effect. However, in ten eyes (15.6%), an obvious deterioration was observed. After an initial improvement, there were no changes in three eyes (4.7%), while in seven eyes (10.9%) a deterioration was observed (Figs. 3a and b).

In only two eyes (3.1%) was progression obvious in a detailed and comprehensive PeriData analysis[13] but not in the GSS index-based evaluation. Therefore, the Brusini GSS chart was found to be helpful and reliable for evaluating the follow-up of visual fields.

Discussion

Detection of the progression of visual-field defects in glaucoma is important when making appropriate clinical decisions. At the present time, there is no satisfactory technique for detecting progressive visual-field loss with great certainty except when the change is rather large.

For follow-up, Brusini GSS charts and PeriData[13] analysis were in agreement in 97% of cases. As a general rule, in order to detect progression, at least four visual fields should be performed over a reasonable period of time.[14] Brusini charts failed to depict progression in 3% of cases. Global indices might not be able to detect changes confined to only small visual-field areas. If SF is increased, the rate of false-negative responses for catch trials should be checked. An increased SF without an increased rate of false responses might indicate pathology, a change in threshold.[7] Therefore, in cases with a high LF, the clinician should also pay attention to SF values. However, for follow-up, these plotted Brusini charts highlight progression, deterioration, stability, and fluctuations.

By means of the Brusini GSS, visual fields can be classified quickly and easily, and with an accuracy of 89%, into the following groups: normal, diffusely, mixed, or locally defective. When the Bebie curve is not available, GSS charts are helpful in characterizing the fields as normal, localized, mixed, or generalized.

The border between normal and defective visual fields in the Brusini GSS chart is 2.6 dB for MD and 6 dB^2 for CLV. For MD, ±2 dB, is considered normal with Program G1 of the Octopus perimeter, and MD values above 1.5 dB are considered questionably normal.[15,16] For CLV, 4 dB^2 is the upper normal limit.[15] A CLV value of 1.4 dB^2 has been suggested to provide an optimal diagnosis.[17] These differences explain the erroneous classification of 5% of the visual fields as normal, and the marked mismatched classification in 1.3% of the 610 visual fields.

With Program G1, the upper normal limit for SF is 2 dB, and values above 1.75 dB may be considered questionable.[15] In evaluating the follow-ups with high LF on GSS charts, care should be taken with high SF values.[14-18] Brusini[6] chose CPSD and CLV values and advised the use of PSD and LV if SF was not available or was very high. In these cases, he advised using LV instead of CLV, correcting LV by 2.5 dB^2. In agreement with Brusini, the present study proposes LV instead of CLV in visual fields with SF values above 1.7 dB.

According to Brusini,[6] GSS was developed for Zeiss-Humphrey perimeters. We suggest implementing current Octopus normal values and the use of LV instead of CLV in order to improve the reliability of GSS and to avoid any confusion which may result from high SF values. In the case of a follow-up in the same patient with both Zeiss-Humphrey and Octopus perimeters, conversion formulas must be applied before the results can be plotted on a Brusini chart.[19] Furthermore, we suggest the addition of an appropriate slot in the GSS, which would permit the examination date of the visual field as well as other important information to be entered.

A license for use of the Brusini charts is available from Dr. P. Brusini, Department of Ophthalmology, Hospital of San Donà di Piave (VE), Italy.

Acknowledgments

Dr. Koçak is a visiting researcher sponsored by the Swiss Scholarship Committee. The Brusini charts have been reproduced with the permission of Dr. P. Brusini.

References

1. Weber J: Topographie der funktionellen Schädigung beim chronischen Glaukom, pp 10-21. Heidelberg: Under Verlage 1992
2. Aulhorn E, Karmeyer H: Frequency distribution in early glaucomatous visual-field defects. Doc Ophthalmol Proc Ser 14:75-83, 1977
3. Hart WM, Becker B: The onset and evaluation of glaucomatous visual-field defects. Ophthalmology 89:268-279, 1982
4. Mikelberg FS, Drance SM: The mode of progression of visual-field defects in glaucoma. Am J Ophthalmol 98:443-445, 1984
5. Gollamudi SR, Liao P, Hirsch J: Evaluation of corrected loss variance as a visual-field index. II. Corrected loss variance in conjunction with mean defect may identify stages of glaucoma. Ophthalmologica 197:144-150, 1988
6. Brusini P: Department of Ophthalmology, Hospital of San Donà di Piave (VE), Italy, 1995
7. Augustiny L, Flammer J: The influence of artificially induced visual-field defects on the visual-field indices. Doc Ophthalmol Proc Ser 42:55-67, 1985
8. Flammer J: The concept of visual-field indices. Graefe's Arch Clin Exp Ophthalmol 224:389-392, 1986
9. Flammer J, Drance SM, Augustiny L, Funkhouser A: Quantification of glaucomatous visual-field defects with automated perimetry. Invest Ophthalmol Vis Sci 26:176-181, 1985
10. Messmer C, Flammer J, Stümpfig D: Influence of betaxolol and timolol on the visual fields of patients with glaucoma. Am J Ophthalmol 112:678-681, 1991
11. Kaiser HJ, Flammer J, Messer C, Stümpfig D, Hendrickson Ph: Thirty-month visual-field follow-up of glaucoma patients treated with β-blockers. J Glaucoma 1:153-155, 1992
12. Flammer J, Jenni F, Bebié H, Keller B: The Octopus Glaucoma G1 Program. Glaucoma 9:67-72, 1987
13. Brusini P, Nicosia S, Weber J: Automated visual field management in glaucoma with the PeriData program. In: Mills RP, Heijl A (eds) Perimetry Update 1990/1991, pp 273-277. Amsterdam/Milano: Kugler & Ghedini Publ 1991
14. Boeglin RJ, Caprioli J, Zulauf M: Long-term fluctuation of the visual field in glaucoma. Am J Ophthalmol 113:396-400, 1992
15. Zulauf M, LeBlanc RP, Flammer J: Normal visual fields measured with Octopus-Program G1. II. Global visual-field indices. Graefe's Arch Clin Exp Ophthalmol 232:516-522, 1994
16. Rutishauser C, Flammer J, Haas A: The distribution of normal values in automated perimetry. Graefe's Arch Clin Exp Ophthalmol 227:513-517, 1989
17. Mandava S, Caprioli J, Zulauf M: A glaucoma pattern index to quantify glaucomatous visual-field loss. J Glaucoma 1:178-183, 1992
18. Zulauf M, Caprioli J: Fluctuation of the visual field in glaucoma. Ophthalmol Clin N Am 4(4):671-697, 1991
19. Zeyen T, Roche M, Brigatti L, Caprioli J: Formulas for conversion between Octopus and Humphrey threshold values and indices. Graefe's Arch Clin Exp Ophthalmol 233:627-634, 1995

PERIMETRIC DAMAGE IN PRIMARY OPEN-ANGLE GLAUCOMA AND IN PSEUDOEXFOLIATION GLAUCOMA
Classification according to the 'Glaucoma Staging System'

CLAUDIA TOSONI[1], PAOLO BRUSINI[2], GIUSEPPE MIGLIORATI[1], GIORGIO BELTRAME[1] and PIERANTONIO BAREA[2]

[1]Department of Ophthalmology, General Hospital of Udine; [2]Department of Ophthalmology, Hospital of San Donà di Piave; Italy

Abstract

The Glaucoma Staging System is a new method to classify glaucomatous visual field defects. This system was used to classify the visual field damage present at diagnosis in 127 patients with primary open-angle glaucoma (POAG) and in 114 patients with pseudoexfoliation glaucoma (PEXG). The damage was significantly more severe in PEXG patients than in POAG patients. The most common defects in POAG patients were the mixed ones, while in PEXG patients a generalized defect was frequently found in advanced cases. A diffuse loss was a common finding in early POAG cases. A purely localized defect was found in very few cases, irrespective of the type of glaucoma.

Introduction

In progressive diseases, such as glaucoma, an accurate staging of severity of damage is useful, not only for research, but also in clinical practice.[1] Over the last few years, computerized automated perimetry has become the most widely used technique for evaluating glaucomatous damage.[2,3] A new method of staging, the 'Glaucoma Staging System' (GSS), which is simple, quick and reliable, and can be used with most of the commercially available computerized perimeters, has recently been introduced.[4] The GSS uses the MD and CPSD (or CLV) indices on a Cartesian coordinate diagram. This nomogram classifies the visual fields in six stages of increasing severity and differentiates visual field defects into three types: generalized, localized and mixed (Fig. 1).

In the present study, we used this system to classify visual field damage in patients with both primary open-angle glaucoma (POAG) and pseudoexfoliation glaucoma (PEXG) to assess the severity of damage and the type of defect at diagnosis.

Address for correspondence: Claudia Tosoni, MD, Via Santa Maria Crocifissa di Rosa 10, 33100 Udine, Italy

Perimetry Update 1996/1997, pp. 349–354
Proceedings of the XIIth International Perimetric Society Meeting
Würzburg, Germany, June 4–8, 1996
edited by M. Wall and A. Heijl

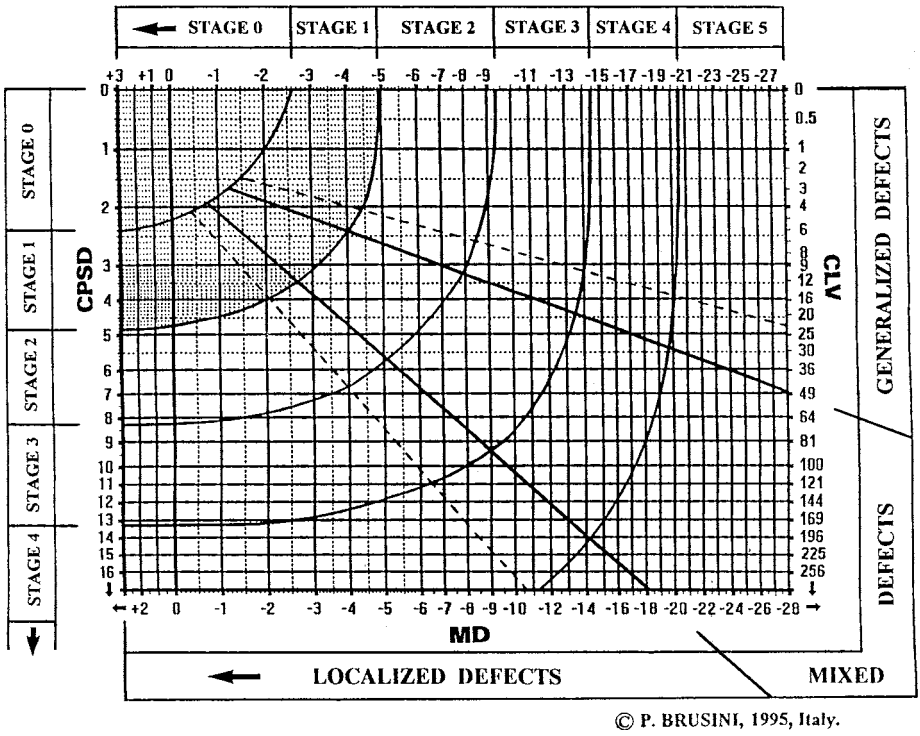

Fig. 1. The Glaucoma Staging System. The intersection of the MD and CPSD (or CLV) indices defines the stage and the type of defect.

Material and methods

We retrospectively reviewed the charts of 127 patients with POAG and 114 patients with PEXG. Other types of glaucoma, such as angle-closure, juvenile and secondary glaucomas, were excluded.

Inclusion criteria were *1.* an intraocular pressure before therapy of 21 mmHg or more; *2.* no specific therapy; *3.* a cup:disc ratio of 0.4 or more, or a difference in cup:disc ratio of 0.2 or more between both eyes with a pressure difference; and *4.* vertical elongation of the cup downwards or upwards to the boundary of the disc.

The occurrence of pseudoexfoliation was registered after slit-lamp examination. Patients with dense cataract or those on miotic therapy were excluded. Automated visual field tests were performed with either the Humphrey 30-2 or the Octopus G1 threshold tests. Details of the patient population are given in Table 1.

We used the first visual field with good reliability indices and without artifacts. The visual field state was classified using GSS. Distribution of GSS stages and type of defect were studied in the two groups of glaucoma patients. An analysis of variance with the general linear model was performed to discover the effects of the glaucoma group on both stage and type of defect. The mean frequency (rank value) of stages and types of defect for both glaucoma groups was compared using a mul-

Table 1. Patient population

	Open-angle glaucoma	*Pseudoexfoliation glaucoma*
Number of patients	127	114
Total number of eyes	232	170
Mean age at diagnosis	64	67
Men/women	63/64	63/51

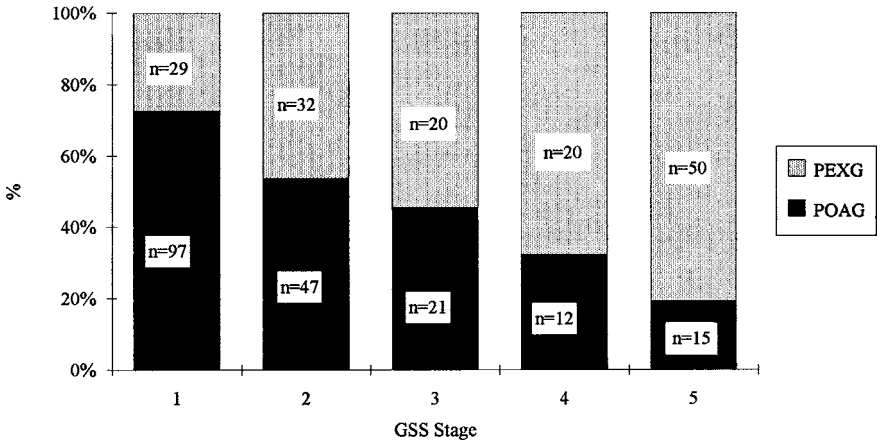

Fig. 2. Distribution of different GSS stages in both glaucoma groups.

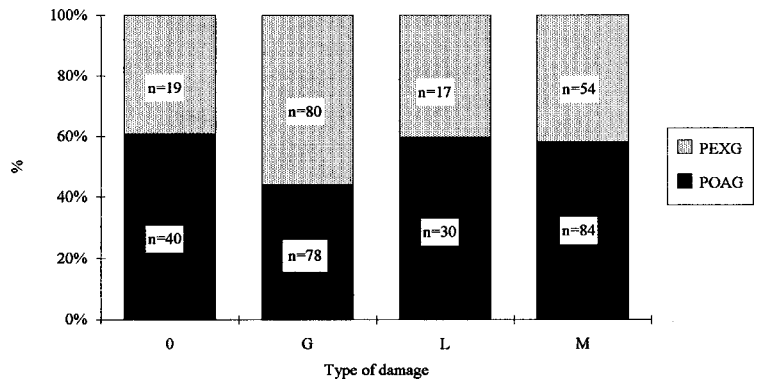

Fig. 3. Distribution of types of defect in both glaucoma groups.

tiple comparison procedure. In the first group, mean values (for stages, n=10) were obtained as the mean of three types of defect for each different stage in PEXG and POAG. In the second group, mean values (for type of defect, n=6) were the mean of five stages for each different type of defect in PEXG and POAG.

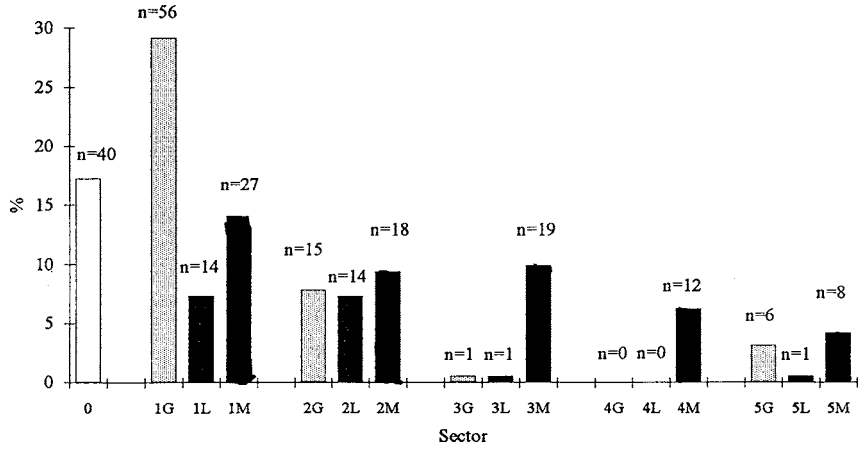

Fig. 4. Distribution of sectors (see text) in POAG.

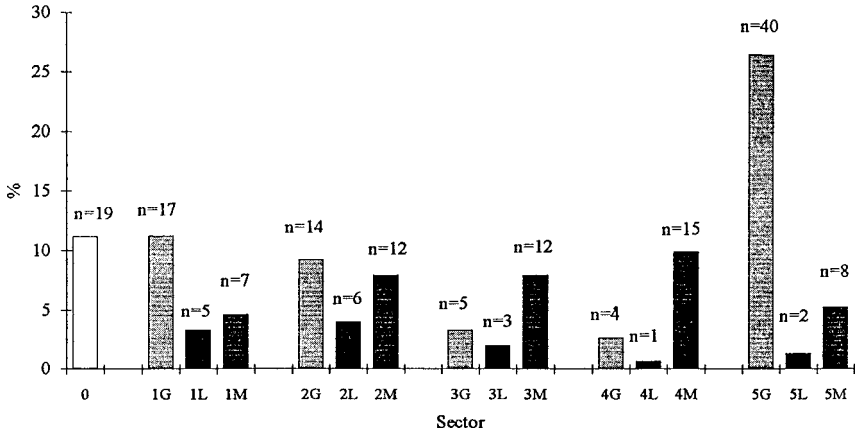

Fig. 5. Distribution of sectors (see text) in PEXG.

Results

The distribution of the different stages in both glaucoma groups at diagnosis is shown in Figure 2, and the distribution of the different types of defect in Figure 3.

The distribution of sectors (sector = combination between stage and type of defect) in the glaucoma groups is reported in Figures 4 and 5.

Comparison between the groups revealed a higher percentage of POAG eyes at Stage 0 (normal visual field; 17.2% versus 11.2%). We did not use Stage 0 in our analysis of data. Eyes classified as Stage 0 were probably only those affected by intraocular hypertension or the pseudoexfoliation syndrome without glaucoma damage. In fact, at follow-up, most cases remained at Stage 0.

It should be noted that in PEXG most patients were at Stage 5 (50 eyes, 30.6%). In this stage, generalized defects were the most frequent (26.8%). The comparison of

Table 2. Multiple comparison of the mean frequency (rank value) of the different stages in the glaucoma groups

GSS stage	*Glaucoma group*	*T grouping*[1]	*Mean rank value*
1	POAG	a	25.50
2	POAG	ab	20.50
2	PEXG	ab	20.17
1	PEXG	bc	17.83
5	PEXG	bc	17.33
4	PEXG	cd	13.67
3	PEXG	cd	13.67
3	POAG	de	10.66
5	POAG	de	9.00
4	POAG	e	6.67

In each glaucoma group, stages with a different letter are significantly different ($p<0.05$)

Table 3. Multiple comparison of the mean frequency (rank value) of the different types of defect for glaucoma type

Type of defect	*Glaucoma group*	*T grouping*[1]	*Mean rank value*
Mixed	POAG	a	21.00
Generalized	PEXG	a	20.30
Mixed	PEXG	a	20.00
Generalized	POAG	b	13.10
Localized	POAG	b	9.30
Localized	PEXG	b	9.30

In each glaucoma group, types of defect with a different letter are significantly different ($p<0.05$)

different stages of severity between the two glaucoma groups is shown in Table 2.

In POAG, low severity stages (1 and 2) were found more frequently, whereas, in PEXG, intermediate and severe stages were usually found at diagnosis. Considering the type of defect, we found that, in POAG, generalized defects were more frequent at Stage 1, and mixed defects more frequent at all other stages. In PEXG, generalized defects were more frequent at Stages 1, 2 and 5, and mixed defects at Stages 3 and 4. However, purely localized defects were uncommon in both groups. In the PEXG group, generalized and mixed defects were found most frequently. On the other hand, in POAG patients, mixed defects appeared to be more prevalent (Table 3).

Discussion

The prognosis for PEXG is generally considered to be severe compared to POAG.[5-10] Cross-sectional studies by Tarkkanen,[11] Horven,[12] Klouman[13] and Aasved[14] have shown more severe damage at diagnosis in PEXG than in POAG. Our study confirms these observations. More than 60% of patients with POAG presented with moderate visual field defects at diagnosis. On the other hand, over 50% of PEXG patients showed severe visual field defects.

The type of defect was similar in the two groups even though the diffuse loss

seemed to be more common in PEXG. In our study, the most common visual field defects in POAG patients were mixed, while, in PEXG patients, a generalized defect was frequently found in advanced cases.

In the first stages, a generalized sensitivity depression was quite common. Diffuse loss of sensitivity is known to be an aspecific feature alteration, usually related to media opacities (*i.e.*, cataract) or miosis, but it is likely that at least a part of these defects are genuine and related to glaucoma. On the other hand, purely localized defects were found in very few cases. A predominantly localized defect with a slight sensitivity depression in apparently normal visual fields was a more common finding. This can clearly be seen when looking at the Bebie curve,[15] available with the Octopus 1-2-3 perimeter and with both Octosmart and Peridata software. In very advanced glaucoma, a localized defect is very rare, because even the 'good points' are somewhat disturbed.

In conclusion, we can confirm the increased severity of PEXG compared to POAG. The Glaucoma Staging System seems to be a useful method for classifying both the severity and type of the defect.

References

1. Brusini P, Tosoni C, Miani F: Suddivisione in stadi del glaucoma cronico semplice: utilità di un linguaggio comune nella ricerca e nella clinica. Min Oftalmol 36:347-350, 1994
2. Heijl A: Computerized perimetry in glaucoma management. Acta Ophthalmol (Kbh) 67:1-12, 1989
3. Langerhorst CT: Automated perimetry in glaucoma. In: Heijl A (ed) Perimetry Update, 1988/89, pp 88-90. Amsterdam/Milano: Kugler & Ghedini Publ 1988
4. Brusini P: Clinical use of a new method for visual field damage classification in glaucoma. Eur J Ophthalmol 6:402-407, 1995
5. Brooks AMV, Gillies WE: The presentation and prognosis of glaucoma in pseudoexfoliation of the lens capsule. Ophthalmology 95(2):271-276, 1988
6. Cambiaggi A, Menci E, Marras A: Il comportamento del campo visivo nel glaucoma pseudoesfoliativo: studio retrospettivo. Boll Ocul (Suppl 2) 74:219-223, 1995
7. Aulhorn E, Karmeyer H: Frequency distribution in early glaucomatous visual field defects. Doc Ophthalmol Proc Ser 14:75-83, 1977
8. Lindblom B, Tohrburn W: Functional damage at diagnosis of primary open-angle glaucoma. Acta Ophthalmol (Kbh) 62:223-229, 1984
9. Lindblom B, Tohrburn W: Prevalence of visual field defects due to capsular and simple glaucoma in Halsingland, Sweden. Acta Ophthalmol (Kbh) 60:353-361, 1982
10. Olivus E, Thorburn W: Prognosis of glaucoma simplex and glaucoma capsulare: a comparative study. Acta Ophthalmol (Kbh) 56:921-934, 1978
11. Tarkkanen A: Treatment of chronic open angle glaucoma associated with pseudoexfoliation. Acta Ophthalmol (Kbh) 43:514-523, 1965
12. Horven I: Exfoliation syndrome: incidence and prognosis of glaucoma capsulare in Massachusetts. Arch Ophthalmol 76:505-511, 1966
13. Klouman OF: Pseudoexfoliation in ophthalmic practice. Acta Ophthalmol (Kbh) 45:822-828, 1967
14. Aasved H: The frequency of optic nerve damage and surgical treatment in chronic simplex glaucoma and capsular glaucoma. Acta Ophthalmol (Kbh) 49:589-600, 1971
15. Brusini P, Tosoni C: Use of Bebie curve for perimetric damage staging in glaucoma. Paper presented at the Octopus User's Meeting, Lucerne, 22-24 March 1994

COMPARISON OF DISC SIZE AND DISC DIAMETER AMONG HEALTHY EYES AND EYES WITH LOW-TENSION GLAUCOMA, PRIMARY OPEN-ANGLE GLAUCOMA, AND OCULAR HYPERTENSION

CHRISTA KRAEMER, EUGEN GRAMER and HUBERT MAIER

University Eye Hospital Würzburg, Germany

Introduction

For the biomorphometrical comparison of different forms of glaucoma (*e.g.*, low-tension, primary open-angle, and pigmentary glaucoma), the size of the optic disc[1] as well as the stage of the visual field defect[2] is a necessary basic requirement. The neuroretinal rim area and the size of excavation depend on the size of the optic disc.[3] For example, a large optic disc has a larger cup-disc ratio[1,3] than a smaller disc. It is a matter of controversy whether eyes with low-tension glaucoma have a larger disc size than eyes with primary open-angle glaucoma (POAG), or healthy eyes.[4-9] If eyes with more advanced field loss had larger discs, this could suggest that the size of the disc is a risk factor in glaucoma.

Purpose

The aim of the present study was to answer the following questions:

1. Are there any quantitative differences in eyes with low-tension glaucoma (LTG) and POAG at the same stage of disease in: *a.* horizontal and vertical diameters of the optic disc; and *b.* disc size?
2. Are there any differences in disc size and disc diameter among eyes with LTG, healthy eyes, and eyes with ocular hypertension (OH)?
3. Do eyes with more advanced field loss have a larger disc size in POAG or in LTG compared to eyes with beginning visual field loss? Is optic disc size a risk factor in glaucoma?

Address for correspondence: Prof. E. Gramer, MD, LLD, University Eye Hospital Würzburg, Josef-Schneider-Strasse 11, D-97080 Würzburg, Germany

Perimetry Update 1996/1997, pp. 355–362
Proceedings of the XIIth International Perimetric Society Meeting
Würzburg, Germany, June 4–8, 1996
edited by M. Wall and A. Heijl

Methods

For a quantifying examination of the horizontal and vertical diameters of the optic disc, we used the Laser Tomographic Scanner (LTS) confocal examination technique. The values were not corrected by the length of the axis, but, for this reason, only eyes with a refraction within ±3 D were included. One hundred and fifty-three eyes of 153 patients were examined with the LTS: 53 eyes with POAG, 30 with LTG, 20 with OH, and 50 healthy eyes. Healthy eyes were defined as eyes with a visual acuity of 1.0 or better and a normal visual field (Octopus 201, Program 31 or G1), for example, the second eye of a patient with a perforating injury in the other eye. Because the LTS does not give disc area directly in mm^2, we also examined 105 eyes of 105 patients using the Heidelberg Retina Tomograph (HRT): 49 eyes with POAG, 26 with LTG, ten with OH, and 20 healthy eyes. In an earlier study, we showed that the disc diameters measured with both confocal instruments were identical.[10]

Inclusion criteria were as follows:

1. a Stage I-IV visual field defect, according to the classification of Aulhorn[11]
2. computer perimetry (Octopus perimeter 201, Program 31, GG Program[12])
3. visual acuity of 0.8 or better
4. refraction within ±3 D.

Low-tension glaucoma was defined as glaucoma with a maximum intraocular pressure of 21 mmHg, confirmed by diurnal tension curves. There were no significant differences among Stages I-IV with regard to the central maximum intraocular pressure within the groups of eyes with POAG and LTG. Significance calculations were carried out using the Mann-Whitney-U-test.

Results

Horizontal and vertical disc diameter: Laser Tomographic Scanner measurements

Figure 1 shows the horizontal and vertical disc diameters of the groups (POAG, LTG, OH, and healthy eyes), including all eyes with Stage I-IV visual field loss. The horizontal diameter did not differ significantly from the vertical one within the four groups, except in the eyes with OH. Neither was there any significant difference in horizontal and vertical diameters among the diagnostic groups.

Figures 2 and 3 and Table 1 show the disc diameters with regard to the stages of disease in eyes with POAG and LTG measured with the LTS. Comparing the differences in Stages I-IV in POAG and LTG, we found a significantly smaller horizontal than vertical disc diameter in Stages I and II in POAG ($p<0.01$), resulting on average in a more longitudinal elliptical form of the disc. In Stages I and II in LTG, there was a significantly smaller vertical than horizontal disc diameter ($p<0.01$). This resulted, on average, in a more transversal elliptical form of the disc. In the advanced Stage IV of the disease, there were no significant differences in eyes with POAG or LTG.

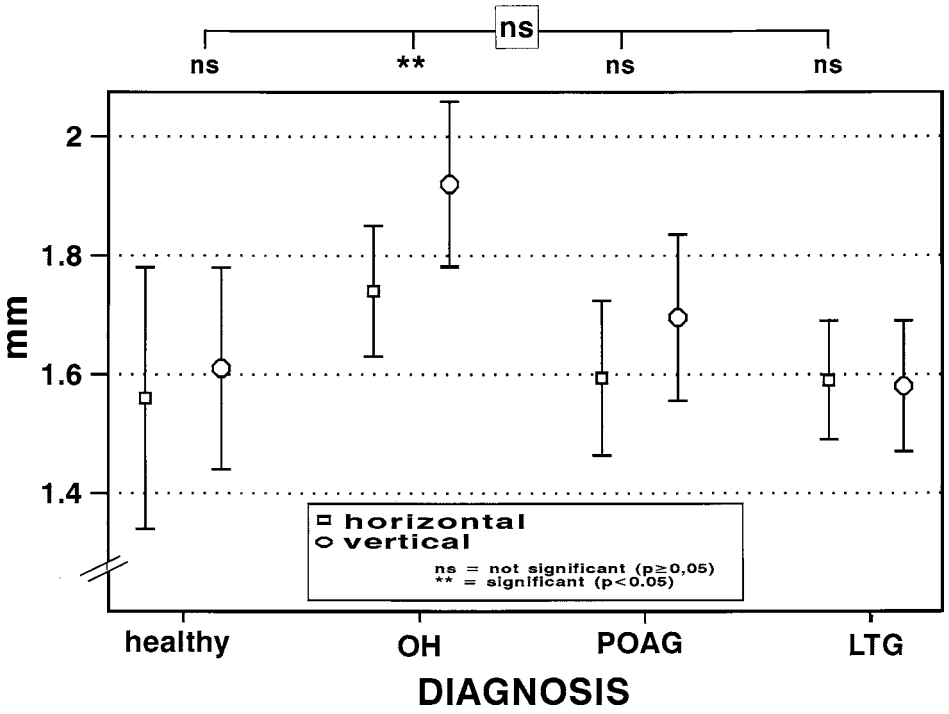

Fig. 1. LTS measurements: correlation between the horizontal and vertical disc diameters (mean value with standard deviation) in healthy eyes, and those with ocular hypertension (OH), primary open-angle glaucoma (POAG), and low-tension glaucoma (LTG) (*n*=153 eyes).

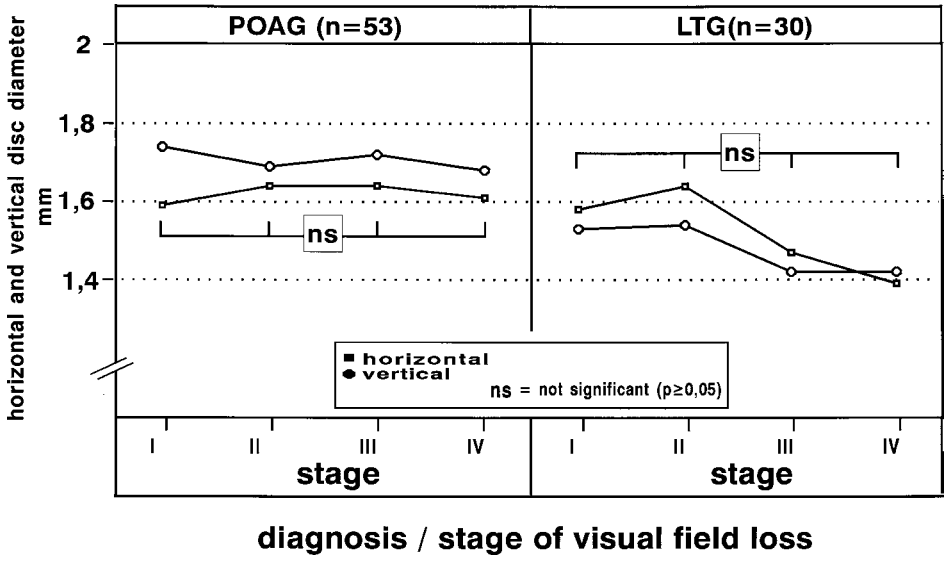

Fig. 2. LTS measurements: horizontal and vertical disc diameters (mean value with standard deviation) in relation to Stages I-IV in POAG (*n*=53) and LTG (*n*=30).

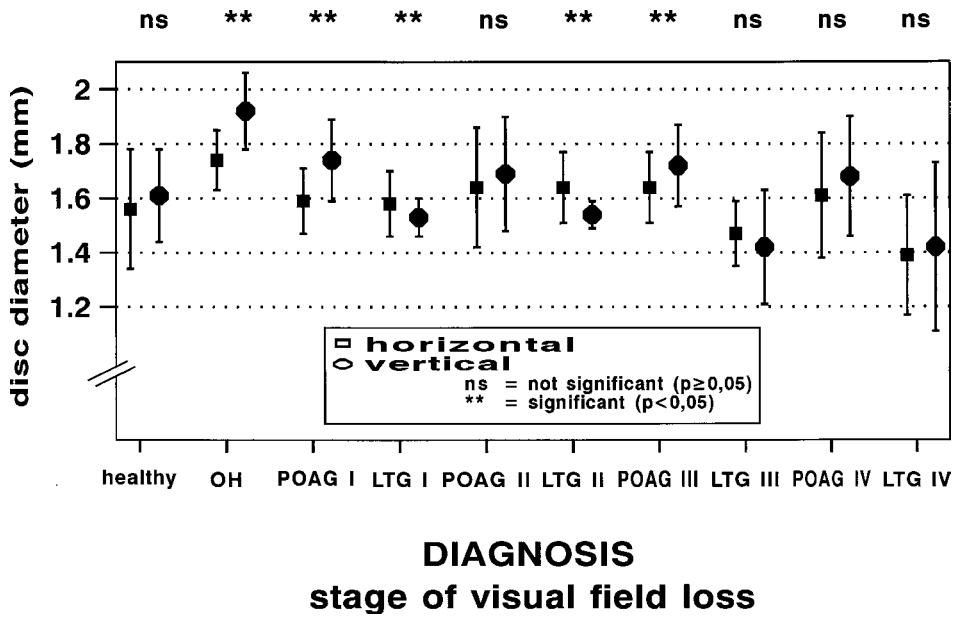

Fig. 3. LTS measurements: horizontal and vertical disc diameters (mean value with standard deviation) in healthy eyes, and eyes with OH, POAG (Stages I-IV) and LTG (Stages I-IV).

Table 1. LTS measurements: horizontal and vertical disc diameters (mean value with standard deviation) in healthy eyes, and eyes with OH, POAG (Stages I-IV) and LTG (Stages I-IV)

Diagnosis	*Stage*	*Patients/ eyes*	*Disc diameter horizontal*	*vertical*	*p*
	I	23	1.59 ± 0.12	1.74 ± 0.15	< 0.001
POAG	II	13	1.64 ± 0.22	1.69 ± 0.21	> 0.05
	III	9	1.64 ± 0.13	1.72 ± 0.15	< 0.01
	IV	8	1.61 ± 0.23	1.68 ± 0.22	> 0.05
	I	10	1.58 ± 0.12	1.53 ± 0.07	< 0.01
LTG	II	9	1.64 ± 0.13	1.54 ± 0.05	< 0.001
	III	5	1.47 ± 0.12	1.42 ± 0.21	> 0.05
	IV	6	1.39 ± 0.22	1.42 ± 0.31	> 0.5
Healthy		50	1.56 ± 0.22	1.61 ± 0.17	> 0.1
OH		20	1.74 ± 0.11	1.92 ± 0.14	< 0.001

Disc diameter and disc size (Heidelberg Retina Tomograph) measurements

Figure 4 and Table 2 show the values for the disc diameters and optic disc size in a further group of patients (n=105) measured with the HRT. The disc diameters were neither significantly different among the groups nor between the stages of POAG and LTG. The disc size was not significantly different among any of the groups (p>0.5).

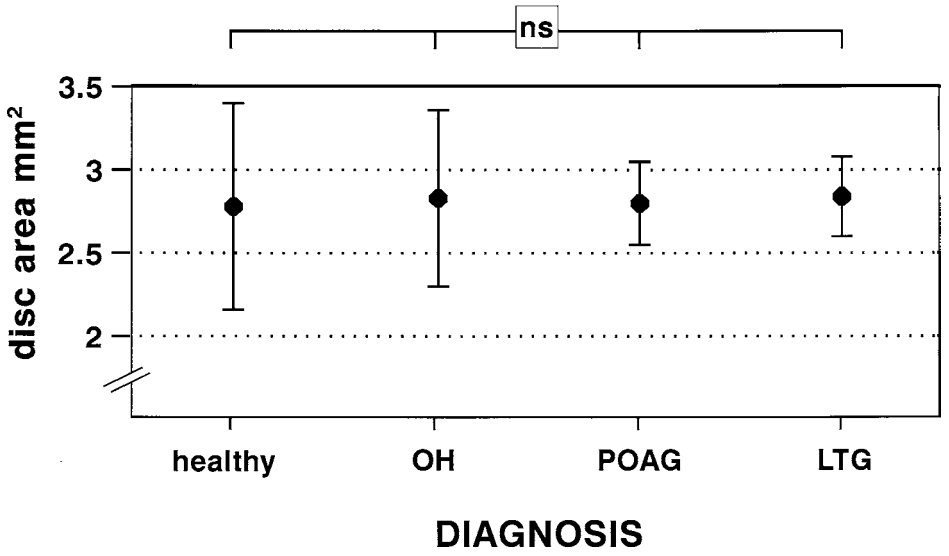

Fig. 4. HRT measurements: disc size (mean value with standard deviation) in healthy eyes, and eyes with OH, POAG and LTG.

Discussion

Disc diameters measured with the LTS and HRT do not indicate larger disc sizes in LTG. Looking at the disc diameters measured with the LTS (see Fig. 3), it appears that discs in eyes with LTG are smaller than those in eyes with POAG, especially in the advanced stages.[13]

We found smaller discs in advanced stages of visual field loss, but this difference was not statistically significant. It has been reported that eyes with multiple defects in the retinal nerve fiber layer,[14] or increased visual field defects, tend to have a smaller optic discs.[15] Other studies have found that the nerve fiber and photoreceptor count is higher in eyes with larger discs, therefore, they have a higher anatomical reserve capacity.[16,17]

However, the differences in disc diameter between the early and advanced stages, measured by us, are not significant, and disc size cannot be calculated from the horizontal and vertical disc diameters alone, because discs may be tilted and the horizontal and vertical diameters may not coincide with the main axis of the oval form of the disc.

Disc diameters measured by the confocal examination technique are in agreement with those measured directly during pars-plana vitrectomy.[18] In our study, the vertical disc diameter in eyes with OH, measured with the LTS, showed a significantly higher value compared to the horizontal disc diameter, but this may be due to the small number of eyes in this group. The measurements with the HRT do not verify this difference, and neither was there a significant difference between the mean disc diameter of eyes with OH compared to eyes from the other diagnostic groups.

A positive correlation between interocular asymmetry of optic disc size of more than 0.01 mm^2 in the same person and greater field loss affecting the eye with the

Table 2. HRT measurements: horizontal and vertical disc diameter and disc size (mean value with standard deviation) in healthy eyes, and eyes with OH, POAG (Stages I-IV) and LTG (Stages I-IV)

Diagnosis		*Eyes/ patients*	*Disc diameter horizontal*	*(mm) vertical*	*p*	*Disc area (mm²)*	*p*
POAG	I	10	1.62 ± 0.31	1.65 ± 0.21	> 0.5	2.67 ± 0.31	
	II	9	1.67 ± 0.17	1.67 ± 0.11	> 0.5	2.78 ± 0.25	
	III	10	1.65 ± 0.22	1.71 ± 0.12	> 0.5	2.82 ± 0.47	
	IV	20	1.65 ± 0.23	1.76 ± 0.31	> 0.1	2.90 ± 0.61	
LTG	I	9	1.74 ± 0.23	1.65 ± 0.11	> 0.1	2.87 ± 0.45	$p > 0.5$
	II	6	1.69 ± 0.12	1.61 ± 0.23	> 0.1	2.72 ± 0.35	
	III	4	1.72 ± 0.31	1.67 ± 0.21	> 0.1	2.87 ± 0.71	
	IV	7	1.69 ± 0.22	1.67 ± 0.25	> 0.1	2.82 ± 0.57	
Healthy		20	1.62 ± 0.15	1.72 ± 0.2	> 0.5	2.78 ± 0.62	
OH		10	1.59 ± 0.22	1.78 ± 0.18	> 0.1	2.83 ± 0.53	

larger disc, seem to support the hypothesis that an eye with a large optic disc may be more vulnerable to a rise in intraocular pressure.[19] But this reported difference may have other reasons, such as different intraocular pressure in each eye.

Differences in disc size between eyes with LTG or POAG, as measured with the HRT, have been reported[4] (on average, 2.4 mm^2 in eyes with LTG, and 2.02 mm^2 in eyes with POAG). Other studies noted a larger disc size in eyes with LTG compared to eyes with POAG, pseudoexfoliative glaucoma and healthy eyes.[5,20] On the other hand, our measurements with the HRT showed no significant difference in disc size between eyes with LTG or POAG.

In another study it was found that eyes with LTG and large visual field defects had smaller discs than those with less visual field loss, and previous findings of unusually large discs in LTG may be substantiated by an artificial selection.[15] The reason for this selection could be the fact that larger discs were more likely to be classified as glaucomatous than small discs.[21]

Conclusions

In eyes with POAG and LTG, HRT and LTS measurements of mean horizontal and vertical disc diameters and mean disc size did not reveal any significant differences. Therefore, *1.* the size of the disc does not appear to be a risk factor in LTG; and *2.* there are no differences in disc diameters of eyes in the early and advanced stages of either POAG or LTG.

Our former studies have shown a larger cup:disc ratio in eyes with LTG,[1,22-25] a smaller mean neuroretinal rim area,[1] a steeper slope and flatter bottom of the excavation,[26,27] and more frequent nerve fiber bundle defects[8] in eyes with LTG compared to eyes with POAG at the same stage of the disease. Furthermore, differences in the topograph of visual field loss in eyes with LTG, POAG, and pigmentary glaucoma[2,25] at the same stage of the disease have been demonstrated. These morphometric disc differences cannot be explained by a larger disc diameter in eyes with LTG than in

POAG. We suggest that eyes with LTG may have less connective tissue in the optic nerve head[22-24] which may be a further risk in LTG with genetic disposition.[22,23,25]

Acknowledgments

This study describes in parts data of the dissertation of Dr. H. Maier.

References

1. Gramer E, Bassler M, Leydhecker W: Cup/disc ratio, excavation volume, neuroretinal rim area of the optic disc in correlation to computer perimetric quantification of visual defects in glaucoma with and without pressure: clinical study with the Rodenstock Optic Nerve Head Analyzer and the program Delta of the Octopus Perimeter 201. Doc Ophthalmol Proc Ser 49:329-348, 1987
2. Gramer E, Althaus G, Leydhecker W: Topography and progression of visual field damage in glaucoma simplex, low tension glaucoma and pigmentary glaucoma with program Delta of Octopus Perimeter 201. Doc Ophthalmol Proc Ser 49:349-363, 1987
3. Gramer E, Siebert M: Optic nerve head measurements: its advantages and its limitations. Int Ophthalmol 13:3-13, 1989
4. Burk ROW, Rohrschneider K, Noack H, Völcker HE: Are large optic nerve heads susceptible to glaucomatous damage at normal intraocular pressure? Graefe's Arch Clin Exp Ophthalmol 230:552-560, 1992
5. Jonas JB: Size of glaucomatous optic discs. Ger J Ophthalmol 1:41-44, 1992
6. Jonas JB, Xu L: Optic disc morphology in eyes after nonarteritic ischemic optic neuropathy. Invest Ophthalmol Vis Sci 34:2260-2265, 1993
7. Jonas JB, Papastathopoulos KL, Panda-Jonas S: Morphology of the retina, choroid and optic nerve in glaucoma. In: Krieglstein GK (ed) Glaucoma Update V, pp 104-117. Heidelberg: Kaden Verlag 1995
8. Mansour AM, Sjoch D, Logani S: Optic disc size in ischemic optic neuropathy. Am J Ophthalmol 106:587-589, 1988
9. Quigley HA, Enger C, Katz J, Sommer A, Scott R, Gilbert D: Risk factors for the development of glaucomatous visual field loss in ocular hypertension. Arch Ophthalmol 112(5):644-649, 1994
10. Maier H, Serguhn S, Gramer E: Darstellbarkeit von Nervenfaserbündeldefekten. Ophthalmologe 92:521-525, 1995
11. Aulhorn E: Visual field defects in chronic glaucoma. In: Heilmann K, Richardson KT (eds) Glaucoma, Conception of a Disease. Stuttgart: George Thieme Verlag 1978
12. Gramer E, Knauth-Spaeth M: Glaukomspezifische Untersuchung des Gesichtsfelds: Eine klinische Studie zum Informationsgehalt der Prüfungsraster des Programms G1 und 31 des Octopus Perimeters 201. In: Gramer E (ed) Glaukom Diagnostik und Therapie, pp 38-59. Stuttgart: Enke 1990
13. Kraemer C, Gramer E, Maier H: Are optic nerve heads larger in low tension glaucoma compared to primary open angle glaucoma? Invest Ophthalmol Vis Sci 37 (Suppl)3:29, 1996
14. Chihara E, Honda Y: Multiple defects in the retinal nerve fiber layer in glaucoma. Graefe's Arch Clin Exp Ophthalmol 230(3):201-205, 1992
15. Jonas JB, Stürmer J, Papaststhopoulos KI, Meier-Gibbons F, Dichtl A: Optic disc size and optic nerve damage in normal pressure glaucoma. Br J Ophthalmol 79(12):1102-1105, 1995
16. Jonas JB, Schmidt AM, Muller-Bergh JA, Schlotzer-Schrehardt UM, Naumann GO: Human optic nerve fiber count and optic disc size. Invest Ophthalmol Vis Sci 33(6):2012-2018, 1992
17. Panda-Jonas S, Jonas JB, Jakobczyk M, Schneider U: Retinal photoreceptor count, retinal surface area and optic disc size in normal human eyes. Ophthalmology 101(3):519-523, 1994
18. Bartz-Schmidt KU, Weber J, Heimann K: Validity of two dimensional data obtained with the Heidelberg Retina Tomograph as verified by direct measurements in normal optic nerve heads. Ger J Ophthalmol 3(6):400-405, 1994
19. Tomita G, Nyman K, Raitta C, Kawamura M: Interocular asymmetry of optic disc size and its

relevance to visual field loss in normal-tension-glaucoma. Graefe's Arch Clin Exp Ophthalmol 232(5):290-296, 1994
20. Tuulonen A, Airaksinen PJ: Optic disc size in exfoliative, primary open angle and low tension glaucoma. Arch Ophthalmol 110(2):211-213, 1992
21. Heijl A, Molder H: Optic disc diameter influences the ability to detect glaucomatous disc damage. Acta Ophthalmol (Kbh) 71(1):122-129, 1993
22. Gramer E: Risk factors in glaucoma: clinical studies. In: Krieglstein GK (ed) Glaucoma Update V, pp 14-31. Heidelberg: Kaden Verlag 1995
23. Gramer E: General risk factors in glaucoma. Ger J Ophthalmol 4 (Suppl) 37: 1995
24. Gramer E, Leydhecker W: Glaukom ohne Hochdruck: Eine klinische Studie. Klin Mbl Augenheilk 186:262-267, 1985
25. Gramer E, Tausch M: The risk profile of the glaucomatous patient. Curr Opin Ophthalmol 6:78-88, 1995
26. Gramer E, Maier H, Messmer EM: A measure of the thickness of the nerve fiber layer and the configuration of the optic disc excavation in glaucoma patients: a clinical study using the laser tomographic scanner. In: Mills RP (ed) Perimetry Update, pp 207-213. Amsterdam/New York: Kugler Publ 1993
27. Maier H, Siebert M, Gramer E: Unterschiede in der Form der Papillenexcavation bei Glaucoma chronicum simplex und Glaukom ohne Hochdruck: eine klinische Studie. In: Gramer E, Kampik A (eds) Pharmakotherapie am Auge, pp 29-71. Berlin/Heidelberg/New York: Springer Verlag 1992

NEURO-OPHTHALMOLOGY

RECONSIDERATION OF VISUAL FIELD INCONGRUENCE

Lars Frisén

Institute of Clinical Neuroscience, Division of Ophthalmology, University of Göteborg, Sweden

Abstract

Forty-nine subjects with homonymous relative visual field defects due to a variety of intracranial lesions were studied by high-pass resolution perimetry. Statistical analysis balanced for learning and fatigue effects revealed significant incongruence in 15 cases, usually with a slightly larger defect contralateral to the lesion. There was no clear relationship between incongruence and locations or natures of underlying lesions. Instead, methodological and pathophysiological considerations suggested that incongruence was the outcome of individually peculiar interactions between fine anatomical details, varying spatial distributions of neural conduction defects, and various measurement problems. Hence, incongruence emerged as an epiphenomenon of negligible clinical relevance.

Introduction

Congruence is a term used to describe certain homonymous visual field defects and denotes closely similar shapes of field remnants in both eyes. Conversely, incongruence designates dissimilar field remnants. Following Wilbrand,[1] incongruence has attracted interest as an aid for topographic diagnosis. Contemporary textbooks continue a long tradition of emphasizing incongruence with lesions of the optic tract.[2,3] However, modern clinical and experimental studies lend little support to this notion.[4-7] Incongruence is more commonly due to lesions of the suprageniculate visual pathways, but its diagnostic value is reduced by considerable interindividual variability.[8]

Previous studies have focused on the location of the outer borders of the field remnants or the so-called absolute part of the field defects. Usually, there are also defects inside the field borders in the form of threshold elevations or relative defects. These may also show incongruence, *e.g.*, in the form of isopter asymmetries (Fig. 1). Study of relative defects is ideally suited for the static threshold approach of computer-assisted perimetry (CAP). Other advantages include freedom from examiner influences and potential for balancing for learning and fatigue effects, none of which could be realized previously. As CAP increasingly replaces traditional forms of perimetry and also shifts emphasis to the field inside some 30° of eccentricity, a CAP

Address for correspondence: Lars Frisén, MD, PhD, Ögondivisionen, Sahglgrenska Sjukhuset, S-413 45 Göteborg, Sweden

Perimetry Update 1996/1997, pp. 365–376
Proceedings of the XIIth International Perimetric Society Meeting
Würzburg, Germany, June 4–8, 1996
edited by M. Wall and A. Heijl

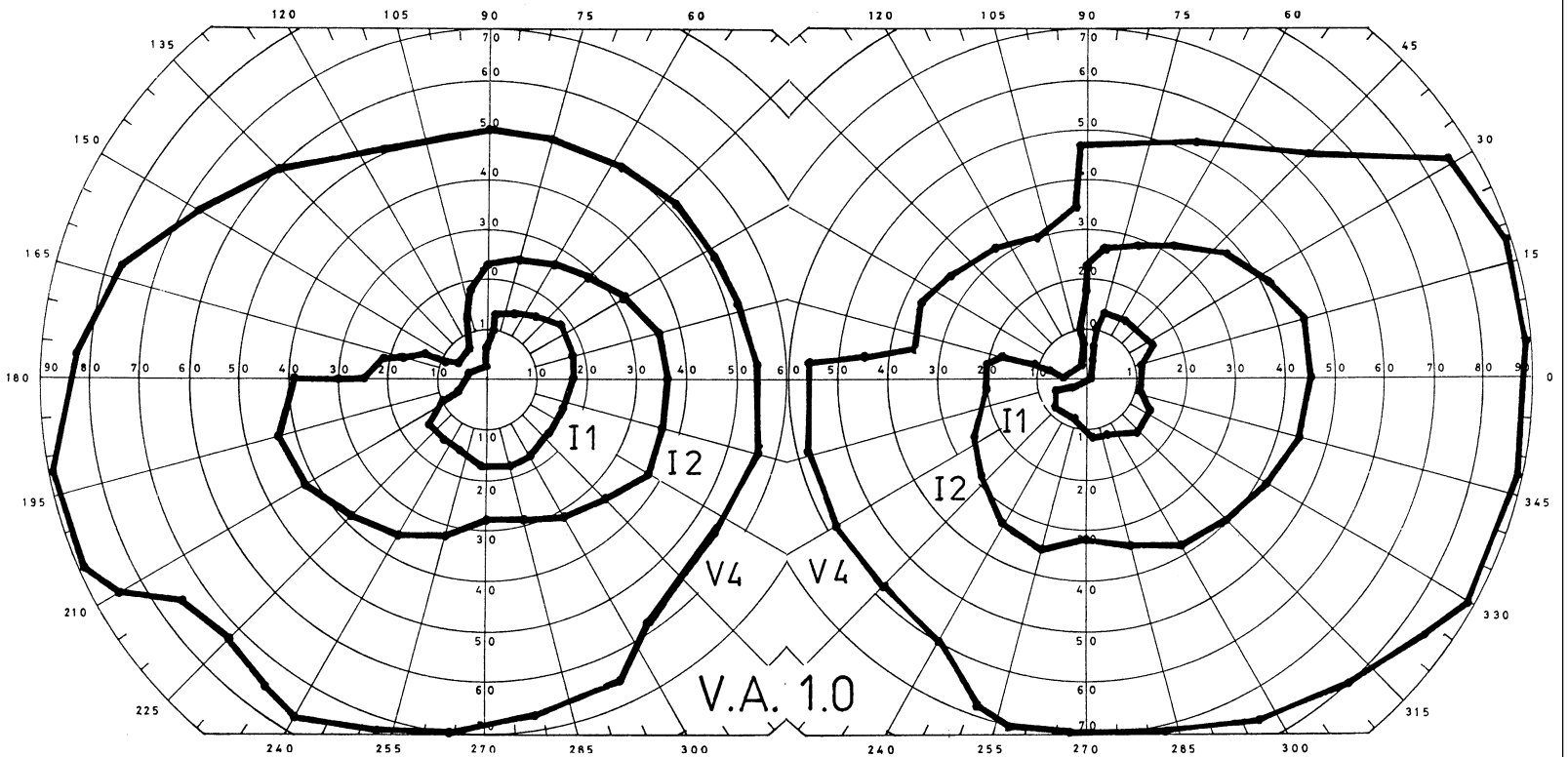

Fig. 1. Results of manual kinetic perimetry in a subject with a right temporal lobe glioma and a left homonymous visual field defect. Note that asymmetry of isopters is not confined to outer borders. Lack of both optic atrophy and a contralateral, relative afferent pupil defect indicated sparing of the optic tract. Inset: target designations (Goldmann format), and decimal visual acuity.

examination of congruence and incongruence in homonymous relative field defects appears well motivated.

This study reports on CAP results from 49 consecutive patients who presented a wide spectrum of locations and natures of lesions. Fields were mapped with high-pass resolution perimetry (HRP), which has a comparatively small variability and a short test duration. HRP results are qualitatively closely similar to those of conventional perimetry; sensitivity and specificity are also closely comparable.[9,10]

Subjects and methods

Visual field records were drawn retrospectively from the local neuro-ophthalmological database. Records were reviewed in order of acquisition, scrutinizing both the graphic plots and the automatically provided statistical indices and the full clinical picture. For inclusion in the present study, the following conditions had to be met:
1. Presence of a purely relative homonymous visual field defect involving more than three test locations in each eye.
2. Computer-assisted or magnetic resonance tomographic evidence of a single intracranial lesion involving the retrochiasmal visual pathways. Lesions had to be reasonably well defined. Traumatic lesions were rejected.
3. Lack of other causes of visual defects.
4. Lack of motor and sensory causes of poor fixation.

Forty-nine pairs of field records met the above criteria. The field defects were classified by inspection as upper quadrant (n = 11), lower quadrant (n = 12), or both (n = 26). Twenty-three pairs showed left homonymous defects. Their laterality was flipped to make all defects right-sided to facilitate the numerical analysis. Mean subject age was 49 ± 14 (SD) years.

Fifty consecutive pairs of normal visual field records were also retrieved, to serve as controls. Laterality was flipped for some, to counteract a possible effect of which eye in each pair was examined first. This made the examination sequences exactly the same in the normal and abnormal groups. Mean subject age was 45 ± 14 years.

Perimetry

HRP was done using the Ophthimus Ring Perimeter (HighTech Vision, Göteborg, Sweden), a computer graphics device for measuring resolution thresholds in 50 locations inside 30° of eccentricity.[10] Targets were ring-shaped, with a bright core and dark borders. Space-average luminance was 20 cd/m^2, equal to the background. Contrast was 0.25. These conditions served to close the gap between detection and resolution thresholds, making the test task very simple. Thresholds were defined as the size of the smallest discernible target at each location, varying target sizes in 0.1 log unit increments. In analogy with the procedure in conventional CAP, this interval will be termed one decibel (dB) in the following. Fixation was monitored by occasionally projecting a target inside the blind spot.

Data reductions

Because most subjects were naive to perimetry, learning and fatigue effects were of great concern.[11-13] The solution selected here was to express severity of the field

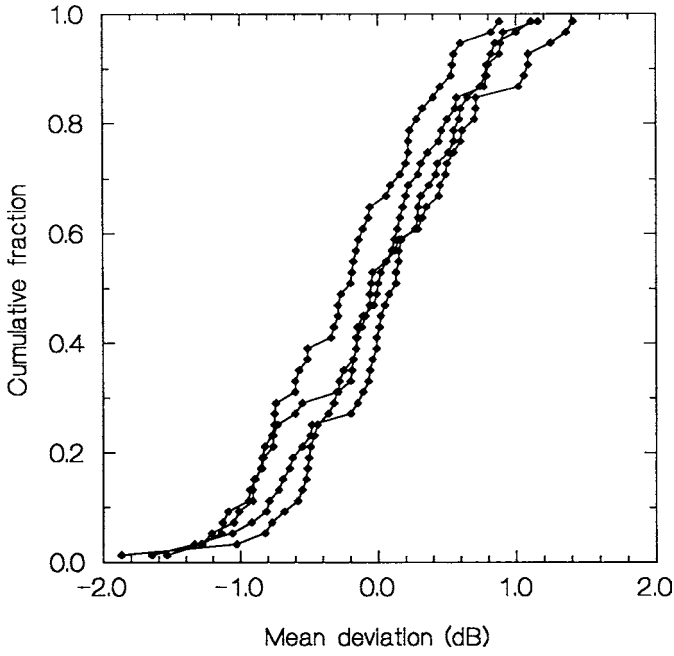

Fig. 2. Cumulative frequency distributions of mean deviations in four test quadrants (upper and lower nasal in the left eye, and upper and lower temporal in the right eye) in 50 normal subjects. See text for full explanation.

Table 1. Comparisons of left (L) and right (R) eye quadrant mean deviations in abnormal hemifields in three patient groups

	Visual field defect		
Statistic *No. of subjects*	*Upper quadrant* *11*	*Lower quadrant* *12*	*Hemifield* *26*
L/R correlation coefficient	0.853 p=0.001	0.875 p<<0.001	0.651 p<<0.001
Linear regressions	L=1.167*R-0.416 p=0.001, 0.709	L=0.754*R+0.359 p<<0.001, 0.425	L=0.699*R+0.821 p<<0.001, 0.169
Linear regressions with origin constraint	L=1.084*R p<<0.001	L=0.857*R p<<0.001	L=0.923*R p<<0.001
No. of incongruent field pairs with larger defect on L/R side	3 / 2	0 / 3	2 / 5

defect relative to the same eye's normal (reference) hemifield, a procedure which also circumvents the problem of other normally occurring interocular differences.[14]

Use of raw threshold data is not appropriate because threshold surface characteristics normally differ between temporal and nasal hemifields. Instead, point-wise deviations from average normal adjusted for age, were used. In normal eyes, these average zero by definition. Reference values were obtained from the normal HRP database, which comprises 215 perimetrically naive subjects, with 30 subjects per decade in the 10-to-80 years age range. Test locations situated on the main meridians were excluded from analysis; the number of remaining locations in each quadrant ranged between eight (upper temporal) and 12 (lower nasal).

For each eye, point-wise deviations were averaged within the reference (left) hemifield and within each quadrant of the test (right) hemifield. Then, the reference hemifield mean deviation was subtracted from mean deviations of the two test quadrants, producing one upper- and one lower-quadrant mean deviation statistic for each eye. Finally, these statistics were compared among pairs of eyes to illuminate congruence.

Statistical analyses used Systat version 5.01 (Systat Inc, Evanston, IL); p values < 0.05 were considered statistically significant.

Results

In the normal subjects, mean deviations for the test quadrants averaged close to 0 dB, as expected (Fig. 2). Approximately 95% of observations were contained inside the ±1.0 dB range, which then can serve to define normal limits. The variability is attributable to normal variants of threshold surface shapes and other individual factors.

Figures 3 to 5 show quadrant mean deviations for patients with homonymous relative visual field defects in the upper or lower quadrants, or both. Generally, magnitudes of defects were similar in each patient's two eyes, with correlation coefficients ranging between 0.69 and 0.88. Linear least squares regressions revealed slopes significantly larger than zero in all instances, whereas constants were not significant (Table 1). Because average normal quadrant deviations equal zero (Fig. 2), it can be argued that the regressions should include the origin. Under this constraint, slopes were close to unity (Table 1).

A statistical definition of incongruence should build on observed distributions in normals of differences between homonymous pairs of test quadrants. These distributions were nearly identical to those shown in Figure 2, so the same cut-off limit, 1.0 dB, was used. So defined, incongruous defects were identified in 25-45% of cases within the three patient groups, depending on the spatial distribution of the field defect (Table 1, Figures 3 to 5, triangular symbols). Incongruence was most common with upper quadrant defects, with three instances (out of 11) of larger defects ipsilaterally, and two contralaterally. For the other defect types, there was a preponderance of larger defects contralaterally.

Among the incongruous field pairs, absolute pair-wise differences in test quadrant mean deviations averaged 1.95 ± 0.62 (SD, $n = 5$) dB for upper quadrant defects, 1.21 ± 0.25 ($n = 3$) for lower quadrant defects, and 1.65 ± 0.32 ($n = 7$) for combined defects. Hence, incongruence in excess of normal interocular variability, 1.0 dB,

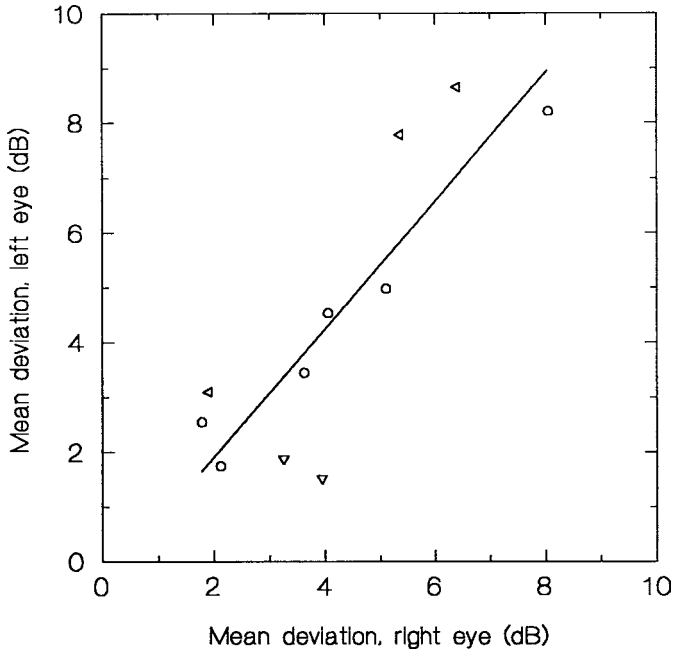

Fig. 3. Quadrant mean deviations in 11 subjects with upper quadrant field defects homonymous to the right. Circles represent cases with congruent defects. Arrowheads represent cases with incongruent defects; arrowheads point to side of greater involvement. Inset: linear least squares regression over all datum points.

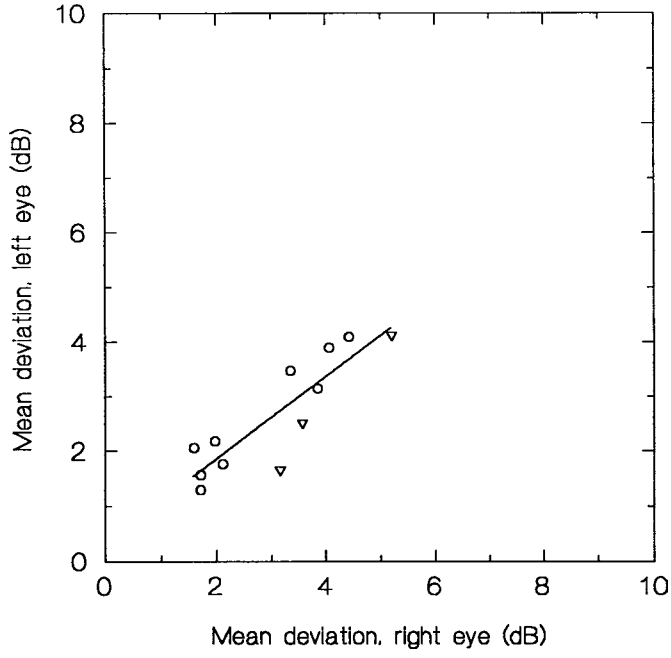

Fig. 4. Quadrant mean deviations in 12 subjects with lower quadrant field defects homonymous to the right. See legend to Figure 3 for explanation of symbols.

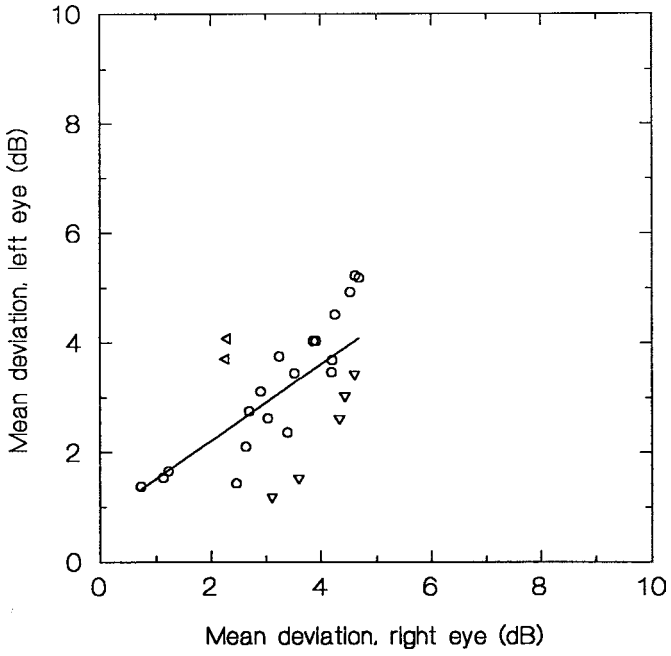

Fig. 5. Hemifield mean deviations in 27 subjects with both upper and lower quadrant field defects homonymous to the right. See legend to Figure 3 for explanation of symbols.

Table 2. Locations and natures of lesions

Location	*No. of cases*	*No. (%) with congruent field defects*	*Pathology (No. if > 1)*
Optic tract, LGB	5	3 (60)	Aneurysm (2), angioma, hematoma, glioma
Temporal	13	10 (77)	Glioma (5), meningioma (2), AVM (2), infarct (2), hematoma, metastasis
Temporoparietal	4	2 (50)	Infarct (4)
Temporo-occipital	5	4 (80)	Infarct (4), AVM
Parietal	3	1 (33)	Hematoma (2), infarct
Parieto-occipital	7	4 (57)	Glioma (2), infarct (2), hematoma (2), giant MS plaque
Occipital	12	10 (83)	Infarct (6), metastasis (3), AVM (2), hematoma

LGB: lateral geniculate body; AVM: arteriovenous malformation

averaged only 0.21-0.95 dB. Its degree did not appear to be related to overall severity of field loss (Figs. 3-5).

As to topography of visual pathway lesions, it was often difficult to decide on precise loci. Major obstacles included inability to directly visualize on neuro-imaging most constituents of the visual pathway, and lesion-mediated distortions of normal

topography. Lesions were often large enough to involve several centimeters worth of pathway. Further, some irregularly shaped lesions might have involved the pathway in widely spaced locations. Hence, only a loose, lobe-centered classification of locus of involvement was possible. Cross-correlation with the nature of the visual field defects revealed no location which was exclusively associated with either congruous or incongruous visual field defects (Table 2).

Discussion

Fifteen of 49 consecutive patients with homonymous relative visual field defects presented some incongruence in the present series for an overall frequency of 31%. Incongruence was most common with upper quadrant field defects, but laterality of the larger defect was variable. Combining all defects, there was a preponderance of larger defects contralateral to the lesion. In most instances, the degree of asymmetry was fairly small, on average exceeding the 95th percentile for normal interocular differences by less than 1.0 dB. Asymmetry of this magnitude may be difficult to detect by inspection of field plots.

Comparisons with previous studies are difficult because of their different focus of attention. Locations of defect borders cannot be compared directly with threshold levels in remaining field areas as studied here. It is possible to examine strengths and weaknesses of each approach, however.

Methodological aspects

Variability

All forms of perimetry are associated with several sources of error, some of which have been clarified only recently. CAP has highlighted a considerable variability associated with visual field examinations and important effects of learning and fatigue.[11-15] Normal variation between individuals is substantial and in part attributable to quantitative variations in the neural substrate.[16-18] Subjects with neurological disorders may be particularly prone to variation. In the present study, reference hemifield mean scores presented a 37% larger range in patients than in controls (5.5 versus 4.0 dB).

Kinetic versus static perimetry

Previous studies depended exclusively on manual kinetic perimetry, which is associated with some unique sources of variation. These include characteristics of target movement (which are difficult to standardize), subject's and examiner's reaction times, and plotting errors. Computer-assisted kinetic perimetry may be better controlled in these cases, but has not found widespread acceptance. In the following, CAP refers to the static counterpart exclusively.

It has long been held that occipital injuries may raise kinetic and static thresholds to different degrees, to produce so-called statokinetic dissociation. Riddoch[19] was the first to report that field remnants in cases with occipital lesions were larger when mapped with moving targets. Later studies have shown similar dissociations with other locations of damage, even of the eye itself. Actually, the normal visual system shows superior sensitivity to movement. Proving larger than normal degrees of dis-

sociation requires instrumental safeguards and analytical tools that were not available to early investigators.[20,21]

Cartographic deformations

Observations originating from a perimetric cupola cannot be transferred to a plane visual field map without introducing errors. Conventional maps, which build on a so-called polar equidistant projection, represent only polar angles and meridional distances correctly, and are inappropriate for area measurements.[22] Because cartographic errors generally increase with increasing eccentricity, visual field borders will generally be more severely affected than observations obtained inside the borders. This is true also for the somewhat different mapping procedures used in CAP, including HRP.[23] However, cartographic errors are immaterial when comparing threshold levels in symmetrical field locations.

CAP and HRP

CAP may not be the best tool for definition of field borders because static border searches tend to become very time-consuming. HRP suffers an another disadvantage in this regard as it uses target size as the test variable. This makes for a somewhat loose rendition of steep threshold gradients. In this context, it should be noted that HRP statistics are not exactly comparable to those of conventional CAP. One important difference applies to variability. In ordinary, differential light sense (DLS) perimetry, variability is influenced by test location and threshold level, none of which play a role in HRP.[24,25] Further, HRP is held to directly reflect the number of functional retinocortical neural channels, whereas the neurophysiological substrate of DLS as yet is incompletely understood.[18] Nevertheless, DLS and HRP field maps are qualitatively closely similar.[9,10]

Role of neural substrate gradients

In the normal visual field, more peripheral parts are served by smaller numbers of neural units, and the actual field borders depend on the very smallest numbers.[16-18] As a first approximation, the same features can be assumed to apply to depressed visual fields, where the numbers of functional neural units presumably are correspondingly reduced.[26] In such circumstances, locations at the very border may be served by very small numbers of neural units, perhaps even single ones. Consequently, the position of the field border may well be excessively sensitive to random events on the axonal level within the underlying lesion. Thresholds measured inside the borders are likely to be served by larger numbers of neural units, and should be less sensitive to such random events.

Depending on larger numbers of neural units, thresholds can be held to reflect the state of the main body of surviving neural units in a way that border mappings never can aspire to do. The reasoning raises the interesting question whether congruence/incongruence should be decided on minority or majority votes, *i.e.*, border mappings or threshold measurements. The decision is simple only in the special case of pure absolute defects, which by definition exclude threshold abnormalities inside the defect border.

The present mode of analysis presupposes elevation of thresholds in more than a few test locations. Spatially restricted field defects, *e.g.*, homonymous scotomata

located to quadrant apices, may well fail to raise quadrant mean deviations beyond the normal range. None of the cases studied here belonged to this category.

Interpretation of incongruence

True incongruence is naturally attributable to dissimilar degrees of damage to homonymous nerve fibers from each eye, predisposed by spatial separation of the two fiber sets or parts of the sets. Whereas such a separation indeed is plausible, it does not follow that its characteristics are exactly the same in all individuals. Indeed, modern measurements have shown that the optic radiation's dimensions and position vary considerably.[27] Similarly, individual variability in fiber arrangements is likely to be substantial. Such variations could suffice to explain why even controlled surgical lesions can produce conflicting results. For example, temporal lobe surgery for epilepsy has variously been reported to produce consistently congruent defects,[28] or consistently incongruent defects, larger on the side of the lesion,[29] or mixed outcomes, sometimes with larger defects on the contralateral side.[30]

There is yet another factor likely to be involved in the production of incongruence, namely the nature of the lesion. The lateral geniculate body (LGB) offers a particularly good example of how different forms of lesions in one and the same well-defined location may cause radically different types of visual field defects. In the LGB, most ischemic lesions are associated with one out of two distinctive (but not pathognomonic) varieties of perfectly congruent homonymous visual field defects, *viz.* quadruple sectoranopia or horizontal sectoranopia. These are attributable to infarction of anterior and lateral choroidal artery territories, respectively.[31,32] On the other hand, infiltration of the LGB by tumor is typically associated with grossly incongruent field defects.[33,34] The difference can be understood in terms of territorial respect. The extent of infarcts are governed by vascular territories, which in the LGB encompass precisely registered synapsing columns from both eyes.[31] Conversely, infiltration by tumor can proceed in a disorderly fashion, *e.g.*, skipping columns or destroying only parts of columns.

Reasoning in reverse, *e.g.*, proposing that all incongruent field defects are caused by tumors, is patently incorrect. Clinical experience dictates that there are several alternatives, including vascular lesions. This is easier to conceive for threshold elevations than for border positions because of the latter's greater dependence on the fates of single axons. Threshold elevations that are uniformly distributed across the visual field can be taken to reflect a spatially uniform block of conduction across the visual pathway, or a spatially uniform attrition of axons at the site of the lesion. Further, non-uniform distributions of threshold elevations can be taken to reflect non-uniform spatial gradients of damage. This latter model has the potential to produce incongruence, by differentially affecting crossing and non-crossing sets of fibers, or parts of these sets. Whether the field defects become larger on one side or the other, or become equal, would then depend on the spatial distribution of the gradient relative to local retinotopic characteristics. Intuitively, the latter should be more loosely defined in the fiber pathways than in the synapsing stations, simply because precise appositioning seemingly is functionally irrelevant in the former and essential in the latter. Similarly, vascular territories may be more variable in the pathways. Hence, even localized infarcts might cause considerable incongruence, provided that they take place outside the LGB and the primary visual cortex. Chances for such an outcome would seem best in locations where visual pathway fibers are spread furthest

apart, *i.e.*, in the temporal lobe and in the occipital lobe (excluding striate cortex).

Conclusions

From the above considerations, it seems sound to view incongruence as the outcome of individually peculiar interactions among fine anatomical details, varying spatial distributions of conduction deficits, and measurement problems. In such circumstances, incongruence holds little promise for clinical relevance.

References

1. Wilbrand H: Die hemianopischen Gesichtsfeld-Formen und das optische Wahrnehmungszentrum: ein Atlas hemianopischer Defekte. Wiesbaden: Bergmann 1890
2. Gloor B: Perimetrie mit besonderer Berücksichtigung der automatischen Perimetrie. Stuttgart: Enke 1993
3. Lachenmayr BJ, Vivell PMO: Perimetry and Its Clinical Correlations. New York, NY: Thieme 1993
4. Frisén L: The neurology of visual acuity. Brain 103:639-670, 1980
5. Newman SA, Miller NR: Optic tract syndrome: neuro-ophthalmological considerations. Arch Ophthalmol 101:1241-1250, 1983
6. Rosenblatt MA, Behrens MM, Zweifach PH, Forman S, Odel JG, Duncan CM, Gross SA: Magnetic resonance imaging of optic tract involvement in multiple sclerosis. Am J Ophthalmol 104:74-79, 1987
7. Reese BE, Cowey A: Segregation of functionally distinct axons in the monkey's optic tract. Nature 331:350-351, 1988
8. Engler U, Zihl J, Pöppel E: Incongruity of homonymous visual field defects. Clin Vis Sci 8:355-363, 1993
9. Lindblom B, Hoyt WF: High-pass resolution perimetry in neuro-ophthalmology: clinical impressions. Ophthalmology 99:700-705, 1992
10. Frisén L: High-pass resolution perimetry: a clinical review. Doc Ophthalmol 83:1-25, 1993
11. Heijl A, Lindgren G, Olsson J: The effect of perimetric experience in normal subjects. Arch Ophthalmol 107:81-96, 1989
12. Martin-Boglind L, Wanger P: The influence of feedback devices, learning and cheating on the results of high-pass resolution perimetry. In: Heijl A (ed) Perimetry Update 1988/89, pp 393-398. Amsterdam/Milano: Kugler & Ghedini Publ 1989
13. Hudson C, Wild JM, O'Neill EC: Fatigue effects during a single session of automated static threshold perimetry. Invest Ophthalmol Vis Sci 35:268-280, 1994
14. Brenton RS, Phelps CD, Rojas P, Woolson RF: Interocular differences of the visual field in normal subjects. Invest Ophthalmol Vis Sci 27:799-805, 1986
15. Bebie H, Fankhauser F, Spahr J: Static perimetry: accuracy and fluctuations. Acta Ophthalmol (Kbh) 54:339-348, 1976
16. Curcio CA, Allen KA: Topography of ganglion cells in human retina. J Comp Neurol 300:5-25, 1990
17. Frisén L: High-pass resolution perimetry and age-related loss of visual pathway neurons. Acta Ophthalmol (Kbh) 69:511-515, 1991
18. Frisén L: High-pass resolution perimetry: central-field neuroretinal correlates. Vision Res 35:293-301, 1995
19. Riddoch G: Dissociation of visual perceptions due to occipital injuries, with especial reference to appreciation of movement. Brain 40:15-57, 1917
20. Hudson C, Wild JM: Assessment of physiologic statokinetic dissociation by automated perimetry. Invest Ophthalmol Vis Sci 33:3162-3168, 1992
21. Plant GT, Laxer KD, Barbaro NM, Schiffman JS, Nakayama K: Impaired visual motion perception in the contralateral hemifield following unilateral posterior cerebral lesions in humans. Brain 116:1303-1335, 1993
22. Frisén L: The cartographic deformations of the visual field. Ophthalmologica 161:38-54, 1970

23. Frisén L: Cartographic deformations in orthogonal perimetric maps. Doc Ophthalmol Proc Ser 42:113-118, 1985
24. Chauhan BC, House PH: Intratest variability in conventional and high-pass resolution perimetry. Ophthalmology 98:79-83, 1991
25. Wall M, Lefante J, Conway M: Variability of high-pass resolution perimetry in normals and patients with idiopathic intracranial hypertension. Invest Ophthalmol Vis Sci 32:3091-3095, 1991
26. Van Buren JM: The Retinal Ganglion Cell Layer. Springfield, IL: Charles C Thomas 1973
27. Ebeling U, Reulen HJ: Neurosurgical topography of the optic radiation in the temporal lobe. Acta Neurochir 92:29-36, 1988
28. Falconer MA, Wilson JL: Visual field changes following anterior temporal lobectomy: their significance in relation to 'Meyer's loop' of the optic radiation. Brain 81:1-14, 1958
29. Babb TL, Wilson CL, Crandall PH: Asymmetry and ventral course of the human geniculostriate pathway as determined by hippocampal visual evoked potentials and subsequent visual field defects after temporal lobectomy. Exp Brain Res 47:317-328, 1982
30. Marino R, Rasmussen T: Visual field changes after temporal lobectomy in man. Neurology 18:825-835, 1968
31. Frisén L, Holmegaard L, Rosencrantz M: Sectorial optic atrophy and homonymous, horizontal sectoranopia: a lateral choroidal artery syndrome? J Neurol Neurosurg Psychiat 41:374-380, 1978
32. Frisén L: Quadruple sectoranopia and sectorial optic atrophy: a distal anterior choroidal syndrome. J Neurol Neurosurg Psychiat 42:590-594, 1979
33. Gunderson CH, Hoyt WF: Geniculate hemianopia: incongruous homonymous field defects in two patients with partial lesions of the lateral geniculate nucleus. J Neurol Neurosurg Psychiat 34:1-6, 1971
34. Shacklett DE, O'Conner PS, Dorwart RH, Linn D, Carter JE: Congruous and incongruous visual field defects with lesions of the lateral geniculate nucleus. Am J Ophthalmol 98:283-290, 1984

MACULAR SPARING IN PATIENTS WITH HEMIANOPSIA
Re-evaluated using static and kinetic fundus perimetry*

KLAUS ROHRSCHNEIDER[1], ROLAND GLÜCK[1], THOMAS FENDRICH[2], REINHARD O.W. BURK[1], FRIEDRICH E. KRUSE[1] and H.E. VÖLCKER[1]

[1]Department of Ophthalmology and [2]Institute of Applied Physics, University of Heidelberg, Heidelberg, Germany

Abstract

Background: It has been suggested that macular sparing in patients with hemianopsia is a perimetric artifact. The authors have re-evaluated this finding by use of their kinetic and static threshold fundus perimetry with the scanning laser ophthalmoscope.
Methods: Twenty eyes of 13 patients with homonymous hemianopsia were examined using conventional Goldmann perimetry as well as automated static and kinetic fundus perimetry with simultaneous documentation of the point of fixation by use of the scanning laser ophthalmoscope.
Results: The findings obtained with either kinetic procedure were identical. Ten eyes showed an area of residual visual field inside the scotomatous hemifield, *i.e.*, a macular sparing. The comparison of the behavior of fixation during fundus perimetry showed no difference between these eyes and those without sparing. There were no straight horizontal movements during stimulus presentation.
Conclusions: The finding of a true macular sparing in patients with homonymous hemianopsia was reliably observed with both kinetic perimetry procedures. The difference, compared to the results obtained by Bischoff *et al*.,[8] is most likely due to the manual static test procedure used by that group. Findings from MRI investigations suggest that different sites of damage cause variable degrees of macular involvement. This supports the authors' conclusion that macular sparing does exist.

Introduction

The observation of a hemianopic visual field defect is a typical finding in patients with specific neurological diseases. While this field defect respects the vertical margin very sharply, there may be a sparing of the macular area, leading to an island of vision in the contralateral and otherwise anopic field. The observation of macular sparing may be helpful in differentiating the location of the site of the pathological process.[1,2] Since the beginning of this century, many hypotheses have been presented to explain the phenomenon of macular sparing,[3-7] three of which are still under

*The authors have no proprietary interest in any of the materials used in this study.

Address for correspondence: Klaus Rohrschneider, MD, Univ.-Augenklinik, Im Neuenheimer Feld 400, D-69120 Heidelberg, Germany

Perimetry Update 1996/1997, pp. 377–385
Proceedings of the XIIth International Perimetric Society Meeting
Würzburg, Germany, June 4–8, 1996
edited by M. Wall and A. Heijl

discussion.[8] Besides the thesis of double representation of the macula in both sides of the occiput,[5,9] incomplete damage may lead to the phenomenon of macular sparing as proposed by Wilbrand in 1926.[6] The third possible explanation is the effect of unstable fixation during visual field examination in patients with hemianopsia. It has been noted that there might be some degree of variation during conventional automated perimetry, even in normals.[10]

Most recently, Bischoff and coworkers have evaluated the finding of macular sparing in hemianopsia, using manual static fundus perimetry, as supplied with the original Rodenstock Scanning Laser Ophthalmoscope (SLO), and have found the sparing to be a perimetric artifact.[8] They concluded that there is a shift of the point of fixation in the direction of the anopic retina in patients with bilateral hemianopsia, leading to an artificial perifoveal island of vision. Nevertheless, this group compared only kinetic conventional visual fields, as obtained using the Goldmann perimeter with the static fields as achieved by manual tracking with the SLO.

Since we have recently developed automated static threshold perimetry[11] and kinetic fundus perimetry[12] for the SLO, both of them with exact documentation of the point of fixation during stimulus presentation, we wanted to re-evaluate these findings in hemianopic patients. We especially wanted to know whether saccadic eye movements exist towards the hemianopic retina which are observable during the stimulus presentation. Additionally, we looked for differences in the observation of macular sparing between static and kinetic perimetry.

Patients and methods

Twenty eyes of 14 patients with homonymous hemianopsia were included in this study (seven males and seven females, aged 22-76 years). The remaining eyes were excluded due to missing visual fields following decreased function up to blindness or reduced compliance. The location and cause of the hemianopsia varied (ischemic insults, tumors [*i.e.*, astrocytoma], chondroma after surgery, intracerebral bleeding following lysis for myocardial infarction). Routine ophthalmic examination included visual acuity, tonometry and stereoscopic fundus examination using the 78-D lens or the Goldmann three-mirror lens.

Conventional kinetic perimetry with the Goldmann perimeter was performed in all eyes included in the study. In addition, ten eyes of five patients underwent computerized static threshold perimetry with the Octopus 500 (Interzeag, Switzerland).

The principle of the SLO (Rodenstock, Ottobrunn, Germany) has been described earlier.[13,14] In brief, the SLO projects a helium neon laser beam (632.8 nm) and an infrared diode laser (780 nm) simultaneously onto the fundus with an image size of 33 by 21°. The HeNe laser used for generation of the background and stimulus illumination is modulated via an acousto-optic modulator.[14] Background illumination was set to 10 cd/m^2. The image of the retina is acquired simultaneously by illumination with infrared laser light through a set of nearly confocal apertures.[15]

We performed kinetic fundus perimetry with the SLO by use of up to three different isopters. Stimulus size was equivalent to Goldmann II (and III), while the stimulus intensity could be varied in 0.1 log steps from 0 to 21 dB, where 0 dB represented the brightest luminance. All eyes were tested with 0 dB, and light inten-

sity was then in most cases decreased to 10 and 15 dB. The actual location of the stimulus at the fundus was controlled by the help of a landmark set by the investigator.[12]

Automated static threshold fundus perimetry was also performed in 15 eyes. We used newly developed software with the help of an additional personal computer, as described earlier.[11] According to further development of the software, the stimulus can be projected exactly onto the predefined position by the help of a landmark setting on the real-time image.[16] During each stimulus presentation (presentation time: 120 msec), the fundus image is digitized and a correction for small movements following the initial landmark definition is performed. Because we were interested in the eye movements during stimulus presentation, we calculated the difference between the location of the landmark prior to each stimulus presentation and in the mean of the subsequent stimulus presentation for all 15 eyes which also underwent static perimetry.

Results

Conventional kinetic perimetry showed macular sparing of 1-8° in size in ten eyes, but we could not observe this phenomenon in the other ten eyes.

Comparison of conventional and fundus perimetry did not reveal any significant difference between the kinetic visual fields, *i.e.*, both techniques were able to detect macular sparing in these ten eyes.

While kinetic and static fundus perimetry typically showed similar results, there was one eye which demonstrated complete macular sparing only during static fundus perimetry, while neither kinetic fundus perimetry nor conventional kinetic perimetry revealed this finding (Fig. 1). During conventional static perimetry, the corresponding location showed a threshold of 6 dB, *i.e.*, only a relative scotoma. On the other hand, we did not find any patient who exhibited macular sparing during kinetic perimetry who failed to present this finding during static perimetry. However, there were five eyes which were not examined using static perimetry.

We did not observe directed eye movements or straight saccades directed towards or against the anopic hemifield in any eye. The location of the mean fixation point was central in all eyes. In addition, we confirmed that sparing was not an artifact due to loss of fixation, since the peripheral border of the scotoma was located in a vertical line through the fovea. Figure 2 demonstrates the direction of eye movements around the mean fixation point where no straight movement towards or against the hemianopic hemisphere can be seen (Table 1). Comparison between the eyes with and without macular sparing did not show any difference either. In addition, the deviation of the single points of fixation was about the same amount for the horizontal and vertical direction (data not shown).

Discussion

The phenomenon of macular sparing in patients with hemianopsia due to visual pathway pathology has been recorded since early in this century.[3,4,6] Following the explanations of Behr in 1909, several theories were proposed to explain this phenomenon. Since the actual radiological methods and the possibilities of exact neurosur-

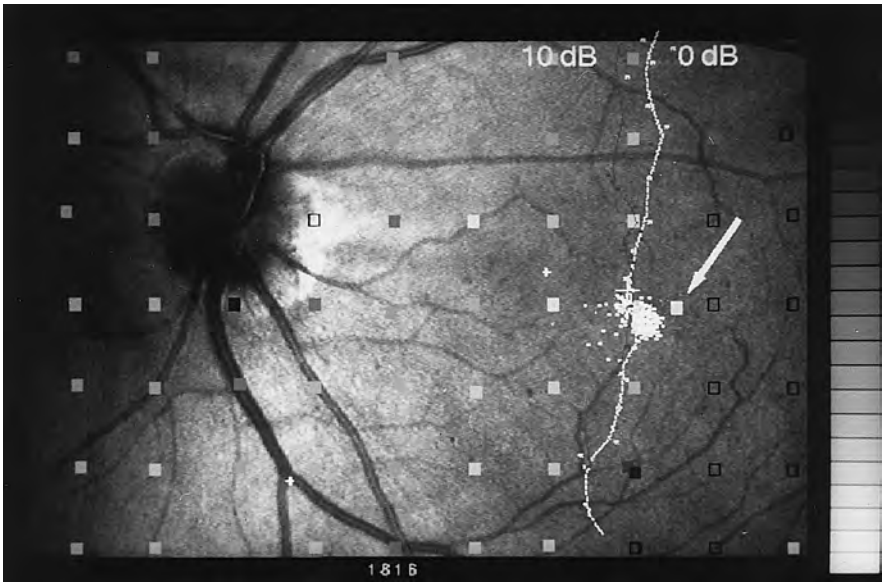

a

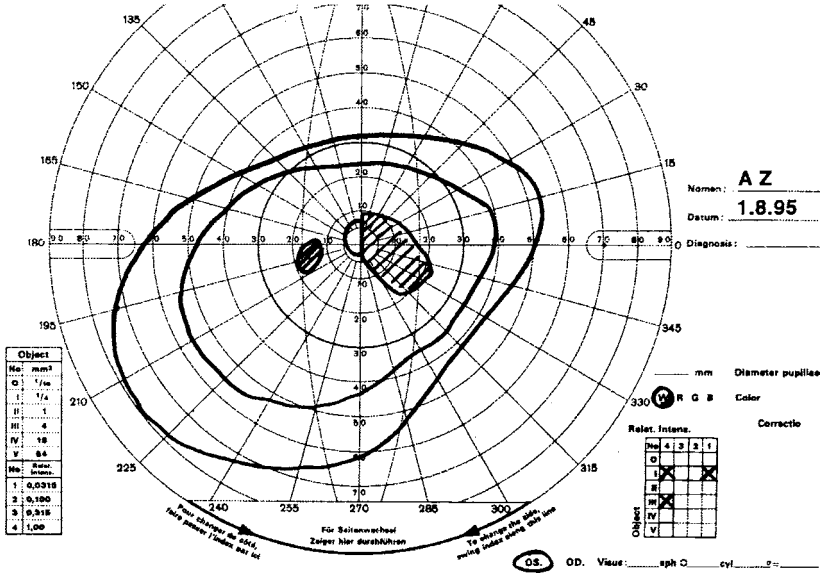

b

Fig. 1. Seventy-six-year-old female patient with different findings during static and kinetic fundus perimetry. *a.* While static threshold fundus perimetry exhibited macular sparing (arrow, stimulus size Goldmann III), kinetic perimetry did not (Goldmann II). The right-hand scale represents the threshold values in 1-dB steps with the highest illumination (0 dB) at the top for static perimetry. The rectangles give the thresholds, where open rectangles are absolute defects. *b.* Conventional kinetic perimetry did not show macular sparing either. *c.* During static perimetry, we observed a relative scotoma (6-dB defect).

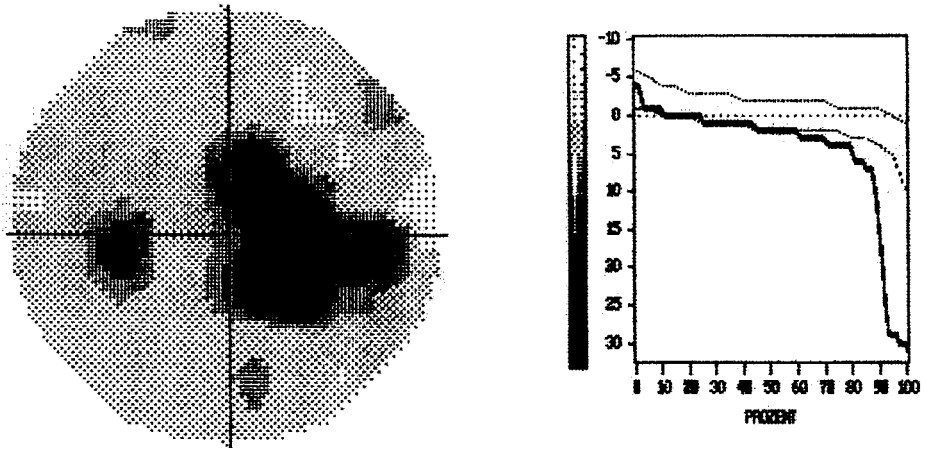

Fig. 1c.

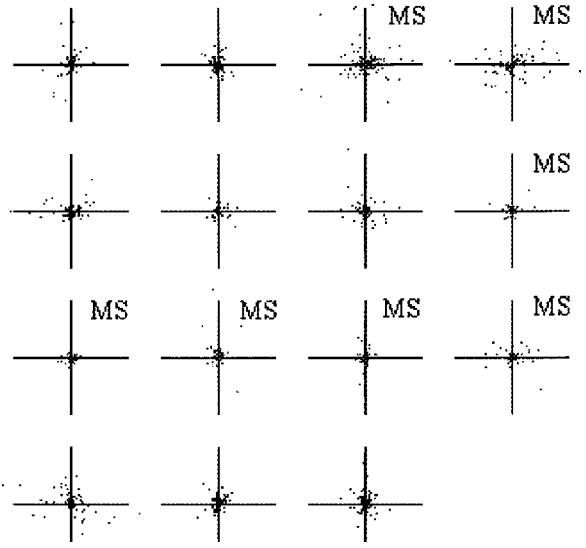

Fig. 2. Direction of eye movements around the mean fixation point (time interval of about 100 msec between landmark setting preceding stimulus presentation and middle of presentation). No straight movement towards or against the hemianopic hemisphere can be seen. There are no differences between eyes with macular sparing (MS) and splitting.

gical removal of well-determined areas of the visual pathway did not exist at that time, there was much speculation about the pathophysiological reasons for the macular sparing in hemianopsia.[7,8,17,18]

Although the phenomenon of macular sparing, especially during kinetic perimetry, has been noted for a long time, it is also known that fixation is not necessarily stable during the perimetric examination.[10,19] There is nearly no possibility for the investigator to correct for little saccades or drifting eye movements, or even to recognize them with the Goldmann perimeter or other conventional cupola perimeters.

Bischoff and coworkers have evaluated the behavior of fixation of hemianopic

Table 1. Data of the deviation between setting of the landmark immediately prior to stimulus presentation and during presentation in the 15 eyes which were examined using automated static fundus perimetry

Patient No	*Eye*	*Fixation stability*			*Count*	*Saccadic eye movements*		
		s_x	s_y	*x/y*		s_x	s_y	*x/y*
1	R	0.21	0.45	0.47	289	0.12	0.13	0.92
1	L	0.23	0.44	0.52	322	0.09	0.07	1.29
2	R	0.71	0.59	1.20	308	0.46	0.25	1.84
2	L	1.19	0.54	2.20	156	0.66	0.20	3.30
3	L	0.41	0.17	2.41	280	0.22	0.07	3.14
4	R	0.23	0.18	1.28	87	0.14	0.08	1.75
4	L	0.49	0.42	1.17	177	0.20	0.21	0.95
5	R	0.13	0.22	0.59	321	0.08	0.04	2.00
5	L	0.21	0.27	0.78	238	0.07	0.03	2.33
6	R	0.43	0.28	1.54	207	0.31	0.17	1.82
6	L	0.38	0.31	1.23	206	0.07	0.08	0.88
7	R	0.34	0.26	1.31	214	0.18	0.08	2.25
7	L	0.48	0.47	1.02	237	0.32	0.14	2.29
8	R	0.15	0.19	0.79	216	0.11	0.08	1.38
8	L	0.24	0.35	0.69	187	0.15	0.24	0.63

Values for stability of fixation are given in degrees (x: horizontally; y: vertically); eye movements during stimulus presentation are reported as saccadic eye movements (degrees). In addition, the total number of stimulus presentations is given (count)

patients using the scanning laser ophthalmoscope and an additional VCR.[8] They observed microsaccades directed towards the seeing hemiretina and back towards the anopic hemifield in a nystagmiform pattern. Since the point of fixation did not pass over the foveola, they concluded that these saccades allowed the patients to detect stimuli which were actually located in non-seeing areas of the visual field. Nevertheless, there are two main points of criticism:

1. The digitization of the actual fundus image is performed at the beginning of the stimulus presentation. The saccades must start after this time since otherwise the image would show a movement of the eye. Regarding the duration and speed of such saccades, it is not possible to reach a point located four or more degrees inside the hemianopic field, even when stimulus duration is 200 msec instead of 100 msec, as reported by Bischoff *et al.*[8] Even if such movements might exist, this would not explain why the sparing only exists for the central area and not for the whole vertical meridian.

2. Comparison between conventional kinetic perimetry, using the Goldmann perimeter, and static fundus perimetry with the SLO (the latter being performed using only a manual technique) leads to additional differences in the observations, as demonstrated in our results (Fig. 1).

Our software enables not only automated static full-threshold fundus perimetry comparable to that with the Octopus to be performed, but also kinetic perimetry with exact knowledge of the actual point of fixation.[11,12] It has to be noted that the original software (version 2.0) distributed by Rodenstock, Germany, does not provide these options. Since there is documentation of the point of fixation immediately before and during stimulus presentation during static perimetry, there is only minimal difference between the proposed and the performed location of each stimulus. In addition, we

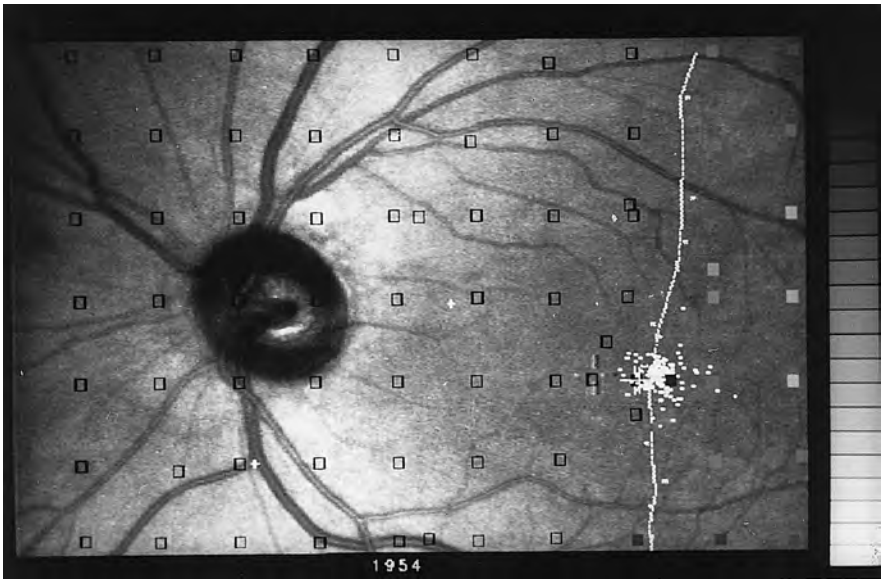

Fig. 3. Macular splitting in both kinetic and static fundus perimetry in a patient with hemianopsia towards the left. The right-hand scale represents the static threshold values in 1-dB steps with the highest illumination (0 dB) at the top (size Goldmann III). The rectangles given the thresholds, where open rectangles are absolute defects. Kinetic stimulus threshold is 0 dB (size Goldmann II).

can calculate whether there are any directed eye movements during this time period. We did not observe movements or saccades such as those reported by Bischoff *et al.*[8] (Table 1). Although the size of saccades may reach the area of macular sparing, it is not likely that we would miss such saccades during the entire examination using our static fundus perimetry. The size of such saccades may reach amplitudes of 4° and speeds of up to 200°/sec.[20,21] Voluntary saccades of up to 50° amplitude reach peak velocities of 500°/sec, and maximum duration is less than 270 msec. For an amplitude of less than 10°, duration is less than 120 msec.[22] We therefore will document each saccadic eye movement which might influence the observation of an artificial macular sparing using our set-up with the SLO.

Since there might be differences between kinetic and static visual field testing, leading to false positive and negative results regarding macular sparing, the comparison between fundus perimetry and conventional cupola perimetry should be performed with the same technique. We demonstrated that it is possible to miss the phenomenon of sparing using not only static perimetry but also kinetic testing (Fig. 1). While the former might be explainable by the grid used during the examination, the latter may be the result of statokinetic dissociation in relative scotomas during kinetic visual field testing. Nevertheless, we found good agreement between both types of fundus examination in other patients, even at the margin of a scotoma (Figs. 3 and 4).

The occurrence of macular sparing should be helpful in differentiation of the location of the damage underlying a hemianopsia. Macular sparing often exists in postgeniculate hemianopsia, while it is absent in pregeniculate damage.[2] More recently it has been reported that MR imaging may also be helpful in differentiating between different locations of occipital damage.[18,23] In addition, the authors report

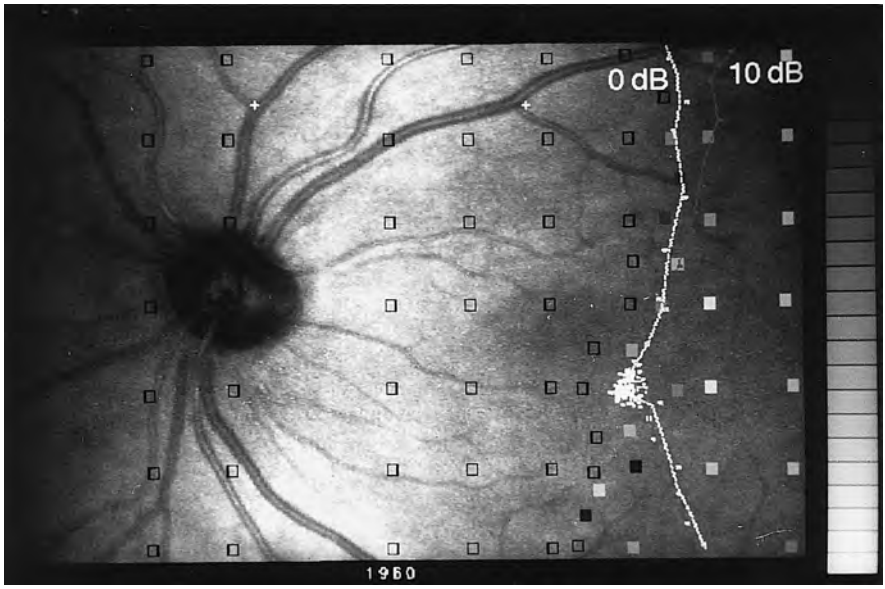

Fig. 4. Example of slight macular sparing in a patient with left hemianopsia. The findings are identical during kinetic and static fundus perimetry. The right-hand scale represents the static threshold values in 1-dB steps with the highest illumination (0 dB) at the top (size Goldmann III). The rectangles give the thresholds, where open rectangles are absolute defects. Values for kinetic stimulus are 0 and 10 dB (size Goldmann II).

that this might allow distinction between patients with and without macular sparing. Sparing occurs "when the occipital pole and operculum are involved by the lesion and when there is sparing of these structures".[18] The former hypothesis of a bilateral representation of the macula leading to the sparing is unsatisfactory. Although such an overlap has been confirmed by electrophysiological studies in non-primates,[9] there is no corresponding finding in humans using MRI examinations.

In conclusion, our fundus perimetry allows exact point-to-point correlation between fundus location and its functions, and supports the existence of macular sparing in a subgroup of hemianopic patients. Since the spared area typically covers 3-5°, there is no need to perform such a time-consuming and expensive examination in daily practice. In addition, the diagnostic value of macular sparing has markedly diminished as neuroradiological methods improve. However, the observation of the fundus may additionally allow typical optic nerve head damage to be checked for, as described by Hoyt and Kommerell in 1973.[24] In addition, our findings show that, in general, kinetic perimetry may be preferred over static procedures when investigating these special patients, since scotoma margins can be detected more accurately (Figs. 3 and 4).[12] Nevertheless, there was one eye which demonstrated a macular sparing of 1.5° during static visual field testing only (Fig. 1). Therefore, in some cases, static perimetry may also be advantageous. However, any form of static perimetry in the central area has the drawback of the need for a high number of stimulus locations, which also makes it time-consuming.

Acknowledgment

Supported in part by the Deutsche Forschungsgemeinschaft DFG Vo 437/2-1.

References

1. Miller NR: Sparing of the macula. In: Miller NR (eds) Walsh and Hoyt's Clinical Neuro-Ophthalmology, Vol 1, 4th Edn, pp 145-147. Baltimore MD: Williams & Wilkins 1991
2. Manor RS: Entoptic phenomena in pregeniculate and postgeniculate hemianopsia with splitting of macula by perimetry. Am J Ophthalmol 108:585-591, 1989
3. Behr C: Zur topischen Diagnose der Hemianopsie. Graefe's Arch Ophthalmol 70:340-402, 1909
4. Rönne H: Ueber die Bedeutung der makularen Aussparung im hemianopischen Gesichtsfeld. Klin Mbl Augenheilk 49:289-312, 1911
5. Lenz G: Die hirnlokalisatorische Bedeutung der Makulaausparung im hemianopischen Gesichtsfeld. Klin Mbl Augenheilk 53:30-63, 1914
6. Wilbrand H: Über die makuläre Aussparung. Z Augenheilk 58:261-268, 1926
7. Huber A: Homonymous hemianopia. Neuro-Ophthalmology 12:351-366, 1992
8. Bischoff P, Lang J, Huber A: Macular sparing as a perimetric artifact. Am J Ophthalmol 119:72-80, 1995
9. Bunt AH, Minckler DS: Foveal sparing: new anatomical evidence for bilateral representation of the central retina. Arch Ophthalmol 95:1445-1447, 1977
10. Eizenman M, Trope GE, Fortinsky M, Murphy PH: Stability of fixation in healthy subjects during automated perimetry. Can J Ophthalmol 27:336-340, 1992
11. Rohrschneider K, Fendrich T, Becker M, Krastel H, Kruse FE, Völcker HE: Static fundus perimetry using the scanning laser ophthalmoscope with an automated threshold strategy. Graefe's Arch Clin Exp Ophthalmol 233:743-749, 1995
12. Rohrschneider K, Becker M, Fendrich T, Völcker HE: Kinetische funduskontrollierte Perimetrie mit dem Scanning-Laser-Ophthalmoskop. Klin Mbl Augenheilk 207:102-110, 1995
13. Webb RH, Hughes GW, Delori FC: Confocal scanning laser ophthalmoscope. Appl Optics 26:1492-1499, 1987
14. Plesch A, Klingbeil U: Konfokales Laser-Scan-System zur Darstellung und Analyse des Fundus. Fortschr Ophthalmol 85:565-568, 1988
15. Van de Velde FJ, Jalkh AE, Elsner AE: Microperimetry with the scanning laser ophthalmoscope. In: Mills RP, Heijl A (eds) Perimetry Update 1990/1991, pp 93-101. Amsterdam/Milano: Kugler & Ghedini 1991
16. Sunness JS, Schuchard RA, Shan N, Rubin GS, Dagnelie G, Haselwood DM: Landmark-driven fundus perimetry using the scanning laser ophthalmoscope. Invest Ophthalmol Vis Sci 36:1863-1874, 1995
17. Huber A: Homonymous hemianopia after occipital lobectomy. Am J Ophthalmol 54:623-629, 1962
18. McFadzean R, Brosnahan D, Hadley D, Mutlukan E: Representation of the visual field in the occipital striate cortex. Br J Ophthalmol 78:185-190, 1994
19. Rohrschneider K, Becker M, Kruse FE, Fendrich T, Völcker HE: Stability of fixation: results of fundus-controlled examination using the scanning laser ophthalmoscope. German J Ophthalmol 4:197-202, 1995
20. Ciuffreda KJ, Kenyon RV, Stark L: Eye movements during reading: further case reports. Am J Optom Physiol Opt 62:844-852, 1985
21. Ciuffreda KJ: Jerk nystagmus: some new findings. Am J Optom Physiol Opt 56:521-530, 1979
22. Collewijn H, Erkelens CJ, Steinman RM: Binocular co-ordination of human horizontal saccadic eye movements. J Physiol (Lond) 404:157-182, 1988
23. Horton JC, Hoyt WF: The representation of the visual field in human striate cortex: a revision of the classic Holmes map. Arch Ophthalmol 109:816-824, 1991
24. Hoyt WF, Kommerell G: Der Fundus oculi bei homonymer Hemianopsie. Klin Mbl Augenheilk 162:456-464, 1973

ANALYSIS OF EARLY VISUAL FIELD DEFECTS IN MULTIPLE SCLEROSIS PATIENTS
Correlation with chromatic sense evaluations and pattern reversal visual-evoked potentials

ANNA POLIZZI, MARCO SCHENONE, GIACOMO BALESTRA, CHIARA CIURLO, GIUSEPPE GATTI, GIANLUIGI MANCARDI, FABIO BANDINI and GUIDO CORALLO

Abstract

Thirty young patients affected by multiple sclerosis (MS) for a period of between two and five years and lacking signs of neuropathy, were examined by means of the Humphrey VFA 640 Program 10-2, high-pass resolution perimetry (HRP), visual-evoked potentials (VEPs), pattern reversal ERG and the Farnsworth-Munsell 100 Hue Test. HRP revealed significant visual field alterations in 50% of patients (functional channels fraction average = 70%); the Humphrey VFA 640 Program 10-2 showed visual field alterations in 15% of cases (foveal threshold average = 36 dB). Alterations in VEP responses and the Farnsworth-Munsell 100 Hue Test were found in 10% and 40% of cases, respectively.

The study demonstrated the sensitivity of HRP and the Farnsworth-Munsell 100 Hue Test in detecting early functional alterations of the optic nerve in MS patients not suffering from ocular symptoms.

Introduction

The early alteration of optic nerve function in patients suffering from multiple sclerosis (MS) has been the object of numerous studies.[1-3] The aim of the present study was to evaluate changes in optic nerve function in a sample of selected patients suffering from MS, but not affected by optic neuritis, using high-pass resolution perimetry (HRP), the Humphrey VFA 640 (10-2 Program), the Farnsworth-Munsell 100 Hue Test, visual-evoked potentials (VEPs) and pattern reversal ERG (PERG).

Material and methods

The data of the MS patients are reported in Table 1. No patients had symptoms of optic neuritis and no patients had current or previous ocular or systemic diseases. Uncooperative subjects were excluded (n = 6). Sixteen normal subjects without ocu-

Address for correspondence: Anna Polizzi, MD, University Eye Clinic of Genoa, S. Martino Hospital, Pad, 9, Largo Rosanna Benzi, 10, 16132 Genova, Italy

Perimetry Update 1996/1997, pp. 387–390
Proceedings of the XIIth International Perimetric Society Meeting
Würzburg, Germany, June 4–8, 1996
edited by M. Wall and A. Heijl

Table 1. MS patient data

Number	16 (32 eyes)
Females/males	13/3
Average age (years)	38.5
Age range (years)	18-55
Average duration of disease (months)	46
range (months)	18-58
Patients on therapy*	10
Patients not on therapy	6

*Therapy: i.v. methylprednisolone for the acute phase during hospitalization: 1 g for three days, 0.50 g for three days, 0.250 g for three days; then oral therapy with prednisone: 50 mg for two days, 25 mg for two days, 12.5 mg for two days

Table 2. Control group

Number	16 (32 eyes)
Females/males	12/4
Average age (years)	36.9
Age range (years)	17-54

lar or systemic diseases, matched for age and sex, were selected as the control group (see Table 2).

All patients underwent:

1. Complete ophthalmological examination (visual acuity, tonometry, fundus examination, ocular motility)
2. HRP (Ring Program);[4-6] in particular, we considered: global deviation (GD), local deviation (LD), and functional channel fraction (FCF)
3. Humphrey VFA 640 (10-2 Program): foveal threshold examination and accurate analysis of the numerical values of the threshold, point-by-point. The 10-2 Program was preferred to the 30-2 as it is shorter and less tiring for this type of patient
4. Farnsworth-Munsel 100 Hue Test, manual[7-10] and computerized versions
5. VEPs (1 cycles/degree and 3.5 cycles/degree) and PERG (1 cycles/degree and 3.5 cycles/degree)[7-10]

One examiner performed the perimetric examination and chromatic sense evaluation in a masked fashion; the tests were conducted on each eye separately. All the patients had previously undergone the psycho-physical test on at least one occasion. The total time for testing was about three and a half hours (excluding the VEPs and PERG examinations). None of the MS patients was affected by ophthalmological diseases. Ocular motility was normal in all MS patients at the time of examination.

Results

The results of the MS patients and the control group data are reported in Tables 3, 4 and 5. Six eyes of the MS patients (18.12%) showed higher threshold levels (analyzed point-by-point) than the control group. The results of HRP were statistically correlated (Mann-Whitney test) with the data obtained from the control group.

Table 3. MS patients

Visual acuity in D (mean)	9.48	(range: 8-10)
IOP mmHg (mean)	15	(range: 11-20)
Temporal pallor of optic disc	20	(62.5%)

Table 4. MS patients

	HRP			*Humphrey 10-2*	*Farnsworth-Munsell 100 Hue Test*		*VEPs (cycles/ degree)*		*PERG (cycles/ degree)*	
	GD	*LD*	*FCF*	*foveal threshold*	*manual*	*computerized*	*1*	*3.5*	*1*	*3.5*
Mean	0.93	0.79	78.5	36.98	229.56	218.07	107.65	116.9	55.41	59.03
SD	1.41	0.42	22.6	7.01	30.95	24.68	34.09	38.3	19.06	13.37

see Table 6 for abbreviations

Table 5. Control group

	HRP			*Humphrey 10-2*	*Farnsworth-Munsell 100 Hue Test*		*VEPs (cycles/ degree)*		*PERG (cycles/ degree)*	
	GD	*LD*	*FCF*	*foveal threshold*	*manual*	*computerized*	*1*	*3.5*	*1*	*3.5*
Mean	0.22	0.60	96.2	37.12	199.5	198.65	105.92	116.2	53.63	58.44
SD	0.37	0.13	8.56	4.63	9.2	11.98	15.88	17.15	11.35	10.21

see Table 6 for abbreviations

Table 6. Statistical correlation (Mann-Whitney test) between MS patients and the control group

HRP	GD	$p = 0.005$
	LD	$p = 0.0012$
	FCF	$p < 0.001$
Humphrey 10-2	foveal threshold	p = NS
Farnsworth-Munsell test	manual	$p = 0.0003$
	computerized	$p = 0.004$
VEPs		p = NS
PERG		p = NS

GD: global deviation; LD: local deviation; FCF: functional channel fraction

The same type of correlation was calculated for the foveal threshold of the Humphrey 10-2 Program, the total score of the Farnsworth-Munsel 100 Hue Test (manual and computerized versions), and for the values of VEPs and PERG (Table 6).

Discussion

Analysis of the central 10° of the visual field using the Humphrey VFA 640 perimeter did not reveal significant alterations in the foveal threshold compared to the control group. The HRP perimetric method, which measured the ganglion cells and functional channel share, showed a statistically significant alteration in the MS patients compared to the control group. The data obtained with the Farnsworth-Munsell 100 Hue Test (manual and computerized versions) showed alterations of the irregular tritan type in 11 patients, and totally irregular alterations in six patients. Furthermore, the difference between the total scores of MS patients and the control group was statistically significant for both tests. VEPs and PERG did not seem to be altered in a statistically significant manner in MS patients. Therefore, the psycho-physical examinations demonstrated a higher sensitivity than the electrophysiological tests with regard to the detection of early alteration of the optic nerve in MS patients.

Conclusions

Two of the examinations performed by us (HRP perimetry and the Farnsworth-Munsell 100 Hue Test) showed a statistically significant alteration in MS patients not suffering from optic neuritis. HRP and the computerized version of the chromatic sense evaluation are extremely valuable in the screening of patients who tire easily, such as those suffering from MS, due to the tests' high sensitivity and the speed and ease with which the examinations can be carried out.

References

1. McAlpine D: Clinical studies. In: McAlpine D et al (eds) Multiple Sclerosis: A Reappraisal. Edinburgh: Churchill Livingstone 1972
2. Meienberg O, Flammer J, Ludin HP: Subclinical visual field defects in multiple sclerosis: demonstration and quantification with automated perimetry and comparison with visually evoked potentials. J Neurol 227:125-133, 1982
3. Brusini P: Subclinical centro-coecal field defects in multiple sclerosis. In: Heijl A (ed) Perimetry Update 1988/89, pp 111-115. Amsterdam/Milano: Kugler & Ghedini Publ 1989
4. Frisén L: High-pass resolution perimetry: recent developments. In: Heijl A (ed) Perimetry Update 1988/89, pp 369-375. Amsterdam/Milano: Kugler & Ghedini Publ 1989
5. Lindblom B, Hoyt WF: High-pass resolution perimetry in neuro-ophthalmology: clinical impressions. Ophthalmology 99:700-705, 1992
6. Wall M: High-pass resolution perimetry in optic neuritis. Invest Ophthalmol Vis Sci 32: 1991
7. Macfadyen DJ, Drance SM, Chisholm IA, Douglas GR, Kozak JF, Paty DW: The Farnsworth-Munsell 100: color vision score and visual evoked potentials in multiple sclerosis. Neuro-Ophthalmology 8/6:289-298, 1988
8. Pinckers A, Verriest G, Cruyseberg JRM: Tests de la vision des couleurs et potentiales évoqué visuels dans la sclérose en plaques. Ophthalmologie 1:45-48, 1987
9. Berninger TA, Heider W: Electrophysiology and perimetry in acute retrobulbar neuritis. Doc Ophthalmol 71:293-305, 1989
10. Frederiksen JL, Larsson HBW, Ottovay E, Stigsby B, Olesen J: Acute optic neuritis with normal visual acuity: comparison of symptoms and signs with psychophysiological, electrophysiological and magnetic resonance imaging data. Acta Ophthalmol (Kbh) 69/3:357-366, 1991

PERSISTENT VISUAL FIELD DEFECTS AFTER CRANIOPHARYNGIOMA SURGERY
A comparison between high-pass resolution and Goldmann perimetry

LENE M. MARTIN[1] and ULRIKA GEDDA[2]

[1]Stockholm University College of Health Sciences; [2]St. Erik Eye Hospital, Stockholm; Sweden

Introduction

High-pass resolution perimetry (HRP) measures spatial resolution within the central 30° visual field.[1,2] The variability is low[3,4] and the method very patient-friendly.[5-7] Several studies show its usefulness in neuro-ophthalmology.[6-11] As an aid in interpretation, the knowledge-based decision support program RIX (Ring Interpretation eXpert) is available.[12] This program has been shown to provide considerable support to the final diagnostic decision in patients with lesions of the visual pathways.[12,13]

The aim of the present study was to compare the visual field findings in surgically treated craniopharyngioma patients, obtained and evaluated using HRP, with automatic interpretation by the RIX program, and kinetic Goldmann perimetry with visual evaluation.

Patients and methods

From a larger group of patients, surgically treated for craniopharyngioma, 16 patients (aged 18-74 years, eight males and eight females) were examined with Goldmann and high-pass resolution perimetry one to 30 years after neurosurgery. They had no other ocular abnormalities. The Goldmann visual fields were evaluated by visual inspection by an independent ophthalmologist, and the HRP fields by the RIX program. The HRP technique has been extensively described elsewhere.[1,2] The RIX program consists of some 200 'if-then' rules and reports abnormal findings from each eye and also, if relevant, a final conclusion based on findings from both eyes. The information included in the program was derived from ten years' personal experience with the HRP technique, documented in several scientific studies.[14] The program also heavily relies on information regarding visual field interpretation from many other

Address for correspondence: Lene Martin, Dr Med Sc, Stockholm University College of Health Sciences, PO Box 1821, S-171 24 Solna, Sweden

Perimetry Update 1996/1997, pp. 391–394
Proceedings of the XIIth International Perimetric Society Meeting
Würzburg, Germany, June 4–8, 1996
edited by M. Wall and A. Heijl

Table 1. Types of defect detected by the two techniques

Defect type	*Goldmann*	*RIX*
Bitemporal defect	4	5
Temporal defect*	3	3
Homonymous defect	2	2
Normal	3	1
Other defects	4	5
Total	16	16

*in these patients, it was only possible to examine one eye

Table 2. Degree of the defects detected with the different techniques

Degree of defect	*No. of patients*
RIX defects equal to Goldmann defects	8
RIX defects more pronounced than Goldmann defects	6
RIX defects less pronounced than Goldmann defects	1

sources in the scientific literature. The RIX program has been in practical use at a number of eye clinics in Scandinavia for at least three years.

Results

It was possible to examine 29 eyes of 16 patients using both techniques. Two patients were blind in one eye and one patient had only a small visual field remnant in one eye. Table 1 shows the types of defect detected by visual evaluation of the Goldmann visual fields and automatic interpretation by the RIX program.

Table 2 lists the differences in degree of defect. One pair of visual fields was judged to be normal using both techniques. In eight patients, the same type and degree of defect was detected by both methods. In two patients with apparently normal Goldmann visual fields, the RIX program reported a paracentral defect on the temporal side in one eye in one patient, and reduced neural capacity in one eye in the other patient. In four other patients, the RIX program reported more pronounced defects than could be seen in the Goldmann visual fields. In one patient, the Goldmann field defect was judged to be a definite upper temporal quadrant defect, while RIX reported a possible, *i.e.*, not quite statistically significant, superotemporal defect.

Visual fields from one of the patients with a more pronounced defect in the HRP field are shown in Figure 1.

Discussion

Visual field examinations were performed in 16 patients (29 eyes) with surgically treated craniopharyngioma, using Goldmann perimetry and HRP. The Goldmann

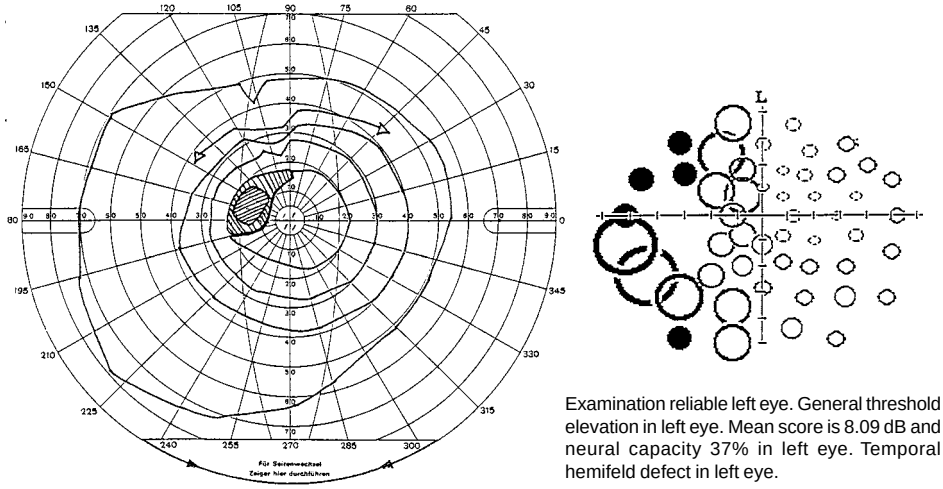

Fig. 1. Note the defect mostly in the upper temporal quadrant in the Goldmann field (left) and the larger rings in the temporal hemifield in the HRP field (right).

visual fields were visually evaluated and the HRP fields were automatically interpreted by the RIX program. In six patients the defects were more pronounced in the HRP than in the Goldmann fields.

Goldmann perimetry has always been regarded as the reference method in neuro-ophthalmology.[15] A good concordance has been reported between automatic perimetry and Goldmann perimetry in chiasmal lesions.[16] During the last decade, several authors have compared the sensitivity of DLS perimetry and of HRP in neurological disorders. The sensitivity of the HRP technique was found to be as good as, or better than, conventional perimetry.[6-11] Even in cases where the Goldmann visual field defects were only detected outside the central 30°, HRP was able to show functional impairment in the corresponding quadrants.[10] Yet, Dannheim and Roggenbuck[8] found no obvious difference between DLS perimetry and HRP in mild to moderate depression of sensitivity in patients with chiasmal lesions. On the other hand, Corallo *et al.*[10] found that HRP could detect initial quadrant defects in patients with slight compression of the chiasm, in whom DLS perimetry results were normal. In the present study, there was no difference between the methods in the evaluation of patients with moderate to large defects, while the automatic interpretation by the RIX program was able to reveal sensitivity depressions in patients with mild defects.

Interpretation of visual field findings is a complex procedure which must be performed in several steps.[17] Previous studies have shown that automatic interpretation can perform at least as well as an experienced observer and better than the average observer.[12,13,17]

In conclusion, the results indicate that the automatic interpretation of HRP visual fields may be somewhat more efficient than visually evaluated kinetic Goldmann perimetry in detecting mild visual field defects in surgically treated craniopharyngioma patients. A larger group of patients is presently being examined in order to verify this observation.

Acknowledgments

The authors are grateful to Elfar Ulfarsson, MD, Department of Neurosurgery, Karolinska Hospital, who was responsible for the craniopharyngioma follow-up project. The current study was supported by a grant from the Karin Sanquist Foundation.

References

1. Frisén L: Resolution theory and high-pass resolution perimetry (HRP). In: Mills RP (ed) Perimetry Update 1992/1993, pp 419-427. Amsterdam/New York: Kugler Publ 1993
2. Frisén L: High-pass resolution perimetry: a clinical review. Doc Ophthalmol 83:1-25, 1993
3. Douglas GR, Drance SM, Mickelberg FS, Schultzer M, Wijsman K: Variability of the Frisén ring perimeter. In: Heijl A (ed) Perimetry Update 1988/89, pp 197-198. Amsterdam/Milano: Kugler & Ghedini Publ 1989
4. House PH, Schulzer M, Drance SM: Characteristics of the normal central visual field measured with resolution perimetry. Graefe's Arch Clin Exp Opthalmol 229:8-12, 1991
5. Martin-Boglind LM, Wanger P: The influence of feed-back devices, learning and cheating on the results of high-pass resolution perimetry. In: Heijl A (ed) Perimetry Update 1988/89, pp 393-398. Amsterdam/Milano: Kugler & Ghedini Publ 1989
6. Lindblom B, Hoyt WH: High-pass resolution perimetry in neuro-ophthalmology: clinical impressions. Ophthalmology 99:700-705, 1992
7. Bynke H: Evaluation of high-pass resolution perimetry in neuro-ophthalmology. In: Heijl A, Mills RP (eds) Perimetry Update 1990/1991, pp 287-290. Amsterdam/Milano: Kugler & Ghedini Publ 1991
8. Dannheim F, Roggenbruck C: Comparison of automated conventional and spatial resolution perimetry in chiasmal lesions. In: Heijl A (ed) Perimetry Update 1988/1989, pp 377-382 Amsterdam/Milano: Kugler & Ghedini Publ 1989
9. Marcini G, Marraffa M, Palmara A, Milan E: La perimetria high-pass resolution nella sindrome chiasmatica. Minerva Oftalmol 33:245-249, 1994
10. Corallo G, Gandolfo E, Grosso S, Bancehro C, Gatti G, Patrone G, Guidi C, Romiti S: Confronto tra perimetria high-pass resolution e perimetria tradizionale in neuro-oftalmologia. Minerva Oftalmol 36:225-230, 1994
11. Wall M, Conway MD, House PH, Allely R: Evaluation of sensitivity and specificity of spatial resolution and Humphrey automatic perimetry in pseudotumor cerebri patients and normal subjects. Invest Ophthalmol Vis Sci 32/13:3306-3312, 1991
12. Martin-Boglind LM, Wanger P: Computer-assisted evaluation of the results of high-pass resolution perimetry: a knowledge-based system. In: Heijl A, Mills RP (eds) Perimetry Update 1990/1991, pp 297-301. Amsterdam/Milano: Kugler & Ghedini Publ 1991
13. Martin-Boglind LM: Computer-assisted interpretation of resolution visual fields from patients with chiasm and retro-chiasm lesions. Ophthalmologica 207/3:148-154, 1993
14. Martin Boglind L: Computer-Assisted Interpretation of Resolution Visual Fields. Basic Studies and Program Development. Thesis, Karolinska Institute 1993
15. Grochwicki M, Vighetto A, Berquet S, Khalfallah Y, Sassolas G: Pituitary adenomas: automatic static perimetry and Goldmann perimetry: a comparative study of 345 visual field charts. Br J Ophthalmol 75:219-221, 1991
16. Wirtschafter JD, Coffman SM: Comparison of manual Goldmann and automated static visual fields using the Dicon 2000 perimeter in detection of chiasmal tumors. Ann Ophthalmol 16:733-741, 1984
17. Kaufmann H, Flammer J, Rutishauser C: Evaluation of visual fields by ophthalmologists and by Octosmart program. Ophthalmologica 201:104-109, 1990

BITEMPORAL INTERMITTENT HEMIANOPIA

M.T. DORIGO[1], R. DE NATALE[2] and L. TOMAZZOLI[2]

[1]University Eye Clinic of Padua, Padua; [2]University Eye Clinic of Verona, Verona; Italy

Introduction

Pituitary adenomas, which are known to be the most frequent cause of chiasmal syndrome, may lead to bitemporal quadranopia or hemianopia of the visual field. The pattern of the visual field defects depends on the size of the adenoma and on the position of the chiasm. Also, reversibility of visual field defects is variable and it may be obtained either by medical or surgical therapy.[1]

In the present paper, we report a rare case of an intermittent bitemporal hemianopia.

Case report

For 20 years, T.L., a 70-year-old female patient, has been affected by recurrent attacks of bitemporal hemianopia. Each attack lasted from 10-20 days and resolved spontaneously.

In February 1995, she was hospitalized due to new visual symptoms. Hormonal tests disclosed a slight increase of prolactin (41 µg/L) with a normal range of 5-25 µg/L. Her visual acuity was 1.0 in both eyes, IOP was 16 mmHg in both eyes, and her optic disc and retinal vessels were normal. The visual field examination, performed with the HFA Program 30-2, documented a variable intermittent bitemporal hemianopia. Computerized tomography showed a cystic sella turcica enlargement without calcification.

Magnetic resonance imaging (MRI) with gadolinium showed a large pituitary supra- and intrasellar cyst, indenting the anterior wall of the third ventricle. A small heterogeneous mass could be seen on the posterior wall of the cyst in the late exposures after the contrast medium. Cerebral angiography was normal.

In 1996 the patient underwent transsphenoidal surgery. Histological examination confirmed the cystic nature of the mass. However, no tissue diagnosis could be made.

Shortly after surgery, the patient was again hospitalized for a new manifestation

Address for correspondence: M.T. Dorigo, MD, University Eye Clinic, Via Giustiniani, 35100 Padova, Italy

Perimetry Update 1996/1997, pp. 395–396
Proceedings of the XIIth International Perimetric Society Meeting
Würzburg, Germany, June 4–8, 1996
edited by M. Wall and A. Heijl

of visual disorders. A repeat MRI examination showed that the cyst had grown into the sella turcica. A transsphenoidal hypophysectomy was performed but, again, no definite diagnosis was possible. Five months after surgery, the patient was free of visual complaints.

Discussion

Sella turcica cysts are relatively uncommon; they may have various pathological mechanisms. Arachnoidal cysts are typical serous cavities lined by neuro-epithelium, but may be of diverse origin, including trauma and inflammation. Some suprasellar cysts apparently arise from congenital anomalies in the floor of the third ventricle. Intrasellar cysts are a common finding in anatomical studies. McGrath encountered 33% in 83 necroscopy specimens.[2] Other cysts arise in the sella itself, and are known as cysts of Ratke's pouch, epithelial cysts or colloidal cysts, depending on their diverse anatomical disposition and histological characteristics.

In the present case, the absence of a histological diagnosis prevented a definite diagnosis, although the recurrent and long visual course, absence of hormonal alterations, MRI images of the cyst, and observation of a yellow colloidal fluid during surgical drainage, all suggest a diagnosis of cystic craniopharyngioma.

We believe that the intermittent hemianopia was correlated with the changing contents of the cyst. Visual disorders occurred at the time the cyst was at its maximum volume, and therefore resulted in compression of the chiasmal structures or the adjacent vessels.

A similar case has been reported by Frisèn *et al.*[3]

References

1. Glaser JS: Neuro-Ophthalmology, p 199. Philadelphia, PA: JB Lippincott Co 1990
2. McGrath P: Cysts of sella and pharyngeal hypophyses. Pathology 2:123, 1971
3. Frisèn L, Sjöstrand J, Norrsell K, Lindgren S: Cyclic compression of the intracranial optic nerve: patterns of visual failure and recovery. J Neurol Neurosurg Psychiatr 39:1109, 1976

OCULAR FUNCTIONAL LOSS DUE TO INTERNAL HYDROCEPHALUS IN A GLAUCOMA PATIENT

Cs. PALOTÁS[1], I. SÜVEGES[1], Zs. KOPNICZKY[2] and P. FOLLMANN[1]

[1]*Semmelweis University School of Medicine, 1st Department of Ophthalmology, Budapest;* [2]*Albert Szent-Györgyi University School of Medicine, Department of Neurosurgery, Szeged; Hungary*

Introduction

In the background of patients with visual loss due to glaucoma, there may be visual defects which could also caused by various other pathological conditions. The almost symptom-free occurrence of circulatory disturbances in the cerebrospinal fluid is rarely found in adults. These disturbances may cause ophthalmological signs by compression and malnutrition of the optic nerve.[1,2] Visual disturbances associated with impaired fluid circulation may appear as papilledema, constricted visual fields, enlarged blind spots and visual obscurations. When hydrocephalus occurs, massive dilation of the third verticle may compress the optic chiasm, causing various types of visual field defect.[3,4] Tumors, stenosis of the aqueduct of Sylvius, and also Von Hippel-Lindau's disease, may be causative factors leading to such alterations.[3,5-7]

In the case of our patient, dilation of the third verticle was only moderate, even though the optic nerve was compressed by the complex circulatory disturbances of the cerebrospinal fluid (CSF) and this, of course, led to the patient's serious ophthalmological complaints. Glaucoma and, due to their importance, the aforementioned issues, are mentioned together in this case report.

Case report

We present the case of a 43-year-old male patient with glaucoma, in whom progressive visual loss and visual field deterioration proved to be caused by CSF disturbances. During his childhood, the patient's acuity was normal in both eyes. The refraction was bilaterally moderate myopia.

From the patient's general case history, it can be seen that dermatological symptoms have been present since 1979. He has had recurring superficial phlebitis and thrombosis in the lower extremities, and therefore has undergone venous surgery four

Address for correspondence: Dr Palotás Csilla, 1st Department of Ophthalmology, Semmelweis Medical University, Tömo u. 25-29, H-1083 Budapest, Hungary

Perimetry Update 1996/1997, pp. 397–403
Proceedings of the XIIth International Perimetric Society Meeting
Würzburg, Germany, June 4–8, 1996
edited by M. Wall and A. Heijl

times. In 1991, he suffered a blunt injury to the left eye caused by a particle of copper and, since then, has experienced gradual visual loss. In 1993, he underwent an operation at another institution, during which a mature cataract of the left eye was extracted extracapsularly and a posterior chamber artificial lens was implanted. During the patient's hospitalization, open-angle glaucoma was detected and the administration of timolol maleate 0.5% eyedrops was initiated. It was not possible to lower the intraocular pressure sufficiently with this regime nor by adding other conservative means. Visual field defects appeared, and the right eye was trabeculectomized in January 1994.

Following surgery, the anterior chamber of the right eye became transiently flat and the patient complained of total visual loss for some days. At that time, the visual acuity in the right eye was only light perception. This significant visual loss was thought to be of vascular origin, therefore, infusion therapy with vasodilators was administered. As a consequence, the visual acuity increased to some extent, becoming 0.3 after the infusions, but this improvement was only partial compared to the normal visual acuity before the disastrous episode of visual loss.

After the permanent visual loss of the right eye following the trabeculectomy, further thorough medical check-ups were carried out in February, March and May, 1994. Alterations in the ocular fundus, circulatory disturbances, and the possibility of neurological pathology were then suspected. In both fundi, the veins were tortuous and dilated, but they were more attenuated on the right side. On both sides, perimetry demonstrated significant concentric contraction of the isopters with superior nasal steps in all isopters (Goldmann kinetic perimetry). Fundus fluorescein angiography, visual-evoked potential (VEP), corneal topography, and orbital color Doppler ultrasonography were all normal. Repeated CT and MRI examinations proposed by neurologists, and angiography of the carotids, demonstrated an enlarged cisterna magna and a typical venous angioma on the left side with moderate dilation of the third ventricle. However, these did not explain the actual complaints of the patient and did not require neurosurgical intervention.

The patient was admitted to the 1st Department of Ophthalmology at Semmelweis University Medical School, Budapest, for further check-up examinations. The repeated pattern visual-evoked potential (PVEP) indicated signs of optic nerve lesions in both eyes. B-scan ultrasonographic examinations revealed optic nerve edema on both sides, and ophthalmoscopy showed hyperemic optic discs with distinct borders and tortuous and dilated central retinal veins which were more attenuated in the right eye.

Neurological and neurosurgical consultations proposed CT and MRI examinations focusing on the optic nerves. On the basis of these findings, the patient was admitted to the Neurosurgical Department at the Szent-Györgyi School of Medicine, Szeged, in November 1994, for detailed check-up examinations, which were followed by a neurosurgical intervention in December 1994. The general physical examinations and laboratory findings were normal.

Orbital CT revealed thickened, irregular optic sheaths on both sides (Figs. 1 and 2), and MRI performed in the coronal plane demonstrated a significantly atrophied optic chiasm. The mid-sagittal cerebral MRI picture showed moderate dilation of the third ventricle, a partial empty sella and an enlarged cisterna magna. An empty sella was also visible on a coronal plane CT of the sella turcica performed by the thin-

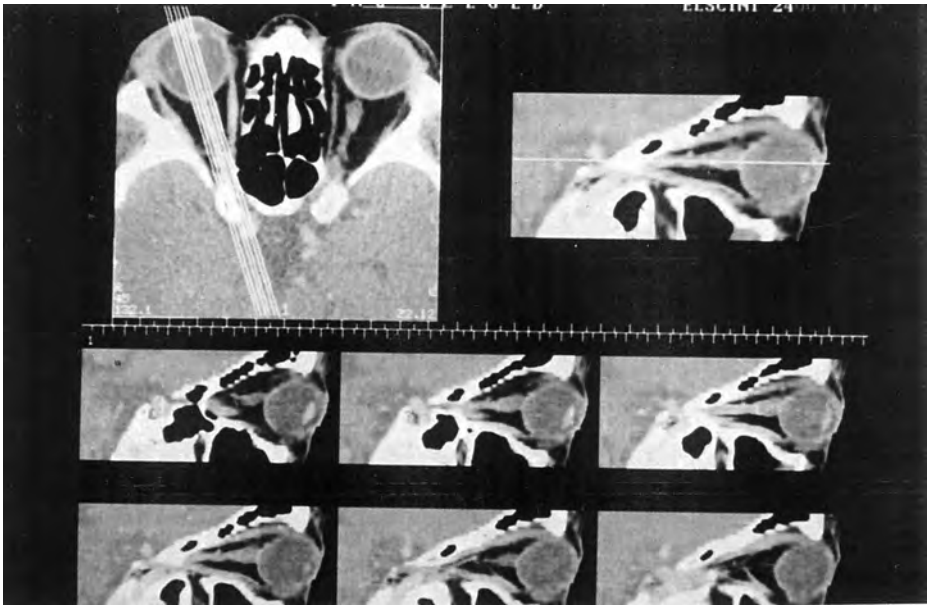

Fig. 1. Orbital CT. Thickened, irregular optic sheaths on the right side.

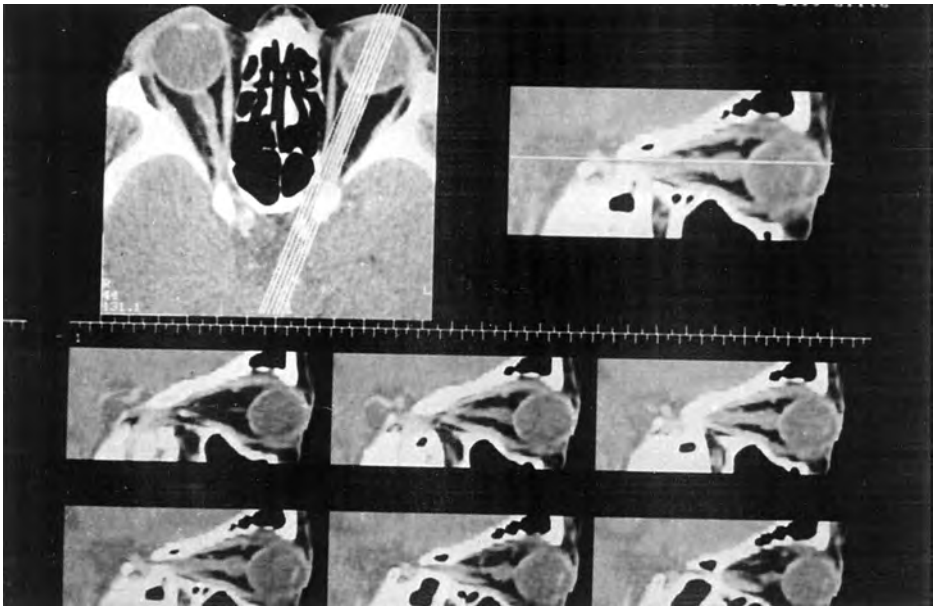

Fig. 2. Orbital CT. Thickened, irregular optic sheaths on the left side.

layer technique. In this CT, the third ventricle appeared to be ballooning downward into the sella, thereby compressing the hypophysis against the wall of the sella. No endocrinological dysfunctions were found.

In a striking picture obtained with contrast material, the intrathecally administered

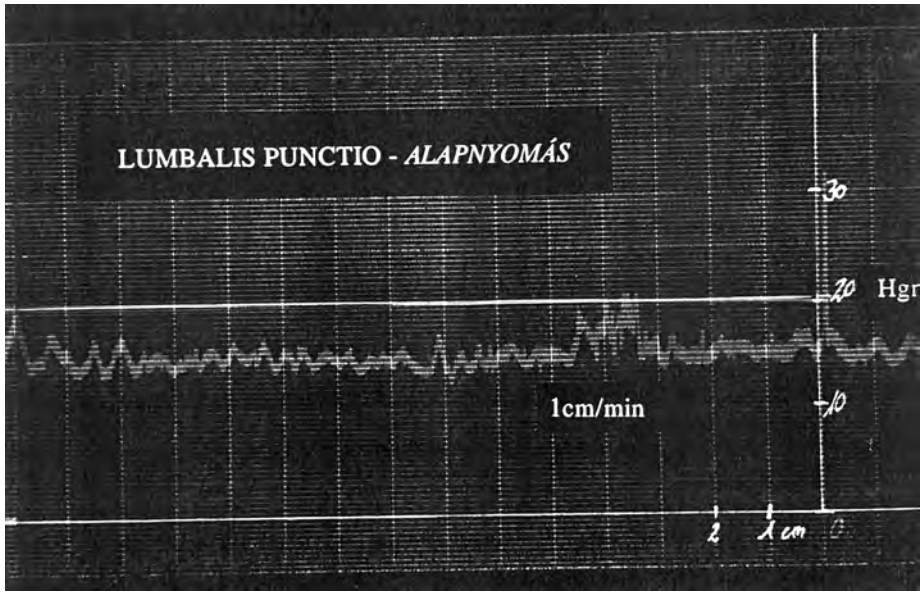

a

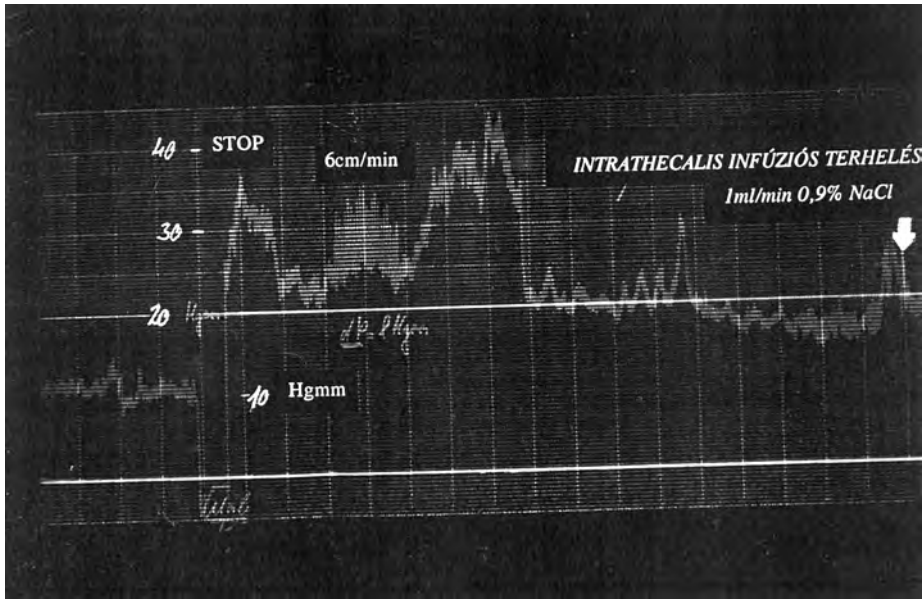

b

Fig. 3a. Basis liquor pressure curve during lumbar puncture. *b.* Intrathecal infusion provocation test with the administration of 1 ml/min of physiological saline.

Omnipack solution streamed upwards into both the subarachnoidal spaces and the cisternae. The cisterna magna was connected to the basal cisternae in the vicinity, and therefore the cisterna was not isolated, and did not exert a space-occupying effect. The contrast material was visible in the right optic sheaths, demonstrating a connection between the subarachnoidal space and the optic sheaths. However, this

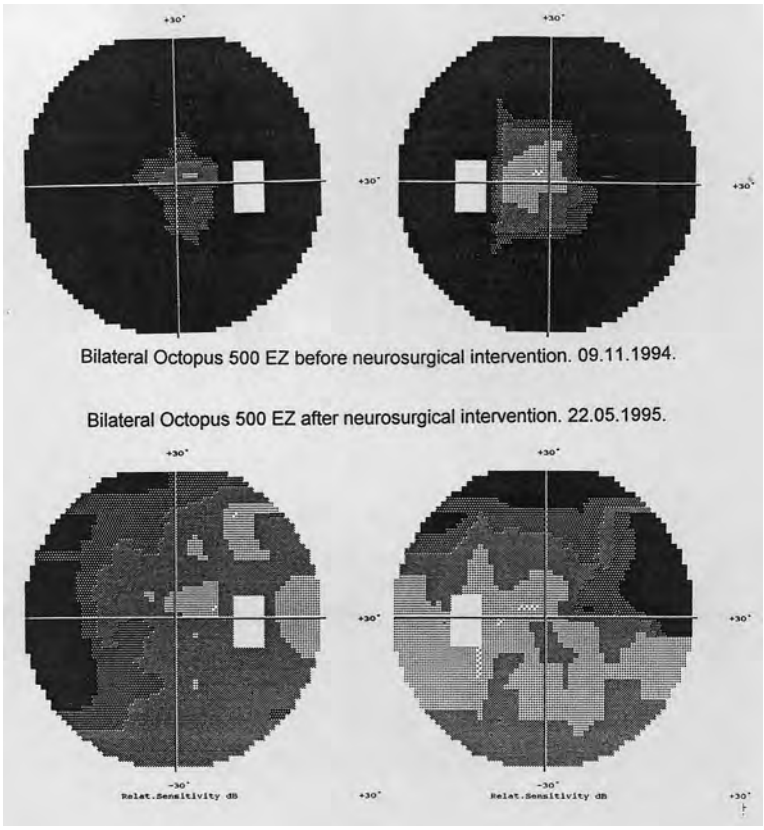

Fig. 4. Pre- and postoperative Octopus perimetry in both eyes.

could not be regarded as pathological *per ciao*, but the asymmetry between the two sides was thought to be of pathological importance.

On the basis of these findings, increased pressure of the CSF was assumed. In the stable, lateral lying position, with the measuring probe at the level of Monroe's foramen, the basal pressure was 15-16 mmHg. During intrathecal infusion of one ml/min of physiological saline, the basal pressure of the CSF gradually increased to 20, 30, and 41 mmHg, and the amplitude of the so-called pulse wave also increased from three to eight mmHg (Fig. 3).

The aim of this provocative test was to determine the resorption capacity of the CSF after having reached a new steady-state condition. The test could not be completed because the patient complained of serious visual loss at the level of 30 mmHg, similar to what he had experienced initially, and a gray net-like picture before both eyes. The test was discontinued, and 11 ml of CSF was released. During the removal of CSF, the patient reported improvement of vision, thus giving functional evidence of the assumed compressive pathomechanism.

On December 12, 1994, implantation of a ventriculoperitoneal Pudenz shunt was carried out. Following the neurosurgical intervention, the patient reported significant subjective visual improvement. Octopus perimetry demonstrated changes in the visual fields, compared to the pre- and postoperative results (Fig. 4).

Since that time, due to a progressive cataract, an extracapsular cataract extraction with posterior chamber artificial lens implantation was carried out in the trabeculectomized right eye on October 25, 1995. The final distance visual acuity was: right eye: 0.1 -2.0 D sph = -0.5 D cyl ax 90° = 0.3; left eye: 0.3 -2.0 D sph = -1.5 D cyl ax 75° = 1.0 partially. At present, the patient has no complaints.

Discussion

The sudden progressive visual disturbances in our glaucoma patient can be explained by the demonstration of hydrocephalus and obstructed passage of the CSF. The subsequent reversal of the field defect upon relieving the hydrocephalus indicates that compression of the optic fibers was the cause of the sudden progressive visual disturbance. The pathological events and the course of the visual disturbance in the present case was very similar to that described by Kupersmith and Bernstein.[6] In that case, the visual disturbance of a 23-year-old woman suffering from Von Hippel-Lindau's disease, and its relief by performing ventriculopleural shunt, were reported.

The case reported here is a good example of the effects of interdisciplinary collaboration within the fields of medicine, and of the results of mutual diagnostic and therapeutic efforts. Against the background of the complaints of an open-angle glaucoma patient, not only the glaucoma, but also cerebrospinal circulatory disturbances – leading to hydrocephalus compressing the optic nerves – was shown. Following the surgical relief of the CSF obstruction, a spectacular improvement in the Octopus visual field was demonstrated.

In addition, from the ophthalmological point of view, the presence of CSF circulatory disturbance in this case may provide further information regarding the ocular circulation-dependent visual loss which is not yet fully understood in glaucoma. From a neurological point of view, it should be stressed that the moderate diffuse dilation of the third ventricle without active signs of obstructive hydrocephalus (lack of transependymal CSF diffusion, retained convexities and subarachnoidal space) led to significant ocular complaints due to compression of the optic nerves, as a consequence of the complex CSF circulatory disturbances.

Detailed examination of the patient and Octopus perimetry prior to and following Pudenz shunt implantation subsequently proved the pathomechanism, which had been assumed to be correct on the basis of the clinical picture.

Summary

The authors report the case of a 43-year-old male patient with glaucoma in whom the cause of progressive loss of vision proved to be caused by a CSF circulatory disturbance. Examinations (ultrasound, VEP, CT, MRI) were performed due to a temporary loss of vision for two to three days immediately after a right eye trabeculectomy, followed by lasting deterioration of vision. The examinations showed CSF circulatory disturbances localized to the optic nerve sheath which caused edema of the optic disc. The patient underwent a ventriculoperitoneal Pudenz shunt implantation, after which no further deterioration of vision was detected. This case demonstrates a correlation between CSF circulatory disturbances, IOP, and deterioration of ocular function (visual acuity, visual field). Attention is drawn to the unusual progression of glaucomatous visual field loss noted after repeated automated perimetry (Octopus 500 EZ). After neurosurgical intervention, the visual field improved, thereby proving the connection between optic nerve involvement and CSF circulatory disturbances.

References

1. Walsh FB, Hoyt WF: Clinical Neuro-Ophthalmology, pp 1968-1976. Baltimore, MD: Williams & Wilkins 1969
2. Salinas-Garsia RF; Smith JL: Binasal hemianopia. Surg-Neurol 10:187-194, 1978
3. Lassman LP, Cullen DP, Howat JML: Stenosis of the aqueduct of Sylvius. Am J Ophthalmol 49:261-266, 1960
4. Wagener HP, Cusick PL: Chiasmal syndromes produced by lesions in the posterior fossa. Arch Ophthalmol 18:887-891, 1937
5. Shapio K, Suiontz H, Shulman K: Unilateral proptosis and visual field defect associated with hydrocephalus. Arch Neurol 33:663-664, 1976
6. Kupersmith MJ, Bernstein A: Visual disturbances in Von Hippel-Lindau disease. Ann Ophthalmol 13:195-197, 1981
7. Udvarhely GB: Neurosurgical diagnosis and treatment of lesions involving the anterior visual pathway. In: Transactions of the New Orleans Academy of Ophthalmology: Symposium on Neuro-Ophthalmology, pp 98-147. St Louis, MO: CV Mosby & Co 1976

PERIMETRIC STUDY OF ASYMPTOMATIC CAROTID OBSTRUCTIVE DISEASE

G. CORALLO[1], E. GANDOLFO[1], P. CAPRIS[1], G.A. OTTONELLO[2], G. BRUSA[2], U. RAITERI[2], E. SEMINO[1], P. TAGLIAVACCHE[1] and M. ZINGIRIAN[1]

[1]Department of Ophthalmology, University of Genoa; [2]Department of Clinical Neurophysiology, S. Martino Hospital; Genoa, Italy

Abstract

Ocular complications in carotid artery obstructive disease generally occur in high-grade stenosis (>90%) or in cases of artery occlusion, and have been described by many authors. Ocular involvement, when carotid stenosis ranges between 70% and 90% (when it is hemodynamically significant, but no occlusion is present), has rarely been studied. Usually, no evidence of ocular ischemia is detectable in these cases. The aim of this study was to perform a functional analysis of patients with uni- or bilateral carotid stenosis of between 70% and 90% and without signs or symptoms of ischemic ocular syndrome, in order to detect the earliest ocular functional alterations due to ischemia.

Thirty-six eyes of 18 patients with these clinical characteristics underwent automated perimetry. Visual field defects were present in 27 eyes (75%). The isolated presence of nerve fiber bundle defects was the most frequent alteration (48%), followed by the isolated presence of global reduction of light sensitivity (22%), and by the combination of these two deficits (22%).

The authors conclude that a subclinical chronic ocular ischemia can be detected by visual field analysis. It is probably a manifestation of a more generalized subclinical chronic ischemic cerebrovascular syndrome.

Introduction

Retinal changes caused by chronic ischemia in stenotic or occlusive carotid disease were described for the first time by Kearns and Hollerhorst in 1963,[1] who called them 'venous-stasis retinopathy'. Also other authors reported chronic ocular manifestations due to carotid occlusive disease. The terms 'ischemic glaucoma',[2] 'ischemic ocular inflammation'[3] and 'neovascular glaucoma'[4] indicate that anterior ischemia is predominant, whereas 'hypotensive retinopathy',[5] 'collateral flow retinopathy'[6] and 'venous-stasis retinopathy'[1] are terms which emphasize the presence of retinal ischemia. The involvement of the whole eye has been named 'ischemic oculopathy',[7] 'ischemic ophthalmopathy'[8] and 'ischemic ocular syndrome'.[9] Ocular changes may

Address for correspondence: Guido Corallo, MD, Clinica Oculistica Università, Largo Rosanna Benzi, 10, Pad. 9, Ospedale S. Martino, 16132 Genova, Italy

Perimetry Update 1996/1997, pp. 405–413
Proceedings of the XIIth International Perimetric Society Meeting
Würzburg, Germany, June 4–8, 1996
edited by M. Wall and A. Heijl

involve the anterior segment, posterior segment, or both. Rubeosis iridis, neovascular glaucoma, retinal hemorrhages, cotton-wool spots, and central arterial occlusion are possible manifestations in these cases.[9-13] They generally occur in high-grade stenosis (>90%) or in occlusion of the internal carotid artery (ICA).

The study of ocular complications associated with carotid obstructive disease is usually performed by means of examination of the anterior and posterior segments and fluorescein angiography. Visual field (VF) examination is rarely utilized in these cases and is considered unnecessary for diagnostic purposes. Nevertheless, automated perimetry may be able to detect the earliest functional deficits in patients affected by hemodynamically significant, but not very severe, carotid stenosis without any signs of ischemic ocular syndrome.

The aim of this study was to investigate the possibility of identifying subclinical, functional ocular alterations by means of automated perimetry, and to correlate these with the severity of carotid stenosis.

Patients and methods

Thirty-six eyes of 18 patients (13 males and five females) affected by obstructive carotid artery disease were examined by automated perimetry (Humphrey 640 VFA, central 30-2 Program). The degree of stenosis was between 70% and 90% in all cases. Ages ranged from 54 to 76 years (mean, 67.5). All the patients in this study were completely asymptomatic for cerebrovascular or ocular disorders.

The patients were first examined at the Department of Clinical Neurophysiology of S. Martino Hospital in Genoa, where they underwent high resolution ecotomography (Biosound 2000, Biosound Inc., Indianapolis) and continuous wave Doppler with spectral analysis (Angioscan III, Unigon Industries, Corp., New York).

The patients were affected by uni- (61.11%) or bilateral stenosis (38.88%) of ICA. (A complete occlusion was never present, but a stenosis greater than 70% was present in at least one side.) In order to evaluate the severity of the stenosis, we adopted the criteria suggested by Hennerici *et al.*[14] All patients underwent a complete ophthalmological examination: biomicroscopic examination of the anterior segment, best corrected visual acuity, tonometry, biomicroscopic examination of the posterior segment, and fluorescein angiography. Only the posterior segment showed some alterations; these were non-specific findings, very common in older patients affected by systemic hypertension or arteriolar sclerosis. Focal and diffuse narrowing of retinal arterioles, increase in arteriolar reflex, retinal veins dilation, and arteriovenous crossing changes are generally not associated with angiographic evidence of microvascular changes.[15-17] Patients with opacification of the media, a familial history of glaucoma, or glaucomatous optic disc alterations, were not included in the study. Some tonometric controls were carried out to make sure ocular pressure was lower than 18 mmHg. Patients with angiographic evidence of retinal vascular disorders were excluded. Patients with refractive errors greater than three diopters or with a history of diabetes and migraine were also excluded. Visual acuity was 20/25 or better in all patients. A summary of the exclusion criteria is shown in Table 1.

According to the literature, we considered a defect to be present when the VF showed at least four adjacent point sensitivities of 5 dB less than surrounding points, or two points with sensitivities of 8 dB less than surrounding points. All VF in our group widely exceeded these minimum conventional limits.

Table 1. Exclusion criteria

Patients were excluded from the study if they met any of the following criteria:
ICA occlusion
ICA stenosis <70% (at least one of two ICA had a stenosis >70%)
Signs and symptoms of ocular ischemia
Focal neurological symptoms
History of amaurosis fugax
Opacification of the media
Ocular pressure >18 mmHg
Optic disc anomalies
Visual acuity <20/25
Refractive error >3 D
History of migraine
Diabetes
Intravenous hyperviscosity syndromes
Any other disease capable of producing VF alterations

General reduction of light sensitivity (GRS) manifests itself by a more or less homogenous reduction of differential sensitivity over the entire VF.

In order to evaluate our visual fields, we analyzed the 'global indices': MD (mean deviation), PSD (pattern standard deviation) and CPSD (corrected pattern standard deviation). In addition, we considered the probability plots results (total deviation and pattern deviation). Mean deviation is the mean elevation or depression of the patient's overall field compared to the normal reference field.

If the deviation is significantly outside the population norms, a '*p*' value is furnished by the computer, and this index is considered abnormal (generally more than 2 dB). For example, a p <2% means that less than 2% of the normal population shows an MD larger than the value found in that test. An abnormal MD value may indicate that the patient has a GRS, or that there is a loss in one part of the VF but not in others. When the MD appears to be the only abnormal index, a GRS is present.

Typical nerve fiber bundle defects (NFBD) or Bjerrum scotomas correspond to the arcuate course of the nerve fibers towards the optic disc. We defined a defect as arcuate on the basis of its topographical aspect on gray scale and, particularly, by considering the topography of pathological points on the pattern deviation plot.

Particular attention was dedicated to preventing artifacts and false positive or false negative responses. The influence of the so-called 'learning effect' was minimized by means of a training examination. In order to avoid the 'demotivation effect', characterized by a fall in attention or a loss of cooperation, the examiner had a preliminary talk with the patients and was constantly present and interactive with them during the entire examination time. The examination was halted every time the cooperation level dropped. Moreover, we carefully evaluated the reliability indices to verify the validity of the examination and to exclude the results in cases of poor cooperation. This method minimized any interference due to patient fatigue, poor cooperation, or to the learning effect**.**

Results

It is not easy to assess a schematic classification of perimetric alterations due to carotid disease. Probably, perimetric defects have a multifactorial origin and may be

caused by both ischemic and/or micro-embolic damage to the different structures involved in visual function (retina, optic nerve and optic pathways).

Visual field abnormalities were detected in 27 of the 36 eyes examined (75%). Nine eyes (25%) showed a normal VF. This finding was bilateral in three of the 18 patients examined (only three patients had a fully normal VF). When considering the 27 eyes showing pathological VF, the isolated presence of NFBD was detected in 48% (13/27), making it the most frequent perimetric defect. This finding was bilateral in five patients and unilateral in three.

The isolated presence of GRS was detected in 22% (6/27). This deficit was unilateral in two patients and bilateral in a further two. The finding of GRS associated with NFBD was present bilaterally in 22% (6/27 eyes, three patients). One patient (2/27 eyes, 7%) showed a deficit distribution, suggesting homonymous quadrantanopic defects.

There were 7/15 patients (46%) affected by VF alterations with asymmetric, mainly unilateral stenosis. Four of these patients (62%) showed bilateral VF defects. Generally, the side where the grade of stenosis was higher and the side showing the worst perimetric results coincided. However, a close relationship between the severity of stenosis and the severity of VF deficits was not detected.

VF defects were often associated with high-grade bilateral stenosis**.** In the three patients with normal bilateral VF, the stenosis was predominantly unilateral and the carotid on the opposite side had a stenosis <50%.

Despite the smallness of our sample, an attempt was made to assess the statistical correlations between the degree of stenosis and the perimetric indices. The method we utilized (Spearman's rank test) revealed no significant correlations.

Discussion

The ocular manifestations of stenotic carotid disease include several clinical pictures: transient episodes of monocular blindness (*amaurosis fugax*), hypotensive retinopathy (also called venous-stasis retinopathy), and the ocular ischemic syndrome. In 1952, Fisher was the first to describe the presence of emboli in retinal arterial branches, and pointed out the association between transient monocular blindness and hemiparesis on the opposite side in patients with carotid artery disease.[18] These phenomena are acute manifestations of carotid artery disease secondary to embolic occlusive events. Obstructive ICA disease may also provoke several chronic ocular manifestations due to slowly progressive ischemia. A large number of different terms were adopted by various authors to indicate these ocular complications: 'hypotensive retinopathy' and 'ischemic ocular syndrome' being two of the most commonly used. Kearns and Hollenhorst[1] pointed out the association between obstructive carotid disease, low perfusion pressure and ocular complications ('venous-stasis retinopathy' or 'hypotensive retinopathy'). This ocular picture is due to a long-term ischemia which generally develops into stenosis of greater than 90% or into complete ICA occlusion. Another ocular picture due to carotid stenosis is that denominated 'ischemic ocular syndrome', which is characterized by severe and chronic panocular ischemia.[4] The ocular lesions involving the posterior segment are similar to those of hypotensive retinopathy, but in this case they are associated with severe ischemia of the anterior segment. Some authors adopt the term of 'ischemic ocular syndrome' to indicate either anterior or posterior segment lesions.

The patients in this study presented with uni- or bilateral stenosis. Stenosis grade, detected by the same physician (GAO) and by the same instruments (Biosound 2000 and Angioscan III), was greater than 70%, but in no case was complete ICA occlusion present. No signs of ocular ischemic syndrome were present at the time of examination. Only non-specific alterations due to age-related arteriolar sclerosis or to systemic hypertension were detectable by ophthalmoscopy.

Visual field defects were present in 75% of examined eyes; this rate suggests the existence of subclinical chronic ischemic damage only detectable by VF analysis. (A list of ocular complications due to carotid disease can be found in Table 2.) This clinical picture is considerably different from the well-known ischemic ocular syndrome and must not be confused with it. Nevertheless, subclinical chronic ocular ischemia may precede the venous stasis retinopathy. In contrast to ischemic ocular syndrome, which induces ocular complications ipsilateral to the side showing ICA occlusion, the alterations in subclinical chronic ischemic oculopathy are frequently bilateral. In ischemic ocular syndrome, the degree of carotid obstruction and the severity of ocular damage are often strictly related. The main differences between ischemic ocular syndrome and subclinical chronic ocular ischemia are listed in Table 3.

Carotid artery occlusion leads to a marked or total ipsilateral reduction in blood flow. Moreover, high-grade ICA stenosis is frequently associated with stenosis of the ophthalmic arteries and with diffuse and severe arteriosclerotic lesions. Consequently, severe damage to the ipsilateral eye may occur. Blood flow reduction leads to increasing ocular ischemia, tissue hypoxia and neovascularization in an attempt to decrease hypoxia itself. The development of a collateral circulation may reduce or delay the damage due to ocular ischemia, but often an ocular ischemic syndrome occurs. These conditions generally denote ipsilateral damage which is easily detectable. When occlusion is unilateral, the fellow eye may show only functional involvement.

The aim of this study was to investigate whether functional deficits were detectable in the case of ICA preocclusion. Moreover, we attempted to investigate whether there is a relationship between uni- or bilateral carotid stenosis and the severity of uni- or bilateral VF alterations.

Our results showed the development of VF alterations in cases of ICA asymptomatic stenosis, suggesting the existence of a subclinical ocular ischemia. A close relationship between uni- or bilateral stenosis and uni- or bilateral VF defects was not demonstrated. It is difficult to find patients affected by ICA stenosis whose opposite ICA is completely normal. Ocular hypoperfusion is often present, and functional damage frequently occurs in these cases. Such damage is only detectable by VF examination. In our series, all the patients had at least one of their two ICA showing a stenosis of greater than 70%, but a low- grade stenosis (from 20% to 50%) was also present in the opposite carotid (Tables 4 and 5).

This slight degree of stenosis may explain the presence of bilateral defects in cases of highly asymmetric stenosis as well. Frequently, in these cases, the eye corresponding to the most stenotic side showed more severe VF alterations.

Probably, the risk factors which lead to the development of a stenosis have also played an important role in the genesis of the VF deficits. Diffuse arteriosclerotic cerebrovascular lesions, systemic hypertension, decreased flow in the ophthalmic artery, and in the choroidal and retinal arterioles, increased blood viscosity, red blood

Table 2. Ocular complications of carotid obstructive disease

Acute manifestations
Amaurosis fugax
Central retinal arterial occlusion or branch retinal arterial occlusion
Ischemic optic neuropathy
Transient monocular blindness and contralateral hemiparesis
Chronic manifestations
Ischemic ocular syndrome
hypotensive retinopathy (venous-stasis retinopathy)
ischemic anterior syndrome
Subclinical chronic ocular ischemia

Table 3. Differences between ischemic ocular syndrome and subclinical chronic ocular ischemia

Ischemic ocular syndrome	*Subclinical chronic ocular ischemia*
Ipsilateral to the most stenotic carotid	Frequently not ipsilateral to the most stenotic carotid
Generally unilateral	Frequently bilateral
Stenosis >90% or carotid occlusion	Stenosis grade <90%
Strict relationship between stenosis grade and ocular damage severity	No rigorous correspondence between stenosis grade and ocular damage severity
Signs and symptoms of ocular ischemia	Asymptomatic
Functional and anatomical damage to the eye	Slight, subclinical damage to the retina and optic nerve
Due to the occlusion of ipsilateral carotid	Multifactorial origin
Generally irreversible	Probably reversible in its early phase
No medical treatment	Medical treatment
Photocoagulation of ischemic areas	

Table 4. Degree of carotid stenosis and perimetric indices: right eye

Patients affected by carotid stenosis		*Global indices (dB)*		
Patients	*Stenosis (%)*	*MD*	*PSD*	*CPSD*
1. BA	80	-4.30	2.00	1.59
2. BE	70	-3.97	6.86	6.27
3. CC	90	-4.77	4.04	3.66
4. CF	80	-11.6	13.85	13.65
5. GA	80	-7.30	7.15	6.74
6. GM	80	-3.78	6.27	6.16
7. IT	50	-3.76	2.54	1.47
8. LN	70	-22.2	8.35	3.54
9. MA	70	-4.07	4.41	3.99
10. MF	80	-15.4	10.50	9.39
11. MR	30	-0.95	2.05	0.88
12. PA	70	-2.22	3.54	2.65
13. PA	70	-5.34	4.78	4.61
14. RA	80	+0.02	2.22	1.78
15. RF	80	-4.20	5.00	4.17
16. RG	70	-2.17	2.19	1.64
17. TF	15	-13.3	7.53	7.04
18. VG	80	-0.38	1.89	1.13

Table 5. Degree of carotid stenosis and perimetric indices: left eye

Patients affected by carotid stenosis			*Global indices (dB)*		
Patients		*Stenosis (%)*	*MD*	*PSD*	*CPSD*
1.	BA	15	-2.99	2.28	1.38
2.	BE	20	-0.14	2.73	1.97
3.	CC	40	-2.61	1.84	1.13
4.	CF	70	-9.56	11.33	11.11
5.	GA	80	-5.13	5.57	5.22
6.	GM	90	-4.60	7.09	7.29
7.	IT	90	-3.78	1.59	0.53
8.	LN	90	-17.1	10.19	10.01
9.	MA	30	-2.76	4.39	4.01
10.	MF	50	-12.2	9.07	8.51
11.	MR	70	-2.53	2.22	1.02
12.	PA	80	-4.38	4.64	3.37
13.	PA	90	-5.82	4.98	4.02
14.	RA	30	+0.01	2.08	1.54
15.	RF	80	-4.60	4.95	4.70
16.	RG	30	-0.50	1.89	1.48
17.	TF	90	-10.2	4.11	2.25
18.	VG	50	-0.38	1.89	1.13

cell (RBC) aggregation and decreased RBC deformation may provoke damage to both eyes at the same time as the carotid stenosis develops.

The lack of a precise correspondence between the severity of stenosis and the severity of VF alterations may be due to a number of factors which may influence the blood flow in the cerebrovascular tree: medical treatment, collateral circulation, patients' age, age on appearance of carotid disease, rapidity of growth, and type of carotid lesions.

Many patients in this study underwent medical treatment with platelet anti-aggregate and other drugs, in order to modify the blood parameters. These therapies may reduce the severity of the carotid disease and provide an explanation of those cases showing minimal VF alterations associated with high-grade uni- or bilateral stenosis. The efficacy of collateral circulation is another important factor. The minimal alterations present in some patients may be due to a good blood supply. Also, the age of the patients, the age of onset, and the rapidity of progression of the stenosis may influence retinal and optic nerve function. Cases of severe and bilateral VF defects associated with unilateral or highly asymmetric stenosis may be due to diffuse arteriosclerotic age-related changes and to a long-standing stenosis.

The anatomopathological aspects of lesions are other important factors; a slight stenosis (40-50%) associated with ulcerative plaques provoking the release of micro-emboli may be more dangerous than a high-grade stenosis (70-80%) without severe micro-embolization phenomena. The commonest perimetric finding in our sample was represented by NFBD. Probably, these are due to the production of micro-emboli from ulcerative plaques of the ICA. These emboli may cause transient occlusions of the retinal arteriolar lumen and subsequently fragment at arteriolar bifurcations, provoking microfocal damage. The presence of isolated NFBD not associated with GRS, relatively circumscribed and not deep, is probably due to a prevalent micro-embolization mechanism. When GRS represents the only alteration, the origin of the

deficit is probably due to progressive chronic hypoperfusion of the eye. The homonymous defects detected in one patient were due to retrochiasmal lesions.

This paper must be considered a preliminary study. There are still too few reported cases to be assessed as a statistical analysis. The demonstration of the existence of functional defects prior to the full clinical picture of ischemic ophthalmopathy represents an interesting result, but further studies are necessary to better investigate the relationship between subclinical ischemic damage to the eye and subclinical damage to the brain.

Conclusions

The high percentage of patients with perimetric alterations suggests that VF examinations should be performed in all cases of hemodynamically significant carotid stenosis. Automated perimetry allows detection of the earliest manifestations of carotid obstructive disease.

This first analysis suggests the existence of a subclinical chronic ischemic oculopathy which can only be detected by automated perimetry. In our opinion, this oculopathy must be considered a new entity, one markedly different from hypotensive retinopathy or venous stasis retinopathy. The lack of a close relationship between the grade of carotid stenosis and the severity of VF alterations, the frequent bilaterality and the presence of solely functional deficits, represent the most important differences. Further studies are necessary to confirm its frequency, characteristics and differences with regard to other ischemic retinal and optic nerve disorders.

References

1. Kearns TP, Hollenhorst RW: Venous-stasis retinopathy of occlusive disease of the carotid artery. Proc Mayo Clin 38:304-312, 1963
2. Smith JL: Unilateral glaucoma in carotid occlusive disease. JAMA 182:683-684, 1962
3. Sturrock GD, Mueller HR: Chronic ocular ischemia. Br J Ophthalmol 68:716-723, 1984
4. Makabe R: Eigenartiges neuvaskulares Glaucom nach Verschluss der Carotis interna. Klin Mbl Augenheilk 164:700-704, 1974
5. Dowling JL, Smith TR: An ocular study of pulseless disease. Arch Ophthalmol 64:236-243, 1960
6. Kearns TP, Siekert RG, Sundt TM: The ocular aspects of bypass surgery of the carotid artery. Mayo Clin Proc 54:3-11, 1979
7. Young LHY, Appen RE: Ischaemic oculopathy: a manifestation of carotid artery disease. Arch Neurol 38:358-361, 1981
8. Ruprecht KW, Naumann G: 'Ischämische Ophthalmopathie': ein Leitsymptom stenosierender Krotisprozesse. Ber Dtsch Ophthalmol Ges 77:891-894, 1980
9. Brown GC, Magargal LE: The ocular ischemic syndrome. Int Ophthalmol 11:239-251, 1985
10. Knox DL: Ischemic ocular inflammation. Am J Ophthalmol 60:995-1002, 1965
11. Dugan JD, Green WR: Ophthalmologic manifestations of carotid occlusive disease. Eye 5:226-238, 1991
12. Kahn M, Green WR, Knox DT et al: Ocular features of carotid occlusive disease. Retina 6:239-252, 1986
13. Ros MA, Magargal LE, Hedges TR et al: Ocular ischemic syndrome: long-term ocular complications. Ann Ophthalmol 19:270-272, 1987
14. Hennerici M, Mohr JP, Rautenberg W et al: Ultrasound imaging and doppler sonography in the diagnosis of the cerebrovascular disease. In: Barnett HYM, Mohr JP, Stein BM et al (eds) Stroke: Pathophysiology. Diagnosis and Management, 2nd Edn, pp 241-268. New York, NY: Churchill Livingstone 1992

15. Gass JDM: Occlusive retinal arterial and arteriolar diseases. In: Gass JDM (ed) Stereoscopic Atlas of Macular Diseases: Diagnosis and Treatment, 3rd Edn, Vol 1, pp 340-368. St Louis, MO: CV Mosby Co 1987
16. Tso MOM, Jampol LM: Pathophysiology of hypertensive retinopathy. Ophthalmology 102:1132, 1982
17. Walsh JB: Hypertensive retinopathy: description, classification, and prognosis. Ophthalmology 89:1127, 1982
18. Fisher M: Transient monocular blindness associated with hemiplegia Arch Ophthalmol 47:167-203, 1952

CLINICAL OBSERVATIONS

THE SIGNIFICANCE OF THE CENTRAL VISUAL FIELD FOR READING ABILITY AND THE VALUE OF PERIMETRY FOR ITS ASSESSMENT

SUSANNE TRAUZETTEL-KLOSINSKI

University Eye Hospital, Department of Pathophysiology of Vision and Neuro-ophthalmology, Tübingen, Germany

Abstract

Reading disability is the main complaint of patients with central field defects. This paper shows the preconditions for reading under normal conditions and in patients with central scotomas.
Methods: Fixation behavior was determined by Tübingen Manual Perimetry (TMP), based on the location of the scotoma and the blind spot. Retinal fixation locus (RFL) and eye movements during reading were recorded simultaneously by a scanning laser ophthalmoscope (SLO). The results of the two methods were compared (n=37 eyes with maculopathy).
Results: A precondition for reading is, on the one hand, a sufficient resolution of the RFL and, on the other, a minimum extent of the reading visual field. In patients with absolute central scotoma, reading ability can be regained by eccentric fixation and additional magnifying aids. In eccentric fixation, the preferred direction of scotoma shift is to the upper or upper/right visual field (93%). A remaining central island (incomplete absolute central scotoma) with persisting central fixation causes reading inability. Fixation behavior showed a high correspondence between SLO and TMP.
Conclusions: The type of field defect and fixation behavior are of great significance for reading ability. The best precondition for regaining reading ability in central scotoma is the use of a single RFL of sufficient resolution together with a reading visual field of sufficient size. Analysis of fixation behavior can explain discrepancies between visual acuity and reading disability. Perimetry is a valuable method for the assessment of fixation behavior. SLO and TMP show high correspondence. SLO has the advantage of quick judgment of fixation behavior, also in alternating RFL, and of simultaneous assessment of morphological, sensory and motor aspects during reading.

Introduction

Reading disability is the main complaint of patients with central field defects. This is important because reading ability is necessary for most information processing, for independence and for general quality of life. This paper shows the preconditions for reading under physiological conditions and in patients with central scotomas.

In a former study we examined the reading process in macular scotoma using an infrared limbus tracker and a modified scanning laser ophthalmoscope (SLO), compared both methods, and showed the value of these techniques.[1] Eccentric fixation,

Address for correspondence: Susanne Trauzettel-Klosinski, MD, Universitäts-Augenklinik, Abt. II, Schleichstrasse 16, D-72076 Tübingen, Germany

Perimetry Update 1996/1997, pp. 417–426
Proceedings of the XIIth International Perimetric Society Meeting
Würzburg, Germany, June 4–8, 1996
edited by M. Wall and A. Heijl

assessed by perimetry, was first shown by Aulhorn[2] in patients with central scotoma. Possibilities and limits of perimetry in the judgment of fixation behavior and reading ability can now be demonstrated by means of the SLO, which allows exact determination of the retinal fixation locus (RFL). This paper focuses on the value of perimetry in assessing fixation behavior and reading ability, while the detailed SLO results are presented elsewhere.[3]

Methods

Perimetry

Tübingen Manual Perimetry (TMP)[4]
Kinetic examination was performed within the 30° field with a test target of ten-minutes diameter and a background luminance of 3.2 cd/m^2. The fixation target consisted of either one circle of 30-minutes diameter or of four circles of 30-minutes diameter (diamond-shaped), midpoints separated by 4° along the horizontal and vertical axes. Size, depth and location of the scotoma were determined. Special attention was paid to the location of the blind spot.

Tübingen Automated Perimetry (TAP)
TAP was performed additionally in some of the patients in the 30° field with the same diamond-shaped fixation target and a background luminance of 10 cd/m^2.

SLO
A modified model 101 SLO (Rodenstock) was used to image the fundus (HeNe or IR laser). The size of the scan field was 35° x 20°. Single targets or texts were scanned directly onto the retina (for details, see ref. 1). The simultaneous representation of text and retina allows exact determination of the RFL during fixation of single targets and during reading. RFL during fixation of single targets and text, and eye movements during reading, were recorded simultaneously on videotape.[5] The temporal resolution was 20 msec (50 fields per second). As the stimuli and fundus were recorded simultaneously, no calibration was necessary to determine the position of the target on the retina (spatial resolution better than 0.2°). RFL was determined for various single targets, words of different length and size, as well as texts.

Patients

Nineteen patients with maculopathy were examined by both methods (37 eyes by TMP, 28 eyes by SLO). Eleven patients had Stargardt's disease, four suffered from age-related maculopathy and five had various kinds of maculopathies. Ten normal subjects underwent fixation and reading tests with the SLO.

Physiological preconditions for reading

Sensory aspects

A visual acuity of about 0.4 is necessary for reading newspaper print at a distance of 25 cm. This resolution is found at the margin of the fovea. Visual acuity decreases

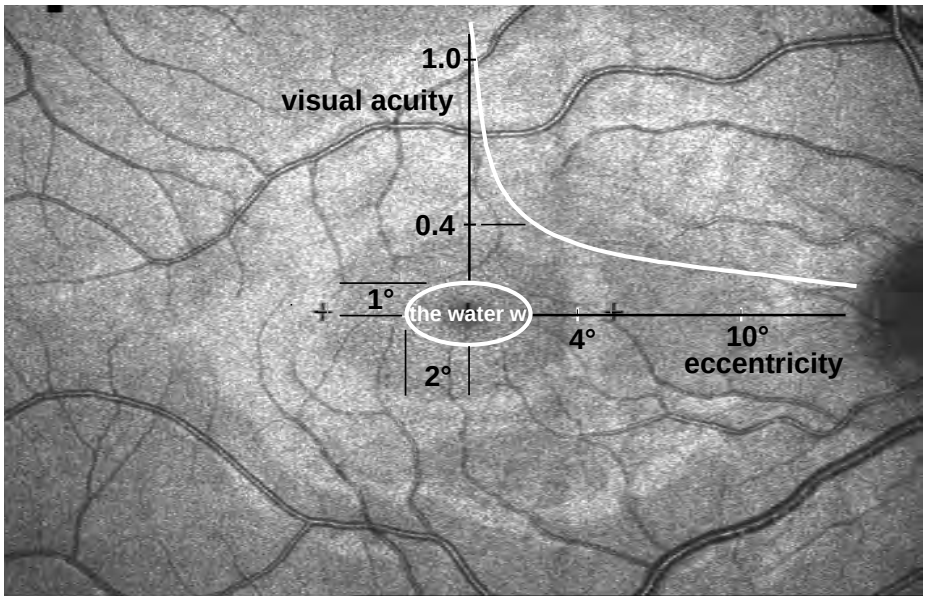

Fig. 1. Retinal resolution (curve) and the minimum reading visual field (ellipse) drawn on an SLO fundus image. *Top:* Visual acuity dependent on eccentricity: rapid decrease of visual acuity with increasing eccentricity. The range of reading ability is limited by the resolution of the retinal area (at 25 cm, 0.4) and by the minimum extent of the reading visual field: 2° to the right and left of the fixation point and 1° above and below (all dimensions related to newspaper print). *Ellipse:* The minimum reading visual field with the corresponding part of the text.

rapidly with increasing retinal eccentricity[6] (Fig. 1). During fixation, an entire complex of letters is perceived and, therefore, a prerequisite for reading is a visual field of a certain minimum extent: 2° to the right and left and 1° above and below the fixation point.[7] Because visual acuity involves recognizing only one test type at a time, the measurement of visual acuity alone is not sufficient to judge reading ability. Therefore, the range of reading ability is limited on the one hand by the resolution of the retinal area used and, on the other, by the minimum extent of the reading visual field. This minimum reading visual field (related to newspaper print) is drawn on a fundus image produced by the SLO (Fig. 1), including the corresponding part of the text. Of course, in a skilled reader, the perceptional area exceeds this minimum.[8]

The retinal area used for reading comprises only a few square millimeters, but the importance of this area is indicated by a disproportionate over-representation in the visual cortex. The central 10° of the visual field, which accounts for about 2% of the total visual field, utilizes more than 50% of the primary visual cortex[9,10] (Fig. 2).

Motor aspects

Accurate eye movements are necessary for well-aimed saccades from one letter complex to the next, which result in a regular stair pattern and a return sweep to the next line – displayed in the eye movement recording (for details, see refs. 1 and 5).

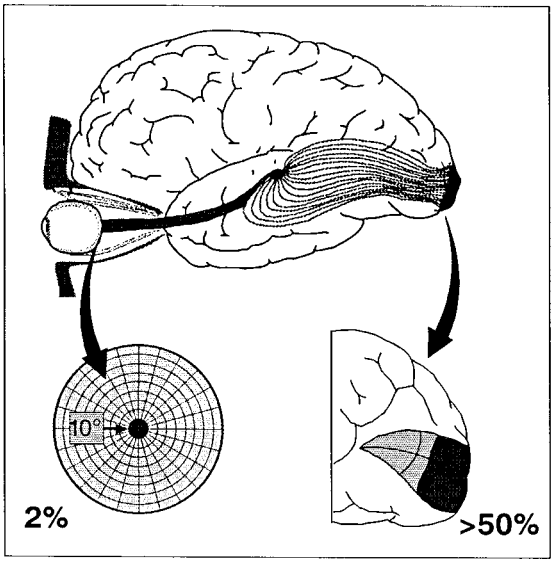

Fig. 2. Over-representation of the central visual field in the visual cortex: the central 10°, which accounts for approximately 2% of the total visual field, utilizes more than 50% of the primary visual cortex (modified from Ref. 11).

Results

The relation of the minimum reading visual field to the 30° visual field and to the text

On the left of Figure 3, the normal situation is depicted. Note that only within the 2×4° area is the text seen clearly, because of the visual acuity curve. It is evident that any kind of field defect affecting the minimum reading visual field disturbs the reading process, for example, in concentric field defects when the central island becomes too small or in hemianotic field defects when half the minimum reading visual field is covered.[12]

In complete absolute central scotoma with central fixation, the reading visual field is totally covered by the scotoma and therefore functionless (Ib), *i.e.*, there is no reading ability (IIb). In these patients, an adaptation process occurs: the patient uses a retinal area at the margin of the scotoma. This new reading visual field now becomes the center of the visual field. Therefore, the scotoma is shifted, as well as the blind spot. The blind spot as the reference scotoma indicates the extent of the shift (Ic). However, the new retinal area used for fixation is of insufficient resolution (IIc). If the text is magnified, reading ability is regained (IId). This is the basis for the application of magnifying visual aids.

Fixation behavior

Perimetric results

Twenty-six eyes showed an absolute central scotoma with a diameter of 3-30°; 21 of

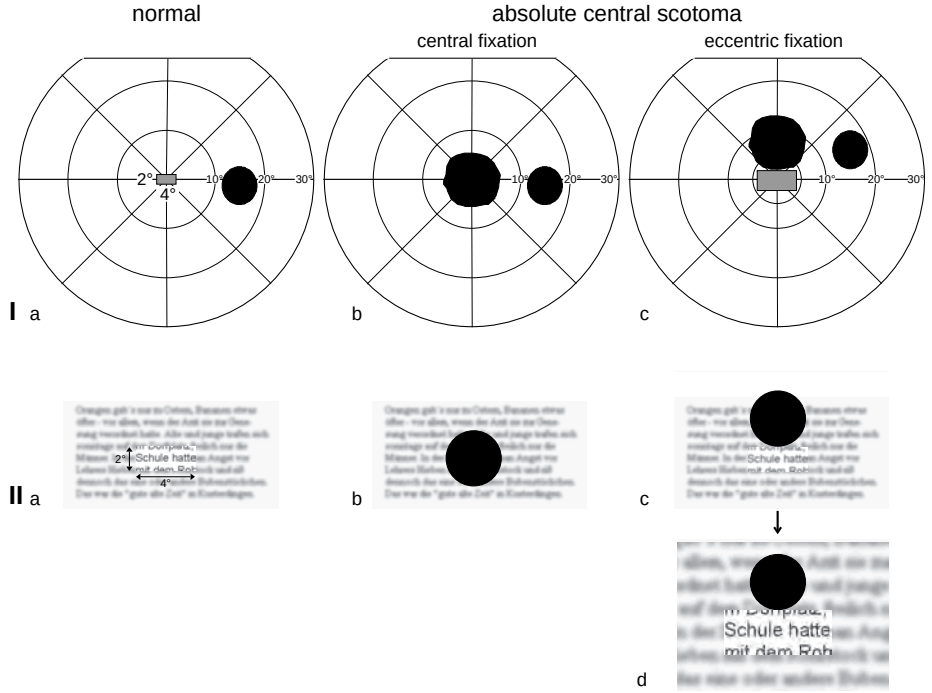

Fig. 3. The relation of the minimum reading visual field to the 30° visual field (I) and to the text (II). Normal subject (a): note that only within the 2° x 4° area can the text be seen clearly. In absolute central scotoma with central fixation, the reading visual field is totally covered by the scotoma and therefore functionless (Ib), there is no reading ability (IIb). In eccentric fixation, a new retinal area at the margin of the scotoma is used for fixation. This new reading visual field now becomes the center of the visual field (Ic). Therefore, the scotoma is shifted, as well as the blind spot. However, the new RFL is of insufficient resolution (IIc). If the text is magnified, reading ability is regained (IId) (modified after Ref. 3).

these eyes (78.4%) shifted the scotoma; 11 patients had a relative central scotoma with a diameter of 4-25° and a depth of 16-32 cd/m^2; eight of these eyes shifted the scotoma. Altogether, 78% showed eccentric fixation.

The preferred direction of scotoma shift was to the upper and upper/right visual field (73% of all eyes), 18 (48.6%) upwards, five (13.5%) upwards/right, and four (10.8%) to the right. Only two eyes (5.4%) shifted the scotoma downwards. When only the eyes with eccentric fixation are considered, the preferred direction of scotoma shift was to the upper and upper/right visual field in 93% of eyes (Fig. 4).

Fixation behavior assessed by SLO

Figure 5 shows the fixation behavior assessed by SLO in a normal person (top). On the left is the central fixation for a single target (cross); on the right, the central fixation for text. The bottom displays eccentric fixation of a patient with juvenile maculopathy; on the left, eccentric fixation of a single target above the lesion; on the right, eccentric fixation of the text. Both subjects are fixating the word ‘was’.

The preferred retinal fixation loci in the total group were above, above/left, and

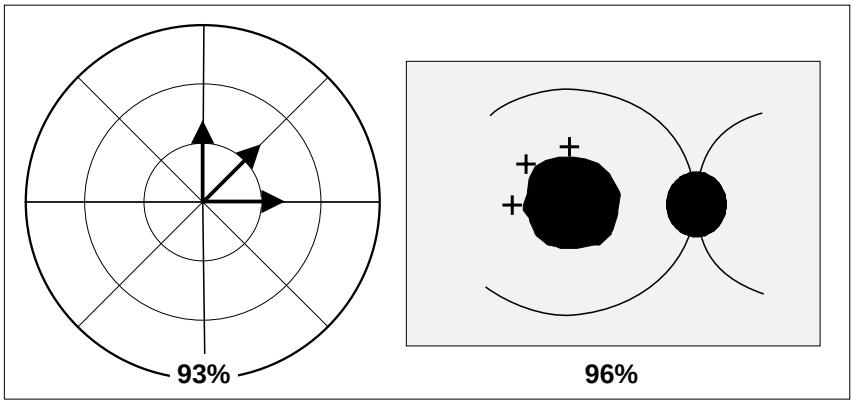

Fig. 4. Direction of scotoma shift assessed by perimetry (left) corresponding to RFL with the SLO (right): 93% of the eyes with eccentric fixation shifted the scotoma upwards, upwards/right or to the right. Accordingly, 96% had their RFL above, above/left and left of the lesion.

left of the lesion (see Fig. 4, right), corresponding to the perimetric results (Fig. 4, left). The results of fixation behavior assessed by TMP and SLO show a high correspondence (74%, see ref. 3). If the absolute central scotoma is incomplete, with a remaining central island, central fixation persists, but the central island is too small for reading. These patients show a discrepancy between visual acuity and reading ability. Sometimes, however, there is a discrepancy between visual acuity and magnification requirement. In such a case, the patient uses two different retinal fixation loci dependent on the size of the stimulus. For small stimuli, requiring high resolution, they use central fixation, for large stimuli and reading text, they use eccentric fixation – with a magnification requirement depending on the eccentricity of the RFL.

Differential diagnosis of fixation behavior in central scotoma by means of the blind spot (Fig. 6)

If the blind spot is in its normal position, there is central fixation. This usually means that, in an absolute central scotoma, there is a central island left with persisting central fixation. This can also be observed in moderate relative scotoma in the beginning stages of maculopathy. When there is a shift of the blind spot, there is eccentric fixation. Two blind spots indicate alternate fixation between two different retinal fixation loci. When the blind spot is absent, there is either a very unstable fixation, or the examination was not done precisely, or the grid for automatic perimetry was of insufficient density (compare also Fig. 7).

Sometimes the question arises of whether a scotoma is central or paracentral. When the blind spot is in its normal location, this indicates a paracentral scotoma. When the blind spot is shifted, this indicates eccentric fixation. Then the blind spot and the scotoma are in the same horizontal line.

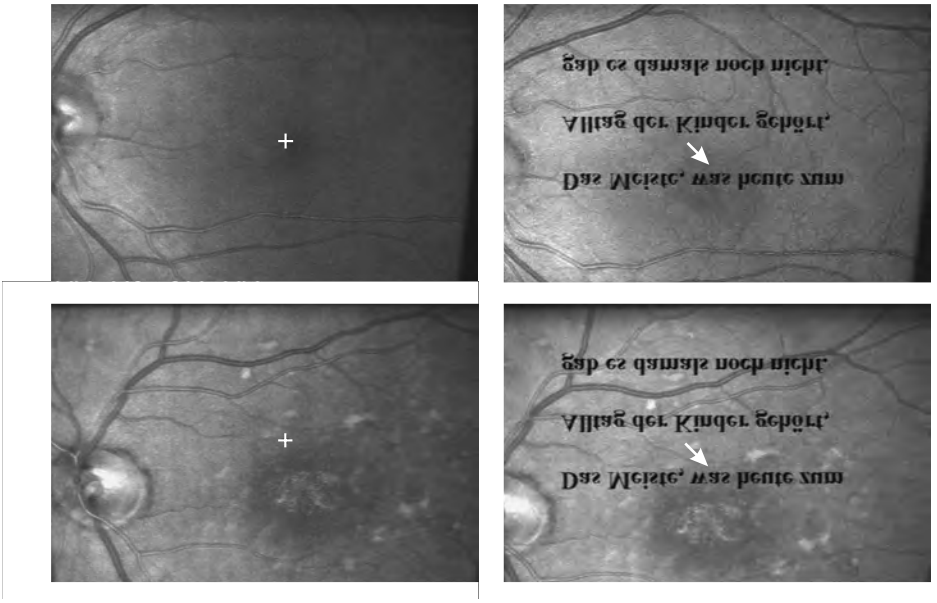

Fig. 5. Top: Fixation behavior assessed by SLO in a normal person. Central fixation for a single target (cross, *left*), central fixation for text (the word 'was', arrow *right*). *Bottom:* Eccentric fixation of a patient with juvenile maculopathy. *Left:* Eccentric fixation of a single target (cross) above the lesion. *Right:* Eccentric fixation of the text (the word 'was', arrow). The text is scanned onto the retina upside down in order to produce an upright image for the test subject.

question	blind spot	diagnosis	visual field
fixation behavior in central scotoma	- normal localization	-central fixation	
	- shifted	- eccentric fixation	
	- 2 blind spots	- alternate fixation (incomplete absolute central scotoma)	
	- not detected	- very unstable fixation - or: not exactly tested - or: grid too large	
central or paracentral scotoma? 	- shifted	- central scotoma with eccentric fixation	
	- normal localization	- paracentral scotoma	

Fig. 6. Differential diagnosis of fixation behavior in central scotoma by means of the blind spot.

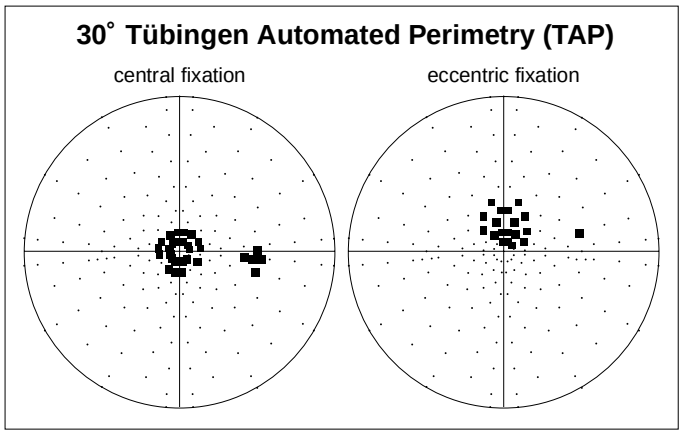

Fig. 7. Central (*left*) and eccentric (*right*) fixation in central scotoma examined by TAP. *Left:* The blind spot can easily be detected when normally located because of the increased number of test targets in this area. *Right:* Shift of central scotoma and blind spot: absence of blind spot in its normal position, absolute defect above it.

Special features in automated perimetry

Figure 7 shows a comparison of central and eccentric fixation examined by TAP. On the left, the absolute central scotoma is located in the visual field center and the blind spot is at its normal position – well-detected by an increased number of test targets in this area. On the right, the shift of central scotoma and blind spot: absence of blind spot at its normal position, absolute defect above it.

Discussion

The range of reading ability is determined by the resolution of the RFL and by the minimum extent of the reading visual field (Fig. 1). Fixation behavior is very important for reading ability. In absolute central scotoma, reading ability can only be regained with eccentric fixation. The insufficient resolution of the new RFL can then be compensated by magnification (Fig. 3, IId). When the absolute central scotoma is incomplete, central fixation persists, but the central island is too small for reading. This explains discrepancies between visual acuity and reading ability.[3]

In summary, the best precondition to regain reading ability in central scotoma is the use of a single RFL of sufficient resolution and size.

The preferred directions of the scotoma shift confirm the findings of Aulhorn.[2] Using the SLO, Guez *et al.*[13] have reported similar results with regard to the RFL. The shift into the upper visual field preferred by about 50% of our patients is most convenient because the lower visual field is more important in everyday life. The preferred RFL should be considered in the localization of retinal laser treatment.

Eccentric fixation is an effective adaptive mechanism. This behavior usually occurs spontaneously (but can be supported by training[14]). That the new RFL can be used as the new center of the visual field, and as the new zero point of the coordi-

nates for eye movements, is an indication of high cortical plasticity (for details, see ref. 3).

Fixation behavior can be very well assessed by perimetry when the blind spot is considered as a reference scotoma.

Even though manual perimetry is superior to automated perimetry for judgment of fixation behavior, automated perimetry can also give valuable information if the grid is of sufficient density. As TAP offers enhanced density of test targets in the area of the normal blind spot, the blind spot can very easily be determined in stable central fixation (Fig. 7, left). The absence of the blind spot is a very conspicuous sign of a shift (Fig. 7, right). The presence of an absolute defect above the normal location confirms this assumption. It is evident that, owing to the lower density of the grid in this area, the (shifted) blind spot can easily be missed. Computerized strategies to improve examination of the blind spot with other automatic perimeters have been proposed by Safran *et al.*[15]

Using the SLO it could be shown that perimetry is a very valuable method for judging fixation behavior in patients with central scotoma. The results of assessing fixation behavior with the SLO and Tübingen Manual Perimeter corresponded very closely.[3] Discrepancies were seen in patients with very unstable fixation or in cases with more than one RFL.

The SLO method has the advantage of the simultaneous assessment of morphological, sensory and motor aspects. It is especially valuable for exact determination of RFL, particularly in cases with very unstable fixation or with more than one RFL, which can clearly be seen with the SLO, but not always with TMP. However, the method is expensive and requires advanced technical equipment.

Perimetry is a valuable method for examining fixation behavior in central scotoma. In patients with discrepancies between visual acuity and reading ability, perimetric results can show the reasons for the reading disability by means of fixation behavior. However, this method is rather time-consuming and requires an experienced perimetrist.

References

1. Trauzettel-Klosinski S, Teschner C, Tornow RP, Zrenner E: Reading strategies in normal subjects and in patients with macular scotoma: assessed by two new methods of registration. Neuro-Ophthalmology 14:15-30, 1994
2. Aulhorn E:P Die Gesichtsfeldprüfung bei macularen Erkrankungen. In: Ber. 73. Zusammenk. der DOG Heidelberg 1975, pp 77-86. München: JF Bergmann 1975
3. Trauzettel-Klosinski S, Tornow RP, Teschner C: Fixation behavior and reading in patients with macular scotoma: assessed by Tuebingen Manual Perimetry and SLO. Neuro-Ophthalmology 16:241-253, 1996
4. Aulhorn E, Harms H: Visual perimetry. In: Jameson D, Hurvich LM (eds) Visual Psychophysics, Vol 7/4, Handbook of Sensory Physiology. Berlin: Springer 1972
5. Trauzettel-Klosinski S, Teschner C, Tornow RP, Durst W, Zrenner E: The reading process: a new approach to the sensory and motoric aspects. Video film, first presentation at the 1st Meeting of the European Neuro-ophthalmological Society EUNOS 1993
6. Wertheim T: Über die indirekte Sehschärfe. Z Psychol 7:172-187, 1894
7. Aulhorn E: Über Fixationsbreite und Fixationsfrequenz beim Lesen gerichteter Konturen. Pflügers Arch Physiol 257:318-328, 1953
8. Rayner, K: Eye movements and the perceptual span in beginning and skilled readers. J Exp Child Psychol 41:211-236, 1986

9. Horton JC, Hoyt WF: The representation of the visual field in human striate cortex. Arch Ophthalmol 109:816-824, 1991
10. McFadzean R, Brosnahan D, Hadley D, Mutuklan E: Representation of the visual field in the occipital striate cortex. Brit J Ophthalmol 78:185-190, 1994
11. Spalding JMK: Wounds of the visual pathway. I. The visual radiation. J Neurol Neurosurg Psychiat 15:99-107, 1952
12. Trauzettel-Klosinki S, Brendler K: Eye movements in reading with hemianopic field defects: the significance of clinical parameters. Graefe's Arch Clin Exp Ophthalmol 1997, in press
13. Guez J-E, Le Gargasson J-F, Rigaudiere F, O'Reagan JK: Is there a systematic location for the pseudo-fovea in patients with central scotoma? Vision Res 33:1271-1279, 1993
14. Nilsson UL, Nilsson SEG: Rehabilitation of the visually handicapped with advanced macular degeneration. Doc Ophthalmol 62:345-367, 1986
15. Safran AB, Mermoud C, Estreicher J, Liebling TM: Evaluation of the blind spot in automated perimetry using a spatially adaptive strategy: optimization of the procedure by means of computerized simulation. In: Mills RP (ed) Perimetry Update 1992/1993, pp 285-292. Amsterdam/ New York: Kugler Publ 1993

PERIMETRIC FOLLOW-UP IN MYOPIC MACULOPATHY

P. CAPRIS[1], G. CORALLO[1], F. ROSSI[1], G. GATTI[1], S. ROVIDA[2] and M. ZINGIRIAN[1]

[1]University Eye Clinic; [2]Biometric and Medical Statistics Institute; Genoa, Italy

Abstract

The clinical evolution of myopic maculopathies (MM) is usually evaluated by means of fundus examination, visual acuity and fluoroangiography. The perimetric evaluation of differential light sensitivity changes in macular diseases, and above all in myopic maculopathies, may be difficult owing to threshold fluctuation.

The aim of this study was to measure the long-term threshold fluctuation (LF) in a group of clinically stable MM patients, in order to evaluate its relationship with depth and topography of visual field defects. This enabled significant criteria to be established to evaluate real sensitivity changes not due to random threshold fluctuation.

Twenty-five subjects who met the following criteria were included in the study: *1.* Diagnosis of MM based on typical ophthalmoscopic and fluoroangiographic findings; *2.* good reliability indices, *3.* visual field defects inside 10° eccentricity; *4.* visual acuity of 0.5 or better without change during the follow-up period; *5.* refraction-5.00/-20.00 D without changes during the follow-up period.

All the subjects included in this study were examined at least three times by automated perimetry. The time interval between examinations was at least three weeks. All visual fields were performed with the Humphrey 640 VFA using the Central 10-2 Program. The LF of stable MM patients was studied. The total mean LF for the entire sample was 1.55 ± 1.03 dB. No statistical correlation was found between LF and sensitivity. The LF was greater in the superior hemifield (0.252 dB). In their sample of more than 6000 light threshold measurements, the authors tried to define the upper limits of threshold change in visual field which might be considered a result of a random fluctuation. In the examinations, a change of more than 4 dB in a single test location was due to random fluctuation in only 2.5%.

These data provide practical guidelines for the evaluation of progressive visual field loss in MM. The implementation of a computerized statistical program for the assessment of MM visual field probability change would seem to be extremely useful and desirable.

Introduction

The degenerative changes in the macula are one of the most important causes of legal blindness in the highly myopic eye. Myopic maculopathies (MM) are characterized by fundus pallor and tessellation, diffuse or local chorioretinal atrophy, posterior staphyloma, lacquer cracks and subretinal neovascularization (SRNV).[1,2] The myopic

Address for correspondence: Paolo Capris, Clinica Oculistica Università di Genova, c/o Pad. 9, V.1e Benedetto XI, 16132 Genova, Italy

Perimetry Update 1996/1997, pp. 427–433
Proceedings of the XIIth International Perimetric Society Meeting
Würzburg, Germany, June 4–8, 1996
edited by M. Wall and A. Heijl

changes in MM have been classified by Avila *et al.*[1] into five grades (M1-M5), according to the severity of the findings.

Subretinal hemorrhages frequently occur when SRNV is present: in 65% according to Hotchkiss and Fine[2] and 78% according to Fried *et al.*[3]

Follow-up of MM is extremely important in order to find the earliest signs of SRNV that can benefit from laser treatment. Usually the follow-up of MM is carried out by measuring far and near visual acuity, by ophthalmoloscopy, fluoroangiography, indocyanine green digital angiography, Amsler grid auto-examination, and perimetry.

Perimetry has often been used to evaluate visual function[4-7], medical therapy[8-13] in myopia and MM, and also the laser treatment effect in age-related macular degeneration (ARMD),[9-15] or surgery in epiretinal membranes.[16] Perimetry is a non-invasive and easy technique for evaluating the modifications of macular light sensitivity in MM. In the advanced stages of MM, a decrease of sensitivity is usually related to sensorial retinal damage. This loss of sensitivity is characteristic of the observed areas of atrophy. The differential light threshold sensitivity in myopia, tested by automatic perimetry, has been studied by many authors.[5,6] A diffuse loss of sensitivity ranging from 0.6-1.77 dB has been demonstrated in myopic eyes in comparison to emmetropic ones.[5,6] This loss is greater in the periphery than inside 10°.[5] The short-term fluctuation (SF) in myopic eyes is normal.[6]

Light threshold, as measured by automated perimetry, is subjected to well-defined physiological short- and long-term fluctuations.[17] Furthermore, these fluctuations are clinically increased in pathological conditions and in stable diseases. Threshold fluctuations have been studied in clinically stable glaucoma[18-24] and in stable ARMD,[25] and significant statistical criteria to evaluate real sensitivity changes have been established. The availability of normal age-matched sensitivity values allows us to detect the earliest visual field defects in glaucoma as in other diseases, such as maculopathies.[24]

An extended statistical package for the assessment of multiple successive field defects in glaucoma (Statpac glaucoma change probability) has been implemented in the Humphrey VFA.[26] Nevertheless, evaluation of sequential perimetric examinations to detect progressive damage in glaucoma, ARMD and MM is a difficult and important problem. The aim of this study was to measure the threshold long-term fluctuation in a group of clinically stable MM patients in order to evaluate its relationship with depth and topography of the visual field defects. This allows identification of significant criteria for evaluating real sensitivity changes not due to random threshold fluctuation.

Material and methods

The clinical charts of 52 myopic patients followed at the Retina Service of the University Eye Clinic of Genoa were reviewed.

Twenty-five subjects who met the following criteria were included in the study:

1. Diagnosis of MM presenting with typical ophthalmoscopic and fluoroangiographic findings, of grades M1-M3 according to Avila's classification.[1] Absence of SRNV and hemorrhages.

2. At least two available automated visual field examinations and at least nine months' follow-up after the first examination.
3. Good reliability indices (Fixation losses <10%; false positive and negative answers <10%).
4. Visual acuity of 0.5 or better (E.T.D.R.S. visual acuity charts), without changes during the follow-up period.[27]
5. Near visual acuity of 2nd De Wecker or better, without changes or 'metamorphopsia' during the follow-up period.
6. Myopic refraction -5.00 D/-20.00 D without changes during the follow-up period.
7. No other eye disease (cataract, glaucoma), or laser or surgical treatment.
8. No change in medical therapy during the follow-up period.

All the subjects included in this study were examined at least three times by automated perimetry. The time interval between examinations was at least three weeks. All visual fields were performed with the Humphrey 640 VFA using the Central 10-2 Program (full threshold strategy), with the central fixation point, including foveal threshold measurement. At the end of the follow-up period, all subjects underwent a fluoroangiographic examination.

Nine subjects were excluded from the study for the following reasons: *1.* appearance of subretinal neovascular membranes; *2.* visual acuity decay; *3.* reliability index deterioration; *4.* voluntary withdrawal; *5.* excessive tiredness; *6.* refractive modification.

At the end of the study, 26 eyes of 16 patients were included in the statistical analysis. In all patients, light threshold values in each series of examinations were compared point-by-point and the long-term fluctuations were measured. The mean and standard deviations were calculated for each test location of each subject in at least the three most recently available visual field examinations. Total long-term fluctuation of each test location was defined as the standard deviation of the mean sensitivity for that location. The total long-term fluctuation of each subject was defined as the mean of standard deviations for each of that subject's test locations. Total long-term fluctuation of the entire sample was the mean of the standard deviations for each test location for all subjects.

Results

One hundred and one visual fields of 26 eyes of 16 patients qualified for the study. All patients had an average of 3.9 visual field examinations (range, 3 to 5). The mean time interval between examinations was 24.5 days, ranging from 18 to 34 days. The mean (±SD) follow-up time of 95.5 (±21.3) days reproduces the clinical condition of perimetric examinations over months and years, in which long-term fluctuation takes place but is sufficiently short to ensure stability of the MM. The patient's mean age (±SD) was 53.4 (±8.3) years (range, 31 to 68). The mean light sensitivity of all visual fields was 27.09 ± 3.13 dB (range, 23.2 to 32.5), and the total mean (±SD) LF for all test locations of the entire sample was 1.55 ± 1.03 dB (range, 0 to 5.29).

The linear regression analysis of LF with differential light sensitivity of the first examination showed no statistically significant correlation. There was a significant relationship between the LF and the refractive error ($p < 0.005$), but no correlation with age (Spearman rank correlation test). The visual field pattern of the Central 10-

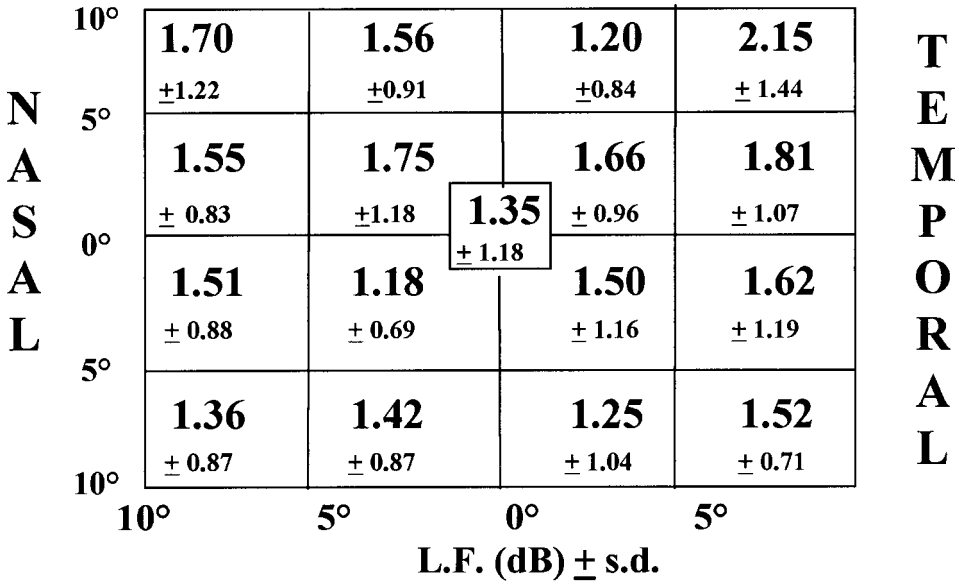

Fig. 1. Mean long-term fluctuation (±SD) of all the patients in the main quadrants at two eccentricities.

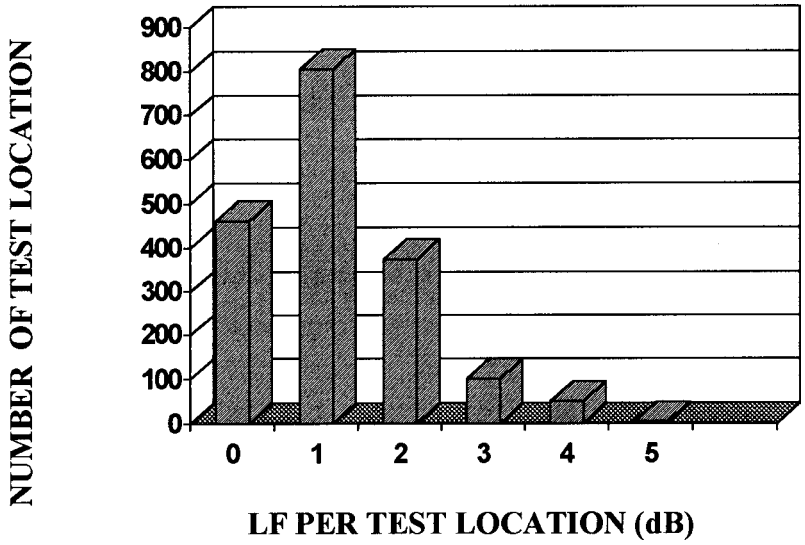

Fig. 2. Frequency distribution of the total long-term fluctuation per test location for the entire sample. The total number of test locations was 1794. Test locations where all sensitivity determinations were 0 dB have been excluded.

2 Program was divided into 16 square zones, four inside 5° and 12 outside, respectively, and the corresponding total LF mean values were calculated in order to evaluate eventual differences related to location and eccentricity (Fig. 1). In ten patients in whom both eyes were examined, the total long-term fluctuation in the

right eye of each subject was compared with the left one (Wilcoxon signed rank test). No significant correlation was found between left and right eyes. The LF was significantly greater in the superior hemifield (mean LF difference: 0.0252 dB; $p < 0.03$), while no difference was found between the temporal and nasal hemifields. In clinical practice, it is more important to know the range and incidence of the measured LF values, therefore the frequency distribution of the entire sample was calculated (Fig. 2).

Discussion

The LF in stable MM patients was studied: the long-time interval between examinations and the exclusion of patients with fundus and visual acuity changes reproduced the clinical condition in which a patient undergoes a perimetric follow-up over months and years. The total LF (±SD) for the entire sample was 1.55 ± 1.03 dB. This value was not statistically related to eccentricity while a significant difference was found between the superior and inferior hemifields. However, this greater LF value in the superior hemifield had no practical clinical interest.

These results are in agreement with other studies[18,19] that also showed a greater LF value in the superior hemifield in glaucomatous VF, while they are in contrast with the results of a correlation between LF and eccentricity found in glaucomatous VF. This can be explained if we consider that the visual field examinations in the present study were only carried out in the central 10°, even if the temporal quadrants could be influenced by the nearness of the blind spot. No significant correlation was found between LF and sensitivity. This is in contrast to the results of other authors who studied LF in glaucoma,[18-20] and also to our previous study on the LF in stable age-related macular degeneration (ARMD).[25] This can be justified by the almost homogeneous sensitivity of the visual fields in our sample in contrast to those of the ARMD patients.

The lack of a significant difference between the right and left eyes can be explained by the random asymmetry of the MM stage, light sensitivity, refractive error, and patient reliability in the group of ten subjects in whom both eyes were tested. In our sample of 6969 light threshold measurements, we tried to define the upper limits of threshold change in visual field, which might be considered a result of random fluctuation. Our results suggest that, in MM, we should consider a test location sensitivity decrease of more than 3 dB as a suspected clinical deterioration; this change was due to random fluctuations in only 8% of locations. A change of more than 4 dB in a single test location was due to random fluctuation in only 2.5% of our examinations.

The evidence that locations with very low light sensitivity frequently correspond with chorioretinal atrophic areas may explain why we found a paradoxically low LF in those areas. These threshold changes are much more important when they are present in many locations, particularly if clustered. The LF in stable glaucoma patients measured by Werner *et al.*[19] (2.8 dB) and Zulauf *et al.*[20] (4.2 dB) was greater than in MM.

In our previous study on LF in ARMD, we obtained a value of 2.15 dB, which could be considered to be clinically superimposable on the LF in MM. These data attempted to provide practical guidelines for the evaluation of progressive visual field

loss in MM. The implementation of a computerized statistical program for the assessment of the maculopathy visual field probability change would seem to be extremely useful and desirable in clinical practice.

Acknowledgments

This work was supported by a grant from CNR (Consiglio Nazionale Ricerche) Progetto finalizzato 'Invecchiamento' Contr. N. 93.00468.PF40 (Italy).

References

1. Avila M, Weiter J, Jalkh A, Trempe C, Pruett R, Schepens C: Natural history of choroidal neovascularization in degenerative myopia. Ophthalmology 91:1573-1581, 1984
2. Hotchkiss ML, Fine SL: Pathologic myopia and choroidal neovascularization. Am J Ophthalmol 90:923-926, 1983
3. Fried M, Siebert A, Meyer-Schwickerath et al: Natural history of Fuch's spot: a long term follow-up study. Doc Ophthalmol 28:215, 1981
4. Risse JF, Gobert F: Champ visuel du myope fort. In: Mondan H, Metge P et al (eds) La Myopie Fort, pp 187-201. Paris: Masson 1994
5. Huang SJ: Early change of visual function in high myopia: measured and analyzed by Octopus automated perimeter. J Jpn Ophthalmol Soc 97/7:881-887, 1993
6. Messenio D, Marra G: L'influenza della ametropie sugli indici perimetrici della perimetria automatizzata. I° Congr Soc Ital Perimetria Part 2, Genoa, November 1989. Minerva Oftalmol 32/2:141-143, 1990
7. Sato Y, Yamashita M, Hayashi K, Tokoro T: Abnormality of visual field in pathological myopia. Acta Soc Ophthalmol Jpn 88/6:977-982, 1984
8. Sacca' S, Gandolfo E, Capris P, Allegri P, Dolci A: Azione di un'associazione antacianosidi-vitamina A-vitamina E sulla soglia luminosa differenziale e sulla fluttuazione a breve termine: studio perimetrico nei miopi. Atti XI Riun Soc Oftalmol Nord-occidentale, Lerici, 3-5 October 1986. Boll Ocul (Suppl)6:269-274, 1986
9. Coscas C, Soubrane G, Ramahefasolo C, Fardeau C: Perifoveal laser treatment for subfoveal choroidal new vessels in age-related macular degeneration. Arch Ophthalmol 109:1258-1264, 1991
10. Jacobs NA, Patterson IH, Broome IJ: The macular threshold: determination of population normal values. Doc Ophthalmol Proc Ser 49:137-142, 1987
11. Fine SL, M.P.S.: Early detection of extrafoveal neovascular membranes by daily central field evaluation. Ophthalmology 92:603-609, 1985
12. Maguire J, Annesley WH et al: Computerized visual field deficit in tears of the retinal pigment epithelium. Br J Ophthalmol 74:556-558, 1990
13. Janknecht P, Soriano JM, Funk J, Hansen LL: Automatic perimetry of the central visual field in diseases of the macula. Klin Mbl Augenheilk 199/4:259-263, 1991
14. Zingirian M: Périmétrie automatisée et pathologie maculaire. J Fr Ophtalmol 641-643, 1989
15. Janknecht P, Soriano JM, Funk J, Jansen LL: Do laser scars grow in spite of successful laser coagulation of subretinal neovascularization? In: Mills RP (ed) Perimetry Update, pp 583-587. Amsterdam/New York: Kugler Publ 1993
16. Villaplana D, Horas M, Casaroli RP, Moreno V, Barraquer J: Automatic perimetry variations found on epiretinal macular membranes. Presented at the 4th Meeting of the European Macula Group, Genoa, June 1996
17. Fankhauser F, Bebi H: Threshold fluctuations, interpolations and spatial resolution in perimetry. Doc Ophthalmol Proc Ser 19:295-309, 1979
18. Werner EB, Bishop KI, Davis P, Krupin T, Petrig B, Sherman C: Visual field variability in stable glaucoma patients. Doc Ophthalmol Proc Ser 49:77-84, 1987
19. Werner EB, Petrig B, Krupin T, Bishop KI: Variability of automated visual fields in clinically

stable glaucoma. In: Heijl A (ed) Perimetry Update 1988/89, pp 167-172. Amsterdam/Milano: Kugler & Ghedini Publ 1989
20. Zulauf M, Caprioli J, Hoffman DC, Tressler CS: Fluctuations of the differential light sensitivity in clinically stable glaucoma patients. In: Mills RP, Heijl A (eds) Perimetry Update 1990/1991, pp 183-188. Amsterdam/Milano: Kugler & Ghedini Publ 1991
21. Heijl A, Lindgren G: Test-retest variability in glaucomatous visual fields. Am J Ophthalmol 108:130-135, 1989
22. Fujimoto N, Adachi-Usami E: Fatigue effects with 10° visual field in automated perimetry. Am J Ophthalmol 25:142-144, 1993
23. Flammer J, Drance SM, Zulauf M: Differential threshold: short- and long-term fluctuation in patients with glaucoma, normal controls, and patients with suspected glaucoma. Arch Ophthalmol 102:704-706, 1984
24. Heijl A, Lindgren G, Olsson J: A package for the statistical analysis of visual fields. Doc Ophthalmol Proc Ser 49:153-168, 1987
25. Capris P, Soldati MR, Di Lorenzo G, Corallo G, Rovida S: Threshold fluctuation in clinically stable age-related macular degeneration. In: Mills RP, Wall M (eds) Perimetry Update 1994/ 1995, pp 383-386. Amsterdam/New York: Kugler Publ 1995
26. Heijl A, Lindgren A, Olsson J, Åsman P, Myers S, Patella M: Extended empirical statistical package for evaluation of single and multiple fields in glaucoma: Statpac 2. In: Mills RP, Heijl A (eds): Perimetry Update 1990/1991, pp 303-315. Amsterdam/Milano: Kugler & Ghedini 1991
27. Ferris FL, Kassoff A, Bresnick GH et al: New visual acuity charts for clinical research. Am J Ophthalmol 94:91-96, 1982

HIGH-PASS RESOLUTION PERIMETRY IN THE EARLY DETECTION OF MACULAR ALTERATIONS IN PATIENTS TAKING HYDROXYCHLOROQUINE

FRANCO BAROSCO, PAOLO BRUSINI, GIUSEPPE DI GIORGIO and MARZIO CHIZZOLINI

Department of Ophthalmology, Ospedale Civile, San Donà di Piave (VE), Italy

Abstract

Twenty-seven patients who received a total cumulative dose of hydroxychloroquine between 18 g and 1270 g for rheumatic diseases, underwent high-pass resolution perimetry (HRP) and computerized automated perimetry (CAP), using the CENTRING Program and 10-2 Program, respectively. The specificity of both methods was examined and found to be good in 20 normal subjects. Significant defects were noted in nearly 40% of eyes examined using HRP and in 5.7% of eyes using CAP. There was no correlation between total drug dose and perimetric defects. HRP is a sensitive and very rapid technique for the follow-up of patients undergoing chronic treatment with synthetic antimalarial drugs.

Introduction

Chloroquine phosphate and its derivative hydroxychloroquine sulphate have been used since the early 1950s in the treatment of rheumatoid arthritis and other rheumatological disorders. These antimalarial drugs are known to produce retinopathy in a cumulative dose-related fashion.[1-4] In recent years antimalarial retinopathy has become rare, probably because rheumatologists switched from chloroquine to hydroxychloroquine, which could be less retinotoxic. The earliest morphological changes are non-specific pigmentary disturbances in the macular area.[5] Once ophthalmoscopically visible changes have occurred in the retina, visual loss can be progressive in spite of cessation of therapy. Visual field defects have been reported to occur prior to overt retinal pigmentary changes, and may progress after cessation of treatment. Computerized automatic perimetry (CAP) appears to be able to detect central and paracentral scotomas before fundus alterations and, sometimes, even before electroretinographic alterations.[6-8] In other retinal and neurological diseases however, high-pass resolution perimetry (HRP) has been shown to be more sensitive than CAP.[9,10] A group of patients treated with hydroxychloroquine for at least two years underwent

Address for correspondence: Franco Barosco, MD, Divisione Oculistica, Ospedale Civile, 30027 San Donà di Piave (VE), Italy

Perimetry Update 1996/1997, pp. 435–439
Proceedings of the XIIth International Perimetric Society Meeting
Würzburg, Germany, June 4–8, 1996
edited by M. Wall and A. Heijl

CAP and HRP examination in order to discover whether HRP could be used in the early detection of a macular alteration.

Material and methods

Fifty-three eyes of 40 patients who had received a different cumulative dose of hydroxychloroquine (mean age 54.2 ± 12.9 years) were entered into the study. In all patients, the total cumulative ingested dose was calculated precisely. The total dose range was from 18 g to 1270 g. Eyes with an intraocular pressure higher than 18 mmHg, a visual acuity lower than 10/10, or a refractive defect higher than 4 diopters (D), were excluded. We also excluded diabetics and subjects who cooperated poorly. No patients' eyes had a history of trauma, surgical intervention or congenital anomalies of the optic disc. Overall, 27 patients satisfied the above inclusion criteria, all of whom underwent an accurate biomicroscopic and fundus examination using a 90-D Volk's lens and, finally, a macular perimetric examination using both CAP and HRP. CAP was performed with a Humphrey Field Analyzer model 640 (Zeiss-Allergan, San Leandro, CA), using the 10-2 threshold test (68 points within the central 10°).

HRP was performed with the Frisén Ophthimus Ring perimeter (Nikon-HighTech Vision, Malmö, Sweden), using the CENTRING Program. This test covers the central 6° using 33 test locations in a fixed, symmetrical pattern, when the subject is tested at 0.5 m display distance. The test strategy is very similar to that of RING. The test time is about three to four minutes. The fixation mark can be adapted to the subject's visual capacity. Appropriate correcting lenses must be used for the selected distance from an ordinary trial lens set. When the test is completed, the computer brings up the result display showing distance, the targets of variable angular sizes between 3.2 min of arc, being the smallest, and 53.6 min of arc, being the greatest, and decibel values, from -4.6 to +7.6, corresponding at each angular degree. The targets used are rings with a light core and dark inner and outer borders. The stimulus value is altered by changing the angular size. If a given target cannot be resolved, it cannot be seen at all because then the ring constituents blend imperceptibly into the background. The examiner begins with a calibration display which is identical to that of the RING test and makes the sitting patient comfortable with the line of sight perpendicular to the front surface of the test display. To perform a CENTRING test, the examiner checks the distance with a measuring tape. The test starts with a demonstration trial before showing a static display of the full target series, in order to acquaint the subject with the size variability. This is followed by test targets of various sizes shown in random locations. The subject is reminded about fixation by periodically flashing a LOOK HERE message onto the screen. Targets are shown for 165 milliseconds, which is just below the reaction time for changing fixation. The perimetric indices referred to in decibels are the 'mean score', the 'mean retest change' and the 'retest SD'. In addition, there are some reliability indices which are similar to the CAP indices. A short learning program preceded the test with both these instruments. As a control group, we also examined 20 eyes of 20 healthy subjects (mean age 49.8 ± 11.2 years) with a refractive defect of less than 4 D.

Fifteen patients underwent electroretinography examination including photopic and scotopic electroretinogram (ERG) using blepharal electrodes. Seven of these showed at least one abnormal visual field either with CAP, HRP, or both. The other

eight patients had a normal visual field whether performed with CAP or HRP. Only five patients consented to undergo a fluoroangiographic examination.

Criteria for abnormality

Using CAP, the tests which showed more than ten significantly depressed points with a $p<2\%$ in the total deviation map of the STATPAC 2 statistical program, were considered abnormal, as were tests showing more than two adjacent depressed points with a $p<2\%$ or one point with a $p<0.5\%$ in the pattern deviation map, but only if within 5°. We considered as borderline those tests in the total deviation map showing more than 20 depressed points with a $p<5\%$, or four to ten points with a $p<2\%$, or the cases in the pattern deviation map that showed two adjacent points with a $p<2\%$, or more than two adjacent points with $p<5\%$, or one point with $p<1\%$.

With HRP, the tests with a CENTRING mean score >1 dB were considered abnormal, as were the eyes presenting with more than two depressed points over the following limits: 5 dB for the nine points within 1°, 6 dB for the eight points located on the 2° parallel, 7 dB for the eight points on the 4°, and 8 dB for the eight points located on the 6°. We also considered abnormal those tests presenting with only one point depressed more than 2 dB over the above-mentioned limits, if the faulty point was located within 4° or was associated with other borderline alterations. Those eyes with a mean score included between 0.1 and 1 dB, those eyes with two depressed points over the above-mentioned limits, or those eyes with only one point depressed by at least 2 dB, were considered borderline.

Results

With the Humphrey 10-2 test, 42 (79.2%) visual fields were normal, eight (15.1%) borderline, and three (5.7%) abnormal. With the CENTRING test, 17 (32.1%) visual fields were considered to be normal, 15 (28.3%) borderline, and 21 (39.6%) abnormal. These differences are statistically significant ($p<0.001$, χ^2 test). In the control group, 17 (85%) normal, one (5%) borderline, and two (10%) abnormal visual fields were found with the 10-2 test. With the CENTRING test, we found 15 (75%) normal, three (15%) borderline, and two (10%) abnormal visual fields. The mean test time was 11’42" ± 1’8" (minimum 9’27", maximum 16’03") with the 10-2 Program, and 2’48" ± 17" (minimum 2’18", maximum 3’35") with the CENTRING Program. We did not observe any significant correlation between the cumulative dose of hydroxychloroquine and perimetric alterations.

Ophthalmoscopic macular examination showed a very light pigmentary change (mottling) keeping within physiological limits in five patients, while it was normal in the other cases. Of the five patients who underwent fluorescein angiography, only one showed some light macular ‘window effect’. In this patient, funduscopic examination was absolutely normal in both eyes, while CAP was normal in the right eye and abnormal in the left, and CENTRING was abnormal in the right eye and borderline in the left.

In all patients who underwent photopic and scotopic ERG, the electrical responses of the retina were normal.

Discussion

Many articles in the literature have reported progressive retinal changes, sometimes even after cessation of antimalarial therapy.[1-4,11] It is possible that central and pericentral perimetric defects could be among the more frequent and, probably, early functional alterations.[6,7,12] Some authors believe there is a relationship not only between hydroxychloroquine retinal toxicity and total dose, but also with daily dose, daily dose for weight, and duration of therapy, and perhaps individual sensitivity may play a role.[3] Carr *et al.*[3] demonstrated a relationship between antimalarial total dose taken and perifoveal retinal threshold elevation, after dark adaptation, to red and blue light. Friedmann[13] reported reversible increases in threshold to white and red test targets which were related to the cumulative dose of chloroquine; these changes were found in the absence of observable macular changes. Mann *et al.*[14] did not find any significant correlation between mean sensitivity, mean defect, corrected loss variance or short-term fluctuation and the drug type, average daily dose or cumulative dose for either chloroquine or hydroxychloroquine, using the Octopus Program 11. They thought that there were probably no changes in retinal function in the majority of patients on antimalarial therapy, but only in those few patients who go on to develop the described 'premaculopathy'. In addition, it is possible that there are changes which are undetected by white-on-white automated perimetry.

It is a much debated question which are the most useful tests for the early detection of hydroxychloroquine maculopathy. Periodic use of an Amsler test and funduscopic examination is specific and inexpensive, but not very sensitive. As retinal damage could progress even after cessation of drug therapy, it stands to reason that we must have a very sensitive, rapid, reproducible, inexpensive and, if possible, specific test at our disposal. In our study, among treated patients, CENTRING visual fields were abnormal in a significantly higher percentage of cases compared to 10-2 visual fields, whereas in the control group the results were similar, if we deem the borderline visual fields to be normal.

Therefore, using the CENTRING Program, HRP appears to be a more sensitive technique than the CAP 10-2 test, at least in this type of patient. There is no general agreement on whether hydroxychloroquine could cause retinal damage too early.[15,16] On this point, our results showed frequent reductions of spatial resolution within the central 6° in many patients who received the antimalarial drug in a 'safe from danger' daily dosage, and for a duration of less than four years. We did not find any correlation between the degree of perimetric defect and the total dose ingested. This seems to confirm the role of individual sensitivity in the development of retinal alterations. We used fluorescein angiography in a small number of patients, and in only one could we confirm a correlation between perimetric defects and macular pigment mottling; in this case, ophthalmoscopy was normal, confirming its inadequacy in the follow-up of patients on antimalarial drugs. In our cases, ERG did not help to show early macular alterations. In fact, this test was also normal in cases with significant perimetric defects.

Former perimetric techniques (for example, static manual perimetry), even if they are very sensitive in revealing small perifoveal scotomas, take much too long to be used for routine diagnosis, screening or follow-up of hydroxychloroquine maculopathy. In this connection, we would emphasize the short duration (mean test time is about one-quarter than of the 10-2) of the CENTRING test. At the present time, there are no studies to confirm our data. Nevertheless, we conclude that HRP-

CENTRING is a very sensitive, fast and fairly inexpensive test, which is useful in the early detection of maculopathy and in the follow-up of patients taking antimalarial drugs. If our results are supported by long-term prospective studies, HRP-CENTRING could be used as a routine test in patients being treated with hydroxychloroquine.

Acknowledgments

The authors would like to thank Mrs Annalisa Caselli, Mrs Donatella Schiavo, Miss Monica Finotto and Miss Roberta Lucci for their valuable help in examining the patients.

References

1. Okun E, Gouras P, Bernstein H, Von Sallmann L: Chloroquine retinopathy: a report of eight cases with ERG and dark adaption findings. Arch Ophthalmol 69:59-71, 1963
2. Bernstein H, Ginsberg J: The pathology of chloroquine retinopathy. Arch Ophthalmol 71:238-245, 1964
3. Carr RE, Gouras P, Gounkel RD: Chloroquine retinopathy: early detection by retinal threshold test. Arch Ophthalmol 75:171-178, 1966
4. Percival SPB, Behrman J: Ophthalmological safety of chloroquine. Br J Ophthalmol 53:101-109, 1969
5. Wetterholm D, Winter FC: Histopathology of chloroquine retinal toxicity. Arch Ophthalmol 71:82-87, 1964
6. Hart WM, Burde RM, Johnston GP, Drews RC: Static perimetry in chloroquine retinopathy: perifoveal patterns of visual field depression. Arch Ophthalmol 102:377-380, 1984
7. Douche C, Bechetoille A, Ebran JM: Surveillance pratique des malades traités par antipaludèens de synthèse. J Fr Ophtalmol 6:689-695, 1983
8. Easterbrook M: Long-term course of antimalarial maculopathy after cessation of treatment. Can J Ophthalmol 27:237-239, 1992
9. Brusini P, Barosco F: Alterazioni della soglia di risoluzione spaziale nelle drusen della testa del nervo ottico. Atti X Convegno SOT. Boll Ocul 74(Suppl 3):219-224, 1994
10. Brusini P, Barosco F: Computerized automated perimetry and high-pass resolution perimetry in diabetic patients. In: Mills RP, Wall M (eds) Perimetry Update 1994/1995, pp 185-188. Amsterdam/New York: Kugler Publ 1995
11. Easterbrook M: The use of Amsler grids in early chloroquine retinopathy. Ophthalmology 91:1368-1372, 1984
12. Easterbrook M, Trope G: Value of Humphrey perimetry in the detection of early chloroquine retinopathy. Proc I Congr Int Soc Ocular Toxicity, Toronto, 1988. Lens Eye Toxic Res 6:258-268, 1989
13. Friedmann AI: The early detection of chloroquine retinopathy with the Friedmann visual field analyser. Ophthalmologica 158(Suppl):583-591, 1969
14. Mann CG, Orr AC, Rubillowicz M, Le Blank RP: Automated static perimetry in chloroquine and hydroxychloroquine therapy. In: Heijl A (ed) Perimetry Update 1988/1989, pp 417-421. Amsterdam/Milano: Kugler & Ghedini Publ 1989
15. Johnson MD, Vine AK: Hydroxychloroquine therapy in massive total doses without retinal toxicity. Am J Ophthalmol 104:139-144, 1987
16. Spalton DJ, Verdon Roe GM, Hughes GRV: Hydroxychloroquine, dosage parameters and retinopathy. Lupus 2:355-358, 1955

VISUAL FIELD ALTERATIONS IN HIV-1 INFECTION

SOEREN THIERFELDER, EUGEN GRAMER and FRANZ GREHN

University Eye Hospital Würzburg, Würzburg, Germany

Abstract

Purpose: Visual field alterations are a common ocular manifestation of HIV-1 infection. It was the aim of this study to analyze their frequency and pathomechanisms.
Method: Since January 1992, 144 HIV-1-infected patients have been submitted to perimetric examinations. The stage of HIV infection was defined according to the CDC classification (CDC I: 1; CDC II: 52; CDC III: 10; CDC IV: 81).
Results: Eighty-one of 144 patients showed perimetric alterations (CDC I: 0; CDC II: 12; CDC III: 6; CDC IV: 63). At CDC II and III, only a diffuse reduction of sensitivity was observed. At CDC IV, a diffuse sensitivity loss occurred in 39 patients. Thirty-five of these patients also showed HIV-associated retinal microangiopathy syndrome. In 19 patients a diffuse reduction of sensitivity combined with an absolute peripheral scotoma caused by cytomegalovirus retinitis was seen. In four patients, bilateral absolute defects of corresponding quadrants or hemifields due to cerebral toxoplasmosis were found. One patient showed bilateral corresponding absolute scotomata due to an intracerebral hemorrhage caused by meningeal Kaposi's sarcoma.
Conclusions: The configuration of visual field alterations in HIV-1-infected patients gave the first clue to their etiology. Thus, exact perimetric examinations are an important tool in the early diagnosis of ocular or cerebral complications in AIDS.

Introduction

Therapeutical advances, with regard to both opportunistic diseases and to HIV infection itself, have increased the life expectancy of HIV-infected patients. However, the preservation of quality of life has become another important aspect of HIV treatment. In this context, ophthalmological examinations including Schirmer's test of tear secretion,[8] accommodometry,[10,17] funduscopy and perimetry, should have become part of the modern interdisciplinary management of HIV-infected patients.

Patients and methods

Since January 1992, 144 HIV-1-infected patients (CDC I: 1; CDC II: 52; CDC III: 10; CDC IV: 81; Table 1) have been examined at the University Eye Hospital,

Address for correspondence: Soeren Thierfelder, MD, University Eye Hospital Würzburg, Josef-Schneider-Strasse 11, D-97080 Würzburg, Germany

Perimetry Update 1996/1997, pp. 441–448
Proceedings of the XIIth International Perimetric Society Meeting
Würzburg, Germany, June 4–8, 1996
edited by M. Wall and A. Heijl

Table 1. CDC classification of HIV infection

I	Acute retroviral syndrome
II	Seropositive, clinically latent HIV infection
III	Lymphadenopathy syndrome
IV	Advanced HIV infection
	a. AIDS-related complex
	b. neurological manifestations
	c. opportunistic infections
	d. opportunistic tumors
	e. further AIDS-associated alterations

Würzburg. All patients underwent a complete ophthalmological examination including computerized perimetry with Program 30-2 of the Humphrey Field Analyzer or, when the patient was in a poor physical condition, with a Goldmann perimeter.

Results

Eighty-one of 144 patients showed visual field alterations (CDC I: 0; CDC II: 12; CDC III: 6; CDC IV: 63).

The most frequent finding was a diffuse reduction of sensitivity without absolute scotomata (see Fig. 1). This pattern was seen in 57 patients (CDC I: 0, CDC II: 12; CDC III: 6; CDC IV: 39) and always occurred in both eyes. Although there was a constant mean defect in consecutive examinations of the same patient, fluctuating locations of the changes were seen. In 35 patients, this type of visual field alteration occurred in combination with HIV-related retinal microangiopathy (CDC II: 12, CDC III: 2, CDC IV: 21), whereas retinal microangiopathy combined with a regular visual field was seen only in two patients. It should be emphasized that none of these 57 patients suffered from any opportunistic ocular disease.

In 19 patients, a diffuse reduction of sensitivity occurred in combination with peripheral absolute scotomata (see Fig. 2). All these patients were staged as CDC IV and were suffering from cytomegalovirus retinitis. These peripheral absolute scotomata occurred long before a reduction in visual acuity, and could be observed even in cases of small retinal inflammatory lesions.

Bilateral absolute scotomata in a pattern of corresponding quadrants or hemifields were found in four patients (see Fig. 3). These patients – also CDC IV – were suffering from cerebral toxoplasmosis, a severe complication of AIDS. In one of them, the perimetric findings gave the first clue to his cerebral disease. All four of these patients have now died in spite of maximum therapy.

One patient (CDC IV) showed only small bilateral paracentral absolute scotomata (see Fig. 4). Computerized tomography revealed an occipital intracerebral hemorrhage resulting from Kaposi's sarcoma of the leptomeninx. In this case, the ophthalmological examination had given the first hint of an intracerebral complication, as there had not been any neurological symptoms besides the described visual field defects. The diagnosis was proved histologically post mortem.

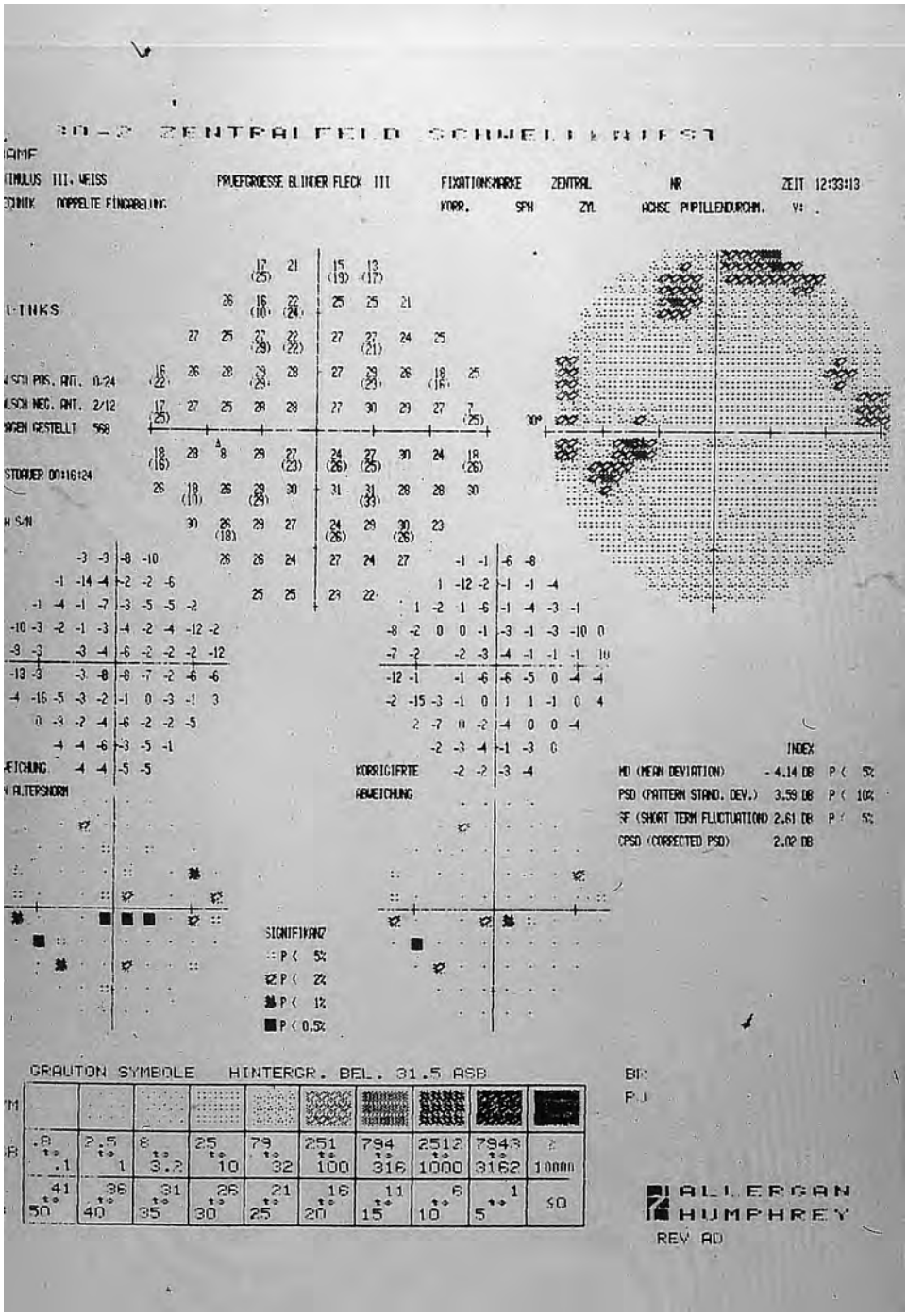

Fig. 1. Diffuse relative reduction of sensitivity in a 31-year-old HIV-1-infected patient (CDC IVa).

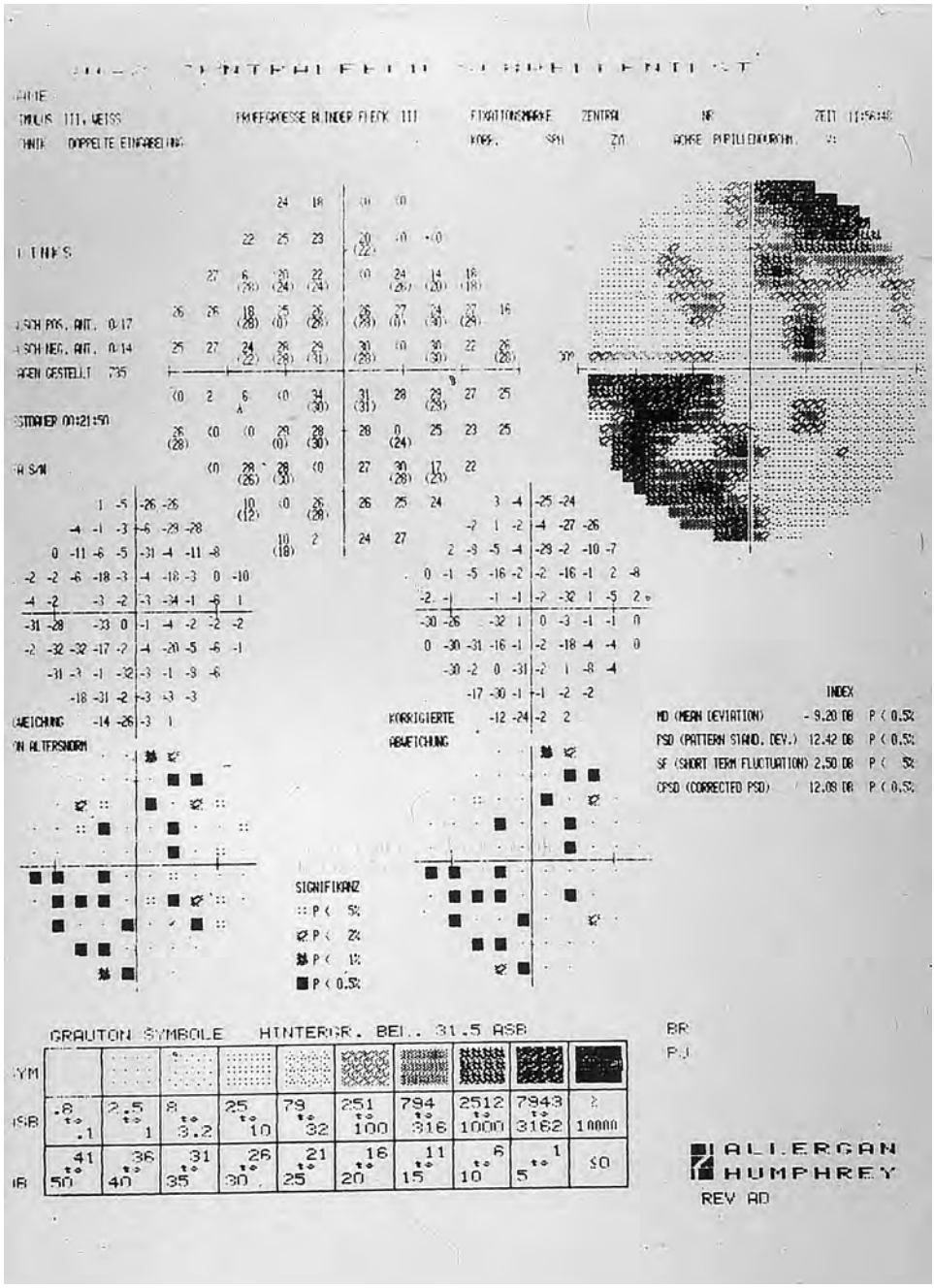

Fig. 2. Visual field of a 43-year-old HIV-1-infected patient suffering from cytomegalovirus retinitis.

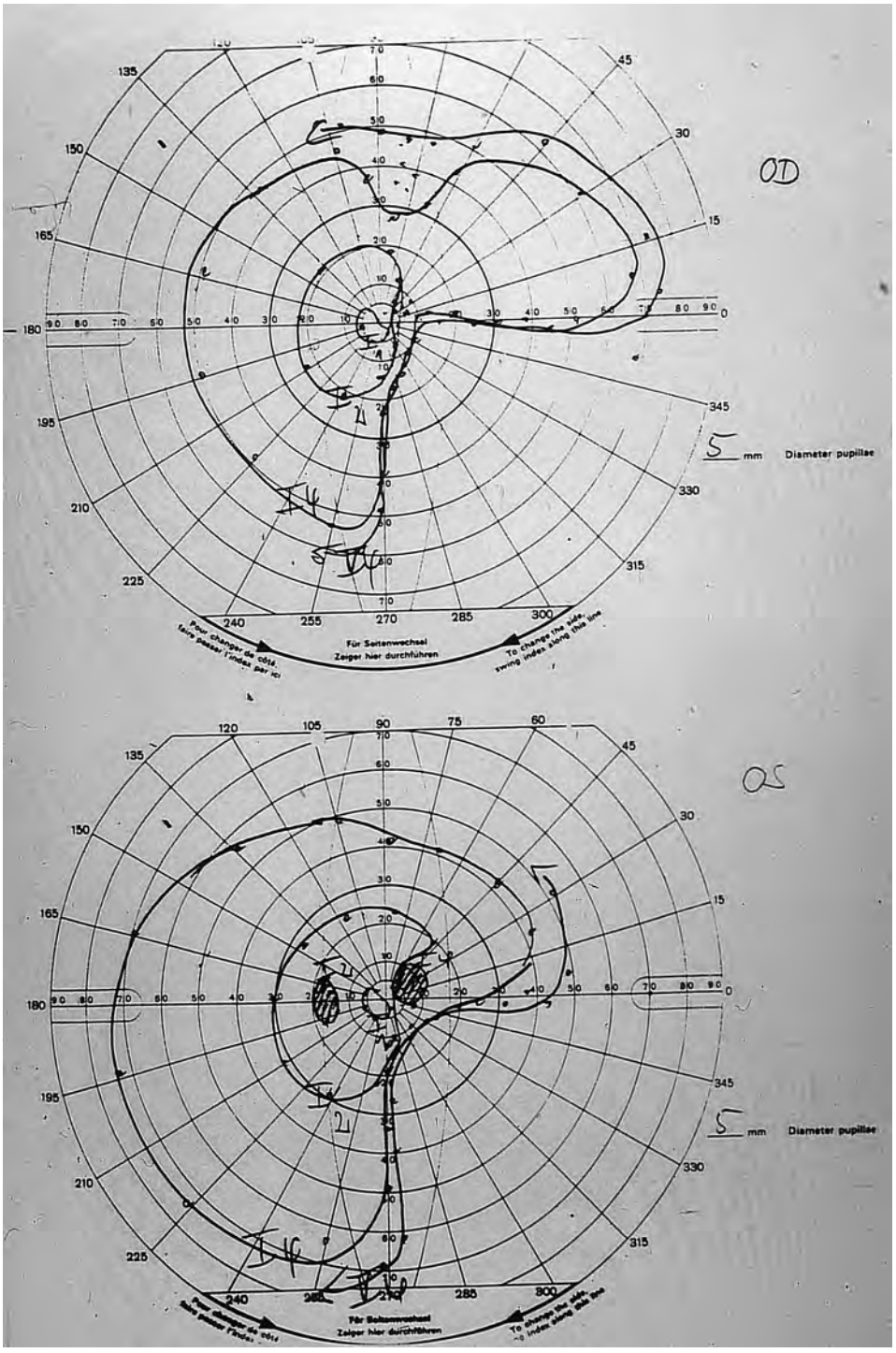

Fig. 3. Visual fields of a 32-year-old HIV-1-infected patient suffering from cerebral toxoplasmosis.

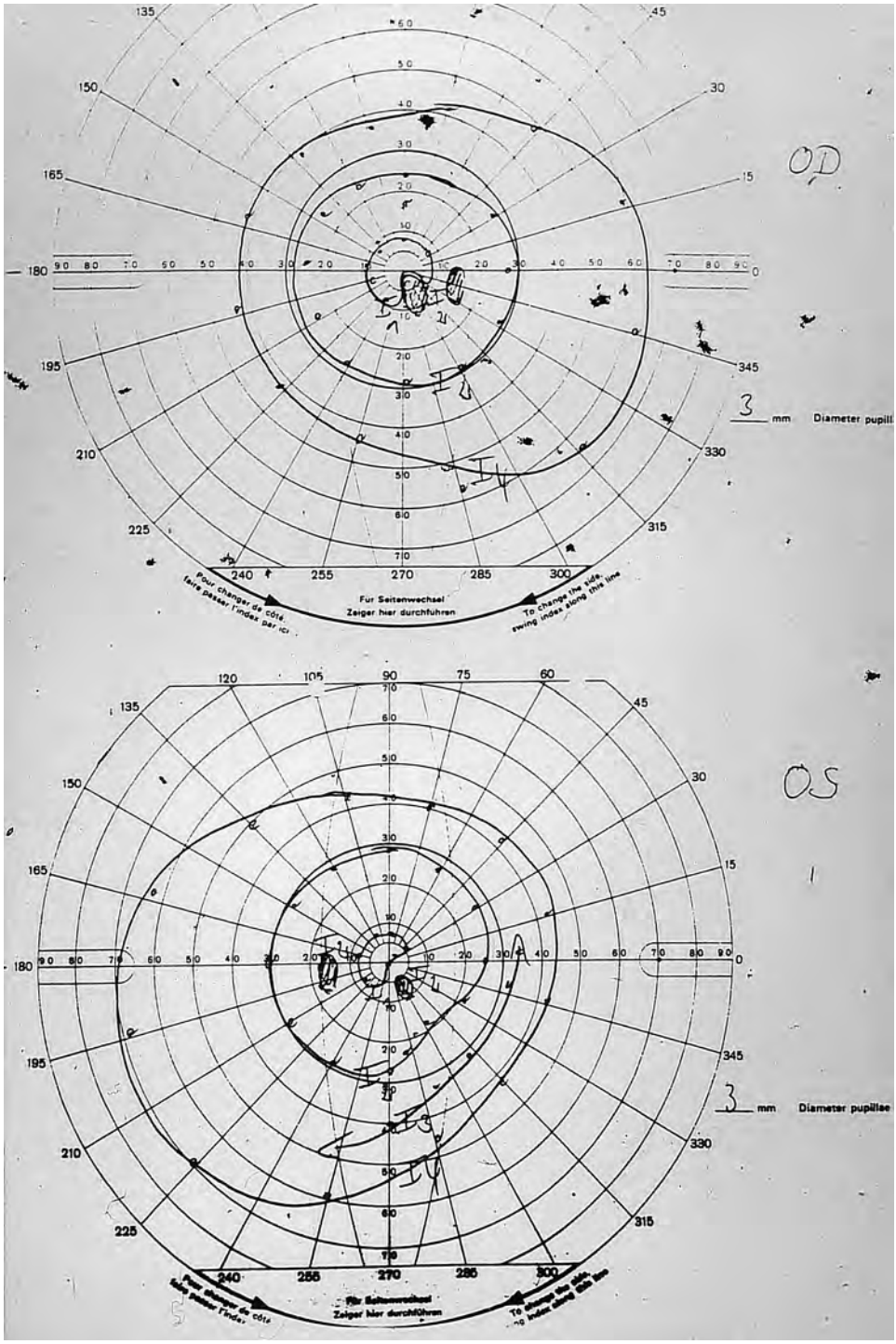

Fig. 4. Paracentral absolute scotoma in a 49-year-old HIV-1-infected patient suffering from Kaposi's sarcoma of the leptomeninx.

Discussion

In HIV-infected patients, several types of visual field alterations can be found. The most frequent defect is bilateral diffuse reduction of sensitivity without absolute scotomata. In contrast to other visual field alterations, it can be observed even in the early stages of HIV infection without opportunistic diseases. The mechanisms of this loss are controversial.[2,3,4,6,11,13,15,15,18] Retinal nerve fiber loss has been postulated.[6,11,13,15,16] However, this supposed retinal nerve fiber loss could not be proved by laser polarimetric *in vivo* measurements.[18] Yet, the strictly bilateral occurrence of this reduction of sensitivity and its fluctuating location in repeated examinations of the same patient lead us to believe that cerebral alterations, *e.g.*, those due to neuronal infection by the neurotropic HIV-1,[1-3,5] are probably responsible.

If absolute scotomata also occur, they appear to suggest opportunistic ocular pathologies, *e.g.*, cytomegalovirus retinitis. In our patients, peripheral absolute scotomata were even observed in patients with full visual acuity and only small retinal inflammatory lesions. They have always extended further than the observed inflammatory retinal areas. This effect is due to early necrosis of the retinal nerve fiber layer caused by cytomegalovirus.[3]

Thus, perimetry may be helpful in the differential diagnosis of both HIV-related retinal microangiopathy, a non-opportunistic ocular manifestation of HIV infection, and cytomegalovirus retinitis, a severe opportunistic infection with a high risk of blindness in the absence of adequate treatment. In some cases, it may be difficult to secure this differential diagnosis from the ophthalmoscopic angle only.

Corresponding bilateral absolute scotomata should raise suspicions regarding cerebral opportunistic complications of AIDS, *e.g.*, cerebral toxoplasmosis of opportunistic tumors. In our five patients suffering from such manifestations of AIDS, two showed visual field alterations before other neurological symptoms could be observed. Thus, exact perimetric examinations are also useful in the early diagnosis of neurological manifestations of AIDS and can improve the patient's prognosis by indicating early treatment.

Conclusions

Visual field alterations are common in HIV-1-infected patients. While the frequent bilateral diffuse reduction of sensitivity already occurs at the so-called 'clinically latent HIV-infection' stage, and does not necessitate any specific treatment, absolute scotomata are a clue to opportunistic complications, *e.g.*, cytomegalovirus retinitis. If absolute scotomata are of a corresponding configuration in both eyes, perimetry should be followed by neurological examinations to disclose any likely cerebral complications of AIDS.

References

1. Barré-Sinoussi F, Chermann JC, Rey F, Nuguyerre MT, Chamaret S, Gruest J, Dauguet C, Axler-Blin C, Vezinet-Brun F, Montagnier L: Isolation of a T-lymphotropic retrovirus from a patient at risk for acquired immune deficiency syndrome (AIDS). Science 220:868-871, 1983
2. Budka H: Morphologisches Korrelat und Pathogenese der HIV-Infektion des Nervensystems. In Möller AA, Backmund H (eds) HIV-Infektion und Nervensystem, pp 33-44, Stuttgart/New York: George Thieme 1991

3. De Girolami U, Hernin D, Girard B, Katlama C, Le Hoang P, Hauw JJ: Pathologic study of the eye and central nervous system in 25 cases of AIDS. Rev Neurol (Paris) 145:819-828, 1989
4. Fabricius EM: Augenmanifestationen bei HIV-Infektionen. Stuttgart: F Enke-Verlag 1992
5. Fuller GN, Guillof RJ, Gazzard B: Neuropathological presentations of AIDS: when to test for HIV. J Roy Soc Med 82:717-720, 1989
6. Geier S, Klauss V, Berninger T, Kronawitter U, Bogner JR, Goebel D: Schäden der Neuroretina und retinale Mikroangiopathie bei Patienten mit AIDS. Ophthalmologe 89(Suppl):77, 1992
7. Gümbel H, Richter R, Klos K, Subklew R, Ohrloff C: Katarakt und Linsentrübung bei HIV + Patienten: Eine quantitative Analyse mit einem automatischen Scheimpflug-Kamera-System. Ophthalmologe 90(Suppl):34, 1993
8. Haas C, Lowenstein W, Chagart A, Carnot F, Chamaret S, Durand H: Chronic lymphocyte sialadenitis related to Gougerot-Sjoegren syndrome disclosing HIV-seropositivity. Ann Med Int (Paris) 140:214-215, 1989
9. Holland GN, Gottlieb MS, Yee RD, Schenker HM, Pettit TH: Ocular disorders associated with severe acquired cellular immunodeficiency syndrome. Am J Ophthalmol 93:393-402, 1992
10. Newsome DA: Non-infectious ocular complications of AIDS. Int Ophthalmol Clin 29:95-97, 1989
11. Nöhmeier C, Geier S, Lachenmayr B, Müller A, Klauss V: Reduktion der Wahrnehmungsschwelle bei Patienten mit AIDS. Ophthalmologe 89(Suppl):77, 1992
12. Pepose JS, Holland GN, Nestor MS, Cochran AJ, Foos RY: Acquired immune deficiency syndrome: pathogenetic mechanisms of ocular disease. Ophthalmology 92:472-484, 1985
13. Quiceno JI, Camparelli E, Sadun A, Munguia D, Grant I, Listhaus A, Lambert B, Freeman WR: Visual dysfunction in patients with acquired immunodeficiency syndrome. Am J Ophthalmol 113:100-101, 1992
14. Szymanski IO, Pullman JM, Underwood JM: Electron microscopic and immunochemical studies in a patient with hepatitis C virus infection and mixed cryoglobulinemia type II. Am J Clin Pathol 102:278-283, 1994
15. Teich SA: Human immunodeficiency virus-related uveitis. Curr Opin Ophthalmol 3:519-526, 1992
16. Tenhula WN, Xu S, Madigan MC, Heller K, Freeman WR, Sadun AA: Morphometric comparisons of optic nerve axon loss in acquired immunodeficiency syndrome. Am J Ophthalmol 113:8-13, 1992
17. Thierfelder S, Mellinghoff-Kreplin G, Hasenfratz G: Klinische Untersuchungen zur Reduktion der Akkommodationsbreite bei Patienten mit HIV-1-Infektion. Klin Mbl Augenheilk 204:523-526, 1994
18. Thierfelder S, Gramer E, Serguhn S: Messungen der retinalen Nervenfaserschichtdicke mittels Laserpolarimetrie bei Patienten mit AIDS im Vergleich zu Gesunden unter Berücksichtigung computerperimetrischer Befunde: eine Pilotstudie unter Einsatz des Nerve-Fiber Analyzer®. Klin Mbl Augenheilk 206:165-169, 1995

ANALYSIS OF THE RELATIONSHIP BETWEEN RETINAL DISEASE AND THE STATIC VISUAL FIELD USING A COMPUTER-ASSISTED COMBINATION SYSTEM

SHIGEKI YAMADA, KEIKO HIGUCHI, TOMOKO SAWADA and AKIHIRO SUGIYAMA

Department of Ophthalmology, Shiga University of Medical Science, Otsu, Japan

Abstract

Many retinal diseases cause visual field defects. Knowledge of the relationship between visual field defects and fundus abnormality is useful for diagnosis and therapy. Therefore, the authors developed a computer system for imposing visual field data on photographs of the fundus. The system is also capable of the analysis of loss due to glaucoma.

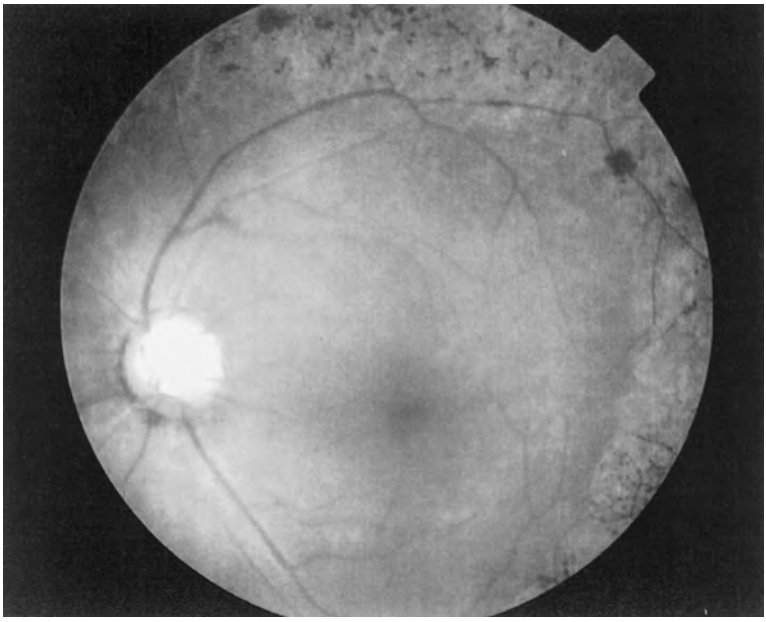

Fig. 1. A case of retinitis pigmentosa.

Address for correspondence: Shigeki Yamada, MD, Department of Ophthalmology, Shiga University of Medical Science Seta, Tsukinowa, Otsu 520-21, Japan

Perimetry Update 1996/1997, pp. 449–456
Proceedings of the XIIth International Perimetric Society Meeting
Würzburg, Germany, June 4–8, 1996
edited by M. Wall and A. Heijl

被検者名：	生年月日：昭和 7年(1932) 8月21日
ＩＤ番号：2499040	コメント：
検査日：平成 7年(1995)11月13日(月) 9:59	検眼：右
測定時間 ： 9分7秒	矯正レンズ：S:+ 4.50 C:+ 0.00 A: 0
検査パターン：緑内障 (125ポイント)	視標呈示回数：327
検査方式：ｽｸﾘｰﾆﾝｸﾞ	肯定応答数： 75
呈示間隔 ： 0.8秒	偽陽性：応答数 0
呈示時間 ： 0.4秒	偽陰性：応答数 0
固視監視レベル：2	固視エラー：応答数/呈示数, 8/20
視標色： 白	コメント：最大輝度 = 1 dB
視標サイズ：Ⅲ	

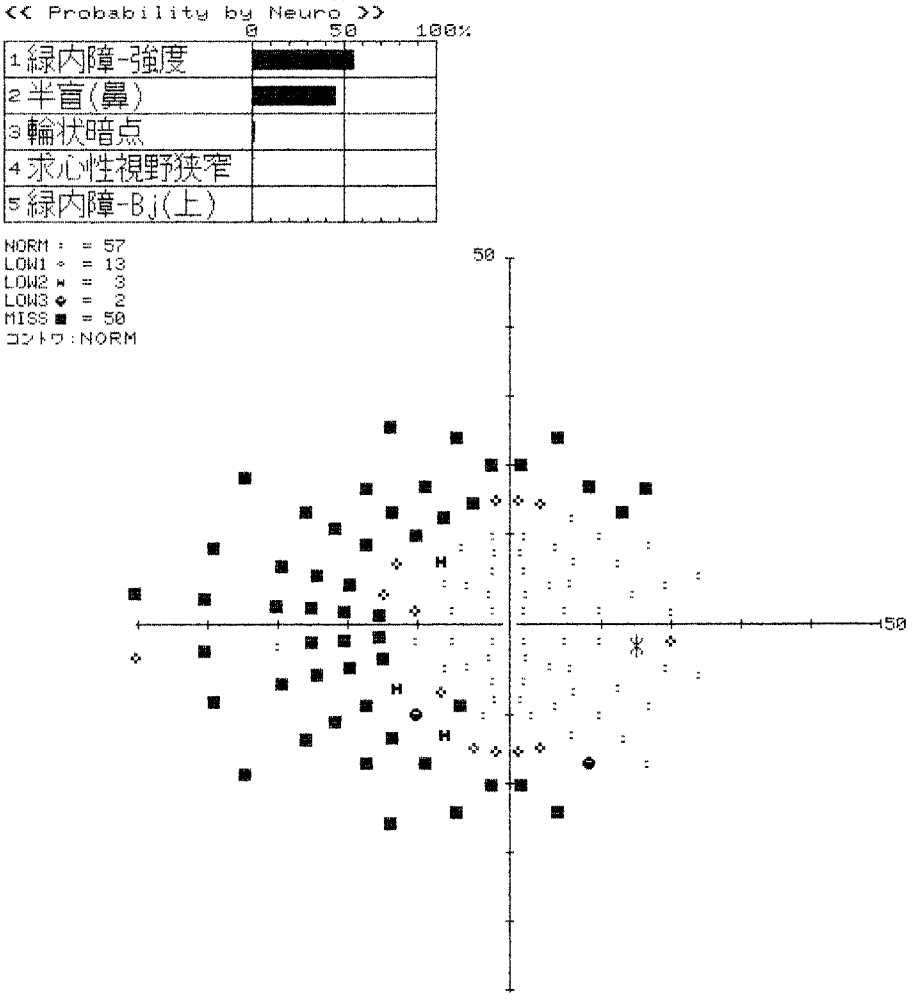

SBP2020

Fig. 2. Visual field of the same case as in Figure 1.

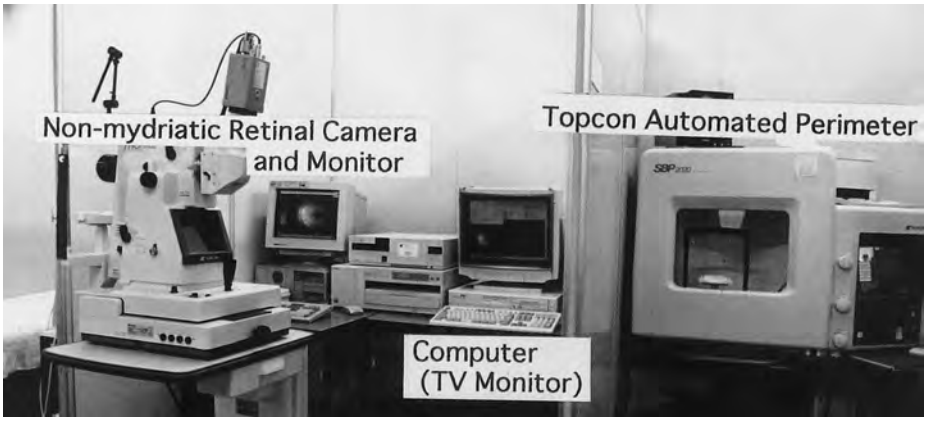

Fig. 3. Analysis system of the relationship between retinal disease and the static visual field.

Introduction

Many retinal diseases cause visual field defects. For example, retinitis pigmentosa (Fig. 1) causes ring scotoma in the early stage, and only the central visual field remains in the progressive stage (Fig. 2). If we reverse Figure 2, turn it upside down and impose it on Figure 1, it shows a more definite relationship between retinal disease and the static visual field. Therefore, using a computer, we developed a system for automatically imposing visual field data on photographs of the fundus (Fig. 3).

Methods

First, we take a photograph of the fundus using a non-mydriatic retinal camera. Then, we measure the static visual field using a Humphrey Field Analyzer or a Topcon automated perimeter. Next, the photographs of the fundus and the visual field data are digitized in a computer, shown on a TV monitor and combined. In the case of local retinal degeneration, the extent of the degeneration corresponds to the extent of the visual field defect (Fig. 4).

The system is also useful for glaucoma patients. It automatically evaluates the visual field, optic nerve head, and also the retinal nerve fiber layer. The program features a nerve fiber layer coordinate system. The nerve fiber coordinate is the angular coordinate, according to the retinal nerve fiber direction referred to in Hogan's model (Fig. 5).[1] Using this nerve fiber coordinate, we analyze three glaucoma parameters and two integrated glaucoma analyses. We apply our system to the visual field defect, the pallor/disc area ratio, and the nerve fiber layer defects. Using this system, the location of the visual field defects, pallor/disc area ratio, and nerve fiber layer defects, are shown as the nerve fiber coordinate angle. We can examine how the three glaucoma parameters correspond. For example, we measure the density of the retinal nerve fiber. Nerve fiber layer defects are low density bundles in the retinal nerve fiber. Therefore, nerve fiber layer defects are shown as cone-shaped peaks.

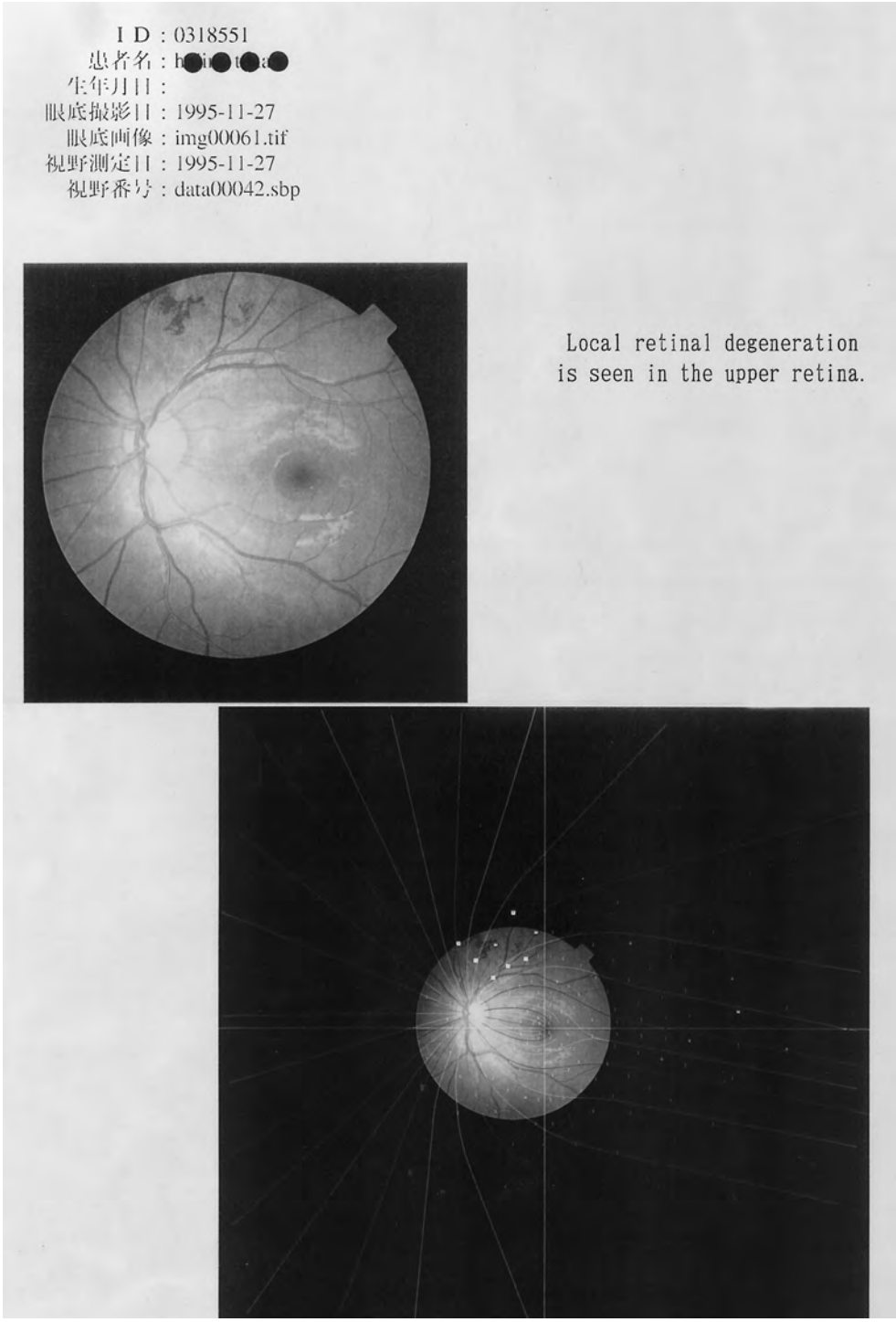

Fig. 4. A case of local retinal degeneration.

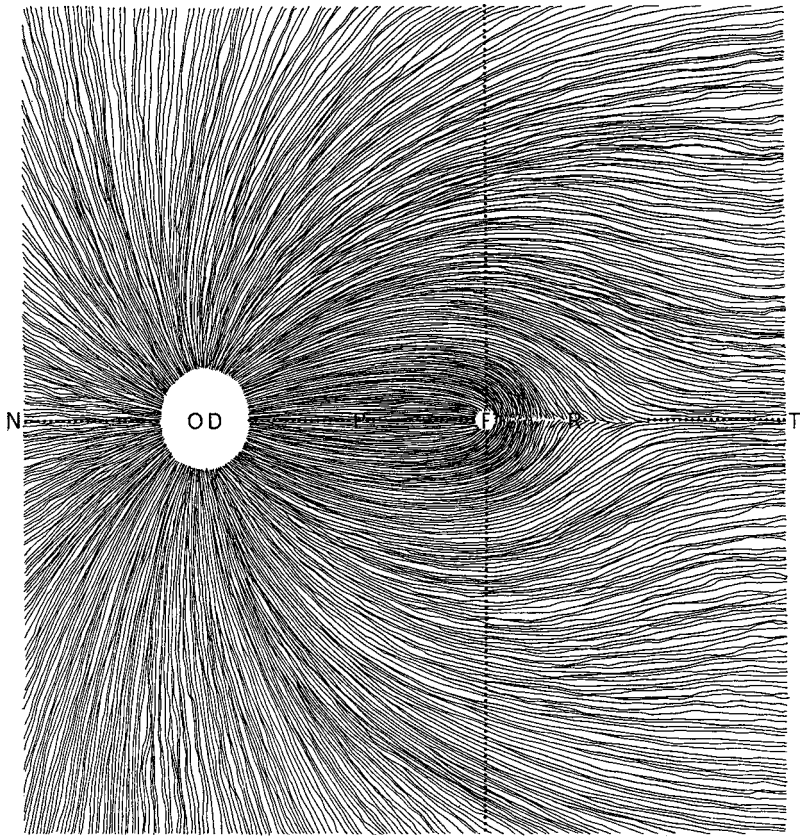

Fig. 5. Hogan's retinal nerve fiber model (Reproduced from Hogan *et al.*[1], by courtesy of WB Saunders).

Results and discussion

Figure 6 shows a progressive glaucoma case. Nerve fiber layer defects are present at 60-130° and 220-270°. Furthermore, we can see an overlapping distribution of the nerve fiber layer defects, the visual field defects and the pallor/disc area ratio. In the case of early glaucoma shown in Figure 7, there are some overlaps of the parameter peaks.

We examined many retinal diseases, such as retinitis pigmentosa, local retinal degeneration, branch retinal vein occlusion, diabetic retinopathy, retinitis centralis, hypertensive retinopathy, myopic fundus, and glaucoma. In these cases, we can seen an overlapping distribution between retinal diseases and the static visual field.

We obtained an adequate correlation of glaucoma parameters in 74 of the 81 glaucoma eyes examined. As is the case in similar systems,[4] the present system may be considered useful in the diagnosis and follow-up treatment of glaucoma.

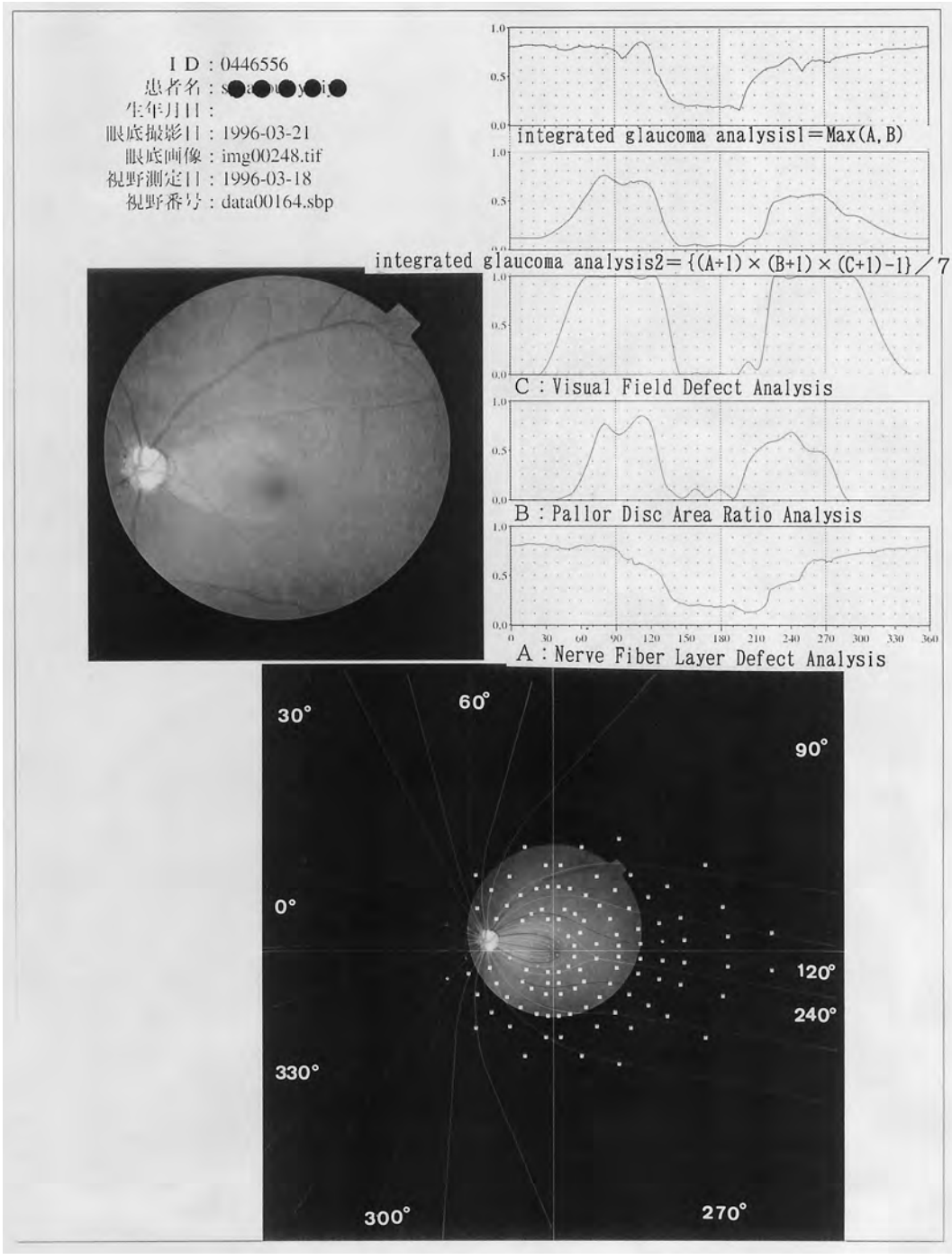

Fig. 6. A case of progressive glaucoma.

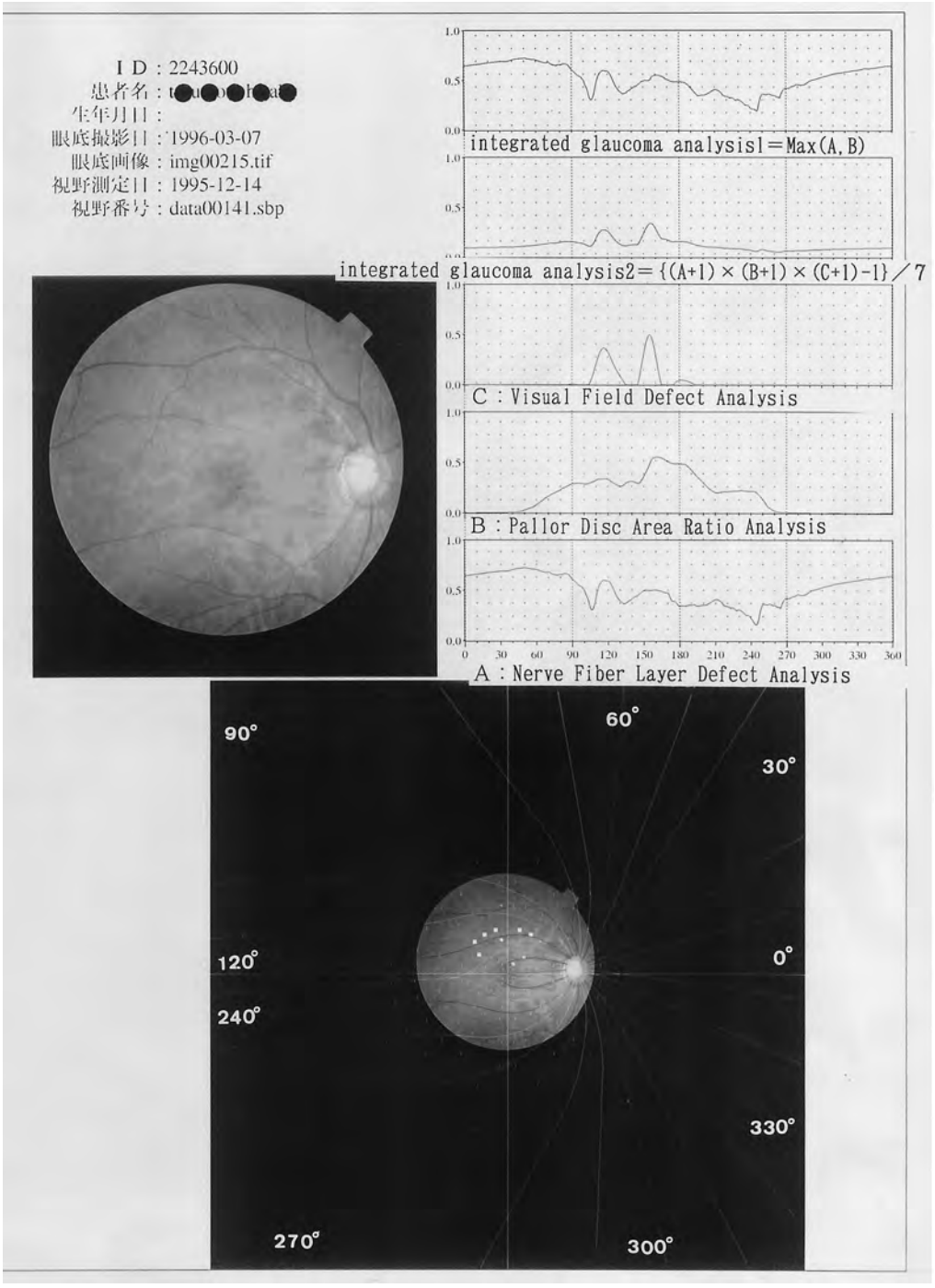

Fig. 7. A case of early glaucoma.

References

1. Hogan MJ, Alvarado JA, Weddell JE: Histology of the Human Eye: An Atlas and Textbook. Philadelphia, PA: WB Saunders 1971
2. Rohit V, George LS, Kenneth WP: The Optic Nerve in Glaucoma. Philadelphia, PA: JB Lippincott 1993
3. Nagin P, Schwartz B, Nanba K: The reproducibility of computerized boundary analysis for measuring optic disc pallor in the normal optic disc. Ophthalmology 92:245-251, 1985
4. Weber J, Dannheim F, Dannheim D: The topographical relationship between optic disk and visual field in glaucoma. Acta Ophthalmol (Kbh) 68:568-574, 1990

MISCELLANEOUS

PREVENT BLINDNESS AMERICA VISUAL FIELD SCREENING STUDY
Sensitivity and specificity revisited*

WILLIAM E. SPONSEL

University of Texas Health Science Center, San Antonio, TX, USA

Introduction

The purpose of the Prevent Blindness America Visual Field Screening Study[1,2] was to assess the diagnostic efficacy and population screening utility of two devices designed to detect glaucomatous visual field loss.

Methods

Henson semi-automated perimetry and Damato patterned-chart campimetry were used. These were performed among: *1.* a normative population in New York; *2.* patients from six glaucoma clinics; and *3.* screening populations in Florida, Ohio, New York, Tennessee, Texas, Utah, and Wisconsin.

Comprehensive history, clinical examination by a glaucoma specialist, and thresholding Humphrey visual fields were available for all normative subjects and glaucoma patients. Population screening was performed by trained volunteers from seven state affiliates of Prevent Blindness America.

The study assessed the capability of two portable and rapidly performed visual function tests to *1.* determine the testing failure rate among manifestly normal eyes; *2.* determine the testing failure rate among eyes with confirmed glaucomatous damage; and *3.* detect glaucomatous or other visual pathology among diverse populations in a traditional screening setting.

Normative (false-positive) study

An ethnically diverse population of 143 bank employees in New York City (aged 18-69, mean 41.5 years; 70 M/73 F) underwent comprehensive ophthalmic examination

*This manuscript summarizes data presented in the *American Journal of Ophthalmology*, Vol. 120, pp 699-708, December, 1975, and presents new data resulting from a survey of participants at the XIIth International Perimetric Society Meeting in Würzburg, June 4-7, 1996.

Address for correspondence: William Eric Sponsel, MD, South Texas Ocular Imaging Center, 7703 Floyd Curl Drive, San Antonio, TX 78284, USA

Perimetry Update 1996/1997, pp. 459–465
Proceedings of the XIIth International Perimetric Society Meeting
Würzburg, Germany, June 4–8, 1996
edited by M. Wall and A. Heijl

on-site by the clinical faculty of the New York Eye and Ear Infirmary. Slit-lamp biomicroscopy, ophthalmoscopy, and applanation tonometry were performed together with history and acuity testing. Each subject also underwent assessments with both the Henson CFA 3000 26-point screening test and the Damato spiral oculokinetic campimetry chart.

Qualification for substudy required the absence of any family or personal history of heritable eye disease or glaucoma, and all the following in both eyes:

intraocular pressure <21 mmHg
cup/disc ratio <0.6
cup/disc asymmetry <0.3
normal Humphrey 30-2

Eighty-five subjects (mean age 39 years) fulfilled all criteria for inclusion in the normative group.

Glaucomatous (true-positive) study

Ninety patients under treatment for primary open-angle glaucoma at clinics in New York, Michigan, Indiana, Chicago, San Francisco, and Los Angeles (mean age 59), underwent their usual ophthalmic examination, together with Henson, Damato, and Humphrey 24-2 or 30-2 Full-Threshold perimetry. All subjects were perimetrically experienced, having undergone at least three prior Humphrey fields; none had previously undergone testing with either the Henson or Damato device.

Eighty-three of the 90 Humphrey fields satisfied standard reliability criteria. Among these, scoring of the Humphrey fields using Anderson's field classification criteria yielded 16 with severe, 23 moderate, 19 early visual field defects, and 25 non-defective fields.

Public screening

One thousand three hundred and fifty-three subjects were evaluated at multiple testing sites in Florida (189), Indiana (134), Ohio (203), Tennessee (189), Texas (184), Utah (190), and Wisconsin (189) between August and October, 1993. At least two volunteer trainees from each PBA state affiliate attended a two-day instruction course on methodology, overseen by Drs Henson and Damato and experienced personnel from the PBA and Glaucoma Advisory Committee.

Subjects failing either screening test were advised to seek the care of an eye-care professional experienced in the treatment of glaucoma. All clinicians reviewing individuals who had failed the screening tests were required to forward their own threshold fields to the PBA study office.

Results

Normative (specificity) study

Eighty of 83 manifestly normal eyes passed the Damato screening test, indicating a false-positive rate of 3.5%, or a specificity of 96.4%. There were no false positives among the 82 subjects completing Henson two-step screening (specificity 100%).

Clinical (sensitivity) study

Among 83 glaucoma suspects and patients, the Henson identified 49 (84%) of the 58 with abnormal Humphrey fields, including 38/39 (97%) of those with moderate or severe loss. The Damato detected 55/68 of those able satisfactorily to complete the test with abnormal Humphrey fields, including 44/48 (92%) with moderate or severe damage.

Population screening

Fifty-five of 1278 subjects tested (4.3%) failed either or both tests. Fourteen of 55 did not complete Damato testing in either eye; nine more completed only one. One-third of those failing the Damato and followed clinically (4/12) were subsequently shown to have normal Humphrey fields.

All 55 subjects completed Henson screening, and 45/55 received subsequent clinical follow-up. Only three of these (6.6%) were found to have normal Humphrey fields.

Conclusions

It appears evident from the foregoing that the Henson perimeter had a very high concordance with the Humphrey, with no false positives in any phase of the study. This latter finding is of great potential advantage in screening, since diseased eyes are likely to be outnumbered 50:1 by normal eyes in the population at large. Moreover, few subjects were unable to complete the Henson, and clinicians receiving patient referrals were highly likely to obtain threshold Humphrey fields as presented with the Henson printout.

The Damato, while very inexpensive and highly portable, was less frequently completed, and when abnormal, was less often acted upon by clinicians. The false-positive rate was also substantially higher with the Damato. Thus, testing attrition and a false-positive rate several-fold higher than the maximal true-positive screening yield are disadvantages of the Damato. Despite this, the Damato has a sensitivity and specificity far superior to tonometry, and can be performed in a comparable time and at substantially less expense than any competing method yet evaluated.

A diagrammatic summary of the diagnostic utility of the Henson and Damato, together with comparative data for tonometry at two different IOP cut-off values, are shown in Figure 1.

Further investigation: assessing the ‘gold standard’

All studies intended to evaluate the diagnostic utility of a new test must be submitted for comparison against an existing ‘gold standard’. The publication of field scoring criteria for grading threshold fields by the Bascom Palmer glaucoma team,[3] as used in the above study, was very important in this regard, providing for the first time a standardized basis for categorizing the extent of Humphrey visual field loss according to clinically-relevant guidelines. The ability of their novel scoring system to discern the extremes of normality, or arbitrary artifact, from early pathology, has not been carefully explored, however.

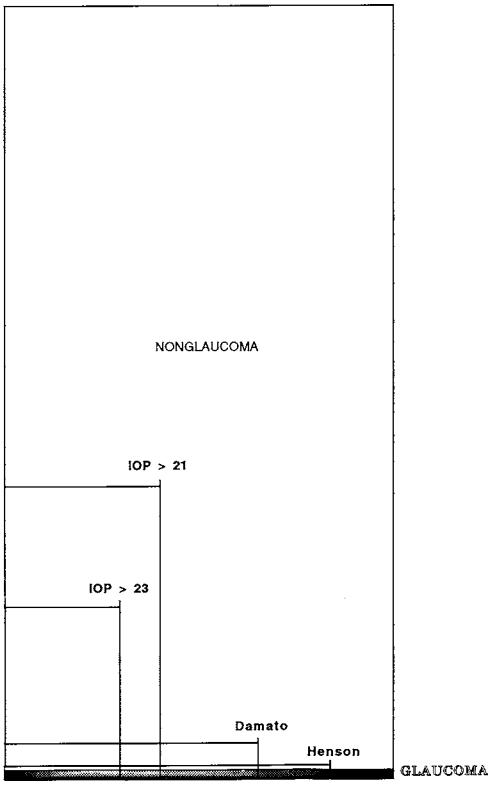

Fig. 1. Diagrammatic representation of the sensitivity and specificity of Henson, Damato, and tonometric criteria for detecting glaucomatous neural damage. The dark band at the bottom represents the estimated 2% of the adult population with glaucoma; the remaining large white rectangle represents those with no glaucoma. The smaller rectangles encompass the population failing each of the screening modalities; note that as the intraocular cut-off pressure increases, the proportion of glaucomas detected drops; the relative proportion of false positives to true positives changes very little throughout the intraocular pressure range 20-28 mmHg, which includes over 90% of open-angle glaucomas. The Damato campimetry chart outperforms tonometry manifoldly, but still produces more false positives than glaucomas. The Henson central field analyzer 3000 detects the majority of glaucomas, with very few false positives. Cut-offs shown for the Henson and Damato in this diagram are conservatively derived from the Prevent Blindness America Glaucoma Screening Study (and are not modified by the additional subjective survey data provided in the present paper).

Although the Henson performed very well as a screening tool in detecting field loss consistent with the Bascom Palmer criteria, perusal of some of the Humphrey visual field data from Phase 2 of the Prevent Blindness Study suggested that strict application of these scoring criteria might produce an underestimate of the Henson's sensitivity. There was almost absolute agreement between the Henson and Humphrey regarding the presence of visual field loss when fields were deemed either moderate or severe by the Humphrey scoring method. The agreement was also absolute for fields deemed normal by the Humphrey scoring algorithm. The only disparity observed arose among nine fields, eight 'early' defects, and a single 'moderate' defect (Fields 1-9). On concurrent Henson field testing, these nine eyes were found to have

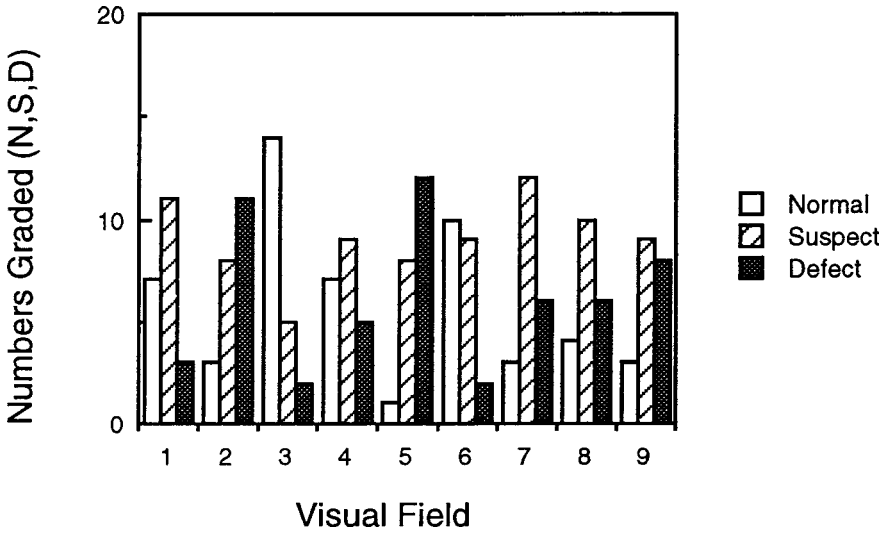

Fig. 2. Results of the survey conducted among visual field experts attending the XII International Perimetric Society Meeting in Würzburg. Each participant was asked to rate nine Humphrey visual fields (see Fields 1-9) which were purportedly defective by Hodapp, Parrish, and Anderson criteria, but not associated with abnormal Henson fields, as 'normal', 'suspect', or 'defect', for possible nerve fiber layer damage. No additional biasing information was provided.

visual fields within normal limits. Preliminary assessment of some of the nine fields for which disparities existed between the Henson and graded Humphreys suggested that the likelihood of pathology in a number of instances was doubtful.

Methods

In order to address this dilemma, a simple questionnaire was prepared and presented, together with the nine contentious Humphrey fields, to members of the International Perimetric Society in attendance at the XII International Meeting in Würzburg. All participants in this survey were highly experienced in the interpretation of glaucomatous visual fields, and each doctor was asked to judge the fields as 'normal', 'suspect' or 'defect' with regard to the presence or absence of nerve fiber layer damage. The questionnaires were administered during the breaks between scientific sessions. Each participant agreed to judge the fields according to his or her own clinical acumen, and no additional information was provided. No reference was made to the Prevent Blindness Study, and all enquiries as to the reasons for the survey were politely deferred. Participants were free to identify themselves, and those who chose to do so are listed in the acknowledgments.

Results

Twenty-one experts from at least eight countries participated in the survey. Their subjective gradings of the nine visual fields are shown in Figure 2. Only one field,

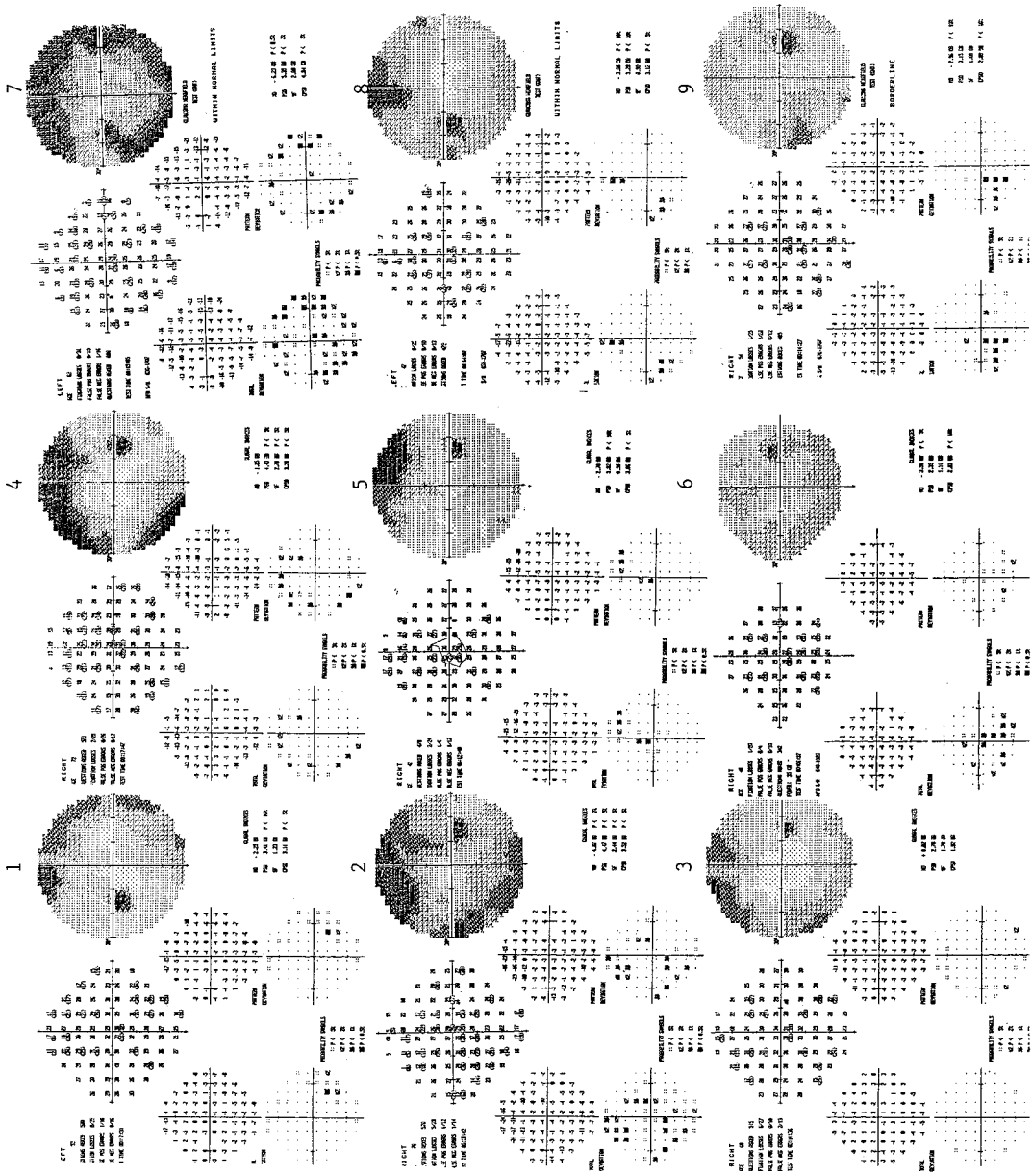

Fields 1-9: The visual fields referred to in Figure 2.

Field 5, was deemed defective by a majority of the expert panel. A majority found Field 3 to be normal. The remaining seven fields were all judged to be equivocal. The specific bias of the refereeing for each field is evident, with Fields 1 and 6 leaning toward normalcy, and Fields 2 and 9 toward pathology.

Conclusions

Since the task of screening is positively to identify bona fide field loss, the Henson appears to have performed commendably, avoiding the difficult diagnostic 'gray zone' which constituted the basis for the above analysis. According to the subjective assessments of the expert judges, the Henson only missed one abnormal field. The consensus among the judges indicates that the specificity of the scoring algorithm used to evaluate the Humphrey fields was imperfect with a consequential underestimate of the sensitivity of both the Henson and Damato.

Given the Henson's speed, the excellent compliance with Henson testing throughout the screenings, the tendency for clinicians to perform appropriate follow-up Humphrey fields when confronted with a Henson printout, and the very high concordance between Humphrey and Henson field assessments, it would appear that the Henson CFA 3000 is uniquely suited to population screenings. One instrument is capable of keeping pace with several exam lanes and, apart from glaucomatous damage, the Henson has detected brain tumors and other neuro-ophthalmic disorders, metabolic retinal disease, and ocular melanoma in our screenings.[4]

Acknowledgments

Thanks are owed to Drs Zingirian (Italy), Stürmer (Switzerland), Béchetoille (France), De la Rosa (Spain), Kitazawa (Japan), Chauhan (Canada), Wishard, Henson, Wild (United Kingdom), Sample, Johnson, and Mills (United States), and to all the other IPS attendees who completed the visual field survey. The author has no financial or other material interest in any of the techniques or instruments discussed. Funding for this work was provided in part by an unrestricted grant from Research to Prevent Blindness.

References

1. Sponsel WE, Ritch R, Stamper R, Higginbotham EJ, Anderson DR, Wilson MR, Zimmerman TJ: Prevent Blindness America Visual Field Screening Study. Am J Ophthalmol 120:699-708, 1995
2. Shields MB: The challenge of screening for glaucoma. Am J Ophthalmol 120:793-795, 1995
3. Hodapp E, Parrish RK II, Anderson DR: Clinical Decisions in Glaucoma, pp 52-61. St Louis, MO: CV Mosby 1993
4. Sponsel WE, Tu E, Lee B: Prevent Blindness America Visual Field Screening Study [Letter]. Am J Ophthalmol 121:735, 1996

COMPARING HUMPHREY VISUAL FIELDS AND CONTRAST SENSITIVITY CHANGES DURING CO_2 SUPPLEMENTATION AND HYPERVENTILATION
Effects of dorzolamide hydrochloride

YOLANDA TRIGO, WILLIAM E. SPONSEL, W. ROWE ELLIOTT III, JOSEPH M. HARRISON and JOSEPH T. KAVANAGH

University of Texas Health Science Center at San Antonio, San Antonio, TX, USA

Abstract

Carbon dioxide (CO_2) is a by-product of active metabolism. Once formed, the CO_2 rapidly reacts with water to form carbonic acid; this reaction is catalytically assisted by the enzyme carbonic anhydrase. In the human 'milieu interne' only 0.2% of the CO^2 formed remains free in the presence of carbonic anhydrase, the rest is catalyzed to carbonic acid. Carbonic anhydrase is so efficient a catalyst that 99% of the enzyme typically present within a tissue must be inhibited to produce a substantive increase in CO_2 concentrations. If a powerful enzyme inhibitor achieves this level of enzyme deactivation, a profound rise in the tissue acidity occurs. This is the mechanism whereby acetazolamide interferes with aqueous production in the ciliary processes, with a resultant fall in intraocular pressure.

In the brain, if the circulation is inadequate to keep up with metabolic needs, CO_2 builds up and cerebral blood flow increases correspondingly. It is known that, at the higher 0_2 tensions, oxygen is more readily released from its carrier hemoglobin, a phenomenon first described by Bohr. Thus, at higher levels of CO_2, both blood flow and oxygen transfer to cerebral tissues increase. The opposite physiological effects are noted at low CO_2 tensions. Recent work has reaffirmed that retinal autoregulation is also dependent on CO_2 concentrations.

Dorzolamide hydrochloride is a topically applied carbonic anhydrase inhibitor which has been shown to produce clinically significant reductions in intraocular pressure in both normal and glaucomatous or ocular hypertensive eyes.[1-6]

If the enzyme inhibitory effects of dorzolamide are uniform throughout the eye, we would expect to see a rise in CO_2 tension throughout all carbonic anhydrase-containing cells. It is known that carbonic anhydrase is abundantly spread throughout the pigmented tissue of the eye, including the retinal pigment epithelium which is adjacent to both the retinal and choroidal blood vessels. The effect of the high CO_2 tension would be to increase both the blood flow and oxygen availability to local tissues, including those responsible for vision. The result of this increased blood flow may be associated with changes in visual function.

Purpose: To determine the effects of dorzolamide on visual function in normal human subjects, while breathing carbon dioxide (CO_2)-enriched air or hyperventilating.

The full report of this study will appear elsewhere.

Address for correspondence: Yolanda Trigo, University of Texas Health Science Center, Department of Ophthalmology, 7703 Floyd Curl Drive, San Antonio, TX 78284-6230, USA

Perimetry Update 1996/1997, pp. 467–469
Proceedings of the XIIth International Perimetric Society Meeting
Würzburg, Germany, June 4–8, 1996
edited by M. Wall and A. Heijl

Methods: Twelve normal healthy subjects (five males and seven non-pregnant, non-lactating females) were enrolled in a double-masked crossover study with placebo control, to assess the effects of dorzolamide 2% on visual function. Each subject was treated in two phases for four days with either dorzolamide 2% or placebo t.i.d. with a two-week wash-out period between phases. Subjects were evaluated at *1.* baseline (normal breathing); *2.* while inhaling a mixture of 5% CO_2 and synthetic air; and *3.* while hyperventilating room air. Subjects maintained an end tidal pCO_2 15% higher than baseline while inhaling the CO_2 mixture, and an end tidal pCO_2 15% lower than baseline while hyperventilating. On Day 4 of each treatment phase, a 10-2 central, full threshold visual field was performed on each subject at each condition, using Humphrey Field Analyzer model 750. Contrast sensitivity to 1 and 4 cycles per degree (cpd) sinusoidal gratings, with a temporal frequency of 7.5 Hz, was also measured in the same subjects under like conditions on Day 2 of each treatment phase, using the NeuroScientific 8010 two-alternative forced choice, staircase method. Three sets of each visual function test were obtained at a prestudy examination. Intraocular pressure (IOP) was measured on each day under each condition, using the Mentor pneumotonometer. The results were analyzed using paired two-tailed *t* tests, and correlations by obtaining Pearson R values and Spearman rank correlation probability analysis.

Results: Dorzolamide appears to exert a positive effect on visual function in several ways:
1. Humphrey MD values during dorzolamide treatment showed a significant increase at the baseline condition compared to MD values during placebo treatment ($p<0.05$). Mean MD values remained positive on dorzolamide and negative on placebo during CO_2 breathing, and decreased significantly during hyperventilation.
2. Contrast sensitivity at 4 CPD decreased with CO_2 supplementation during placebo treatment ($p<0.01$), but there was no significant change during dorzolamide treatment ($p>0.05$).
3. Contrast sensitivity at 1 cpd decreased from baseline during both dorzolamide and placebo-treatment phases ($p<0.05$ and $p<0.01$, respectively) with drug treatment tending to have a modulating effect on hyperventilation-associated visual decrease.

Mean IOP values were not significantly different from baseline or during CO_2 breathing in the treatment phase or placebo phase ($p=0.3$). However, during hyperventilation in both treatment phases, there was a significant decrease in IOP. A mean decrease of 1.5 mmHg was associated with dorzolamide treatment ($p=0.002$) relative to both baseline and CO_2 breathing, which was three-fold greater than the IOP decrease observed in the placebo-treated eye.

Conclusions: Dorzolamide appears to enhance visual function in normal subjects under normal conditions, and prevents visual decrease during hyper- and hypocapnia.

Discussion: Dorzolamide appears to enhance visual function in normal subjects under normal conditions, and prevents visual decrease during hyper- and hypocapnia. The most pronounced effect of dorzolamide occurred during hypercapnia in contrast sensitivity at 4 cpd. Humphrey mean MD remained positive during hypercapnia as well. During hypocapnia, the modulating effect of dorzolamide was evident at 1 cpd.

Further investigation is required to clarify the findings reported above.

Acknowledgments

Supported by a research grant from Merck Research Laboratories, unrestricted grants from Research to Prevent Blindness, with equipment support from Humphrey Zeiss.

References

1. Lippa EA, Schumann JS, Higginbotham EJ, Kass MA, Weinreb RN, Skuta GL, Epstein DL, Shaw B, Holder DJ, Deasy DA, Wilensky JT: MK-507 vs sezolamide: comparative efficacy of two topically active carbonic anhydrase inhibitors. Ophthalmology 98:308-312, 1991
2. Hurvitz LM, Kaufman PL, Robin AL, Weinreb RN, Crawford K, Shaw B: New developments in the drug treatment of glaucoma. Drugs 41:514-532, 1991

3. Podos SM, Searle JB: Topically active carbonic anhydrase inhibitors for glaucoma. Arch Ophthalmol 109:38-40, 1991
4. Lippa EA, Carlson LE, Ehinger B, Eriksson LO, Finnstrom K, Holmin C, Nilsson SEG, Nyman K, Raitta C, Rinvold A, Tarkkanen A, Vegge T, Deasy D, Holder D, Ytteborg J: Dose-response and duration of action of dorzolamide, a topical carbonic anhydrase inhibitor. Arch Ophthalmol 110:495-499, 1992
5. Wilkerson M, Cyrlin M, Lippa EA, Esposito D, Deasy DA, Panebianco D, Fazio R, Yablonski M, Shields MB: Four-week safety and efficacy study of dorzolamide, a novel, active topical carbonic anhydrase inhibitor. Arch Ophthalmol 111:1343-1350, 1993
6. Strahlman E, Tipping R, Vogel R: A double-masked, randomized 1 year study comparing dorzolamide (Trusopt), timolol, and betaxolol. Arch Ophthalmol 113:1009-1016, 1995

APPLICATION OF VIDEO DISPLAY UNITS FOR CAMPIMETRIC PURPOSES
Luminance characteristics and calibration procedures

T.J. DIETRICH[1], M. FRIEDRICH[1], B. SELIG[1], N. BENDA[2] and U. SCHIEFER[1]

[1]University Eye Hospital, Department II; [2]Department of Medical Biometry; Tübingen, Germany

Abstract

Video display units (VDUs) provide many advantages in campimetry: in contrast to conventional bowl projection perimeters, presentation of stimuli that are darker than the surrounding background can be realized.

However, all cathode-ray tubes (CRTs) show an inhomogeneous distribution of luminance, resulting in differences of up to 50%. For campimetric purposes, a homogeneous background luminance is necessary. A new calibration routine, which has been integrated into the software of the Tübingen computer campimeter (TCC), generates a homogeneous background luminance with a maximum deviation of 10%. For this, a background image is used which has been calculated by the interpolation of numerous luminance measurements at 48 different locations on the screen. Thus, the quality requirements for perimeters can be maintained.

Additionally, it could also be shown that the luminance characteristics depend on the location on the screen. For stimulus presentation in campimetric threshold measurements, the luminance characteristics were also interpolated, resulting in an exactly calculated luminance difference at every screen location. In this way, the advances of VDUs for campimetric purposes can be used without loss of quality in psychophysical examinations.

Acknowledgment

Supported by the Tübingen Fortüne Program (Nos. 97 and 167).

Address for correspondence: T.J. Dietrich, MD, University Eye Hospital, Department II, Schleichstrasse 12-16, D-72076, Tübingen, Germany

Perimetry Update 1996/1997, p. 471
Proceedings of the XIIth International Perimetric Society Meeting
Würzburg, Germany, June 4–8, 1996
edited by M. Wall and A. Heijl

FIXATION CONTROL FOLLOWING REPEATED MACULAR THRESHOLD MEASUREMENTS

T. HALDA[1] and B. KOVÁCS[2]

[1]United Health Care Providers; [2]Department of Ophthalmology, University of Pécs; Pécs, Hungary

Abstract

The macular thresholds of a laser operator were studied before and after all-green (532 nm) photocoagulation. The macula threshold program of the Dicon AP 2000 perimeter determines the sensitivity of the macula by 14-point thresholding along the vertical and horizontal axes. The center points are the same for both axes. According to the authors' standards, fixation was correct if no significant difference was found between the two average values of the central points of the meridian, using the paired *t* test. One in 14 'cross examinations' demonstrated fixation error. Laser light has a reversible effect on the sensitivity of the macular threshold which can be detected by static perimeter and lasts for half an hour. In special cases, the method is considered suitable for controlling macular fixation.

Introduction

Perimetry fixation can be controlled by direct or indirect methods. Fixation can be controlled visually or indirectly by the Heijl-Krakau method. We present an indirect method for the control of fixation in the most sensitive area of the retina.

Controlling fixation during measurement of the macula area is hindered by two problems. Firstly, the receptor sensitivity and density are very high in the macular area, so that a little parafixation can cause significant changes in sensitivity. In other words, on the tip of the visual hill, small slopes indicate significant differences in levels. Therefore, for measurements carried out near the macula, the accuracy of fixation is very important. Secondly, a 'visually' small movement cannot be perceived safely, the control of fixation is subjective, and it cannot be measured or reproduced.

These problems occur when carrying out repeated macular measurements with a Dicon 2000 automatic perimeter.

Address for correspondence: T. Halda, Semmelweis u.5., 7623 Pécs, Hungary

Perimetry Update 1996/1997, pp. 473–477
Proceedings of the XIIth International Perimetric Society Meeting
Würzburg, Germany, June 4–8, 1996
edited by M. Wall and A. Heijl

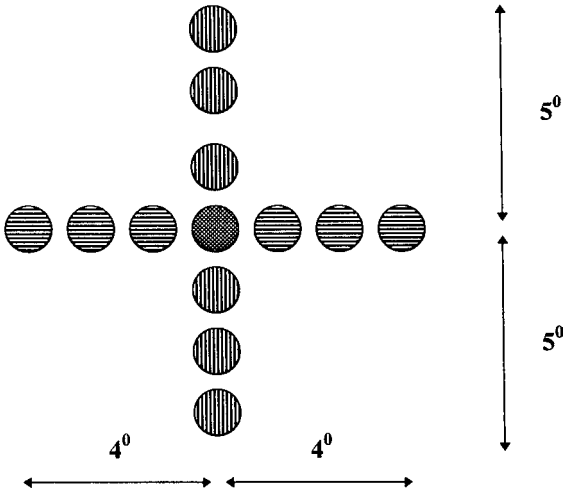

Fig. 1. Arrangements of the stimuli.

Methods

The equipment operates with fixed light emission diodes (LEDs) at a wavelength of 570 nm. Its macular program was originally intended for examining patients with age-related macular degeneration (AMD). Macular threshold identification in the LED matrix was originally used to test the blind spot. The person being examined fixates on a LED in the center of the matrix. For facilitation of the fixation, the area is bordered by four red LEDs. The accuracy of fixation can be controlled through a centrally placed periscope. With the equipment's macula program, the threshold is determined at 7-7 points, in an 8°-10° range.

During the control of the macular fixation, we capitalized on the fact that the sensitivity of the center (at 0°) was determined both horizontally and vertically (Fig. 1). According to our definition, fixation was correct when there was no significant difference between the two independently determined values.

The application of the method is illustrated by a series of experiments (Table 1).

Several articles have been published on the damaging effect of laser light on the operator's macular function.[1,2] Therefore, the short wavelength argon blue, which can cause irreversible damage, was withdrawn from the therapy regimen. Regular control of macular function is recommended to those carrying out laser treatment (so that changes can be detected while still at a reversible stage).

In our series of measurements, Jacobs and Harris' method was used with certain changes.[3] Horizontal and vertical stimulus thresholds were determined with a Dicon 2000 automatic perimeter. We used a background illumination of 31.5 asb and a 2-mm^2 spot size. Measuring was continued beyond the stimulus threshold in 0.2-log units until the stimulus could be identified twice. Horizontal and vertical macular stimulus thresholds were examined using two parameters. Peak sensitivity was determined at the fixation point. The average sensitivity of the macula was the average sensitivity of the three central points, including the peak. The operator's macular

Table 1. Design of measurement

Series No. 1
Perimetry: before and after treatment sessions
(0.5 hour, standard panphotocoagulation)
No. of tests: 12-13
Series No. 2 (Simulation of clinical use of the laser)
Target: matt black test bar in place of eye
No lens used
Viewing with biomicroscope
Series parameters:
500 burns in repeat mode
350 mW energy
0.1 sec
0.5 mm spot size
Perimetry: before exposure
after 0.5, 1, 2, 4 hours' exposure
No. of tests: 5-22

Table 2. Fixation controls

Series No. 1
4 'cross-examinations'
after treatment - right eye
difference: 1.96 ± -0.55 asb
$n = 13$
$p<0.004$ (paired t test)
Series No. 2
10 'cross-examinations'
no significant difference
$n = 5\text{-}22$
p: $1.00 \leq 0.01$ (paired t test)

threshold sensitivity was measured before and immediately after the laser treatments.

This series of measurements was repeated in experimental circumstances at standardized laser exposure and time intervals.

After the measurement, independently determined central sensitivity was compared among the 14 independent groups. During the 'cross examinations' in the first series, the 'before' treatment sensitivities in the right eye and the two-paired t test showed significant differences ($p \leq 0.004$) (Table 2). Because of this, the results in the right eye examined in the out-patient unit were omitted from the evaluation. The t values of the tests controlling the other 13 fixations fell between 1.00 and 0.1; in these cases, fixation was therefore regarded as being correct.

In the out-patients (the first series), a 1.42 ± 1.58 asb stimulus decrease in the level of the threshold was detected after treatment. This was significant with the Wilcoxon single rank test ($z=0.043$).

In experimental circumstances (the second series) the peak sensitivity in the right eye showed a significant decrease of 2.28 ± 0.79 asb half an hour after the laser exposure ($z=0.0098$). The vertical average sensitivity in the left eye also decreased by 4.44 ± 4.31 asb ($z=0.0051$).

After half an hour, no significant decreases were detected.

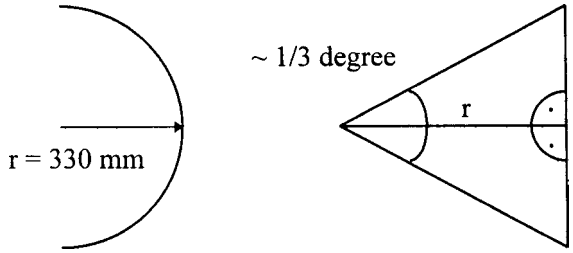

Fig. 2. Object-size estimation.

Results

In special cases, the method is considered to be suitable for controlling macular fixation.

The accuracy of the method is determined by the physical dimension of the LEDs, the radius of the bowl and the distance between the given fixation point and the macula. In our case: 2-mm^2-sized LEDs were placed on the surface of a bowl with a 330-mm radius. Therefore, we can calculate that the test object's size is one-third of a degree. In the case of good fixation, no difference can be detected, and therefore accuracy is within this value (Fig. 2).

Laser light has a reversible effect on the sensitivity of the macular threshold; this effect can be detected by static perimetry and lasts for half an hour.

Discussion

Advantages: The AP 2000 macula program enables fixation to be controlled, which was not possible before. It is very accurate.
Disadvantages: The correctness of fixation can only be evaluated after a complete series of measurements. It can only be used for evaluating a series of measurements carried out on the same person.

The method is suitable for controlling the fixation of individual measurements. It is only a matter of using software repeatedly indicating and determining the threshold sensitivity of an assigned point, and then checking this point at random using a visual field examination. These results must be evaluated separately. Statistically significant difference indicates that the fixation was not correct.

The method is suitable for the preliminary quantitative determination of the fixation range needed. The nearer we mark the point of fixation to the fovea, the stricter we can make the conditions.

The stimulus repeatedly appearing in the fixation point can cause psychological pressure in connection with the correct execution of the fixation.

References

1. Berninger T, Canning C et al: Using argon laser blue light reduces ophthalmologists' color contrast sensitivity. Arch Ophthalmol 107:1453-1458, 1989
2. Gündüz K, Arden G: Changes in colour contrast sensitivity associated with operating argon lasers. Br J Ophthalmol 73:241-246, 1989
3. Jacobs N, Harris M: Definition of normal macular thresholds on the Dicon AP 2000 autoperimeter. Acta Ophthalmol (Kbh) 69:253-255, 1991

INDEX OF AUTHORS